Lecture Notes in Physics 885

Angelo Vulpiani
Fabio Cecconi
Massimo Cencini
Andrea Puglisi
Davide Vergni *Editors*

Large Deviations in Physics

The Legacy of the Law of Large Numbers

Springer

Lecture Notes in Physics

Volume 885

For further volumes:
http://www.springer.com/series/5304

The Lecture Notes in Physics

The series Lecture Notes in Physics (LNP), founded in 1969, reports new developments in physics research and teaching-quickly and informally, but with a high quality and the explicit aim to summarize and communicate current knowledge in an accessible way. Books published in this series are conceived as bridging material between advanced graduate textbooks and the forefront of research and to serve three purposes:

- to be a compact and modern up-to-date source of reference on a well-defined topic
- to serve as an accessible introduction to the field to postgraduate students and nonspecialist researchers from related areas
- to be a source of advanced teaching material for specialized seminars, courses and schools

Both monographs and multi-author volumes will be considered for publication. Edited volumes should, however, consist of a very limited number of contributions only. Proceedings will not be considered for LNP.

Volumes published in LNP are disseminated both in print and in electronic formats, the electronic archive being available at springerlink.com. The series content is indexed, abstracted and referenced by many abstracting and information services, bibliographic networks, subscription agencies, library networks, and consortia.

Proposals should be sent to a member of the Editorial Board, or directly to the managing editor at Springer:

Christian Caron
Springer Heidelberg
Physics Editorial Department I
Tiergartenstrasse 17
69121 Heidelberg/Germany
christian.caron@springer.com

Angelo Vulpiani • Fabio Cecconi •
Massimo Cencini • Andrea Puglisi • Davide Vergni
Editors

Large Deviations in Physics

The Legacy of the Law of Large Numbers

Springer

Editors

Angelo Vulpiani
Dipartimento di Fisica
Università di Roma Sapienza
Roma
Italy

Fabio Cecconi
Massimo Cencini
Andrea Puglisi
Istituto Sistemi Complessi
Consiglio Nazionale delle Ricerche
Roma
Italy

Davide Vergni
Istituto per le Applicazioni del Calcolo
Consiglio Nazionale delle Ricerche
Roma
Italy

ISSN 0075-8450 ISSN 1616-6361 (electronic)
Lecture Notes in Physics
ISBN 978-3-642-54250-3 ISBN 978-3-642-54251-0 (eBook)
DOI 10.1007/978-3-642-54251-0
Springer Heidelberg New York Dordrecht London

Library of Congress Control Number: 2014940148

Preface

Probability theory was at its origin, almost solely, centered around games of chance (cards and dice). With the *Ars Conjectandi*, Jakob Bernoulli, while obtaining the first version of the theorem now known as the Law of Large Numbers (LLN), moved the theory of probability away from being primarily a vehicle for calculating gambling odds. This step has been crucial by showing that the probability theory might have an important role in the understanding of a variety of problems in many areas of the natural sciences and human experiences.

In 1913, when the tsar Nicholas II called for celebrations of the 300th Anniversary of the Romanov rule, the great Russian mathematician Andrei Andreyevich Markov responded by organizing a symposium aimed at commemorating a different anniversary. Markov took the occasion to celebrate the bicentenary of Bernoulli's *Ars conjectandi*: Bernoulli actually completed his book by 1690, but the book was only published posthumously in 1713 by his nephew Niklaus because of family quarrels.

Nowadays, one century after Markov, the autocratic tsarist government is over and we can take the occasion to celebrate the Law of Large Numbers with no need of extra scientific pretexts.

The LLN is at the base of a scientific legacy whose relevance cannot be overestimated. We can start mentioning the great visionary idea of the ergodic hypothesis by Ludwig Boltzmann. The ergodicity issue, originally introduced in the context of the statistical mechanics and then developed as an autonomous branch of measure theory, can be seen as the generalization of the LLN to non-independent variables. This topic is still an active research field in mathematical physics. In addition, it constitutes the starting point of the numerical methods used in statistical mechanics, namely the molecular dynamics and the Monte Carlo methods.

The most important physical properties of macroscopic objects are determined by mean values, whose mathematical base is guaranteed by the LLN. But, in many cases, also the fluctuations can be important. The control of "small" fluctuations around the mean value is provided by the Central Limit Theorem (CLT), whose general relevance was established for the first time in 1812 with the book *Théorie Analytique des Probabilités* by Pierre Simon Laplace. From a physical point of

view, however, even very small fluctuations can be dramatically important. As a paradigmatic example, we can mention the treatment of the Brownian motion, which among the many still in progress applications brought conclusive evidence for the atomic hypothesis.

Beyond their conceptual importance, thanks to their link to response functions via the fluctuation-dissipation theorem, fluctuations are becoming more and more important in present-day applications, especially via the recently established fluctuation relations. Their relevance is amplified in small (micro- and nano-) systems, and in materials (as granular matter) where the number of effective elementary constituents is not as large as in gases or liquids. In such systems large excursions from the average cannot be neglected, therefore it is necessary to go beyond the Gaussian approximation, i.e. beyond the realm of validity of the CLT. The proper technical tool to study such strong fluctuations is the Large Deviation Theory (LDT), which generalizes the CLT.

The first general mathematical formulation of the Large Deviation Theory is due to Harald Cramér in the 1930s. However, the very first application of LDT can be ascribed to Boltzmann who, using combinatorial arguments, had been able to show the relevance of the entropy as a bridge between microscopic and macroscopic levels.

This book encompasses some recent developments of the fundamental limit theorems – LLN, CLT and LDT – of the probability theory in statistical physics, in particular: ergodicity breaking, non-equilibrium and fluctuation relations, disordered systems, computational methods, systems with long-range interactions, Brownian motors, chaotic dynamics, anomalous diffusion and turbulence.

Rome, Italy
December 2013

Angelo Vulpiani
Fabio Cecconi
Massimo Cencini
Andrea Puglisi
Davide Vergni

Contents

1 From the Law of Large Numbers to Large Deviation Theory in Statistical Physics: An Introduction 1
Fabio Cecconi, Massimo Cencini, Andrea Puglisi, Davide Vergni, and Angelo Vulpiani
1.1 Introduction 1
1.2 An Informal Historical Note 3
1.2.1 Law of Large Numbers and Ergodicity 4
1.2.2 Central Limit Theorems 9
1.2.3 Large Deviation Theory 11
1.3 LDT for the Sum and Product of Random Independent Variables 13
1.3.1 A Combinatorial Example 13
1.3.2 Product of Random Variables 15
1.4 Large Deviation Theory: Examples From Physics 17
1.4.1 Energy Fluctuations in the Canonical Ensemble 17
1.4.2 Multiplicative Cascade in Turbulence 18
1.4.3 Chaotic Systems 19
1.4.4 Disordered Systems 21
1.4.5 Entropy Production in Markov Processes 24
References 26

2 Ergodicity: How Can It Be Broken? 29
Giancarlo Benettin, Roberto Livi, and Giorgio Parisi
2.1 The Ergodic Hypothesis 30
2.1.1 The Fundamental Physical Ideas 30
2.1.2 A Well-Posed Mathematical Setting 33
2.2 Ergodicity Breaking 36
2.2.1 Ergodicity Breaking in the Fermi-Pasta-Ulam Model at Low Energies 37
2.2.2 Ergodicity Breaking Induced by Breather States in the Discrete Nonlinear Schrödinger Equation 47

2.3 Ergodicity Breaking at Equilibrium 53
2.3.1 General Concepts 53
2.3.2 The Gibbs States 54
2.3.3 The Local DRL Equilibrium States 60
2.4 Glassy System 62
2.4.1 A Heuristic Construction: Finite Volume States 62
2.4.2 The Case of Many States 65
References 68

3 Large Deviations in Stationary States, Especially Nonequilibrium ... 71
Giovanni Jona-Lasinio
3.1 Introduction 71
3.2 Assumptions 73
3.3 The Fundamental Formula 74
3.4 Time Reversal and Its Consequences 78
3.5 Long Range Correlations 80
3.6 Fluctuations of the Current and Dynamical Phase Transitions 81
3.7 Universality in Current Fluctuations and Other Results 83
3.8 Nonequilibrium Phase Transitions 84
3.9 Large Deviations for Reaction-Diffusion Systems 85
3.10 Thermodynamic Interpretation of the Large Deviation Functional 85
3.11 Concluding Remarks and Additional References 89
References 90

4 Fluctuation-Dissipation and Fluctuation Relations: From Equilibrium to Nonequilibrium and Back 93
Paolo Adamo, Roman Belousov, and Lamberto Rondoni
4.1 Concise History 93
4.2 The Brownian Motion and the Langevin Equation 95
4.3 The Fluctuation-Dissipation Relation 99
4.4 Evolution of Probability Distributions 103
4.4.1 Ergodicity and Mixing 107
4.5 Linear Response 108
4.6 Onsager-Machlup: Response from Small Deviations 112
4.7 Fluctuation Relations: Response from Large Deviations 118
4.7.1 The Gallavotti-Cohen Approach 119
4.7.2 Fluctuation Relations for the Dissipation Function 121
4.7.3 Green-Kubo Relations 125
4.7.4 Jarzynski Equality 126
4.8 t-Mixing and General Response Theory 127
4.9 Concluding Remarks 129
References 131

5 Large Deviations in Disordered Spin Systems 135
Andrea Crisanti and Luca Leuzzi
5.1 Some General Results on Large Deviations 135
5.1.1 An Example: The Mean Field Ising Model 139
5.2 Sample-to-Sample Free Energy Fluctuations and Replica Trick ... 142
5.2.1 Random Ising Chain 143
5.2.2 Replica Trick 145
5.2.3 Replicas in the Random Ising Chain 147
5.2.4 From Small to Large Deviations 148
5.2.5 Random Directed Polymer 151
5.2.6 Mean-Field Spin-Glass 151
5.2.7 Positive Large Deviations 153
5.2.8 Spherical Spin-Glass Model and Gaussian Random Matrices 154
5.3 Sample-to-Sample Fluctuation of the Overlap 155
5.3.1 Back to the Replicated Random Ising Chain 156
5.3.2 Random Field Ising Model 158
5.4 A Final Word 159
References 159

6 Large Deviations in Monte Carlo Methods 161
Andrea Pelissetto and Federico Ricci-Tersenghi
6.1 Introduction 161
6.2 Data Reweighting 163
6.3 Multiple Histogram Method 168
6.4 Umbrella Sampling and Simulated Tempering 172
6.4.1 Umbrella Sampling 172
6.4.2 Simulated Tempering 173
6.4.3 Equivalence of Simulated Tempering and Umbrella Sampling 174
6.5 Generalizing the Umbrella Method: Multicanonical Sampling 178
6.6 Parallel Tempering 184
6.6.1 General Considerations 184
6.6.2 Some General Rigorous Results 186
6.6.3 Optimal Choice of Temperatures 187
6.6.4 Improving Parallel Tempering 189
6.7 Conclusions 190
References 190

7 Large Deviations Techniques for Long-Range Interactions 193
Aurelio Patelli and Stefano Ruffo
7.1 Long-Range Interactions 193
7.2 Some Useful Results of Large Deviations Theory 198
7.3 Thermodynamic Functions From Large Deviations Theory 199

7.4 Applications 202
7.4.1 Three-States Potts Model 203
7.4.2 The Blume-Capel Model 205
7.4.3 A System with Continuous Variables: The XY Model ... 208
7.4.4 Negative Susceptibility: ϕ^4 Model 212
7.4.5 The Free Electron Laser 215
7.5 The Min-Max Procedure and a Model with Short and Long-Range Interactions 216
7.6 Conclusions and Perspectives 219
References 219

8 Large Deviations of Brownian Motors 221
Alessandro Sarracino and Dario Villamaina
8.1 Introduction 221
8.2 Nonequilibrium Fluctuations and Brownian Motors 224
8.2.1 Kinetic Ratchets 225
8.2.2 Molecular Motors 227
8.3 Experiments in Granular Systems 231
8.3.1 Velocity Fluctuations of a Self-Propelled Polar Particle 232
8.3.2 Asymmetric Rotor in a Granular Gas 234
8.4 Conclusions 238
References 239

9 Stochastic Fluctuations in Deterministic Systems 243
Antonio Politi
9.1 Introduction 243
9.2 Kolmogorov-Sinai Entropy 245
9.3 Lyapunov Exponents 250
9.3.1 Pesin Relation 253
9.4 Non Hyperbolicity 254
9.4.1 A 3d Map 256
9.5 Space-Time Chaos 257
9.6 Stable Chaos 259
References 261

10 Anomalous Diffusion: Deterministic and Stochastic Perspectives 263
Roberto Artuso and Raffaella Burioni
10.1 Introduction 263
10.2 Stochastic Anomalous Transport 264
10.2.1 Moments and Scaling 264
10.2.2 A Few Observations About Lévy Stable Laws 267
10.2.3 An Extension: Continuous Time Random Walks 269
10.2.4 Topological Effects in Subdiffusion: Weak Anomalous Diffusion and Random Walks on Graphs 272

10.2.5 Topological Effects in Superdiffusion: Strong Anomalous Diffusion and Quenched Lévy Walks 277
10.3 Deterministic Anomalous Transport 281
10.3.1 A Brief Tour of Intermittency 281
10.4 Chain of Intermittent Maps 284
10.4.1 Subdiffusion 287
10.4.2 Superdiffusion 287
10.5 Deterministic vs Stochastic Approximation 289
10.6 A Final Warning 291
References 291

11 Large Deviations in Turbulence 295
Guido Boffetta and Andrea Mazzino
11.1 Introduction 295
11.2 Global Scale Invariance and Kolmogorov Theory 296
11.3 Accounting for the Fluctuations: The Multifractal Model 299
11.3.1 The Statistics of Velocity Gradient 302
11.3.2 The Statistics of Acceleration 303
11.3.3 Multiplicative Processes for the Multifractal Model 305
11.4 Fluctuations of the Energy Dissipation Rate 307
11.5 Conclusions 309
References 309

Index 311

Contributors

Paolo Adamo Department of Mathematical Sciences, Politecnico di Torino, Torino, Italy

Roberto Artuso Dipartimento di Scienza e Alta Tecnologia, Università degli Studi dell'Insubria, Como, Italy

Roman Belousov Department of Mathematical Sciences, Politecnico di Torino, Torino, Italy

Giancarlo Benettin Dipartmento di Matematica Pura e Applicata, Università di Padova, Padova, Italy

Guido Boffetta Dipartimento di Fisica and INFN, University of Torino, Torino, Italy

Raffaella Burioni Dipartimento di Fisica, INFN Gruppo Collegato di Parma, Università degli Studi di Parma, Parma, Italy

Fabio Cecconi Istituto dei Sistemi Complessi, Consiglio Nazionale delle Ricerche, Rome, Italy

Massimo Cencini Istituto dei Sistemi Complessi, Consiglio Nazionale delle Ricerche, Rome, Italy

Andrea Crisanti Dipartimento di Fisica, Università di Roma "Sapienza" and Istituto dei Sistemi Complessi, Consiglio Nazionale delle Ricerche, Rome, Italy

Giovanni Jona-Lasinio Dipartimento di Fisica and INFN, Università di Roma "Sapienza", Rome, Italy

Luca Leuzzi Istituto per i Processi Chimico-Fisici, Consiglio Nazionale delle Ricerche and Dipartimento di Fisica, Università di Roma "Sapienza", Rome, Italy

Roberto Livi Dipartimento di Fisica, Università di Firenze, Sesto Fiorentino, Italy

Andrea Mazzino INFN and CINFAI Consortium, DICCA – University of Genova, Genova, Italy

Giorgio Parisi Dipartimento di Fisica, Università di Roma "Sapienza", Rome, Italy

Aurelio Patelli Dipartimento di Fisica e Astronomia and INFN, Università di Firenze, Sesto Fiorentino, Italy

Andrea Pelissetto Dipartimento di Fisica and INFN, Università "Sapienza", Rome, Italy

Antonio Politi SUPA, Institute for Complex Systems and Mathematical Biology, King's College, University of Aberdeen, Aberdeen, UK

Andrea Puglisi Istituto dei Sistemi Complessi, Consiglio Nazionale delle Ricerche, and Dipartimento di Fisica, Università "Sapienza", Rome, Italy

Federico Ricci-Tersenghi Dipartimento di Fisica and INFN, Università "Sapienza", Rome, Italy

Lamberto Rondoni Department of Mathematical Sciences, Politecnico di Torino, Torino, Italy

Stefano Ruffo Dipartimento di Fisica e Astronomia, INFN and CNISM, Università di Firenze, Sesto Fiorentino, Italy

Alessandro Sarracino Istituto dei Sistemi Complessi, Consiglio Nazionale delle Ricerche, and Dipartimento di Fisica, Università "Sapienza", Rome, Italy

Davide Vergni Istituto per le Applicazioni del Calcolo, Consiglio Nazionale delle Ricerche, Rome, Italy

Dario Villamaina Laboratoire de Physique Théorique et Modèles Statistiques, UMR 8626, Université Paris Sud 11 and CNRS, Orsay, France

Angelo Vulpiani Dipartimento di Fisica, Università "Sapienza" and Istituto dei Sistemi Complessi, Consiglio Nazionale delle Ricerche, Rome, Italy

Chapter 1
From the Law of Large Numbers to Large Deviation Theory in Statistical Physics: An Introduction

Fabio Cecconi, Massimo Cencini, Andrea Puglisi, Davide Vergni, and Angelo Vulpiani

Abstract This contribution aims at introducing the topics of this book. We start with a brief historical excursion on the developments from the law of large numbers to the central limit theorem and large deviations theory. The same topics are then presented using the language of probability theory. Finally, some applications of large deviations theory in physics are briefly discussed through examples taken from statistical mechanics, dynamical and disordered systems.

1.1 Introduction

Describing the physical properties of macroscopic bodies via the computation of (ensemble) averages was the main focus of statistical mechanics at its early stage. In fact, as macroscopic bodies are made of a huge number of particles, fluctuations were expected to be too small to be actually observable. Broadly speaking, we can say that the theoretical basis of statistical descriptions was guaranteed by the law of large numbers. Boltzmann wrote: *In the molecular theory we assume that the laws of the phenomena found in nature do not essentially deviate from the limits that they*

F. Cecconi • M. Cencini
Istituto dei Sistemi Complessi, Consiglio Nazionale delle Ricerche, Via dei Taurini 19, Rome, I-00185, Italy
e-mail: fabio.cecconi@roma1.infn.it; massimo.cencini@cnr.it

A. Puglisi (✉) • A. Vulpiani
Istituto dei Sistemi Complessi, Consiglio Nazionale delle Ricerche, and Dipartimento di Fisica, Università "Sapienza", Piazzale Aldo Moro 5, Rome, I-00185, Italy
e-mail: andrea.puglisi@roma1.infn.it; angelo.vulpiani@roma1.infn.it

D. Vergni
Istituto per le Applicazioni del Calcolo, Consiglio Nazionale delle Ricerche, Via dei Taurini 19, Rome, I-00185, Italy
e-mail: davide.vergni@cnr.it

A. Vulpiani et al. (eds.), *Large Deviations in Physics*, Lecture Notes in Physics 885,
DOI 10.1007/978-3-642-54251-0_1,

would approach in the case of an infinite number of infinitely small molecules, while Gibbs[1] remarked ... *[the fluctuations] would be in general vanishing quantities, since such experience would not be wide enough to embrace the more considerable divergences from the mean values* [1].

Although very small, the importance of fluctuations was recognized quite early to find conclusive evidence for the atomistic hypothesis. At the end of the nineteenth century, atomic theory was still considered, by influential scientists as Ostwald and Mach, useful but non real for the building of a consistent description of nature: *The atomic theory plays a part in physics similar to that of certain auxiliary concepts in mathematics; it is a mathematical model for facilitating the mental reproduction of facts* [1].

The situation changed at the beginning of the twentieth century, when Einstein realized the central role played by the fluctuations and wrote: *The equation* [NA: for the energy fluctuations $\langle E^2\rangle - \langle E\rangle^2 = kT^2C_V$, $C_V = \partial\langle E\rangle/\partial T$ being the specific heat] *we finally obtained would yield an exact determination of the universal constant* [NA: the Avogadro number], *if it were possible to determine the average of the square of the energy fluctuations of the system; this is however not possible according to our present knowledge*. For macroscopic objects the equation for the energy fluctuations cannot actually be used for the determination of the Avogadro number. However, Einstein's intuition was correct as he understood how to relate the Avogadro number to a macroscopic quantity—the diffusion coefficient D—obtained by observing the fluctuations of a Brownian particle—D indeed describes the long time ($t \to \infty$) behavior of particle displacement $\langle (x(t) - x(0))^2\rangle \simeq 2Dt$, which is experimentally accessible. The theoretical work by Einstein and the experiments by Perrin gave a conclusive evidence of atomism: the celebrated relationship between the diffusion coefficient (measurable at the macroscopic level) and the Avogadro number N_A (related to the atomistic description) is

$$D = \frac{RT}{6N_A\pi\eta a},$$

where T and η are the temperature and dynamic viscosity of the fluid respectively, a the radius of the colloidal particle, $R = N_Ak$ is the perfect gas constant and k is the Boltzmann constant.

Einstein's seminal paper on Brownian motion contains another very important result, namely the first example of Fluctuation-Dissipation Theorem (FDT): a relation between the fluctuations (given by correlation functions) of an unperturbed system and the mean response to a perturbation. In the specific case of Brownian motion, FDT appears as a link between the diffusion coefficient (a property of the unperturbed system) and the mobility, which measures how the system reacts to a small perturbation.

[1] Who, by the way, already knew the expression for the mean square energy fluctuations.

Beyond their conceptual relevance and the link with response functions, fluctuations in macroscopic systems are quantitatively extremely small and hard to detect (but for the case of second order phase transition in equilibrium systems). However, in recent years statistical mechanics of small systems is becoming more and more important due to the theoretical and technological challenges of micro- and nano-physics. In such small systems[2] since large excursions from averages values become increasingly important, it is mandatory to go beyond the Gaussian approximation (i.e. beyond the realm of validity of the central limit theorem) by means of the large deviation theory.

Next section presents a non-exhaustive historical survey from the law of large numbers to large deviation theory. Then, in Sect. 1.3 we illustrate with two examples how large deviation theory works. Section 1.4 illustrates some applications of large deviations in statistical physics.

1.2 An Informal Historical Note

Perhaps the most straightforward way to understand the connection between Law of Large Numbers (LLN), the Central Limit Theorem (CLT) and the Large Deviation Theory (LDT) is to consider a classical topic of probability theory, namely the properties of the empirical mean

$$y_N = \frac{1}{N}\sum_{j=1}^{N} x_j \tag{1.1}$$

of a sequence $\{x_1, \ldots, x_N\}$ of N random variables. Three basic questions naturally arise when N is very large:

(a) The behavior of the empirical mean y_N, the possible convergence to an asymptotic value and its dependence on the sequence;
(b) The statistics of small fluctuations of y_N around $\langle y_N \rangle$, i.e., of $\delta y_N = y_N - \langle y_N \rangle$ when $|\delta y_N|$ is "small";
(c) The statistical properties of rare events when such fluctuations are "large".

In the simplest case of sequences $\{x_1, \ldots, x_N\}$ of independent and identically distributed (i.i.d.) random variables with expected value $\langle x \rangle$ and with finite variance, the law of large numbers answers point (a): the empirical average gets close and closer to the expected value $\langle x \rangle$ when N is large:

$$\lim_{N\to\infty} P\left(|y_N - \langle x \rangle| < \epsilon\right) \to 1\,. \tag{1.2}$$

[2]We note that sometimes even in macroscopic systems (e.g. granular materials) the number of effective elementary constituents (e.g. the seeds) is not astonishingly large as in gases or liquids.

In the more general case of dependent variables, in principle, the empirical mean may depend on the specific sequence of random variables. This is the essence of the ergodic problem which generalizes the LLN and had a crucial role for the development of statistical mechanics.

Issue (b) is addressed by the central limit theorem. For instance, in the simple case of i.i.d. variables with expected value $\langle x \rangle$ and finite variance σ^2, the CLT describes the statistics of small fluctuations, $|\delta y_N| \lesssim O(\sigma/\sqrt{N})$, around the mean value when N is very large. Roughly speaking, the CLT proves that, in the limit $N \gg 1$, the quantity

$$z_N = \frac{1}{\sigma\sqrt{N}} \sum_{j=1}^{N} (x_j - \langle x \rangle) \tag{1.3}$$

is normally distributed, meaning that

$$p(z_N = z) \simeq \frac{1}{\sqrt{2\pi}} e^{-\frac{z^2}{2}} , \tag{1.4}$$

independently of the distribution of the random variables. Under suitable hypothesis the theorem can be extended to dependent (weakly correlated) variables.

Finally, the last point (c) is the subject of large deviation theory which, roughly, states that in the limit $N \gg 1$

$$p(y_N = y) \sim e^{-N\mathscr{C}(y)} . \tag{1.5}$$

Unlike the central limit theorem result with the "universal" limit probability density (1.4), the detailed functional dependence of $\mathscr{C}(y)$—the Cramér or rate function—depends on the probability distribution of $\{x_1, \ldots, x_N\}$. However, $\mathscr{C}(y)$ possesses some general properties: it is zero for $y = \langle y_N \rangle$ and positive otherwise, moreover—when the variables are independent (or weakly correlated)—it is a convex function. Clearly, whenever the CLT applies, $\mathscr{C}(y)$ can be approximated by a parabola around it minimum in $\langle y \rangle$.

As frequently occurring in the development of science, the actual historical path did not follow the simplest trajectory: (a) then (b) and at the end (c). Just to mention an example, Boltzmann introduced the ergodic problem and developed—ante litteram—some aspects of large deviations well before the precise mathematical formulation of the central limit theorem.

1.2.1 Law of Large Numbers and Ergodicity

In the origins, the calculus of probabilities was, to a large extent, a collection of specific rules for specific problems, mainly a matter for rolling dice and card games. For instance, the works by Pascal and Fermat originated by practical questions

in gambling raised by the chevalier de Méré (a French nobleman in love with gambling) [2].

1.2.1.1 J. Bernoulli

J. Bernoulli gave the first important contribution moving the theory of probability away from gambling context with the posthumous book *Ars Conjectandi* (The art of conjecturing), published in 1713 and containing the LLN.[3] In modern terms, if $\{x_1, \ldots, x_N\}$ are i.i.d. with finite variance and expected value $\langle x \rangle$ then for each $\epsilon > 0$ and if $N \to \infty$

$$P\left(\left|\frac{1}{N}\sum_{j=1}^{N} x_j - \langle x \rangle\right| > \epsilon\right) \to 0 \,. \tag{1.6}$$

A particularly important case of the above result is

$$P(|f_N - p| > \epsilon) \to 0 \,, \tag{1.7}$$

where f_N is the frequency of an event over N independent trials, and p is its occurrence probability in a single trial. The result (1.7) stands at the basis of the interpretation of probability in terms of frequencies.

1.2.1.2 Boltzmann

Boltzmann introduced the ergodic hypothesis while developing statistical mechanics [3]. In modern language, we can state the ergodic problem as follows. Consider a deterministic evolution law U^t in the phase space Ω,

$$\mathbf{X}(0) \to \mathbf{X}(t) = U^t \mathbf{X}(0) \,,$$

and a probability measure $d\mu(\mathbf{X})$ invariant under the evolution U^t, meaning that $d\mu(\mathbf{X}) = d\mu(U^{-t}\mathbf{X})$. The dynamical system $\{\Omega, U^t, d\mu(\mathbf{X})\}$ is ergodic, with respect to the measure $d\mu(\mathbf{X})$, if, for every integrable function $A(\mathbf{X})$ and for almost all initial conditions $\mathbf{X}(t_0)$, time and phase average coincide:

$$\overline{A} \equiv \lim_{\mathscr{T}\to\infty} \frac{1}{\mathscr{T}} \int_{t_0}^{t_0+\mathscr{T}} A(\mathbf{X}(t))\mathrm{d}t = \int A(\mathbf{X}) d\mu(\mathbf{X}) \equiv \langle A \rangle \,, \tag{1.8}$$

where $\mathbf{X}(t) = U^{t-t_0}\mathbf{X}(t_0)$.

[3] The most rudimentary form of the LLN seems to be credited to Cardano.

It is worth recalling why the ergodic hypothesis was so important for the development of statistical mechanics. Simplifying, Boltzmann's program was to derive thermodynamics for macroscopic bodies—composed by, say, $N \gg 1$ particles—from the microscopic laws of the dynamics. Thermodynamics consists in passing from the $6N$ degrees of freedom to a few macroscopic, experimentally accessible quantities such as, e.g., the temperature and pressure. An experimental measurement is actually the result of a single observation during which the system passes through a very large number of microscopic states. Denoting with $\mathbf{q}_i$ and $\mathbf{p}_i$ the position and momentum vectors of the i-th particle, the microscopic state of the N-particles system at time t is described by the $6N$-dimensional vector $\mathbf{X}(t) \equiv (\mathbf{q}_1(t), \ldots, \mathbf{q}_N(t); \mathbf{p}_1(t), \ldots, \mathbf{p}_N(t))$, which evolves according to the Hamilton equations. The measurement of an observable $A(\mathbf{x})$ effectively corresponds to an average performed over a very long time (from the microscopic point of view): $\overline{A}_{\mathscr{T}} = (1/\mathscr{T}) \int_{t_0}^{t_0+\mathscr{T}} A(\mathbf{X}(t))\mathrm{d}t$. The theoretical calculation of the time average $\overline{A}_{\mathscr{T}}$, in principle, requires both the knowledge of the microscopic state at time t_0 and the determination of its evolution. The ergodic hypothesis eliminates both these necessities, provided we know the invariant measure. In statistical mechanics of, e.g., isolated systems a natural candidate for the invariant measure $d\mu(\mathbf{X})$ is the microcanonical measure on the constant energy surface $H = E$.

To the best of our knowledge the first precise result on ergodicity, i.e. the validity of (1.6) for non independent stochastic processes has been obtained by A.A. Markov, for a wide class of stochastic processes (now called Markov Chains). Consider an aperiodic and irreducible Markov Chain with M states, transition probabilities $\{P_{i\to j}\}$, and invariant probabilities $\pi_1, \pi_2, \ldots, \pi_M$, and an observable A which takes value A_j on the state j, then for almost all the realizations $\{j_t\}$ we have

$$\overline{A} \equiv \lim_{T\to\infty} \frac{1}{T} \sum_{t=1}^{T} A_{j_t} = \sum_{j=1}^{N} A_j \pi_j = \langle A \rangle \,, \tag{1.9}$$

where j_t indicates the state of the chain at time t of a "walker" performing a trajectory according to the transition probabilities $\{P_{i\to j}\}$. There is a curious story at the origin of the above result [4]. Markov, who was an atheist and a strong *critic* of both the tsarist government and the Orthodox Church, at the beginning of the twentieth century had a rather hot diatribe with the mathematician Nekrasov, who had opposite political and religious opinions. The subject of the debate was about the statistical regularities and their role for the problem of free will. Nekrasov noted that the LLN of Bernoulli is based on the independence of successive experiments, while, among human beings, the situation is rather different, hence the LLN cannot, in any way, explain the statistical regularities observed in social life. Such a remark led Markov to find an example of non independent variables for which a generalized LLN holds; in a letter to a colleague he wrote:

> I considered variables connected in a simple chain, and from this came the idea of the possibility of extending the limit theorems of the calculus of probability also to a complex chain.

The ergodic problem in deterministic systems is much more difficult than its analogous for Markov chains. It is rather natural, both from a mathematical and a physical point of view, to wonder under which conditions a dynamical system is ergodic. At an abstract level for a dynamical system $(\Omega, U^t, d\mu(\mathbf{X}))$, the problem has been tackled by Birkhoff and von Neumann who proved the following fundamental theorems:

Theorem 1.1. *For almost every initial condition* $\mathbf{X}_0$ *the time average*

$$\overline{A}(\mathbf{X}_0) \equiv \lim_{\mathscr{T}\to\infty} \frac{1}{\mathscr{T}} \int_0^{\mathscr{T}} A(U^t \mathbf{X}_0) \mathrm{d}t \tag{1.10}$$

exists.

Theorem 1.2. *A necessary and sufficient condition for the system to be ergodic, is that the phase space* Ω *be metrically indecomposable. The latter property means that* Ω *can not be subdivided into two invariant (under the dynamics* U^t*) parts each of positive measure.*

Sometimes instead of metrically indecomposable the equivalent term "metrically transitive" is used. Theorem 1.1 is rather general and not very stringent, in fact time average $\overline{A}(\mathbf{X}_0)$ can depend on the initial condition. The result of Theorem 1.2, while concerning the foundations of statistical mechanics, remains of poor practical utility, since, in general, it is almost impossible to decide whether a given system satisfies the condition of metrical indecomposability. So that, at a practical level, Theorem 1.2 only shifts the problem.

1.2.1.3 Ergodicity and Law of Large Numbers in Statistical Mechanics

Strictly speaking, the ergodicity is a too demanding property to be verified and proved in systems of practical interest. Khinchin in his celebrated book *Mathematical Foundation of the Statistical Mechanics* [5] presents some important results on the ergodic problem which overcome the formal mathematical issues.

The general idea of his approach is based on the following facts:

(a) In the systems which are of interest to statistical mechanics the number of degrees of freedom is very large;
(b) In statistical mechanics, the important observables are not generic (in mathematical sense) functions, so it is enough to restrict the validity of the ergodic hypothesis (1.8) just to the relevant observables;
(c) One can accept that Eq. (1.8) does not hold for initial conditions $\mathbf{X}_0$ in a region of small measure (which goes to zero as $N \to \infty$).

Khinchin considers a separable Hamiltonian system i.e.:

$$H = \sum_{n=1}^{N} H_n(\mathbf{q}_n, \mathbf{p}_n) \tag{1.11}$$

and a special class of observables (called *sum functions*) of the form

$$f(\mathbf{X}) = \sum_{n=1}^{N} f_n(\mathbf{q}_n, \mathbf{p}_n) \tag{1.12}$$

where $f_n = O(1)$. Interesting examples of sum functions are the pressure, the kinetic energy, the total energy and the single-particle distribution function. Notice that a change $O(1)$ in a single f_n results in a relative variation $O(1/N)$ in $f(\mathbf{X})$: the sum functions are "good" macroscopic functions, since they are not so sensitive to microscopic details.

The main result, obtained using the LLN, is:

$$\text{Prob}\left(\frac{|\overline{f} - \langle f \rangle|}{|\langle f \rangle|} \geq K_1 N^{-1/4}\right) \leq K_2 N^{-1/4} \tag{1.13}$$

where K_1 and K_2 are $O(1)$.

The restriction to the separable structure of the Hamiltonian, i.e. (1.11), had been removed by Mazur and van der Linden [6]. They extended the result to systems of particles interacting through a short range potential. Let us stress that in the Khinchin result, as well as in the generalization of Mazur and van der Linden, basically the dynamics has no role and the existence of good statistical properties follows from the LLN, i.e. using the fact that $N \gg 1$.

1.2.1.4 Ergodicity at Work in Statistical Mechanics

We conclude this short excursus on LLN and ergodicity mentioning some important uses of such topics in statistical physics.

The Boltzmann ergodic hypothesis and the result (1.9) for Markov chains are the conceptual starting point for two powerful computational methods in statistical mechanics: molecular dynamics and Monte Carlo method, respectively. In the first approach one assumes (without a mathematical proof) ergodicity[4] and computes time averages from the numerical integration of the "true" Hamilton's equations. In the Monte Carlo approach one selects an ergodic Markov chain[5] with the correct equilibrium probability. Of course, in practical computations, one has to

[4]It is now well known, e.g. from KAM theorem and FPU simulations, that surely in some limit ergodicity fails, however it is fair to assume that the ergodic hypothesis holds for liquids or interacting gases.

[5]Note that, at variance with the molecular dynamics, the Monte Carlo dynamics is somehow artificial (and not unique), therefore the dynamical properties, e.g. correlation functions, are not necessarily related to physical features.

face nontrivial problems, firstly how to estimate the typical time necessary to have a good average and how to control the errors.

Another interesting application is the following: consider a simple multiplicative process: $x_N = a_N x_{N-1}$ where $\{a_j\}$ are i.i.d. positive. Using the LLN[6] it is simple to show that for almost all the realizations one has $x_N \sim e^{\lambda N}$, where $\lambda = \langle \ln a \rangle$ or more formally $P(|(1/N)\ln(x_N/x_0) - \lambda| > \epsilon) \to 0$ as $N \to \infty$. Let us now repeat the problem for non commutative random matrices $\{\mathbb{A}_j\}$, i.e. the multiplicative process $\mathbb{X}_N = \mathbb{A}_N \mathbb{X}_{N-1}$, we can wonder about the limit for $N \to \infty$ of $(1/N)\ln||\mathbb{X}_N||/||\mathbb{X}_o||$, where $||(.)||$ indicates a norm. At first glance the above problem can sound rather artificial, on the contrary it is important for disordered systems[7] and chaotic dynamics. In the 1960s Furstenberg and Kester [7] have proven, under suitable general conditions, the existence of the limit $(1/N)\ln||\mathbb{X}_N||/||\mathbb{X}_o||$ for almost all the realizations: assume that $\langle \ln^+ ||\mathbb{A}_j|| \rangle < \infty$ (where $\ln^+ x = 0$ if $x \leq 1$ and $\ln^+ x = \ln x$ otherwise) then the limit $\lambda_1 = \lim_{N\to\infty}(1/N)\ln||\mathbb{X}_N||/||\mathbb{X}_o||$ exists with probability 1. This result had been extended to deterministic ergodic system by Oseledec [8] in the case the $\{\mathbb{A}_j\}$ are obtained linearizing the dynamics along the trajectory.

1.2.2 Central Limit Theorems

1.2.2.1 The Beginning

The first version of the CLT is due to A. de Moivre who studied the asymptotic behavior of the sum

$$S_N = x_1 + \ldots + x_N$$

in the specific case of binomial random variables with $P(x_j = 1) = p$ and $P(x_j = 0) = 1 - p$. Starting from the binomial distribution and the Stirling approximation de Moivre discovered that

$$\lim_{N\to\infty} P\left(a \leq \frac{S_N - Np}{\sqrt{Np(1-p)}} \leq b\right) = \frac{1}{\sqrt{2\pi}} \int_a^b e^{-\frac{1}{2}x^2} dx \,. \tag{1.14}$$

The history of the CLT as universal law, i.e. not only for dichotomic variables, began with Laplace who was able to prove a generalization of the de Moivre's result. With the use of the characteristic functions and asymptotic methods of approximating

[6] It is enough to consider the variables $t_j = \ln x_j$ and $q_j = \ln a_j$, and then, noting that $t_N = q_1 + q_2 + \ldots + q_N$, one can use the LLN and obtain the result.

[7] For instance the discrete one-dimensional Schrödinger equation with a random potential can be written in terms of a product of 2×2 random matrices.

integrals, Laplace proved that, for the case where $\{x_i\}$ are i.i.d. discrete variables with mean value $\langle x \rangle$ and variance $\sigma^2 < \infty$:

$$\lim_{N\to\infty} P\left(a \le \frac{S_N - N\langle x\rangle}{\sqrt{N\sigma^2}} \le b\right) = \frac{1}{\sqrt{2\pi}} \int_a^b e^{-\frac{1}{2}x^2} dx \,. \tag{1.15}$$

1.2.2.2 The Russian School and Lindeberg

The first mathematical detailed treatment of the CLT, i.e. the validity of (1.15) for generic i.i.d. (even non discrete) with finite variance, is due to the Russian school with Chebyshev and Markov who used in a rigorous way the method of the characteristic functions and moments [9].

A generalization of the CLT for independent variables with different distribution is due to Lindeberg (around 1920) who proved that, if $\langle x_j \rangle = 0$ (this is not a real limitation) and $0 < \sigma_j^2 < \infty$, under the hypothesis that, for any τ,

$$\lim_{N\to\infty} \frac{1}{D_N^2} \sum_{n=1}^{N} \int_{|x|>\tau D_N} x^2 p_{x_n}(x) dx = 0 \,, \quad \text{where} \quad D_N^2 = \sum_{n=1}^{N} \sigma_n^2 \,, \tag{1.16}$$

one has

$$\lim_{N\to\infty} P\left(a \le \frac{S_N}{\sqrt{D_N^2}} \le b\right) = \frac{1}{\sqrt{2\pi}} \int_a^b e^{-\frac{1}{2}x^2} dx \,. \tag{1.17}$$

Intuitively the Lindeberg condition means that each variance σ_n^2 must be small respect to D_N^2: for any τ and for N large enough one has $\sigma_n < \tau D_N$ for all $n \le N$.

Feller and Lévy found that the Lindeberg condition is not only sufficient but also necessary for the validity of the CLT [9].

1.2.2.3 Modern Times

The case of independent variables is quite restrictive, so it is interesting to wonder about the possibility of extending the validity of CLT to non independent variables. Intuition suggests that if the correlation among variables is weak enough a CLT is expected to hold. Such an argument is supported by precise rigorous results [10]. We just mention the basic one. Consider a stationary process with zero mean and correlation function $c(k) = \langle x_{n+k} x_n \rangle$. If the correlation is summable,

$$\sum_{k=1}^{\infty} c(k) < \infty \,, \tag{1.18}$$

it is possible to prove that

$$\lim_{N\to\infty} P\Big(a \le \frac{S_N}{\sqrt{N\sigma_{\text{eff}}^2}} \le b\Big) = \frac{1}{\sqrt{2\pi}} \int_a^b e^{-\frac{1}{2}x^2} dx \,, \tag{1.19}$$

where $\sigma_{\text{eff}}^2 = \sigma^2 + 2\sum_{k=1}^{\infty} c(k)$. In other words σ^2 is replaced by σ_{eff}^2; note that for $N \gg 1$

$$\langle S_N \rangle \simeq 2\sigma_{\text{eff}}^2 N \ . \tag{1.20}$$

The previous result is rather important in the context of diffusion. Interpreting N as a discrete time, Eq. (1.20) simply expresses the diffusive behavior of S_N with diffusion coefficient σ_{eff}^2. Violation of the condition (1.18) are thus at the origin of anomalous diffusive behaviors, for instance to observe $\langle S_N \rangle \sim N^\alpha$ with $\alpha > 1$ and $\sigma < \infty$ it is necessary to have $\sum_{k=1}^{\infty} c(k) = \infty$, i.e. strongly correlated random variables. Another possible violation is when $\sigma = \infty$, in such case CLT can be generalized and this is the subject of the infinitely divisible and Lévy stable distributions.

1.2.3 Large Deviation Theory

The large deviation theory studies the rare events and can be seen as a generalization of the CLT, as it describes not only the "typical" fluctuations but also the very large excursions.

The first general mathematical formulation of LDT has been introduced in the 1930s mainly by Cramér for i.i.d. random variables $x_1, x_2, \ldots$ with mean value $\langle x \rangle$. Under the rather general assumption of existence of the moment generating function $\langle \mathrm{e}^{qx} \rangle$ in some neighborhood of $q = 0$, it is possible to prove that for the "empirical mean" $y_N = (x_1 + \ldots + x_N)/N$

$$\lim_{N\to\infty} \frac{1}{N} \ln P(y_N > y) = -\mathscr{C}(y) \tag{1.21}$$

provided $y > \langle x \rangle$ and $P(x > y) > 0$. Of course, by repeating the previous reasoning for the variable reflected with respect to the mean (i.e. $x \to 2\langle x \rangle - x$), one proves the complementary result for $y_N < y < \langle x \rangle$. The Cramér function $\mathscr{C}(y)$ depends on the probability distribution of x, is positive everywhere but for $y = \langle x \rangle$ where it vanishes. In addition, it is possible to prove that is convex, i.e. $\mathscr{C}'' > 0$.

Roughly speaking, the essence of the above result is that for very large N the probability distribution function of the empirical mean takes the form

$$p(y_N = y) \sim e^{-N\mathscr{C}(y)} \,. \tag{1.22}$$

It is interesting to remind that the first LDT calculation has been carried out by Boltzmann. He was able to express the asymptotic behavior of the multinomial probabilities in terms of relative entropy, see Sect. 1.3.1. In his approach a crucial physical aspect is the statistical interpretation of the entropy as a bridge between microscopic and macroscopic levels.

Let us note that, in general, the Cramér function (for independent or weakly correlated variables) must obey some constraints:

(i) $\mathscr{C}(y) > 0$ for $y \neq \langle y \rangle = \langle x \rangle$;
(ii) $\mathscr{C}(y) = 0$ for $y = \langle y \rangle$;
(iii) $\mathscr{C}(y) \simeq (y - \langle y \rangle)^2/(2\sigma^2)$, where $\sigma^2 = \langle (x - \langle x \rangle)^2 \rangle$, if y is close to $\langle y \rangle$.

Properties (i) and (ii) are consequences of the law of large numbers, and (iii) is nothing but the central limit theorem.

Moreover, the Cramér function $\mathscr{C}(y)$ is linked via a Legendre transform

$$\mathscr{C}(y) = \sup_q \{qy - L(q)\} \,, \tag{1.23}$$

to the cumulant generating function of the variable x

$$L(q) = \ln \langle e^{qx} \rangle \,. \tag{1.24}$$

The result (1.23) is easily understood by noticing that the average $\langle e^{qNy_N} \rangle$ can be written in two equivalent ways,

$$\langle e^{qNy_N} \rangle = \langle e^{qx} \rangle^N = e^{NL(q)}$$

$$\langle e^{qNy_N} \rangle = \int e^{qNy_N} \, p(y_N) dy_N \sim \int e^{[qy - \mathscr{C}(y)]N} dy \,,$$

yielding

$$\int e^{[qy - \mathscr{C}(y)]N} dy \sim e^{NL(q)} \,. \tag{1.25}$$

In the limit of large N, a steepest descent evaluation of the above integral provides

$$L(q) = \sup_y \{qy - \mathscr{C}(y)\} \,, \tag{1.26}$$

which is the inverse of (1.23). Due to the convexity of $\mathscr{C}(y)$, Eqs. (1.23) and (1.26) are fully equivalent. For a nice general discussion on large deviations see the booklet by Varadhan [11].

For dependent variables, in analogy with the central limit theorem, we expect that if the dependence is weak enough a large deviations description such as (1.22) holds, where the Cramér function depends on the specific features of the correlations.

We sketch in the following the case of ergodic Markov chains with a finite number of states.

Consider a sequence $\mathscr{S}^{(N)} = (s_1, s_2, \ldots, s_N)$ where s_t denotes the state of the chain at time t. Given a function of state, $f(s_t)$, the Cramér function of the sum

$$F_N = \frac{1}{N} \sum_{t=1}^{N} f(s_t) \tag{1.27}$$

can be explicitly computed [12]. From the transition probabilities $P_{i\to j}$ for any real q we can define the matrix

$$\mathbb{P}_{ij}^{(q)} = P_{i\to j} \mathrm{e}^{q f_i} \tag{1.28}$$

where f_i is the value of the function $f(s_t)$ when $s_t = i$. Denoting with $\zeta(q)$ the largest eigenvalue of $\mathbb{P}^{(q)}$, whose uniqueness is ensured by the Perron-Frobenius theorem for positive-entry matrices [13], the Cramér function is given by the formula

$$\mathscr{C}(F) = \sup_q \{qF - \ln \zeta(q)\}\,, \tag{1.29}$$

which generalizes (1.23) to Markov chains.

For general non independent variables, $L(q)$ is defined as

$$L(q) = \lim_{N\to\infty} \frac{1}{N} \ln\langle e^{q\sum_{n=1}^{N} x_n}\rangle\ ,$$

and (1.23) is exact whenever $\mathscr{C}(y)$ is convex, otherwise Eq. (1.23) just gives the convex envelop of the correct $\mathscr{C}(y)$.

1.3 LDT for the Sum and Product of Random Independent Variables

1.3.1 A Combinatorial Example

A natural way to introduce the large deviation theory and show its deep relation with the concept of entropy is to perform a combinatorial computation. Consider the simple example of a sequence of independent unfair-coin tosses. The possible outcomes are head $(+1)$ or tail (-1). Denote the possible result of the n-th toss by x_n, where head has probability π, and tail has probability $1-\pi$. Let y_N be the mean value after $N \gg 1$ tosses,

$$y_N = \frac{1}{N}\sum_{n=1}^{N} x_n. \tag{1.30}$$

The number of ways in which K heads occur in N tosses is $N!/[K!(N-K)!]$, therefore, the exact binomial distribution yields

$$P\left(y_N = \frac{2K}{N} - 1\right) = \frac{N!}{K!(N-K)!}\pi^K(1-\pi)^{N-K} \ . \tag{1.31}$$

Using Stirling's approximation and writing $K = pN$ and $N - K = (1-p)N$ one obtains

$$P(y_N = 2p-1) \sim e^{-NI(\pi,p)} \ , \tag{1.32}$$

where

$$I(\pi, p) = p\ln\frac{p}{\pi} + (1-p)\ln\frac{1-p}{1-\pi} \ . \tag{1.33}$$

$I(\pi, p)$ is called "relative entropy" (or Kullback-Leibler divergence), and $I(\pi, p) = 0$ for $\pi = p$, while $I(\pi, p) > 0$ for $\pi \neq p$. It is easy to repeat the argument for the multinomial case, where $x_1, \ldots, x_N$ are independent variables that take m possible different values $a_1, a_2, \ldots, a_m$ with probabilities $\{\pi\} = \pi_1, \pi_2, \ldots, \pi_m$.[8] In the limit $N \gg 1$, the probability of observing the frequencies $\{f\} = f_1, f_2, \ldots, f_m$ is

$$P(\{f\} = \{p\}) \sim e^{-NI(\{\pi\},\{p\})}$$

where

$$I(\{\pi\},\{p\}) = \sum_{j=1}^{m} p_j \ln\frac{p_j}{\pi_j}$$

is called "relative entropy" of the probability $\{p\}$, with respect to the probability $\{\pi\}$. Such a quantity measures the discrepancy between $\{p\}$ and $\{\pi\}$ in the sense that $I(\{\pi\},\{p\}) = 0$ if and only if $\{p\} = \{\pi\}$, and $I(\{\pi\},\{p\}) > 0$ if $\{p\} \neq \{\pi\}$.

From the above computation one understands that it is possible to go beyond the central limit theory, and to estimate the statistical features of extreme (or tail) events, as the number of observations grows without bounds. Writing $I(\pi, p)$ in terms of $y = 2p - 1$, we have the asymptotic behavior of the probability density:

$$p(y) \sim e^{-N\mathscr{C}(y)} \ , \tag{1.34}$$

[8] Such a result has been obtained by Boltzmann, who firstly noted the basic role of the entropy [14].

with

$$\mathscr{C}(y) = \frac{1+y}{2}\ln\frac{1+y}{2\pi} + \frac{1-y}{2}\ln\frac{1-y}{2(1-\pi)} \,. \tag{1.35}$$

For p close to π, i.e. $y \simeq \langle y \rangle$, a Taylor expansion of $\mathscr{C}(y)$ reproduces the central limit theorem.

1.3.2 Product of Random Variables

Large deviation theory accounts for rare events pertaining to the tails of the probability density function (pdf) of the *sum* of random variables. Ironically, one of the best examples to appreciate its importance is the *product* of random variables such as

$$M_N = \prod_{k=1}^{N} \beta_k \,, \tag{1.36}$$

where $\{\beta_k\}$ are real and positive random variables. The statistical properties of the product M_N can be straightforwardly related to those of the sum of random numbers by noticing that

$$M_N = \prod_{k=1}^{N} \beta_k = e^{N\left(\frac{1}{N}\sum_{k=1}^{N} x_k\right)} = e^{N y_N} \qquad \text{with} \qquad x_k = \ln \beta_k \,, \tag{1.37}$$

where again $y_N = (1/N)\sum_{k=1}^{N} \ln \beta_k$ denotes the empirical mean. Below, we illustrate the importance of LDT product of random numbers partially following Ref. [15], using a simple example which allows us to use the results of the previous section. In particular, we can take $\beta_k = \mathrm{e}$ and e^{-1} (i.e. $x_k = \ln \beta_k = \pm 1$) with probability π and $1-\pi$, respectively, so that we can write $P(M_N = \mathrm{e}^K \mathrm{e}^{-(N-K)}) = P(y_N = 2K/N - 1)$ as given by Eq. (1.31). Therefore, we can directly compute the moments of order q

$$\langle M_N^q \rangle = (\pi \mathrm{e}^q + (1-\pi)\mathrm{e}^{-q})^N \,. \tag{1.38}$$

Using Eq. (1.34) we can write the moments as

$$\langle M_N^q \rangle = \langle \mathrm{e}^{N q\, y_N} \rangle \approx \int \mathrm{d}y\, \mathrm{e}^{-N(\mathscr{C}(y) - q\, y)} \approx \mathrm{e}^{-N \inf_y \{\mathscr{C}(y) - q\, y\}} \,, \tag{1.39}$$

where in the second equality we used the LDT result with the Cramér function $\mathscr{C}$ given by Eq. (1.35) and, in the third, we made a steepest descent estimate of the

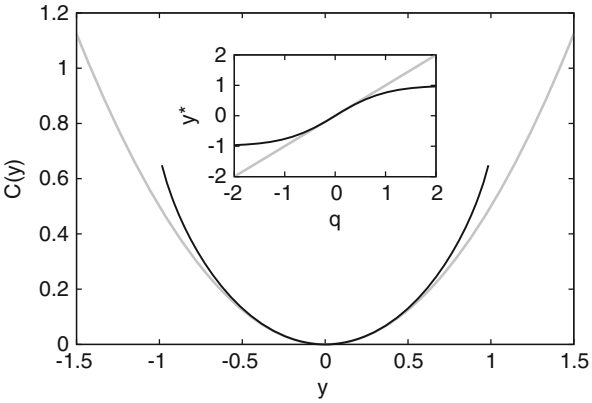

Fig. 1.1 Comparison between the Cramér function (1.35) (*black*) and its parabolic approximation $\tilde{\mathscr{C}}$ (*grey*), for $\pi = 1/2$. *Inset*: $y^*(q)$ vs q, as obtained using LDT or CLT

integral; both steps require N to be large. Using Eq. (1.35), a rather straightforward computation shows that the minimum in Eq. (1.39) is realized at $y^*(q) = (\pi e^q - (1-\pi)e^{-q})/(\pi e^q + (1-\pi)e^{-q})$, with

$$\inf_y\{\mathscr{C}(y) - q\, y\} = \mathscr{C}(y^*) - q\, y^* = -\ln\left(\pi e^q + (1-\pi)e^{-q}\right)\,, \tag{1.40}$$

so that we recover the result (1.38).

Now to appreciate the importance of rare events, we can disregard them by repeating the estimate of the moments using the CLT. In practice, this amounts to Taylor expanding $\mathscr{C}$ in (1.35) around its minimum $y = 2\pi - 1$, i.e. to approximate $\mathscr{C}$ with the parabola

$$\tilde{\mathscr{C}}(y) = \frac{(y + 1 - 2\pi)^2}{8\pi(1-\pi)}\,. \tag{1.41}$$

This approximation corresponds to assume a lognormal distribution for the product M_N [16]. The moments can be computed by finding the minimum in (1.39) with $\mathscr{C}$ replaced by its parabolic approximation $\tilde{\mathscr{C}}$. A straightforward computation gives $y^* = 2\pi - 1 + 4\pi(1-\pi)q$ and $\inf_y\{\tilde{\mathscr{C}}(y) - q\, y\} = \tilde{\mathscr{C}}(y^*) - q\, y^* = -q(2\pi - 1 + (1-\pi)q)$, which leads to moments very different from the correct ones (1.38) also for moderate values of q. Moreover, the fast growth of the moments ($\sim \exp(\text{const.}Nq^2)$) makes the lognormal distribution not uniquely determined by the values of its moments [17]. Figure 1.1 shows the Cramér function (1.39) and its parabolic approximation. The minimum position $y^*(q)$ obtained with the lognormal deviates from the correct value also for moderate values of q (see inset).

In the above example, the CLT (and thus the lognormal approximation) does not take into account the fact that y_N cannot exceed 1, which is the value corresponding to a sequence consisting of N consecutive $\beta_k = \mathrm{e}$. Such a sequence has an exponentially small probability to appear, but it carries an exponentially large contribution compared to the events described by CLT.

For an introductory discussion of LDT in multiplicative processes see Ref. [15].

1.4 Large Deviation Theory: Examples From Physics

1.4.1 Energy Fluctuations in the Canonical Ensemble

The large deviation theory finds a rather natural application in statistical mechanics, e.g. for the fluctuations of the energy e per particle in a system of N particles at temperature T:

$$p(e) \simeq \frac{1}{\mathscr{Z}_N} \exp\{-N\beta[e - Ts(e)]\} \ ,$$

where $s(e)$ is the microcanonical entropy per particle. Since $\int p(e)de = 1$, the constant $\mathscr{Z}_N$ (partition function) turns out to be

$$\mathscr{Z}_N \sim \exp\{-N\beta f(T)\} \ ,$$

where $f(T)$ is the free energy per particle

$$f(T) = \min_e \{e - Ts(e)\} \ .$$

The value e^* for which the function $e - Ts(e)$ reaches its minimum is determined by

$$\frac{1}{T} = \frac{\partial s(e)}{\partial e} \ , \tag{1.42}$$

i.e. it is the value such that the corresponding microcanonical ensemble has temperature T. It is rather obvious what is the Cramér function and its physical meaning:

$$\mathscr{C}(e) = \beta[e - Ts(e) - f(T)] \ .$$

Let us note that the value of e such that $\mathscr{C}(e)$ is minimum (zero) is nothing but $e^* = \langle e \rangle$ given by (1.42). The Gaussian approximation around e^* is

$$\mathscr{C}(e) \simeq \frac{1}{2}\mathscr{C}''(e^*)(e - e^*)^2 \ ,$$

and therefore $\langle (e - e^*)^2 \rangle = 1/[N\mathscr{C}''(e^*)]$, since

$$\langle (e - e^*)^2 \rangle = \frac{k_B}{N} T^2 c_V \ ,$$

where $c_V = \partial \langle e \rangle / \partial T$ is the specific heat per particle. The convexity of the Cramér function has a clear physical meaning: $c_V(T)$ must be positive. The case of non-convex Cramér function corresponds to phase transitions, i.e. non-analytic $f(T)$.

1.4.2 Multiplicative Cascade in Turbulence

Turbulent flows are characterized by fluctuations over a wide range of scales, with a disordered alternation of quiescent regions and sparse bursting events—*intermittency* [18]. Intermittency of this kind is well captured by multiplicative processes which, in turbulence, find their justification in the phenomenology of the energy cascade [18]: the nonlinear process by which velocity fluctuations flow from the large scales (of injection) to the small ones, where they are dissipated by molecular diffusion. The book in Ref. [18] provides a detailed discussion of turbulence within the framework of LDT (and the multifractal model). Here we just illustrate a simple d-dimensional multiplicative process, inspired to turbulence, able to generate an intermittent signal similar to those experimentally observed.

At step $N = 0$ consider a (mother) hypercube of side ℓ_0 (the forcing scale) where energy dissipation is nonrandom and equal to ϵ_0. The $N = 1$ step is obtained subdividing the hypercube in 2^d (daughter) hypercubes of side $\ell_0/2$ (powers of 2 are just for simplicity). In each daughter hypercube the energy dissipation is obtained by multiplying ϵ_0 by independent random variables $w \geq 0$ (such that $\langle w \rangle = 1$ and $\langle w^q \rangle < \infty$ for any $q > 0$). At the n-th step we thus have 2^{Nd} hypercubes of side $\ell_N = \ell_0 2^{-N}$, with energy dissipation

$$\epsilon_N = w_N \epsilon_{N-1} = \prod_{k=1}^{N} w_k \epsilon_0 \,. \tag{1.43}$$

Although the prescription $\langle w \rangle = 1$ ensures that $\langle \epsilon_N \rangle = \epsilon_0$, the multiplicative process is non-conservative, i.e. the value of the energy dissipation of a specific hypercube of side ℓ_N is not equal to the sum of the energy dissipation in the daughters hypercube at scale $\ell_N/2$. Moreover, as discussed in Sect. 1.3.2, large fluctuations are typical of product of random variables, so that we can expect that for N large intermittency shows up. For instance, the choice

$$w = \begin{cases} \beta^{-1} & \text{with prob.} \quad \beta \\ 0 & \text{with prob.} \quad 1-\beta \end{cases} \qquad 0 < \beta \leq 1 \,, \tag{1.44}$$

corresponds to a popular model known as β-model for turbulence [19]. Clearly, with (1.44) at the N-th step energy dissipation will be different from zero only in a fraction $\beta^N = 2^{N \log_2 \beta} = (\ell_0/\ell_N)^{\log_2 \beta}$ of the $2^{Nd} = (\ell_0/\ell_N)^d$ hypercubes, in other terms energy dissipation will distribute on a fractal of dimension $D_F = d - \log_2(1/\beta)$. This qualitatively explains the sparseness of bursting events. However, whenever different from zero energy dissipation will be equal to $\beta^{-N}\epsilon_0$. Therefore, to account for the unevenness of energy dissipative values in each hypercube where it is different from zero, one possibility is to generalize (1.44) by assuming that β is not a fixed value but a realization of i.i.d. random variables with a given pdf $p(\beta)$ [20]. Essentially this leads the energy dissipation to be a multifractal measure [18], which can be characterized in terms of the moments

$$\langle \epsilon_N^q \rangle = \int \prod_{k=1}^{N} \beta_k \, p(\beta_k) d\beta_k \epsilon_0^q \beta_k^{-q} \,. \tag{1.45}$$

To compute the moments in the limit $N \to \infty$ we can proceed similarly to (1.39). In particular, we have $\epsilon_N = \epsilon_0 (\ell_N/\ell_0)^{-y_N}$ with $y_N = \sum_{k=1}^{N} \log_2 \beta_k / N$. LDT implies that $p(y_N = y) \sim (\ell_N/\ell_0)^{\mathscr{C}(y)/\log 2}$, so that estimating the integral in (1.45) with the saddle point method we obtain

$$\langle \epsilon_N^q \rangle = \epsilon_0^q \left(\frac{\ell_N}{\ell_0} \right)^{\tau_q} \quad \text{with} \quad \tau_q = \inf_y \left\{ \frac{\mathscr{C}(y)}{\log 2} - y(q-1) \right\} \,. \tag{1.46}$$

In general, τ_q will be a nonlinear function of q: the signature of multifractality and intermittency. Conversely, in the model (1.44) with β non-random, $\tau^q = (q-1)(d - D_F)$ is a linear function. The exponents τ_q is linked to the scaling behavior of moments of the difference of velocities, the so-called structure functions, which are directly accessible experimentally. As shown in Ref. [20] a careful choice of $p(\beta)$ allows for reproducing the behavior of the structure functions' exponents which display a seemingly universal nonlinear dependence on q.

1.4.3 Chaotic Systems

The most characterizing feature of chaotic systems is the sensitive dependence on initial conditions: starting from nearby initial conditions, trajectories exponentially diverges. The classical indicators of the degree of instability of trajectories are the Lyapunov Exponents (LE), that quantify the mean rate of divergence of trajectories which start infinitesimally close. For the sake of simplicity we consider a $1d$ discrete time dynamical system

$$x(t+1) = f(x(t)) \tag{1.47}$$

and given an initial condition $x(0)$, we look at two trajectories, $x(t)$ and $\tilde{x}(t)$ starting from $x(0)$ and $\tilde{x}(0) = x(0) + \delta x(0)$, respectively, where $|\delta x(0)| \ll 1$. Denoting with $\delta x(t) = |x(t) - \tilde{x}(t)|$ the distance between the two trajectories, we expect that for non-chaotic systems $|\delta x(t)|$ remains bounded or increases algebraically in time, while for chaotic systems it grows exponentially

$$|\delta x(t)| = |\delta x(0)| e^{\gamma t} \,, \tag{1.48}$$

where

$$\gamma = \frac{1}{t} \ln \frac{|\delta x(t)|}{|\delta x(0)|} \,, \tag{1.49}$$

is the local exponential rate of divergence between trajectory.

The Maximum Lyapunov Exponent, characterizing the sensitivity to initial conditions, is defined by the limit

$$\lambda_{\max} = \lim_{t\to\infty} \lim_{|\delta x(0)|\to 0} \frac{1}{t} \ln \frac{|\delta x(t)|}{|\delta x(0)|} . \tag{1.50}$$

Note that γ is fluctuating while $\lambda_{\max}$ is a non-fluctuating quantity, but it can depend on $x(0)$. It is easy to understand that the existence of the limit in Eq. (1.50) is a generalization of LLN for dependent variables. In order to obtain $\delta x(t)$ from $\delta x(t-1)$, in the case of an infinitesimal $|\delta x(t-1)|$ one can use a simple Taylor expansion of the first order and the local exponent γ can be computed as

$$\gamma = \frac{1}{t} \ln \frac{|\delta x(t)|}{|\delta x(0)|} = \frac{1}{t} \sum_{k=1}^{t} \ln |f'(x(k-1))| . \tag{1.51}$$

The Maximum Lyapunov Exponent is nothing but

$$\lambda_{\max} = \lim_{t\to\infty} \frac{1}{t} \sum_{k=1}^{t} \ln |f'(x(k-1))| ,$$

and, if the system is ergodic, it does not depend on $x(0)$. Moreover, in simple cases, it is possible to obtain also the Cramér function of γ. Let us consider the tent map

$$x(t+1) = f(x(t)) = \begin{cases} \dfrac{x(t)}{p} & 0 \le x(t) < p \\ \dfrac{1-x(t)}{1-p} & p \le x(t) \le 1, \end{cases} \tag{1.52}$$

with $p \in (0,1)$. The derivative of the map takes only two values, $1/p$ and $1/(p-1)$, moreover the map can be shown to generate a memory-less process so that the sum (1.51) can be interpreted as the sum of Bernoullian random variables

$$\xi_j = \begin{cases} -\ln p & \text{with prob. } p \\ -\ln(1-p) & \text{with prob. } 1-p. \end{cases}$$

Therefore the effective Lyapunov exponent on a time interval t is

$$\gamma(t) = -\frac{k \ln p + (t-k)\ln(1-p)}{t} \qquad \text{with prob.} \qquad \binom{t}{k} p^k (1-p)^{t-k} ,$$

where k is the number of occurrences of $\xi_j = -\ln p$. Using the Stirling approximation, with some algebra it is possible to obtain the probability of the occurrence

of γ in a time interval t as $P_t(\gamma) \simeq \exp(-t\mathscr{C}(\gamma))$ where the Cramér function is given by

$$\mathscr{C}(\gamma) = \left[\frac{\gamma + \ln(1-p)}{\ln \frac{1-p}{p}} \ln \left(\frac{\gamma + \ln(1-p)}{p \ln \frac{1-p}{p}} \right) - \frac{\gamma + \ln p}{\ln \frac{1-p}{p}} \ln \left(- \frac{\gamma + \ln p}{(1-p) \ln \frac{1-p}{p}} \right) \right]. \tag{1.53}$$

The Cramér function has its minimal value in $\gamma = -p \ln p - (1-p)\ln(1-p)$ (where it also vanishes) which is the Maximum Lyapunov Exponent, and the Taylor expansion of Eq. (1.53) around this minimum provides the Central Limit Theorem for the sum (1.51). Unfortunately this computation can be performed almost only for piecewise linear maps.

For generic dynamical systems

$$\mathbf{x}(t+1) = \mathbf{f}(\mathbf{x}(t))$$

there exists a theorem due to Oseledec that under very general hypothesis, states the existence of the Lyapunov exponents. But a major difficulty arises, i.e., the product of Eq. (1.51) cannot be factorized because of the non commutativity of the Jacobian matrix with entries $A_{ij} = \partial f_i / \partial x_j$.

1.4.4 Disordered Systems

Products of matrices and Oseledec's limit theorem find a natural application to the study of statistical mechanics of disordered systems. Indeed, their thermodynamical properties can be recast, via transfer matrix formalism, as the evaluation of the asymptotic properties of products of matrices. The presence of randomness induced by disorder introduces sample to sample fluctuations of observables which require proper averaging procedures over different disorder realizations. In this case the transfer-matrix approach involves products of *random matrices*.

As an example, which already includes all the difficulties, consider an array of N binary variables $\sigma_i = \pm 1$ (spins) whose interaction is defined by the Hamiltonian,

$$H(\boldsymbol{\sigma}) = -J \sum_{i=1}^{N} \sigma_i \sigma_{i+1} + \sum_{i=1}^{N} h_i \sigma_i, \tag{1.54}$$

where J determines a ferromagnetic internal coupling between nearest neighbor sites and $\{h_i\}_{i=1}^N = \mathbf{h}$ represent a set of local magnetic fields acting on site, each independently extracted from a distribution $\rho(h)$. Typically, $\rho(h)$ is chosen to be a Gaussian or a bimodal distribution and usually periodic boundary conditions are assumed, $\sigma_{i+N} = \sigma_i$. For finite N, the system has 2^N possible configurations, however we are interested in the thermodynamic limit $N \to \infty$, where extensive

thermodynamics quantities becomes independent of N and the choice of boundary conditions is irrelevant.

Once a given realization of the disorder is assigned, $\mathbf{h} = \{h_i\}_{i=1}^{N}$, the equilibrium thermodynamics of the N-spin chain is determined by the free-energy:

$$f_N(\beta, \mathbf{h}) = -\frac{1}{\beta N} \ln Z_N(\beta, \mathbf{h}), \tag{1.55}$$

where

$$Z_N(\beta, \mathbf{h}) = \sum_{\sigma_1} \dots \sum_{\sigma_N} e^{-\beta(J\sigma_1\sigma_2 - h_1\sigma_1)} \cdots e^{-\beta(J\sigma_N\sigma_1 - h_N\sigma_N)} \tag{1.56}$$

is the partition function of the system, the summation covers all the 2^N spin configurations and $\beta = 1/(k_B T)$. In principle, the free-energy (1.55) for every finite N is a random variable, because it depends on the disorder realizations, however, as we shall see in the transfer matrix formalism, a straightforward application of Oseledec's limit theorem implies that

$$\lim_{N\to\infty} f_N(\beta, \mathbf{h}) = \lim_{N\to\infty} -\frac{1}{\beta N} \langle \ln Z_N(\beta, \mathbf{h}) \rangle_h, \tag{1.57}$$

where the average $\langle \dots \rangle_{\mathbf{h}}$ is meant over the random field distribution. Result (1.57) can be interpreted as follows, in the thermodynamic limit $f_N(\beta, \mathbf{h})$ is a non-random quantity as it converges to its limit average over the disorder, for almost all disorder configurations. In an equivalent physical language, when $N \to \infty$, f_N is practically independent of $\{h_i\}_{i=1}^{N}$, and it is a self-averaging observable with respect to sample to sample disorder fluctuations.

The transfer matrix approach amounts to re-writing the partition function

$$Z_N = \sum_{\{\sigma_i\}} \prod_{i=1}^{N} e^{-\beta(J\sigma_i\sigma_{i+1} - h_i\sigma_i)} = Tr\left(\prod_{i=1}^{N} \mathbf{T}[i] \right) \tag{1.58}$$

as an iterated matrix product in indexes $\sigma_2, \sigma_3, \dots, \sigma_N$ and the summation over σ_1 as a trace operation, where the 2×2 fundamental matrix $\mathbf{T}[i]$ has entries: $T(\sigma_i, \sigma_{i+1}) = \exp[\beta(J\sigma_i\sigma_{i+1} - h_i\sigma_i)]$, more explicitly:

$$\mathbf{T}[i] = \begin{bmatrix} e^{\beta(J-h_i)} & e^{-\beta(J+h_i)} \\ e^{-\beta(J-h_i)} & e^{\beta(J+h_i)} \end{bmatrix} . \tag{1.59}$$

In the thermodynamic limit, the free energy per spin is given by the maximum Lyapunov exponent λ_1 of the product of matrices in Eq. (1.58):

$$-\beta f(\beta, \mathbf{h}) = \lim_{N\to\infty} \frac{1}{N} \ln\left[Tr\left(\prod_{i=1}^{N} \mathbf{T}[i] \right) \right] = \lambda_1. \tag{1.60}$$

When the field $h_i = H$ is the same on every site (no disorder), the computation of free-energy is particularly simple because the product involves identical symmetric matrices: $Z_N = Tr(\mathbf{T}^N) = \mu_+^N + \mu_-^N$ being $\mu_\pm$ the eigenvalues of $\mathbf{T}$. Therefore the free energy coincides with the logarithm of the maximum eigenvalue of $\mathbf{T}$: $f(\beta, H) = -\beta^{-1} \ln(\mu_+)$, where

$$\mu_\pm = e^{\beta J} \cosh(\beta H) \pm \sqrt{\cosh^2(\beta H) 2e^{2\beta J} \sinh(2\beta J)}.$$

When h_i is not constant, the matrices (1.59) are not commuting, and the asymptotic behavior of the random matrix product has to be numerically evaluated. Practically, one resorts to compute the exponential growth rate of an arbitrary initial vector $\mathbf{z}_0 = (u_0, v_0)$, with positive components, under the effect of the iterated matrix multiplication $\mathbf{z}_{n+1} = \mathbf{T}[n]\mathbf{z}_{n-1}$,

$$\lambda_1 = \lim_{N\to\infty} \frac{1}{N} \ln\left(\frac{|\mathbf{z}_N|}{|\mathbf{z}_0|} \right) = \lim_{N\to\infty} \frac{1}{N} \sum_{n=0}^{N-1} \ln\left(\frac{|\mathbf{z}_{n+1}|}{|\mathbf{z}_n|} \right).$$

Oseledec's theorem grants that, under rather general conditions, the above limit exists and it is a non-random quantity (self averaging property). Then, the computation of free-energy of a one-dimensional random field Ising model to some extent constitutes a physical example of the application of the law of large numbers. Moreover the self-averaging property of the free-energy in the context of disordered systems corresponds to the ergodicity condition for dynamical systems.

A large deviation approach can be formulated also for the fluctuations of the free-energy of a random field Ising model at finite N around its thermodynamic limit value. The transfer random-matrix formalism makes the characterization of large deviations an application of the generalized Lyapunov exponents. It is easy to compute the asymptotic behavior of $\langle |\mathbf{z}_n|^q \rangle$ for $q = 1, 2, 3, \ldots$ and therefore compute the generalized Lyapunov exponents

$$L(q) = \lim_{n\to\infty} \frac{1}{n} \ln \langle |\mathbf{z}_n|^q \rangle. \tag{1.61}$$

It is possible to show that $L(1)$ is the logarithm of the largest eigenvalue of $\langle \mathbf{T} \rangle$ while $L(2)$ is the logarithm of the largest eigenvalue of $\langle \mathbf{T}^{\otimes 2} \rangle$ where $\langle \mathbf{T}^{\otimes 2} \rangle$ is the tensorial product $\langle \mathbf{T} \otimes \mathbf{T} \rangle$ and so on for $\langle \mathbf{T}^{\otimes 3} \rangle$, etc. In such a way we have an exact bound $\lambda_1 \leq L(q)/q$ for $q = 1, 2, \ldots$. To consider $L(1)$ instead of λ_1 corresponds, in physical terms, to consider an annealed average, i.e. $\ln \langle Z_N \rangle$ instead of $\langle \ln Z_N \rangle$. The knowledge of $L(q)$, for all q, is equivalent to the knowledge of the Cramér function $C(\gamma)$.

1.4.5 Entropy Production in Markov Processes

A recent application of the theory of large deviations concerns the dynamical behaviour of deterministic and stochastic systems at large times.

Consider a continuous time Markov process with a finite number of states, whose evolution is such that: if the system is in state x, it remains in such a state for a random time $t \geq 0$ extracted with a probability density $p(t) = \omega(x)e^{-\omega(x)t}$ and then jumps to a new state x' with transition probability $\frac{w(x \to x')}{\omega(x)}$. The functions $w(x \to x')$ are said to be the transition rates of the Markov process and $\omega(x) = \sum_{x'} w(x \to x')$ is the total exit rate from x. It is useful to introduce also a notion of *time-reversed state* $\overline{x}$ for a given state x: for the so-called "even" variables, such as positions or forces, one has $\overline{x} \equiv x$, while for "odd" variables, such as velocities, one has $\overline{x} \equiv -x$. For what follows, a further assumption is crucial: if $w(x \to x') > 0$ then $w(\overline{x'} \to \overline{x}) > 0$.

From the above definitions, a trajectory of time-length t can be written as $\Omega_0^t = \{(x_0, t_0), (x_1, t_1), (x_2, t_2), \ldots, (x_n, t_n)\}$, where the system undergoes n jumps visiting states x_i in temporal order from $i = 0$ to $i = n$ and stays in each of them for a waiting time t_i, with $\sum_i t_i = t$. Its time-reversal reads $\overline{\Omega_0^t} = \{(\overline{x}_n, t_n), (\overline{x}_{n-1}, t_{n-1}), \ldots, (\overline{x}_2, t_2), (\overline{x}_1, t_1), (\overline{x}_0, t_0)\}$.

The probability $P_x(t)$ of finding the system in state x at time t evolves according to the master equation:

$$\frac{dP_x(t)}{dt} = \sum_{x'} P_{x'}(t) w(x' \to x) - \omega(x) P_x(t). \tag{1.62}$$

We denote by P_x^{inv} the steady state solution of (1.62). The particular steady state where $P_{x'}^{\text{inv}} w(x' \to x) = P_{\overline{x}}^{\text{inv}} w(\overline{x} \to \overline{x'})$ is a steady state which is said to satisfy *detailed balance*. The detailed balance conditions imply that the probability of occurrence of any trajectory is invariant under time-reversal $P(\Omega_0^t) = P(\overline{\Omega_0^t})$: in short, a *movie* of the system of any time-length cannot be discriminated to be played in the forward or backward direction. Markov processes describing physical systems at thermal equilibrium (or isolated), satisfy the detailed balance conditions. On the contrary, the presence of external forces and/or internal dissipation leads to steady states with physical currents, with the consequent breakdown of the detailed balance conditions.

Following a series of studies [21–24], a "fluctuating entropy production functional" has been proposed in [25] for the general case of Markov processes. The functional, for a trajectory which in the time $[0, t]$ includes n jumps, reads

$$W_t(\Omega_0^t) = \sum_{i=1}^{n} \ln \frac{w(x_{i-1} \to x_i)}{w(\overline{x_i} \to \overline{x_{i-1}})}. \tag{1.63}$$

It is immediate to verify that in a steady state satisfying detailed balance $W_t = -\ln[P^{\text{inv}}_{x_0}/P^{\text{inv}}_{\overline{x}_n}]$ and therefore—given the finiteness of the space of states—one has $\lim_{t\to\infty}\frac{W_t}{t} = 0$. Otherwise, as discussed below, $\lim_{t\to\infty}\frac{\langle W_t\rangle}{t} > 0$.

More precisely, a large deviation principle for the stochastic variable W_t can be obtained, such that its associated Cramér function satisfies a particular relation, called "Fluctuation-Relation". An instructive way to derive it is the following [25]. Let us define the joint probability $p_x(W_t, t)$ of finding the system at time t in state x with a value of the entropy production (measured starting from time 0) W_t; we also define the vector $\mathbf{p}(W_t, t) = \{p_{x_1} \dots p_{x_M}\}$ where M is the number of possible states for the system. It is not difficult to realize that its evolution is governed by a modified master equation that reads

$$\frac{dp_x(W_t,t)}{dt} = \sum_{x'} p_{x'}\left[W_t - \Delta W(x'\to x), t\right] w(x'\to x) - \omega(x)\, p_x(W_t,t). \tag{1.64}$$

With $\Delta W(x'\to x) = \ln\frac{w(x'\to x)}{w(\overline{x}\to\overline{x'})}$. If we consider the generating function for W_t conditioned to state x, i.e.

$$g_x(s,t) = \int d\, W_t e^{-sW_t}\, p_x(W_t,t), \tag{1.65}$$

we find for its time evolution, immediately descending from Eq. (1.64):

$$\frac{dg_x}{dt} = \sum_{x'} w(x'\to x) e^{-s\Delta W(x'\to x)} g_{x'}(s,t) - \omega(x) g_x(s,t) =$$

$$\sum_{x'} w(x'\to x)^{1-s} w(\overline{x}\to\overline{x'})^s g_{x'}(s,t) - \omega(x) g_x(s,t) = [L(s)\mathbf{g}(s,t)]_x \tag{1.66}$$

where we have used the definition of $\Delta W(x'\to x)$. The initial conditions for Eq. (1.66) is $g_x(s,0) = \int d\, W_t e^{-sW_t} P_x(0)\delta(W_t) = P_x(0)$, so that

$$g_x(s,t) = \sum_y [e^{Lt}(s)]_{xy} P_y(0). \tag{1.67}$$

Finally, summing over all possible states x, weighted with their probability, we get the unconditioned generating function, that reads

$$g(s,t) = \sum_{x,y} P_x(t)[e^{Lt}(s)]_{xy} P_y(0). \tag{1.68}$$

The Perron-Frobenius theorem guarantees that $L(s)$ has a unique maximal eigenvector $\tilde{g}(s) > 0$ with real eigenvalue $-\mu(s)$. This allows one to define the limit

$$\lim_{t\to\infty} -\frac{1}{t}\ln g(s,t) = \mu(s). \tag{1.69}$$

It is immediate to verify that $\mu(s)$ is the time-rescaled cumulant generating function for the steady state of the variable W_t. Its Legendre transform is the Cramér function for the large deviations of the same variable, i.e.

$$p(W_t) \approx \exp\left[t \sup_s \left(s\frac{W_t}{t} + \mu(s)\right)\right] \approx \exp[t\mathscr{C}(W_t/t)]. \tag{1.70}$$

From its definition in Eq. (1.66), it is straightforward to realize that $L^*(s) = L(1-s)$ and therefore $\mu(s) = \mu(1-s)$. This immediately reflects into the following relation for the Cramér function of $w_t = W_t/t$:

$$\mathscr{C}(w_t) - \mathscr{C}(-w_t) = w_t, \tag{1.71}$$

which is known as Steady State Fluctuation Relation (SSFR).

In the limit of an infinite space of states ($M \to \infty$) problems may arise in the derivation sketched above, when the inverse transform is operated to retrieve the large deviation rate function $\mathscr{C}(w_t)$. In some cases a modified SSFR holds true instead of Eq. (1.71): to recover the validity of formula (1.71) one has to measure a different entropy production, modified by adding so-called "boundary terms", as discussed in [26–28].

Notwithstanding the problems for unbounded spaces, the result (1.70) together with (1.71) is remarkable: the "entropy production" measured on very long trajectories tends to be sharply peaked around its average value, which is positive for non-equilibrium systems and zero otherwise. Moreover, if the trajectories have finite time-length, one can observe also *negative* fluctuations, representing a sort of "finite size violation" of the second principle of thermodynamics, but with exponentially small probability.

References

1. J. Mehra, *The Golden Age of Theoretical Physics* (World Scientific, Singapore, 2001)
2. I. Todhunter, *History of the Mathematical Theory of Probability from the Time of Pascal to that of Laplace* (BiblioBazaar, Charleston, 2009)
3. C. Cercignani, *Ludwig Boltzmann: The Man Who Trusted Atoms* (Oxford University Press, Oxford, 2007)
4. L. Graham, J.M. Kantor, *Naming Infinity: A True Story of Religious Mysticism and Mathematical Creativity* (Harvard University Press, Cambridge, 2009)
5. A. Khinchin, *Mathematical Foundations of Statistical Mechanics* (Dover, New York, 1949)
6. P. Mazur, J. van der Linden, J. Math. Phys. **4**, 271 (1963)
7. H. Furstenberg, H. Kesten, Ann. Math. Stat. **31**, 457 (1960)
8. V.I. Oseledec, Trans. Moscow Math. Soc. **19**, 197 (1968)
9. H. Fischer, *A History of the Central Limit Theorem* (Springer, Berlin, 2010)

10. W. Hoeffding, H. Robbins, Duke Math. J. **15**, 773 (1948)
11. S.R.S. Varadhan, *Large Deviations and Applications* (Society for Industrial and Applied Mathematics, Philadelphia, 1984)
12. H. Touchette, Phys. Rep. **478**, 1 (2009)
13. G. Grimmett, D. Stirzaker, *Probability and Random Processes* (Oxford University Press, Oxford, 2001)
14. R.S. Ellis, Physica D **133**, 106 (1999)
15. S. Redner, Am. J. Phys. **58**, 267 (1990)
16. J. Aitchison, J.A.C Brown, *The Lognormal Distribution* (Cambridge University Press, Cambridge, 1963)
17. S.A. Orszag, Phys. Fluids **13**, 2211 (1970)
18. U. Frisch, *Turbulence: The Legacy of A. N. Kolmogorov* (Cambridge University Press, Cambridge, 1995)
19. E.A. Novikov and R.W. Stewart, Isv. Akad. Nauk. USSR Ser. Geophys. **3**, 408 (1964)
20. R. Benzi, G. Paladin, G. Parisi, A. Vulpiani, J. Phys. A **17**, 3521 (1984)
21. D.J. Evans, E.G.D. Cohen, G.P. Morriss, Phys. Rev. Lett. **71**, 2401 (1993)
22. G. Gallavotti, E.G.D. Cohen, Phys. Rev. Lett. **74**, 2694 (1995)
23. D.J. Evans, D.J. Searles, Adv. Phys. **51**, 1529 (2002)
24. J. Kurchan, J. Phys. A.: Math. Gen. **31**, 3719 (1998)
25. J.L. Lebowitz, H. Spohn, J. Stat. Phys. **95**, 333 (1999)
26. R. van Zon, E.G.D. Cohen, Phys. Rev. Lett. **91**, 110601 (2003)
27. F. Bonetto, G. Gallavotti, A. Giuliani, F. Zamponi, J. Stat. Phys. **123**, 39 (2006)
28. A. Puglisi, L. Rondoni, A. Vulpiani, J. Stat. Mech. P08010 (2006)

Chapter 2
Ergodicity: How Can It Be Broken?

Giancarlo Benettin, Roberto Livi, and Giorgio Parisi

Abstract The introduction of the ergodic hypothesis can be traced back to the contributions by Boltzmann to the foundations of Statistical Mechanics. The formulation of this hypothesis was at the origin of a long standing debate between supporters and opponents of the Boltzmann mechanistic formulation of thermodynamics. The great intuition of the Austrian physicist nevertheless inspired the following contributions that aimed at establishing rigorous mathematical basis for ergodicity. The first part of this chapter will be devoted to reconstructing the evolution of the concept of ergodicity, going through the basic contributions by Birkhoff, Khinchin, Kolmogorov, Sinai etc. The second part will be focused on more recent case studies, associated with the phenomenon known as "ergodicity breaking" and its relations with physical systems. In particular, we describe how it can be related to the presence of exceedingly large relaxation time scales that emerge in nonlinear systems (e.g., the Fermi-Pasta-Ulam model and the Discrete Nonlinear Schrödinger Equation) and to the coexistence of more than one equilibrium phase in disordered systems (spins and structural glasses).

G. Benettin
Dipartmento di Matematica Pura e Applicata, Università di Padova, Via Trieste 63, Padova, I-35121, Italy
e-mail: benettin@math.unipd.it

R. Livi (✉)
Dipartimento di Fisica, Università di Firenze, Via Sansone 1, Sesto Fiorentino, I-50019, Italy
e-mail: livi@fi.infn.it

G. Parisi
Dipartimento di Fisica, Università di Roma "Sapienza", Piazzale Aldo Moro 5, Rome, I-00185, Italy
e-mail: giorgio.parisi@roma1.infn.it

A. Vulpiani et al. (eds.), *Large Deviations in Physics*, Lecture Notes in Physics 885,
DOI 10.1007/978-3-642-54251-0_2, © Springer-Verlag Berlin Heidelberg 2014

2.1 The Ergodic Hypothesis

2.1.1 The Fundamental Physical Ideas

Providing a mechanical foundation to thermodynamics was the main goal of statistical mechanics, that was conceived on the basis of an atomistic view of matter. The mathematical model of a monoatomic ideal gas summarized some of the basic ingredients of this approach. The gas is constituted by a large number N of mechanical particles, with equal mass m and no internal structure, that are contained into a volume V and interact among themselves and with the walls of the container by elastic collisions. On the basis of classical mechanics this model could be studied, in principle, by integrating the equations of motion starting from any initial condition. Accordingly, such a mechanical representation should exclude any need of introducing a thermodynamic description of the system, its evolution in time being completely determined by the laws of mechanics. On the other hand, as argued by Boltzmann already in 1872 [1], computing the trajectories of a macroscopic number of particles (approximately 10^{23} in a mole of gas) is practically unfeasible, and is even unnecessary if one aims to know only the few interesting macroscopic properties of the gas, like pressure or density. The alternative proposal is to replace the detailed microscopic description of the system by convenient hypotheses of statistical nature. On one hand, this needs the introduction of the idea of *probability of microscopic states* in the phase space of the system. This concept can be used to compute statistical averages of any physically interesting observable. On the other hand, it is obviously crucial understanding the link between the microscopic dynamical description and the macroscopic statistical one, i.e. *in which sense deterministic dynamics is compatible with probability and supports it.*

This problem of connecting in some way dynamics and probability is known as *the ergodic problem*; investigating it gave rise to deep developments and perspectives, including a well-posed mathematical theory, known as *ergodic theory*, started by Birkhoff around 1920, still growing and producing beautiful questions and results. The central idea suggested by Boltzmann is the so-called *ergodic hypothesis*. Before describing it in some detail, we wish to stress that Boltzmann's program of deducing thermodynamics from dynamics through probabilistic considerations, appeared at that time intrinsically weak and open to easy criticism. Boltzmann's theory was challenged, in particular, by two paradoxes, attributed to Loschmidt and Zermelo. The first one is known as the *reversibility paradox*: since all the microscopic evolution processes of the ideal gas model (i.e., elastic collisions and free flight between collisions) are reversible—so that, for each possible microscopic trajectory, the reversed trajectory is possible as well—dynamics cannot be consistent with the intrinsic irreversibility of thermodynamics.[1] The second one is called the

[1] It is worth pointing out that the second law of thermodynamics allows to reach the conclusion that in the absence of external forcing a thermodynamic system evolves spontaneously to its equilibrium state, that corresponds to an extremal point (maximum) of the state function entropy.

recurrence paradox and it is based on Poincare's recurrence theorem: a mechanical conservative system made of a finite number of particles in a finite phase space (like the above gas model, at finite total energy) during its evolution will return arbitrarily close to any initial state (apart a set of initial data of zero Lebesgue measure). This implies that, contrary to everyday experience, a gas in a container, after having expanded freely and reached its equilibrium state, sooner or later will return arbitrarily close to its initial out-of-equilibrium state.

Let us briefly illustrate the essence of the Boltzmann's ergodic hypothesis, still making reference for simplicity to the above elementary gas model. The phase space of the system, traditionally denoted Γ, has dimension $6N$ (three coordinates and three momenta per particle). Following Boltzmann, we introduce in Γ and in the dynamics a discretization. First of all, since the microscopic dynamics conserves energy, we focus the attention on a thin layer Γ_E between energies E and $E + \delta E$, with some given δE so small to be physically not appreciable. The volume of the layer will be denoted Ω_E. The layer is then divided into very small cells of equal volume—so small, say, that microscopic states in the same cell are physically indistinguishable. A cell, in this discretized picture, identifies a possible microscopic state, and the dynamics, if time is similarly discretized, is replaced by a deterministic jump from cell to cell. In this framework, the essential assumptions of Boltzmann's theory are the following:

- A macroscopic state—a state, say, in which the values of all thermodynamic variables like (possibly local) temperature or density are specified—consists of a bunch of microscopic states, i.e. of cells, compatible with those values.
- All microscopic states, or cells, have the same a priori probability; correspondingly, the overall volume ω of the cells associated to a given macroscopic state, normalized to Ω_E i.e. ω/Ω_E, has the meaning of a priori probability that the state is realized. The location of the set in Γ_E is not relevant, only its volume is. Such an assumption is usually referred to as the a priori *equiprobability of microscopic states*. Notice that the interpretation of the volume as probability is consistent, because the microscopic evolution preserves volume.
- The above probabilistic assumption is in turn supported by a nontrivial dynamical assumption, known as Boltzmann's ergodic hypothesis: *in an infinite time any trajectory, starting in any cell, goes one after the other through all cells of Γ_E, thus spending in any set of cells of overall volume ω a fraction of time proportional to ω*. An equivalent assumption (frequently referred to as Boltzmann's ergodic hypothesis in textbooks) is that for any observable (any function on Γ), its time average over an infinite trajectory equals its phase average, i.e. the average computed by the above a priori probability.

Such a "coarse grained" description of phase space and dynamics, which avoids mathematical formalism and introduces quickly the main physical ideas, might appear mathematically rough and weak. As a matter of fact, as first shown by Birkhoff, everything can be turned into a clean mathematical framework, leading to the notion of microcanonical measure and of ergodicity; see Sect. 2.1.2 below.

The above assumptions do not use in any deep way the fact that the number N of particles in the system is large: they remain meaningful even for a system of, say, two particles. N large is instead essential for a fourth statement, which however, at least for our ideal gas model, is not anymore an assumption but a computation:

– For large N, the equilibrium state (uniform density and temperature, in our gas example, up to negligible fluctuations) occupies the overwhelming majority of Ω_E, while all the other nonequilibrium states occupy absolutely negligible volumes. See for comments classical textbooks, among them [2].

Correspondingly, a system started out of equilibrium will reach, after a transient, the equilibrium state, and stay there almost forever. However, *large fluctuations occasionally leading the system from equilibrium to an out-of-equilibrium state are not forbidden*, although they are extremely rare events—so rare that there is no chance to see them in a human life and even in the Universe lifetime. In this view the irreversibility of the usual thermodynamic description, which excludes such large fluctuations, appears to be an approximation, although of course a beautiful one, actually better and better for larger and larger N. Boltzmann's view, including fluctuations, makes a conceptual step beyond the standard thermodynamic picture. It is worthwhile to stress that thanks to the inclusion of fluctuations, the paradoxes are solved: concerning recurrence, the far from equilibrium initial state occupies an extremely thin set in Γ_E; the fluctuation leading the system back there, is an extremely rare event, which however is not forbidden and sooner or later, after possibly many Universe lifetimes, will occur. Concerning reversibility, in a similar way a reversed trajectory, along which, say, entropy decreases, occurs for an extremely small set of initial data (as small as the arrival lower entropy state, since dynamics preserves volumes), and so is extremely unlike, but is not forbidden.[2]

In the same years when Boltzmann developed his fundamental scientific theory, the American physicist J.W. Gibbs worked out his equilibrium ensemble theory, that certainly took inspiration and, on its turn, influenced further contributions by Boltzmann. On the other hand, despite Gibbs' approach yields essentially the same practical consequences of Boltzmann theory of equilibrium thermodynamic states, it is worth stressing that the conceptual basis are quite different. In his approach Boltzmann makes reference to the statistical properties of a single, although "typical", dynamical trajectory of a given system: a typical trajectory spends in each volume ω of Γ_E a time proportional to ω, thus giving probability ω/Ω_E to that set. In Gibbs' thoughts, instead, probability plays a more primitive role. The basic idea is that a macroscopic state of a system is an "ensemble" of microscopic states, all existing simultaneously; states are distributed with some given probability density ρ_t, depending on time, in Γ_E or, for systems in contact with a thermal bath so that energy is not conserved, in the whole phase space Γ. The density ρ_t includes all the macroscopic information one has on the system, and is itself the macroscopic state

[2]This is the basic consideration that inspired even the modern formulation of the so-called fluctuation theorem [3].

of the system. Initially ρ_0 depends on the way the system is prepared—for example (with reference to the model of ideal gas we are dealing with), with all the molecules in one corner of the vessel, the velocities possibly having a preferred direction, or similar prescriptions. Different points evolve independently in time according to the laws of microscopic dynamics: *precisely like having an ensemble of independent non interacting mental replicas of the system at hand.* The microscopic evolution makes the ensemble density ρ_t evolve in time; at each time, ρ_t can be used to compute the expectation of any observable. Natural very basic questions, in this approach, include the search for equilibrium ensembles, i.e. probability densities that stay invariant, as well as the possible convergence (in a sense to be made precise) of an initial nonequilibrium ensemble to an equilibrium one.

We shall come back to both the Boltzmannn and the Gibbs approaches in the next paragraph, after introducing the modern mathematical setting of the ergodic problem.

2.1.2 A Well-Posed Mathematical Setting

Boltzmann and Gibbs (as well as Maxwell and Einstein, who also gave fundamental contributions to kinetic theory) did not worry too much about the mathematical precision of the physical ideas they introduced. A convenient mathematical setting, known as ergodic theory, was produced by mathematicians like Birkhoff, von Neumann and Khinchin, starting around 1930. The basic notion is that of a dynamical system. For this, one needs three objects: (i) A phase space where motion takes place, actually some manifold M of finite dimension. (ii) A deterministic law of motion, such that for any initial state $x \in M$ and any time $t \in \mathbb{R}$, the state at time t (the solution of the microscopic equations of motion of the system), denoted $\Phi^t(x)$, is univocally determined. For each $t \in \mathbb{R}$, Φ^t is a map: $M \to M$ and, since $\Phi^0 =$ identity, the inverse of Φ^t is Φ^{-t}, and the composition rule $\Phi^t \circ \Phi^s = \Phi^{t+s}$ holds, the set of all maps

$$\Phi = \{\Phi^t, t \in \mathbb{R}\}$$

is a one-parameter group, called *flow*. (iii) A measure μ in M, normalized so as $\mu(M) = 1$, preserved by the dynamics: that is, for any measurable $A \subset M$ and any $t \in \mathbb{R}$,

$$\mu(\Phi^{-t}(A)) = \mu(A)\,, \qquad \text{where} \qquad \Phi^{-t}(A) = \{x \in M : \Phi^t(x) \in A\}\,.$$

Within ergodic theory, *the triplet* (M, μ, Φ) *is known as a dynamical system.*[3]

[3] Variants that we shall not considered here include the discrete case $t \in \mathbb{Z}$ and the non-invertible cases $t \in \mathbb{R}^+$ and $t \in \mathbb{N}$.

For comments and simple examples we demand to textbooks like [4]. The only example we are here interested in is that of an isolated Hamiltonian system with n degrees of freedom. Let Γ denote its $2n$-dimensional phase space and Γ_E be any surface of constant energy (a true surface, not anymore a layer as before). The Hamiltonian dynamics is known to preserve the volume in Γ, and this in turn induces the conservation of a measure μ_L, called *Liouville measure*, on each Γ_E; a possible definition is

$$\mathrm{d}\mu_L = C \, \frac{\mathrm{d}\Sigma}{\|\nabla H\|} \, ,$$

where $\mathrm{d}\Sigma$ is the Euclidean area on Γ_E, ∇H is the gradient of the Hamiltonian H and $\|\,.\,\|$ denotes Euclidean norm; C is just a normalization constant.[4] The triplet (Γ_E, μ_L, Φ) is, in ergodic theory, a Hamiltonian dynamical system.[5]

For any measurable function $M \to \mathbb{R}$, let $\langle f \rangle$ denote its phase average:

$$\langle f \rangle = \int_M f \, \mathrm{d}\mu \, .$$

The first (highly) nontrivial result in ergodic theory is the so-called *Birkhoff–Khinchin ergodic theorem*, stating that *For any measurable f, and almost any $x \in M$,the time average*

$$\overline{f}(x) = \lim_{t\to\infty} \frac{1}{T} \int_0^T f(\Phi^t(x)) \, \mathrm{d}t$$

exists, is equal to the corresponding backwards average, and moreover $\langle \overline{f} \rangle = \langle f \rangle$.

Now we are ready to introduce the mathematical notion of ergodicity. For any measurable set $A \subset M$, let $T_A(x, T)$ be the time spent in A up to time T by the motion starting in x, and

$$\tau_A(x) = \lim_{T\to\infty} \frac{1}{T} T_A(x, T) \, .$$

A possible formal definition of ergodicity, closely following Boltzmann's ergodic hypothesis, is

E1: *for any measurable $A \subset M$, and almost any $x \in M$, it is $\tau_A(x) = \mu(A)$.*

[4] Where the gradient is smaller, nearby surfaces of constant energy are, so to speak, more separated; correspondingly, the measure associated to the same area of Γ_E is larger. The measure μ_L keeps the Boltzmann original attitude of looking at the $2n$-dimensional volume in a thin layer between nearby surfaces of constant energy, just turning it into a precise mathematical language.

[5] One might also consider the whole Γ in place of Γ_E and the volume in Γ in place of μ_L: an easier point of view, which however does not lead to any interesting result because the dynamics never mixes different constant energy surfaces.

A necessary and sufficient condition (and so an equivalent definition of ergodicity), also interpreting Boltzmann's thoughts, is

E2: *for any measurable* $f : M \to \mathbb{R}$, *almost everywhere it is* $\overline{f}(x) = \langle f \rangle$.

Let us come to the Gibbs' view. Let ρ_t be a probability density on M (an ensemble) evolving in time; the dynamics obviously preserves probability (the probability of being at time t in $A \subset M$ is the same as being in $\Phi^{-t}(A)$ at time 0), and consequently

$$\rho_t(\Phi^t(x)) = \rho_0(x) \, .$$

A trivial equilibrium state, known as the *microcanonical ensemble*, is the constant one, $\rho^*(x) = 1$ for any $x \in M$ (recall the normalization $\mu(M) = 1$). Are there other candidates? It is easy to prove that ρ^* is the only invariant density (among measurable functions), if and only if E1, E2 hold. So, a further property equivalent to E1, E2, to be possibly used as definition of ergodicity, is[6]

E3: *there exists only one (measurable) equilibrium state, namely* ρ^*.

It is quite remarkable that the mathematical notion of ergodicity keeps the central ideas of both the Boltzmann and the Gibbs approaches, formalizing them together. In fact, none of the properties E1–E3 was used by Birkhoff as his primitive notion of ergodicity, but a fourth still equivalent one[7]:

E4: *let* A *be an invariant subset of* M (i.e., $\Phi^{-t}(A) = A$). *Then* A *is trivial, i.e.* $\mu(A) = 0$ *or* 1.

Besides ergodicity a second notion, called *mixing*, plays a fundamental role in ergodic theory. The idea is that any initial set A, transported by the dynamics, spreads uniformly over M; formally, the definition is

M1: *for any measurable* $A, B \subset M$, *it is*

$$\lim_{t \to \infty} \mu(\Phi^{-t}(A) \cap B) = \mu(A)\mu(B) \, . \tag{2.1}$$

This turns out to be equivalent to the decay of all time correlations, indeed an alternative equivalent definition of mixing:
M2: *for any square–summable observables* $f, g : M \to \mathbb{R}$, *it is*

$$\lim_{t \to \infty} \int_M f(\Phi^t(x)) g(x) \mathrm{d}\mu(x) = \int_M f(x) \mathrm{d}\mu(x) \int_M g(x) \mathrm{d}\mu(x) \, . \tag{2.2}$$

[6] Usually reported as: *any measurable constant of motion* (i.e. $f(\phi^t(x)) = f(x)$ for any x) *is trivial, i.e. almost everywhere constant in* M; the restriction to ρ positive and normalized is irrelevant.

[7] E4 is known as *metrical indecomposability of* M: no decomposition of M into A and $M \setminus A$ can be invariant, unless it is trivial.

Mixing is shown to be stronger than ergodicity. A particular case of (2.2), but equivalent to the general one, is when g is an initial Gibbs distribution ρ_0. The trivial replacement $x' = \Phi^t(x)$, recalling $\int_M \rho_0 \mathrm{d}\mu = 1$, turns M2 into

M2': *for any initial* ρ_0 *and any* f, *it is*

$$\lim_{t\to\infty} \langle f \rangle_{\rho_t} = \langle f \rangle_{\rho^*} , \qquad \text{where} \qquad \langle f \rangle_\rho = \int_M f(x)\rho(x)\, \mathrm{d}\mu(x) .$$

In this weak sense, any initial probability density ρ_0 approaches, for $t \to \infty$, the equilibrium density ρ^*. Quite clearly, the notion of mixing appropriately formalizes Gibbs' question whether a system, no matter how prepared, asymptotically reaches equilibrium.

The notion of mixing also allows to better understand the reversibility paradox: (2.2) shows that in a mixing system, *in spite of the reversibility of the microscopic dynamics, Gibbs macroscopic states behave irreversibly*, without contradiction. Similarly, (2.1) shows that in a mixing system, *the dilution of a set* A *over* M, *in spite of the reversibility of the dynamics, is one way*.[8]

Deciding whether a given system is ergodic or mixing, is quite hard, apart from very elementary model examples. It is especially hard in the realm of statistical mechanics, that is when the number of degrees of freedom is large. Even for simple models of gases, like hard spheres in a cubic box, the question is not yet completely solved. Very few is known concerning systems of (nonlinearly) coupled oscillators. A crucial question concerns the time scales entering the game: a system might be ergodic and mixing, but evolve so slowly towards equilibrium, that for any human time scale it could appear as not evolving at all and "frozen" in some non-equilibrium state. A few important examples will be discussed in the next section.

2.2 Ergodicity Breaking

The lack of ergodicity in models with many degrees of freedom provides a kind of paradox in statistical mechanics, and is often referred to as *ergodicity breaking*. In recent years, it has been realized that the breaking of ergodicity is more frequent than previously expected, and characterizes a series of physical models of great phenomenological interest.

[8]This happens of course also if we change t in $-t$, i.e. there is no preferred direction of time. A deep discussion could be opened here. Take a common gas and consider a low entropy initial condition, for example with all molecules initially confined in a corner of the container. *For most initial states satisfying such condition, both in the forward and in the backward evolution of the system, with perfect symmetry, the gas evolves towards equilibrium and entropy increases.* This is not always told to students, when discussing about the "arrow of time".

In fact, one should consider that, despite ergodicity has played a basic role for enabling a solid conceptual basis for statistical mechanics, i.e. for a mechanical approach to thermodynamics, only a few mathematical models can be rigorously proved to be ergodic. Their list reduces essentially to billiard-like systems[9] and, in the direction of statistical mechanics, to systems of a few hard discs in a box: the ergodicity of a (not too dense) gas of N discs or spheres in a box, for large N, is conjectured but not completely mathematically demonstrated. Very few is known concerning physically realistic models, like gases of molecules interacting with typical intermolecular potentials, possibly including internal vibrational or rotational degrees of freedom. Even less understood are models of many nonlinearly coupled oscillators, say nonlinear discrete vibrating strings, or membranes, or crystals. Among them, the first and most studied system is certainly the Fermi-Pasta-Ulam (FPU) model, introduced to describe the relaxation to thermodynamic equilibrium in a chain of nonlinearly coupled oscillators. Such a system has been studied mainly numerically, although relevant theoretical investigations do exist. As a matter of fact, the system exhibits nice ergodic properties[10] at large enough energy (or temperature), although, likely, it is never ergodic in the strict mathematical sense; at lower energies instead the behavior is *very* complex and, so to speak, more far from ergodicity than at higher energies. An account including just a few results, extracted from the very wide literature on the subject, is presented in the next subsection.

2.2.1 *Ergodicity Breaking in the Fermi-Pasta-Ulam Model at Low Energies*

In 1954 Enrico Fermi, John Pasta and Stanislaw Ulam, universally known by the acronym FPU, decided to use one of the first electronic computers ever constructed—the MANIAC I,[11] of the Los Alamos National Laboratory—to numerically integrate the microscopic equations of motion of a Hamiltonian system, elementary but interesting for statistical physics, aiming to understand its ergodic and statistical properties.

Enrico Fermi does not need any presentation; its interest in the ergodic problem is not surprising, since already in 1923 he published an important paper on the

[9] One point bounces elastically inside a bounded region. The ergodic properties depend in a non trivial way on the shape of the boundary. The first example, due to Sinai [5, 6], represented an important breakthrough in ergodic theory.

[10] This means, essentially, that the system behaves nicely, as if it were ergodic, if one does not look at the behavior of microscopic degrees of freedom, but restricts the observation to macroscopic observables, possibly to a selected subset of them. Such a point of view was proposed by Khinchin [7]. It looks physically deep, but never gave rise to a well-posed mathematical theory.

[11] Mathematical Analyzer, Numerical Integrator (or perhaps Numerator, Integrator) and Computer.

subject [8].[12] John Pasta was a computer scientist, certainly a pioneer in the field. Stanislaw Ulam was a mathematician, expert mainly in diffusion equations, mostly known as the inventor of the so-called "Monte–Carlo" methods in statistical problems.

The resulting paper[13] [11] was a quite innovative one, from several points of view.

- It started a new research field, nowadays highly developed and known as "molecular dynamics", aiming at understanding the macroscopic properties of a system starting "ab initio", i.e. from its microscopic laws of motion. Clusters of hundreds or even thousands of computers nowadays are normally used, mainly by chemical physicists, to investigate larger and larger systems, in particular quantum ones.
- It started a new branch of mathematics: as it is not much known, the modern theory of integrable nonlinear wave equations like KdV, mKdV or NLS—including relevant phenomena like solitons—precisely originated as an effort to understand the unexpected phenomena observed by FPU [12].
- It raised concrete questions in ergodic theory that after almost 60 years, in spite of the great progress of the theory and the enormous progress of computers,[14] still are poorly understood.

In the next paragraph we shall quickly describe the model and the early results, then we shall provide examples of more recent investigations.

The model and the early results The FPU model is a chain of particles connected by nonlinear springs, with Hamiltonian

$$H(q_1, \cdots, q_N, p_1, \cdots, p_N) = \frac{1}{2}\sum_{j=1}^{N} p_j^2 + \sum_{j=1}^{N+1} V(q_{j+1} - q_j)\,, \qquad (2.3)$$

where

$$V(r) = \frac{1}{2}r^2 + \frac{\alpha}{3}r^3 + \frac{\beta}{4}r^4\,,$$

[12] Such a paper contains a mathematical theorem which suitably generalizes a well known result by Poincaré [9], followed by an heuristic application to the ergodic problem. This latter part is open to criticism (a crucial regularity that Fermi assumes to be generic, is not).

[13] Quite interestingly, the paper remained for several years an internal report of the Los Alamos Laboratories [10], and only in 1965 it got published in Fermi's Collected Papers [11].

[14] MANIAC I is referred to as capable of 10^4 "operations" per second. This means a possible ratio 10^5, compared to common nowadays cpu's; a cluster of 100 cpu's—a quite common object—rises the ratio to 10^7. This means that what is easily done, nowadays, in 1 h, would have required about 400,000 years of computation on MANIAC I.

α and β being the nonlinearity constants ($\beta > 0$; the sign of α is irrelevant). The mass of the particles and the elastic constant of the springs are set equal to one. We shall here consider (as FPU did) fixed end conditions, i.e. $q_0 = q_{N+1} = 0$; periodic boundary conditions are also widely studied. As it can be easily checked, the only quantities that determine the dynamics up to a rescaling are the products $\alpha^2\varepsilon$ and $\beta\varepsilon$, where $\varepsilon = E/N$ is the specific energy, E denoting of course the total energy of the chain.

The normal modes of the linear chain ($\alpha, \beta = 0$), as it is well known, are given by

$$Q_k = \sqrt{\tfrac{2}{N+1}} \sum_{n=1}^{N} q_n \, \sin \frac{\pi k n}{N+1} \,, \qquad P_k = \sqrt{\tfrac{2}{N+1}} \sum_{n=1}^{N} p_n \, \sin \frac{\pi k n}{N+1} \,, \tag{2.4}$$

$k = 1, \ldots, N$, while the dispersion relation (frequency vs. mode index k) is

$$\omega_k = 2 \sin \frac{\pi k}{2N+2} \,; \tag{2.5}$$

the harmonic energy associated to each mode k is finally

$$E_k = \frac{1}{2}\big(P_k^2 + \omega_k^2 Q_k^2\big) \,. \tag{2.6}$$

Relevant observables of the problem are the mode energies E_k and their time averages, namely

$$\overline{E}_k(t) = \frac{1}{t} \int_0^t E_k(Q_k(t'), P_k(t')) \, \mathrm{d}t' \,, \qquad k = 1, \ldots, N \,. \tag{2.7}$$

The authors could work only with a small number of particles, typically $N = 32$, up to short times, of the order of 10^4 or slightly larger; this however was enough to them, to understand that some serious obstacle to ergodicity and mixing did exist. The aim of the work was indeed understanding how, and on which time scale, the model, if prepared in a state far from statistical equilibrium, does approach equilibrium. To this purpose, the authors gave initially all of the energy to only one normal mode, actually the lowest one ($k = 1$), expecting a progressive involving in the dynamics of all modes, till energy equipartition. With great surprise, they did not find any tendency to equipartition, rather they observed the formation of a strange state in which only a few modes did effectively share energy, and moreover, the dynamics appeared to be close to a quasi-periodic one, with no trace of the expected "molecular chaos". In their very words:

> Let us here say that the results of our numerical computations show features which were, from the beginning, surprising to us. Instead of a gradual, continuous flow of energy from the first mode to the higher modes, all of the problems show an entirely different behavior. (...) Instead of a gradual increase of all the higher modes, the energy is exchanged, essentially, among only a certain few. It is, therefore, very hard to observe the rate of 'thermalization' or mixing in our problem, and this was the initial purpose of the calculation.

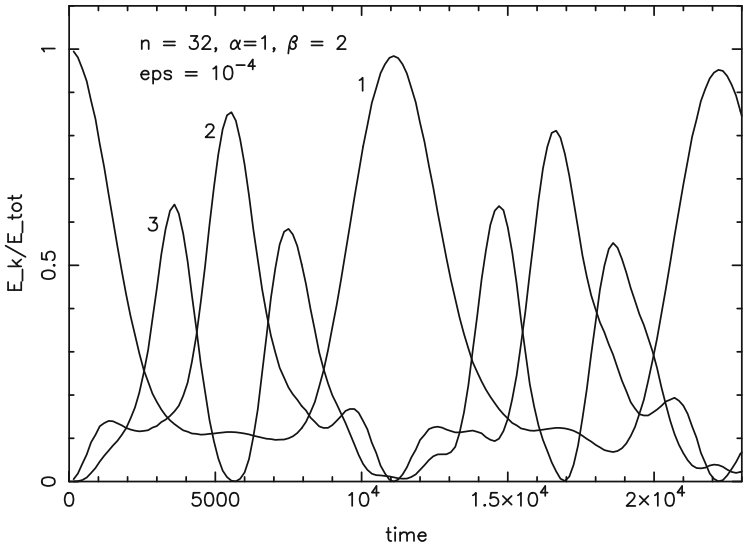

Fig. 2.1 The instantaneous values of the energies E_k, $k = 1, 2, 3$, versus t, for $N = 32$, $\alpha = 1$, $\beta = 2$, $\varepsilon = 2 \times 10^{-4}$, all energy initially given to mode $k = 1$

The sense of surprise, and the consciousness to be in front of a real novelty, is still present, several years later, in Ulam's introduction to the FPU paper in [11]:

> The results of the computations were interesting and quite surprising Fermi. He expressed to me the opinion that they really constituted a little discovery in providing intimations that the prevalent beliefs in the universality of 'mixing and thermalization' in non-linear systems may not be always justified.

Figure 2.1, a modern remake of one of the original FPU figures, shows the time behavior of $E_k(t)$ vs. t, $k = 1, 2, 3$, for a small model with $N = 32, \alpha = 1, \beta = 2$, at low energy $\varepsilon = 10^{-4}$, only mode $k = 1$ being initially excited. The presence of quasi-periodicity is rather evident. Recurrences on even larger times were observed a few years later[15] in [13], see Fig. 2.2. If we look at the time averages $\overline{E}_k$, the lack of energy equipartition, and thus of ergodicity and equilibrium, is even more clear. Figure 2.3 shows $\overline{E}_k(t)$ vs. the averaging time t, in the same conditions of the previous Figs. 2.1 and 2.2, for $k = 1, \ldots, N$; the clear impression is that each of the $\overline{E}_k$'s reaches its own asymptotic value, different from the equipartition value $1/N$.

At sufficiently high energies, as first recognized in [14], the situation completely changes: regularity disappears, and the system reaches rather quickly energy equipartition; see Fig. 2.4, where ε is raised to $\varepsilon = 10^{-2}$. The difference with respect to Fig. 2.3 is striking.

[15]Reference [13] was published only in 1972, but the results certainly circulated since 1961, see Ulam's introduction to FPU in [11].

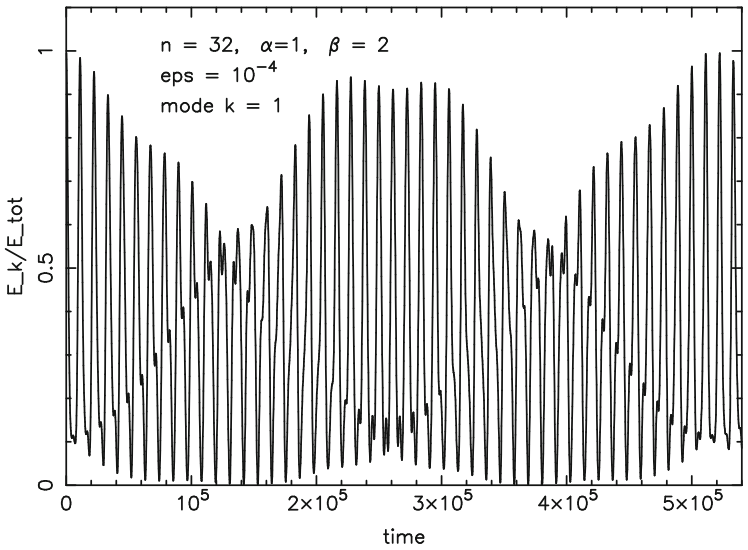

Fig. 2.2 The instantaneous value of E_1, on a ten times larger time interval, in the same conditions as Fig. 2.1

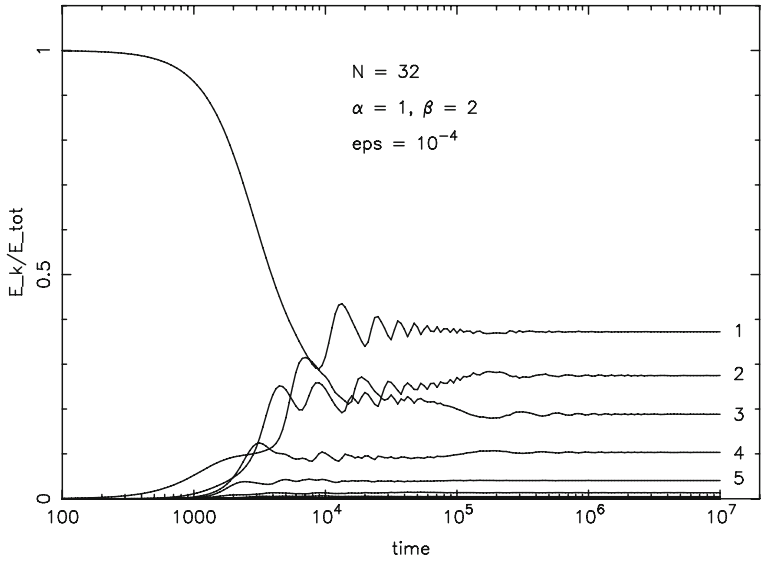

Fig. 2.3 The averaged energies $\overline{E}_k(t)$ vs. t for the first few modes (semi-log scale), in the same conditions as in Fig. 2.1

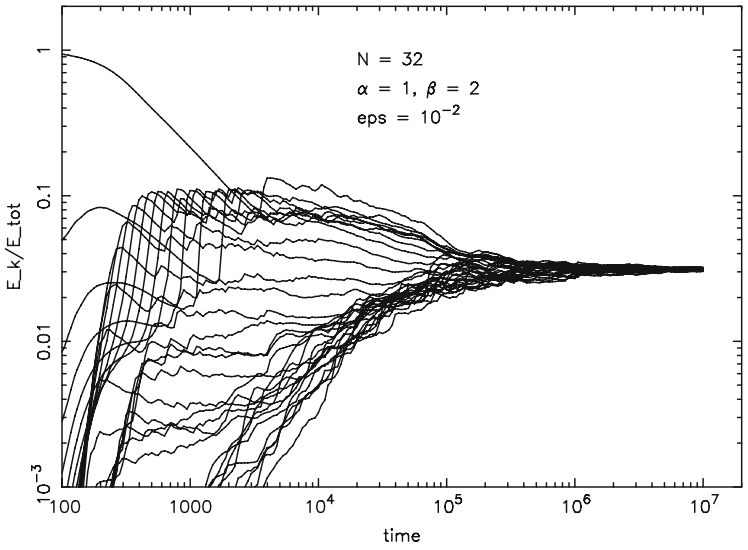

Fig. 2.4 The averaged energies $\overline{E}_k(t)$ vs. t (log-log scale), at larger specific energy $\varepsilon = 10^{-2}$. Parameters as in the previous figures

The debate on the FPU problem continued for several years, having in mind, as the main goal, the localization of a threshold below which ergodicity breaks. The underlying theoretical paradigm was, basically, KAM theory: indeed the idea of a critical nonlinearity, and the evidence of quasi-periodicity at low nonlinearities, remind that theory. The idea of a threshold, however, soon appeared to be rough: different indicators, different choices of the initial conditions, perhaps even different personal attitudes of the authors in interpreting data, led to quite different conclusions, and results, mainly concerning the crucial question of the persistence of the ergodicity breaking—no matter how defined—in the thermodynamic limit, could not provide a clear answer. In the early eighties of last century, however, the point of view significantly changed, and two important new ideas entered the game.

(i) The state observed by FPU, in which only a few normal modes do share energy, is not really asymptotic in time, rather it represents a kind of metastable situation, or intermediate state, which on a *much larger* time scale slowly evolves and possibly reaches equipartition. That is: on larger times, ergodicity is possibly recovered even at low energies. The new point of view was introduced, and supported by heuristic theoretical reasoning and some numerical calculations, in [15, 16]. It should be stressed that the cultural background, in the meanwhile, had changed: in statistical mechanics, the theory of spin glasses, with metastability and associated long times, entered the discussion; in dynamical systems, Nekhoroshev theory developed as complementary to KAM theory and introduced, as a generic scenario, the possible presence of long time scales, when a natural perturbative parameter is small.

(ii) The intermediate state, and specifically the quasi-periodicity characterizing it, reflects the closeness of the FPU model to an integrable[16] model, which however is not the linear chain, but the so-called Toda model: on the time scale observed by FPU, at the low nonlinearities they did work, FPU and Toda are hardly distinguishable. This point of view was first proposed and supported in [17], but apart a few exceptions, it was not much further exploited till very recently [20].

The literature on the subject, after the above cornerstone papers i.e. in the last 30 years, is rather wide, and let us say somehow disorienting: a coherent picture of the FPU phenomenon still looks far away. The state of the art dated a few years ago can be found in [18, 19]; the points of view there expressed, however, are rather deeply different and, consequently, hard to summarize. In the remaining part of this section we shall limit ourselves to present only very few recent numerical results, with the only aim to quickly illustrate the two above ideas and to show, at least, the complexity of the problem. The main question we shall have in mind is whether the FPU phenomena are significant for statistical mechanics, i.e., if they persists in the limit of large N at fixed ε.

An excerpt of recent results Among recent papers, the ones that mainly are concerned with the persistence in the thermodynamic limit of the FPU phenomenon—that we now appropriately describe as necessity of quite large time scales for ergodicity, and ergodicity breaking for shorter observation times—are [20–24]. We shall limit ourselves to very few results taken from (some of) them. We need to consider values of N much larger than 32 as in FPU,[17] moreover the initial data too need to be more adapted to a statistical mechanics approach: in particular for large N the equivalent of the FPU-like initial conditions is not exciting a single or a few modes, but some fraction of N, moreover with random initial phases (see [23] for a study of the crucial role of phases in the thermodynamic limit). Figure 2.5 illustrates the presence of two time scales in the problem. The figure refers to a model with $N = 1{,}023$, $\alpha = 1$, $\beta = 2$, small $\varepsilon = 10^{-4}$, the lowest 10 % of modes being initially excited (see the rectangle marked $t = 0$). The figure shows the time averages[18] $\overline{E}_k(t)$ vs. k/N, at different times in geometric progression.

[16] We shall not define integrability here. In the very essence, an integrable system is a system having many constants of motion—as many as the number of degrees of freedom—and *all* motions are quasi periodic. Ergodicity is far away, and statistical approaches like using a microcanonical measure are meaningless.

[17] How many degrees of freedom do already represent the thermodynamic limit, is a delicate question discussed rather widely in [24]. Basically, the more ε is small, the larger N needs to be to reasonably approach the thermodynamic limit. *Taking instead the limit* $\varepsilon \to 0$ *at fixed large* N (no matter how large) *is not appropriate:* the limits are in the reverse order. The exchange of the limits, although very spontaneous having finite computational resources, might lead to a wrong picture of the thermodynamic limit behavior.

[18] With a minor change of the definition of $\overline{E}_k$, namely

$$\overline{E}_k(t) = \frac{1}{t/3} \int_{(2/3)t}^{t} E_k(Q_k(t'), P_k(t'))\, \mathrm{d}t' \,;$$

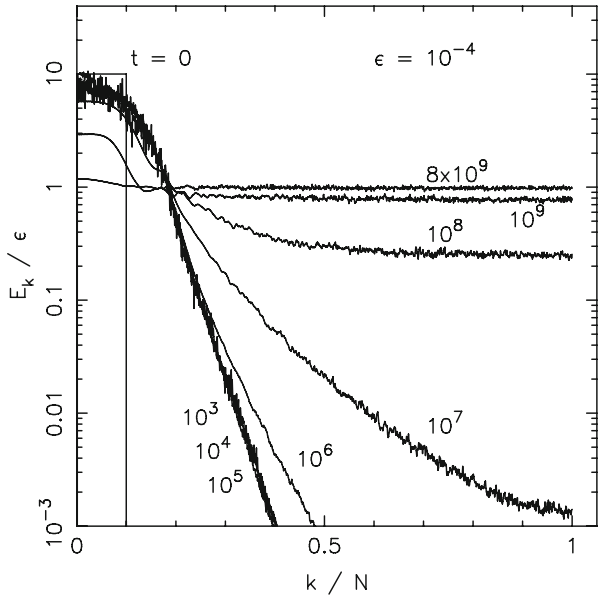

Fig. 2.5 The shape of the averaged energy spectrum of normal modes $\overline{E}_k(t)$ plotted vs. k/N, at selected times t (marked in the figure) in geometric progression. Energy initially equidistributed among modes with $0 < k/N < 0.1$, see the *rectangle* marked $t = 0$. Each point is the average over 24 random extractions of the initial phases. Parameters: $N = 1{,}023$, $\alpha = 1$, $\beta = 2$, $\varepsilon = 10^{-4}$

The phases of the excited modes are chosen randomly, moreover, just to clean the curves, an average over 24 different random choices of the phases is added. The figure shows that quite soon, already at $t \simeq 10^3$, a well defined profile is formed, in which only some low frequency modes effectively take part to energy sharing, the energies of the remaining ones decaying exponentially with k/N. The energy profile keeps its form nearly unchanged for a rather large time scale, definitely much larger than the time needed to form it; only on *much* larger times, say $t = 10^9$ or 10^{10}, the system does approach energy equipartition, the high-frequency modes being progressively involved into the energy sharing. The first profile, i.e. the one formed at $t = 10^3$, is clearly the analog of the FPU state, in which ergodicity appears to be broken. Similarly to the glassy behavior, however, on much larger times ergodicity is recovered. A similar behavior can be found for different initial excitations, see [20].

For given parameters and initial conditions (for example, 10 % of modes initially excited as above), let us denote $T(N, \varepsilon)$ the large time scale, i.e. the equilibrium or ergodicity time. T of course needs to be appropriately defined, and some arbitrariness necessarily enters the definition; the idea in [24] is to look at the time of

similar averages in a running window (of amplitude proportional to t) are in principle equivalent to the usual time averages from $t = 0$, but are less "lazy" to change, and better show the evolution of the time averages on the appropriate time-scale.

the raise of the tail in Fig. 2.5, making it quantitative through an appropriate index; here we cannot be more precise (see the quoted paper for details) and proceed by assuming $T(N, \varepsilon)$ is somehow defined. The numerical evidence, see [24], is that:

– By increasing N at fixed ε, $T(N, \varepsilon)$ converges to a limit value $T_\infty(\varepsilon)$, representing the time scale for ergodicity in the thermodynamic limit for a given ε.
– $T_\infty(\varepsilon)$ grows, for $\varepsilon \to 0$, following a power law[19]:

$$T_\infty(\varepsilon) \sim \varepsilon^{-a} , \qquad a = 9/4 . \tag{2.8}$$

This seems to be the time scale at which, in the thermodynamic limit, ergodicity is re-established.

Let us quickly come to point (ii) above. The Toda model, let us recall, has Hamiltonian as in (2.3), but the potential V is replaced by

$$V_T(r) = U(e^{\lambda r} - 1 - \lambda r) .$$

For all values of the parameters U, λ, the model is exactly integrable [25, 26]. For the particular choice

$$U = \tfrac{1}{4}\alpha^{-2} , \qquad \lambda = 2\alpha ,$$

the Toda potential follows the FPU one up to third order, namely

$$V_T(r) = \tfrac{1}{2}r^2 + \tfrac{1}{3}\alpha r^3 + \tfrac{1}{4}\beta_T r^4 + \tfrac{1}{5}\gamma_T r^5 + \cdots$$

with

$$\beta_T = \tfrac{2}{3}\alpha^2 , \qquad \gamma_T = \tfrac{1}{3}\alpha^3 , \qquad \ldots$$

So, the FPU model is closer to a certain Toda model than to the linear chain: roughly speaking, the distance of FPU to the linear chain is $\alpha\sqrt{\varepsilon}$, while the distance to Toda is $|\beta - \beta_T|\varepsilon$, much smaller at low ε.

As understood in [17], the Toda model provides the best integrable approximation to FPU, and it turns out that the dynamics of FPU, within the first time scale—the one in which ergodicity is broken—is almost indistinguishable from the Toda dynamics. Figure 2.6, actually a remake of a figure in [17], shows the instantaneous values of the energies $E_k(t)$ for a Toda model with small $N = 32$, in

[19] If instead N is kept fixed, even if large, then $T(N, \varepsilon)$, for small ε below a certain ε_N, abandons the power law to follow a stretched exponential $T(N, \varepsilon) \sim e^{1/\varepsilon^\gamma}$, $\gamma = 1/8$. This is different from the thermodynamic limit. Performing the limits in the correct way is numerically painful but necessary.

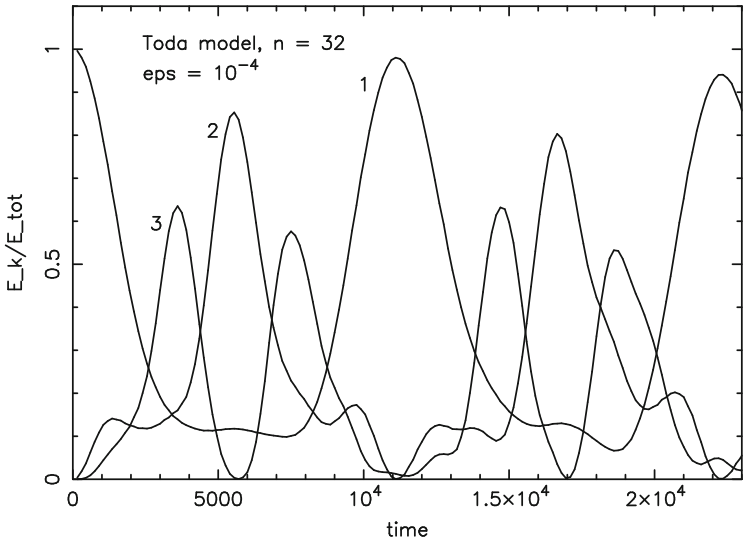

Fig. 2.6 The analog of Fig. 2.1, for the Toda model with the same $N = 32$, in the same conditions

conditions identical to those of Fig. 2.1. The similarity of the two figures is striking. The similarity persists for larger N, see [20]. Figure 2.7 is instead the analog of Fig. 2.5: same N, same conditions. Quite clearly, the Toda model has only the first time scale; the tail never raises and ergodicity is never recovered. The profile of the energy spectrum in Fig. 2.7 is hardly distinguishable from the profile appearing in Fig. 2.5, up to $t = 10^5$. Further evidences of the role of the Toda model as a good integrable approximation of FPU during the shorter time scale, as well as the progressive loss of integrability on larger times, can be found in [20].

Part of such a rich phenomenology and complexity of the FPU model is present in other one-dimensional models, like the so-called FPU β-model ($\alpha = 0$) or the "discrete ϕ^4" model: with however some important differences, also due to the fact that an integrable nonlinear approximation like Toda in such other models does not exist (at least, is not known). In higher dimension 2 or 3, very few modern results do exist. The most recent and detailed one is probably [27], devoted to dimension 2; the essential result is that some phenomena like the presence of two time scales, in higher dimension, do persist, but the large time scale is not as large as in dimension one: a power law like in (2.8) is indeed found, but with smaller exponent $a = 5/4$ or even $a = 1$, depending on the model.

Whether or not the nontrivial behavior of the FPU models is relevant in physical reality, is hard to say. For sure, they provide a beautiful example of the possible complexity in the realization of ergodicity and mixing in some large systems, interesting in principle for statistical mechanics.

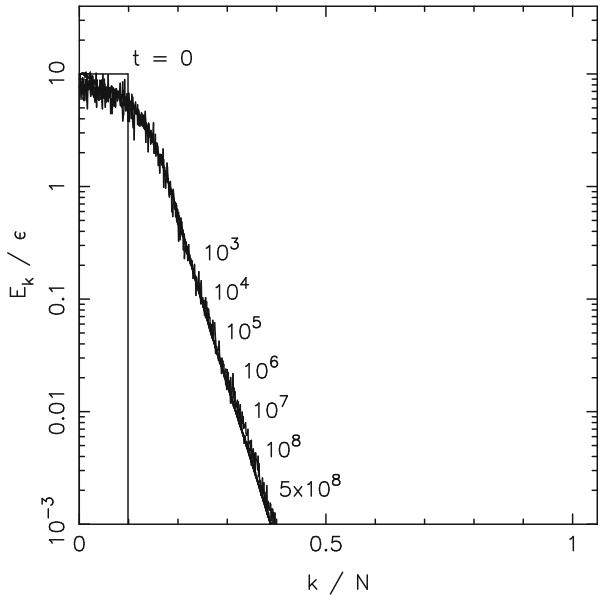

Fig. 2.7 The analog of Fig. 2.5, for the Toda model with the same $N = 1{,}023$, in the same conditions

2.2.2 *Ergodicity Breaking Induced by Breather States in the Discrete Nonlinear Schrödinger Equation*

The ergodicity breaking mechanism in the FPU model is associated to the exceedingly large time scales characterizing its approach to equilibrium at low energies, where the model is close to integrability. A similar phenomenon occurs in the Discrete Nonlinear Schrödinger Equation (DNLSE), despite the basic dynamical mechanism and its statistical implications are quite different. In fact, the DNLSE exhibits ergodicity breaking for high values of the energy, where it is quite far from any integrable limit. In particular, it exists a *negative temperature* region of the model, where the spontaneous formation of localized excitations in the form of breathers prevents any practically accessible convergence to equilibrium. This peculiar non-equilibrium mechanism is expected to yield relevant consequences for many of the physical problems described by the DNLSE.

Generalities of the model The Discrete Nonlinear Schrödinger Equation has been widely investigated in various domains of physics as a model of propagation of nonlinear excitations [28, 29]. In fact, it provides an effective description of electronic transport in biomolecules [30] as well as of nonlinear waves propagation in a layered photonic or phononic systems [31,32]. More recently, a renewed interest for this multipurpose equation emerged in the physics of gases of cold atoms trapped in periodic optical lattices (e.g., see Ref. [33] and references therein for a recent survey).

The one-dimensional DNLSE reads

$$i\dot{z}_n = -2|z_n|^2 z_n - z_{n+1} - z_{n-1} \tag{2.9}$$

and it can be derived from the Hamiltonian

$$H = \sum_{n=1}^{N} |z_n|^4 + z_n^* z_{n+1} + z_n z_{n+1}^*, \tag{2.10}$$

where $z_n(t)$ is a complex variable that can be interpreted as the "wave function" at site n on a chain made of N sites. Boundary conditions for the moment are unspecified. Notice that Eq. (2.9) and Hamiltonian (2.10) are fully classical. As described in [33] they can be derived through a suitable procedure as the classical limit of a genuine quantum model. This is the reason why the dynamical variables, $z_n(t)$, keep track of this quantum origin. On the other hand, the canonical transformation $z_n \equiv (p_n + \imath q_n)/\sqrt{2}$ allows to rewrite Hamiltonian (2.10) by the usual classical canonically conjugated variables of momentum, p_n, and position, q_n, as follows

$$H = \sum_{n=1}^{N} (p_n^2 + q_n^2)^2 + 2(p_{n+1}p_n + q_{n+1}q_n), \tag{2.11}$$

The sign of the quartic term is assumed to be positive (in the language of cold atoms this corresponds to a repulsive interaction), while the sign of the hopping term is irrelevant, due to the symmetry associated with the canonical (gauge) transformation $z_n \to z_n e^{i\pi n}$. At variance with its continuum version, the DNLSE is not integrable and this is the property that makes it interesting not only for dynamics but also for thermodynamics. In fact, it has only two conserved quantities, the energy H and the total norm (or total number of particles),

$$A = \frac{1}{2} \sum_{n=1}^{N} (p_n^2 + q_n^2) \quad . \tag{2.12}$$

As a consequence, the equilibrium phase-diagram is two-dimensional, as it involves the energy density $h = H/N$ and the particle density $a = A/N$. The first reconstruction of the diagram was carried out in Ref. [34], where the authors derived the thermodynamics of the DNLSE model by assuming the existence of a grand-canonical measure.[20] In fact, the grand-canonical ensemble seems the appropriate one for the statistical mechanics description of a model like the DNLSE, where both

[20]Explicit calculations of gran-partition function of the DNLSE were carried out by transfer integral techniques.

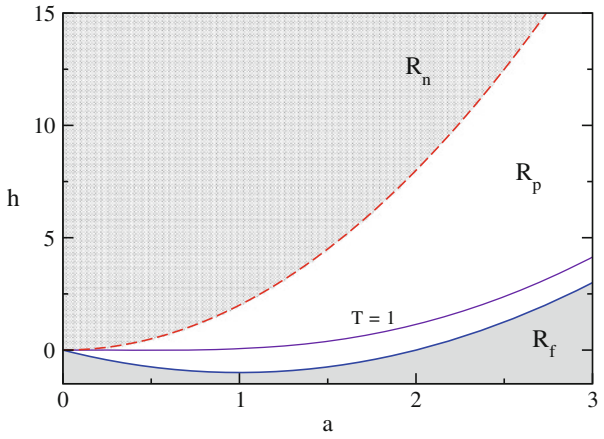

Fig. 2.8 Equilibrium phase diagram (a, h) of the DNLSE. The positive temperature region R_p lies between the ground state (*solid blue line*) and the infinite temperature isothermal (*dashed red line*). The *purple line* corresponds to the isothermal at temperature $T = 1$. The "negative temperature" region R_n extends above the infinite temperature line. Below the ground state extends the physically forbidden region R_f

the total energy and the total mass are conserved quantities. It can be easily realized that the ground state of Hamiltonian (2.10) is identified by the relation

$$h = a^2 - 2a$$

that is the lower curve in Fig. 2.8. The corresponding temperature and chemical potential are $T = 0$ and $\mu = 2(a - 1)$, respectively. The upper curve in Fig. 2.8 is identified by the relation

$$h = 2a^2$$

and corresponds to the infinite temperature line (random phases) with $T = \infty$ and $\mu = -\infty$.

Many interesting aspects concern the thermodynamics of the DNLSE in the region in between these two curves (e.g., see [35]). Here we are rather interested to discuss the ergodicity breaking mechanism characterizing the region above the infinite temperature line.

Thermodynamics in the region of negative temperatures It was conjectured already in [34] that the region R_n should correspond to negative temperatures. Actually, this can be argued by the following considerations. The hypersurface in phase space corresponding to constant energy, H, and number of particles, A, is a compact manifold, being the interception between the constant energy hypersurface and the hypersphere corresponding to constant number of particles. According to Weierstrass' Theorem, the energy H has to be bounded for any value of A. Making

reference to the microcanonical statistical ensemble, in this case the entropy S is a function of the energy $E = H$ defined on a finite interval $I = [E_{min}, E_{max}]$, where $E_{min} = A^2/N - 2A$ is the ground-state energy and $E_{max} = A^2$ corresponds to all the energy concentrated into a single site (notice that this "upper" state is N-fold degenerate). Since $S(E)$ has to be a differentiable function and certainly has two minima in correspondence of the extrema of I, there must be a maximum of S inside I and this maximum is located at $E^* = 2A^2/N$ (i.e., it corresponds to the $T = \infty$ line). The microcanonical definition of temperature T is

$$\frac{1}{T} = \frac{\partial S}{\partial E} \quad , \tag{2.13}$$

which is a positive quantity in the interval $[E_{min}, E^*]$ and, accordingly, a negative one in the interval $[E^*, E_{max}]$. This conclusion can be rigorously verified, by obtaining an explicit analytic expression for T by differential geometry methods [36]. On the other hand, while in the region R_p of Fig. 2.8 there are equilibrium states for any value of T (e.g., see the purple line, corresponding to the isothermal $T = 1$), equilibrium states for negative temperatures (i.e. in the region R_n of Fig. 2.8) cannot exist. This peculiar feature of the DNLSE was first realized by B. Rumpf [37]. From a thermodynamic point of view, the presence of negative temperature states indicates that the entropy of a system is locally a decreasing function of the internal energy (quite an unusual thermodynamic scenario!). In a series of papers, Rumpf provided a solid theoretical argument that excludes the existence of negative temperature equilibrium states in the DNLSE [38–40]. More precisely, he showed that also in R_n the maximum entropy criterion for equilibrium implies that the system eventually evolves to a delocalized, incoherent background state at infinite temperature, superposed to a single breather that collects the "excess" of energy. This mechanism of relaxation to equilibrium by an energy collapse of a finite fraction of energy onto a single site is, on the other hand, counterintuitive, if not astonishing: it is reminiscent of the formation of a black hole in the Universe or of a vortex in a fluid. As it was already observed in [34], in the region R_n the energy density is sufficiently high to allow for the spontaneous formation of *breathers* through the well known dynamical mechanism of modulational instability. This mechanism appears when a nonlinear wave propagates in discrete space (the lattice of the DNLSE). For a suitable mathematical description see [41–43]. Here we prefer to illustrate it by an intuitive argument. Propagating nonlinear waves are typical dynamical structures of models like the DNLSE. In general, they propagate at different speed in points where they have different amplitude, like the sea waves that eventually fold onto themselves, before spreading. But sea waves are in a continuum medium (water), while nonlinear waves on a lattice are not allowed to fold, because lattice points have to maintain their original order. Accordingly, at some instant of time when the nonlinear wave would like to fold it occurs a shock wave (singularity) that concentrates a large fraction of wave amplitude (i.e., energy) onto a few lattice sites. This is the first step of the dynamical process yielding the formation of an exponentially localized time-periodic state, the so called *breather*.

The reason why the breather is periodic can be understood again by a simple argument. The concentration of a large amount of energy in a few sites essentially amounts to decouple these sites from the rest of the lattice, as one can easily infer from the very structure of Hamiltonian (2.10). In practice, the breather is a very close approximation to a single nonlinear oscillator located at some lattice site, very weakly interacting with the nearby sites (where its amplitude is exponentially small w.r.t. the site where it is localized). Since the single nonlinear oscillator is known to go through a periodic evolution (with an energy dependent period), the same holds for the breather. In a rigorous mathematical approach one can prove that breathers can be intended as continuation of a single oscillator solution to a lattice solution by methods based on the implicit function theorem. Their dynamical stability is guaranteed if their frequency is not resonant with those of linear lattice waves (for details see [44–47]).

Relaxation dynamics in the region of negative temperatures Studying these dynamical properties of the DNLSE equation demands numerical integration of Eq. (2.9) by suitable algorithms: in this case a Yoshida symplectic algorithm [48] is an appropriate choice, since it applies to non separable Hamiltonians, like (2.11). According to the argument by Rumpf [37–40], one should expect that, after having selected an initial condition in R_n, the dynamics should go through the formation of breathers that eventually merge into each other, thus relaxing to the equilibrium state, where the background obeys random phase statistical properties ($T = \infty$) and the energy excess is collected into a single *black hole*, as a result of a coarsening process among breathers. But this is not what the integration of the DNLSE equation tells us, as shown in Fig. 2.9.

In fact, if one takes a randomly seeded initial condition, where the number of particles is on average equally distributed on the lattice sites, with a sufficiently large amplitude to be located in R_n, dynamics produces spontaneously some breathers superposed to a radiation-like background. Breathers are not solitons, meaning that they are not conserved dynamical structures when they interact among themselves. *A fortiori* they go through inelastic collisions with the background waves. On the other hand, breathers typically form in lattice regions quite far from each other, so that their mutual interaction is practically negligible. In fact, they are quasi-static dynamical structures and their mobility is very much reduced with respect to the speed of sound of linear lattice waves. Accordingly, they can interact among themselves mainly through the background field (collisions among breathers cannot be excluded, but they are extremely rare events). On the other hand, a breather, due to its very nature of localized excitation, is on average weakly coupled to the background, the less the larger is its amplitude. It can be easily concluded that only large-deviation events driven by the background fluctuations can destabilize a breather and destroy it. This is what one can observe in Fig. 2.9, where breathers evolve before being eventually reabsorbed into the background. Their lifetime, that can be exceedingly long, depends on their amplitude. On the other hand, for a breather that disappears there is a new one that is spontaneously formed in another lattice region, in such a way that the average number of breathers in the lattice is kept practically constant. Numerical simulations show that this dynamical

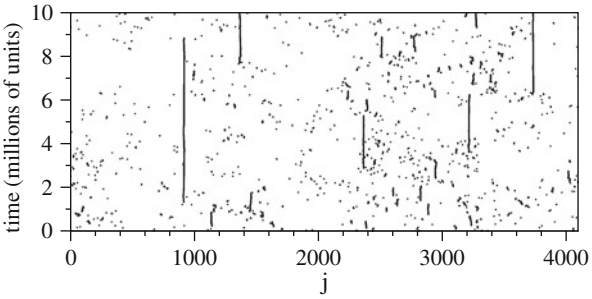

Fig. 2.9 Evolution in time of the local amplitude in a *negative temperature state* with $a = 1$ and $h = 2.4$. Notice that we are just above the line $h = 2a^2$ ($T = \infty$) in Fig. 2.8. The plot has been obtained by drawing a *black dot* at any lattice point n where the amplitude $|z_n|^2$ overtakes the threshold value 10, expressed in the adimensional units of the DNLSE model. The choice of this threshold value can be motivated on the basis of refined mathematical arguments (see [49]). In practice, a breather state is unambiguously signaled when the local amplitude overtakes this threshold value. The vertical scale in expressed in millions of proper time units of the model, thus indicating that there are breathers with very different lifetimes. On the other hand they keep on being destroyed and formed again, in such a way that there is an average number of localized solution at any time distributed all over the lattice. In this figure we are dealing with quite a large one, i.e. $N = 4{,}096 = 2^{12}$. This number has not been chosen by chance: using a chain length equal to a power of 2 allows to optimize the algorithm performances [48]

regime is still observed after $\mathcal{O}(10^7)$ proper time units (an intrinsic limit due to the maximum available computing resources for integrating a lattice made of $\mathcal{O}(10^3)$ sites). Notice that, if the same kind of initial conditions are used in R_p, the DNLSE chain is found to relax to thermodynamic equilibrium in $\mathcal{O}(10)$ proper time units. Very approximate analytic estimates indicate that the time needed to reach equilibrium in R_n could be astronomical even in a finite lattice [50]. The dynamical mechanisms yielding the formation of breathers and ruling their stability in practice keep the evolution far from the predicted equilibrium state, that is practically unreachable. The breaking of ergodicity is due to the very presence of breathers, that amount to localized periodic solution ("islands" in phase space) very weakly overlapping among themselves and with the surrounding "chaotic" sea, representing the background field. As discussed in the previous section for the FPU model, also in this case relaxation dynamics inhibits a fast equilibration. Anyway, in the DNLSE case, the ergodicity breaking effect is even more dramatic, since it is a genuine nonperturbative phenomenon, associated with the spontaneous formation of nonlinear excitations named *breathers*.

In this perspective, it should be pointed out that this is a phenomenon with relevant physical consequences. Actually, despite the dynamical regime observed in numerical simulations cannot be considered a genuine thermodynamic equilibrium state, nonetheless it exhibits robust statistical properties. In particular, if one measures the temperature of this *transient* states by formula (2.13), one finds that its time average converges to a negative value. Moreover, an energy fluctuation produced at any lattice point typically produces a breather state, rather than being

equally redistributed into the background field (as it happens in R_p). This definitely clarifies the peculiar scenario we are dealing with: the equilibrium state can emerge from a large-deviation event (the collapse of a macroscopic fraction of energy onto a single site), whose probability is practically zero, even over a time comparable with the age of the universe.

2.3 Ergodicity Breaking at Equilibrium

2.3.1 General Concepts

We have seen in the previous sections that the key idea behind ergodicity breaking in the dynamics is the existence of more that one equilibrium state (in the dynamic context the equilibrium states are defined as the average over a trajectory of time length going to infinity). Different equilibrium states may be obtained in the infinite time limit starting from different initial configurations. It is clear that the notion of ergodicity breaking is strictly tied to that of equilibrium state. In the dynamic approach systems with finite number of degrees of freedom may be non-ergodic. In the simplest case this non-ergodicity is due to the existence of conserved quantities, however we have already seen that this is not the only possible source of non ergodicity.

In this section we would like to discuss the precise definition of an equilibrium state not from a dynamical view point, but from a static viewpoint, i.e. in the framework of the standard ensembles of equilibrium thermodynamics. In other words we do not use the Boltzmann approach of averaging over the time, but we suppose that the dynamics has been such to carry the system in equilibrium configuration. We thus follow the Gibbs-Einstein approach of introducing a probability measure over the configurations, i.e. to consider an ensemble of configurations to which we associate the appropriate weigh [51, 52] (different options are the micro-canonical, the canonical and the grand-canonical ensemble).

Usually it is said that if the dynamics reaches the micro-canonical distribution at large times, the system is ergodic, so that the reader may wonder which kind of ergodicity breaking may be present in the micro-canonical (or in the canonical) ensemble. We shall see that the question is well posed and that ergodicity breaking in the ensemble approach is a rather subtle phenomenon that may be present only in the infinite volume limit and it is absent for systems with a finite number of degrees of freedom.

Indeed in this approach the breaking of ergodicity in the equilibrium ensemble is associated to the coexistence of more than one equilibrium phase of the system and to first order phase transitions. We shall see later that this conventional view point reflects only part of the reality and in glassy systems we may have coexistence of many equilibrium phases in absence of a first order phase transition.

In the case of a finite system the microcanonical or the canonical ensembles are obviously well defined (in most of the cases) and they are clearly unique. We assume

(as usually happens) that the two ensembles become equivalent for large enough systems and in the following we will consider mostly the case of the canonical ensemble:

$$\rho_G(A) \equiv \langle A(C)\rangle_G = \int d\mu(C)A(C)\,, \quad d\mu(C) = Z(\beta)^{-1}\exp(-\beta H(C))d(C)\,, \tag{2.14}$$

where C is a generic configuration of the system and the partition function ($Z(\beta)$) is such that $\int d\mu(C) = 1$. The previous equation defines the Gibbs state ρ_G.

Things become more complex in the infinite volume systems. In order to study what happens in the infinite volume limit there are two complementary approaches:

- We consider the infinite volume system as a limit of finite volume systems.
- We consider directly the infinite volume system.

We will discuss both approaches in the following.

2.3.2 The Gibbs States

The study of the infinite volume limit contains many subtle points also if we consider the simplest cases, bounded Hamiltonians with a finite range interaction. In this case it is quite simple to prove that the free energy density is well defined [51, 52], unfortunately the situation is much more complex if we consider the limiting behavior of the probability distribution of the configurations and of the expectation values of the observables.

Crucial phenomena as phase transitions are present only in the infinite volume limit: we would like to control this limit in details; the issues at stakes are quite subtle: some of the key mechanisms that lead to phase transitions where discovered after the second world war. Here we will only discuss some of the general principles without studying the models where the phenomena we describe are realized.

We clarify here the language we use and we give a few mathematical definitions in order to be precise.

The first point we have to address is the definition of a state of a system. We could use either a probabilistic language or a more algebraic setting; we choose the second possibility because we find it more elegant. We prefer to use this algebraic approach also because the notion of a state can be easily extended to an infinite system, while we cannot naively define a probability distribution over infinite configurations.

The reader should notice that the word *state* is often used in mathematics, with different underlying meanings; we will use the following definition [53–58]. Let $\mathscr{A}$ be the algebra of observables.[21] An example of this algebra in spin models are the

[21] In classical statistical mechanics it is an Abelian algebra with identity while it would be a non-Abelian algebra in the quantum case.

functions of a finite number of spins. We say that a linear functional ρ over the algebra $\mathscr{A}$ is a state if for all elements (A) of the algebra:

$$A \geq 0 \Rightarrow \rho(A) \geq 0, \quad ||\rho|| = 1\,, \tag{2.15}$$

where this second condition (the norm of ρ is one) is equivalent to $\rho(A = 1) = 1$. Sometimes we will use the standard notation of statistical mechanics:

$$\rho(A) = \langle A \rangle_\rho\,. \tag{2.16}$$

To any finite volume state we can associate a normalized probability distribution of the configurations: it associates to any function its expectation value. The advantage of this algebraic setting is that positive linear functionals on algebras are extremely well studied and many mathematical results are available. Moreover the whole approach translates immediately to statistical quantum mechanics, where quantum phenomena like Bose-Einstein condensation cannot so easily be dealt in a probabilistic approach.

Let us start to discuss a physical implementation: we consider a system in D dimension in a box of size Λ and we assume that each of the D coordinates of the particles (or of the spins) are in the interval $[-\Lambda/2 : \Lambda/2]$. The free energy density f is given by

$$-\beta f = \lim_{\Lambda \to \infty} \Lambda^{-D} \log(Z_\Lambda)\,, \tag{2.17}$$

where the partition function Z_Λ is computed using an Hamiltonian H_Λ that depends only on the degrees of freedom inside the box (with some appropriate boundary conditions, e.g. periodic boundary conditions, open boundary conditions, fixed boundary conditions).

We say that a sequence of states ρ_k of increasing size Λ_k ($\lim_{k\to\infty} \Lambda_k = \infty$) converges to ρ if

$$\lim_{k \to \infty} \rho_k(A) = \rho(A)\,, \tag{2.18}$$

for all observables that depend only on degrees of freedom inside a box of fixed arbitrary size R.

In the nutshell we fix an arbitrary box of size R and we ask that the observables inside the box do not depend on Λ_k in the limit where $\Lambda_k \to \infty$ (obviously this construction is possible only for $\Lambda_k > R$ and this happens for large k). In other words we impose some kind of weak topology on the space of states[22]: the crucial point is that A does not depend on k.

[22]The experienced reader may ask why we have introduced the extra length R that may seems to be unnecessary. One would be tempted to assume that the volume average in the box of side Λ_k of the observable should become k independent for large k. This simpler formulation does not have problems as far the expectation values of the observables are space independent. In the most

The existence of a limit for the state when the volume goes to infinity (i.e. $k \to \infty$) is less evident than the existence of a limit for the free energy.

We could assume (or prove, if we are smart enough) that the limit in Eq. (2.18) exists and in this way we could define an infinite volume equilibrium state. However this construction may be non-unique. When we consider finite volume systems we should specify the boundary conditions (e.g. periodic, free, fixed) and the result may depend on the choice of these boundary conditions. Moreover there is no warranty that the sequence of states ρ_k converges to something. In many case, using compactness arguments (i.e. generalizations of the Bolzano-Weierstrass theorem), we could prove that there is a subsequence of the k's such that the ρ_k have a limit [57], but the limit may depend on the subsequence (as we shall see later in an explicit example).

Let us neglect all these problems: we consider only one kind of boundary condition (e.g. periodic) and we assume that we are lucky enough that the infinite volume limit is well defined (as it happens in the ferromagnetic Ising model at positive temperature). In this way we arrive to define in an unique way the infinite volume Gibbs state ρ_G.

The introduction of the notion of pure states in statistical physics has the main goal, as we said before, to allow a clear definition of ergodicity breaking. As we shall see later in more details a crucial notion is the one of *clustering*: a state is called clustering if connected correlation functions (defined below) computed in such state go to zero at large distance. There exist plenty of systems where the previously defined infinite volume Gibbs state has the unwanted property that its correlation functions do not satisfy the clustering properties [51, 53, 58].

Physical consistency requires that, when a system is in a given phase, intensive quantities do not fluctuate: this is possible only if correlation functions are clustering. Moreover the equilibrium linear response theorem tells us that the response to a small external perturbation is proportional to the appropriate connected correlation function. If the connected correlation functions do not vanish at large distance a small perturbation would propagate to the whole system and this is unphysical.

Let us discuss in details ergodicity breaking in this context. We will see that there are two phenomena (i.e. clustering and purity) that are related.

2.3.2.1 Clustering and Purity

Connected correlation functions play a crucial role in equilibrium statistical mechanics [51, 53]: in the case of two observables we have:

$$\langle AB \rangle_c \equiv \langle AB \rangle - \langle A \rangle \langle B \rangle \,. \tag{2.19}$$

general case where no (even approximate) translational invariance is present we have better to stick to the formulation we use in the main text.

Connected correlations functions should be familiar to the reader as far the linear response theorem relates the connected correlation functions to the response function. It is natural to require that the connected correlation functions vanishes at large distance: for example in spin systems

$$\lim_{x\to\infty} \langle \sigma(x)\sigma(y)\rangle_c = 0 \tag{2.20}$$

This *clustering* requirement corresponds to ask that the variance of intensive quantities (e.g. the average of the spins in a box) goes to zero when the size of the box goes to infinity. On the contrary, if connected correlation functions would not go to zero, the integrated response to local perturbation would propagate to the whole space and this is an unphysical result.

A state that satisfies the clustering condition is called a clustering state. As we have already remarked the Gibbs state may be not a clustering state. A possible way to find clustering states (i.e. states that have a physical interpretation) is based on the idea that a non-clustering state can be interpreted as the linear combination of two clustering state. From the mathematical view point this procedure corresponds to decompose a non-clustering state as a sum (or an integral) of clustering states. We shall see now how it can be done starting from a simple example.

A popular example of a system, where this decomposition is possible, is given by a ferromagnetic system at zero external magnetic field in the low temperature region, where a spontaneous magnetization is present.

When a spontaneous magnetization is present (e.g. 0.5) the typical configurations can be of the following types:

- The proportion of spins that are positive is definitely greater than 50 % (i.e. 75 %) and the probability of negative spins is definitively less than 50 % (i.e. 75 %).
- We have the opposite situation with positive and negative spins interchanged.

Configurations where positive spins are around 50 % of the total number is possible, but their probability is exponentially small when the volume goes to infinity.

If we call p_+ and p_- respectively the probability of positive or negative spins ($p_+ + p_- = 1$), we find that in this state the expectation value of the magnetization is $m = p_+ - p_-$. In this situation a spontaneous magnetization m is present (we could also have a state of magnetization equal to $-m$).

We can compute the correlation function and we have for x not near to y (i.e. for $x - y$ large):

$$\langle \sigma(x)\rangle_G = 0\,, \quad \langle \sigma(x)\sigma(y)\rangle_G \approx m^2\,. \tag{2.21}$$

The resulting infinite volume Gibbs state will be a statistical mixture of two clustering states having positive or negative magnetization. We can write

$$\rho_G = \frac{1}{2}\rho_+ + \frac{1}{2}\rho_-\,, \quad \rho(\sigma(x))_\pm \equiv \langle \sigma(x)\rangle_\pm = \pm m\,, \tag{2.22}$$

Here it is possible to prove that these two states with given magnetization are clustering.

This decomposition of the Gibbs state into two or more clustering states is the simplest example of ergodicity breaking in equilibrium setting and it corresponds to the existence of two or more equilibrium phases.

Sometimes in the literature the words *clustering* and *ergodic* are used with the same meaning. We can understand the reason if we come back to the dynamics evolution described in the previous section: it is easy to see that if we consider the evolution of a non ergodic system in time, the time correlation functions are not clustering. Let us consider a system with a dynamics such that the quantity $A(t)$ is conserved. If we consider an ensemble of trajectories having the same initial value for $A(0)$ it is evident that

$$\langle A(t) = A(0) \rangle \,, \qquad \langle A(t)A(t') \rangle = A(0)^2 \,, \quad \langle A(t)A(t') \rangle_c = 0 \,. \tag{2.23}$$

If the initial probability distribution is not concentrated at only one value of A and we have a non trivial distribution of A at the initial time $P(A)$ we find that the

$$\langle A(t)A(t') \rangle_c = \langle A(t)A(t') \rangle - \langle A(t) \rangle \langle A(t') \rangle = \langle A^2(0) \rangle - \langle A(0) \rangle^2 \neq 0 \,. \tag{2.24}$$

A general analysis may be done much more deeply in the case of translational invariant systems. We can introduce the concept of purity of a state [54–56]. A state in a given set is pure if it cannot be written as linear combination with positive weight of different states in the same set. More precisely, if the state ρ is pure and the w's are positive,

$$\rho = w_1 \rho_1 + w_2 \rho_1 \tag{2.25}$$

implies that $\rho = \rho_1 = \rho_2$.

In the case of a finite system the canonical state is not pure: e.g. it is the integral of microcanonical states. Indeed for a finite system we have that

$$\langle A \rangle_\beta^c = \frac{\int dE \exp(-\beta E + S(E)) \langle A \rangle_E^{\mu c}}{\int dE \exp(-\beta E + S(E))} \,, \tag{2.26}$$

where the superscript c and μc denote respectively the canonical and the microcanonical distribution and E and $S(E)$ are respectively the total energy and the total entropy. The previous equation can be written as

$$\rho_\beta^c = \frac{\int dE \exp(-\beta E + S(E)) \rho_E^{\mu c}}{\int dE \exp(-\beta E + S(E))} \,. \tag{2.27}$$

In the infinite volume limit the situation changes (e.g. microcanonical states with a finite difference of total energy becomes identical) and the previous formula collapses to

$$\rho_\beta^c = \rho_{e(\beta)}^{\mu c} \,, \tag{2.28}$$

where $\rho_e^{\mu c}$ is the microcanonical state as function of the energy *density* e and $e(\beta)$ is an appropriate function.

In the case of translational invariant systems a classical result implies that if we consider the space of translational invariant states the condition of purity coincides with clustering. Now the Aloaglu theorem [59,60] tells us that a state can be written in an unique way as linear combination of pure states (that for this reason are also called extreme states). The conclusion is that we can write in full generality the relation

$$\rho_G = \int d\nu(\lambda)\rho_\lambda \,, \tag{2.29}$$

where $d\nu(\lambda)$ is a measure over the pure clustering states that are label by λ.

2.3.2.2 The Gibbs Rule

It should have not escaped to the reader that the phenomenon of spontaneous magnetization in ferromagnets is present only in zero magnetic field. When constant *non-zero* external magnetic field h is present, one of the two magnetizations are selected depending on the sign of the magnetic field. A non-zero external magnetic field lifts the degeneracy between these two states. However we obtain two different results in the limit of zero magnetic field depending on the sign of the magnetic field:

$$\rho_\pm = \lim_{h \to 0^\pm} \rho(h) \,. \tag{2.30}$$

Therefore we could have avoided the decomposition into clustering states and considered only what happens at non zero magnetic field. At the end we perform the limit of zero magnetic field only *after* the infinite volume limit [61].

This observation may be formalized by considering a system with an Hamiltonian that depends on some parameters p that belong to a vector space. If we neglect continuous symmetries, under some technical hypothesis on the differentiability in the Banach space of all interactions (whose physical meaning is not clear) it can be proved that for a generic choice of the parameters p the Gibbs states is clustering [62].

More detailed results can be proved in this approach. Let us suppose that for some choice of the parameters two different states are obtained depending on the direction (in the space of Hamiltonians) from which we reach these points and two different phases coexist. These points form a manifold of codimension one in the space of Hamiltionians. If there are points where three different phases coexist (e.g. the triple point where gas liquid and solid coexist) they form a manifold of codimension two. Generally speaking the $n + 1$ phases may be present only on a manifold of

codimension n, i.e. we must impose n conditions (one for each additional phase). This is essentially the well known Gibbs rule for phase coexistence that is valid in most of the common situations.

2.3.3 The Local DRL Equilibrium States

The previous discussion is based on approaching the infinite volume system as a sequence of finite volume systems. However it would be interesting to discuss the whole question directly for the infinite volume system.

The problem of dealing with an actual infinite system is that the Hamiltonian is infinite and that Eq. (2.18) does not make senses. We have to find a different way to say that our state ρ is a Gibbs distribution. Dobrushin, Lanford and Ruelle (DRL) [63] have proposed the following condition for a system with finite range interaction. Let us divide the systems in three space regions, a first one(that we call S), such that the space is partitioned in two other region: the interior of S (I) and its exterior E: S is essentially the boundary of a finite region (I). Only E is infinite; S and I are finite. The region S is thick enough that there is no direct interaction among the interior and the exterior. The DLR condition requires that

$$P(C_I|C_S) \propto \exp\left(-\beta H(C_I, C_S)\right) , \tag{2.31}$$

where $P(C_I|C_S)$ is the probability of an interior configuration (C_I) conditioned to the surface configuration (C_S) and $H(C_I, C_S)$ is the part of the Hamiltonian that depends only on the interior configuration (it is defined apart from an irrelevant additive constant).

If the condition (2.31) is satisfied for any region S the state is a local (DRL) equilibrium state. It is trivial to verify that the previously constructed Gibbs state is a DLR state so this notion extends the concept of Gibbs state directly to the infinite volume system.

Since we are able now to consider the set of all possible DLR states (a convex set), it would be natural to find the extreme points of this set (i.e. the pure states according to Aloaglu theorem) and to identify them as possible phases of the system. This is a very nice definition of state, unfortunately it is non-constructive, because in the general case we do not know to construct all the DLR states. We can mimic the discussion in the previous section and look for clustering DLR states. A general theorem tell us that, if we consider the set of translational invariant DLR states, clustering states and pure states do coincide [59, 60]: this results makes us very happy.

It would be natural to conjecture that in the general case clustering DLR states and pure DRL states do coincide. However such an intuitive results is not established. It is likely that we should put some extra conditions. The most physically relevant situation is the case of random systems with a translational

invariant probability distribution of the quenched disorder (e.g. impurities in semiconductors). Here each realization of the disorder is not invariant under translation, however the ensemble is invariant. Unfortunately also in this situation it is not clear if the notions of clustering DRL states and pure states do coincide.

2.3.3.1 Some Considerations on Random Systems

We will give now an example of a situation where the Boltzmann-Gibbs distribution does not have a limit when the volume diverges. We consider a ferromagnetic Ising model with a small random magnetic field at low temperature in three dimensions.

The heuristic analysis goes as follows. In a finite box of size L there are two relevant finite volume states, the one with positive magnetization and the one with negative magnetization. In a first approximation, valid at small field and temperature, the difference in free energy of the two states is proportional to $2\sum_i h_i$, which is a number of order $L^{3/2}$. Therefore (with the exception of rare choices of the random field) for a given value of L only one state dominates. However, when increasing L, there will be an infinite number of values of L where we will go from the situation where the magnetization is positive to a situation where the magnetization is negative (and viceversa). The magnetization itself does not have a limit when the volume goes to infinity.[23]

A definite limit may be obtained by taking the limit by subsequences, i.e. choosing only those value of L for which the magnetization is positive. A different limit is obtained if we choose only those value of L for which the magnetization is negative.

Once the infinite volume limit has been taken we can decompose the state into extremal DLR states. Here the typical relevant states for the infinite volume limit are those with positive or negative magnetization. If we choose the first approach (limit by appropriate subsequences) we will find a pure state that is a clustering state.

Similar and more complex phenomena are frequent both in random and in non-random system (e.g. those having quasi-periodic or chaotic ground states). In these case a special care is needed in order to obtain the infinite volume limit. When the naive infinite volume limit does not exist, it is often said the system has a chaotic dependence on the volume. Sometimes in discussing the infinite volume limit one use the metastate construction described in [57], although other different approaches are possible [58, 64], however a presentation of these approaches would take too much space; the interested reader should look to the original papers.

[23]The limit may not exist also in non-random systems: the simplest example is a two dimensional Ising model that is ferromagnetic in the y direction (with periodic boundary conditions) and antiferromagnetic in the x direction with fixed boundary conditions (positive at the left and negative on the right). It is possible to check that at low temperatures two different states are obtained in the infinite L limit, depending on the parity of L.

2.4 Glassy System

It has been suggested that glassy systems (spin glasses, structural glasses, colloids...) may have many equilibrium states, also in a situation where there is no first order phase transition. These systems are characterized by an extremely slow approach to the infinite volume limit. On phenomenological ground we can conjecture that this extreme slowness is due to the existence of many states and to the large amount of time needed to jump from one state to another. This old observation is strongly supported by the discovery that infinite many states do exist in the corresponding mean field models, where analytic and rigorous results have been obtained.

These states are very different on a microscopical level, however they look quite similar as far as most of the intensive quantities are concerned. The coexistence of many states for generic values of the parameters is a complete violation of the Gibbs rule. A careful analysis has showed that this is possible only if some identities (that sometimes go under the name of stochastic stability) are valid [65–67]: they are extremely powerful and they can be used to arrive at a general classification of the structure of these states.

In this situation the approach described in the previous section may be non-optimal [57]. The mathematical construction is quite heavy and the number of equilibrium states is quite likely an uncountable number. In order to bypass this difficulty it is convenient to consider the finite volume pure states that will be described in the next section.

2.4.1 A Heuristic Construction: Finite Volume States

We have seen that the construction of infinite volume pure states is thorny. We find convenient to introduce the heuristic concept of *pure states in a finite volume* [58]. This concept is crystal clear from a physical point of view. However it can be difficult to state it in a rigorous way (i.e. to prove existence theorems) mostly because the notion of finite volume pure states (or phases) is deeply conditioned by the physical properties of the system under consideration. In order to prove theorems on finite volume pure states one needs a very strong rigorous command of the physical properties of finite, large statistical systems. We stress that we will use the concepts of finite volume states only as tools to interpret formulae that are mathematically well defined.

Most of the research in mathematical physics has been devoted to the study of the pure states of an infinite system. Unfortunately the concept of pure states of an infinite system may be too rigid to capture all the statistical properties of a finite system: here we need, as we will see later, more sophisticated tools, i.e. finite volume pure states. We stress that the finite volume pure states we introduce here

are mathematically *very different* from the pure states for an infinite system that are normally used in the literature.[24]

Let us see how approximate pure states or phases in a large but *finite* system can be defined, using a definition of state that is different from the usual one that we have seen for non-random systems. We will give only a rough definition that concentrates more on the physics of the system. Our strategy is to mimic the definition of pure states of an infinite system and to apply it to the physical relevant situation of a finite (and large) system (which is the only one accessible by numerical simulations and by experiments).

We consider a system in a box of linear size L, containing a total of N spins. We partition the configuration space[25] into regions (lumps in the notation of Talagrand [68]), labeled by α, and we define averages restricted to these regions [58]: *these regions will correspond to our finite volume pure states or phases*. It is clear that in order to produce something useful we have to impose sensible constraints on the form of these partitions.

We require that the restricted averages on these regions are such that connected correlation functions are small[26] at large distance x. In the case of a ferromagnet the two regions are defined by considering the sign of the total magnetization. The first region includes configurations with a positive total magnetization, the second region selects configurations with a negative total magnetization. There are ambiguities for those configurations that have exactly zero total magnetization, but the probability that such a configuration can occur is exponentially small at low temperature.[27]

Physical intuition tells us that this decomposition exists (at least for familiar systems), otherwise it would make no sense to speak about the spontaneous magnetization of a ferromagnetic sample, or to declare that a finite amount of water (at the melting point) is in the solid or liquid state. Moreover all numerical simulations gather data that are based on these kinds of notions, since the systems that we can store in a computer are always finite. The concept of finite volume states is preeminent from the physical point of view: infinite volume states are mainly an attempt to capture their properties in an amenable mathematical setting. This decomposition of a finite but large system into phases makes sense, although its translation in a rigorous mathematical setting has not been done (also because

[24] It is very easy to arrive to contradictions if one does not make a clear distinction between these two different concepts.

[25] In the Ising case the configuration space contains 2^N points.

[26] The precise definition of *small at large distance* in a finite volume system can be phrased in many different ways. For example we can introduce a function $g(x)$ which goes to zero when x goes to infinity and require that the connected correlation functions evaluated in a given phase are smaller than $g(x)$. Of course the function $g(x)$ should be carefully chosen in order to avoid to give trivial results; one should also prove the independence of the results from the choice of g in a given class of functions.

[27] The probability distribution in a finite volume pure state is not the Gibbs one: the DLR relations, which tell us that the probability distribution is locally a Gibbs distribution, are violated, but the violation should go to zero in the large volume limit.

working in the infinite volume setting is much simpler, and in most cases informative enough).

According to the previous discussion the *finite* volume Gibbs measure can be decomposed in a sum of such finite volume pure states. The states of the system are labeled by α: we can write

$$\langle A\rangle_G = \sum_\alpha w_\alpha \langle A\rangle_\alpha \equiv \sum_\alpha w_\alpha A_\alpha \,, \tag{2.32}$$

with the normalization condition

$$\sum_\alpha w_\alpha = 1 \,. \tag{2.33}$$

Things become more interesting if we consider quantities that depend on two configurations (let us call them σ and τ). In the case of spin systems a well studied quantity is the overlap between two configurations [69, 70]:

$$q(\sigma,\tau) = \frac{1}{N}\sum_{i=1,N} \sigma_i \tau_i \,. \tag{2.34}$$

If there would be only one state we would have that for large systems, neglecting correlations,

$$\langle q\rangle = \frac{1}{N}\sum_{i=1,N} m_i^2 \,, \quad \langle q^2\rangle \approx \langle q\rangle^2 \,. \tag{2.35}$$

In the presence of many states we would have

$$\langle q\rangle = \sum_{\alpha,\beta} w_\alpha w_\beta q_{\alpha,\beta} \quad , \quad \langle q^2\rangle \approx \sum_{\alpha,\beta} w_\alpha w_\beta q^2_{\alpha,\beta} \,, \tag{2.36}$$

where

$$q_{\alpha,\beta} = \frac{1}{N}\sum_{i=1,N} m_i^\alpha m_i^\beta \,, \quad m_i^\alpha \equiv \langle \sigma_i\rangle_\alpha \,. \tag{2.37}$$

The interesting case is when

$$\mathrm{Var}(q) \equiv \langle q^2\rangle - \langle q\rangle^2 \neq 0 \,. \tag{2.38}$$

In presence of an unique infinite volume states intensive quantities like q do not fluctuate. If $\mathrm{Var}(q) \neq 0$ the one state picture cannot be correct. We can interpret this result using the finite volume pure state approach and from the previous formulae we get

$$\mathrm{Var}(q) \approx \sum_{\alpha,\beta} w_\alpha w_\beta \left(q_{\alpha,\beta} - \langle q \rangle\right)^2 . \tag{2.39}$$

Similar arguments can be presented for the probability distribution of q that should be equal to

$$P(q) \approx \sum_{\alpha,\beta} w_\alpha w_\beta \delta(q_{\alpha,\beta} - q) . \tag{2.40}$$

If we take care of the correlations inside a single state we find that a better approximation would be to substitute the δ function with a smooth function of very small width (vanishing when the volume goes to infinity).[28]

2.4.2 The Case of Many States

It is interesting to note that in usual situations in Statistical Mechanics the classification into phases is not very rich. For usual materials, in the generic case, there is only one phase: such a classification is not very interesting. In slightly more interesting cases (e.g. symmetry breaking) there may be two states. For example, if we consider the configurations of a large number of water molecules at 0°, we can classify them as water or ice: here there are two states. In slightly more complex cases, if we tune carefully a few external parameters like the pressure or the magnetic field, we may have coexistence of three or more phases (a tricritical or multicritical point).

In all these cases the classification is simple and the number of states is small as a consequence of the Gibbs rule. On the contrary, in the mean field theory of some glassy systems the number of states is very large (it goes to infinity with N), and a very interesting nested classification of states is possible [69]. We stress that this behavior implies that the Gibbs rule is not valid in these cases. We have seen that Gibbs rule states that in order to have coexistence of $n + 1$ phases we must tune n parameters. Here no parameters are tuned and the number of coexisting phases is infinite! This is possible only if some conditions are satisfied: they are the Ghirlanda-Guerra identities and their generalizations (that sometimes are called stochastic stability) [58, 65–67].

2.4.2.1 Stochastic Stability

If we consider a generic random system, there are general identities that are valid almost everywhere in Hamiltonian space: they have been proved firstly in a mean

[28] This refinement is not crucial in the infinite volume limit.

field setting and later on generalized to some short range realistic models: it is reasonable to conjecture that they are valid in general (in some cases they have been proved [71]). These identities have remarkable consequences.

In order to decide if an ensemble of systems with Hamiltonian H is stochastically stable, we have to consider the free energy of an auxiliary system with the following Hamiltonian:

$$H + \varepsilon H_R \,, \tag{2.41}$$

where ε is a small parameter and H_R is a random Hamiltonian, i.e. is a generic element in an appropriate set of random Hamiltonians.

The interesting quantity is the dependence of the free energy density ($f(\varepsilon)$) on the parameter ε after we average over the different choices of H_R. If the average free energy $f(\varepsilon)$ is a differentiable function of ε (and the limit where the volume goes to infinity commutes with the derivative with respect to ε) the system is *stochastically stable*. In the nutshell, stochastic stability tells us that the Hamiltonian H does not has any special features and that its properties are analogous to those of similar random systems (H may contain quenched random disorder). These conditions are the opposite of the situation described in the Gibbs rule where a perturbation induces a first order transition. The requirement that in presence of many states a random perturbation does *not* induce a first order transition is a very strong one.

Let us give a very simple example of the Ghirlanda-Guerra identities. Let us consider a random system where the random coupling are indicated by J and by an overline the average over J. For each realization of the system we can compute the probability distribution $P_J(q)$ and consider its ensemble average

$$P(q) = \overline{P_J(q)} \,. \tag{2.42}$$

The function $P(q)$ usually has a smooth limit when the volume goes to infinity (i.e. $P^\infty(q)$), in contrast with the individual $P_J(q)$ that may have a strong volume dependence.

We are interested to know how much the function $P_J(q)$ fluctuates from system to system. In the case where

$$P_J(q) \approx P^\infty(q) = \delta(q - q^*) \tag{2.43}$$

the answer is trivial (i.e. no fluctuations), so that the interesting case is when $P^\infty(q)$ is not a single delta function. A first information of the fluctuation is encoded in the function

$$P^\infty_{1,2,3,4}(q_{1,2}, q_{3,4}) = \lim_{N\to\infty} \overline{P_J(q_{1,2})\, P_J(q_{3,4})} \,. \tag{2.44}$$

The Girlanda-Guerra identities tell us that $P^\infty_{1,2,3,4}$ is not an arbitrary function, but it is given by

$$P^{\infty}_{1,2,3,4}(q_{1,2}, q_{3,4}) = \left(\frac{2}{3} + \frac{1}{3}\delta(q_{1,2} - q_{3,4})\right) P^{\infty}(q_{1,2}) P^{\infty}(q_{3,4}) \,. \tag{2.45}$$

Of course we are assuming that all these functions have a limit when the volume goes to infinity.

Stochastic stability is a very strong property. Many properties can be derived from stochastic stability. Maybe, the most extraordinary one is ultrametricity [69]. For a given system we can consider three equilibrium configuration and we can define the corresponding overlaps. Let us order the configurations in such a way that $q_{1,2} \geq q_{1,3} \geq q_{2,3}$ The system is ultrametric if the probability of finding

$$q_{1,3} \neq q_{2,3} \tag{2.46}$$

is equal to zero.

For a certain time it was believed that stochastic stability could be an independent property from ultrametricity, however there have been recently many papers suggesting the contrary, and this line of research culminated in the general proof of Panchenko that stochastic stability *does* imply ultrametricity [72].

At the end of the game we find the following surprising result. In the case where the function $P_J(q)$ fluctuates when we change the parameters of the system, we can define its functional probability distribution $\mathscr{P}[P]$. This functional order parameter is a description of the probability of $P_J(q)$ when we change the disorder.[29] The functional probability distribution $\mathscr{P}[P]$ is an object that should have an infinite volume limit, i.e. $\mathscr{P}^{\infty}[P]$.

In general the functional probability distribution $\mathscr{P}^{\infty}[P]$ tell us many important information on the structure of states in the infinite volume limit. If stochastic stability is satisfied it is relatively easy to prove [73] that the functional probability distribution $\mathscr{P}^{\infty}[P]$ has it support on functions $P(q)$ of the form

$$P(q) = \sum_{s} c_s \delta(q - q_s) \,. \tag{2.47}$$

with $\sum_s c_s = 1$. Much more work is needed to prove that the distribution $\mathscr{P}^{\infty}[P]$ has it support on functions $P(q)$ of the form

$$P(q) = \sum_{\alpha,\beta} w_\alpha w_\beta \delta(q_{\alpha,\beta} - q) \,, \tag{2.48}$$

where the probability distribution of the $q_{\alpha,\beta}$'s and the w_α's has an explicit form that can be computed from the knowledge of $P^{\infty}(q)$. Explicit formulae can be written,

[29] It may be possible that also for non-random systems we have a similar description where the average over the number of degrees of freedom plays the same role of the average over the disorder.

but they are too complex to be discussed here (they can be generated using Ruelle probability cascade [74]).

We have seen that there are systems where the structure of ergodicity breaking that is quite different from the conventional one; in these systems the Gibbs rule is not valid and it is substituted by its antithesis, the stochastic stability identities. It is conjectured that this is the situation in the case of glassy systems both for random and non-random systems. One can prove that this alternative scenario is present in many mean field models [69, 75]. It is quite possible that the same scenario holds also in the finite dimensional case (and in particular for some three dimensional systems). Rigorous theorems for the moment are still lacking, however there is plenty of numerical evidence (and also some experimental indications) that this pattern of ergodicity breaking is realized in some finite dimensional glassy systems like spin glasses [76,77] and structural glasses [78]. Recent very large scale simulations [76, 77] show that the predictions of this approach do agree very well for three-dimensional Ising spin glasses at zero magnetic field.

References

1. L. Boltzmann, *Vorlesungen über Gastheorie* (Barth, Leipzig 1898). English translation: *Lectures on Gas Theory* (University of California Press, 1966)
2. G.E. Uhlenbeck, G.W. Ford, *Lectures in Statistical Mechanics* (American Mathematical Society, Providence, 1963)
3. G. Gallavotti, E.G.D. Cohen, Phys. Rev. Lett. **74**, 2694 (1995); G. Gallavotti, E.G.D. Cohen, J. Stat. Phys. **80**, 931 (1995)
4. I.P. Cornfeld, S.V. Fomin, Ya. G. Sinai, *Ergodic Theory* (Springer, Berlin, 1982)
5. Ya. G. Sinai, Doklady Akad. Nauk SSSR **153**, 1261 (1963). [English version: Sov. Math Dokl. **4**, 1818 (1963)]
6. Ya. G. Sinai, Russ. Math. Surv. **25**, 137 (1970)
7. A.I. Khinchin, *Mathematical Foundations of Statistical Mechanics* (Dover, New York 1949; translated from Russian)
8. E. Fermi, Phys. Zeits. **24**, 261 (1923)
9. H. Poincaré, *Les Méthodes Nouvelles de la Méchanique Céleste*, vol. 1 (Gautier–Villars, Paris, 1892)
10. E. Fermi, J. Pasta, S. Ulam, Los-Alamos internal report, Document LA-1940 (1955)
11. E. Fermi, J. Pasta, S. Ulam, in *Enrico Fermi Collected Papers*, vol. II (The University of Chicago Press/Accademia Nazionale dei Lincei, Chicago/Roma, 1965), pp. 977–988
12. N.J. Zabusky, M.D. Kruskal, Phys. Rev. Lett. **15**, 240 (1965)
13. J. Tuck, M.T. Menzel, Adv. Math. **9**, 399 (1972)
14. F.M. Izrailev, B.V. Chirikov, Sov. Phys. Dokl. **11**, 30 (1966)
15. E. Fucito, F. Marchesoni, E. Marinari, G. Parisi, L. Peliti, S. Ruffo, A. Vulpiani, J. Phys. **43**, 707 (1982)
16. R. Livi, M. Pettini, S. Ruffo, M. Sparpaglione, A. Vulpiani, Phys. Rev. A **28**, 3544 (1983)
17. E.E. Ferguson, H. Flashka, D.W. McLaughlin, J. Comput. Phys. **45**, 157 (1982)
18. Chaos focus issue: *The "Fermi-Pasta-Ulam" problem—the first 50 years*. Chaos **15**, 015104 (2005)
19. G. Gallavotti (Ed.): *The Fermi-Pasta-Ulam Problem: A Status Report*. Lecture Notes in Physics, vol. 728 (Springer, Berlin/Heidelberg, 2008)

20. G. Benettin, H. Christodoulidi, A. Ponno, The Fermi-Pasta-Ulam problem and its underlying integrable dynamics. J. Stat. Phys. **144**, 793 (2001)
21. L. Berchialla, L. Galgani, A. Giorgilli, DCDS-A **11**, 855 (2004)
22. L. Berchialla, A. Giorgilli, S. Paleari, Phys. Lett. A **321**, 167 (2004)
23. G. Benettin, R. Livi, A. Ponno, J. Stat. Phys. **135**, 873 (2009)
24. G. Benettin, A. Ponno, J. Stat. Phys. **144**, 793 (2011)
25. M. Hénon, Phys. Rev. B **9**, 1921 (1974)
26. H. Flaschka, Phys. Rev. B **9**, 1924 (1974)
27. G. Benettin, G. Gradenigo, Chaos **18**, 013112 (2008)
28. J. Eilbeck, P. Lomdahl, A. Scott, Physica D **16**, 318 (1985)
29. P.G. Kevrekidis, *The Discrete Nonlinear Schrödinger Equation* (Springer, Berlin 2009)
30. A. Scott, *Nonlinear Science: Emergence and Dynamics of Coherent Structures* (Oxford University Press, Oxford, 2003)
31. A.M. Kosevich, M.A.J. Mamalui, Exp. Theor. Phys. **95**, 777 (2002)
32. G. Tsironis, D. Hennig, Phys. Rep. **307**, 333 (1999)
33. R. Franzosi, R. Livi, G. Oppo, A. Politi, Nonlinearity **24**, R89 (2011)
34. K. Rasmussen, T. Cretegny, P. Kevrekidis, N. Gronbech-Jensen, Phys. Rev. Lett. **84**, 3740 (2000)
35. S. Iubini, S. Lepri, A. Politi, Phys. Rev. E **86**, 011108 (2012)
36. R. Franzosi, J. Stat. Phys. **143**, 824 (2011)
37. B. Rumpf, Phys. Rev. E **69**, 016618 (2004)
38. B. Rumpf, Europhys. Lett. **78**, 26001 (2007)
39. B. Rumpf, Phys. Rev. E **77**, 036606 (2008)
40. B. Rumpf, Physica D **238**, 2067 (2009)
41. A.M. Morgante, M. Johansson, G. Kopidakis, S. Aubry, Physica D **162**, 53 (2002)
42. I. Daumont, T. Dauxois, M. Peyrard, Nonlinearity **10**, 617 (1997)
43. J. Carr, J.C. Eilbeck, Phys. Lett. A **109**, 201 (1985)
44. A.J. Sievers, S. Takeno, Phys. Rev. Lett. **61**, 970 (1988)
45. R.S. MacKay, S. Aubry, Nonlinearity **7**, 1623 (1994)
46. S. Flach, C.R. Willis, Phys. Rep. **295**, 181 (1998)
47. J.C. Eilbeck, M. Johansson, in *Localization and Energy Transfer in Nonlinear Systems*, ed. by L. Vazquez, R.S. MacKay, M.P. Zorzano (World Scientific, Singapore, 2003), p. 44 and references therein
48. H. Yoshida, Phys. Lett. A **150**, 262 (1990)
49. S. Iubini, R. Franzosi, R. Livi, G.-L. Oppo, A. Politi, New J. Phys. **15**, 023032 (2013)
50. M. Johansson, K.O. Rasmussen, Phys. Rev. E **70**, 066610 (2004)
51. See any book of Statistical Mechanics, e.g. G. Parisi, *Statistical Field Theory* (Perseus Books, New York, 1998)
52. M. Aizenman, S. Goldstein, J.L. Lebowitz, Comm. Math. Phys. **62**, 279 (1978)
53. D. Ruelle, *Statistical Mechanics* (Benjamin, New York, 1969)
54. R. Haag, D. Kastler, J. Math. Phys. **5**, 848 (1964)
55. D. Kastler, D.W. Robinson, Comm. Math. Phys. **3**, 151 (1966)
56. H.O. Georgii *Gibbs Measures and Phase Transitions* (de Gruyter Studies in Mathematics, Berlin, 1988)
57. C.M. Newman, D.L. Stein, Phys. Rev. E **55**, 5194 (1997)
58. E. Marinari, G. Parisi, F. Ricci-Tersenghi, J.J. Ruiz-Lorenzo, F. Zuliani, J. Stat. Phys. **98**, 973 (2000)
59. D. Ruelle, *Rigorous Results: Statistical Mechanics* (World Scientific, River Edge, 1999)
60. O. Bratteli, D.W. Robinson, *Operator Algebras and Quantum Statistical Mechanics/ C*-and W*-Algebras, Symmetry Groups, Decomposition of States* (Springer, Heidelberg, 2003)
61. D. Ruelle, Ann. Phys. **69**, 364 (1972)
62. D. Ruelle, Comm. Math. Phys. **53**, 195 (1977)
63. O.E. Lanford, D. Ruelle, Comm. Math. Phys. **13**, 194 (1969); R.L. Dobrushin, Theor. Probab. Appl. **15**, 458–486 (1970)

64. M. Aizenman, J. Wehr, Phys. Rev. Lett. **62**, 2503 (1989); Comm. Math. Phys. **130**, 489 (1990)
65. S. Ghirlanda, F. Guerra, J. Phys. A **31**, 9149 (1998)
66. M. Aizenman, P. Contucci, J. Stat. Phys. **92**, 765 (1998)
67. G. Parisi, arXiv:cond-mat/9801081 (1998, preprint)
68. M. Talagrand, Prob. Theory Rel. Fields **117**, 303 (2000)
69. M. Mézard, G. Parisi, M.A. Virasoro, *Spin Glass Theory and Beyond* (World Scientific, Singapore, 1987)
70. G. Parisi, The overlap in glassy systems, arXiv:cond-mat/1310807, preprint, in *Stealing the Gold: A Celebration of the Pioneering Physics of Sam Edwards* ed. by P.M. Goldbart, N. Goldenfeld, D. Sherrington (Oxford University Press, Oxford, 2005)
71. P. Contucci, C. Giardina, Ann. Henri Poincare **6**, 915 (2005); J. Stat. Phys. **126**, 917 (2007)
72. D. Panchenko, Ann. Prob. **41**, 1315 (2013); *The Sherrington-Kirkpatrick Model* (Springer, New York, 2013)
73. G. Parisi, M. Talagrand, Comp. Rend. Math. **339**, 303 (2004)
74. D. Ruelle, Comm. Math. Phys. **108**, 225 (1987)
75. T.R. Kirkpatrick, D. Thirumalai, P.G. Wolynes, Phys. Rev. A **40**, 1045 (1989)
76. R. Banos et al., J. Stat. Mech. P06026 (2010)
77. R. Banos et al., Phys. Rev. Lett. **105**, 177202 (2010)
78. P.G. Wolynes, V. Lubchenko, *Structural Glasses and Supercooled Liquids: Theory, Experiment, and Applications* (Wiley, Hoboken, 2012)

Chapter 3
Large Deviations in Stationary States, Especially Nonequilibrium

Giovanni Jona-Lasinio

Abstract Over the last 10 years, in collaboration with L. Bertini, A. De Sole, D. Gabrielli and C. Landim, we developed a general approach to nonequilibrium diffusive systems known as *Macroscopic Fluctuation Theory*. Our theory has been inspired by stochastic models of interacting particles (stochastic lattice gases). It is based on the study of rare fluctuations of macroscopic variables in stationary states and is applicable to a wide class of systems. The present overview emphasizes the main ideas and provides a guide to the literature including contributions from other authors.

3.1 Introduction

Since the first attempts to construct a nonequilibrium thermodynamics, a guiding idea has been that of local equilibrium. This means the following. Locally on the macroscopic scale it is possible to define thermodynamic variables like density, temperature, chemical potentials. . . which vary smoothly on the same scale. Microscopically this implies that the system reaches local equilibrium in a time which is short compared to the times typical of macroscopic evolutions as described for example by hydrodynamic equations. So what characterizes situations in which this description applies is a separation of scales both in space and time.

The simplest nonequilibrium states one can imagine are stationary states of systems in contact with different reservoirs and/or under the action of external fields. In such cases there are currents (electrical, heat, matter of various chemical constitutions . . .) through the system whose macroscopic behavior is encoded in transport coefficients like the diffusion coefficient, the conductivity or the mobility.

G. Jona-Lasinio (✉)
Dipartimento di Fisica and INFN, Universit'a di Roma Sapienza, Piazzale Aldo Moro 5, Rome, I-00185, Italy
e-mail: gianni.jona@roma1.infn.it

A. Vulpiani et al. (eds.), *Large Deviations in Physics*, Lecture Notes in Physics 885,
DOI 10.1007/978-3-642-54251-0_3,

The ideal would be to approach the study of these states starting from a microscopic model of atoms interacting with realistic forces and evolving with Newtonian dynamics. This is beyond the reach of present day mathematical tools and much simpler models have to be adopted in the reasonable hope that some essential features are adequately captured.

In the last decades stochastic lattice gases have provided a very useful laboratory for studying properties of stationary nonequilibrium states (SNS). Besides many interesting results specific to the different models considered, the following features of general significance have emerged.

1. Local equilibrium and hydrodynamic equations have been derived rigorously from the microscopic dynamics for a wide class of stochastic models.
2. A definition of nonequilibrium thermodynamic functionals has emerged via a theory of dynamic large fluctuations, moreover a general equation which they have to satisfy has been established [5]. This is a time independent Hamilton-Jacobi (H-J) equation whose independent arguments are the local thermodynamic variables and requires as input the transport coefficients. These coefficients can be either calculated explicitly for given models or obtained from measurements so that H-J can be used also as a phenomenological equation.
3. Nonequilibrium long range correlations have been observed experimentally in various types of fluids [27]. In our simplified models mathematically they appear to be a generic consequence of H-J [5, 11] and their origin can be traced back to the violation of time reversal invariance [10].
4. The analysis of large fluctuations of thermodynamic variables, e.g. the density, has shown that phase transitions exist far from equilibrium that are not possible in equilibrium. In particular this has been demonstrated in the case of the weakly asymmetric exclusion process which macroscopically is described by a viscous Burgers equation [12].
5. An analysis of the fluctuations of the currents averaged over long times has revealed the possibility of different dynamical regimes, which are interpreted as dynamical phase transitions in which translational invariance in time is spontaneously broken. Such phase transitions have actually been proved to exist in some well known models [7, 9].

As we shall see the results we are referring to are a consequence of a basic large deviation formula describing, when the number of degrees of freedom tend to infinity, the joint fluctuations of the density and the current. This approach is now known as *Macroscopic Fluctuation Theory* [4, 5] which can be considered as a more refined form of fluctuating hydrodynamics. As a general comment we may say that this theory goes beyond the theory developed long ago by Onsager [43] and by Onsager-Machlup [44], to which it reduces for states close to equilibrium. This statement will be made more precise in the following.

The topics discussed are dispersed through several papers and the present article may serve as a guide to the literature.

3.2 Assumptions

We introduce in this section some general assumptions for the macroscopic description of out of equilibrium driven diffusive systems which are characterized by conservation laws. For simplicity of notation, we restrict to the case of a single conservation law, e.g. the conservation of the mass described locally by a density ρ. The system is in contact with boundary reservoirs, characterized by their chemical potential λ, and under the action of an external field E. We denote by $\Lambda \subset \mathbb{R}^d$ the bounded region occupied by the system, by x the macroscopic space coordinates and by t the macroscopic time. We shall consider also the case in which λ and E depend explicitly on the time t.

In the sequel we shall use the same letter ρ both for space-time dependent paths $\rho(t, x)$ and time independent profiles $\rho(x)$. When it is necessary to emphasize the time dependence we shall write $\rho(t)$ omitting the x dependence.

1. The macroscopic state is completely described by the local density $\rho(t, x)$ and the associated current $j(t, x)$.
2. The macroscopic evolution is given by the continuity equation together with the constitutive equation which express the current as a function of the density. Namely,

$$\begin{cases} \partial_t \rho(t) + \nabla \cdot j(t) = 0, \\ j(t) = J(t, \rho(t)), \end{cases} \tag{3.1}$$

   where we omit the explicit dependence on the space variable $x \in \Lambda$. For driven diffusive systems the constitutive equation takes the form

$$J(t, \rho) = -D(\rho)\nabla\rho + \chi(\rho)\, E(t) \tag{3.2}$$

   where the *diffusion coefficient* $D(\rho)$ and the *mobility* $\chi(\rho)$ are $d \times d$ positive matrices.
3. The transport coefficients D and χ satisfy the local Einstein relation

$$D(\rho) = \chi(\rho)\, f''(\rho), \tag{3.3}$$

   where f is the equilibrium free energy per unit of volume which is a local function of ρ.
4. The Eqs. (3.1) and (3.2) have to be supplemented by the appropriate boundary condition on $\partial\Lambda$ due to the interaction with the external reservoirs. If $\lambda(t, x)$, $x \in \partial\Lambda$, is the chemical potential of the external reservoirs, this boundary condition reads

$$f'\big(\rho(t, x)\big) = \lambda(t, x), \qquad x \in \partial\Lambda. \tag{3.4}$$

We can now make more precise in what sense our setting goes beyond Onsager's near equilibrium theory. Our systems may admit nonlinear hydrodynamic equations. In second place we can consider states far from equilibrium: take as an example a one dimensional system in contact with two reservoirs at the boundaries characterized by the chemical potentials λ_1, λ_2. Near equilibrium means that $|\lambda_1 - \lambda_2|$ is small. In our theory we do not have any restriction.

In the case of stochastic microscopic models with time independent driving, the above macroscopic description is derived in the diffusive scaling limit [5, 9, 23, 36, 50]. The extension to time dependent driving does not present special problems.

Given time-independent chemical potential $\lambda(x)$ and external field $E(x)$, we denote by $\bar{\rho}_{\lambda,E}$ the stationary solution of (3.1)–(3.4),

$$\begin{cases} \nabla \cdot J(\bar{\rho}) = \nabla \cdot \Big(- D(\bar{\rho}) \nabla \bar{\rho} + \chi(\bar{\rho})\, E \Big) = 0, & x \in \Lambda, \\ f'(\bar{\rho}(x)) = \lambda(x), & x \in \partial\Lambda. \end{cases} \tag{3.5}$$

Observe that if the field E is gradient, $E = \nabla U$, and if it is possible to choose the arbitrary constant in the definition of U such that $U(x) = \lambda(x)$, $x \in \partial\Lambda$, then the stationary solution satisfies $f'\big(\bar{\rho}_{\lambda,E}(x)\big) = U(x)$ and the stationary current vanishes, $J(\bar{\rho}_{\lambda,E}) = 0$. Conversely, given any profile $\bar{\rho}(x)$ it is possible to choose $\lambda(x)$ and $E(x)$ so that $\bar{\rho}$ solves (3.5) and moreover $J(\bar{\rho}) = 0$. It is indeed enough to set $\lambda(x) = f'(\bar{\rho}(x))$, $x \in \partial\Lambda$, and $E(x) = \nabla f'(\bar{\rho}(x))$, $x \in \Lambda$. Therefore in general equilibrium states in presence of boundary conditions and external fields are inhomogeneous.

3.3 The Fundamental Formula

We first suppose that the boundary conditions and the external field do not depend on time. A large part of this paper discusses the consequences of the following formula, first derived in [7,9], describing the joint fluctuations of the density and the current in a thermodynamic system obeying the equations of the previous section. Given trajectories $\rho(t,u)$ for the density and $j(t,u)$ for the current, up to a prefactor according to the macroscopic fluctuation theory we have

$$\mathbb{P}\big(\rho(t,u), j(t,u), \ \ t \in [0,T]\big) \sim \exp\{-\epsilon^{-d} \beta \mathscr{G}_{[0,T]}(\rho, j)\} \tag{3.6}$$

Here $\mathbb{P}$ is the stationary probability measure, ϵ the ratio between the microscopic length scale (say the typical intermolecular distance) and the macroscopic one. The temperature β in the following will be kept constant and equal to 1.

$$\mathscr{G}_{[0,T]}(\rho, j) = \begin{cases} V(\rho(0)) + \mathscr{I}_{[0,T]}(j) \text{ if } \partial_t \rho + \nabla \cdot j = 0 \\ +\infty \qquad\qquad\qquad\quad \text{otherwise} \end{cases} \tag{3.7}$$

$V(\rho)$ is the large deviation functional of the invariant measure and provides the probability of the initial condition $\rho(0)$. We shall refer to it as the *quasi potential*. The other term, which determines the probability of the chosen trajectory, is given by

$$\mathscr{I}_{[0,T]}(j) \;=\; \frac{1}{4}\int_0^T dt\,\big\langle [j(t)-J(\rho(t))],\, \chi(\rho(t))^{-1}[j(t)-J(\rho(t))]\big\rangle \tag{3.8}$$

where $J(\rho) = -D(\rho)\nabla\rho + \chi(\rho)E$ and $\langle , \rangle$ means space integration.

A heuristic derivation of the above formula for a lattice gas in the case of a fixed initial configuration can be given as follows. The basic microscopic model is given by a stochastic lattice gas with a weak external field and particle reservoirs at the boundary. More precisely, let $\Lambda \subset \mathbb{R}^d$ be a smooth domain and set $\Lambda_N = N\Lambda \cap \mathbb{Z}^d$; we consider a Markov process on the state space X^{Λ_N}, where X is a subset of $\mathbb{N}$, e.g. $X = \{0, 1\}$ when an exclusion principle is imposed. The number of particles at the site $i \in \Lambda_N$ is denoted by $\eta_i \in X$ and the whole configuration by $\eta \in X^{\Lambda_N}$. The dynamical evolution is given by a continuous time Markov process on the state space X^{Λ_N}. This is specified by transition rates $c_{i,j}(\eta)$ describing the jump of a particle from a site i to its nearest neighbor j and rates $c_i^{\pm}(\eta)$ describing the appearance or loss of a particle at the boundary site i. The reservoirs are characterized by a chemical potential λ. We assume that the rates satisfy the local detailed balance condition [10] with respect to a Gibbs measure associated to some Hamiltonian $\mathscr{H}$. Typically, for a nonequilibrium model, we can consider Λ the cube of side one and the system under a constant force E/N. Moreover we choose the chemical potential λ so that $\lambda(j/N) = \lambda_0$ if the first coordinate of j is 0, $\lambda(j/N) = \lambda_1$ if the first coordinate of j is N, and impose periodic boundary conditions in the other directions.

To define the current denote by $\mathscr{N}_t^{i,j}$ the number of particles that jumped from i to j in the macroscopic time interval $[0, t]$. At the boundary we adopt the convention that $\mathscr{N}_t^{i,j}$ represents the number of particles created at j due to the reservoir at i if $i \notin \Lambda_N$, $j \in \Lambda_N$ and that $\mathscr{N}_t^{i,j}$ represents the number of particles that left the system at i by jumping to j if $i \in \Lambda_N$, $j \notin \Lambda_N$. The difference $J_t^{i,j} = \mathscr{N}_t^{i,j} - \mathscr{N}_t^{j,i}$ is the net number of particles flown across the bond $\{i, j\}$ in the time interval $[0, t]$. In other words, given a path $\eta(s)$, $0 \le s \le t$, the instantaneous current $dJ_t^{i,j}/dt$ is a sum of δ–functions localized at the jump times across the bond $\{i, j\}$ with weight $+1$, respectively -1, if a particle jumps from i to j, respectively from j to i.

We now define the empirical current density

$$j^N(t,x) = \frac{1}{N^{d+1}}\sum_{k=1}^{d}\sum_i \delta(x - i/N)\,\frac{dJ_t}{dt}^{i,i+e_k} \tag{3.9}$$

Fix a current profile $j(t, x)$ and an initial configuration η^N; in order to make $j(t, x)$ typical, we introduce an external field F. Let ρ be the solution of

$$\begin{cases} \partial_t \rho + \nabla \cdot j = 0 \\ \rho(0,x) = \rho_0(x) \end{cases} \tag{3.10}$$

and $F : [0,T] \times \Lambda \to \mathbb{R}^d$ be the vector field such that

$$\begin{aligned} j &= J(\rho) + \chi(\rho)F \\ &= -\frac{1}{2} D(\rho)\nabla\rho + \chi(\rho)\{\nabla H + F\} \end{aligned}$$

We introduce a perturbed measure $\mathbb{P}^{N,F}_{\eta^N}$ which is obtained by modifying the rates as follows

$$c^F_{i,j}(\eta) \;=\; c_{i,j}(\eta)\, e^{N^{-1}F(t,i/N)\cdot(j-i)}$$

One can show by a direct calculation for which we refer to [9] that

$$\begin{aligned} \frac{d\mathbb{P}^N_{\eta^N}}{d\mathbb{P}^{N,F}_{\eta^N}} &\sim \exp\Big\{ - N^d \frac{1}{2} \int_0^T dt\, \langle F, \chi(\rho) F\rangle \Big\} \\ &= \exp\big\{ - N^d \mathscr{I}_{[0,T]}(j) \big\} \end{aligned}$$

Moreover, under $\mathbb{P}^{N,F}_{\eta^N}$, as $N \to \infty$, $j^N(t,x)$ converges to $j(t,x)$. Therefore,

$$\begin{aligned} &\mathbb{P}^N_{\eta^N}\Big(j^N(t,x) \approx j(t,x), \quad (t,u) \in [0,T] \times \Lambda \Big) \\ &= \mathbb{E}^{N,F}_{\eta^N}\Big(\frac{d\mathbb{P}^N_{\eta^N}}{d\mathbb{P}^{N,F}_{\eta^N}}\; \mathbb{1}_{\{j^N \approx j\}} \Big) \sim e^{-N^d \mathscr{I}_{[0,T]}(j)} \end{aligned}$$

where $\mathbb{E}^{N,F}_{\eta^N}$ denotes expectation with respect to the perturbed probability measure $\mathbb{P}^{N,F}_{\eta^N}$. Introducing now the empirical density

$$\pi^N(u) = \frac{1}{N^d} \sum_{x \in \Lambda_N} \delta(u - x/N)\eta_x$$

we can write the fundamental formula (3.6) in the more precise form

$$\mathbb{P}\big(\pi^N \approx \rho(t,u),\, j^N \approx j(t,u), \quad t \in [0,T]\big) \sim \exp\{-N^d \beta \mathscr{G}_{[0,T]}(\rho, j)\} \tag{3.11}$$

We emphasize that we need to allow general non–gradient external fields F. On the other hand for the large deviation principle of the density it is sufficient to

consider gradient external fields. The latter is therefore a special case and can be recovered from (3.6) and (3.7) as we will now show.

The large deviation functional for the trajectories of the density can be obtained by projection. We fix a path $\rho = \rho(t,x)$, $(t,x) \in [0,T] \times \Lambda$. There are many possible trajectories $j = j(t,x)$, differing by divergence free vector fields, such that the continuity equation is satisfied. By minimizing $\mathscr{I}_{[0,T]}(\rho, j)$ over all such paths j

$$I_{[0,T]}(\rho) = \inf_{\substack{j: \\ \nabla\cdot j = -\partial_t \rho}} \mathscr{I}_{[0,T]}(j) \tag{3.12}$$

Let F be the external field which generates the current j according to

$$j = -D(\rho)\nabla\rho + \chi(\rho)(E+F)\ .$$

and minimize with respect to F. We show that the infimum above is obtained when the external perturbation F is a gradient vector field whose potential H solves

$$\partial_t \rho = \nabla\cdot\Big(D(\rho)\nabla\rho - \chi(\rho)\big[E + \nabla H\big]\Big) \tag{3.13}$$

which is a Poisson equation for H.

Write

$$F = \nabla H + \tilde{F} \tag{3.14}$$

Using (3.13) we get

$$\mathscr{I}_{[0,T]}(j) = \frac{1}{4}\int_0^T dt\,\Big\{\langle \nabla H, \chi(\rho)\nabla H\rangle + \langle \tilde{F}, \chi(\rho)\tilde{F}\rangle\Big\}$$

Therefore the infimum is obtained when $\tilde{F} = 0$. Then $I_{[0,T]}(\rho)$ can be written

$$I_{[0,T]}(\rho) = \frac{1}{4}\int_0^T dt\,\big\langle \nabla H(t), \chi(\rho(t))\nabla H(t)\big\rangle \tag{3.15}$$

$$= \frac{1}{4}\int_{T_1}^{T_2} dt\,\Big\langle \big[\partial_t\rho + \nabla\cdot J(\rho)\big]\, K(\rho)^{-1}\big[\partial_t\rho + \nabla\cdot J(\rho)\big]\Big\rangle$$

where the positive operator $K(\hat{\rho})$ is defined on functions $u : \Lambda \to \mathbb{R}$ vanishing at the boundary $\partial\Lambda$ by $K(\hat{\rho})u = -\nabla\cdot\big(\chi(\hat{\rho})\nabla u\big)$. Compare (3.15) with the large deviation functional of Freidlin-Wentzell theory [29].

3.4 Time Reversal and Its Consequences

To the time reversed process corresponds the adjoint generator with respect to the invariant measure. Let us define the operator inverting the time of a trajectory $[\theta f](t) = f(-t)$ for f scalar and $[\theta j](t) = -j(-t)$ for the current. The stationary adjoint process, that we denote by $\mathbb{P}^{N,a}_{\mu^N}$, is the time reversal of $\mathbb{P}^N_{\mu^N}$, i.e. we have $\mathbb{P}^{N,a}_{\mu^N} = \mathbb{P}^N_{\mu^N} \circ \vartheta^{-1}$. Then at the level of large deviations we have

$$\begin{aligned} &\mathbb{P}^N_{\mu^N}\Big(\pi^N \approx \rho,\ j^N \approx j \quad t \in [-T,T]\Big) \\ &= \mathbb{P}^{N,a}_{\mu^N}\Big(\pi^N \approx \vartheta\rho,\ j^N \approx \vartheta j \quad t \in [-T,T]\Big) \end{aligned} \tag{3.16}$$

which implies

$$\mathscr{G}_{[-T,T]}(\rho, j) = \mathscr{G}^a_{[-T,T]}(\vartheta\rho, \vartheta j) \tag{3.17}$$

where $\mathscr{G}^a_{[-T,T]}$ is the large deviation functional for the adjoint process.

The previous relationship has far reaching consequences. By dividing both sides by $2T$ and taking the limit $T \to 0$ we find

$$\begin{aligned} -\Big\langle \frac{\delta V}{\delta\rho}, \nabla\cdot j\Big\rangle &= -\big\langle J(\rho) + J^a(\rho), \chi(\rho)^{-1} j\big\rangle \\ &+\frac{1}{2}\big\langle J(\rho) + J^a(\rho), \chi(\rho)^{-1}[J(\rho) - J^a(\rho)]\big\rangle \end{aligned} \tag{3.18}$$

which has to be satisfied for any ρ and j. Integrating by parts the left hand side we obtain

$$J(\rho) + J^a(\rho) = -2\chi(\rho)\nabla\frac{\delta V}{\delta\rho} \tag{3.19}$$

$$\big\langle J(\rho), \chi(\rho)^{-1} J(\rho)\big\rangle = \big\langle J^a(\rho), \chi(\rho)^{-1} J^a(\rho)\big\rangle \tag{3.20}$$

The first of these equations is a fluctuation-dissipation relation for the current which inserted into the second gives the equation for the quasi potential V

$$\Big\langle \nabla\frac{\delta V}{\delta\rho}, \chi(\rho)\nabla\frac{\delta V}{\delta\rho}\Big\rangle - \Big\langle \frac{\delta V}{\delta\rho}, \nabla\cdot J(\rho)\Big\rangle = 0 \tag{3.21}$$

This is the Hamilton-Jacobi equation associated to the following variational characterization of V

$$V(\rho) = \inf_{\substack{\rho:\, \rho(-\infty)=\bar\rho \\ \rho(0)=\rho}} I_{[-\infty,0]}(\rho) \tag{3.22}$$

This characterization follows by considering the functional I as an action functional in the variables ρ and $\partial_t \rho$ and performing a Legendre transform. The associated Hamiltonian is

$$\mathscr{H}(\rho, \pi) = \left\langle \nabla\pi \cdot \chi(\rho)\nabla\pi \right\rangle + \left\langle \nabla\pi \cdot J(\rho) \right\rangle \tag{3.23}$$

where π is the conjugate momentum.

Consider a trajectory connecting the density profiles ρ_{t_1} and ρ_{t_2}. From time reversal we have

$$V(\rho_{t_1}) + I_{[t_1,t_2]}(\rho) = V(\rho_{t_2}) + I^a_{[-t_2,-t_1]}(\theta\rho) \tag{3.24}$$

By taking $\rho_{t_1} = \bar{\rho}$, which implies $V(\rho_{t_1}) = 0$, $\rho_{t_2} = \rho$, the inf over all possible trajectories and time intervals we obtain the variational expression of V with the minimizer defined by

$$I^a_{[-\infty,0]}(\theta\rho) = 0 \tag{3.25}$$

that is $\theta\rho$ must be a solution of the adjoint hydrodynamics. The adjoint hydrodynamics follows immediately recalling the relationship between J and J^a

$$J^a(\rho) = -2\chi(\rho)\nabla\frac{\delta V}{\delta\rho} - J(\rho)$$

We have

$$\partial_t \rho + \nabla J^a = \partial_t \rho + \nabla\{D(\rho)\nabla\rho - \chi(\rho)(E + 2\nabla\frac{\delta V}{\delta\rho})\} = 0 \tag{3.26}$$

The minimizer is therefore the time reversal of the relaxation solution of this equation connecting ρ to $\bar{\rho}$. The optimal field to create the fluctuation is $F = 2\nabla\frac{\delta V}{\delta\rho}$, that is minus twice the dissipative thermodynamic force.

From the Hamilton-Jacobi equations it follows that the hydrodynamic equations for the process and its adjoint can be written respectively

$$\partial_t \rho = \nabla \cdot \left(\chi(\rho)\nabla\frac{\delta V}{\delta\rho}\right) + \mathscr{A}(\rho) \tag{3.27}$$

$$\partial_t \rho = \nabla \cdot \left(\chi(\rho)\nabla\frac{\delta V}{\delta\rho}\right) - \mathscr{A}(\rho) \tag{3.28}$$

This can be seen as follows. Decompose the current $J(\rho)$

$$J(\rho) = J_{\mathrm{S}}(\rho) + J_{\mathrm{A}}(\rho), \tag{3.29}$$

with

$$J_{\mathrm{S}}(\rho) = -\chi(\rho)\,\nabla\frac{\delta V_{\lambda,E}(\rho)}{\delta\rho} \tag{3.30}$$

and $J_{\mathrm{A}}(\rho) = J(\rho) - J_{\mathrm{S}}(\rho)$. The Hamilton-Jacobi equation implies that for every ρ

$$\int_{\Lambda} dx\; J_{\mathrm{S}}(\rho)\cdot\chi(\rho)^{-1}J_{\mathrm{A}}(\rho) = 0\;. \tag{3.31}$$

From (3.19)

$$J^{a}(\rho) = J_{\mathrm{S}}(\rho) - J_{\mathrm{A}}(\rho) \tag{3.32}$$

The orthogonality condition for the currents implies also

$$\left\langle \frac{\delta V}{\delta\rho}\,,\,\mathscr{A}(\rho)\right\rangle = 0$$

with $\mathscr{A}(\rho) = -\nabla J_{\mathrm{A}}$.

We shall refer to $J_{\mathrm{S}}(\rho)$ as the *symmetric* current and to $J_{\mathrm{A}}(\rho)$ as the *antisymmetric* current. This terminology refers to symmetric and antisymmetric part of the underlying Markovian microscopic dynamics [5,6,9]. More precisely, the generator of the evolution can be decomposed into a symmetric and an antisymmetric part which are respectively even and odd under time reversal. We emphasize that the decomposition (3.29) depends non trivially on $\lambda\,, E\,$.

3.5 Long Range Correlations

We are concerned only with *macroscopic correlations* which are a generic feature of nonequilibrium models. Microscopic correlations which decay as a summable power law disappear at the macroscopic level.

We introduce the *pressure* functional as the Legendre transform of the quasi-potential V

$$G(h) = \sup_{\rho}\left\{\langle h\rho\rangle - V(\rho)\right\}$$

By Legendre duality we have the change of variable formulae $h = \frac{\delta V}{\delta\rho}$, $\rho = \frac{\delta G}{\delta h}$, so that the Hamilton-Jacobi equation can then be rewritten in terms of G as

$$\left\langle \nabla h\cdot\chi\Big(\frac{\delta G}{\delta h}\Big)\nabla h\right\rangle + \left\langle \nabla h\cdot J\Big(\frac{\delta G}{\delta h}\Big)\right\rangle = 0 \tag{3.33}$$

where h vanishes at the boundary of Λ. As for equilibrium systems, G is the generating functional of the correlation functions.

We define

$$C_n(x_1, \ldots, x_n) = \frac{\delta^n G}{\delta h(x_1) \cdots \delta h(x_n)} \Big|_{h=0} \tag{3.34}$$

By expanding (3.33) around the stationary state and writing the pair correlation function in the form

$$C(x, y) = C_{\text{eq}}(x)\delta(x - y) + B(x, y)$$

where

$$C_{\text{eq}}(x) = D^{-1}(\bar{\rho}(x))\chi(\bar{\rho}(x))$$

we obtain the following equation for B

$$\mathscr{L}^\dagger B(x, y) = \alpha(x)\delta(x - y) \tag{3.35}$$

where $\mathscr{L}^\dagger$ is the formal adjoint of the elliptic operator $\mathscr{L} = L_x + L_y$ given by, using the usual convention that repeated indices are summed,

$$L_x = D_{ij}(\bar{\rho}(x))\partial_{x_i}\partial_{x_j} + \chi'_{ij}(\bar{\rho}(x))E_j(x)\partial_{x_i} \tag{3.36}$$

and

$$\alpha(x) = \partial_{x_i}\left[\chi'_{ij}\big(\bar{\rho}(x)\big)\, D^{-1}_{jk}\big(\bar{\rho}(x)\big)\bar{J}_k(x)\right]$$

where $\bar{J} = J(\bar{\rho}) = -D(\bar{\rho}(x))\nabla\bar{\rho}(x) + \chi(\bar{\rho}(x))E(x)$ is the macroscopic current in the stationary profile. Therefore if $\alpha(x)$ is non-vanishing the inhomogenous equation (3.35) has a non trivial solution and long range correlations are present. The existence of such correlations in lattice gases and in particular in the symmetric simple exclusion process was first established, using fluctuating hydrodynamics, in [49]. Remark that χ independent of ρ implies $\alpha = 0$. Equations for the correlation functions of any order have been derived in [11].

3.6 Fluctuations of the Current and Dynamical Phase Transitions

Currents involve time in their definition so it is natural to consider space-time thermodynamics. According to our fundamental formula the *cost functional* to produce a current trajectory $j(t, x)$ is

$$\mathscr{I}_{[0,T]}(j) \;=\; \frac{1}{4}\int_0^T dt\,\big\langle [j(t)-J(\rho(t))],\, \chi(\rho(t))^{-1}[j(t)-J(\rho(t))]\big\rangle \tag{3.37}$$

in which we recall that $J(\rho) = -D(\rho)\nabla\rho + \chi(\rho)E$. where $\rho = \rho(t,u)$ is obtained by solving the continuity equation $\partial_t\rho + \nabla\cdot j = 0$.

Among the many problems we can discuss within this theory, the fluctuations of the time average of the current $\mathscr{J}_N$ over a large time interval have been analysed [7, 9]. Let $J(x)$ be the time average of $j(t,x)$ that we assume divergence free, i.e.

$$J(x) = \frac{1}{T}\int_0^T j(x,t)dt \tag{3.38}$$

In [15] Bodineau and Derrida addressed this problem in one space dimension by postulating an "*additivity principle*" which relates the fluctuation of the time averaged current in the whole system to the fluctuations in subsystems. However their approach does not always apply. In fact the probability of observing a given divergence free time averaged fluctuation J can be described by a functional $\Phi(J)$ which we characterize, in any dimension, in terms of a variational problem for the functional $\mathscr{I}_{[0,T]}$

$$\Phi(J) = \lim_{T\to\infty}\;\inf_j \frac{1}{T}\,\mathscr{I}_{[0,T]}(j)\;, \tag{3.39}$$

where the infimum is carried over all paths $j = j(t,u)$ having time average J. The static additivity principle postulated in [15] gives the correct answer only under additional hypotheses which are not always satisfied.

Let us denote by U the functional obtained by restricting the infimum in (3.39) to divergence free current paths j, i.e.

$$U(J) = \inf_\rho \frac{1}{4}\big\langle [J-J(\rho)],\, \chi(\rho)^{-1}[J-J(\rho)]\big\rangle, \tag{3.40}$$

where the infimum is carried out over all the density profiles $\rho = \rho(u)$ satisfying the appropriate boundary conditions. From (3.39) and (3.40) it follows that $\Phi \le U$. In one space dimension the functional U is the one introduced in [15]. While Φ is always convex the functional U may be non convex. In such a case $U(J)$ underestimates the probability of the fluctuation J. In [7, 9] we interpreted the lack of convexity of U, and more generally the strict inequality $\Phi < U$, as the occurrence of a dynamical phase transition.

There are cases in which $\Phi = U$. Sufficient conditions on the transport coefficients D, χ for the coincidence of Φ and U can be given [9]. Consider the case when the matrices $D(\rho)$ and $\chi(\rho)$ are multiples of the identity, i.e., there are strictly positive scalar functions still denoted by $D(\rho)$, $\chi(\rho)$, so that $D(\rho)_{i,j} = D(\rho)\delta_{i,j}$, $\chi(\rho)_{i,j} = \chi(\rho)\delta_{i,j}$, $i,j = 1,\dots,d$. Let us first consider the case with no external field, i.e. $E = 0$; if

$$D(\rho)\chi''(\rho) \le D'(\rho)\chi'(\rho), \quad \text{for any } \rho, \tag{3.41}$$

where $'$ denotes the derivative, then $\Phi = U$. In this case U is necessarily convex. Moreover if

$$D(\rho)\chi''(\rho) = D'(\rho)\chi'(\rho), \quad \text{for any } \rho, \tag{3.42}$$

then we have $\Phi = U$ for any external field E.

To exemplify situations in which $\Phi < U$ consider the fluctuations of the time averaged current for periodic boundary conditions. Two models have been discussed so far. The Kipnis–Marchioro-Presutti (KMP) model [8, 37], which is defined by a harmonic chain with random exchange of energy between neighboring oscillators, and the exclusion process. In the case of the KMP model we have $U(J) = (1/4)J^2/\chi(m) = (1/4)J^2/m^2$, where m is the (conserved) total energy. For J large enough, $\Phi(J) < U(J)$. This inequality is obtained by constructing a suitable travelling wave current path whose cost is less than $U(J)$ [9]. A similar result has been obtained by Bodineau and Derrida [16] for the periodic simple exclusion process with external field. For the KMP process this phenomenon is rather striking as it occurs even in equilibrium, i.e. without external field. This result has been verified in numerical simulations which provide an estimate of the critical J_c at which the transition takes place [33].

The behavior of $\mathscr{I}$ and Φ under time reversal shows that Φ satisfies a fluctuation relationship akin to the Gallavotti-Cohen theorem for the entropy production [30]. The anti-symmetric part of Φ is equal to the power produced by the external field and the reservoirs independently of the details of the model

$$\Phi(J) - \Phi(-J) = \Phi(J) - \Phi^a(J) = -\langle J, E\rangle + \int_{\partial\Lambda} d\Sigma\, \lambda_0\, J\cdot\hat{n}, \tag{3.43}$$

the right hand side of this equation is the power produced by the external field and the boundary reservoirs (recall E is the external field and λ_0 the chemical potential of the boundary reservoirs). From this relationship one derives a macroscopic version of the fluctuation theorem for the entropy production.

For an extensive analysis of fluctuation theorems see [20].

3.7 Universality in Current Fluctuations and Other Results

From the functional $\Phi(J)$ the moments of the time averaged current can be obtained and an interesting universal expression has been obtained in [2] for a one dimensional system on a ring. Let $Q(t) = \int_0^t j(t')dt'$ the total integrated current during the time interval $(0, t)$. Define the generating function of the cumulants of Q

$$\psi_J(s) = \lim_{t\to\infty} \frac{\ln\langle \exp -sQ\rangle}{t} = \Phi^*(s) \tag{3.44}$$

where the brackets denote an average over the time evolution during $(0, t)$. $\Phi^*(s)$ is the Legendre transform of $\Phi(J)$. In [2] the authors estimate $\Phi(J)$ and they obtain

$$\lim_{t\to\infty} \frac{\langle Q^{2n}\rangle_c}{t} = B_{2n-2}\frac{2n!}{n!(n-1)!} D(\frac{-\chi\chi''}{8D^2})^n N^{2n-2} \tag{3.45}$$

where B_{2n-2} are the Bernoulli numbers. This is an interesting universal relationship which follows from the MFT. For the study of cumulants in higher dimension see the recent preprint [1].

The fundamental formula can be used also in the study of non stationary states. By a direct calculation Derrida and Gerschenfeld [24] evaluated the generating function of the moments of Q_t for the symmetric simple exclusion process with a step initial condition. Then they showed [25] that their results can be obtained and extended using the macroscopic fluctuation theory. The distribution of Q_t has generically the non-gaussian decay $\exp[-q^3/t]$. For further results on non stationary states see [40].

3.8 Nonequilibrium Phase Transitions

Are there phase transitions forbidden in equilibrium but possible in nonequilibrium?

We consider the weakly asymmetric simple exclusion process which is characterized at the macroscopic scale by $D = 1$ and $\chi = \rho(1-\rho)$. We fix boundary conditions on the segment $[0, 1]$ $\rho(0) = \rho_0$ and $\rho(1) = \rho_1$. We take a constant external field E which may push the current in the same direction or opposite to the boundary conditions. The hydrodynamic equation for this model is the viscous Burgers equation

$$\partial_t \rho = \Delta\rho - \nabla\chi(\rho)E \tag{3.46}$$

The interesting case is the second one. For E sufficiently large there are density profiles where $V(\rho)$ is non-differentiable, i.e. there is a discontinuity in the first derivative [12] which is interpreted as a first order phase transition.

The reason for this phenomenon is that the variational principle defining $V(\rho)$ admits two minimizers. It can be shown that in the limit $E = \infty$ this is the case if the density profile ρ is suitably chosen. Then by a continuity argument one shows that this persists when the external field E is large. Such a situation is not possible in equilibrium due to the convexity of $V(\rho)$. For a follow-up to our work [12] see [19].

3.9 Large Deviations for Reaction-Diffusion Systems

Unlike the models discussed so far, the so-called *Glauber + Kawasaki* process is not a lattice gas in the sense that the number of particles is not locally conserved. A reaction term allowing creation/annihilation of particles is added in the bulk. The hydrodynamics is

$$\partial_t \rho = \Delta\rho + b(\rho) - d(\rho) = \Delta\rho + v \tag{3.47}$$

where the reaction terms b and d are polynomials in ρ.

The large deviation functional for the density was first calculated in [35]

$$I_{[0,T]}(\rho) = \int_0^T dt \left\{ \frac{1}{4} \langle \nabla H, \rho(1-\rho)\nabla H \rangle \right.$$
$$\left. + \left\langle b(\rho), \left(1 - e^H + He^H\right) \right\rangle + \left\langle d(\rho), \left(1 - e^{-H} - He^{-H}\right) \right\rangle \right\} \tag{3.48}$$

where the external potential H is connected to the fluctuation ρ by

$$\partial_t \rho = \Delta\rho - \nabla \cdot \left(\rho(1-\hat{\rho})\nabla H\right) + b(\rho)e^H - d(\rho)e^{-H} \tag{3.49}$$

The hydrodynamic equation has a local source term v and it is natural to consider the joint fluctuations of ρ, $J(\rho) = -\nabla\rho$, $v = b(\rho) - d(\rho)$. A large deviation formula extending (3.6) to this case has been obtained in [17] with large deviation functional

$$\mathscr{I}_0(\rho, j, v) = \int_0^T dt \left\langle \left\{ \frac{1}{4} \frac{\left(j - J(\rho)\right)^2}{\chi(\rho)} + \Phi\left(\rho, v\right) \right\} \right\rangle, \tag{3.50}$$

where

$$\Phi(\rho, v) = b(\rho) + d(\rho) - \sqrt{v^2 + 4d(\rho)b(\rho)} + v \ln \left(\frac{\sqrt{v^2 + 4d(\rho)b(\rho)} + v}{2b(\rho)} \right). \tag{3.51}$$

ρ, j and v are connected by the equation

$$\partial_t \rho = -\nabla j + v \tag{3.52}$$

3.10 Thermodynamic Interpretation of the Large Deviation Functional

In this section we discuss two different interpretations of the quasi potential [13]. The first one deals with the appearance of the quasi potential in a thermodynamic transformation, the second with its connection with Shannon entropy.

The energy exchanged between the system and the external reservoirs and fields in a thermodynamic transformation during the time interval $[0, T]$ is

$$W_{[0,T]} = \int_0^T dt \Big\{ - \int_{\partial\Lambda} d\sigma(x)\, \lambda(t,x)\, j(t,x)\cdot \hat{n}(x) + \int_\Lambda dx\, j(t,x)\cdot E(t,x) \Big\}, \quad (3.53)$$

where $\hat{n}$ is the outer normal to $\partial\Lambda$ and $d\sigma$ is the surface measure on $\partial\Lambda$. The first term on the right hand side is the energy provided by the reservoirs while the second is the energy provided by the external field.

Fix time dependent paths $\lambda(t,x)$ of the chemical potential and $E(t,x)$ of the driving field. Given a density profile ρ, let $\rho(t,x)$, $j(t,x)$, $t \geq 0$, $x \in \Lambda$, be the solution of (3.1)–(3.4) with initial condition ρ. We claim that

$$\begin{aligned} W_{[0,T]} &= \int_0^T dt \Big\{ - \int_{\partial\Lambda} d\sigma\, f'(\rho(t))\, j(t)\cdot \hat{n} + \int_\Lambda dx\, j(t)\cdot E(t) \Big\} \\ &= \int_0^T dt \int_\Lambda dx \Big\{ - \nabla \cdot \big[f'(\rho(t))\, j(t) \big] + j(t)\cdot E(t) \Big\} \\ &= \int_0^T dt \int_\Lambda dx \big[- f'(\rho(t)) \nabla \cdot j(t) - f''(\rho(t)) \nabla u(t) \cdot j(t) + j(t)\cdot E(t) \big] \\ &= \int_0^T dt\, \frac{d}{dt} \int_\Lambda dx\, f(\rho(t)) \;+\; \int_0^T dt \int_\Lambda dx\; j(t)\cdot \chi(\rho(t))^{-1} j(t), \end{aligned} \quad (3.54)$$

where F is the equilibrium free energy functional,

$$F(\rho) = \int_\Lambda dx\; f(\rho(x)). \quad (3.55)$$

We used the continuity equation (3.1), the Einstein relation (3.3), and the constitutive equation (3.2).

Consider at time $t = 0$ a stationary nonequilibrium profile $\bar{\rho}_0$ corresponding to some driving (λ_0, E_0). This system is put in contact with new reservoirs at chemical potential λ_1 and a new external field E_1. For $t > 0$ the system evolves according to the hydrodynamic equation (3.1)–(3.4) with initial condition $\bar{\rho}_0$, time independent boundary condition λ_1 and external field E_1. Along such a path we have

$$\begin{aligned} W_{[0,T]} = F(\rho(T)) - F(\rho(0)) &+ \int_0^T dt \int_\Lambda dx\, J_{\mathrm{S}}(\rho(t)) \cdot \chi(\rho(t))^{-1} J_{\mathrm{S}}(\rho(t)) \\ &+ \int_0^T dt \int_\Lambda dx\, J_{\mathrm{A}}(\rho(t)) \cdot \chi(\rho(t))^{-1} J_{\mathrm{A}}(\rho(t)). \end{aligned} \quad (3.56)$$

where J_{S} is computed by using the quasi potential V_{λ_1, E_1}, that is the quasi potential corresponding to the stationary state with external driving λ_1, E_1. We have used the orthogonality of J_{S} and J_{A} under constant boundary conditions.

By definition (3.30) of the symmetric part of the current and by an integration by parts,

$$\int_0^T dt \int_\Lambda dx\, \nabla \cdot J(\rho(t))\, \frac{\delta V_{\lambda_1,E_1}(\rho(t))}{\delta \rho} = -\int_0^\infty dt \int_\Lambda dx\, \partial_t \rho(t)\, \frac{\delta V_{\lambda_1,E_1}(\rho(t))}{\delta \rho}. \tag{3.57}$$

Therefore

$$\begin{aligned} W_{[0,T]} = {} & F(\rho(T)) - F(\bar\rho) + V_{\lambda_1,E_1}(\bar\rho_0) - V_{\lambda_1,E_1}(\rho(T)) \\ & + \int_0^T dt \int_\Lambda dx\, J_{\mathrm{A}}(\rho(t)) \cdot \chi(\rho(t))^{-1} J_{\mathrm{A}}(\rho(t)). \end{aligned} \tag{3.58}$$

This equation shows that in the transformation considered the variation of the quasi potential in the interval $[0, T]$ represents the energy dissipated by the thermodynamic force $-\nabla \frac{\delta V_{\lambda,E}(\rho)}{\delta \rho}$. To understand the meaning of the last term let us consider first a stationary state. Since the quasi potential $V_{\lambda,E}$ is minimal in the stationary profile, recalling the decomposition of the current (3.29) we deduce that $J_{\mathrm{S}}(\bar\rho_{\lambda,E}) = 0$; namely, the stationary current coincides with the total current and is purely antisymmetric. In view of Eq. (3.56) the amount of energy per unit of time needed to maintain the system in the stationary profile $\bar\rho_{\lambda,E}$ is

$$\int_\Lambda dx\, J_{\mathrm{A}}(\bar\rho_{\lambda,E}) \cdot \chi(\bar\rho_{\lambda,E})^{-1} J_{\mathrm{A}}(\bar\rho_{\lambda,E}). \tag{3.59}$$

In (3.58) the antisymmetric current $J_{\mathrm{A}}(t)$ is computed not at density profile $\bar\rho_{\lambda(t),E(t)}$ but at the solution $\rho(t)$ of the hydrodynamic equation. However due to the orthogonality between J_{S} and J_{A}, it is still possible an unambiguous identification of the dissipation associated with the thermodynamic force $-\nabla \frac{\delta V_{\lambda,E}(\rho)}{\delta \rho}$ interpreting the rest as energy necessary to keep the system out of equilibrium. In the more general case of time dependent external driving Eq. (3.57) fails as additional terms appear.

The transformation considered is the nonequilibrium analog of the one discussed in [47, Ch. 7] to define *availability*, that is the maximal work [41] obtainable in the transformation. While a definition of thermodynamic potentials, that is functionals of the state of the system, does not appear possible in nonequilibrium thermodynamics, the quasi potential is the natural extension of the availability.

In [13] by interpreting the ideas in [45] we defined in a nonequilibrium setting the renormalized work as the total work minus the energy dissipated to keep the system out of equilibrium. Fix, therefore, $T > 0$, a density profile ρ, and space-time dependent chemical potentials $\lambda(t) = \lambda(t, x)$ and external field $E(t) = E(t, x)$, $0 \le t \le T$, $x \in \Lambda$. Let $\rho(t) = \rho(t, x)$, $j(t) = j(t, x)$, $t \ge 0$, $x \in \Lambda$, be the solution of (3.1)–(3.4) with initial condition ρ. We thus defined the renormalized work

$$W^{\mathrm{ren}}_{[0,T]} = W_{[0,T]} - \int_0^T dt \int_\Lambda dx\, J_{\mathrm{A}}(t, \rho(t))\, \cdot \chi(\rho(t))^{-1} J_{\mathrm{A}}(t, \rho(t)). \tag{3.60}$$

where

$$J(t,\rho) = J_{\mathrm{S}}(t,\rho) + J_{\mathrm{A}}(t,\rho), \qquad J_{\mathrm{S}}(t,\rho) = -\chi(\rho)\,\nabla\frac{\delta V_{\lambda(t),E(t)}(\rho)}{\delta\rho}$$

with $J(t,\rho)$ given by (3.2) and $V_{\lambda(t),E(t)}$ is the quasi potential relative to the state $\lambda(t), E(t)$ with frozen t. We do not discuss further this topic and for more details we refer the reader to [13].

From an operational point of view however the contributions to dissipation of the symmetric and antisymmetric currents are not easily separable. While ΔF can be obtained from equilibrium measurements, the other terms require a preliminary knowledge of the quasi potential, a generically nonlocal quantity. It can be estimated from measurements of the density correlation functions, in principle an infinite number. In fact V is the Legendre transform of the generating functional of density correlation functions [5]. The operational aspects will be discussed in more detail in a forthcoming paper [14].

We now discuss in the case of stochastic lattice gases an interesting relationship between the quasi potential and the relative entropy between the initial and the final state of the system. We refer again to [13]. Recall that $\Lambda \subset \mathbb{R}^d$ is the macroscopic volume, and denote by Λ_ϵ the corresponding subset of the lattice with spacing ϵ, so that the number of sites in Λ_ϵ is approximately $\epsilon^{-d}|\Lambda|$. Given the chemical potential λ of the boundary reservoirs and the external field E, let $\mu_{\Lambda_\epsilon}^{\lambda,E}$ be the stationary measure of a driven stochastic lattice gas.

Given (λ_0, E_0) and (λ_1, E_1), we claim that

$$\lim_{\epsilon\to 0} \epsilon^d\, S\big(\mu_{\Lambda_\epsilon}^{\lambda_0,E_0}\big|\mu_{\Lambda_\epsilon}^{\lambda_1,E_1}\big) = \beta\, V_{\lambda_1,E_1}(\bar\rho_0), \tag{3.61}$$

where $\beta = 1/\kappa T$, and $\bar\rho_0$ is the stationary profile corresponding to (λ_0, E_0).

We present a simple heuristic argument leading to (3.61). In view of the definition of the relative entropy of two probability distributions we have

$$\epsilon^d\, S\big(\mu_{\Lambda_\epsilon}^{\lambda_0,E_0}\big|\mu_{\Lambda_\epsilon}^{\lambda_1,E_1}\big) = \epsilon^d \sum_\eta \mu_{\Lambda_\epsilon}^{\lambda_0,E_0}(\eta)\log\frac{\mu_{\Lambda_\epsilon}^{\lambda_0,E_0}(\eta)}{\mu_{\Lambda_\epsilon}^{\lambda_1,E_1}(\eta)}.$$

By approximating the distributions $\mu_{\Lambda_\epsilon}^{\lambda_i,E_i}$ with their large deviation asymptotics we obtain

$$\begin{aligned}\epsilon^d\, S\big(\mu_{\Lambda_\epsilon}^{\lambda_0,E_0}\big|\mu_{\Lambda_\epsilon}^{\lambda_1,E_1}\big) &\approx \epsilon^d\beta\sum_\eta \mu_{\Lambda_\epsilon}^{\lambda_0,E_0}(\eta)\big[V_{\lambda_1,E_1}(\rho_\epsilon(\eta)) - V_{\lambda_0,E_0}(\rho_\epsilon(\eta))\big]\\ &\approx \beta\big[V_{\lambda_1,E_1}(\bar\rho_0) - V_{\lambda_0,E_0}(\bar\rho_0)\big] = \beta\, V_{\lambda_1,E_1}(\bar\rho_0)\,,\end{aligned}$$

where $\rho_\epsilon(\eta)$ denotes the density profile associated to the microscopic configuration η. In the final step we used the law of large numbers for the microscopic density profile under the probability $\mu_{\Lambda_\epsilon}^{\lambda_0, E_0}$.

To clarify the meaning of (3.61) we call the reader's attention to the following apparent but false counter examples. Let, for instance, μ_ϵ^β be the Gibbs measure for a one-dimensional Ising model at zero magnetic field and inverse temperatures β_0 and β_1 on a ring with ϵ^{-1} sites. The magnetization satisfies a large deviation formula and its typical value is zero for both ensembles so that the right hand side of (3.61) vanishes. On the other hand, by a direct computation, for $\beta_0 \neq \beta_1$, $\lim_\epsilon \epsilon S(\mu_\epsilon^{\beta_0} | \mu_\epsilon^{\beta_1}) > 0$.

However this example does not contradict (3.61) as we are comparing two ensembles in which we varied the temperature and not the magnetic field. In this example, the correct formulation of (3.61) would be in terms of the large deviation function for the energy, that is the extensive variable conjugated the the intensive parameter that has been changed.

3.11 Concluding Remarks and Additional References

Over the last decade the macroscopic fluctuation theory has been used in the study of several problems. Whenever the comparison has been possible, it is remarkable that a perfect agreement has been found between the results obtained by this theory and the microscopic approaches. This agreement provided a strong motivation already in the early stages of development of the theory. In [5] we derived from the Hamilton-Jacobi equation the quasi potential for the nonequilibrium symmetric simple exclusion process from the Hamilton-Jacobi equation obtaining the same result as [26] from the exact calculation of the invariant measure. Moreover the MFT led to the prediction of rather surprising properties of diffusive systems, such as the existence of phase transitions not permitted in equilibrium, the possibility of phase transitions in the large deviation functional of the current, the universality of the cumulants of the current on the ring geometry. The theory requires as input the transport coefficients. Therefore all the systems characterized by the same coefficients behave in the same way.

The quasi potential $V(\rho)$ induces a splitting of the total current into a symmetric and an antisymmetric part under time reversal which is crucial also for the analysis of the energy balance in thermodynamic transformations. The study of transformations from one state to another one is a most relevant subject and has been addressed by several authors in different contexts. For instance, following the basic papers [21, 32, 34], the case of Hamiltonian systems with finitely many degrees of freedom has been recently discussed in [28,31] while the case of Langevin dynamics is considered in [22]. See also [3, 18, 42]. For a detailed study of thermodynamic transformations from the standpoint of the macroscopic fluctuation theory we refer to [13].

A very general approach to the theory of nonequilibrium thermodynamic transformations was initiated by Oono and Paniconi [45] and pursued in the work of Hatano, Sasa, Tasaki [32, 48]. While in [32] a stochastically perturbed dynamical system underlies the analysis, in [48] a guiding idea is to keep as much as possible the phenomenological character of classical thermodynamics without reference to an underlying microscopic dynamics. In this work the authors discuss the operational definition of nonequilibrium thermodynamic observables in concrete situations and generalize basic operations like decomposition, combination and scaling of equilibrium thermodynamics to nonequilibrium states. The possibility of experimental tests is then examined. In more recent papers by Komatsu, Nakagawa [38] and by Komatsu, Nakagawa, Sasa, Tasaki, [39] the problem of constructing microscopic ensembles describing stationary states of both stochastic and Hamiltonian systems, is considered. Expressions for the nonequilibrium distribution function are proposed either exact or valid up to a certain order in the parameters keeping the system out of equilibrium and some consequences are worked out. All these works, although different in spirit from our approach, have provided a stimulus and a source of inspiration especially in connection with the study of thermodynamic transformations.

In [46] Öttinger developed an approach to nonequilibrium called GENERIC (*general equation for the nonequilibrium reversible-irreversible coupling*) based on a separation in the macroscopic evolution equations of dissipative and conservative terms which reminds of our decomposition (3.27).

References

1. E. Akkermans, T. Bodineau, B. Derrida, O. Shpielberg, Universal current fluctuations in the symmetric simple exclusion process and other diffusive systems. arxiv:1306.3145 (2013)
2. C. Appert-Rolland, B. Derrida, V. Lecomte, F. van Wijland, Universal cumulants of the current in diffusive systems on a ring. Phys. Rev. E **78**, 021122 (2008)
3. E. Aurell, K. Gawedzki, C. Mejía-Monasterio, R. Mohayaee, P. Muratore-Ginanneschi, Refined Second Law of Thermodynamics for fast random processes (2012, Preprint). `arXiv:1201.3207`
4. L. Bertini, A. De Sole, D. Gabrielli, G. Jona-Lasinio, and C. Landim, Fluctuations in stationary nonequilibrium states of irreversible processes. Phys. Rev. Lett. **87**, 040601 (2001)
5. L. Bertini, A. De Sole, D. Gabrielli, G. Jona-Lasinio, C. Landim, Macroscopic fluctuation theory for stationary non-equilibrium states. J. Stat. Phys. **110**, 635 (2002)
6. L. Bertini, A. De Sole, D. Gabrielli, G. Jona-Lasinio, C. Landim, Minimum dissipation principle in stationary non-equilibrium states. J. Stat. Phys. **116**, 831 (2004)
7. L. Bertini, A. De Sole, D. Gabrielli, G. Jona-Lasinio, C. Landim, Current fluctuations in stochastic lattice gases. Phys. Rev. Lett. **94**, 030601 (2005)
8. L. Bertini, D. Gabrielli, J. Lebowitz, Large deviations for a stochastic model of heat flow. J. Stat. Phys. **121**, 843 (2005)
9. L. Bertini, A. De Sole, D. Gabrielli, G. Jona-Lasinio, C. Landim, Non equilibrium current fluctuations in stochastic lattice gases. J. Stat. Phys. **123**, 237 (2006)
10. L. Bertini, A. De Sole, D. Gabrielli, G. Jona-Lasinio, C. Landim, Stochastic interacting particle systems out of equilibrium. J. Stat. Mech.: Theory Exp. P07014 (2007)

11. L. Bertini, A. De Sole, D. Gabrielli, G. Jona-Lasinio, C. Landim, Towards a nonequilibrium thermodynamics: a self-contained macroscopic description of driven diffusive systems. J. Stat. Phys. **123**, 857 (2009)
12. L. Bertini, A. De Sole, D. Gabrielli, G. Jona-Lasinio, C. Landim, Lagrangian phase transitions in nonequilibrium thermodynamic systems. J. Stat. Mech.: Theory Exp. L11001 (2010)
13. L. Bertini, D. Gabrielli, G. Jona-Lasinio, C. Landim, Thermodynamic transformations of nonequilibrium states. J. Stat. Phys. **149**, 773 (2012); Clausius inequality and optimality of quasistatic transformations for nonequilibrium stationary states. Phys. Rev. Lett. **110**, 020601 (2013)
14. L. Bertini, A. De Sole, D. Gabrielli, G. Jona-Lasinio, C. Landim, Macroscopic Fluctuation Theory, Paper in preparation
15. T. Bodineau, B. Derrida, Current fluctuations in diffusive systems: an additivity principle. Phys.Rev. Lett. **92**, 180601 (2004)
16. T. Bodineau, B. Derrida, Distribution of current in non-equilibrium diffusive systems and phase transition. Phys. Rev. E **72**, 066110 (2005)
17. T. Bodineau, M. Lagouge, Current large deviations in a driven dissipative model. J. Stat. Phys. **139**, 201 (2010)
18. E. Boksenbojm, C. Maes, K. Netočný, J. Pešek, Heat capacity in nonequilibrium steady states. Europhys. Lett. EPL **96**, 40001 (2011)
19. G. Bunin, Y. Kafri, D. Podolsky, Cusp singularities in boundary-driven diffusive systems. J. Stat. Phys. **152**, 112 (2013)
20. R. Chetrite, K. Gawedzki, Fluctuation relations for diffusion processes. Commun. Math. Phys. **282**, 469 (2008)
21. G.E. Crooks, Entropy production fluctuation theorem and the nonequilibrium work relation for free energy differences. Phys. Rev. E **60**, 2721 (1999)
22. S. Deffner, E. Lutz, Information free energy for nonequilibrium states (2012, Preprint). `arXiv:1201.3888`
23. B. Derrida, Non equilibrium steady states: fluctuations and large deviations of the density and of the current. J. Stat. Mech.: Theory Exp. P07023 (2007)
24. B. Derrida, A. Gerschenfeld, Current fluctuations in one dimensional diffusion systems with a step initial density profile. J. Stat. Phys. **137**, 978 (2009)
25. B. Derrida, A. Gerschenfeld, Current fluctuations of the one dimensional symmetric simple exclusion process with step initial condition. J. Stat. Phys. **136**, 1 (2009)
26. B. Derrida, J. Lebowitz, E. Speer, Large deviation of the density profile in the steady state of the open symmetric simple exclusion process. J. Stat. Phys. **107**, 599 (2002)
27. J.R. Dorfman, T.R. Kirkpatrick, J.V. Sengers, Generic long-range correlations in molecular fluids. Annu. Rev. Phys. Chem. **45**, 213 (1994)
28. M. Esposito, C. Van den Broeck, Second law and Landauer principle far from equilibrium. EPL **95**, 40004 (2011)
29. M.I. Freidlin, A.D. Wentzell, *Random Perturbations of Dynamical Systems*, 2nd edn. (Springer, New York, 1998)
30. G. Gallavotti, E.D.G. Cohen, Dynamical ensembles in stationary states. J. Stat. Phys. **80**, 931 (1995)
31. H-H. Hasegawa, J. Ishikawa, K. Takara, D.J. Driebe, Generalization of the second law for a nonequilibrium initial state. Phys. Lett. A **374**, 1001 (2010); K. Takara, H-H. Hasegawa, D.J. Driebe, Generalization of the second law for a transition between nonequilibrium states. Phys. Lett. A **375**, 88 (2010)
32. T. Hatano, S. Sasa, Steady-state thermodynamics of Langevin systems. Phys. Rev. Lett. **86**, 3463 (2001)
33. P.I. Hurtado, P.L. Garrido, Spontaneous symmetry breaking at the fluctuating level. Phys. Rev. Lett. **107**, 180601 (2011)
34. C. Jarzynski, Nonequilibrium equality for free energy differences. Phys. Rev. Lett. **78**, 2690 (1997)

35. G. Jona-Lasinio, C. Landim, M.E. Vares, Large deviations for a reaction-diffusion model. Prob. Theory Relat. Fields **97**, 339 (1993)
36. C. Kipnis, C. Landim, *Scaling Limits of Interacting Particle Systems* (Springer, Berlin, 1999)
37. C. Kipnis, C. Marchioro, E. Presutti, Heat flow in an exacly solvable model. J. Stat. Phys. **27**, 65 (1982)
38. T. Komatsu, N. Nakagawa, Expression for the stationary distribution in nonequilibrium steady states. Phys. Rev. Lett. **100**, 030601 (2008)
39. T. Komatsu, N. Nakagawa, S. Sasa, H. Tasaki, Entropy and nonlinear nonequilibrium thermodynamic relation for heat conducting steady states. J. Stat. Phys. **142**, 127 (2011)
40. P.L. Krapivsky, B. Meerson, Fluctuations of current in nonstationary diffusive lattice gases. Phys. Rev. E **86**, 031601 (2012)
41. L.D. Landau, E.M. Lifshitz, Course of theoretical physics, in *Statistical Physics*, vol. 5, 3rd edn. (Pergamon, Oxford/Edinburgh/New York, 1980)
42. C. Maes, K. Netocny, A nonequilibrium extension of the Clausius heat theorem (2012). arXiv:1207.3423
43. L. Onsager, Reciprocal relations in irreversible processes. I. Phys. Rev. **37**, 405 (1931); Reciprocal relations in irreversible processes. II. Phys. Rev. **38**, 2265 (1931)
44. L. Onsager, S. Machlup, Fluctuations and irreversible processes. Phys. Rev. **91**, 1505 (1953); Fluctuations and irreversible process. II. Systems with kinetic energy. Phys. Rev. **91**, 1512 (1953)
45. Y. Oono, M. Paniconi, Steady state thermodynamics. Prog. Theor. Phys. Suppl. **130**, 29 (1998)
46. H.C. Öttinger, *Beyond Equilibrium Thermodynamics* (Wiley, Hoboken, 2005)
47. A.B. Pippard, *Elements of Classical Thermodynamics for Advanced Students of Physics* (Cambridge University Press, New York, 1957)
48. S. Sasa, H. Tasaki, Steady state thermodynamics. J. Stat. Phys. **125**, 125 (2006)
49. H. Spohn, Long range correlations for stochastic lattice gases in a non equilibrium steady state. J. Phys. A **16**, 4275 (1983)
50. H. Spohn, *Large Scale Dynamics of Interacting Particles* (Springer, Berlin, 1991)

Chapter 4
Fluctuation-Dissipation and Fluctuation Relations: From Equilibrium to Nonequilibrium and Back

Paolo Adamo, Roman Belousov, and Lamberto Rondoni

Abstract The fluctuation-dissipation relation is a most remarkable classical result of statistical physics, which allows us to understand nonequilibrium properties of thermodynamic systems from observations of equilibrium phenomena. The modern transient fluctuation relations do the opposite: they allow us to understand equilibrium properties from nonequilibrium experiments. Under proper conditions, the transient relations turn into statements about nonequilibrium steady states, even far from equilibrium. The steady state relations, in turn, generalize the fluctuation-dissipation relations, as they reduce to them when approaching equilibrium. We will review the progress made since Einstein's work on the Brownian motion, which gradually evolved from the theory of equilibrium macroscopic systems towards an ever deeper understanding of nonequilibrium phenomena, and is now shedding light on the physics of mesoscopic systems. In this evolution, the focus also shifted from small to large fluctuations, which nowadays constitute a unifying factor for different theories. We will conclude illustrating the recently introduced *t-mixing* property and discussing a fully general and simple response formula, which applies to deterministic dynamics and naturally extends the Green-Kubo theory.

4.1 Concise History

The study of fluctuations in statistical mechanics received the ultimate impulse from Einstein's work on the Brownian motion [1], in which the first fluctuation-dissipation relation was derived, and from Einstein's paper [2], which turned Boltzmann's celebrated equation

P. Adamo • R. Belousov • L. Rondoni (✉)
Department of Mathematical Sciences, Politecnico di Torino, Corso Duca degli Abruzzi 24, Torino, I-10129 Italy
e-mail: adamatrice@gmail.com; belousov.roman@gmail.com; lamberto.rondoni@polito.it

A. Vulpiani et al. (eds.), *Large Deviations in Physics*, Lecture Notes in Physics 885,
DOI 10.1007/978-3-642-54251-0_4,

$$S = k_B \log W \tag{4.1}$$

in one expression for the probability $P(\Delta S)$ of a fluctuation out of an equilibrium state resulting in an entropy jump ΔS:

$$P(\Delta S) = e^{\Delta S / k_B} \tag{4.2}$$

In the following 100 years, Einstein's work was developed by so many scientists that it would be too long to list them here.[1] In particular, Nyquist obtained a formula applicable to linear electrical circuits for spectral densities and correlation functions of the thermal noise in terms of their impedance [5]. The same formula is valid for mechanical systems, if the correspondence of mechanical and electrical quantities is properly established. Onsager found the complementary result, computing the transport coefficients in terms of thermal fluctuations [6, 7].

In the 1950s, authors such as Callen and Welton [8], Callen and Greene [9], Green [10–12], and Kubo [13] gave further contributions to the fluctuation-dissipation theory, while Onsager and Machlup provided a generalization for fluctuation paths of Einstein's formula (4.2), [14, 15]. Alder and Wainwright later discovered that long time tails in the velocity autocorrelation functions prevent the existence of the self-diffusion coefficient in two-dimensional fluids [16], a phenomenon further studied by Kadanoff and Swift for systems near a critical point [17]. Physicists such as Cohen, Dorfman, Kirkpatrick, Oppenheim, Procaccia, Ronis and Spohn investigated the long range correlations in nonequilibrium steady states [18–20].

In the 1970s Hänggi and Thomas obtained certain "nonequilibrium fluctuation theorems" [21, 22], using a kind of terminology that became quite popular 20 years later, after another corner stone had been laid: the transient time correlation function formalism. Developed by Visscher [23], Dufty and Lindenfeld [24], Cohen [25], and Morriss and Evans [26], it yields an exact relation between nonlinear steady state response and transient fluctuations in the thermodynamic fluxes.

More recent results in dynamical systems theory allowed the derivation of nonequilibrium fluctuation response relations, similar to those of equilibrium states, [27–29]. Numerous nonequilibrium extensions of the fluctuation dissipation theorem have been obtained in other contexts, see e.g. Refs. [30–34] and references therein.

The 1993 paper by Evans et al. [35] on the fluctuations of the entropy production rate of a deterministic particle system, modeling a shearing fluid, opened the way to a unifying framework for a variety of nonequilibrium phenomena, under a mathematical expression nowadays called *Fluctuation Relation* (FR). Within this context, fluctuation relations for transient states were derived by Evans and Searles

[1] We recall a few of them, with the intent to show how prolific this research line has been for over a century, and how it has gradually shifted from equilibrium to nonequilibrium problems. Recent reviews on the subject include [3, 4].

in 1994 [36, 37], while in 1995 Gallavotti and Cohen fully formalized the theory of steady state relations for systems of the Anosov type [38, 39]. These FRs are exact and general. They extend the Green-Kubo and Onsager relations to far from equilibrium states, in the sense that they reduce to those relations in the vicinity of the equilibrium regime [40–43]. Among the recent results, transient relations, such as the Jarzynski equality, have been obtained independently and have motivated much research e.g. in biophysics [44, 45]. Indeed, fluctuations are not directly observable in macroscopic systems, while they are substantial in small systems or small parts of macroscopic systems.[2]

With an eye kept on recent developments and open problems, the purpose of the present paper is to review the main results obtained through the specialized literature in a non-technical fashion accessible to a wide audience. The most recent results will be considered in the context of deterministic dynamics.

4.2 The Brownian Motion and the Langevin Equation

Observing with a microscope the pollen suspended in a glass of water, one realizes that pollen grains move erratically and incessantly, although no work is done on them to balance the energy dissipated by the viscosity of the fluid, and although the water appears to be still. This phenomenon was named after the botanist Robert Brown, who tried unsuccesfully to explain it [47], and remained a puzzle until Einstein tackled it in terms of kinetic theory, to prove that atoms exist.

The puzzle arises observing the equation of motion for the velocity of one spherical particle of mass m and radius a in a fluid of viscosity η, which reads:

$$\frac{\mathrm{d}\mathbf{v}}{\mathrm{d}t} = -\frac{6\pi a\eta}{m}\mathbf{v} \tag{4.3}$$

and predicts the exponentially decaying behaviour

$$\mathbf{v}(t) = \mathbf{v}(0)\exp(-t/\tau)\,, \quad \text{with} \quad \tau = \frac{m}{6\pi a\eta}\,. \tag{4.4}$$

Here $\mathbf{v}(0)$ is the initial velocity, $\mathbf{v}(t)$ the velocity at a subsequent time t and τ is a characteristic time depending on the properties of both water and pollen, which takes values of order 10^{-4} s for particles of radius $a \sim 10^{-4}$ m and mass 10^{-7} g. Consequently, the particle should come to rest in less than a few milliseconds, but it does not.

Einstein's theory [1] boldly solved the riddle, introducing an ingredient which had been previously thought to be uninfluential: a stochastic force f_R acting on

[2] An exception is provided by gravitational waves detectors, whose resolution is so high that their thermal fluctuations are revealed [46].

the pollen grains, resulting from many random collisions with the water molecules and bearing no memory of events occurring at different times. This idea required Eq. (4.3) to be replaced by a new dynamical law, which was proposed by Langevin 3 years later [48]:

$$\frac{\mathrm{d}\mathbf{v}}{\mathrm{d}t} = -\frac{6\pi a\eta}{m}\mathbf{v} + f_R(t)\,, \tag{4.5}$$

Here, the acceleration f_R is greater at higher temperatures T, but averages to zero at all temperatures, $\langle f_R \rangle = 0$, because the average work done on the pollen particles by the force mf_R must vanish. Would this not be the case, there would be an overall loss of energy in time, and pollen would sooner or later stop moving, while water would cool down. This has never been observed. Furthermore, the lack of memory, can be idealized assuming that the force acting at times t and $t' \neq t$ are uncorrelated, i.e.

$$\left\langle \left(f_R \circ S^t\right)\left(f_R \circ S^{t'}\right)\right\rangle = q\delta(t-t') \tag{4.6}$$

where S^t represents the time evolution for a time t,[3] q is a constant and δ is Dirac's delta function. Here and above, $\langle . \rangle$ represents averages over all possible realizations of the process, or over all possible initial conditions, if pollen and water behave as prescribed by classical mechanics.[4]

Because f_R cannot be known more precisely than on average and as expressed by (4.6), even $\mathbf{v}(t)$ can only be known in statistical terms. These, however, are fully satisfactory. Indeed, the behaviour of a single pollen particle yields practically no insight on the phenomenon, whereas the collective behaviour of all pollen particles does. The problem can then be tackled as follows. Let Γ be a point in the phase space of all pollen particles and water molecules. Then, treat f_R formally as a known function and integrate (4.5), with initial condition $\mathbf{v}(0) = \mathbf{v}_0$. For simplicity, assume the motion takes place in a 1-dimensional space. The result is:

$$v(t) = e^{-\gamma t}v_0 + \int_0^t e^{-\gamma(t-t')} f_R(t')\mathrm{d}t' \tag{4.7}$$

[3] So that $f_R \circ S^t x = f_R(S^t x)$, with $S^t x$ the position of a Brownian particle initially in x, after a time t.

[4] There are various points of view on the significance of the random term f_R. Some view Nature as intrinsically deterministic and randomness merely as the result of incomplete information. Others take the laws of Nature as ultimately stochastic, and determinism just as a convenient idealization in the description of certain phenomena. We adopt a pragmatic standpoint: mathematical models, whether stochastic or deterministic, are meant to describe non-exhaustively complementary features of natural phenomena. Depending on the feature of interest, one kind of model may be more convenient or may bear deeper insight than the other.

where $\gamma = 6\pi a\eta/m$. Taking the average, one obtains $\langle v \circ S^t \rangle = e^{-\gamma t} v_0$, because this operation can be taken (quite generally) inside the integral and $\langle f_R \rangle = 0$. Therefore, *on average*, the velocity behaves as predicted by Eq. (4.4). Analogously, multiplying two subsequent values of v and averaging, yields:

$$\langle \left(v \circ S^{t_1}\right) \left(v \circ S^{t_2}\right) \rangle = e^{-\gamma(t_1+t_2)} v_0^2 + \int_0^{t_1} \mathrm{d}t_1' \int_0^{t_2} \mathrm{d}t_2' \, e^{-\gamma(t_1+t_2-t_1'-t_2')} q\delta(t_1'-t_2') \tag{4.8}$$

Considering separately the case with $t_1 > t_2$ and that with $t_2 > t_1$, some algebra eventually yields:

$$\langle \left(v \circ S^{t_1}\right) \left(v \circ S^{t_2}\right) \rangle = \frac{q}{2\gamma} \left[e^{-\gamma|t_1-t_2|} - e^{-\gamma(t_1+t_2)} \right] + e^{-\gamma(t_1+t_2)} v_0^2 \tag{4.9}$$

For large times t_1 and t_2, the system is found in a steady state, characterized by

$$\langle \left(v \circ S^{t_1}\right) \left(v \circ S^{t_2}\right) \rangle \simeq \frac{q}{2\gamma} e^{-\gamma|t_1-t_2|} \tag{4.10}$$

and, in particular, by mean energy per Brownian particle given by

$$\langle E \rangle = \lim_{t\to\infty} \frac{m}{2} \langle \left(v \circ S^t\right)^2 \rangle = \frac{mq}{4\gamma} \tag{4.11}$$

Assuming this corresponds to the equilibrium with the heat bath at temperature T constituted by the fluid, the equipartition principle, $\langle E \rangle = k_B T/2$, leads to:

$$q = \frac{2k_B T\gamma}{m} \tag{4.12}$$

It is now possible to make predictions on the behaviour of an observable quantity: the position of pollen particles. Assume that all particles are initially clustered in position x_0. Integrating the velocity and averaging, one obtains:

$$\begin{aligned} \left\langle \left(x \circ S^t - x\right)^2 \right\rangle &= \left\langle \int_0^t v \circ S^{t_1} \, \mathrm{d}t_1 \int_0^t v \circ S^{t_2} \, \mathrm{d}t_2 \right\rangle \\ &= \left(v_0^2 - \frac{k_B T}{m} \right) \frac{\left(1 - e^{-\gamma t}\right)^2}{\gamma^2} + \frac{k_B T}{m} \left[\frac{2t}{\gamma} - \frac{2\left(1 - e^{-\gamma t}\right)}{\gamma^2} \right], \end{aligned} \tag{4.13}$$

which grows asymptotically linearly in time, with diffusion coefficient D and mobility μ given by:

$$D = \lim_{t\to\infty} \frac{\left\langle \left(x \circ S^t - x\right)^2 \right\rangle}{t} = \frac{2k_B T}{m\gamma}, \quad \mu = \frac{D}{k_B T} \tag{4.14}$$

In the 3-dimensional case with spherical particles of radius a and mass m, one eventually obtains the celebrated Einstein-Smoluchowski relation:

$$D = \frac{k_B T}{6\pi\eta a} = \frac{\mathscr{R} T}{6\pi\eta a} \cdot \frac{1}{N_A}\,, \tag{4.15}$$

where $\mathscr{R}$ is the universal gas constant and N_A Avogadro's number.

Equation (4.15) turned out to be extremely important, since it connected the experimentally easily accessible macroscopic quantity $\left\langle (\mathbf{x} \circ S^t)^2 \right\rangle$ with Avogadro's number, which could thus be estimated.[5] Perrin's experiments [49] confirmed the validity of the theory and convinced practically everybody that atoms could be counted, hence that they really existed.

There are two interesting limits that can be taken in Eq. (4.5): $\eta/m \to \infty$ and $\eta/m \to 0$. Keeping m fixed, the first limit corresponds to a fluid with high viscosity, while the second limit corresponds to an inviscid fluid. In the first case, the effect of the molecular impacts is negligible and the description of a macroscopic object in a liquid is restored. In the second case, only molecular impacts can perturb the motion of the object of mass m, as it happens to particles of molecular sizes which, obeying microscopic reversible laws, perform effectively random motions, unaware of any viscous damping. Viscosity is, indeed, a collective effect which emerges when in very large numbers molecules act on a sufficiently large surface of a moving object.

The intermediate situation in which viscosity and random molecular impacts are of comparable magnitude, which is of interest for the Brownian motion, unveils one level of description, the mesoscopic level, which differs substantially from the well understood microscopic and macroscopic levels. The ingenuity of this theory lies in its ability to identify three coexisting but separate scales of observations: the microscopic scale (which we describe as deterministic and reversible), the mesoscopic scale (which we describe as stochastic and irreversible), and the macroscopic scale (which we describe as deterministic and irreversible). The phenomena observed at the different scales obviously coexist, but pertain to such widely separated domains of reality that totally different kinds of description are required to represent them. However, fluctuations at the mesoscopic scale shed light on the whole picture, as we will see later.

Equation (4.15) constitutes the first Fluctuation-Dissipation Relation (FDR), in the sense that it links the equilibrium fluctuations of the particles positions (which correspond to the mesoscopic scale) with the macroscopic property η of the fluid, which characterizes nonequilibrium, dissipative, phenomena.

The great generality of such a result can be understood observing that many different phenomena can be treated by means of equations mathematically indistinguishable from Eq. (4.5). For instance, an RC circuit at temperature T is described by the following equation:

[5] At that time, the numerical value of N_A was unknown.

$$R\frac{\mathrm{d}Q}{\mathrm{d}t} + \frac{1}{C}Q = f_R \tag{4.16}$$

where Q is the charge in the capacitor of capacitance C, $U(t) = CQ(t)$ is the voltage across the resistance R, and f_R represents the random motion of the electrons, which averages to zero, but varies randomly in time, as the consequence of thermal agitation. If f_R has the properties assumed earlier for the Brownian motion, the mathematical analysis is identical. In particular, in place of Eq. (4.10) one has $\langle Q(t)Q(t')\rangle = k_B TC \exp(-|t-t'|/RC)$, which describes a phenomenon known as the Johnson-Nyquist noise .

Remark. This illustrates how the FDR allows the calculation of nonequilibrium properties by means of equilibrium experiments: no external forces drag the pollen particles in the liquid, yet we compute the viscosity they would experience if dragged; no emf pushes the electrons, yet we compute the resistance encountered when they are pushed.

4.3 The Fluctuation-Dissipation Relation

The above theory can be cast in a more general context, useful to analyze a very wide spectrum of situations of e.g. technological interest. Assume that the friction acts as a memory term in the equations of motion, so that Eq. (4.5) is replaced by:

$$\dot{v}(t) = -\int_{-\infty}^{t} \gamma(t-t')v(t')\,\mathrm{d}t' + f_R(t) \tag{4.17}$$

which reduces to the previous form, if $\gamma(t) = \text{const}\cdot\delta(t)$. To obey the principle of causality, one may take $\gamma(t) = 0$ for $t < 0$. Then,

$$\int_{-\infty}^{t} \gamma(t-t')v\circ S^{t'}\,\mathrm{d}t' = \int_{-\infty}^{\infty} \gamma(t-t')v\circ S^{t'}\,\mathrm{d}t' \tag{4.18}$$

is a convolution integral, which suggests a solution by Fourier transforms. Introducing the Fourier transforms and anti-transforms as:

$$\tilde{z}(\omega) = \frac{1}{2\pi}\int_{-\infty}^{\infty} z(t)e^{-i\omega t}\mathrm{d}t\ , \quad \text{and} \quad z(t) = \int_{-\infty}^{\infty} \tilde{z}(\omega)e^{i\omega t}\mathrm{d}\omega \tag{4.19}$$

one obtains

$$\tilde{v}(\omega) = \frac{\tilde{f}_R(\omega)}{i\omega + \tilde{\gamma}(\omega)} \tag{4.20}$$

At this stage, many possible routes can be taken, by assuming different relations between γ and f_R. For this purpose let us introduce the power spectrum I_z of a given signal z,[6] i.e. the square absolute value of the Fourier components of z. Thanks to the Wiener-Khinchin theorem, this is given by:

$$I_z(\omega) = \frac{1}{2\pi} \int_{-\infty}^{\infty} \phi_z(t) e^{-i\omega t} \mathrm{d}t \tag{4.21}$$

where ϕ_z is the steady state autocorrelation function of z:

$$\phi_z(t) = \left\langle \left(z \circ S^{t_0}\right) \left(z \circ S^{t_0+t}\right) \right\rangle \tag{4.22}$$

which does not depend on t_0 because of stationarity. If we perform a Fourier analysis of Eq. (4.5), with $\gamma = 6\pi a\eta/m$ and the following definitions:

$$v(t) = \sum_{n=-\infty}^{\infty} v_n e^{i\omega_n t} \,, \quad f_R(t) = \sum_{n=-\infty}^{\infty} f_n e^{i\omega_n t} \,, \tag{4.23}$$

we obtain

$$v_n = \frac{f_n}{i\omega_n + \gamma} \,, \quad \text{and} \quad I_v(\omega) = \frac{I_f(\omega)}{\omega^2 + \gamma^2} \tag{4.24}$$

the first of which is clearly a special instance of Eq. (4.20). The simplest case corresponds to constant I_f. In that case, the stochastic term f_R is called a *white noise*, and the power spectrum of the velocity takes the form of a Lorentzian curve, characteristic of equilibrium states. One further obtains:

$$\phi_v(t_1 - t_2) = \left\langle \left(v \circ S^{t_1}\right) \left(v \circ S^{t_2}\right) \right\rangle = \frac{\pi I_f}{\gamma} e^{-\gamma|t_1 - t_2|} \tag{4.25}$$

which yields $I_f^{(BM)} = \gamma k_B T/\pi m$, if the equipartition of energy applies.

Question. Assuming Eq. (4.17) as the relevant equation of motion, could $I_f(\omega)$ be obtained as a generalization of the Brownian motion expression $I_f^{(BM)}$?

For instance, let $\tilde{\gamma} = Re[\tilde{\gamma}] + iIm[\tilde{\gamma}]$ be given in terms of its real and imaginary parts, and require I_f to be expressed by:

$$I_f(\omega) = \frac{2k_B T}{m} Re\left[\tilde{\gamma}(\omega)\right] \tag{4.26}$$

[6]The terminology originates in the context of electrical circuits, where the power spectrum represents the electrical power dissipated at various frequencies.

Which relation between γ and f_R would lead to (4.26) with positive $Re\,[\tilde{\gamma}(\omega)]$, as appropriate for power spectra? One finds that the relation

$$\langle f_R(t_1) f_R(t_2)\rangle = \frac{k_B T}{m}\left[\gamma(t_1 - t_2) + \gamma(t_2 - t_1)\right] , \tag{4.27}$$

which means that the viscosity is affected by the properties of the bath and vice versa, suffices to obtain the desired result. If $\gamma(t)$ takes the form $\gamma\delta(t)$, we fall back in the original situation with δ-correlated noise and $I_f(0) = k_B T\gamma/\pi m = I_f^{(BM)}$. To generalize the expression for the mobility, observe that one can pose:

$$\begin{aligned}
\mu = \frac{D}{k_B T} &= \lim_{t\to\infty} \frac{\left\langle (x \circ S^t - x)^2 \right\rangle}{2tk_B T} \\
&= \lim_{t\to\infty} \frac{1}{2tk_B T} \int_0^t \mathrm{d}t_1 \int_0^t \mathrm{d}t_2 \left\langle \left(v \circ S^{t_1}\right)\left(v \circ S^{t_2}\right)\right\rangle \qquad (4.28)\\
&= \lim_{t\to\infty} \frac{1}{2tk_B T} \int_0^t \mathrm{d}t_1 \int_0^t \mathrm{d}t_2 \left\langle v\left(v \circ S^{t_2 - t_1}\right)\right\rangle \qquad (4.29)\\
&= \lim_{t\to\infty} \frac{1}{k_B T t} \int_0^t (t - s)\left\langle v\,(v \circ S^s)\right\rangle \mathrm{d}s \qquad (4.30)\\
&= \frac{1}{k_B T} \lim_{t\to\infty} \int_0^t \left\langle v\,(v \circ S^s)\right\rangle \mathrm{d}s \qquad (4.31)
\end{aligned}$$

where (4.29) holds, because we consider a steady state, while (4.30) and (4.31) are derived with a little bit of algebra, provided the following is satisfied:

$$\left| \int_0^\infty s\phi_v(s)\mathrm{d}s \right| < \infty . \tag{4.32}$$

The equality between μ and (4.31) is one example of Green-Kubo relation, which suggests the following generalization of the mobility,

$$\mu(\omega) = \frac{1}{2\pi k_B T} \int_0^\infty \mathrm{d}t \left\langle v\left(v \circ S^t\right)\right\rangle e^{-i\omega t} , \tag{4.33}$$

for the diffusion coefficient to equal $D = k_B T\mu(0)$. Further manipulations yield:

$$I_v(\omega) = \frac{1}{2\pi} \int_{-\infty}^{\infty} \phi_v(t) e^{-i\omega t}\mathrm{d}t = k_B T\left[\mu(\omega) + \mu(-\omega)\right] = 2k_B T Re\left[\mu(\omega)\right] \tag{4.34}$$

Recalling Eq. (4.20), one has $|\tilde{v}(\omega)|^2 = |\tilde{f_R}(\omega)|^2 / \left[\omega^2 + \tilde{\gamma}(\omega)^2\right]$, which implies:

$$I_v(\omega) = \frac{I_f(\omega)}{\omega^2 + \tilde{\gamma}(\omega)^2} = \frac{2k_B T}{m} \frac{Re[\tilde{\gamma}(\omega)]}{\omega^2 + \tilde{\gamma}(\omega)^2} \tag{4.35}$$

Then we can recover ϕ_v in two different ways, the first using the above equation:

$$\phi_v(t) = \int I_v(\omega) e^{i\omega t} \mathrm{d}t = \frac{k_B T}{m} \int_{-\infty}^{\infty} \mathrm{d}t e^{i\omega t} \left[\frac{1}{i\omega + \tilde{\gamma}(\omega)} + \frac{1}{-i\omega + \tilde{\gamma}(\omega)^*} \right] \tag{4.36}$$

where * represents complex conjugation; the second using Eq. (4.34). Comparing term by term, we deduce:

$$\mu(\omega) = \frac{1}{m\left[i\omega + \tilde{\gamma}(\omega)\right]} \tag{4.37}$$

which is called a *Fluctuation-Dissipation Relation of first kind* , whereas

$$Re\left[\tilde{\gamma}(\omega)\right] = \frac{m}{2k_B T} I_f(\omega) = \frac{m}{4\pi k_B T} \int_{-\infty}^{\infty} \mathrm{d}t e^{-i\omega t} \left\langle f_R f_R \circ S^t \right\rangle \tag{4.38}$$

is called a *Fluctuation-Dissipation Relation of second kind* . The first kind gives the complex mobility (admittance, in general) in terms of the autocorrelation of the velocity (flow, in general). The second kind gives the complex viscosity (impedance, in general) in terms of the autocorrelation of the the random force. As explained in Ref. [50], these two kinds of FDR imply that the response of a system to external actions which perturb its equilibrium is linked to the spontaneous thermal fluctuations in absence of perturbing forces. The FDR of the first kind has to be considered more fundamental than the second, since it refers to experimentally accessible quantities (the flows), while the second kind relies on the rather problematic distinction between frictional and random forces.

To conclude this section, it is interesting to analyze the procedure we have followed: given the result we wanted to obtain, we have searched for the conditions that produce it. Consequently, the model we have constructed certainly yields the desired result. The question is now to look for the systems of physical interest which satisfy the imposed conditions. This is standard practice in physics, often more useful than the straight logical deductions from general principles, which are frequently cumbersome or even impossible. For instance, in statistical physics, one typically relies on macroscopic observations to infer the form of the molecular interaction potentials, not vice versa. The theory of Brownian motion is of the other kind: some general ideas on the microscopic dynamics led to predictions on the macroscopic behaviour, which were subsequently experimentally verified.

4.4 Evolution of Probability Distributions

This section recalls some basic notions of dynamical systems theory, introducing the notation which will be used later. Consider a dynamical system defined by an evolution equation on a phase space $\mathscr{M}$:

$$\dot{\Gamma} = F(\Gamma) , \quad \Gamma \in \mathscr{M} \tag{4.39}$$

whose trajectories for each initial condition Γ are given by $\{S^t\Gamma\}_{t\in\mathbb{R}}$, where S^t is the operator that moves Γ to its position after a time t, hence $S^0\Gamma = \Gamma$. We will consider time reversal invariant dynamics, i.e. the dynamics for which

$$IS^t\Gamma = S^{-t}I\Gamma , \quad \forall\Gamma \in \mathscr{M} \tag{4.40}$$

holds, where the linear operator $I : \mathscr{M} \to \mathscr{M}$ is an involution (I^2 =identity) representing a time reversal operation [in Hamiltonian dynamics, where $\Gamma = (\mathbf{q}, \mathbf{p})$, one usually takes $I(\mathbf{q}, \mathbf{p}) = (\mathbf{q}, -\mathbf{p})$]. Furthermore, we will consider evolutions such that $\{S^t\}_{t\in\mathbb{R}}$ satisfies the group property $S^tS^s = S^{t+s}$. The time averages of a phase variable $\phi : \mathscr{M} \to \mathbb{R}$, along a trajectory starting at Γ, will be denoted by:

$$\overline{\phi}(\Gamma) = \lim_{t\to\infty} \frac{1}{t} \int_0^t \phi\,(S^s\Gamma)\,\mathrm{d}s \tag{4.41}$$

If the dynamics represent a thermodynamic system, in which Γ is a single microscopic state, the time average should not depend on Γ,[7] and could be obtained as a phase space average, with respect to a given probability distribution μ:

$$\overline{\phi}(\Gamma) = \int_{\mathscr{M}} \phi(X)\,\mathrm{d}\mu(X) = \langle\phi\rangle_\mu , \quad \text{for almost every } \Gamma \in \mathscr{M} \tag{4.42}$$

This is the case when the dynamical system $(S, \mathscr{M}, \mu)$ is ergodic (cf. Sect. 4.4.1). Ergodicity is a very strong property, which is not strictly obeyed by most of the systems of physical interest. It can be however assumed to hold very often, because physics is usually concerned with a small set of observables and for systems made of exceedingly large numbers of particles, cf. [51].

Once $\mathscr{M}$ is endowed with a probability distribution μ_0, $\mu_0(\mathscr{M}) = 1$ and $\mu_0(E) \geq 0$ for all allowed events $E \subset \mathscr{M}$, the dynamics in $\mathscr{M}$ may be used to induce an evolution in the space of probabilities. One may assume that the subsets of the phase space have a certain probability, which they carry along where the dynamics moves them. As a consequence, the probability distribution on $\mathscr{M}$ changes in time, and one may introduce a set of distributions $\{\mu_t\}_{t\in\mathbb{R}}$ as follows:

[7] Except a negligible set of phase space points.

$$\mu_t(E) = \int_E \mathrm{d}\mu_t = \int_{S^{-t}E} \mathrm{d}\mu_0 = \mu_0(S^{-t}E) \tag{4.43}$$

where $S^{-t}E$ is the preimage of E a time t earlier. This relation simply means that the probability of $S^{-t}E$ at the initial time, belongs to E at time t. With this definition, probability is conserved in phase space and flows like a compressible fluid, in general.[8] Taking much care, the evolution of the probability distributions may be used to define an evolution of the observables, introducing

$$\langle\phi\rangle_t = \int_{\mathscr{M}} \phi \, \mathrm{d}\mu_t \tag{4.44}$$

As the mean values of the phase functions completely characterize the system, one often refers to μ_t as to the *state* of the system at time t. A probability measure μ is called *invariant* if $\mu(E) = \mu(S^{-t}E)$ for all t and all measurable sets E.

At times μ_t has a density f_t, i.e. $\mathrm{d}\mu_t(\Gamma) = f_t(\Gamma)\mathrm{d}\Gamma$. In that case, the evolution of μ_t follows from the evolution of the normalized non-negative function f_t, determined by Eq. (4.43). Operating the change of coordinates $Y = S^t X$, i.e. $X = S^{-t}Y$, in the last integral of the following expression

$$\mu_t(E) = \int_E f_t(X)\,\mathrm{d}X = \int_{S^{-t}E} f_0(X)\,\mathrm{d}X \tag{4.45}$$

one obtains:

$$\int_E f_t(X)\,\mathrm{d}X = \int_E f_0(Y)J^{-t}(Y)\,\mathrm{d}Y \tag{4.46}$$

where $J^{-t}(Y) = |(\partial S^{-t}X/\partial X)|_Y$ is the Jacobian of the transformation. As Eqs. (4.43–4.46) hold for all allowed subsets of $\mathscr{M}$, one can write

$$f_t(X) = f_0(S^{-t}X)J^{-t}(X) \tag{4.47}$$

For Hamiltonian dynamics, $J^{-t}(X) = 1$, hence $f_t(X) = f_0(S^{-t}X)$. In general, for the evolution of the observables one obtains:

$$\langle\phi\rangle_t = \int_{\mathscr{M}} \phi(\Gamma) f_t(\Gamma)\mathrm{d}\Gamma = \int_{\mathscr{M}} \phi(\Gamma) f_0(S^{-t}\Gamma)J^{-t}(\Gamma)\mathrm{d}\Gamma \tag{4.48}$$

Introducing $Y = S^t\Gamma$ in the last integral, so that $\mathrm{d}\Gamma = J^t(Y)\mathrm{d}Y$, one finds:

$$\langle\phi\rangle_t = \int_{\mathscr{M}} \phi(S^tY) f_0(Y)J^{-t}(S^tY)J^t(Y)\mathrm{d}Y \tag{4.49}$$

[8] In case of Hamiltonian dynamics, and more generally in the case of the so-called *adiabatically incompressible* systems, probabilities flow like incompressible fluids.

To make this expression more explicit, recall that probability is transported by the phase space points like mass is transported in a fluid. Then, the evolution equation for a density f in the phase space is given by a formal continuity equation:

$$\frac{\partial f}{\partial t} = -\nabla_\Gamma \cdot (Ff) \ , \quad \frac{\mathrm{d}f}{\mathrm{d}t} = \frac{\partial f}{\partial t} + \nabla_\Gamma f \cdot F = -f \nabla_\Gamma \cdot F = -f\Lambda \tag{4.50}$$

where $\Lambda = \nabla_\Gamma \cdot F$, called phase space expansion rate, is the divergence of the vector field F on $\mathscr{M}$, cf. Eq. (4.39). Equations (4.50) generalize the Liouville equation to non-Hamiltonian dynamics. Because the global existence and uniqueness of solutions of the equations of motion is practically assured for all particles systems of physical interest,[9] one may safely assume that the solutions of the Liouville equation also exist and can be constructed by means of formal calculations. Various procedures are available for this purpose. For example, let us introduce the f-Liouvillean operator $\mathscr{L}$:

$$\mathscr{L} = -i \left(\nabla_\Gamma \cdot F + F \cdot \nabla_\Gamma\right) \ , \quad \text{so that} \quad \frac{\partial f}{\partial t} = -i\mathscr{L} f \tag{4.51}$$

and let us express $\partial f_t / \partial t$ to first order in the time increment Δt:

$$\frac{\partial f_t}{\partial t}(\Gamma) = -i \left(\mathscr{L} f_t\right)(\Gamma) = \frac{f_{t+\Delta t}(\Gamma) - f_t(\Gamma)}{\Delta t} + O\left(\Delta t\right) \tag{4.52}$$

It follows that

$$f_{\Delta t}(\Gamma) = (1 - i\mathscr{L}\Delta t)\, f_0(\Gamma) + O\left(\Delta t^2\right)$$
$$f_{2\Delta t}(\Gamma) = (1 - i\mathscr{L}\Delta t)\, f_{\Delta t}(\Gamma) + O\left(\Delta t^2\right) = (1 - i\mathscr{L}\Delta t)^2\, f_0(\Delta) + O\left(\Delta t^2\right) \tag{4.53}$$
$$\vdots \tag{4.54}$$
$$f_{n\Delta t}(\Gamma) = (1 - i\mathscr{L}\Delta t)^n\, f_0(\Gamma) + nO\left(\Delta t^2\right) \tag{4.55}$$

Taking $\Delta t = t/n$, so that $\Delta \to 0$ and $nO\left(\Delta t^2\right) \to 0$ as $n \to \infty$, one obtains:

$$f_t(\Gamma) = \lim_{n\to\infty} \left(1 - \frac{it\mathscr{L}}{n}\right)^n f_0(\Gamma) = \sum_{n=0}^{\infty} \frac{(-it\mathscr{L})^n}{n!} f_0(\Gamma) \equiv e^{-it\mathscr{L}} f_0(\Gamma) \tag{4.56}$$

[9] Global solution means that particles do no cease to exist after a while; Uniqueness implies that the same particles do not exist at once along distinct trajectories. If these properties are violated, one typically concludes that the equations of motion do not suit the problem at hand.

The question is now to connect Eq. (4.56) with Eq. (4.47), to give a more useful expression of the corresponding evolution operators. One can write

$$Y = S^t X = S^{t/n}\left(S^{t/n}\left(\cdots S^{t/n}\left(X\right)\cdots\right)\right) \tag{4.57}$$

Hence, the chain rule yields

$$\left.\frac{\partial Y}{\partial X}\right|_{X_i} = \left(\left.\frac{\partial S^{t/n} X}{\partial X}\right|_{X_{n-1}}\right)\left(\left.\frac{\partial S^{t/n} X}{\partial X}\right|_{X_{n-2}}\right)\cdots\left(\left.\frac{\partial S^{t/n} X}{\partial X}\right|_{X_0}\right) \tag{4.58}$$

where $X_j = S^{jt/n} X_0$, and X_0 is the initial point of a trajectory. One can expand to first order each derivative in brackets as follows:

$$\left.\frac{\partial\left(S^{t/n} X\right)}{\partial X}\right|_{X_j} = \left.\frac{\partial}{\partial X}\left(X + F\Delta t + O(\Delta t^2)\right)\right)\right|_{X_j} \tag{4.59}$$

and further

$$\left.\frac{\partial\left(S^{t/n} X\right)}{\partial X}\right|_{X_j} = \mathbb{1} + \left.\frac{\partial F}{\partial X}\right|_{X_j} \Delta t + O\left(\Delta t^2\right) = e^{\left.\frac{\partial F}{\partial X}\right|_{X_j} \Delta t} + O\left(\Delta t^2\right) ,$$

$\mathbb{1}$ being the identity matrix. Substituting Eq. (4.60) in Eq. (4.58), and noting that the exponential operators do not commute in general, the $n \to \infty$ limit leads to a so-called left ordered exponential, which can also be expressed as a Dyson series:

$$\begin{aligned} e_L^{\int_0^t T(S^s X)\mathrm{d}s} = \mathbb{1} &+ \int_0^t \mathrm{d}t_1\, T(S^{t_1} X) + \int_0^t \mathrm{d}t_1 \int_0^{t_1} \mathrm{d}t_2\, T(S^{t_1} X) T(S^{t_2} X) \\ &+ \int_0^t \mathrm{d}t_1 \int_0^{t_1} \mathrm{d}t_2 \int_0^{t_2} \mathrm{d}t_3\, T(S^{t_1} X) T(S^{t_2} X) T(S^{t_3} X) + \ldots \end{aligned} \tag{4.60}$$

where the time dependent matrix

$$T(S^s X) = \left.\frac{\partial F}{\partial X}\right|_{S^s X} \tag{4.61}$$

is the Jacobian matrix of F computed at the point $S^s X$. Considering that the identity $\det(e^L) = \exp(\mathrm{Tr} L)$ holds for left ordered exponentials as well, one obtains:

$$\det\left(e_L^{\int_0^t T(S^s X)\mathrm{d}s}\right) = \exp\left\{\int_0^t \nabla_\Gamma \cdot F\left(S^s X\right)\mathrm{d}s\right\} = \int_0^t \Lambda\left(S^s X\right)\mathrm{d}s \tag{4.62}$$

This implies that:

$$J^t(X) = e^{\int_0^t \Lambda(S^u X)\mathrm{d}u} = e^{\int_{-t}^0 \Lambda(S^{t+s}X)\mathrm{d}s} = \frac{1}{J^{-t}(S^t X)} = \frac{1}{J^{-t}(Y)} \tag{4.63}$$

where we have taken $u = t + s$ in the second integral. Equation (4.63) is obvious for compressible fluids: a fluid element about X varies in a time t by a factor which is the inverse of the variation of the fluid element about Y, when tracing backwards its trajectory. Consequently $J^{-t}(S^t X)J^t(X) = 1$, and Eq. (4.47) may be rewritten as:

$$f_t(X) = f_0(S^{-t}X)e^{\int_{-t}^0 \Lambda(S^s X)\mathrm{d}s} \tag{4.64}$$

while Eq. (4.49) takes the interesting form

$$\langle\phi\rangle_t = \int_{\mathscr{M}} \big(\phi \circ S^t\big)(X)\ f_0(X)J^{-t}(S^t X)J^t(X)\,\mathrm{d}X = \langle\phi \circ S^t\rangle_0 \tag{4.65}$$

4.4.1 Ergodicity and Mixing

Let us recall some notion concerning invariant probability distributions. Let μ be one such distribution. Then, the following statements are equivalent:

E1. For every integrable phase function one has $\overline{\phi}(\Gamma) = \langle\phi\rangle_\mu$, where $\langle\phi\rangle_\mu \equiv \int \phi\ \mathrm{d}\mu$, except for a set of vanishing μ probability;

E2. Except for a set of vanishing μ probability, $\tau_E(\Gamma) = \mu(E)$, where $E \subset \mathscr{M}$ is a μ-measurable set and

$$\tau_E(\Gamma) = \lim_{t\to\infty} \frac{1}{t}\int_0^t \chi_E\,(S^s\Gamma)\,\mathrm{d}s\ ; \quad \text{with } \chi_E\,(\Gamma) = \begin{cases} 1 & \text{if } \Gamma \in E \\ 0 & \text{else} \end{cases} \tag{4.66}$$

is the the mean time in E;

E3. Let ϕ be μ-integrable and let $\phi(S^t\Gamma) = \phi(\Gamma)$ for all t and all Γ. Then $\phi(\Gamma) = C$ μ-almost everywhere, for a given $C \in \mathbb{R}$;

E4. The dynamical system $(S, \mathscr{M}, \mu)$ is *metrically indecomposable*, i.e. given the invariant set E (which means $S^{-t}E = E$), either $\mu(E) = 0$ or $\mu(E) = 1$.

We call *ergodic* the dynamical systems that verify these statements.

Remark. Ergodicity is a very strong property becasue ϕ can be any integrable function. Physics needs much less; only several phase variables are physically relevent.

The following statments are equivalent too:

M1. For every pair of measurable sets $D, E \subset \mathscr{M}$ one has:

$$\lim_{t\to\infty} \mu\left(S^{-t}D \cap E\right) = \mu(D)\mu(E) \tag{4.67}$$

M2. For all $\phi, \psi \in L_2(\mathscr{M}, \mu)$ the following holds:

$$\lim_{t\to\infty} \left\langle \left(\phi \circ S^t\right) \psi \right\rangle_\mu = \langle \phi \rangle_\mu \langle \psi \rangle_\mu \tag{4.68}$$

We call *mixing* the dynamical systems that verify these two statements. Mixing is an even stronger property than ergodicity, in the sense that mixing systems are also ergodic, whereas not all ergodic systems are mixing.

For mixing Hamiltonian dynamics one can prove that an initial state characterized by a probability density f_0 eventually converges to the *microcanonical* ensemble. Indeed, for every square integrable phase function ϕ, one can write:

$$\begin{aligned} \langle \phi \rangle_t &= \int \phi(\Gamma) f_t(\Gamma) \mathrm{d}\Gamma \\ &= \int \phi(\Gamma) \left(f_0 \circ S^{-t}\right)(\Gamma) \mathrm{d}\Gamma = \int \left(\phi \circ S^t\right)(\Gamma) f_0(\Gamma) \mathrm{d}\Gamma \end{aligned} \tag{4.69}$$

The equalities in (4.69) are due to the fact that the Hamiltonian dynamics preserve phase space volumes. Now, assuming that the uniform distribution $\mathrm{d}\Gamma$ is normalized, $\int \mathrm{d}\Gamma = 1$, the mixing condition implies that the last integral obeys

$$\lim_{t\to\infty} \left\langle \left(\phi \circ S^t\right) f_0 \right\rangle_{\mathrm{d}\Gamma} = \langle \phi \rangle_{\mathrm{d}\Gamma} \langle f_0 \rangle_{\mathrm{d}\Gamma} = \langle \phi \rangle_{\mathrm{d}\Gamma} \cdot 1 = \langle \phi \rangle_{\mathrm{d}\Gamma} \tag{4.70}$$

which is the convergence to the microcanonical average for all phase functions.

Remark. This proof is deceitfully simple. In general, convergence to a steady state is quite hard to prove. Although it is a very strong property, in general mixing does not suffice to prove convergence to a steady state, because it amounts to the decay in time of the microscopic correlations within already stationary macroscopic states.

4.5 Linear Response

Let us address the problem of the response of a given system to external actions. As an example, consider a system of N particles in contact with a thermal bath at inverse temperature β, and the following Hamiltonian:

$$H(\Gamma) = H_0(\Gamma) + \lambda A(\Gamma) \,, \tag{4.71}$$

where λ is a small parameter and A perturbs the canonical equilibrium expressed by $f_0 = \exp(-\beta H_0)/\int \mathrm{d}\Gamma \exp(-\beta H_0)$. After some time, a new canonincal equilibrium is established which, to the first order in λ, is given by:

$$f = \frac{e^{-\beta H_0} e^{-\beta\lambda A}}{\int \mathrm{d}\Gamma e^{-\beta H_0} e^{-\beta\lambda A}} = \frac{e^{-\beta H_0}\left[1 - \beta\lambda A + O(\beta^2\lambda^2 A^2)\right]}{\int \mathrm{d}\Gamma e^{-\beta H_0}\left[1 - \beta\lambda A + O(\beta^2\lambda^2 A^2)\right]}$$
$$\simeq f_0 \frac{1 - \lambda\beta A}{1 - \lambda\beta \langle A\rangle_0} \simeq f_0(\Gamma)\left[1 - \lambda\beta\left(A(\Gamma) - \langle A\rangle_0\right)\right] \tag{4.72}$$

where, $\langle\cdot\rangle_0$ denotes averaging with respect to f_0. The effect of the perturbation on a given observable ϕ, is then expressed by:

$$\langle\phi\rangle - \langle\phi\rangle_0 = \int \mathrm{d}\Gamma \phi(\Gamma)\left[f(\Gamma) - f_0(\Gamma)\right] \simeq -\lambda\beta\left[\langle\phi A\rangle_0 - \langle\phi\rangle_0\langle A\rangle_0\right] \tag{4.73}$$

which is the correlation of the observble ϕ with the perturbation A, with respect to the state expressed by f_0. Taking $\phi = A = H_0$, one obtains an expression for the heat capacity at constant volume C_V, which expresses the response of the system to temperature variations. Indeed, defining C_V as

$$C_V = \frac{\partial\langle H_0\rangle_0}{\partial T} = \frac{\mathrm{d}\beta}{\mathrm{d}T}\frac{\partial\langle H_0\rangle_0}{\partial\beta} = \frac{\langle H_0^2\rangle_0 - \langle H_0\rangle_0^2}{k_{_B} T^2} \tag{4.74}$$

one obtains:

$$\frac{\partial\langle H_0\rangle}{\partial\beta} = \lim_{\lambda\to 0}\frac{\langle H_0\rangle - \langle H_0\rangle_0}{\lambda\beta} = -\left[\langle H_0^2\rangle_0 - \langle H_0\rangle_0^2\right] = -k_{_B} T^2 C_V \tag{4.75}$$

More in general, consider time dependent perturbations of form $-\mathscr{F}(t)A(\Gamma)$:

$$H(\Gamma, t) = H_0(\Gamma) - \mathscr{F}(t)A(\Gamma) \tag{4.76}$$

and split the corresponding evolution operator in two parts:

$$i\mathscr{L}_0 f = \{f, H_0\}\ , \quad i\mathscr{L}_{\mathrm{ext}}(t) f = -\mathscr{F}(t)\{f, A\} \tag{4.77}$$

where $\{\cdot\}$ are the Poisson brackets. One has $i\mathscr{L}_0 f_0 = 0$, which means that f_0 is invariant for the unperturbed dynamics. Then, the solution of the Liouville equation

$$\frac{\partial f}{\partial t} = -i\left(\mathscr{L}_0 + \mathscr{L}_{\mathrm{ext}}(t)\right) f \tag{4.78}$$

can be expressed by:

$$f_t(\Gamma) = e^{it\mathscr{L}_0} f_0(\Gamma) - i\int_0^t \mathrm{d}t' e^{-i(t-t')\mathscr{L}_0}\mathscr{L}_{\mathrm{ext}}(t') f_{t'}(\Gamma)$$
$$= f_0(\Gamma) - i\int_0^t \mathrm{d}t' e^{-i(t-t')\mathscr{L}_0}\mathscr{L}_{\mathrm{ext}}(t') f_0(\Gamma) + \text{higher order in } \mathscr{L}_{\mathrm{ext}} \tag{4.79}$$

as proved by inspection. If the deviations from the unperturbed system are considered small, the higher orders in $\mathscr{L}_{\text{ext}}$ can be omitted. Then Eq. (4.73) implies:

$$\langle \phi \rangle_t - \langle \phi \rangle_0 \simeq \int \mathrm{d}\Gamma \phi(\Gamma) \int_0^t \mathrm{d}t' e^{-i(t-t')\mathscr{L}_0} \mathscr{F}(t') \{ f_0, A \} \tag{4.80}$$

where

$$\{ f_0, A \} = \{ H_0, A \} \frac{\partial f_0}{\partial H_0} = \beta f_0 \frac{\mathrm{d}A}{\mathrm{d}t} \tag{4.81}$$

Eventually, one obtains:

$$\langle \phi \rangle_t - \langle \phi \rangle_0 \simeq \int_0^t \mathrm{d}t' R(t-t') \mathscr{F}(t') \tag{4.82}$$

where $R(t)$ is the response function:

$$R(t) = \beta \left\langle \dot{A} \left(\phi \circ S^t \right) \right\rangle_0 = \beta \int \mathrm{d}\Gamma f_0(\Gamma) \frac{\mathrm{d}A}{\mathrm{d}t}(\Gamma) e^{it\mathscr{F}_0} \phi(\Gamma) \tag{4.83}$$

Once again, the macroscopic nonequilibrium behaviour of a given system has been related solely to the correlations of microscopic fluctuating quantities, computed with respect to the relevant equilibrium ensemble.

Equation (4.82) suggests that even the linear response is in general affected by memory effects. From this point of view, the Markovian behaviour seems to be either very special or a crude approximation, implying, for instance, that all nonequilibrium fluids have a viscoelastic behaviour. In practice, however, in normal fluids and normal conditions the memory terms decay exponetially fast, so that the Markovian approximation is by and large justified. The viscoelastic behaviour is indeed noticeable only in complex fluids or under extreme conditions, i.e. exceedingly far from equilibrium.

Question. Can this formalism be extended to perturbations of nonequilibrium steady states? For instance, to steady states whose dynamics is dissipative, hence not Hamiltonian, as in the important case of viscous hydrodynamics [4]?

Recently, it has been shown that the approach we have outlined does indeed apply, if the steady state is represented by a regular probability density, as commonly happens in the presence of noise, cf. Refs. [4, 28].

Differently, the invariant phase space probability distribution of a dissipative system μ, say, is typically singular and supported on a fractal attractor. Consequently, it is not obvious anymore that the statistical features induced by a perturbation can be related to the unperturbed statistics. The reason is that even very small perturbations may lead to microscopic states whose probability vanishes in the unperturbed state μ. In such a case, the information contained in μ is irrelevant.

Indeed, Ruelle [52] showed that in certain cases[10] a perturbation $\delta\Gamma$ about a microstate Γ and its evolution $S^t\delta\Gamma$ can be decomposed in two parts, $(S^t\delta\Gamma)_\parallel$ and $(S^t\delta\Gamma)_\perp$, respectively perpendicular and parallel to the fibres of the attractor:

$$S^t\delta\Gamma = (S^t\delta\Gamma)_\parallel + (S^t\delta\Gamma)_\perp$$

The first addend can be related to the dynamics on the attractor, while the second may not.

Later, it has been pointed out [53] that this difficulty should not concern the systems of many interacting particles which are of statistical mechanics interest. In those cases, rather than the full phase space, one considers the much lower dimensional projections, afforded by a few physically relevant observables. Hence, one is typically interested in the marginals of singular phase space measures, on spaces of sufficiently lower dimension, which are usually regular [54, 55]. These facts can be briefly recalled as follows. Ruelle showed that the effect of a perturbation $\delta F(t) = \delta F_\parallel(t) + \delta F_\perp(t)$ on the response of a generic (smooth enough) observable ϕ is given by:

$$\langle\phi\rangle_t - \langle\phi\rangle_0 = \int_0^t R_\parallel^{(\phi)}(t-\tau)\delta F_\parallel(\tau)d\tau + \int_0^t R_\perp^{(\phi)}(t-\tau)\delta F_\perp(\tau)d\tau \qquad (4.84)$$

where the subscript 0 denotes averaging with respect to μ, $R_\parallel^{(\phi)}$ may be expressed in terms of correlation functions evaluated with respect to μ, while $R_\perp^{(\phi)}$ depends on the dynamics along the stable manifold, hence it may not.

Let us adopt the point of view of Ref. [53]. For a d-dimensional dissipative dynamical system consider, for simplicity, an impulsive perturbation $\Gamma \to \Gamma + \delta\Gamma$, such that all components of $\delta\Gamma$ vanish except one, denoted by $\delta\Gamma_i$. The probability distribution μ is correspondingly shifted by $\delta\Gamma$, and turns into a non-invariant distribution μ_0, whose evolution μ_t tends to μ in the $t \to \infty$ limit. For every measurable set $E \subset \mathscr{M}$, $\mu_0(E)$ is given by $\mu(E - \delta\Gamma)$,[11] and $\mu_t(E)$ is computed as explained in Sect. 4.4. Taking $\phi(\Gamma) = \Gamma_i$, one obtains:

$$\langle\Gamma_i\rangle_t - \langle\Gamma_i\rangle_0 = \int \Gamma_i \, \mathrm{d}\mu_t(\Gamma) - \int \Gamma_i \, \mathrm{d}\mu(\Gamma) \qquad (4.85)$$

Approximate the singular μ by means of piecewise constant distributions, introducing an ϵ-partition made of a finite set of d-dimensional hypercubes $\Lambda_k(\epsilon)$ of side ϵ and centers Γ_k. We define an ϵ-approximation of μ and of μ_t in terms of the probabilities $P_k(\epsilon)$ and $P_{t,k}(\epsilon;\delta\Gamma)$ of the hypercubes $\Lambda_k(\epsilon)$:

$$P_k(\epsilon) = \int_{\Lambda_k(\epsilon)} \mathrm{d}\mu(\Gamma) \,, \quad P_{t,k}(\epsilon) = \int_{\Lambda_k(\epsilon)} \mathrm{d}\mu_t(\Gamma) \,. \qquad (4.86)$$

[10] Concerning certain smooth, uniformly hyperbolic dynamical systems.

[11] The set $E - \delta\Gamma$ is defined by $\{\Gamma \in \mathscr{M} : \Gamma + \delta\Gamma \in E\}$.

This yields the coarse grained invariant density $\rho(\Gamma;\epsilon)$:

$$\rho(\Gamma;\epsilon) = \sum_k \rho_k(\Gamma;\epsilon)\ , \quad \text{with} \quad \rho_k(\Gamma;\epsilon) = \begin{cases} P_k(\epsilon)/\epsilon^d & \text{if } x \in \Lambda_k(\epsilon) \\ 0 & \text{else} \end{cases} \tag{4.87}$$

If Z_i is the number of one-dmensional bins of form $\left[\Gamma_i^{(q)} - \epsilon/2, \Gamma_i^{(q)} + \epsilon/2\right)$, $q \in \{1, 2, \ldots, Z_i\}$, in the i-th direction, marginalizing the approximate distribution yields the following quantities:

$$p_i^{(q)}(\epsilon) = \int_{\Gamma_i^{(q)} - \frac{\epsilon}{2}}^{\Gamma_i^{(q)} + \frac{\epsilon}{2}} \left\{ \int \rho(\Gamma;\epsilon) \prod_{j \neq i} \mathrm{d}\Gamma_j \right\} \mathrm{d}\Gamma_i \tag{4.88}$$

Each of them is the invariant probability that the coordinate Γ_i of Γ lie in one of the Z_i bins. Similarly, one gets the marginal of the evolving approximate probability $p_{t,i}^{(q)}(\epsilon)$. In both cases, dividing by ϵ, one obtains the coarse grained marginal probability densities $\rho_i^{(q)}(\epsilon)$ and $\rho_{t,i}^{(q)}(\epsilon)$, as well as the ϵ-approximate response function:

$$B_i^{(q)}(\Gamma_i, \delta\Gamma, t, \epsilon) = \frac{1}{\epsilon}\left[p_{t,i}^{(q)}(\epsilon) - p_i^{(q)}(\epsilon)\right] = \rho_{t,i}^{(q)}(\epsilon) - \rho_i^{(q)}(\epsilon) \tag{4.89}$$

Reference [53] shows that the right hand side of Eq. (4.89) tends to a regular function of Γ_i under the $Z_i \to \infty, \epsilon \to 0$ limits. Consequently, $B_i^{(q)}(\Gamma_i, \delta\Gamma, t, \epsilon)$ yields an expression similar to that of standard response theory, in the sense that it depends solely on the unperturbed state, although that is supported on a fractal set. There are exceptions to this conclusion, most notably those discussed by Ruelle. But for systems of many interacting particles this is the expected result. The idea is that the projection procedure makes unnecessary the explicit calculation of $R_\perp^{(\phi)}$ in Eq. (4.84). This does not mean that $R_\perp^{(\phi)}$ is necessarily negligible [56]. However, apart from peculiar situations, it does not need to be explicitly computed and the response may be referred only to the unperturbed dynamics, as in the standard theory.

4.6 Onsager-Machlup: Response from Small Deviations

The classical theory of fluctuations was developed by Onsager and Machlup [14] and Machlup and Onsager [15] in order to quantify the probability of temporal fluctuations paths, and not just of fluctuation values. Their theory is based on the following assumptions:

A1. Onsager regression hyptothesis: the decay of a system from a nonequilibrium state produced by a spontaneous fluctuation obeys on average the macroscopic law describing the decay from the same state produced by a macroscopic constraint that has been suddenly removed;

A2. The observables and the random forces are Gaussian random variables (i.e. their probability density of m values taken at m consecutive instants of time is an m-dimensional Gaussian);

A3. The probability density $P(\Gamma)$ of the microstate Γ obeys Boltzmann's principle:

$$k_B \log P(\Gamma) = \mathscr{S}(\Gamma) + \text{const} \tag{4.90}$$

A4. The state $S^t\Gamma$ is statistically independent of the state $S^{t'}\Gamma$ for $|t - t'| > \tau_d$, τ_d being the very short decorrelation time[12];

A5. The microscopic dynamics is time reversal invariant;

A6. The vector of observables $\alpha = (\alpha_1, \ldots, \alpha_n)$ is chosen so that its evolution is Markovian. This is possible if n is neither too small nor too large. This choice is system dependent and must satisfy the following criteria

- Each component α_i of α must represent a macroscopic quantity referring to a subsystem containing very many particles;
- α_i must be an algebraic sum of molecular variables, so that by the Central Limit Theorem its fluctuations (not the large deviations) are Gaussians centered on its average (equilibrium) value;
- α_i must be an even function of the molecular variables that are odd under time reversal (a manifestation of the microscopic time reversal invariance);

A7. The system is in local thermodynamic equilibrium;

A8. The fluxes $\dot{\alpha}_i$ depend linearly on the thermodynamic forces X_i:

$$\dot{\alpha}_i = \sum_{j=1}^{n} L_{ij} X_j \ , \qquad X_i = \sum_{j=1}^{n} R_{ij} \dot{\alpha}_j \ ; \tag{4.91}$$

A9. The process is stationary: i.e. given the times $t_1, t_2, \ldots, t_p$ and the n-dimensional vectors $\alpha^{(1)}, \alpha^{(2)}, \ldots, \alpha^{(p)}$, the probabilities $F_{i,p}$, $i = 1, \ldots, n$, that each component of the observable vector is smaller by value than the corresponding component of the vector sequence $\alpha^{(k)}$ at the corresponding times t_k satisfy:

[12] Onsager and Machlup observe that (cf. Footnote 2 of Ref. [14]): *"This statement is, of course, charged with meaning, and requires elaborate precautions about ergodicity, etc. It may be said to hold for systems which 'forget' their initial states in a 'reasonably' short time. It is, however, precisely the choice of time scale that matters. In a sufficiently long time, all physical systems 'forget'."*

$$F_{i,p}\left(\alpha_i \leq \alpha_i^{(k)}, t_k, k = 1, \ldots, p\right) = F_{i,p}\left(\alpha_i \leq \alpha_i^{(k)}, t_k + \tau, k = 1, \ldots, p\right) \tag{4.92}$$

for all τ and, analogously, the corresponding probability densities $f_{i,p}$, satisfy

$$f_{i,p}\left(\alpha_i = \alpha_i^{(k)}, t_k, k = 1, \ldots, p\right) = f_{i,p}\left(\alpha_i = \alpha_i^{(k)}, t_k + \tau, k = 1, \ldots, p\right) \tag{4.93}$$

where

$$F_{i,p}\left(\alpha_i \leq \alpha_i^{(k)}, t_k, k = 1, \ldots, p\right) = \int_{-\infty}^{\alpha_i^{(1)}} \mathrm{d}\alpha_i^{(1)} \cdots \int_{-\infty}^{\alpha_i^{(p)}} \mathrm{d}\alpha_i^{(p)} f_{i,p}\left(\alpha_i = \alpha_i^{(k)}, t_k, k = 1, \ldots, p\right) \tag{4.94}$$

For simplicity, let α be the vector of the deviations from the equilibrium values. Then, the entropy $\mathscr{S}$ is a function of the observables α, which can be expanded about its equilibrium value $\mathscr{S}_0$ as:

$$\mathscr{S} = \mathscr{S}_0 - \frac{1}{2}\sum_{i,j=1}^{n} s_{ij}\alpha_i\alpha_j + \text{higher order in } \alpha \tag{4.95}$$

There is no linear term in α because $\mathscr{S}_0$ is the maximum of $\mathscr{S}$. Correspondingly, the thermodynamic forces are expressed (to the same order of approximation) by

$$X_i = \frac{\partial \mathscr{S}}{\partial \alpha_i} = -\sum_{j=1}^{n} s_{ij}\alpha_j\,, \qquad i = 1, \ldots, n \tag{4.96}$$

which implies

$$\sum_{j=1}^{n}\left[R_{ij}\dot{\alpha}_j + s_{ij}\alpha_j\right] = 0\,, \qquad i = 1, \ldots, n \tag{4.97}$$

To compute the evolution of the state α, we may introduce a function Φ depending on the rate of change of the state and another, Ψ, depending on the state itself or, equivalently because of Eq. (4.96), on the thermodynamic forces:

$$\Phi\left(\dot{\alpha}, \dot{\beta}\right) = \frac{1}{2}\sum_{i,j=1}^{n} R_{ij}\dot{\alpha}_i\dot{\beta}_j\,, \quad \Psi(X, Y) = \frac{1}{2}\sum_{i,j=1}^{n} L_{ij}X_iX_j \tag{4.98}$$

These functions characterize the real evolution when $\dot{\alpha} = \dot{\beta}$ are the real evolving fluxes and when $X = Y$ are the real thermodynamic forces, in which case one has:

$$\dot{\mathscr{S}} = 2\Phi\left(\dot{\alpha}, \dot{\alpha}\right) = 2\Psi\left(X, X\right) \tag{4.99}$$

Nonetheless they are defined for other evolutions as well. In particular, if the molecular chaos is accounted for by the following random perturbation of Eq. (4.97),

$$\sum_{j=1}^{n} \left[R_{ij}\dot{\alpha}_j + s_{ij}\alpha_j \right] = \epsilon_i \ , \quad \langle \epsilon_i \rangle = 0 \ , \qquad i = 1, \ldots, n \tag{4.100}$$

where ϵ_i is a random force which allows different paths with different probabilities and which does no net work, Φ and Ψ are defined for those paths. Assumption **A2** here is used to express the statistics of the ϵ_i's. Assumption **A5** is used to exclude rotating systems and external magnetic fields, which would imply further terms, and later an asymmetry e.g. in the transition probabilities. Assumption **A7** allows us to consider the thermodynamic quantities $\alpha, \dot{\alpha}$ etc.

Let $f_{i,1}\left(\alpha_i^{(1)}, t_1\right)$ be the probability density for the i-th observable to take values close to $\alpha_i^{(1)}$ at time t_1. By assumptions **A1** and **A3**, it is independent of t_1. Let $f_{i,1}\left(\alpha_i^{(k)}, t_k | \alpha_{i-1}^{(k-1)}, t_{k-1}\right)$ be the conditional probability density for the i-th observable to take values close to $\alpha_i^{(k)}$ at time t_k, given that it was $\alpha_{i-1}^{(k-1)}$ at time t_{k-1}. Because of the Markov property **A6**, which makes use of **A4**, and becasue of **A3**, one thus has:

$$\begin{aligned} & f_{i,p}\left(\alpha_i = \alpha_i^{(k)}, t_k, k = 1, \ldots, p\right) \\ & \quad = f_{i,1}\left(\alpha_i^{(p)}, t_p | \alpha_{i-1}^{(p-1)}, t_{p-1}\right) \cdots f_{i,1}\left(\alpha_i^{(2)}, t_2 | \alpha_i^{(1)}, t_1\right) f_{i,1}\left(\alpha_i^{(1)}, t_1\right) \qquad (4.101) \\ & \quad = f_{i,1}\left(\alpha_i^{(p)}, t_p | \alpha_{i-1}^{(p-1)}, t_{p-1}\right) \cdots f_{i,1}\left(\alpha_i^{(2)}, t_2 | \alpha_i^{(1)}, t_1\right) e^{\mathscr{S}(\alpha^{(1)})/k_B} \qquad (4.102) \end{aligned}$$

with the constraints

$$\lim_{\tau \to 0} f_{i,1}\left(\alpha_i, t_1 + \tau | \alpha_i^{(1)}, t_1\right) = K\delta\left(\alpha - \alpha^{(1)}\right) \tag{4.103}$$

because $\tau \to 0$ is the limit in which α deterministically approaches $\alpha^{(1)}$, and

$$\lim_{\tau \to \infty} f_{i,1}\left(\alpha_i, t_1 + \tau | \alpha_i^{(1)}, t_1\right) = e^{\mathscr{S}(\alpha^{(1)})/k_B} \tag{4.104}$$

because of the correlations loss **A4** between the times t_1 and $t_1 + \tau$, and because of **A3**. Solving the Langevin equation (4.100), $f_{i,1}\left(\alpha_i, t_1 + \tau | \alpha_1^{(1)}, t_1\right)$ can be explicitly given. For ease of explications, let us now refer to the case with $n = 1$, the general case being trivially related to that. We then consider the equation:

$$R\dot{\alpha} + s\alpha = \epsilon \tag{4.105}$$

which leads to

$$f_1\left(\alpha, t+u|\alpha^{(0)}, t\right) = \frac{s\exp\left\{-\frac{s\left(\alpha-\alpha^{(0)}e^{-su/R}\right)^2}{2k_B\left(1-e^{-2su/R}\right)}\right\}}{\sqrt{2\pi}k_B\sqrt{1-e^{-2su/R}}} \tag{4.106}$$

With this information and with Ito's discretization convention:

$$R\frac{\alpha^{(k)}-\alpha^{(k-1)}}{\delta\tau}+s\alpha^{(k-1)}=\epsilon(t_k)\,,\quad \text{i.e. } \alpha^{(k)}-\left(1-\frac{s\delta\tau}{R}\right)\alpha^{(k-1)}=\frac{\delta\tau}{R}\epsilon(t_k) \tag{4.107}$$

substituting in Eq. (4.102), with fixed α and $\alpha^{(0)}$, and recalling **A4**, **A6**, one eventually obtains:

$$f_1\left(\alpha, t+\tau|\alpha^{(0)}, t\right) = \left(\frac{1}{2k_B}\right)^p\left(\frac{sR}{\pi\delta\tau}\right)^{p/2}\times$$

$$\int \mathrm{d}\alpha^{(1)}\cdots\int \mathrm{d}\alpha^{(p)}\exp\left\{-\frac{R}{4k_B}\sum_{k=1}^{p}\left[\dot{\alpha}^{(k)}+\frac{s}{R}\alpha^{(k+1)}\right]^2\delta\tau\right\} \tag{4.108}$$

$$\tag{4.109}$$

Under the $p\to\infty$, $\delta\tau\to 0$ limits, with $\tau = p\delta\tau$, the sum in the exponential tends to the integral along the path:

$$\int_t^{t+\tau}\left[\dot{\alpha}(t')+\frac{s}{R}\alpha(t')\right]^2\mathrm{d}t' \tag{4.110}$$

which must be minimized to find the most likely path. Analogously, the n-dimensional case, after diagonalization, yields

$$\Phi\left(\dot{\alpha},\dot{\alpha}\right)=\frac{1}{2}\sum_{i=1}^{n}R_i\alpha_i^2\,;\quad \Psi\left(X,X\right)=\frac{1}{2}\sum_{i=1}^{n}\frac{1}{R_i}X_i^2=\frac{1}{2}\sum_{i=1}^{n}\frac{s_i^2}{R_i}\alpha_i^2 \tag{4.111}$$

and the integral to be minimized to achieve the maximum probability is

$$\int_t^{t+\tau}\sum_{i=1}^{n}\left[\dot{\alpha}_i(t')+\frac{s_i}{R_i}\alpha_i(t')\right]^2\mathrm{d}t'. \tag{4.112}$$

The integrand can be expressed as

$$\mathscr{L}\left(\alpha,\dot{\alpha}\right)=2\Phi\left(\dot{\alpha},\dot{\alpha}\right)-2\dot{\mathscr{S}}(\alpha)+2\Psi\left(X(\alpha),X(\alpha)\right) \tag{4.113}$$

and the path of minimum integral follows from the standard Lagrangian formalism:

$$\frac{\mathrm{d}}{\mathrm{d}t}\frac{\partial \mathscr{L}}{\partial \dot{\alpha}} - \frac{\partial \mathscr{L}}{\partial \alpha} = 0\,, \quad \text{which yields} \quad R_j \ddot{\alpha}_j - \frac{s_j^2}{R_j}\alpha_j = 0\,, \quad j = 1, \ldots, n \tag{4.114}$$

Interestingly, each of the n 2nd order differential equations (4.114) is equivalent to two first order equations. Indeed, their general solution

$$\alpha_j(t) = C_{j1}\, e^{-s_j t/R_j} + C_{j2}\, e^{s_j t/R_j} \tag{4.115}$$

requires $C_{j2} = 0$ when the $t \to \infty$ limit is considered – in which case we have the relaxation to equilibrium from a nonequilibrium initial condition – while it requires $C_{j1} = 0$ when the previous history, beginning with a previous equilibrium state at $t = -\infty$, is considered. But then, one may think of the first case as a solution of the differential equation

$$\dot{\alpha}_j + \frac{s_j}{R_j}\alpha_j = 0 \tag{4.116}$$

and the second case as corresponding to

$$\dot{\alpha}_j - \frac{s_j}{R_j}\alpha_j = 0\,. \tag{4.117}$$

We thus have two possible evolutions, which are symmetric under time reversal: one describes the relaxation to equilibrium, in accord with the hydrodynamic laws; the other treats fluctuations away from the equilibrium, and is the first example of the so-called *adjoint hydrodynamics* [57]. In the large n limit, the most probable path becomes the only path of positive probability. Therefore, Onsager and Machlup obtained a justification of hydrodynamics for macroscopic systems, starting from a mesoscopic description, in which the molecular chaos appears in the form of noise.

Remark. Because these results are crucially based on the Gaussian distributions, they are restricted to small deviations, from which the linear response about equilibrium states can be properly derived.

Considering large, rather than small deviations, this theory has been generalized to fluctuations about nonequilibrium steady states and which are not symmetric under time reversal [57]. This lack of symmetry has been interpreted as the cause of macroscopic irreversibility. For dissipative deterministic particle systems, that are time reversal invariant, it has been shown that similar asymmetries may arise, when particles interact [58]. This confirms the importance of microscopic interactions for the irreversible macroscopic behaviour.

4.7 Fluctuation Relations: Response from Large Deviations

In 1993, the paper [35] addressed the question of the fluctuations of the entropy production rate in a pioneering attempt towards a unified theory of a wide range of nonequilibrium phenomena. In particular, a *Fluctuation Relation* (FR) was there derived and tested. Obtained on purely dynamical grounds, it constitutes one of the few general exact results for systems almost arbitrarily far from equilibrium, while close to equilibrium it is consistent with the Green-Kubo and Onsager relations. This FR reads:

$$\frac{\mathrm{Prob}_\tau(\sigma \approx A)}{\mathrm{Prob}_\tau(\sigma \approx -A)} = e^{\tau A} \tag{4.118}$$

where A and $-A$ are average values of the normalized power dissipated in a driven system, denoted by σ, in a long time τ, and $\mathrm{Prob}_\tau(\sigma \approx \pm A)$ is the steady state probability of observing values close to $\pm A$.

Remark. Because this relation holds asymptotically in the observation time τ, it constitutes a *large deviation* result: for large τ, any $A \neq \langle\sigma\rangle$ lies many standard deviations away from the mean. In other words, it corresponds to a large (macroscopic) deviation from the macroscopically observable value $\langle\sigma\rangle$. The standard deviation typically shrinks as $O(\tau^{-1/2})$ with τ.

The FR (4.118) was derived for the following *time reversal invariant dissipative isoenergetic* model of a 2-dimensional shearing fluid:

$$\begin{cases} \dfrac{d}{dt}\mathbf{q}_i = \dfrac{\mathbf{p}_i}{m} + \gamma\, y_i \hat{\mathbf{x}} \\ \dfrac{d}{dt}\mathbf{p}_i = \mathbf{F}_i(\mathbf{q}) + \gamma p_i^{(y)} \hat{\mathbf{x}} - \alpha_{th}\mathbf{p}_i \end{cases} \tag{4.119}$$

where γ is the shear rate in the y direction, $\hat{\mathbf{x}}$ is the unit vector in the x-direction, and the friction term α_{th}, called "thermostat" , takes the form

$$\alpha_{th}(\Gamma) = -\frac{\gamma}{\sum_{i=1}^N \mathbf{p}_i^2} \sum_{i=1}^N p_i^{(x)} p_i^{(y)} \tag{4.120}$$

as prescribed by Gauss' principle of least constraint, in order to keep fixed the internal energy $H_0 = \Phi^{\mathrm{WCA}} + K$, where Φ^{WCA} is the potential by which particles interact, which was assumed to be the so-called WCA-potential [59], and K is the kinetic energy of the system.

This molecular dynamics model was chosen by the authors of [35] because its phase space expansion rate Λ is proportional to α_{th}. Hence a dynamical quantity, which can be expressed in terms of the probability distribution in the phase space,

could be related to the irreversible entropy production or, alternatively, to the energy dissipation rate divided by $\sum \mathbf{p}_i^2$. The FR is parameter-free and, being dynamical in nature, it applies almost arbitrarily far from equilibrium as well as to small systems. This makes the FR a milestone of contemporary nonequilibrium statistical mechanics.

Gallavotti and Cohen accurately delineated the mathematical context in which the result of [35] had been framed, introducing the Chaotic Hypothesis [38, 39, 60, 61]:

Chaotic Hypothesis: *A reversible many-particle system in a stationary state can be regarded as a transitive Anosov system for the purpose of computing its macroscopic properties.*

Anosov systems can indeed be proven to have probability distributions of the kind assumed in [35]. The result is a steady state FR for the fluctuations of Λ, which we call Λ-FR and which will be described below. As the Anosov property practically means a high degree of randomness, analogous results have been obtained first for finite state space Markov chains and later for many other stochastic processes [62–64]. Stochastic processes are easier to handle than deterministic dynamics, but ambiguities affect their observables, except for special cases. The reader is addressed to the numerous existing review papers, such as Refs. [3, 4, 34]. We focus now on some specific results for deterministic dynamics.

4.7.1 The Gallavotti-Cohen Approach

The idea proposed by Gallavotti and Cohen is that dissipative, reversible, transitive Anosov maps, $S : \mathscr{M} \to \mathscr{M}$, are idealizations of nonequilibrium particle systems [39]. That the system evolves with discrete or continuous time was thought to be a side issue [39]. The Λ-FR for Anosov maps relies on time reversibility and on the fact that these dynamical systems admit arbitrarily fine *Markov* partitions [65]. These are subdivisions of $\mathscr{M}$ in cells with disjoint interiors and with boundaries forming invariant sets, which in two dimensions consist of pieces of stable and unstable manifolds. Gallavotti and Cohen further assumed that the dynamics is transitive, i.e. that a typical trajectory explores all regions of $\mathscr{M}$, as finely as one wishes. This structure justifies the probability (Lyapunov) weights of Eq. (1) in Ref. [35], from which the Λ-FR emerges.

Let the dynamics be given by $X_{k+1} = SX_k$ and introduce the phase space expansion rate $\Lambda(X) = \log J(X)$, where J is the Jacobian determinant of S. The dynamics is called *dissipative* if $\langle \Lambda \rangle < 0$, where $\langle . \rangle$ is the steady state phase space average. Then, consider the dimensionless phase space contraction rate e_τ, obtained along a trajectory segment $w_{X,\tau}$ with origin at $X \in \mathscr{M}$ and duration τ, defined by:

$$e_\tau(X) = \frac{1}{\tau \langle \Lambda \rangle} \sum_{k=-\tau/2}^{\tau/2-1} \Lambda(S^k X) \tag{4.121}$$

Let J^u be the Jacobian determinant of S restricted to the unstable manifold V^+, i.e. the product of the asymptotic separation factors of nearby points, along the directions in which distances asymptotically grow at an exponential rate. *If the system is Anosov*, the probability that $e_\tau(X) \in B_{p,\epsilon} \equiv (p-\epsilon, p+\epsilon)$ equals, in the fine Markov partitions and long τ limits, with the sum of weights of form

$$w_{X,\tau} = \prod_{k=-\tau/2}^{\tau/2-1} \frac{1}{J^u(S^k X)} \tag{4.122}$$

which are assigned to the cells containing the points X such that $e_\tau(X) \in B_{p,\epsilon}$. Then, denoting by $\pi_\tau(B_{p,\epsilon})$ the corresponding probability, one can write

$$\pi_\tau(e_\tau(X) \in B_{p,\epsilon}) \approx \frac{1}{M_\tau} \sum_{X: e_\tau(X) \in B_{p,\epsilon}} w_{X,\tau} \tag{4.123}$$

where M_τ is a normalization constant. *If the support of the physical measure is* $\mathscr{M}$, as in the case of moderate dissipation [66], time-reversibility and dissipation guarantee that the range of possible fluctuations includes a symmetric interval $[-p^*, p^*]$, with $p^* > 0$, and one can consider the ratio

$$\frac{\pi_\tau(B_{p,\epsilon})}{\pi_\tau(B_{-p,\epsilon})} \approx \frac{\sum_{X, e_\tau(X) \in B_{p,\epsilon}} w_{X,\tau}}{\sum_{X, e_\tau(X) \in B_{-p,\epsilon}} w_{X,\tau}} , \tag{4.124}$$

where each X in the numerator has a counterpart in the denominator. Denoting by I the involution which replaces the initial condition of a given trajectory with the initial condition of the reversed trajectory, time-reversibility yields:

$$\Lambda(X) = -\Lambda(IX) , \quad w_{IX,\tau} = w_{X,\tau}^{-1} \quad \text{and} \quad \frac{w_{X,\tau}}{w_{IX,\tau}} = e^{-\tau\langle\Lambda\rangle p} \tag{4.125}$$

if $e_\tau(X) = p$. Taking small ϵ in $B_{p,\epsilon}$, the division of each term in the numerator of (4.124) by its counterpart in the denominator approximately equals $e^{-\tau\langle\Lambda\rangle p}$, which then equals the ratio in (4.124). Therefore, in the limit of small ϵ, infinitely fine Markov partition and large τ, the authors of [39] obtain the following theorem:
Gallavotti-Cohen Theorem. *Let* $(\mathscr{M}, S)$ *be dissipative and reversible and assume that the chaotic hypothesis holds. Then, in the* $\tau \to \infty$ *limit, one has*

$$\frac{\pi_\tau(B_{p,\epsilon})}{\pi_\tau(B_{-p,\epsilon})} = e^{-\tau\langle\Lambda\rangle p} . \tag{4.126}$$

with an error in the argument of the exponential which can be estimated to be p- *and* τ*-independent.*

If the Λ-FR (hence the chaotic hypothesis on which it is based) holds, the function $C(p;\tau,\epsilon) = (1/\tau\langle -\Lambda\rangle)\log\left[\pi_\tau(B_{p,\epsilon})/\pi_\tau(B_{-p,\epsilon})\right]$ tends to a straight line of slope 1 for growing τ, apart from small errors. If Λ can be identified with a physical observable, the Λ-FR is a parameter-free statement about the physics of nonequilibrium systems. Unfortunately, Λ differs from the dissipated power in general, [43], hence alternative approaches have been developed.

4.7.2 Fluctuation Relations for the Dissipation Function

Question. If the FR has been observed to hold for the energy dissipation of a given system, which mechanisms are responsible for that?

In attempts to answer this question, various results have been achieved and others clarified. In particular:

1. Transient, or ensemble, FRs have been derived, which differ in nature from the steady state FRs;
2. Classes of infinitely many identities have been obtained to characterize equilibrium and nonequilibrum states;
3. A novel ergodic notion, now knonw as *t-mixing*, has been introduced;
4. A quite general response formula has been derived.

These further develoments originated with a paper by Evans and Searles [36], who proposed the first transient fluctuation relation for the *Dissipation Function* Ω, which is formally similar to Eq. (4.118). In states close to equilibrium, Ω can be identified with the *entropy production rate*, $\sigma = JVF^{ext}/k_B T$, where, J is the (intensive) flux due to the thermodynamic force F^{ext}, V and T are the volume and the kinetic temperature, respectively [36, 37]. This relation, called transient Ω-FR, is obtained under virtually no hypothesis, except for *time reversibility*; it is transient because it concerns non-invariant ensembles of systems, instead of the steady state. The approach stems from the belief that the complete knowledge of the invariant measure implied by the Chaotic Hypothesis is not required to understand the few properties of physical interest, like thermodynamic relations do not depend on the details of the microscopic dynamics [67].

Let $\mathscr{M}$ be the phase space of the system at hand, and $S^\tau : \mathscr{M} \to \mathscr{M}$ be a reversible evolution corresponding to $\dot{\Gamma} = F(\Gamma)$. Take a probability measure $d\mu_0(\Gamma) = f_0(\Gamma)d\Gamma$ on $\mathscr{M}$, and let the observable $\mathscr{O} : \mathscr{M} \to I\!R$ be odd with respect to the time reversal, i.e. $\mathscr{O}(I\Gamma) = -\mathscr{O}(\Gamma)$. Denote its time averages by

$$\overline{\mathscr{O}}_{t,t+\tau}(\Gamma) \equiv \frac{1}{\tau}\mathscr{O}_{t_0,t_0+\tau}(\Gamma) \equiv \frac{1}{\tau}\int_{t_0}^{t_0+\tau} \mathscr{O}(S^s\Gamma)ds\,. \tag{4.127}$$

For a density f_0 that is even under time reversal [$f_0(I\Gamma) = f_0(\Gamma)$], define the

Dissipation function:

$$\Omega(\Gamma) = -\frac{d}{d\Gamma}\ln f_0\Big|_{\Gamma}\cdot\dot{\Gamma} - \Lambda(\Gamma)\,, \quad \text{so that}$$
$$\overline{\Omega}_{t,t+\tau}(\Gamma) = \frac{1}{\tau}\left[\ln\frac{f_0(S^t\Gamma)}{f_0(S^{t+\tau}\Gamma)} - \Lambda_{t,t+\tau}\right] \tag{4.128}$$

For a compact phase space, the uniform density $f_0(\Gamma) = 1/|\mathscr{M}|$ implies $\Omega = \Lambda$, which was the case of the original FR. The existence of the logarithmic term in (4.128) is called *ergodic consistency*, a condition met if $f_0 > 0$ in all regions visited by all trajectories $S^t\Gamma$.

For $\delta > 0$, let $A_\delta^\pm = (\pm A - \delta, \pm A + \delta)$, and let $E(\mathscr{O} \in (a,b))$ be the set of points Γ such that $\mathscr{O}(\Gamma) \in (a,b)$. Then, we have $E(\overline{\Omega}_{0,\tau} \in A_\delta^-) = IS^\tau E(\overline{\Omega}_{0,\tau} \in A_\delta^+)$ and:

$$\frac{\mu_0(E(\overline{\Omega}_{0,\tau}\in A_\delta^+))}{\mu_0(E(\overline{\Omega}_{0,\tau}\in A_\delta^-))} = \frac{\int_{E(\overline{\Omega}_{0,\tau}\in A_\delta^+)} f_0(\Gamma)d\Gamma}{\int_{E(\overline{\Omega}_{0,\tau}\in A_\delta^+)} f_0(S^\tau X)e^{-\Lambda_{0,\tau}(X)}dX}$$
$$= \frac{\int_{E(\overline{\Omega}_{0,\tau}\in A_\delta^+)} f_0(\Gamma)d\Gamma}{\int_{E(\overline{\Omega}_{0,\tau}\in A_\delta^+)} e^{-\Omega_{0,\tau}(X)} f_0(X)dX} = \left\langle e^{-\Omega_{0,\tau}}\right\rangle^{-1}_{\overline{\Omega}_{0,\tau}\in A_\delta^+} \tag{4.129}$$

where by $\langle\cdot\rangle_{\overline{\Omega}_{0,\tau}\in A_\delta^+}$ we mean the average computed with respect to μ_0 under the condition that $\overline{\Omega}_{0,\tau} \in A_\delta^+$. This implies the

Transient Ω-FR:

$$\frac{\mu_0(E(\overline{\Omega}_{0,\tau}\in A_\delta^+))}{\mu_0(E(\overline{\Omega}_{0,\tau}\in A_\delta^-))} = e^{[A+\epsilon(\delta,A,\tau)]\tau}\,, \tag{4.130}$$

with $|\epsilon(\delta, A, \tau)| \le \delta$, an error term due to the finiteness of δ.

Remarks. (i) The transient Ω-FR refers to the non-invariant probability distribution μ_0. Time reversibility is basically the only ingredient of its derivation.

(ii) From an experimental point of view, its similarity with the steady state FR is deceitful: rather than expressing a statistical property of fluctuations of a given system, it expresses a property of the initial ensemble of identical systems.

(iii) In order for Ω to be the energy dissipation, f_0 has to be the equilibrium ensemble corresponding to the given dissipative dynamics, which is invariant when the forcing terms (but not the thermostats) are switched off.

(iv) Consequently, *the transient Ω-FR yields a property of the equilibrium state by means of nonequilibrium experiments.* This closes the circle with the FDR, which does the opposite.

The steady state Ω-FR requires further hypotheses. In the first place let averaging begin at time t, i.e. consider

$$\frac{\mu_0(E(\overline{\Omega}_{t,t+\tau} \in A_\delta^+))}{\mu_0(E(\overline{\Omega}_{t,t+\tau} \in A_\delta^-))} \,. \tag{4.131}$$

Taking $\hat{t} = t + \tau + t$, performing the transformation $\Gamma = IS^{\hat{t}}W$ in the integral defining $\mu_0(E(\overline{\Omega}_{t,t+\tau} \in A_\delta^-))$, with $W \in \mathscr{M}$, and doing some algebra yields:

$$\begin{aligned}\frac{\mu_0(E(\overline{\Omega}_{t,t+\tau} \in A_\delta^+))}{\mu_0(E(\overline{\Omega}_{t,t+\tau} \in A_\delta^-))} &= \left\langle \exp\left(-\Omega_{0,\hat{t}}\right)\right\rangle^{-1}_{\overline{\Omega}_{t,t+\tau} \in A_\delta^+} \\ &= e^{[A+\epsilon(\delta,t,A,\tau)]\tau} \left\langle e^{-\Omega_{0,t}-\Omega_{t+\tau,2t+\tau}}\right\rangle^{-1}_{\overline{\Omega}_{t,t+\tau} \in A_\delta^+} \end{aligned} \tag{4.132}$$

where $|\epsilon(\delta, t, A, \tau)| \leq \delta$. Here, the second line follows from the first because $\Omega_{0,\hat{t}} = \Omega_{0,t} + \Omega_{t,t+\tau} + \Omega_{t+\tau,\hat{t}}$, with the central contribution made approximately equal to A by the condition $\overline{\Omega}_{t,t+\tau} \in A_\delta^+$. Recall that $\mu_0(E) = \mu_t(S^t E)$, where μ_t is the evolved probability distribution, with density f_t. Then, taking the logarithm and dividing by τ Eq. (4.132) produces:

$$\begin{aligned}\frac{1}{\tau} \ln \frac{\mu_t(E(\overline{\Omega}_{0,\tau} \in A_\delta^+))}{\mu_t(E(\overline{\Omega}_{0,\tau} \in A_\delta^-))} &= \\ &= A + \epsilon(\delta, t, A, \tau) - \frac{1}{\tau} \ln \left\langle e^{-\Omega_{0,t}-\Omega_{t+\tau,2t+\tau}}\right\rangle_{\overline{\Omega}_{t,t+\tau} \in A_\delta^+} \\ &\equiv A + \epsilon(\delta, t, A, \tau) + M(A, \delta, t, \tau) \end{aligned} \tag{4.133}$$

because $E(\overline{\Omega}_{0,\tau}) = S^t E(\overline{\Omega}_{t,t+\tau})$.

If μ_t tends to a steady state μ_∞ when $t \to \infty$, the (exact) relation (4.133) should change from a statement on the ensemble f_t, to a statement on the statistics generated by a single typical trajectory. But to be of practical use, this identity requires $M(A, \delta, t, \tau)$ to behave properly. If in the steady state, i.e. after the $t \to \infty$ limit, $M(A, \delta, t, \tau)$ is negligible in the $\delta \to 0$ and $\tau \to \infty$ limits, one obtains the:
Steady State Ω-FR. *For any tolerance $\epsilon > 0$, there is a sufficiently small $\delta > 0$ such that*

$$\lim_{\tau\to\infty} \frac{1}{\tau} \ln \frac{\mu_\infty(E(\overline{\Omega}_{0,\tau} \in A_\delta^+))}{\mu_\infty(E(\overline{\Omega}_{0,\tau} \in A_\delta^-))} = A + \eta \,, \quad \textit{with} \;\; \eta \in (-\epsilon, \epsilon) \tag{4.134}$$

For this to be the case, one needs some assumption. Indeed, $M(A, \delta, t, \tau)$ could diverge with t, making fruitless the $\tau \to \infty$ limit. If on the other hand $M(A, \delta, t, \tau)$ remains bounded by a finite $M(A, \delta, \tau)$, $\lim_{\tau\to\infty} M(A, \delta, \tau)$ could still exceed ϵ.

The first difficulty is simply solved by the observation that the divergence of $M(A, \delta, t, \tau)$ implies that one of the probabilities on the left hand side of Eq. (4.133) vanishes, hence that A or $-A$ are not observable in the steady state. If no value A is observable, the steady state Ω-FR loses interest, because there are no fluctuations in the steady state. Therefore, let us assume that A and $-A$ are observable. To proceed, observe that Eqs. (4.128) lead to

$$f_s(\Gamma) = f_0\left(S^{-s}\Gamma\right) e^{-\Lambda_{-s,0}(\Gamma)} = f_0(\Gamma) e^{\Omega_{-s,0}(\Gamma)} \tag{4.135}$$

which implies the following relation, first derived by Evans and Morriss [68]:

$$\left\langle e^{-\Omega_{0,s}} \right\rangle_0 = 1 \,, \quad \text{for every } s \in I\!R \,. \tag{4.136}$$

Suppose now that the correlation with respect to f_o of $\exp(-\Omega_{0,s})$ with $\exp(-\Omega_{s,t})$, decays instantaneously in time. In that case, one can write:

$$1 = \left\langle e^{-\Omega_{0,t}} \right\rangle_0 = \left\langle e^{-\Omega_{0,s}-\Omega_{s,t}} \right\rangle_0 = \left\langle e^{-\Omega_{0,s}} \right\rangle_0 \left\langle e^{-\Omega_{s,t}} \right\rangle_0 \,, \tag{4.137}$$

hence

$$\left\langle e^{-\Omega_{s,t}} \right\rangle_0 = 1 \,, \quad \text{for all } s \text{ and } t \tag{4.138}$$

and the values of the exponentials in the conditional average of Eq. (4.133) do not depend on the condition $\overline{\Omega}_{t,t+\tau} \in A_\delta^+$, so that:

$$\left\langle e^{-\Omega_{0,t}} \cdot e^{-\Omega_{t+\tau,2t+\tau}} \right\rangle_{\overline{\Omega}_{t,t+\tau} \in A_\delta^+} = \left\langle e^{-\Omega_{0,t}} \cdot e^{-\Omega_{t+\tau,2t+\tau}} \right\rangle_0 = 1 \,. \tag{4.139}$$

Then, the logarithmic correction term in (4.133) identically vanishes for all t, τ, and the Ω-FR is verified at all $\tau > 0$. This idealized situation does not need to be realized, but tests performed on molecular dynamics systems [69] indicate that the typical situation is similar to this; typically, there is a constant K such that

$$0 < \frac{1}{K} \leq \left\langle e^{-\Omega_{0,t}-\Omega_{t+\tau,2t+\tau}} \right\rangle_{\overline{\Omega}_{t,t+\tau} \in A_\delta^+} \leq K \,. \tag{4.140}$$

As a matter of fact, the de-correlation or Maxwell time, t_M, expresses a physical property of the system, thus it does not depend on t or τ. Its order of magnitude is that of the mean free time. If $\tau \gg t_M$, the boundary terms $\Omega_{t-t_M,t}$ and $\Omega_{t+\tau,t+\tau+t_M}$ are typically small compared to $\Omega_{t,t+\tau}$. Hence, $\Omega_{t-t_M,t}$ and $\Omega_{t+\tau,t+\tau+t_M}$ are expected to contribute only a fraction of order $O(t_M/\tau)$ to the arguments of the exponentials in the conditional average. One may then write:

$$\left\langle e^{-\Omega_{0,t}} \cdot e^{-\Omega_{t+\tau,2t+\tau}} \right\rangle_{\overline{\Omega}_{t,t+\tau} \in A_\delta^+} \approx \tag{4.141}$$

$$\approx \left\langle e^{-\Omega_{0,t-t_M}} \cdot e^{-\Omega_{t+\tau+t_M,2t+\tau}} \right\rangle_{\overline{\Omega}_{t,t+\tau} \in A_\delta^+} \tag{4.142}$$

$$\approx \left\langle e^{-\Omega_{0,t-t_M} \cdot e^{-\Omega_{t+\tau+t_M,2t+\tau}}} \right\rangle_0 \tag{4.143}$$

$$\approx \left\langle e^{-\Omega_{0,t+t_M}} \right\rangle_0 \left\langle e^{-\Omega_{t+\tau+t_M,2t+\tau}} \right\rangle_0 = O(1) \,, \tag{4.144}$$

with improving accuracy for growing t and τ, since t_M is fixed. If these scenarios are realized, Eq. (4.140) follows and $M(A, \delta, t, \tau)$ vanishes as $1/\tau$, with a characteristic scale of order $O(t_M)$.

Remark. The assumption that Eqs. (4.141)–(4.144) hold is not usual in dynamical systems theory. It is a kind of mixing property which, however, refers to non-invariant probability distributions, differently from the standard notion of mixing.

Various other relations can be obtained following the same procedure. For instance, for each odd $\mathscr{O}$, any $\delta > 0$, any t and any τ the following transient FR holds:

$$\frac{\mu_0(\overline{\mathscr{O}}_{0,\tau} \in A_\delta^+)}{\mu_0(\overline{\mathscr{O}}_{0,\tau} \in A_\delta^-)} = \langle \exp\left(-\Omega_{0,\tau}\right) \rangle^{-1}_{\overline{\mathscr{O}}_{0,\tau} \in A_\delta^+} \,, \tag{4.145}$$

which is another relation expressing some property of the equilibrium state by means of nonequilibrium dynamics.

4.7.3 Green-Kubo Relations

As mentioned at the beginning of this section, the present theory affords a derivation of the Green-Kubo relations and stresses the role of the physical time scales. Take, for instance, a Nosé-Hoover thermostatted system [68], with internal energy H_0, in which the interaction between particles and reservoir is represented by an additional degree of freedom (s, p_s) and the whole (Hamiltonian) system has energy:

$$H = H_0 + 3NkT \ln(s) + \frac{p_s^2}{2Q} \tag{4.146}$$

where H_0 is the energy of the system alone. The equilibrium state density is *microcanonical* in the original frame but *canonical* in the extended frame:

$$f_c(\Gamma, \alpha) = \frac{e^{-\beta\left(H_0 + Q\alpha^2/2\right)}}{\int d\alpha \, d\Gamma \;\; e^{-\beta\left(H_0 + Q\alpha^2/2\right)}} \,, \tag{4.147}$$

where $Q = 2K_0\tau^2$, $\alpha = ps/Q$ is a phase variable with its own equation of motion, and K_0 is the reservoir's target kinetic energy [68]. This yields

$$f_c(\alpha) = \int d\Gamma f_c(\Gamma, \alpha) = \sqrt{\frac{\beta Q}{2\pi}} \, \exp\left[-\beta Q \alpha^2/2\right] \tag{4.148}$$

Therefore, the distribution of $\alpha_{0,t}$ is Gaussian in equilibrium, and near equilibrium it can be assumed to remain such, around its mean, for large t. To use the FR together with the Central Limit Theorem, the values A and $-A$ must be a small number of standard deviations away from $\langle\Omega\rangle$. For a system subject to an external field F_e which induces a current J, Ref. [70] proved that

$$\tau\sigma_{J_\tau}(F_e) = 2L(F_e)k_B T/V + O((F_e)^2/\tau N)\,,$$

where J_τ is the variable obtained integrating J for a time τ, and σ_{J_τ} its variance,

$$L(F_e) = \beta V \int_0^\infty dt\langle (J\circ S^t - \langle J\rangle_{F_e})(J - \langle J\rangle_{F_e})\rangle_{F_e}\,,$$

$\langle\cdot\rangle_{F_e}$ is the phase space average at field F_e and $L(0) = \lim_{F_e\to 0} L(F_e)$ is the corresponding linear transport coefficient. When τ grows, $A = 0$ gets more and more standard deviations away from $\langle\Omega\rangle$, which is $O(F_e^2)$, for small F_e, while the standard deviation tends to a positive constant, since that of α tends to $1/\sqrt{\beta Q}$. Assume for simplicity that the variance of $\Omega_{0,\tau}(F_e)$ is monotonic in F_e at fixed τ, and in τ at fixed F_e. Then, there is $\tau_\sigma(F_e, A)$ such that the variance is large if $\tau < \tau_\sigma(F_e, A)$. At the same time, τ has to be larger than a given $\tau_\delta(F_e, A)$ for the steady state Ω-FR to apply to the values A and $-A$, with accuracy δ. Assume that also $\tau_\delta(F_e, A)$ is monotonic in F_e. To derive the Green-Kubo relations, one then needs $\tau_\delta(F_e, A) < \tau < \tau_\sigma(F_e, A)$ for $F_e \to 0$, which is possible because the distribution tends to a Gaussian centered in zero, when F_e tends to zero and τ is fixed. Letting $\sigma^2(\overline{\Omega}_{0,\tau})$ be the variance of the PDF of the phase variable $\overline{\Omega}_{0,\tau}$, one eventually obtains:

$$\langle\Omega\rangle = \frac{\tau}{2}\sigma^2(\overline{\Omega}_{0,\tau}) \quad \text{i.e. } L(0) = \lim_{F_e\to 0}\frac{\langle J\rangle_{F_e}}{F_e} = \beta V\int_0^\infty dt\,\langle J\left(J\circ S^t\right)\rangle_{F_e=0}\,. \tag{4.149}$$

4.7.4 Jarzynski Equality

Among the transient relations, the one independently obtained by Jarzynski is noteworthy. Consider a finite particle system, in equilibrium with a much larger system, constituting a heat bath at temperature T. Assume that the overall system is described by a Hamiltonian of the form

$$\mathscr{H}(\Gamma;\lambda) = H(x;\lambda) + H_E(y) + h_i(x, y) \tag{4.150}$$

where x and y denote the positions and momenta of the particles in, respectively, the system of interest and the bath, h_i represents the interaction between system and bath, and λ is an externally controllable parameter. This system can be driven away

from equilibrium, performing work, by acting on λ. Let $\lambda(0) = A$ and $\lambda(\tau) = B$ be the initial and final values of λ for a given evolution protocol $\lambda(t)$. Suppose the process is repeated many times to build the statistics of the work done, varying λ from A to B always in the same manner. Let ρ be the PDF of the externally performed work W. This is not the thermodynamic work done on the system, if the process is not performed quasi statically [71], but it is a measurable quantity. The Jarzynski equality predicts that [44]:

$$\left\langle e^{-\beta W}\right\rangle_{A\to B} = \int dW\, \rho(W) e^{-\beta W} = e^{-\beta[F(B)-F(A)]} \tag{4.151}$$

where $\beta = 1/k_B T$, and $[F(B) - F(A)]$ is the free energy difference between the initial equilibrium state with $\lambda = A$ and the equilibrium state which is eventually reached for $\lambda = B$. The average $\langle e^{-\beta W}\rangle_{A\to B}$ is the average over all works done in varying λ from A to B. While the process always begins in the equilibrium state corresponding to $\lambda = A$, the system does not need to be in equilibrium when λ reaches the value B. However, the equilibrium state with $\lambda = B$ exists and is unique, hence $F(B)$ is well defined. Equation (4.151) is supposed to hold whichever protocol one follows to change λ from A to B, hence also arbitrarily far from equilibrium (large $\dot{\lambda}$); therefore the presence of the equilibrium quantities $F(A)$ and $F(B)$ in Eq. (4.151) is remarkable. From the thermodynamic point of view, one observes that the externally measured work does not need to coincide with the internal work (which would not differ from experiment to experiment, if performed quasistatically). From an operational point of view, it does not matter whether the system is in local equilibrium or not: certain forces are applied, certain motions are registered, hence certain works are recorded. The Jarzynski equality is a transient relation and, similarly to the transient Ω-FR, rests on minimal conditions on the microscopic dynamics.

Remark. The Jarzynski Equality, analogously to the transient FRs, connects equilibrium to nonequilibrium properties of physical systems, allowing us to compute equilibrium properties by performing nonequilibrium experiments. This is the task complementary to the one performed by the FDR.

4.8 t-Mixing and General Response Theory

Observing that Eq. (4.65), implies:

$$\left\langle e^{-\Omega_{s,t}}\right\rangle_0 = \left\langle e^{-\Omega_{0,t-s}}\right\rangle_s \tag{4.152}$$

the correlations decay of Eqs. (4.141)–(4.144) appears to be one special case of a property which can be expressed as follows:

$$\lim_{t\to\infty}\left[\left\langle \psi\left(\phi\circ S^t\right)\right\rangle_0 - \langle\psi\rangle_0\langle\phi\rangle_t\right] = 0 \tag{4.153}$$

Consider the particular case in which $\psi = \Omega$. The fact that $\langle \Omega \rangle_0 = 0$, because Ω is odd and f_0 is even under time reversal, reduces Eq. (4.153) to the simpler expression

$$\lim_{t\to\infty} \left\langle \Omega \left(\phi \circ S^t\right)\right\rangle_0 = 0 \tag{4.154}$$

If the convergence of this limit is faster than $O(1/t)$, one further has:

$$\int_0^\infty \left\langle \Omega \left(\phi \circ S^t\right)\right\rangle_0 \, \mathrm{d}t \in \mathbb{R} \tag{4.155}$$

a condition which has been called *t-mixing*.

Let us now consider the response of observables, starting from an equilibrium state, but evolving arbitrarily far from equilibrium:

$$\langle \phi \rangle_t - \langle \phi \rangle_0 = \int_0^t \frac{\mathrm{d}}{\mathrm{d}s} \langle \phi \rangle_s \, \mathrm{d}s = \int_0^t \mathrm{d}s \frac{\mathrm{d}}{\mathrm{d}s} \int \mathrm{d}\Gamma f_s(\Gamma) \phi(\Gamma) \tag{4.156}$$

Substituting the expression for f_s given by Eq. (4.135), we obtain

$$\frac{\mathrm{d}}{\mathrm{d}s} \int \mathrm{d}\Gamma f_s(\Gamma) \phi(\Gamma) = \int \mathrm{d}\Gamma f_0(\Gamma) e^{\Omega_{-s,0}(\Gamma)} \Omega\left(S^{-s}\Gamma\right) \phi(\Gamma) \tag{4.157}$$

Introducing $X = S^{-s}\Gamma$, $\Gamma = S^s X$, with the Jacobian determinant given by $|\partial\Gamma/\partial X| = \exp(\Lambda_{0,s}(X)$, the above equation takes the form:

$$\frac{\mathrm{d}}{\mathrm{d}s} \langle \phi(\Gamma) \rangle_s = \int \mathrm{d}X f_0(S^s X) e^{\Omega_{-s,0}(S^s X)} e^{\Lambda_{0,s}(X)} \Omega\left(X\right) \phi(S^s X) \tag{4.158}$$

Observe that

$$\Omega_{-s,0}(S^s X) = \int_{-s}^0 \mathrm{d}u \, \Omega\left(S^u S^s X\right) = \int_0^s \mathrm{d}z \, \Omega(S^z X) = \Omega_{0,s}(X) \tag{4.159}$$

so that, using Eq. (4.128), we obtain:

$$\begin{aligned} \frac{\mathrm{d}}{\mathrm{d}s} \langle \phi(\Gamma) \rangle_s &= \int \mathrm{d}X \, \phi\left(S^s X\right) \Omega(X) e^{\Omega_{0,s}(X)} e^{\Lambda_{0,s}(X)} f_0(S^s X) \\ &= \int \mathrm{d}X \, \Omega(X) \phi\left(S^s X\right) f_0(X) = \langle \Omega \left(\phi \circ S^s\right)\rangle_0 \end{aligned} \tag{4.160}$$

which is the integrand of Eq. (4.155). Therefore, we have the totally general **Response Formula:**

$$\langle \phi \rangle_t = \langle \phi \rangle_0 + \int_0^t \mathrm{d}s \, \langle \Omega \left(\phi \circ S^s\right)\rangle_0 \tag{4.161}$$

Moreover, if the t-mixing condition holds for all observables ϕ, the fact that

$$\langle \phi \rangle_t \overset{t\to\infty}{\longrightarrow} \langle \phi \rangle_0 + \int_0^\infty \mathrm{d}s \ \langle \Omega \, (\phi \circ S^s) \rangle_0 \in \mathbb{R} \tag{4.162}$$

implies that the system under investigation converges to a steady state. This proof is as simple as the one based on standard mixing for the convergence to the microcanonical ensemble, but is much more general, since it holds for dissipative dynamics as well. The relation between standard mixing and t-mixing is still to be largely understood. However one interesting aspect is the following.

Remark. While standard mixing concerns the decay of correlations among the evolving microstates of a given steady state, t-mixing concerns the decay of correlations among evolving macrostates. For this reason, the t-mixing property implies the convergence to a steady state, whereas the mixing property in general does not.

Mixing assumes the state to be stationary, making irrelevant the issue of relaxation. The derivation of convergence to a microcanonical state, illustrated in Sect. 4.4.1, is thus very fortunate.[13] That derivation is soley possible because, in the case of mixing with respect to a stationary probability density, one may formally interpret the evolving transient probability densities as evolving *observables* as well. This way one combines in one mathematical object two physically distinct entities: the distribution of microscopic states and a macroscopic (supposedly) measurable observable.[14] In reality, this extends quite a bit the meaning of mixing, which concerns the decay of correlations among the successive *micro*-states within a given *invariant* macrostate. Consequently, the argument does not carry over the much more common case of dissipative dynamics and of singular invariant distributions.[15]

4.9 Concluding Remarks

We have summarised the hystorical development of response theory, from Einstein's ingenius works to the recentmost theories for the steady states of deterministic systems. We have illustrated how the FDR and its consequences allow us to infer nonequilibrium properties of macroscpic systems from observations on equilibrium states. Those results were based on a theory of small fluctuations, which allowed

[13] An argument similar to that outlined in Sect. 4.4.1 applies if the dynamics is mixing with respect to other invariant densities.

[14] Something similar happens when the equilibrium thermodynamic entropy of a physical object is expressed by the equilibrium average of the logarithm of the equilibrium density, which is the Gibbs entropy.

[15] The analogy concerning the identification of the thermodynamic entropy with the Gibbs entropy continues: if the steady state is singular, the Gibbs entropy does not represent any thermodynamic entropy at all.

frequent recourse to the Central Limit Theorem and Gaussian approximations. The modern theories concerned with the large deviations have produced the complementary result: evaluation of equilibrium properties from nonequilibrium experiments.

We have seen that the transient relations are almost tautological: they hold very generally as long as the microscopic dynamics are time reversal invariant. From this point of view, besides the most important fact of providing information on equilibrum states, they afford useful tests for the validity of the models adopted in the investigation of nonequilibrium phenomena. The steady state Ω-FR, instead, can be obtained from the time reversibility and from the Ω-autocorrelation decay, expressed with respect to the equilibrium ensemble. This is an unusual condition in dynamical systems theory, since correlations are usually referred to the invariant measures. The result is a novel ergodic property, now called *t-mixing*.

The t-mixing condition has been suggested by the work on the large deviations of the dissipation function, as a natural condition under which the steady state FR holds. Its use in the investigation of other questions led us to a completely general response formula, which holds whether a perturbed system eventually settles on a steady state or it does not. In both cases, for any observable ϕ, it gives the observable value $\langle\phi\rangle_t$ at any instant of time t, as the time integral of the correlation function of Ω with ϕ, computed with respect to the corresponding equlibrium ensemble μ_0. This completes the Green-Kubo theory as, somewhat surprisingly, it makes the equilibrium ensemble play a fundamental role even for systems driven very far from equilibrium. The counterpart is that, far from equilibrium Ω may not be recognized as a standard thermodynamic property, although it continues to represent the dissipated energy.

The other important issue is that the theory illustrated above is fully dynamical and does not require the large system limit. Therefore, it may be useful in the study of small (meso- as well as micro-scopic) objects. This is indeed the case but, again, for small systems the meaning of ensembles differs from that of macroscpic objects, thus care must be taken in interpreting the corresponding results.

In the context of dissipative reversible dynamics we have thus closed the circle, going from equilibrium to non-equilibrium descriptions and vice versa. Open questions are numerous. Among issues that seem to be within close reach, we mention: (a) the relation between standard mixing and t-mixing, which is not a merely mathematical question, and (b) the applicability of both transient and steady state FR, especially those involving two observables, such as Eq. (4.145). The role of the dissipation function Ω, which is a kind of thermodynamic potential in the theory outlined above, and its relation to specific situations is perhaps the most interesting of the present challenges, especially with regard to the response formula Eq. (4.161). We believe that the t-mixing notion and Eq. (4.161) are among the most significant results emerging from the deterministic theory of the FRs.

Acknowledgements This work has received funding from the European Research Council under the EU Seventh Framework Programme (FP7/2007–2013)/ERC grant agreement n. 202680. The EU is not liable for any use made on the information contained herein.

References

1. A. Einstein, The motion of elements suspended in static liquids as claimed in the molecular kinetic theory of heat. Ann. Phys. **17**, 549 (1905)
2. A. Einstein, Theory of opalescence of homogeneous liquids and mixtures of liquids in the vicinity of the critical state. Ann. Phys. **33**, 1275 (1910)
3. L. Rondoni, C. Mejía-Monasterio, Fluctuations in nonequilibrium statistical mechanics: models, mathematical theory, physical mechanisms. Nonlinearity **20**, R1 (2007)
4. U. Marini Bettolo Marconi, A. Puglisi, L. Rondoni, A. Vulpiani, Fluctuation-dissipation: response theory in statistical physics. Phys. Rep. **461**, 111 (2008)
5. H. Nyquist, Thermal agitation of electric charge in conductors. Phys. Rev. **32**, 110 (1928)
6. L. Onsager, Reciprocal relations in irreversible processes. I. Phys. Rev. **37**, 405 (1931)
7. L. Onsager, Reciprocal relations in irreversible processes. II. Phys. Rev. **38**, 2265 (1931)
8. H.B. Callen, T.A. Welton, Irreversibility and generalized noise. Phys. Rev. **83**, 34 (1951)
9. H.B. Callen, R.F. Greene, On a theorem of irreversible thermodynamics. Phys. Rev. **86**, 702 (1952)
10. M.S. Green, Brownian motion in a gas of noninteracting molecules. J. Chem. Phys. **19**, 1036 (1951)
11. M.S. Green, Markoff random processes and the statistical mechanics of time-dependent phenomena. J. Chem. Phys. **20**, 1281 (1952)
12. M.S. Green, Markoff random processes and the statistical mechanics of time-dependent phenomena. II. Irreversible processes in fluids. J. Chem. Phys. **22**, 398 (1954)
13. R. Kubo, Statistical-mechanical theory of irreversible processes. I. General theory and simple applications to magnetic and conduction problems. J. Phys. Soc. Jpn. **12**, 570 (1957)
14. L. Onsager, S. Machlup, Fluctuations and irreversible processes. Phys. Rev. **91**, 1505 (1953)
15. S. Machlup, L. Onsager, Fluctuations and irreversible process. II. Systems with kinetic energy. Phys. Rev. **91**, 1512 (1953)
16. B.J. Alder, T.E. Wainwright, Velocity autocorrelations for hard spheres. Phys. Rev. Lett. **18**, 988 (1967)
17. L.P. Kadanoff, J. Swift, Transport coefficients near the liquid-gas critical point. Phys. Rev. **166**, 89 (1968)
18. I. Procaccia, D. Ronis, I. Oppenheim, Light scattering from nonequilibrium stationary states: the implication of broken time-reversal symmetry. Phys. Rev. Lett. **42**, 287 (1979)
19. T.R. Kirkpatrick, E.G.D. Cohen, J.R. Dorfman, Kinetic theory of light scattering from a fluid not in equilibrium. Phys. Rev. Lett. **42**, 862 (1979)
20. H. Spohn, *Large Scale Dynamics of Interacting Particles* (Springer, Heidelberg, 1991)
21. P. Hänggi, H. Thomas, Linear response and fluctuation theorems for nonstationary stochastic-processes. Z. Phys. B **22**, 295 (1975)
22. P. Hänggi, Stochastic-processes .2. Response theory and fluctuation theorems. Helv. Phys. Acta **51**, 202 (1978)
23. W.M. Visscher, Transport processes in solids and linear-response theory. Phys. Rev. A **10**, 2461 (1974)
24. J.W. Dufty, M.J. Lindenfeld, Non-linear transport in the Boltzmann limit. J. Stat. Phys. **20**, 259 (1979)
25. E.G.D. Cohen, Kinetic-theory of non-equilibrium fluids. Physica A **118**, 17 (1983)
26. G.P. Morriss, D.J. Evans, Application of transient correlation functions to shear flow far from equilibrium. Phys. Rev. A **35**, 792 (1987)
27. M. Falcioni, S. Isola, A. Vulpiani, Correlation functions, relaxation properties in chaotic dynamics, statistical mechanics. Phys. Lett. A **144**, 341 (1990)
28. G. Boffetta, G. Lacorata, S. Musacchio, A. Vulpiani, Relaxation of finite perturbations: beyond the fluctuation-response relation. Chaos **13**, 806 (2003)
29. D. Ruelle, Differentiation of SRB states. Commun. Math. Phys. **187**, 227 (1997)

30. F. Corberi, E. Lippiello, M. Zannetti, Fluctuation dissipation relations far from equilibrium. J. Stat. Mech. **2007**, P07002 (2007)
31. M. Baiesi, C. Maes, An update on nonequilibrium linear response. New J. Phys. **15**, 013004 (2013)
32. T. Speck, U. Seifert, Restoring a fluctuation-dissipation theorem in a nonequilibrium steady state. Europhys. Lett. **74**, 391 (2006)
33. T. Speck, U. Seifert, Extended fluctuation-dissipation theorem for soft matter in stationary flow. Phys. Rev. E **79**, 040102 (2009)
34. R. Chetrite, K. Gawedzki, Fluctuation relations for diffusion processes. Commun. Math. Phys. **282**, 469 (2008)
35. D.J. Evans, E.G.D. Cohen, G.P. Morriss, Probability of second law violations in shearing steady flows. Phys. Rev. Lett. **71**, 2401 (1993)
36. D.J. Evans, D.J. Searles, Equilibrium microstates which generate second law violating steady states. Phys. Rev. E **50**, 1645 (1994)
37. D.J. Evans, D.J. Searles, Steady sates, invariant measures, response theory. Phys. Rev. E **52**, 5839 (1995)
38. G. Gallavotti, E.G.D. Cohen, Dynamical ensembles in nonequilibrium statistical mechanics. Phys. Rev. Lett. **94**, 2694 (1995)
39. G. Gallavotti, E.G.D. Cohen, Dynamical ensembles in stationary states. J. Stat. Phys. **80**, 931 (1995)
40. G. Gallavotti, Extension of Onsager's reciprocity to large fields, the chaotic hypothesis. Phys. Rev. Lett. **77**, 4334 (1996)
41. G. Gallavotti, D. Ruelle, SRB states and nonequilibrium statistical mechanics close to equilibrium. Commun. Math. Phys. **190**, 279 (1997)
42. L. Rondoni, E.G.D. Cohen, Orbital measures in non-equilibrium statistical mechanics: the Onsager relations. Nonlinearity **11**, 1395 (1998)
43. D.J. Evans, D.J. Searles, L. Rondoni, On the application of the Gallavotti-Cohen fluctuation relation to thermostatted steady states near equilibrium. Phys. Rev. E **71**, 056120 (2005)
44. C. Jarzynski, Nonequilibrium equality for free energy differences. Phys. Rev. Lett. **78**, 2690 (1997)
45. C. Bustamante, J. Liphardt, F. Ritort, The nonequilibrium thermodynamics of small systems. Phys. Today **58**, 43 (2005)
46. M. Bonaldi et al., Nonequilibrium steady-state fluctuations in actively cooled resonators. Phys. Rev. Lett. **103**, 010601 (2009)
47. R. Brown, A brief account of microscopical observations made in the months of June, July, and August, 1827 on the particles contained in the pollen of plants; and on the general existence of active molecules in organic and inorganic bodies. Philos. Mag. **4**, 161 (1828)
48. P. Langevin, Sur la theorie du mouvement brownien. C. R. Acad. Sci. (Paris) **146**, 530 (1908). Translated in Am. J. Phys. **65**, 1079 (1997)
49. J. Perrin, *Les Atomes* (Alcan, Paris, 1913)
50. R. Kubo, M. Toda, N. Hashitsume, *Statistical Physics II: Nonequilibrium Statistical Mechanics* (Springer, Berlin, 1985)
51. A.I. Khinchin, *Mathematical Foundations of Statistical Mechanics* (Dover, New York, 1949)
52. D. Ruelle, General linear response formula in statistical mechanics, and the fluctuation-dissipation theorem far from equilibrium. Phys. Lett. A **245**, 220 (1998)
53. M. Colangeli, L. Rondoni, A. Vulpiani, Fluctuation-dissipation relation for chaotic non-Hamiltonian systems. J. Stat. Mech. **2012**, L04002 (2012)
54. D.J. Evans, L. Rondoni, Comments on the entropy of nonequilibrium steady states. J. Stat. Phys. **109**, 895 (2002)
55. F. Bonetto, A. Kupiainen, J.L. Lebowitz, Absolute continuity of projected SRB measures of coupled Arnold cat map lattices. Ergod. Theory Dyn. Syst. **25**, 59 (2005)
56. B. Cessac, J.-A. Sepulchre, Linear response, susceptibility and resonances in chaotic toy models. Physica D **225**, 13 (2007)

57. L. Bertini, A.D. Sole, D. Gabrielli, G. Jona-Lasinio, C. Landim, Macroscopic fluctuation theory for stationary non-equilibrium states. J. Stat. Phys. **107**, 635 (2002)
58. A. Gamba, L. Rondoni, Current fluctuations in the nonequilibrium Lorentz gas. Physica A **340**, 274 (2004); C. Giberti, L. Rondoni, C. Vernia, Asymmetric fluctuation-relaxation paths in FPU models. Physica A **365**, 229 (2006); C. Paneni, D.J. Searles, L. Rondoni, Temporal asymmetry of fluctuations in nonequilibrium states. J. Chem. Phys. **124**, 114109 (2006); C. Paneni, D.J. Searles, L. Rondoni, Temporal asymmetry of fluctuations in nonequilibrium steady states: links with correlation functions and nonlinear response. J. Chem. Phys. **128**, 164515 (2008)
59. J.D. Weeks, D. Chandler, H.C. Andersen, Role of repulsive forces in determining the equilibrium structure of simple liquids. J. Chem. Phys. **54**, 5237 (1971)
60. G. Gallavotti, Reversible Anosov diffeomorphisms, large deviations. Math. Phys. Electron. J. **1**, 1 (1995)
61. G. Gallavotti, Fluctuation theorem revisited (2004), http://arXiv.org/cond-mat/0402676
62. J. Kurchan, Fluctuation theorem for stochastic dynamics. J. Phys. A **31**, 3719 (1998)
63. J.L. Lebowitz, H. Spohn, A Gallavotti-Cohen-type symmetry in the large deviation functional for stochastic dynamics. J. Stat. Phys. **95**, 333 (1999)
64. C. Maes, The fluctuation theorem as a Gibbs property. J. Stat. Phys. **95**, 367 (1999)
65. Ya.G. Sinai, *Lectures in Ergodic Theory*. Lecture Notes in Mathematics (Princeton University Press, Princeton, New Jersey, USA, 1977)
66. D.J. Evans, E.G.D. Cohen, D.J. Searles, F. Bonetto, Note on the Kaplan-Yorke dimension and linear transport coefficients. J. Stat. Phys. **101**, 17 (2000)
67. D.J. Evans, D.J. Searles, L. Rondoni, The steady state fluctuation relation for the dissipation function. J. Stat. Phys. **128**, 1337 (2007)
68. D.J. Evans, G.P. Morriss, *Statistical Mechanics of Nonequlibrium Liquids* (Academic, New York, 1990)
69. B. Johnston, D.J. Evans, D.J. Searles, L. Rondoni, Time reversibility, correlation decay and the steady state fluctuation relation for dissipation. Entropy **15**, 1503 (2013)
70. D.J. Searles, D.J. Evans, Ensemble dependence of the transient fluctuation theorem. J. Chem. Phys. **113**, 3503 (2000)
71. E.G.D. Cohen, D. Mauzerall, A note on the Jarzynski equality. J. Stat. Mech. **2004**, P07006 (2004)

Chapter 5
Large Deviations in Disordered Spin Systems

Andrea Crisanti and Luca Leuzzi

Abstract This contribution is an introduction to the use of large deviations to study properties of disordered systems. We present some features of the application of the theory of large deviations to models with random bonds or fields. Proceeding by examples, starting from the mean field Ising model we introduce the notation for the rate function and the cumulant generating function for small and large deviations. By means of the replica theory we analyze sample-to-sample free energy and overlap fluctuations. In particular, we address the random Ising chain, random directed polymers, mean-field spin-glasses both with Ising and spherical spins and the random field Ising model. For pedagogical aims, we put more emphasis on low dimensional systems, where product of random matrices can be employed, leaving out more advanced methods, focusing on the basic ideas behind the application of large deviations.

5.1 Some General Results on Large Deviations

In this section we shall introduce some definitions and recall some general results on large deviations. The presentation will be informal because our primary scope is the application of large deviations to disordered systems, rather than the study of large deviations themselves. For a more rigorous definition we refer to, e.g., Ref. [1], for a

A. Crisanti
Dipartimento di Fisica, Università di Roma "Sapienza", Piazzale Aldo Moro 5, Rome, I-00185, Italy
e-mail: andrea.crisanti@roma1.infn.it

L. Leuzzi (✉)
Istituto per i Processi Chimico-Fisici, Consiglio Nazionale delle Ricerche Piazzale Aldo Moro 5, Rome, I-00185, Italy
e-mail: luca.leuzzi@cnr.it

A. Vulpiani et al. (eds.), *Large Deviations in Physics*, Lecture Notes in Physics 885,
DOI 10.1007/978-3-642-54251-0_5,

review on large deviations see, e.g., Ref. [2]. The reader interested in the application of product of Random Matrices to low dimensional disordered systems, and more, is referred to Ref. [3].

To set up the problem consider a physical observable A_N of a system made of N spins. If A_N depends on the system configuration, the magnetization density for example, then A_N will be a fluctuating quantity. If (quenched) disorder is present, the observable A_N, e.g., the free energy density, can depend on it and its fluctuations will, as well, stem from it. Its probability distribution (density) depends on the system size N, but usually it becomes more and more concentrated around a value a^* as N increases, and values of A_N different form a^* become more and more unlikely as N increases. The value a^* is called *the most probable* or *typical* value of A_N. The existence of this typical value is an expression of the Law of Large Numbers, which in its weak form states that A_N converges to a^* as $N \to \infty$ with probability 1:

$$P\left(|A_N - a^*| \geq \epsilon\right) \to 0 \qquad \text{as } N \to \infty \tag{5.1}$$

for all $\epsilon > 0$. In physics this property is usually referred to as *self-averaging*, to stress the fact that probability density of A_N converges for $N \to \infty$ to the delta function $\delta(A_N - a^*)$.

Beside the existence of the typical value, it is of interest to understand how fast A_N converges in probability to its typical value. It turns out that often the convergence is *exponential*, that is, if P_N is the probability density of A_N, then

$$\lim_{N\to\infty} -\frac{1}{N} \ln P_N(A_N = a) = I(a) \tag{5.2}$$

with $I(a)$ a continuous function called, in this context, *rate function*.

An equivalent statement is that the asymptotic form of P_N is

$$P_N(A_N = a) \sim g(N, a)\, e^{-N\, I(a)}, \qquad N \gg 1. \tag{5.3}$$

where $g(N, a)$ is a slowly varying function compared to the exponential. The meaning of the sign "$\sim$" is that expressed in Eq. (5.2). Whenever $P_N(A_N)$ satisfies (5.2), or (5.3), we say that it obeys a *large deviation principle* with the rate function $I(a)$. The rate function is always non-negative, otherwise the probability distribution function would diverge as $N \to \infty$, and takes its (global) minimum value for $a = a^*$. Since $I(a)$ is defined up to a constant we can always set $I(a^*) = 0$.

If $I(a)$ only displays one global minimum it is easy to recover the Law of Large Number. If Ω is a sub-set of possible values of A_N then, using (5.3) and Laplace's approximation, we have

$$P(A_N \in \Omega) = \int_\Omega da\, P_N(A_N = a)$$
$$\sim \int_\Omega da\, g(a,N)\, e^{-N\, I(a)}$$
$$\sim e^{-N \inf_{a\in\Omega} I(a)}, \qquad N \gg 1. \tag{5.4}$$

Therefore $P(A_N \in \Omega) \to 0$ exponentially fast if $a^* \notin \Omega$, and hence $P(A_N \in \Omega) \to 1$ exponentially fast if $a^* \in \Omega$. The large deviations principle hence extends the law of large number in the sense that it provides informations on how fast is the convergence.

It should be stressed that the rate function $I(a)$ may possess more than one global minimum. In this case the law of large numbers may not hold. In physics the typical value a^* determined by a global minimum of $I(a)$ is called an *equilibrium state*. The presence of multiple global minima is then associated with the coexistence of different equilibrium phases. If the rate function possesses local minima, in addition to one or more global minima, these are identified with *metastable states*. The rate functions are indeed closely related to thermodynamic potentials.

Let us go back to the case of single global minimum, and make the additional assumption that $I(a)$ is twice differentiable at $a = a^*$, so that we can approximate it as

$$I(a) = \frac{1}{2} A^* (a - a^*)^2. \tag{5.5}$$

where $A^* = d^2 I(a)/da^2|_{a=a^*}$. Then from (5.3), dropping the irrelevant slow term $g(a,N)$, it follows

$$P_N(A_N = a) \sim \exp\left[-\frac{NA^*}{2}(a - a^*)^2\right]. \tag{5.6}$$

This Gaussian approximation is valid for values of $a - a^*$ up to $O(N^{-1/2})$, and hence describes the *small* deviations of A_N around the typical value a^*. One then essentially recovers the Central Limit Theorem. Values of a for which the quadratic approximation of $I(a)$ cannot be used are the *large* deviations. These arguments can be extended also to the case in which $I(a)$ does not possess a quadratic Taylor expansion around its minimum. We shall see more on these later. The central point here is that the knowledge of $I(a)$ provides information on both small and large deviations.

Unfortunately, a direct calculation of the rate function $I(a)$ in a general case is a rather difficult task. A useful and rather general method to have access to $I(a)$ consists in perturbing the measure to make unlikely rare events appear. From the knowledge of the "strength" needed to make a value $A_N = a$ likely one can infer

the rate function $I(a)$. Practically, one defines the cumulant generating function of a as

$$W_N(k) \equiv \frac{1}{N} \ln \int_{\mathbb{R}} da\, P_N(A_N = a)\, e^{Nka} \tag{5.7}$$

where $k \in \mathbb{R}$. When P_N obeys a large deviation principle, we can compute the large-N limit of $W_N(k)$ using the Laplace integration method,

$$W(k) = \lim_{N\to\infty} W_N(k) = \lim_{N\to\infty} \frac{1}{N} \ln \int_{\mathbb{R}} da\, e^{N[ka - I(a)]} = \sup_{a\in\mathbb{R}} [ka - I(a)]. \tag{5.8}$$

$W(k)$ is then the *Legendre* transform of $I(a)$. If $I(a)$ is differentiable this is also expressed as

$$W(k) = ka - I(a) \tag{5.9}$$

where $a = a(k)$ is the solution of

$$\frac{d}{da} I(a) = k. \tag{5.10}$$

The cumulant generating function $W_N(k)$, and hence $W(k)$, is a convex function of k by construction. The Legendre transform can then be inverted, leading to

$$\Gamma(a) = \sup_{k\in\mathbb{R}} [ka - W(k)] \tag{5.11}$$

where $\Gamma(a)$ is the convex envelope of $I(a)$. If $W(k)$ is differentiable we can write the Legendre transform as

$$\Gamma(a) = ka - W(k) \tag{5.12}$$

where $k = k(a)$ is the solution of

$$\frac{d}{dk} W(k) = a. \tag{5.13}$$

A simple calculation shows that if $I(a)$ has the quadratic form (5.5), then

$$W(k) = ka^* + \frac{1}{2} \frac{k^2}{A^*} \tag{5.14}$$

and $\Gamma(a) = I(a)$.

5.1.1 An Example: The Mean Field Ising Model

To illustrate the above statements we consider the Mean Field Ising Model, where the calculation can be explicitly carried out. The model is defined by the Hamiltonian

$$H = -\frac{1}{N}\sum_{i<j}^{1,N}\sigma_i\sigma_j \tag{5.15}$$

where $\sigma_i = \pm 1$ are Ising spins. As observable we take the magnetization density

$$m_N = \frac{1}{N}\sum_{i=1}^{M}\sigma_i\,. \tag{5.16}$$

When the system is in equilibrium with a thermal bath at temperature T the probability that the magnetization density takes a given value m is

$$P_N(m_N = m) = \frac{1}{Z_N}\sum_{\sigma_1,\ldots\sigma_N} e^{-\beta H}\,\delta\left(m - \frac{1}{N}\sum_{i=1}^{M}\sigma_i\right) \tag{5.17}$$

where Z_N is the partition function

$$Z_N = \sum_{\sigma_1,\ldots\sigma_N} e^{-\beta H}. \tag{5.18}$$

A standard calculation leads to the asymptotic result

$$\sum_{\sigma_1,\ldots\sigma_N} e^{-\beta H}\,\delta\left(m - \frac{1}{N}\sum_{i=1}^{M}\sigma_i\right) \sim e^{N\phi(m)}, \qquad N \gg 1 \tag{5.19}$$

valid for large N, where

$$\phi(m) = \frac{\beta}{2}m^2 - \frac{1+m}{2}\ln\left(\frac{1+m}{2}\right) - \frac{1-m}{2}\ln\left(\frac{1-m}{2}\right). \tag{5.20}$$

From this expression it also follows

$$Z_N = \int_{-1}^{1} dm \sum_{\sigma_1,\ldots\sigma_N} e^{-\beta H}\,\delta\left(m - \frac{1}{N}\sum_{i=1}^{M}\sigma_i\right) \sim e^{N\phi(m^*)}, \qquad N \gg 1 \tag{5.21}$$

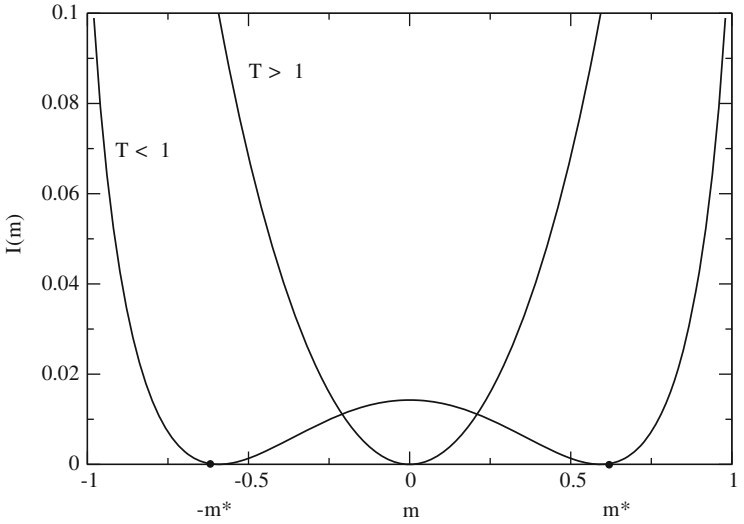

Fig. 5.1 The rate function $I(m)$ of the mean-field Ising model above ($T > 1$) and below ($T < 1$) the Curie-Weiss transition point $T_c = 1$

with m^* given by

$$m^* = \arg \sup_{m\in[-1,1]} \phi(m) \quad \Rightarrow \quad \frac{d}{dm}\phi(m)\Big|_{m^*} = 0. \tag{5.22}$$

Using $\phi(m)$ from (5.20) one gets the well known result

$$m^* = \tanh(\beta m^*) \tag{5.23}$$

for the Mean Field Ising Model.

Collecting all contributions we see that $P_N(m)$ obeys a large deviation principle $P_N(m) \sim e^{-NI(m)}$ with rate function

$$I(m) = \phi(m^*) - \phi(m). \tag{5.24}$$

The form of $I(m)$ depends on T, see Fig. 5.1. For temperatures $T > 1$ ($\beta < 1$) $I(m)$ is a convex function, with a single global minimum at $m^* = 0$. For these temperatures $\Gamma(m)$ coincides with $I(m)$. When T decreases, and becomes smaller than 1, $\beta > 1$, $I(m)$ develops two local minima at $m^* = \pm|m^*|$, $|m^*| \neq 0$, and it is no more convex in the whole interval $m \in [-1, 1]$. In this temperature range $\Gamma(m)$ does not coincides with $I(m)$ in the whole interval $m \in [-1 : 1]$.

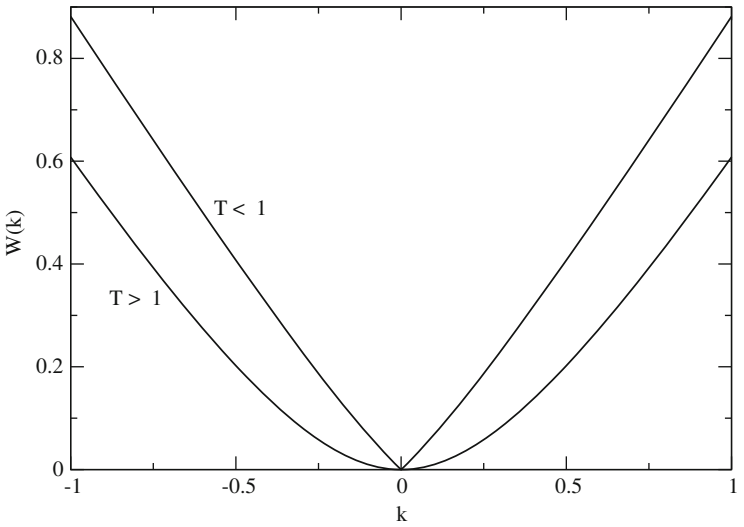

Fig. 5.2 The cumulant generating function $W(k)$ of the mean-field Ising model above ($T > 1$) and below ($T < 1$) the Curie-Weiss transition point $T_c = 1$

From the definition of $W_N(k)$ it follows that

$$\frac{d}{dk} W_N(k) = \langle a \rangle_k^{(N)} \tag{5.25}$$

where $\langle \cdots \rangle_k^{(N)}$ denotes averaging with the weight $P_N(A_N = a)e^{Nka}$. Then, under the hypothesis that $W(k)$ exists and is differentiable, using the Laplace method we have

$$W'(k) = \frac{d}{dk} W(k) = \arg\sup_{a \in \mathbb{R}} [ak - I(a)]. \tag{5.26}$$

For the Mean Field Ising model we thus find

$$\lim_{k \to 0^{\pm}} W'(k) = 0 \qquad T > 1 \tag{5.27}$$

while

$$\lim_{k \to 0^{\pm}} W'(k) = \pm |m^*| \qquad T < 1 \tag{5.28}$$

and $W(k)$ has a cusp for $T < 1$, see Fig. 5.2. Since k has the same role as a uniform external field, Eq. (5.28) expresses the well known fact that when an infinitesimal external field applied to a Ferromagnetic system in equilibrium tends to zero, the

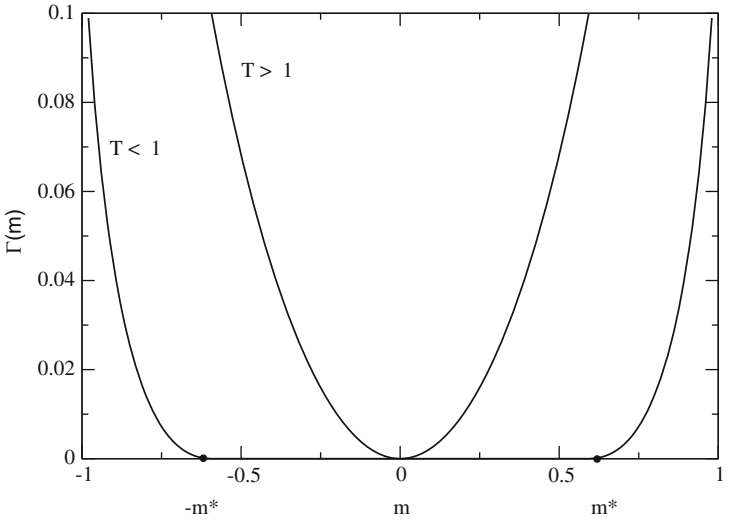

Fig. 5.3 The Legendre Transform $\Gamma(m)$ of the generating function $W(k)$ for the mean-field Ising model above ($T > 1$) and below ($T < 1$) the Curie-Weiss transition point $T_c = 1$

magnetization parallel to the field does not vanish if the system temperature is below its critical temperature. Direct consequence of Eq. (5.28) is that $\Gamma(m)$ and $I(m)$ do not coincide for $T < 1$. Indeed, a direct calculation shows that for $T < 1$

$$\Gamma(m) = \begin{cases} I(m) & |m| > |m^*| \\ \\ 0 & m \in [-m^*, m^*] \end{cases} \tag{5.29}$$

as shown in Fig. 5.3.

5.2 Sample-to-Sample Free Energy Fluctuations and Replica Trick

In systems with quenched disorder each system realization will be characterized by a different configuration of disorder. We will call such a realization a *sample*. The thermodynamic properties fluctuate from sample to sample. Most of them are, however, self-averaging, if the disorder does not have long range correlations [4]. Standard example is the free energy, just to name one, on which we will mainly concentrate. This means that in the large volume limit the free energy per variable of different samples deviates arbitrarily little from the typical value

$$f = -\lim_{N\to\infty} \frac{\overline{\ln Z_N}}{\beta N} \tag{5.30}$$

where Z_N is the partition function of a given disordered sample. Here, and in the following, the bar indicates the average over the realizations of disorder. In this specific framework we anticipate that, besides being interesting by themselves, large deviations are also interesting because intrinsically related to the *replica method*, i.e., the mathematical method used to perform the disorder average.

5.2.1 Random Ising Chain

To introduce the problem consider a one dimensional random Ising chain with Hamiltonian,

$$H = -\sum_{i=1}^{N} (J_i \sigma_i \sigma_{i+1} + h_i \sigma_i) \tag{5.31}$$

where periodic boundary condition $\sigma_{N+1} = \sigma_1$ are assumed. The couplings J_i between spins σ_i and σ_{i+1} and/or the magnetic field h_i are independent random variables. For any quenched realization of disorder the free energy density of a chain made of N spins is

$$y_N = -\frac{1}{\beta N} \ln Z_N . \tag{5.32}$$

and, since it depends on J_i and h_i, it is a random quantity. The self-averaging property assures that in the limit of large N its probability distribution converges to $\delta(y_N - f)$, and, hence, $y_N \to f$ for almost all realization of disorder. However, for finite N the free energy y_N fluctuates from sample to sample. The probability distribution function of y_N depends in a complicate way on the probability distributions of couplings and local fields. Nevertheless, for large, though finite N, the fluctuations of y_N about f can be characterized using large deviations.

The partition function Z_N of the Ising chain can be computed from the product

$$Z_N = \mathrm{Tr} \prod_{i=1}^{N} \mathbf{L}_i \tag{5.33}$$

of the random transfer matrices

$$\mathbf{L}_i = \begin{bmatrix} e^{\beta(J_i+h_i)} & e^{\beta(-J_i+h_i)} \\ e^{-\beta(J_i+h_i)} & e^{-\beta(-J_i+h_i)} \end{bmatrix}. \tag{5.34}$$

In this context a theorem due to Oseledec [5] ensures that for – almost – all realizations of $\mathbf{L}_i$, the limit of

$$\lim_{N\to\infty} \frac{1}{N} \ln \left[\mathrm{Tr} \prod_{i=1}^{N} \mathbf{L}_i \right] = \lambda_1 \tag{5.35}$$

exists and is equal to the largest Lyapunov exponent λ_1 of the product matrix $\prod_{i=1}^{N} \mathbf{L}_i$. The exponent λ_1 can be related to the rate of growth of a generic vector $\xi(0) \in \mathbb{R}^2$ under repeated applications of the matrix $\mathbf{L_i}$:

$$\lambda_1 = \lim_{N\to\infty} \frac{1}{N} \ln R(N) \tag{5.36}$$

where

$$R(N) = \frac{|\xi(N)|}{|\xi(0)|}, \qquad \xi(i+i) = \mathbf{L}_i\, \xi(i). \tag{5.37}$$

The Oseledec's Theorem for products of random matrices, from the point of view of the statistical mechanics of disordered systems, is a statement on the self-averaging property of the free energy y_N of the disordered spin system whose average free energy, cf. Eq. (5.30), is $f = -\lambda_1/\beta$. Once f is known, the thermodynamic properties of the model can be derived.

The exponent λ_1, and hence f, is a non-random quantity. To study the sample-to-sample fluctuations one then considers the so called effective Lyapunov exponent

$$\gamma_N = \frac{1}{N} \ln \left[\mathrm{Tr} \prod_{i=1}^{N} \mathbf{L}_i \right] \sim \lambda_1, \qquad N \gg 1,$$

related to the rate of growth of a generic vector $\xi(0) \in \mathbb{R}^2$ under the application of N random matrices $\mathbf{L}_i$. The exponent γ_N *is* a fluctuating quantity, and information on its probability distribution can be obtained through the generalized Lyapunov exponents $L(q)$ [6],

$$L(q) = \lim_{N\to\infty} \frac{1}{N} \ln \overline{[R(N)]^q} \tag{5.38}$$

which plays the role of the generating functional $W(k)$, cf. Eq. (5.8), in the context of large deviation theory. For large N the probability distribution of γ_N obeys a large deviation principle

$$P_N(\gamma_N = \gamma) \sim e^{-NS(\gamma)} \tag{5.39}$$

with $S(\lambda_1) = 0$. The rate or *entropy* function $S(\gamma)$ gives the number of sequences $(\mathbf{L}_1, \ldots, \mathbf{L}_N)$ with $\gamma_N \in [\gamma, \gamma + d\gamma]$. The rate function $S(\gamma)$ is related to $L(q)$ by the Legendre transform

$$L(q) = \max_{\gamma} [q\gamma - S(\gamma)] \tag{5.40}$$

which, once inverted, yields $S(\gamma)$, or its convex envelope if $L(q)$ is not differentiable.

By expanding $L(q)$ in powers of q around $q = 0$ we have

$$L(q) = q\lambda_1 + \frac{1}{2}\sigma^2 q^2 + O(q^2) \tag{5.41}$$

where $\lambda_1 = dL(q)/dq|_{q=0}$ and the variance σ^2 (not to be confused with the Ising spin) is

$$\sigma^2 = \lim_{N\to\infty} \frac{1}{N}\left[\overline{[\ln R(N)]^2} - \left[\overline{\ln R(N)}\right]^2\right] = \lim_{N\to\infty} \beta^2 N\left[\overline{y_N^2} - \overline{y_N}^2\right] \tag{5.42}$$

as follows by direct differentiation of Eq. (5.38), see also Eqs. (5.7) and (5.8). Note that a finite σ^2 implies

$$\overline{y_N^2} - \overline{y_N}^2 \sim \frac{1}{N} \qquad \text{for} \quad N \gg 1,$$

i.e., normal fluctuations. The inversion of the Legendre transform leads to

$$S(\gamma) = \frac{1}{2\sigma^2}(\gamma - \lambda_1)^2 \tag{5.43}$$

cf. also Eqs. (5.5) and (5.14), and hence

$$P_N(y_N = y) \sim \exp\left[-\frac{N\beta^2}{2\sigma^2}(y - f)^2\right], \qquad N \gg 1. \tag{5.44}$$

The analysis of one-dimensional systems can be efficiently done in terms of products of matrices. While this approach can in principle be extended to higher dimensional systems, its use becomes less and less useful as the dimension of the system increases. The main reason is that for dimensions greater than one the size of the matrices increases exponentially with the number of spins, making the approach practically unfeasible.

5.2.2 *Replica Trick*

Since the thermodynamic properties of disordered systems are obtained from the disorder averaged free energy, in higher dimensional system the difficulty of averaging a logarithm is usually overcome using the *replica method*. This procedure is essentially the identity

$$\overline{\ln Z_N} = \lim_{n\to 0} \frac{\overline{(Z_N)^n} - 1}{n} \quad . \tag{5.45}$$

For integer n, $(Z_N)^n$ can be expressed as

$$(Z_N)^n = \prod_{a=1}^{n} Z_N^a$$

and may be interpreted as the partition function of n independent identical replicas $a = 1, \ldots, n$ of the system.

The generalized exponents $L(q)$ are directly related to the replica method. Defining the cumulant generating function, cf. Eqs. (5.7) and (5.32), as

$$-\beta W_N(n) = \frac{1}{N} \ln \overline{(Z_N)^n} = \frac{1}{N} \ln \int dy\, P_N(y_N = y)\, e^{-\beta N n y} \tag{5.46}$$

one readily sees that

$$-\beta W(n) = -\beta \lim_{N\to\infty} W_N(n) = L(n). \tag{5.47}$$

In the replica method one usually considers the (annealed) free energy density *per* replica $f(n) = W(n)/n$ because the average free energy per spin f, cf. Eq. (5.30) is, then, obtained as

$$f = -\lim_{N\to\infty} \frac{1}{\beta N} \overline{\ln Z_N} = \lim_{n\to 0} f(n). \tag{5.48}$$

Expanding $f(n)$ in powers of n, and using (5.41), we have

$$f(n) = f - \frac{\mu}{2} n + O(n^2) \tag{5.49}$$

where $f = -\lambda_1/\beta$, while $\mu = \sigma^2/\beta^2$ measures the strength of the free energy sample to sample fluctuations.

Analytic calculations of $f(n)$ are usually constrained to integer n, for which the replica method can be applied. This leads to the problem of extrapolating $f(n)$ evaluated for $n = 1, 2, 3 \ldots$ down to $n = 0$. This problem is well known in higher dimensional disordered systems, such as the Sherrington-Kirkpatrick model [18, 19], a mean-field model for spin-glasses, see Sect. 5.2.6, where the naive computation and extrapolation of $f(n)$ to $n = 0$ leads to an unphysical negative entropy. This is associated with the occurrence of a phase transition at finite temperature and a consequent breaking of the replica permutation symmetry. In presence of large fluctuations, though, a "naive" extrapolation may lead to wrong results even for one-dimensional systems, where no replica symmetry breaking is known to occur.

5.2.3 Replicas in the Random Ising Chain

In one-dimensional Ising chains, where we can use transfer matrices, the function $f(n)$ can be computed for integer positive n from the direct product of transfer matrices. Indeed it can be shown that [7]:

$$L(n) = \ln ||\overline{\mathbf{L}^{\otimes n}}|| \tag{5.50}$$

where $\otimes$ denotes the ordinary direct product, and $||\overline{\mathbf{L}^{\otimes n}}||$ the largest, in modulus, eigenvalue of $\overline{\mathbf{L}^{\otimes n}}$. The results can then be compared with the direct numerical calculation of λ_1 using Eq. (5.36).

As a specific example we consider the one-dimensional Ising chain (5.31) with uniform external field $h_i = h$ and bimodal random couplings:

$$P(J_i) = \frac{1}{2}\left[\delta(J_i - J) + \delta(J_i + J)\right] . \tag{5.51}$$

This model is known to possess a positive zero-temperature entropy [8,9]. Since the coupling constant can assume only two values, $\pm J$, we have

$$\overline{\mathbf{L}^{\otimes n}} = \frac{1}{2}\left[\begin{pmatrix} e^{\beta(J+h)} & e^{-\beta J} \\ e^{-\beta J} & e^{\beta(J-h)} \end{pmatrix}^{\otimes n} + \begin{pmatrix} e^{\beta(-J+h)} & e^{\beta J} \\ e^{\beta J} & e^{\beta(-J-h)} \end{pmatrix}^{\otimes n}\right]. \tag{5.52}$$

The size of the matrix is $2^n \times 2^n$ and the diagonalization can be easily performed, at least for values of n not too large.

Figure 5.4 shows $f(n)$ evaluated at integer n, the extrapolated $f(n \to 0)$ and the correct $f = -\lambda_1/\beta$ values for high and low temperature. For high temperature the values of $f(n)$ for integer n sit very close to a linear function, and the straightforward extrapolation to $n \to 0$ leads to a result in very good agreement with $-\lambda_1/\beta$. At low temperature the values of $f(n)$ evaluated at integer n deviate from a linear function and the agreement between the naive $f(n \to 0)$ extrapolation and $-\lambda_1/\beta$ is lost.

In Fig. 5.5 (left panel) the free energy $f = -\lambda_1/\beta$ and the result from the naive extrapolation $f(n \to 0)$ are compared as function of temperature. At high temperatures the two curves coincide. As the temperature T decreases the naive extrapolation $f(n \to 0)$ starts to deviate from f, and eventually decreases with T leading to an unphysical solution with negative entropy. This is a scenario similar to that observed in the Sherrington-Kirkpatrick model when the replica permutation symmetry is not broken. Here, however, the origin of the unphysical result can be traced back to the increase of sample-to-sample fluctuations of the free energy as the temperature decreases. There is no relationship to replica symmetry breaking and spin-glass transition. This is evidenced in Fig. 5.5 (right panel) which shows that the strength μ of the free energy sample-to-sample fluctuations is larger where the naive extrapolation $f(n \to 0)$ fails.

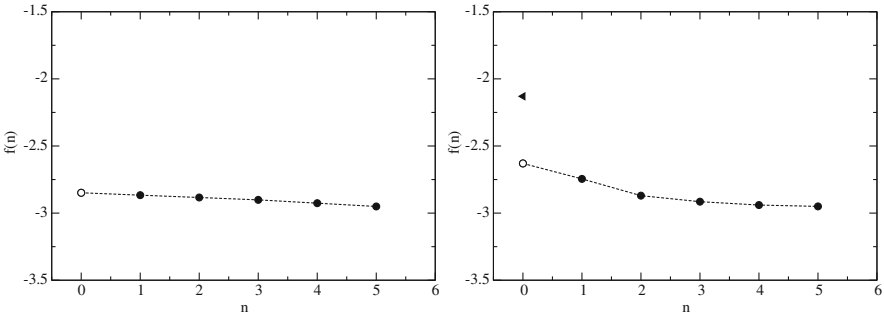

Fig. 5.4 Annealed free energy density per replica $f(n)$ of the random Ising chain at high (*left panel*) and low (*right panel*) temperature. The exact average free energy density $f = -\lambda_1/\beta$ is identified by a *triangle*

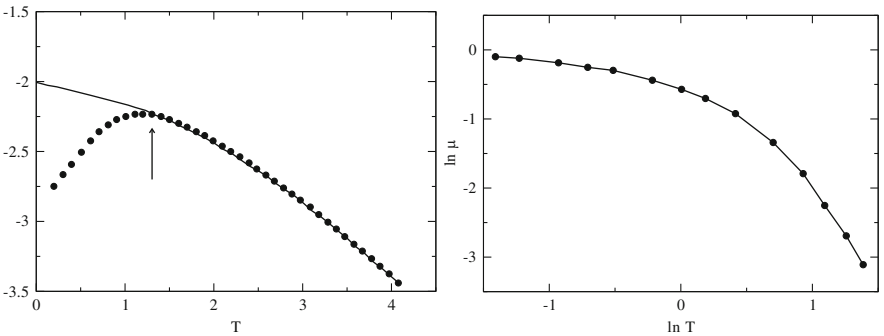

Fig. 5.5 *Left panel*: Free energy $f = -\lambda_1/\beta$ (*line*) and naive extrapolation $f(n \to 0)$ (*dots*) of the annealed free energy density per replica as function of temperature for the random Ising chain. *Right panel*: The sample-to-sample fluctuation strength $\mu = \sigma T$ vs. T on a log-log plot

5.2.4 From Small to Large Deviations

We have seen that if the coefficient of n^2 in the expansion of $W(n)$ is non-zero then the fluctuations of y_N about the typical value f are normal, that is $O(N^{-1/2})$ as $N \gg 1$, cf. Eqs. (5.41, 5.42 and 5.47). But what if, instead, this coefficient vanishes? To address this question we go back to the cumulant generating function $W_N(n)$. From its definition, Eq. (5.46), it follows that

$$-\beta N W_N(n) = \sum_{k\geq 1} \frac{C_k}{k!} n^k \qquad ; \qquad C_k \equiv \left.\frac{\partial \ln \overline{Z_N^n}}{\partial n^k}\right|_{n=0} \tag{5.53}$$

where C_k is the kth cumulant of $\ln Z_N = -\beta N y_N$, that is

$$C_1 = \overline{\ln Z_N}, \qquad C_2 = \overline{(\ln Z_N)^2} - \left(\overline{\ln Z_N}\right)^2,$$

and so on. It is sufficient to take successive derivatives of Eq. (5.46) with respect to n, and evaluate them at $n = 0$. Thus, if $W_N(n)$ is known, the cumulants are identified with the coefficients of its Taylor expansion around $n = 0$. In particular, the coefficient of the n^2 term in the expansion

$$C_2 = \beta^2 N^2 [\overline{y_N^2} - \overline{y_N}^2] \tag{5.54}$$

gives a measure of the fluctuations of y_N about the average value $\overline{y_N}$ evaluated for *finite* N. This expression is indeed valid for *any* N and not only in the limit $N \gg 1$.

From Eq. (5.53) readily follows:

$$-\beta W(n) = \lim_{N\to\infty} \frac{1}{N} \sum_{k\geq 1} \frac{C_k}{k!} n^k \equiv \sum_{k\geq 1} \frac{c_k}{k!} n^k \tag{5.55}$$

where $c_k = \lim_{N\to\infty} C_k/N$. If the cumulant $C_k \sim o(N)$, then the corresponding n^k term is missing in the expansion. Consequence of this is that a $c_2 \neq 0$ implies normal fluctuations $\overline{y_N^2} - \overline{y_N}^2 \sim N^{-1}$. Vice versa, if $C_2 \sim N^{1-a}$ with $a > 0$, so that the n^2 is missing, means

$$\overline{y_N^2} - \overline{y_N}^2 \sim \frac{1}{N^{1+a}}. \tag{5.56}$$

As a consequence, the absence of the n^2 term in the expansion of $W(n)$ signals anomalous fluctuations. In this case, to have the correct scaling of C_2 with N, one has to go back to $W_N(n)$, the calculation of which is, in general, more difficult than that of $W(n)$.

As emphasized above, C_2 is associated with the sample-to-sample fluctuations in a finite system about the average value $\overline{y_N}$, and not about the asymptotic value $f = \lim_{N\to\infty} \overline{y_N}$. While to access the first one we need $W_N(n)$, information on the latter can be directly obtained from $W(n)$. Indeed, let us assume that the probability distribution of y_N obeys a large deviation principle

$$P_N(y_N = y) \sim e^{-NS(y)},$$

with $S(f) = 0$ and $S(y) > 0$ if $y \neq f$. From Eqs. (5.46) and (5.47) it follows, via a saddle point integration, that

$$\beta W(n) = \inf_y [S(y) + \beta n y]. \tag{5.57}$$

The rate $S(y)$ can now be obtained by inverting the Legendre transform:

$$S(y) = \beta[W(n) - ny] \tag{5.58}$$

where n is eliminated in favor of y using

$$\frac{d}{dn}W(n) = y. \tag{5.59}$$

We recall that, strictly speaking, $W(n)$ gives the convex envelope of $S(y)$. Moreover, if the moments $\overline{Z_N^n}$ grow more than exponentially with n for $n \gg 1$, then the probability distribution is not uniquely determined by $W(n)$ [10, 11]. Nevertheless, $W(n)$ yields information on small deviations of y_N from f. We have indeed seen, as, for example, Eqs. (5.41), (5.43) and (5.44), that if

$$W(n) = fn - \frac{\mu}{2}n^2 + O(n^3) \tag{5.60}$$

with $\mu > 0$, $-W(n)$ is a convex function of n. It follows

$$S(y) = \frac{\beta}{2\mu}(y - f)^2 \tag{5.61}$$

and, hence, $\overline{(y-f)^2} \sim N^{-1}$. Otherwise stated, this expresses the fact that the Gaussian approximation is valid for (small) deviations $y - f$, up to order $O(N^{-1/2})$.

Consider now the case in which the term n^2 is missing, and $W(n)$ takes the form

$$W(n) = fn - \frac{\mu_+}{3}n^3 + O(n^4), \qquad n \geq 0 \tag{5.62}$$

where as before $\mu_+ > 0$ for convexity. The restriction $n \geq 0$ is now necessary since $-W(n)$ given by Eq. (5.62) is not convex for $n < 0$. Use of Eqs. (5.58) and (5.59), and a simple calculation, shows that this form of $W(n)$ leads to

$$\frac{S(y)}{\beta} = \frac{2}{3\sqrt{\mu_+}}(f - y)^{3/2}, \qquad f - y \geq 0. \tag{5.63}$$

The restriction $f - y \geq 0$ is a consequence of the constraint $n \geq 0$, because positive values of n favors smaller values of y, see, e.g., Eq. (5.46). This is similar to what we have seen in the example of the Mean Field Ising model (Sect. 5.1.1) where positive (negative) values of k select positive (negative) value of magnetization m. From Eq. (5.63) it follows that for large N

$$\overline{(f - y)} \sim N^{-2/3}, \qquad \overline{(f - y)^2} \sim N^{-4/3}, \qquad f - y \geq 0. \tag{5.64}$$

To gain informations on the region $f - y \leq 0$, we need $W(n)$ for negative n. In principle $W(n)$ for positive and negative n may have different functional forms. Under the hypothesis that

$$W(n) = fn + \frac{\mu_-}{3}n^3 + O(n^4), \qquad n \leq 0 \tag{5.65}$$

with $\mu_- > 0$, we have

$$\frac{S(y)}{\beta} = \frac{2}{3\sqrt{\mu_-}}(y-f)^{3/2}, \qquad f - y \le 0. \tag{5.66}$$

and the constraint in the scaling, cf. Eq. (5.64), can thus be removed. Note that the scaling $\overline{(f-y)} \sim N^{-2/3}$ requires $\mu_+ \neq \mu_-$, i.e. a non symmetric probability distribution, otherwise the average vanishes by symmetry. Were this the case, the $\overline{(f-y)}$ scaling is valid only if we restrict the energy domain to $f - y \ge 0$ (or ≤ 0).

The above arguments can be extended to a generic power of n. If the first non-vanishing term in the expansion of $W(n) - fn$ is proportional to n^m with $m \ge 3$, then a straightforward calculation shows that

$$\overline{(f-y)} \sim N^{-(m-1)/m}, \qquad \overline{(f-y)^2} \sim N^{-2(m-1)/m}. \tag{5.67}$$

Again, if the probability distribution is symmetric the scaling for $\overline{(f-y)}$ is valid if restricted to $f - y \ge 0$ (or ≤ 0), otherwise it vanishes by symmetry at any N.

5.2.5 Random Directed Polymer

A cumulant generating function of the form (5.62) has been found using a replica calculation in the study of random directed polymers [12, 13]. From the above arguments it then follows that the probability distribution of the extensive free energy Y_L of polymers of length L for small deviations from the typical value Lf is

$$P_L(Y_L = Y) \sim \exp\left[-a_\pm |Lf - Y|^{3/2} L^{-1/2}\right], \qquad L \gg 1 \tag{5.68}$$

where we take either a_+ or a_- depending on the sign of $Lf - Y$. This form, and the associated scaling

$$\overline{(Lf - Y)} \sim L^{1/3}, \qquad L \gg 1 \tag{5.69}$$

are in agreement with both analytical [14, 15] and numerical [16, 17] results.

5.2.6 Mean-Field Spin-Glass

The large deviation scenario depicted in Sect. 5.2.4 is found, for example, in the Sherrignton-Kirkpatrick model, a mean field spin-glass model defined by the Hamiltonian [18, 19]

$$\mathscr{H} = -\frac{1}{2}\sum_{i\neq j}^{1,N} J_{ij}\,\sigma_i\sigma_j \tag{5.70}$$

where $\sigma = \pm 1$ are Ising spins and the symmetric couplings J_{ij} are independent identically distributed quenched Gaussian random variables of zero mean and variance equal to $1/N$. All pairs of spins (i, j) interacts, and the scaling of the variance ensures a well defined thermodynamic limit as $N \to \infty$. Using the replica method the (annealed) free energy density per replica $f(n) = W(n)/n$ can be computed for integer n [18, 19].

For high temperature the symmetry under permutation of the n replicas is unbroken and one has $W(n) = fn$, the naive extrapolation $n \to 0$ is trivially correct. This result can be seen as the limiting case $m \to \infty$ of the general case just discussed, cf. Eq. (5.67). Therefore in this phase, called *replica symmetric*, one has

$$\overline{(f - y)} \sim N^{-1}, \qquad \overline{(f - y)^2} \sim N^{-2}. \tag{5.71}$$

If we turn to $W_N(n)$ an explicit calculation shows [20] that

$$\beta\,\overline{y_N} = -\frac{\beta^2}{4} - \ln 2 - \frac{1}{4N}\ln(1-\beta^2) + o(N^{-1}) \tag{5.72}$$

$$\beta C_2/N = -\frac{1}{2N}\left[\beta^2 + \ln(1-\beta^2)\right] + o(N^{-1}). \tag{5.73}$$

From this result we see that C_2/N diverges as $\beta \to 1^-$ signaling the spin glass transition at the critical temperature $T_c = 1$. Indeed, the $1/N$ terms contain the contributions from the fluctuations about the saddle point used to evaluate $W(n)$, so that the divergence of C_2/N signals the instability of the high temperature replica symmetric phase.

Below T_c the phase space is broken into a large, yet entropically not extensive, number of degenerate locally stable states, and the replica permutation symmetry is broken both in the zero replicas limit and for positive small values of n. The study of the model below T_c becomes then rather difficult. For temperature slightly below T_c, working with a *truncated* version of the SK model [21–23] Kondor found [24]

$$f(n) = f_P(\tau) - \frac{9}{5{,}120}n^5 + \cdots, \qquad n \le n_s(\tau) = \frac{4}{3}\tau + \cdots \tag{5.74}$$

where the so-called Parisi free energy $f_P(\tau)$ can be computed in the truncated model around the critical temperature as [23]

$$f_P(\tau) = \frac{\tau^3}{12} + \frac{\tau^4}{24} + \frac{\tau^5}{20} + \cdots; \quad \tau \equiv \frac{1-T^2}{2} \tag{5.75}$$

or it can be computed in the original SK model,[1] where also the non variational part of the free energy is included and τ is defined as $\tau = (T_c - T)/T_c$ [35]

$$f_P(\tau) = -\ln 2 - \frac{1}{4} + \tau \ln 2 - \frac{\tau}{4} - \frac{\tau^2}{4} - \frac{\tau^3}{12} + \frac{\tau^4}{24} - \frac{\tau^5}{120} + \cdots ; \tag{5.76}$$

For $n > n_s(\tau)$ the replica symmetric solution remains stable.

From this result, it follows that the first non-vanishing term in the expansion of $W(n) - fn$ is proportional to n^6, and so, from the above general result, cf. Eq. (5.67), we conclude that [25]

$$\overline{(f - y)} \sim N^{-5/6}, \qquad \overline{(f - y)^2} \sim N^{-5/3}. \tag{5.77}$$

Using scaling argument one may also infer that $C_2 \sim N^{1/3}$.

The above prediction has been tested in recent years in numerical simulations also significantly below T_c and, in particular, at $T = 0$ [26–33]. Kondor's computation has been extended down to zero temperature and for higher orders in n [34,35], generalizing Eq. (5.74) to the following expression valid at *any* temperature:

$$f(n) - f_P = -\frac{9}{640}\left(\frac{n}{T}\right)^5 [T\dot{q}(0)]^3 + O(n^7), \tag{5.78}$$

where $\dot{q}(0)$ is the derivative of the overlap parameter function $q(x)$ characterizing the infinite Replica Symmetry Breaking (RSB) spin-glass phase evaluated at $x = 0$.[2] As $T = T_c$, $\dot{q}(0) = 1/2$, thus leading back to Kondor's result. As $T \to 0$, the resolution of Parisi anti-parabolic equation for the ∞-RSB Ansatz [36], yields $T\dot{q}(0) = 0.743$ [37,38]. In all cases, the $N^{-5/6}$ scaling for free energy density large deviations is confirmed at all temperatures, including $T = 0$, thus allowing for a direct comparison with the results of numerical simulations.

5.2.7 *Positive Large Deviations*

A different scenario arises for positive large fluctuations of free energy, i.e., *above* the typical value f. In this case the probability distribution of y does not follow a large deviation principle as in Eq. (5.39) but, rather,

[1] The computations differ for two reasons. First, the small perturbative parameter τ is defined in two different ways and $\tau_{\text{exact}} = \tau_{\text{trunc}} - \tau_{\text{trunc}}^2/2$. Second, the truncated model represents the exact one near the critical point but already at the fourth order in τ the free energy behavior differs.

[2] The function $q(x)$ is the continuous order parameter characterizing the spin-glass phase in presence of a continuous, that is, an infinite number, of breakings of replica symmetry. It is always zero in the paramagnetic phase and it becomes continuously non zero and x-dependent at the transition point to the spin-glass phase. The variable x, defined in the interval $[0, 1]$, is the so called RSB parameter labeling the RSB's in the continuous limit [23,36,46].

$$P_N(y) \sim e^{-N^2 S_2(y)} \tag{5.79}$$

i.e., the rate function scales as N^{-2} [27, 39, 44]. In the SK model the rate function takes the form [39]

$$S_2(y) = -a\,[T\dot{q}(0)]^{-6/5}\,(f-y)^{12/5} + o\left((f-y)^{12/5}\right) \tag{5.80}$$

$$a = \left(-\frac{7}{12\,C}\right)^{7/5}; \qquad C = 0.64(2)$$

thus leading to the same scaling (5.77) when small deviations are matched. On top of this the exponent $12/5$ is in good agreement with zero temperature numerical simulations [27]. The computation is much more complicated than in the negative deviation case, where the rate function scale linearly in N. In the first place because as $y > f$, the large deviation rate function $S(y) \to \infty$ and one has to work with a negative number of replicas. Namely, n is chosen as proportional to the size N with a negative coefficient. The large size limit eventually corresponds to $n \to -\infty$.

The $O(N^2)$ scaling for the rate function is not something special related to the replica symmetry breaking solution of mean-field spin-glasses. In the case of Gaussian random matrices, indeed, this kind of large deviations appears in different fields [39]. Let us consider, as an instance, the simpler, replica symmetric, spherical mean-field spin-glass model.

5.2.8 *Spherical Spin-Glass Model and Gaussian Random Matrices*

Let us consider the Hamiltonian (5.70) with *soft* spins, rather than *hard* Ising spins $\sigma = \pm 1$, with a global *spherical constraint*

$$\sum_{i=1}^{N} \sigma_i^2 = N \quad . \tag{5.81}$$

At zero temperature the energy of this model is equal to the largest eigenvalue (with a minus sign in front) of a random Gaussian matrix of dimension $N \times N$. For random Gaussian matrices the small deviations of the largest eigenvalue are described by the Tracy-Widom distribution [40] and the probability that the largest eigenvalue is lower than its typical value – else said that the energy is higher than its typical value – goes like Eq. (5.79).

The $O(N^2)$ large deviation behavior plays, indeed, an important role to determine, e.g., the expected number of minima of a random polynomial [41] or in the framework of the anthropic principle in string theory [42]. In the latter case a crucial point is the estimate of the probability that *all* eigenvalures of a Gaussian matrix are positive (or negative) [43]. This turns out to behave as

$$P_N \sim e^{-b\theta N^2}; \qquad \theta = \frac{\ln 3}{4} \tag{5.82}$$

where the so called Dyson index b is $b = 1$ for matrices whose entries belong to the Gaussian orthogonal ensemble, $b = 2$ for elements extracted from a Gaussian unitary ensemble and $b = 4$ for self-dual Hermitian matrices of the Gaussian symplectic ensemble [44, 45].

5.3 Sample-to-Sample Fluctuation of the Overlap

The use of large deviation is not restricted to the study of free energy fluctuations. Other quantities can be analyzed. Here we consider the *overlap* parameter. In disordered magnetic systems such as spin glasses the couplings between spins can be of either sign. Consequence of this is that it is not possible to satisfy simultaneously all constraints and the system becomes *frustrated*. This results in a large number of equivalent equilibrium states that cannot be characterized only in terms of free energy and a single-valued order parameter as in non-disordered systems. To have a characterization of this phase one introduces the notion of distance between equilibrium states through the overlap q and its probability distribution.

Given two spin configurations $\{\sigma_i\}$ and $\{\tau_i\}$ their mutual overlap is

$$q_N = \frac{1}{N} \sum_{i=1}^{N} \sigma_i \, \tau_i \tag{5.83}$$

The overlap q_N is a fluctuating quantity and its probability distribution in equilibrium at temperature T is given by

$$P_{J,N}(q) = \frac{1}{(Z_N)^2} \sum_{\sigma_1,\ldots\sigma_N} \sum_{\tau_1,\ldots\tau_N} e^{-\beta H(\sigma)} \, e^{-\beta H(\tau)} \, \delta\left(q - \frac{1}{N} \sum_{i=1}^{M} \sigma_i \, \tau_i\right) \tag{5.84}$$

where Z_N is the partition function. We have added the subscript J because in general $P_{J,N}$ depends on the particular realization of the couplings (disorder), *even* in the limit $N \to \infty$. In other words, the structure of the equilibrium states may vary with the disorder realization in thermodynamic limit as well: $P_{J,N}$ is not self-averaging.

The disorder average $\overline{P_J}$ can ben computed using the replica method, see e.g., Refs. [46, 47]. The cumulant generating function $W_{J,N}(k)$ associated with $P_{J,N}(q_N = q)$ is

$$
\begin{aligned}
e^{NW_{J,N}(k)} &= \int_{-1}^{1} dq\; P_{J,N}(q)\, e^{Nkq} \\
&= \frac{1}{(Z_N)^2} \sum_{\sigma_1,\dots\sigma_N} \sum_{\tau_1,\dots\tau_N} \exp\left[-\beta H(\sigma) - \beta H(\tau) + k \sum_i \sigma_i\, \tau_i \right] \\
&= Z_N^{(2)}(k)/(Z_N)^2
\end{aligned}
\tag{5.85}
$$

where $Z_N^{(2)}(k)$ is the partition function of two replicas of the system coupled by the term $k \sum_i \sigma_i\, \tau_i$. Then $\overline{W_{J,N}(k)}$ can be obtained from the moments $\overline{(Z_N)^n}$ and $\overline{[Z_N^{(2)}(k)]^n}$ using the replica trick, cf. Eq. (5.45).

5.3.1 Back to the Replicated Random Ising Chain

Here we shall not enter into the details of the replica approach, but rather consider the case of the random Ising chain (5.31) where transfer matrices can be used. In the previous section we have seen that the partition function of the Ising chain can be written as a product of the 2×2 (random) matrices $\mathbf{L}_i$, see Eqs. (5.33) and (5.34). Similarly the 2-replica partition function can be written as a product of 4×4 matrices. Then in term of matrices the cumulant generating function (5.85) reads

$$
W_{J,N}(k) = \frac{1}{N} \ln \left[\mathrm{Tr} \prod_{i=1}^{N} [\mathbf{A}_i \mathbf{B}(k)] \right] - \frac{2}{N} \ln \left[\mathrm{Tr} \prod_{i=1}^{N} \mathbf{L}_i \right] \tag{5.86}
$$

where

$$
\mathbf{A}_i = \mathbf{L}_i \otimes \mathbf{L}_i \quad , \tag{5.87}
$$

with $\mathbf{L}_i$ defined in Eq. (5.34), and $\mathbf{B}(k)$ is the diagonal matrix

$$
\mathbf{B}(k) = \begin{bmatrix} e^{k} & 0 & 0 & 0 \\ 0 & e^{-k} & 0 & 0 \\ 0 & 0 & e^{-k} & 0 \\ 0 & 0 & 0 & e^{k} \end{bmatrix} . \tag{5.88}
$$

The Oseledec theorem [5] ensures that $W(k) = \lim_{N\to\infty} W_{J,N}(k)$ exists, and is equal to

$$
W(k) = \lambda(k) - \lambda(0) \tag{5.89}
$$

where $\lambda(k)$ is the maximum Lyapunov exponent of the product of random matrices $\mathbf{M}_i = \mathbf{A}_i\mathbf{B}(k)$ and $\lambda(0) = 2\lambda_1$, see Eq. (5.36). We have suppressed the subscript J because the Oseledec theorem also ensures that the Lyapunov exponent takes the same value for almost all realization of disorder, i.e., it is self-averaging quantity, and hence $\overline{W_J(k)} = W(k)$. For large positive (negative) k the integral in (5.85) is dominated by the extreme $q = +1\ (-1)$, and $W(k) \sim \pm k$ as $k \to \pm\infty$.

If $W(k)$ is differentiable for all $k \in \mathbb{R}$, then the Gärtner-Ellis theorem [48, 49], see also [2], ensures that q_N satisfies a large deviation principle with rate function given by

$$\Gamma(q) = \sup_{k\in\mathbb{R}} [kq - W(k)] \tag{5.90}$$

implying that $P_{J,N}(q_N = q)$ is itself a self-averaging quantity, converging to a delta function as $N \to \infty$. The non-self-averaging character of $P_{J,N}(q_N = q)$ thus requires that, as $N \to \infty$, it rather becomes a smooth, non-trivial, function with a finite bounded support $[q_{\min}, q_{\max}]$. As a consequence

$$W(k) \sim \begin{cases} kq_{\min} & \text{if } k \sim 0^- \\ \\ kq_{\max} & \text{if } k \sim 0^+ \end{cases} \tag{5.91}$$

so that $W(k)$ is not differentiable at $k = 0$.

Note that while $P_J(q) = \lim_{N\to\infty} P_{J,N}(q_N = q)$ is not self-averaging, its support $[q_{\min}, q_{\max}]$ is self-averaging and, moreover,

$$q_{\min,\max} = \lim_{k\to 0^{\mp}} \frac{d}{dk} W(k) \tag{5.92}$$

This result can be considered as a distinctive feature of a replica symmetry breaking [46].

On the basis of these results it follows that $P_{J,N}(q_N = q)$ obeys a large deviation principle

$$P_{J,N}(q_N = q) \sim A_J(q)\, e^{-NS_J(q)}, \qquad N \gg 1 \tag{5.93}$$

with $S_J(q) = 0$ if $q \in [q_{\min}, q_{\max}]$ and $S_J(q) > 0$ if $q \notin [q_{\min}, q_{\max}]$. The rate function may depend on the disorder realization, but its convex envelop $\Gamma(q)$ given by Eq. (5.90) is self-averaging.

We have derived these results using the theory of the products of random matrices, however their validity is more general and can be extend to other random systems where random matrices cannot be used, see e.g. Ref. [50].

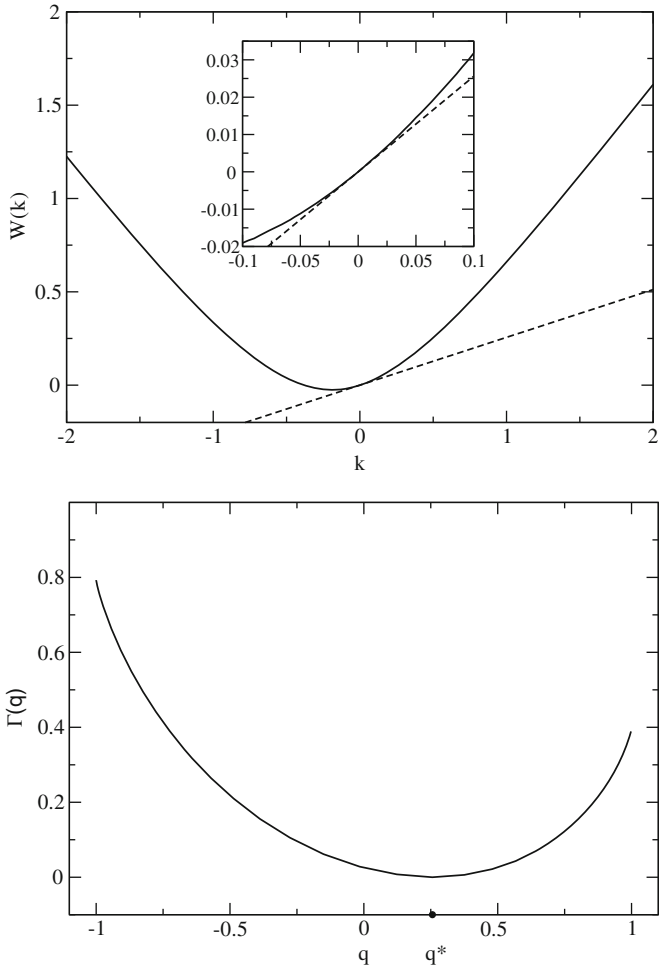

Fig. 5.6 The cumulant generating function $W(k)$ (*top*) and its Legendre Transform $\Gamma(q)$ (*bottom*) for the random Ising chain with $J_i = 1$ and $h_i = \eta_i - \eta_{i+1}$, where $P(\eta_i) = \delta(\eta_i^2 - 1)$, at zero temperature. A closer look of $W(k)$ about $k = 0$, inset *top panel*, reveals that its derivative $W'(k)$ is continuous as $k \to 0^{\pm}$, so that $q_{\min} = q_{\max} = q^* = W'(k = 0)$

5.3.2 *Random Field Ising Model*

We conclude this section by reporting some results for the random Ising chain with $J_i = 1$ and random fields $h_i = \eta_i - \eta_{i+1}$, where η are independent identically distributed random variables taking the value ± 1 with equal probability. As a consequence of the site correlation of the field h_i frustration is important, and the zero temperature entropy does not vanishes. The function $W(k) = \lambda(k) - \lambda(0)$, evaluated from the Lyapunov exponent of the product of random matrices, is shown in Fig. 5.6 for zero temperature. The function is smooth and differentiable for all k,

indicating that $P_{J,N}(q_N = q) \sim \delta(q - q^*)$ as $N \to \infty$. The value of q^* is obtained from the slope of $W(k)$ at the origin: $q^* = \lim_{k\to 0} W'(k) \simeq 0.256$. Its non-zero value confirms the relevance of frustration, though there is no replica symmetry breaking. For other results for the random Ising chain along these lines see, e.g., Ref. [51].

5.4 A Final Word

This contribution is an introduction to the use of large deviations to study properties of disordered systems. We have intentionally put more emphasis on low dimensional systems, where product of random matrices can be employed, for its pedagogical impact. The intent was indeed to write a simple and easy introduction to the subject, leaving out all unnecessary mathematics and advanced methods, focusing on the basic ideas behind the application of large deviations to disordered systems. As a consequence the contribution does not pretend to be exhaustive, nor self-contained. The reader interested in details on calculations is then referred to the references.

References

1. S.R.S. Varadhan, *Large Deviations and Applications* (Society of Industrial and Applied Mathematics, Belfast, 1984)
2. U. Touchette, Phys. Rep. **478**, 1 (2009)
3. A. Crisanti, G. Paladin, A. Vulpiani, *Products of Random Matrices in Statistical Physics*. Springer Series in Solid State Sciences, vol. 104 (Springer, Berlin/Heidelberg, 1993)
4. M. Lifshitz, S.A. Gredeskul, L.A. Pastur, *Introduction to the Theory of Disordered Systems* (Wiley, New York, 1988)
5. V.I. Oseledec, Trans. Mosc. Math. Soc. **19**, 197 (1968)
6. G. Paladin, A. Vulpiani, Phys. Rep. **156**, 147 (1987)
7. J.P. Bouchaud, A. Geroges, D. Hansel, P. Le Doussal, J.M. Maillard, J. Phys. A **19**, L1145 (1986)
8. M. Puma, J.F. Fernandez, Phys. Rev. B **18**, 1931 (1978)
9. B. Derrida, H.J. Hilhorst, J. Phys. A **16**, 2641 (1983)
10. T. Carleman, C. R. Acad. Sc. Paris **174**, 1680 (1922)
11. S.A. Orszag, Phys. Fluids **13**, 2211 (1970)
12. M. Kardar, Phys. Rev. Lett. **55**, 2235 (1985)
13. M. Kardar, Nucl. Phys. B [FS20] **290**, 582 (1987)
14. Y.C. Zhang, J. Stat. Phys. **57**, 1123 (1989)
15. J.P. Bouchaud, H. Orland, J. Stat. Phys. **61**, 877 (1990)
16. M. Mézard, J. Phys. (Fr.) **51**, 1831 (1990)
17. T. Halpin-Healy, Phys. Rev. A **44**, R3415 (1991)
18. D. Sherrington, S. Kirkpatrick, Phys. Rev. Lett. **35**, 1792 (1975)
19. S. Kirkpatrick, D. Sherrington, Phys. Rev. B **17**, 4384 (1978)
20. G. Toulouse, B. Derrida, in *Proceedings of 6th Brazilian Symposium on Theoretical Physics*, Rio de Janeiro (CNPQ 1981, Brasilia), ed. by E. Ferreira, B. Koller (1980), p. 143
21. A. Bray, M.A. Moore, J. Phys. C Solid State Phys. **12**, 79 (1979)

22. E. Pytte, J. Rudnick, Phys. Rev. B **19**, 3603 (1979)
23. G. Parisi, Phys. Rev. Lett. **43**, 1754 (1979)
24. I. Kondor, J. Phys. A **16**, L127 (1983)
25. A. Crisanti, G. Paladin, H.-J. Sommers, A. Vulpiani, J. Phys. I (Fr.) **2**, 1325 (1992)
26. J.-P. Bouchaud, F. Krzakala, O.C. Martin, Phys. Rev. B **68**, 224404 (2003)
27. A. Andreanov, F. Barbieri, O.C. Martin, Eur. Phys. J. B **41**, 365 (2004)
28. S. Boettcher, Europhys. Lett. **67**, 453 (2004)
29. S. Boettcher, Eur. Phys. J. B **46**, 501 (2005)
30. H.G. Katzgraber, M Körner, F. Liers, M. Jünger, A.K. Hartmann, Phys. Rev. B **72**, 094421 (2005)
31. K.F. Pal, Physica A **367**, 261 (2006)
32. T. Aspelmeier, A. Billoire, E. Marinari, M.A. Moore, J. Phys. A **41**, 324008 (2008)
33. M. Palassini, J. Stat. Mech. P10005 (2008)
34. G. Parisi, T. Rizzo, Phys. Rev. Lett. **101**, 117205 (2008)
35. G. Parisi, T. Rizzo, Phys. Rev. B **79**, 134205 (2009)
36. G. Parisi, J. Phys. A **13**, 115 (1980)
37. A. Crisanti, T. Rizzo, Phys. Rev. E **65**, 046137 (2002)
38. R. Oppermann, M.J. Schmidt, D. Sherrington, Phys. Rev. Lett. **98**, 127201 (2007)
39. G. Parisi, T. Rizzo, Phys. Rev. B **81**, 094201 (2010)
40. C.A. Tracy, H. Widom, Comm. Math. Phys. **159**, 151 (1994); C.A. Tracy, H. Widom, Comm. Math. Phys. **177**, 727 (1996)
41. J.-P. Dedieu, G. Malajovich, J. Complex. **24**, 89 (2008)
42. L. Susskind, arXiv:hep-th/0302219v1; R. Bousso, J. Polchinski, Sci. Am. **291**, 60–69 (2004); L. Susskind, *The Cosmic Landscape: String Theory and the Illusion of Intelligent Design* (Little, Brown & Co., New York, 2005)
43. A. Aazami, R. Easther, J. Cosmol. Astropart. Phys. 013 (2006)
44. D.S. Dean, S.N. Majumdar, Phys. Rev. Lett. **97**, 160201 (2006)
45. D.S. Dean, S.N. Majumdar, Phys. Rev. E **77**, 041108 (2008)
46. M. Mézard, G. Parisi, M. Virasoro, *Spin Glass Theory and Beyond* (World Scientific, Singapore, 1988)
47. K.H. Fischer, J.A. Hertz, *Spin Glasses* (Cambridge University Press, Cambridge, 1991)
48. J. Gärtner, Theory Probab. Appl. **22**, 24 (1977)
49. R.S. Ellis, Ann. Probab. **12**, 1 (1984)
50. S. Franz, G. Parisi, M. Virasoro, J. Phys. I (Fr.) **2**, 1869 (1992)
51. A. Crisanti, G. Paladin, M. Serva, A. Vulpiani, Phys. Rev. E **49**, R953 (1994)

Chapter 6
Large Deviations in Monte Carlo Methods

Andrea Pelissetto and Federico Ricci-Tersenghi

Abstract Numerical studies of statistical systems aim at sampling the Boltzmann-Gibbs distribution defined over the system configuration space. In the large-volume limit, the number of configurations becomes large and the distribution very narrow, so that independent-sampling methods do not work and importance sampling is needed. In this case, the dynamic Monte Carlo (MC) method, which only samples the relevant "equilibrium" configurations, is the appropriate tool.

However, in the presence of ergodicity breaking in the thermodynamic limit (for instance, in systems showing phase coexistence) standard MC simulations are not able to sample efficiently the Boltzmann-Gibbs distribution. Similar problems may arise when sampling rare configurations. We discuss here MC methods that are used to overcome these problems and, more generally, to determine thermodynamic/statistical properties that are controlled by rare configurations, which are indeed the subject of the theory of large deviations.

We first discuss the problem of data reweighting, then we introduce a family of methods that rely on non-Boltzmann-Gibbs probability distributions, umbrella sampling, simulated tempering, and multicanonical methods. Finally, we discuss parallel tempering which is a general multipurpose method for the study of multimodal distributions, both for homogeneous and disordered systems.

6.1 Introduction

Statistical mechanics was developed at the end of the nineteenth century to provide a theoretical framework to thermodynamics. However, the complexity of the formulation made ab initio calculations essentially impossible: only ideal

A. Pelissetto • F. Ricci-Tersenghi (✉)
Dipartimento di Fisica and INFN, Università "Sapienza", Piazzale Aldo Moro 5, Rome, I-00185, Italy
e-mail: andrea.pelissetto@roma1.infn.it; federico.ricci@roma1.infn.it

A. Vulpiani et al. (eds.), *Large Deviations in Physics*, Lecture Notes in Physics 885,
DOI 10.1007/978-3-642-54251-0_6,

(noninteracting) systems could be treated exactly, the two-dimensional Ising model being a notable exception. To understand the behavior of more complex systems, crude approximations and phenomenological models, in most of the cases only motivated by physical intuition, were used. The understanding of statistical systems changed completely in the late 1950s, when computers were first used [1–4]. The first *machine calculations* showed that the behavior of macroscopic systems containing a large number of molecules (of the order of the Avogadro's number, $N_A \approx 6.022 \cdot 10^{23}$) could be reasonably reproduced by relatively small systems with a number of molecules of the order of 10^2–10^3, which could be simulated with the computer facilities of the time. These results, which, for many years, were met with skepticism by the more theoretically-oriented part of the statistical-mechanics community, opened a new era: theoreticians had their own laboratory, in which they could analyze the behavior of different systems under well-controlled *theoretical* conditions. Since then, numerical methods have been extensively used and have provided quantitatively accurate predictions for the behavior of many condensed-matter systems. Similar methods have also been employed in many other fields of science, from high-energy physics (in the 1970s the first lattice QCD simulations were performed) to astrophysics, chemistry, biology, statistics, etc.

The Monte Carlo (MC) method is one of the most powerful techniques for the simulation of statistical systems. Since the Boltzmann-Gibbs distribution is strongly concentrated in configuration space, MC methods implement what is called *importance sampling*: points in configuration space are not generated randomly, but according to the desired probability distribution. In practice, in a MC simulation one only generates typical configurations, i.e. those that most contribute to thermodynamic averages. From a mathematical point of view, a MC algorithm is a Markov chain that (a) is stationary with respect to the Boltzmann-Gibbs distribution and (b) satisfies ergodicity (mathematicians call the latter property irreducibility). If these two conditions are satisfied, time averages converge to configuration averages: hence, by using the MC results one can compute ensemble averages for the system at hand. While condition (a) is usually easy to satisfy—the Metropolis algorithm is a general purpose method to define a Markov chain that satisfies (a)—condition (b) is more subtle. Indeed, in the presence of phase transitions or of quenched disorder, a statistical system may show an infinite number of inequivalent thermodynamic states in the infinite-volume limit, which in turn implies ergodicity breaking for any (physical or MC) local dynamics. For instance, consider the Ising model in a finite volume with some boundary conditions that do not break the up-down symmetry (for instance, the usual periodic boundary conditions). Since the symmetry is exactly preserved, the magnetization per site m is exactly zero. However, if the temperature T is low enough, in any MC simulation of a sufficiently large system one observes that the system magnetizes, i.e. m is equal either to m_0 or to $-m_0$. This result can be easily understood. The correct distribution $P(m)$ of the magnetization has maxima $P_{\max}$ at $\pm m_0$ and a minimum $P_{\min}$ at $m = 0$. The important point is that the ratio $P_{\min}/P_{\max}$ is extremely small, of the order of e^{-aN^p}, $a, p > 0$, where N is the number of system variables. To obtain the correct average one should sample all relevant configurations, i.e., both those that have $m \approx m_0$ and those that have

$m \approx -m_0$. But these two regions of configuration space are separated by a barrier of rare configurations, i.e. that occur with an exponentially small probability and which, therefore, are never sampled—importance sampling MC samples only the typical configuration space. Hence, any simulation gets stuck in one of the two minima, ergodicity is lost, and therefore MC does not provide the correct answer.

In this contribution we wish to discuss MC methods that are used to overcome the problem of ergodicity breaking and, more generally, to determine thermodynamic/statistical properties that are controlled by rare configurations, which are indeed the subject of the theory of large deviations [5]. In this contribution we will first discuss the problem of data reweighting, then we will introduce a family of methods that rely on non-Boltzmann-Gibbs probability distributions, umbrella sampling, simulated tempering, and multicanonical methods. Finally, we will discuss parallel tempering which is a general multipurpose method for the study of multimodal distributions, both for homogeneous and disordered systems.

6.2 Data Reweighting

In this contribution we shall work in the canonical ensemble, considering configurations x distributed according to the Boltzmann-Gibbs probability density

$$\pi_\beta(x) = \frac{e^{-\beta H(x)}}{Z_\beta} ,$$

where $H(x)$ is the energy function and the normalizing constant Z_β is the partition function at inverse temperature β. Note that the energy function H is extensive, i.e., proportional to the number N of system variables; in the thermodynamic limit $N \to \infty$, the distribution $\pi_\beta(x)$ becomes peaked around its maximum. We indicate by $\langle\cdot\rangle_\beta$ the average with respect to $\pi_\beta(x)$.

The dynamic MC method which uses importance sampling can efficiently sample from a distribution which is strongly concentrated in the space of configurations as $\pi_\beta(x)$ is for large values of N. Thus, a MC run at β_0 allows us to compute any interesting thermodynamic quantity at β_0. However, suppose that we are also interested in the behavior at a different temperature β_1: do we need to run a new MC simulation or can we re-use the data collected at β_0? The answer mainly depends on the energy function $H(x)$, on how close β_1 and β_0 are, and, though this is usually much less relevant, on the amount of data collected at β_0.

In this context one useful technique is called *data reweighting* [6–8]. If $A(x)$ is any observable, its average at β_1 can be expressed as

$$\langle A\rangle_{\beta_1} = \frac{\sum_x A(x)e^{-\beta_1 H(x)}}{\sum_x e^{-\beta_1 H(x)}} = \frac{\sum_x A(x)e^{-\Delta\beta H(x)}e^{-\beta_0 H(x)}}{\sum_x e^{-\Delta\beta H(x)}e^{-\beta_0 H(x)}} = \frac{\langle A\, e^{-\Delta\beta H}\rangle_{\beta_0}}{\langle e^{-\Delta\beta H}\rangle_{\beta_0}} , \tag{6.1}$$

where $\Delta\beta = \beta_1 - \beta_0$.

Though in principle this formula solves the problem, in practice it is only useful if the two averages at β_0 can be computed with reasonable accuracy. But this is not obvious. Since H is extensive, the calculation of averages involving $e^{-\Delta\beta H}$ is a large-deviation problem for $N \to \infty$. Therefore, accurate results are only obtained if rare configurations, i.e. configurations that have an exponentially small probability for $N \to \infty$, are correctly sampled. From a physical point of view the origin of the difficulties can be understood quite easily. Problems arise because configurations sampled by the MC at β_0 are not those giving the largest contribution to $\langle A\rangle_{\beta_1}$, since $\pi_{\beta_1}(x)$ and $\pi_{\beta_0}(x)$ are strongly concentrated on different configurations. If we call D_β the set of typical configurations of $\pi_\beta(x)$,[1] then the estimate of $\langle A\rangle_{\beta_1}$ obtained by data reweighting is reliable only if the configurations obtained at β_0 sample well enough D_{β_1}. Usually this requirement is stated by saying that the energy histograms at inverse temperatures β_0 and β_1 should overlap. This statement is qualitatively correct, although of little practical use, given that we do not know the energy histogram at β_1 (this is something we would like to compute from the data measured at β_0).

Data reweighting provides also the answer to a second problem that arises in many different contexts, that of computing free energy differences. In the canonical ensemble one would consider the Helmholtz free energy $F(\beta) = -\beta^{-1} \ln Z_\beta$. Given $F(\beta_0)$, one can compute $F(\beta_1)$ by using

$$\beta_1 F(\beta_1) - \beta_0 F(\beta_0) = -\ln\langle e^{-\Delta\beta H}\rangle_{\beta_0} = \ln\langle e^{\Delta\beta H}\rangle_{\beta_1} \,. \tag{6.2}$$

The same type of averages appear here as in Eq. (6.1) and indeed, this type of computations suffers from the same problems discussed above.

We wish now to make this qualitative discussion quantitative. For this purpose, let us compute the statistical error on $\langle A\rangle_{\beta_1}$. Since this quantity is expressed as a ratio of two mean values, the variance of the estimator can be obtained by using the general expression

$$\sigma^2_{\rm est} \equiv \mathrm{var}\left(\frac{\frac{1}{n}\sum_i A_i}{\frac{1}{n}\sum_i B_i}\right) = \frac{1}{n}\frac{\langle A\rangle^2}{\langle B\rangle^2}\left\langle \mathscr{O}^2\right\rangle (1 + 2\tau_{\mathscr{O}}) + O(n^{-2}) \,, \tag{6.3}$$

where n is the number of measurements performed,

$$\mathscr{O} = \frac{A}{\langle A\rangle} - \frac{B}{\langle B\rangle} \,, \tag{6.4}$$

and $\tau_{\mathscr{O}}$ is the integrated autocorrelation time associated with $\mathscr{O}$. Equation (6.3) is valid as $n \to \infty$, neglecting corrections of order n^{-2}. In our case the relevant quantity is $\left\langle \mathscr{O}^2\right\rangle$. If we specialize Eq. (6.4) to our case, we obtain

[1] A precise definition of D_β is not necessary for our purposes. For example, we can consider for D_β the smallest set of configurations such that $\sum_{x\in D_\beta} \pi_\beta(x) > 1 - \varepsilon$.

$$\langle \mathscr{O}^2 \rangle_0 = \left\langle \left(\frac{A e^{-\Delta\beta H}}{\langle A e^{-\Delta\beta H} \rangle_0} - \frac{e^{-\Delta\beta H}}{\langle e^{-\Delta\beta H} \rangle_0} \right)^2 \right\rangle_0 = \left\langle \left(\frac{A}{A_1} - 1 \right)^2 \frac{e^{-2\Delta\beta H}}{\langle e^{-\Delta\beta H} \rangle_0^2} \right\rangle_0$$
$$= \frac{Z_0^2}{Z_1^2} \left\langle \left(\frac{A}{A_1} - 1 \right)^2 \right\rangle_2 \langle e^{-2\Delta\beta H} \rangle_0 = \frac{Z_0 Z_2}{Z_1^2} \left\langle \left(\frac{A}{A_1} - 1 \right)^2 \right\rangle_2 .$$

Here we have introduced $\beta_2 = 2\beta_1 - \beta_0$, $\langle \cdot \rangle_{\beta_i}$ has been written as $\langle \cdot \rangle_i$, and $A_1 = \langle A \rangle_1$. In terms of the Helmholtz free energy $F(\beta)$ we have

$$\langle \mathscr{O}^2 \rangle_0 = \left\langle \left(\frac{A}{A_1} - 1 \right)^2 \right\rangle_2 e^{Nf(\beta_0, \beta_1)} ,$$

where

$$Nf(\beta_0, \beta_1) = 2\beta_1 F(\beta_1) - \beta_0 F(\beta_0) - \beta_2 F(\beta_2) .$$

The extensivity of the free energy $F(\beta)$ implies that f is finite for $N \to \infty$. It is easy to show that f is a positive function and increases as $|\beta_0 - \beta_1|$ increases. Indeed, using $E = \partial(\beta F)/\partial\beta$ and $C_V = \partial E/\partial T$ at constant volume (in our language at constant N), we can rewrite

$$Nf(\beta_0, \beta_1) = \int_{\beta_0}^{\beta_1} [E(\beta') - E(\beta' + \beta_1 - \beta_0)] d\beta' =$$
$$= \int_{\beta_0}^{\beta_1} \left[\frac{\beta' - \beta_0}{\beta'^2} C_V(\beta') + \frac{\beta_1 - \beta'}{(\beta' + \beta_1 - \beta_0)^2} C_V(\beta' + \beta_1 - \beta_0) \right] d\beta' .$$

The positivity of the specific heat immediately implies that $f(\beta_0, \beta_1) > 0$. For $|\beta_1 - \beta_0| \ll 1$ we can expand $f(\beta_0, \beta_1)$ in powers of $\beta_1 - \beta_0$, obtaining

$$f(\beta_0, \beta_1) = \frac{c_V}{\beta_0^2} (\beta_1 - \beta_0)^2 , \tag{6.5}$$

where $c_V = C_V/N$ is the specific heat per system variable at $\beta = \beta_0$. Collecting all terms we obtain for the variance of the estimate

$$\frac{\sigma_{\text{est}}^2}{\langle A \rangle_1^2} = \frac{1}{n} \frac{\langle (A - A_1)^2 \rangle_2}{A_1^2} e^{Nf(\beta_0, \beta_1)} (1 + 2\tau_{\mathscr{O}}) + O(n^{-2}) .$$

Since Eq. (6.1) is a ratio, the estimate is also biased. The bias can be easily computed in the case of independent sampling (if correlations are present formulae are more involved, but the conclusions reported below remain unchanged). Using

$$\text{bias}\left(\frac{\frac{1}{n}\sum_i A_i}{\frac{1}{n}\sum_i B_i}\right) = \left\langle \frac{\frac{1}{n}\sum_i A_i}{\frac{1}{n}\sum_i B_i}\right\rangle - \frac{\langle A\rangle}{\langle B\rangle} =$$

$$= \frac{1}{2n}\frac{\langle A\rangle}{\langle B\rangle}\left[\text{var}\mathscr{O} - \frac{\text{var}A}{\langle A\rangle^2} + \frac{\text{var}B}{\langle B\rangle^2}\right] + O(n^{-2}) \,, \qquad (6.6)$$

we easily check that also the bias is proportional to $\exp[Nf(\beta_0,\beta_1)]$.

We can also compute the error $\sigma_{\Delta F}$ on the free-energy difference as computed by using Eq. (6.2). We have

$$\sigma^2_{\Delta F} = \left[\frac{\langle e^{-2\Delta\beta H}\rangle_0}{\langle e^{-\Delta\beta H}\rangle_0^2} - 1\right](1+2\tau) \approx \frac{Z_2 Z_0}{Z_1^2}(1+2\tau) = e^{Nf(\beta_0,\beta_1)}(1+2\tau) \,,$$

where τ is the integrated autocorrelation time associated with $e^{-\Delta\beta H}$. Note that the same exponential factor occurs also here.

The presence of the exponential term sets a bound on the width of the interval in which data reweighting can be performed. Requiring $\sigma_{\rm est}/\langle A\rangle_1 \ll 1$ we obtain

$$\frac{1}{n}\exp[Nf(\beta_0,\beta_1)] \ll 1 \,,$$

which implies for small values of $\Delta\beta = \beta_0 - \beta_1$ the condition

$$|\Delta\beta| \ll \Delta\beta_{\rm max} \equiv \beta_0\sqrt{\ln n/(Nc_V)} \,. \qquad (6.7)$$

Notice that this bound depends on the model under study (through the specific heat c_V at β_0) and on the system size, as $N^{-1/2}$, while the dependence on the number of measurements is only logarithmic. The dependence of $\Delta\beta_{\rm max}$ on $(Nc_V)^{-1/2}$ can be physically explained: energy fluctuations at β_0 are of order $(Nc_V)^{1/2}$ and are thus comparable to the energy difference $E_0 - E_1 \propto Nc_V\Delta\beta_{\rm max}$, only if $\Delta\beta_{\rm max}$ scales like $(Nc_V)^{-1/2}$.

The origin of the function f can be better understood by a physical argument which relies on the intuitive idea of the histogram overlaps. Indeed, the probability that a configuration x generated according to $\pi_{\beta_0}(x)$ is in D_{β_1} is given by

$$\sum_{x\in D_{\beta_1}} \pi_{\beta_0}(x) = e^{\beta_0 F(\beta_0)} \sum_{x\in D_{\beta_1}} e^{-\beta_0 H(x)} \simeq$$

$$\simeq e^{\beta_0 F(\beta_0)} e^{S(\beta_1)-\beta_0 E(\beta_1)} \equiv e^{\Delta S - \beta_0 \Delta E} \,, \qquad (6.8)$$

where $S = \beta(E-F)$ is the entropy. To obtain the second equality we have assumed that all configurations in D_{β_1} have the same energy $E(\beta_1)$ and that their number is $e^{S(\beta_1)}$, which is fully justified in the thermodynamic limit. Given that both ΔS and ΔE are extensive, the probability in Eq. (6.8) is exponentially small in N.

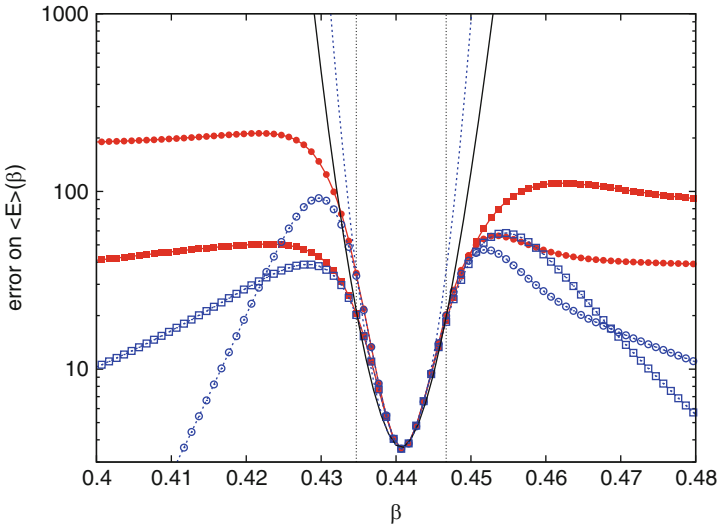

Fig. 6.1 Error on the energy $E(\beta)$ for two different sets of data (we use *squares* and *circles* to distinguish them). We report: (*empty symbols*) the error computed using Eq. (6.3), (*solid symbols*) the error computed using the jackknife method, (*continuous line*) $c\, e^{Nf/2}$ obtained by using Onsager's expression for the free energy, (*dashed line*) $c\, e^{Nf/2}$ using the approximation in Eq. (6.5) and the value of the specific heat at the critical point; c is the error at the critical point. The *vertical dotted lines* give the interval in which we have 100 "good" measures, as defined in the text

The corresponding large deviation (or Cramér) function is given by $\Omega(\beta_0, \beta_1) = \Delta s - \beta_0 \Delta e$, with $s = S/N$ and $e = E/N$. For small $|\beta_1 - \beta_0|$ we have

$$N\Omega(\Delta\beta) = \int_{T_0}^{T_1} dT \left(\frac{C_V}{T} - \frac{C_V}{T_0} \right) \approx -\frac{C_V \Delta\beta^2}{2\beta_0^2} \approx -\frac{1}{2} Nf(\beta_0, \beta_1) \,,$$

where C_V is the specific heat at β_0. The number of "good" measurements for the estimate of $\langle A \rangle_{\beta_1}$ (i.e., those in D_{β_1}) is then $n \exp(-Nf/2)$. The reweighting is reliable if this number is much larger than 1, which again implies condition in Eq. (6.7).

To give an example on how the method works, let us consider the Ising model on a square lattice of size $N = 100^2$ and let us perform a simulation at the critical inverse temperature $\beta_c = \log(\sqrt{2} + 1)/2$. We wish to compute $\langle E \rangle_\beta$ in an interval around the critical point. In Fig. 6.1 we report the statistical error on this quantity obtained by reweighting 10^4 independent measurements. The error computed by using Eq. (6.3) first increases significantly and then decreases exponentially as $|\beta - \beta_c|$ becomes large. This behavior is due to the fact that the reweighted dataset becomes dominated by a single data point and fluctuations within the reweighted dataset disappear. However, this decrease is inconsistent with the exact expression we have derived above—and also with physical intuition—which shows that the

error should always increase as $|\beta - \beta_c|$ increases. The origin of this discrepancy is related to the fact that, as we move out of the critical point, not only does the error on the energy increase, but also the error on the error increases, hence also the error becomes unreliable. It is important to stress that in any case $\sigma_{\rm est}$ cannot be computed by using Eq. (6.3) as soon as the error becomes large. Indeed, that relation is an asymptotic formula valid as long as the neglected corrections (of order n^{-2}) are small. But it is clear that, when the leading term is large, also the corrections become relevant, making the formula unsuitable for the computation of the error. In this case, a more robust method should be used, like the jackknife method [9, 10]. The jackknife error behaves better, but also this method becomes unreliable when the reweighted dataset concentrates on very few data points (those with the largest or smallest energy, depending on the sign of $\Delta\beta$). In practice, the jackknife error converges for large $|\beta - \beta_c|$ to the absolute value of the difference between the two largest (or smallest) energy data points. It is interesting to compare the error determined from the numerical data with the exact result. Hence, in the figure we also report $c\exp(Nf/2)$, where c is the error at the critical point and f has been computed by using Onsager's expression [11, 12] for the free energy. It is clear that the error computed from the MC data becomes immediately unreliable as soon as $|\beta - \beta_c| \gtrsim 0.01$. Indeed, the true error increases quite fast and becomes enormous outside this small interval. For instance, for the extreme case $\beta = 0$ we have $f(\beta_c, 0) = 0.473$ so that $\exp(Nf/2) \sim 10^{1027}$. In Fig. 6.1 we also report the interval in which we have at least $m = 100$ good measures, where m is defined by $n\exp(-Nf/2)$, as discussed above. In this range the jackknife and the asymptotic error estimates agree, as expected. Moreover, in this interval also the quadratic approximation in Eq. (6.5) is quite accurate.

6.3 Multiple Histogram Method

Given that the reweighting method can cover only a limited temperature range of width $\Delta\beta_{\rm max}$ around the temperature β_0 where the original data were collected, one could improve it by running new simulations at β_1, with $|\beta_1 - \beta_0| > \Delta\beta_{\rm max}$, but such that, combining all measured data, the entire range (β_0, β_1) is covered. More generally, suppose one has performed MC simulations at R different inverse temperatures $\{\beta_i\}_{i=1,\ldots,R}$. What is the best way to combine these R datasets to estimate average values $\langle A\rangle_\beta$ at any β?

The most naive method would consist in performing a weighted average of the reweighted data. To explain the shortcomings of this approach, let us assume $R = 2$ and, for instance, let us consider a value of β between β_1 and β_2 which is closer to β_1 than to β_2. A formally correct strategy to compute an average $\langle A\rangle_\beta$ could be the following. We first use the data at β_1 to obtain an estimate A_1 with error σ_1 and then the data at β_2 to obtain an estimate A_2 with error σ_2. Since β is not close to β_2, A_2 has a somewhat large error; but, what is worse, also the error estimate σ_2 has a somewhat large error. Hence, σ_2 as estimated from the data could be largely

underestimated, as we have seen in Sect. 6.2. Finally, one could combine the two estimates as

$$A_{12} = \frac{A_1\sigma_1^{-2} + A_2\sigma_2^{-2}}{\sigma_1^{-2} + \sigma_2^{-2}} \ .$$

But, if σ_2 is largely underestimated, we would give too much weight to A_2, adding essentially noise and not signal to A_1. In these cases A_{12} would be a worst estimate than A_1.

A much better method has been proposed by Ferrenberg and Swendsen [13].[2] Before presenting the method let us define a few fundamental quantities. For simplicity, let us assume that the system is discrete so that the energy takes discrete values. Then, we introduce the density of states $\rho(E)$ which is defined such that

$$Z_\beta = \sum_E \rho(E) e^{-\beta E} \ ,$$

and the energy histogram variable $h(E_0, \beta)$ defined by

$$h(E_0, \beta) = \langle \delta_{E,E_0} \rangle_\beta = \frac{1}{Z_\beta} \sum_E \rho(E) \delta_{E,E_0} e^{-\beta E} = \frac{1}{Z_\beta} \rho(E_0) e^{-\beta E_0} \ . \tag{6.9}$$

The latter quantity has the important property

$$\mathrm{var}\,[h(E_0, \beta)] = \langle \delta^2_{E,E_0} \rangle_\beta - \langle \delta_{E,E_0} \rangle^2_\beta = h(E_0, \beta)[1 - h(E_0, \beta)] \approx h(E_0, \beta) \ ,$$

where we have used the obvious property $\delta^2_{E,E_0} = \delta_{E,E_0}$ and, in the last step, that $h(E_0, \beta) \ll 1$.

We can now define the method. Suppose we have taken n_i independent measurements[3] at β_i and let us denote with $N_i(E)$ the number of measures with energy E. The ratio $N_i(E)/n_i$ is an estimator of the histogram variable $h(E, \beta_i)$. Using Eq. (6.9) we can estimate $\rho(E)$ using the data at β_i as

$$\rho_i(E) \approx n_i^{-1} N_i(E) e^{\beta_i E} Z_i \ ,$$

where Z_i, the partition function at β_i, has still to be determined. The variance of the estimator of $\rho_i(E)$ can be easily computed if one assumes that Z_i is known exactly. Indeed, with this assumption

[2] It is interesting to observe that, for $R = 2$, the multiple histogram method is equivalent to Bennett's acceptance ratio method [14] which was developed for liquid systems.

[3] In the case the measures are correlated with an autocorrelation time τ_i, then an effective $\tilde{n}_i = n_i/(2\tau_i + 1)$ should be used in all following formulae.

$$\sigma_i^2(E) = n_i^{-1}\mathrm{var}\,[\rho(E)] = n_i^{-1} e^{2\beta_i E} Z_i^2 \mathrm{var}\,[h(E,\beta_i)] = \\ = n_i^{-1} e^{2\beta_i E} Z_i^2 h(E,\beta_i) = n_i^{-1} e^{\beta_i E} Z_i \rho(E)\ .$$

In the usual error analysis one would replace $\rho(E)$ in the r.h.s. with its estimator ρ_i. Since we know that this estimator may be very imprecise—it provides an accurate estimate of $\rho(E)$ only if E is a typical energy at inverse temperature β_i—we do not do it here. This is a crucial point in the method and it is the one that guarantees the robustness of the results. It is also important to stress that σ_i is not the "true" error, since Z_i is also a random variable which has to be determined. However, we will only use σ_i to write down a weighted average of the estimators $\rho_i(E)$. For this purpose, it is not necessary that the weights are correct variances or estimates thereof.[4] A robust estimate of the density of states using all R datasets is given by a weighted average, where each estimate $\rho_i(E)$ enters with a weight proportional to $1/\sigma_i^2(E)$:

$$\rho(E) = \sum_{i=1}^{R} \rho_i(E) \frac{1/\sigma_i^2(E)}{\sum_{j=1}^{R} 1/\sigma_j^2(E)} = \frac{\sum_{i=1}^{R} N_i(E)}{\sum_{j=1}^{R} n_j\, e^{-\beta_j E}\, Z_j^{-1}}\ . \tag{6.10}$$

At this point it is important to stress two important differences between this method and the naive method presented at the beginning. First, observe that for any given E, the only runs that contribute to the determination of $\rho(E)$ are those for which $N_i(E) \neq 0$. This means that we are using the data at β_i only where they are relevant. Moreover, the estimate of the error σ_i is robust, since it follows from an exact identity for the histogram variable.

Equation (6.10) still depends on the unknown partition functions Z_i. They can be determined in a self-consistent way by noticing that

$$Z_k = \sum_E \rho(E) e^{-\beta_k E} = \sum_E \frac{\sum_{i=1}^{R} N_i(E)}{\sum_{j=1}^{R} n_j\, e^{(\beta_k-\beta_j)E}\, Z_j^{-1}}\ . \tag{6.11}$$

which can be rewritten as

$$\sum_E \frac{\sum_{i=1}^{R} N_i(E)}{\sum_{j=1}^{R} n_j\, e^{(\beta_k-\beta_j)E}\, (Z_k/Z_j)} = 1\ .$$

[4] We remind the reader of a few basic facts. If A_i are different estimates of the same quantity, i.e., they all satisfy $\langle A_i\rangle = a$, any weighted average $A_{\rm wt} = \sum w_i A_i$, $\sum_i w_i = 1$, is correct in the sense that $\langle A_{\rm wt}\rangle = a$. Usually, one takes $w_i = k\sigma_i^{-2}$ (k is the normalization factor) because this gives the optimal estimator, that is the one with the least error. Here, however, robustness and not optimality is the main issue.

The consistency condition gives us R equations for the partition function ratios Z_i/Z_j. Since the number of independent ratios is $R-1$, one would expect only $R-1$ independent equations and, indeed, the R equations are linearly dependent:

$$\sum_{k=1}^{R} n_k \sum_E \frac{\sum_{i=1}^{R} N_i(E)}{\sum_{j=1}^{R} n_j\, e^{(\beta_k-\beta_j)E}\,(Z_k/Z_j)} = \sum_E \sum_{i=1}^{R} N_i(E) = \sum_{i=1}^{R} n_i \ .$$

To solve the problem one proceeds iteratively. We define $\hat{Z}_k = Z_k/Z_1$ and rewrite Eq. (6.11) as

$$\hat{Z}_k = \sum_E \frac{\sum_{i=1}^{R} N_i(E)}{\sum_{j=1}^{R} n_j\, e^{(\beta_k-\beta_j)E}\,\hat{Z}_j^{-1}} \ .$$

A first estimate of $\hat{Z}_k$ can be obtained by using the data reweighting method presented before.[5] The first estimate the $\hat{Z}_i$'s is plugged on the r.h.s. and the l.h.s. provides a new estimate, which is used again in the r.h.s. to get a third estimate and so on. Since we are only able to compute the ratios of the partition functions, we do not obtain at the end $\rho(E)$ but rather $\rho(E)/Z_i$ for all values of i. However, this is enough to compute averages of functions of the energy since

$$\langle g(E)\rangle_{\beta_i} = \sum_E g(E) e^{-\beta_i E}[\rho(E)/Z_i] \ .$$

or ratios of partition functions

$$\frac{Z_\beta}{Z_i} = \sum_E e^{-\beta E}[\rho(E)/Z_i] \ .$$

The procedure we have presented can be generalized to allow us to compute averages of generic observables $A(x)$. In this case, the basic quantities are the joint histogram with respect to E and A

$$h(E_0, A_0, \beta) = \langle \delta_{E,E_0}\delta_{A,A_0}\rangle_\beta \ ,$$

its estimator $N_i(E_0, A_0)/n_i$, and the density of states $\rho(E_0, A_0)$ which counts the number of states such that $E = E_0$ and $A = A_0$. Repeating the same steps as before, we end up with

$$\rho(E, A) = \frac{\sum_{i=1}^{R} N_i(E, A)}{\sum_{j=1}^{R} n_j\, e^{-\beta_j E}\, Z_j^{-1}} \ .$$

[5] If the inverse temperatures β_i are ordered, one could determine Z_i/Z_{i-1} by using the reweighting method and then $\hat{Z}_i = (Z_i/Z_{i-1})(Z_{i-1}/Z_{i-2})\ldots Z_2/Z_1$.

Once $\rho(E, A)/Z_i$ is known, any average involving E and A can be directly computed.

It is worth noticing that the use of histograms in the multiple histogram method (which is in general information degrading) is not strictly necessary if one is able to save the full configurations or, at least, the measurements $A_{i,t}$ and $E_{i,t}$ at each MC time t. Indeed, the consistency equations can be rewritten as

$$\hat{Z}_k = \sum_{i,t} \frac{1}{\sum_{j=1}^{R} n_j \, e^{(\beta_k - \beta_j) E_{i,t}} \, \hat{Z}_j^{-1}} \,,$$

where $E_{i,t}$ is the t-th energy measurement at β_i, while the average of any quantity at any inverse temperature β can be computed as

$$\langle A \rangle_\beta = \hat{Z}_\beta^{-1} \sum_{i,t} \frac{A_{i,t}}{\sum_j n_j \, e^{(\beta - \beta_j) E_{i,t}} \, \hat{Z}_j^{-1}} \,,$$

with

$$\hat{Z}_\beta = \sum_{i,t} \frac{1}{\sum_j n_j \, e^{(\beta - \beta_j) E_{i,t}} \, \hat{Z}_j^{-1}} \,.$$

Remember that each term entering the sums in the denominators is exponential in N. Much care needs to be taken in doing these sums, since the summations involve terms of very different sizes, and even a single term can exceed the range of floating-point numbers. The suggestion is to work with the logarithms of these terms.

6.4 Umbrella Sampling and Simulated Tempering

6.4.1 Umbrella Sampling

In the previous sections we have shown how to use several runs at $\beta_1 < \ldots < \beta_R$ to compute averages for any β in the interval $[\beta_1, \beta_R]$ and to compute free energy differences. The umbrella sampling (US) method was introduced by Torrie and Valleau [15] to perform the same tasks by means of a single simulation. The idea consists in performing MC simulations with a non-Boltzmann-Gibbs distribution function of the form

$$\pi(x) = \frac{1}{Z_\pi} \sum_{i=1}^{R} \alpha_i e^{-\beta_i H(x)} \,, \tag{6.12}$$

where i runs over the R different temperatures, Z_π is the normalizing factor, and α_i are positive constants that should be carefully chosen as described below. By sampling the distribution in Eq. (6.12) one aims at sampling in a single run the configurations that are typical for all β_i's and, as a consequence, all configuration space which is relevant for the computation of $\langle A \rangle_\beta$ with $\beta_1 \leq \beta \leq \beta_R$. In order for the method to work two requirements should be satisfied. First of all, the temperatures should be finely spaced, so that typical configurations at inverse temperature β_i overlap with those at $\beta_{i\pm1}$. If this does not occur, the system is unable to move in configuration space and does not visit the typical configuration domain of all β_i's. This condition is the same that occurs in the application of the data reweighting method. Using the results presented in Sect. 6.2 and, in particular, Eq. (6.7), we can conclude that $|\beta_i - \beta_{i+1}|$ should scale as $(c_V N)^{-1/2}$: if the system size is increased, temperatures should be closer. A second important condition fixes the coefficients α_i or, more precisely, their ratios. We require that the typical configuration domains at each β_i have approximately the same probability under π. Using the notations of Sect. 6.2, the probability of the typical domain D_{β_k} is given by

$$\sum_{x \in D_{\beta_k}} \pi(x) = \frac{1}{Z_\pi} \sum_i \alpha_i \sum_{x \in D_{\beta_k}} e^{-\beta_i H(x)} \approx \frac{1}{Z_\pi} \alpha_k Z_k \ .$$

Therefore, we require

$$\frac{1}{Z_\pi} \alpha_i Z_i = \frac{1}{Z_\pi} \alpha_j Z_j \qquad \Rightarrow \qquad \frac{\alpha_i}{\alpha_j} = \frac{Z_j}{Z_i} = e^{\beta_i F(\beta_i) - \beta_j F(\beta_j)} \ . \tag{6.13}$$

Hence the ratios α_i / α_j must be related to the free-energy differences. This is a shortcoming of the method, since these differences are exactly one of the quantities one wishes to compute from the simulation. However, the algorithm is correct, though not optimal, for any choice of the α_i's, so that it is enough to have a very rough estimate of the free-energy differences to run a US simulation. Note that we only fix the ratios of the α_i's: this is not a limitation since one can always set, say, $\alpha_1 = 1$, by redefining Z_π. Once the US simulation has been performed, one can compute averages with respect to the Boltzmann-Gibbs distribution by using

$$\langle A \rangle_\beta = \frac{\langle A \, e^{-\beta H} (\sum_i \alpha_i e^{-\beta_i H})^{-1} \rangle_\pi}{\langle e^{-\beta H} (\sum_i \alpha_i e^{-\beta_i H})^{-1} \rangle_\pi} \ . \tag{6.14}$$

6.4.2 Simulated Tempering

As the US method, also the simulated tempering (ST) method [16, 17] aims at sampling the configurations that are typical at a set of inverse temperatures $\beta_1 < \ldots < \beta_R$ and, indeed, it represents a stochastic version of the US method. In the ST

case, one enlarges the configuration space by adding an index i which runs from 1 to R. Hence, a configuration in the ST simulation is a pair (x, i). Configurations are sampled with probability ($\alpha_i > 0$)

$$\Pi(x, i) = \frac{\alpha_i e^{-\beta_i H}}{Z_i} . \tag{6.15}$$

As in the US method, the temperatures and the coefficients α_i should be carefully chosen, using the same criteria we discussed in the US case. In particular, also the ST method requires an a priori determination of the free energy differences. As we discuss in Sect. 6.4.3, the ST and the US method are essentially equivalent, although the ST has a practical advantage: it is trivial to modify a standard MC code into a ST code (we discuss in Sect. 6.4.3 how to implement ST), while significant more work is needed to implement the US method.

6.4.3 *Equivalence of Simulated Tempering and Umbrella Sampling*

Madras and Piccioni [18] have analyzed the US and ST methods and shown their equivalence under very general conditions, that are usually satisfied in practical applications. We will present here their results trying to avoid all mathematical details. Let us first extend the US method to a general family of probabilities. Consider a state space S and a family of probability functions $\pi_i(x)$, $i = 1, \ldots R$, defined on S. We assume the state space S to be discrete, to avoid mathematical subtleties, but the arguments can be easily extended to the continuous case. In physical terms S is the space of the configurations, while π_i are the Boltzmann-Gibbs distributions $e^{-\beta_i H}/Z_i$. A general *umbrella probability* is given by

$$\pi(x) = \sum_i a_i \pi_i(x) \qquad\qquad \sum_i a_i = 1, \qquad a_i > 0 .$$

The coefficients a_i are related to the coefficients α_i defined before by $a_i = \alpha_i Z_i / Z_\pi$, while the optimality condition in Eq. (6.13), which is not assumed to be satisfied in the following, becomes $a_i/a_j = 1$.

By means of a single MC simulation (i.e., by considering a Markov chain that has π as stationary distribution) one generates a set of points $x_1, \ldots, x_n$ in S. If $A(x)$ is a function defined on S, the sample average converges to the average with respect to π as $n \to \infty$:

$$\frac{1}{n} \sum_{k=1}^{n} A(x_k) \to \sum_x \pi(x) A(x) = \langle A \rangle_\pi .$$

One can also obtain averages with respect to any of the probabilities π_i, by simply reweighting the data. Equation (6.14) can be rewritten as

$$\langle A\rangle_i = \sum_x \pi_i(x)A(x) = \frac{\langle \pi_i A/\pi\rangle_\pi}{\langle \pi_i/\pi\rangle_\pi} \ . \tag{6.16}$$

Let us now formulate the ST method in the same framework. The idea is to enlarge the state space S to

$$S' = S \times \{1 \ldots, R\}$$

(we shall often call the additional index a *label*) and consider the probability $\Pi(x,i) = a_i \pi_i(x)$ on S'.

We first show that the ST and the US methods generate equally distributed points in S. Suppose that we use a general MC algorithm on S' (mathematically, a Markov chain that has Π as stationary distribution) to generate data (x_1, i_1), ..., (x_n, i_n). If $A(x)$ is a function defined on S, the sample mean converges to Π-averages as $n \to \infty$:

$$\frac{1}{n}\sum_{k=1}^{n} A(x_k) \to \sum_{x,i} A(x)\Pi(x,i) = \sum_{x,i} A(x)a_i\pi_i(x) = \sum_x A(x)\pi(x) \ .$$

Roughly speaking, this means that, if we start the MC in equilibrium, $x_1, \ldots x_n$ are distributed according to the umbrella sampling distribution, as if they had been obtained by a MC US simulation.

The fact that the US and the ST methods generate data with the same distribution probability does not imply that dynamics are equivalent in the two methods and one may wonder whether, by enlarging the state space, one can define algorithms that can speed up significantly simulations. After all, there is a well-known example in which this strategy works very nicely: the Swendsen-Wang (or cluster) algorithm [19] for the Ising model is indeed obtained [20] by enlarging the configuration space of the Ising spins $\{s_i\}$ to $\{s_i\} \times \{b_{\langle ij\rangle}\}$, where $b_{\langle ij\rangle}$ are the bond occupation variables. For the case of the US and ST methods, this issue has been investigated in Ref. [18], for the case in which each system is updated by means of the Metropolis algorithm.

Let us first define the specific update considered in Ref. [18] for ST. This is not the most general one, but it corresponds to the update used in practical implementations. If (x,i) is the present configuration, an iteration consists first in updating the label i, followed by an update of the configuration x. Labels are updated using the conditional probability of the labels at fixed x: a new label j is chosen with probability $a_j\pi_j(x)/\sum_k[a_k\pi_k(x)] = a_j\pi_j(x)/\pi(x)$. Then, a new configuration $y \in S$ is chosen by using a MC method appropriate for the system with probability π_j, i.e. the system is updated with a Markov chain $T_j(x,y)$ which is stationary with respect to π_j (we remind the reader that this corresponds to the condition $\sum_x \pi_j(x)T_j(x,y) = \pi_j(y)$, a formula which will be often used in the following). The transition matrix is therefore

$$P(x,i;y,j) = \frac{a_j \pi_j(x)}{\pi(x)} T_j(x,y) \ . \tag{6.17}$$

Note that one often uses the Metropolis algorithm to update the labels, by proposing, for instance, $i \to i \pm 1$. This choice is certainly (slightly) more efficient, but should not change the general conclusions: the label dynamics should not be the relevant part of the algorithm. The Markov process in Eq. (6.17) induces a Markov process on S whose transition matrix is obtained by summing $P(x,i;y,j)$ over j:

$$P_s(x,y) = \sum_j P(x,i;y,j) = \frac{1}{\pi(x)} \sum_j a_j \pi_j(x) T_j(x,y) \ . \tag{6.18}$$

Such a process has $\pi(x)$ as equilibrium distribution, since

$$\sum_x \pi(x) P_s(x,y) = \sum_j a_j \sum_x \pi_j(x) T_j(x,y) = \sum_j a_j \pi_j(y) = \pi(y) \ .$$

We will finally show that under very general conditions, if the T_j are Metropolis updates, also P_s is a Metropolis update:

(a) Assume that the probabilities $\pi_i(x)$ satisfy the following condition: for any pair $x, y \in S$ we have either $\pi_i(x)/\pi_i(y) < 1$ for all i's or $\pi_i(x)/\pi_i(y) \geq 1$ for all i's. This is obviously satisfied for Boltzmann-Gibbs distributions. Given x and y one computes the energies $E(x)$ and $E(y)$. If $E(x) > E(y)$ then $e^{-\beta_i E(x)}/e^{-\beta_i E(y)} < 1$ for all $\beta_i > 0$. If the energies satisfy the opposite inequality, also the ratio of the Boltzmann-Gibbs factors satisfies the opposite inequality for all $\beta_i > 0$.

(b) The Metropolis update consists in two steps: a proposal in which a new configuration y is proposed, and an acceptance step. We assume that the proposal does not depend on the label i. For the Boltzmann-Gibbs distribution, this means that, given configuration x, we propose a new configuration y with a method which does not depend on temperature. Moreover—most practical algorithms satisfy this condition—we require the proposal matrix to be symmetric: the probability of proposing y given x is the same as that of proposing x given y.

For the Metropolis update, if $K(x,y)$ is the proposal matrix, we have [21]

$$T_i(x,y) = K(x,y) \min\left(1, \frac{\pi_i(y)}{\pi_i(x)}\right) \qquad x \neq y \ ,$$

$$T_i(x,x) = 1 - \sum_{y \neq x} T_i(x,y) \ .$$

Inserting this expression in Eq. (6.18), we obtain for $x \neq y$

$$P_s(x,y) = \frac{1}{\pi(x)} \sum_j a_j \pi_j(x) K(x,y) \min\left(1, \frac{\pi_j(y)}{\pi_j(x)}\right).$$

Now, assume that $\pi_i(y)/\pi_i(x) > 1$ for all i (we use here assumption (a)). In this case we have also $\pi(y)/\pi(x) > 1$ and

$$P_s(x,y) = \frac{1}{\pi(x)} \sum_j a_j \pi_j(x) K(x,y) = K(x,y) \ .$$

In the opposite case we have instead

$$P_s(x,y) = \frac{1}{\pi(x)} \sum_j a_j \pi_j(x) K(x,y) \frac{\pi_j(y)}{\pi_j(x)} = K(x,y) \frac{\pi(y)}{\pi(x)} \ .$$

Hence

$$P_s(x,y) = K(x,y) \min\left(1, \frac{\pi(y)}{\pi(x)}\right) \ .$$

But this is the transition matrix of a Metropolis update with respect to the probability $\pi(x)$. Hence, for the Metropolis case there is a complete equivalence between the US and the ST methods. Madras and Piccioni [18] have also considered the case in which condition (a) is not satisfied, proving that in this case ST is no better than the US method (they prove that the probability of null transitions in the US method is equal or smaller than that in the ST).

Finally, let us compare how averages are computed in the US and in ST methods. To compute averages with respect to π_i in the US method one uses formula (6.16). This formula also holds for the ST:

$$\langle A \rangle_i = \frac{\langle \pi_i A/\pi \rangle}{\langle \pi_i/\pi \rangle} \ , \tag{6.19}$$

where averages $\langle \cdot \rangle$ without any subscript refer to the ST measure $\Pi(x,i)$. However, in ST simulations, one usually considers

$$\langle A \rangle_i = \frac{\langle A\, I_i \rangle}{\langle I_i \rangle} \ , \tag{6.20}$$

where $I_i(x,j) = \delta_{ij}$ for every point $(x,j) \in S'$. That is, in Eq. (6.20) only data at β_i are used for estimating $\langle A \rangle_i$. The two expressions (6.19) and (6.20) are clearly different, but not that unrelated. Indeed, one could also determine $\langle A \rangle_i$ by reweighting the data measured at β_k:

$$\langle A \rangle_i = \frac{\langle A \pi_i I_k/\pi_k \rangle}{\langle \pi_i I_k/\pi_k \rangle} = A_{i,k} \ .$$

The average in Eq. (6.20) corresponds to $A_{i,i}$. Let us now show that the estimator in Eq. (6.19) is roughly a weighted average of the $A_{i,k}$. Let us define

$$\frac{1}{b_i} = \left\langle \frac{\pi_i}{\pi} \right\rangle .$$

Then, note that in systems of physical interest the supports of the distributions π_i are mostly disjoint: if x is such that $\pi_i(x)$ is significantly larger than zero, then $\pi_k(x)$ is very small for all $k \neq i$. In physical terms it means that, if we have a configuration that is typical at temperature β_i, such a configuration will be not be typical at all other temperatures. If this holds, then we can approximate

$$\frac{1}{\pi(x)} \approx \sum_k \frac{I_k}{a_k \pi_k(x)} , \tag{6.21}$$

so that Eq. (6.19) can be rewritten as

$$\langle A \rangle_i \approx \sum_k \frac{b_i}{a_k} \left\langle A \frac{I_k \pi_i}{\pi_k} \right\rangle .$$

Hence, the estimator in Eq. (6.19) is essentially equivalent to the following weighted average of the $A_{i,k}$:

$$\langle A \rangle_i \approx \sum_k \frac{b_i}{a_k} \left\langle \frac{\pi_i I_k}{\pi_k} \right\rangle A_{i,k} . \tag{6.22}$$

Using Eq. (6.19) to estimate $\langle A \rangle_i$, one is taking into account not only the data with label i, but all data by means of a proper reweighting as shown by Eq. (6.22). Of course, Eq. (6.22) is not quantitatively correct, since in practical implementations there must be configurations that are typical for two distributions (otherwise, the algorithm would not work): for them the approximation made in Eq. (6.21) fails. However, the argument gives a direct physical interpretation of Eq. (6.19) as some kind of, though not exact, reweighting of the data. Note that, when reweighting is used, there is always the technical problem of determining the weights of the average (see Sect. 6.3). No such problem arises here: everything is fixed in Eq. (6.19).

6.5 Generalizing the Umbrella Method: Multicanonical Sampling

Umbrella sampling, like simulated or parallel tempering, provides a way to sample in the same run different probability distributions along a *connected configuration path* $\mathscr{P}$, i.e., a connected subset of the configuration space S such that, if $x \in \mathscr{P}$,

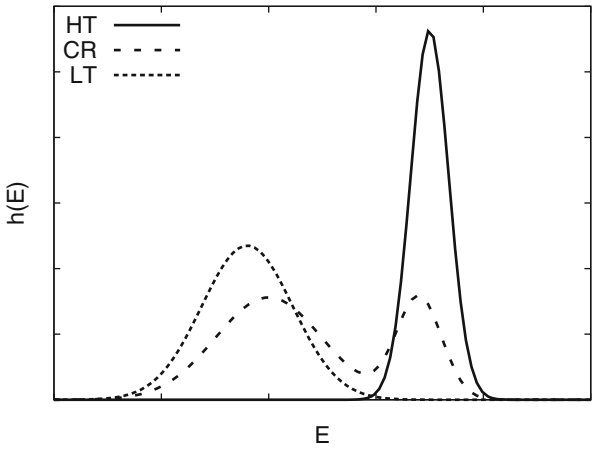

Fig. 6.2 A sketch of the energy distributions in the Potts model for $q > 4$ (first-order transition): the high-temperature (*HT*) and low-temperature (*LT*) distributions are unimodal, while at the critical temperature (*CR*) the distribution is bimodal

x is a typical configuration of at least one of the probabilities $\pi_i(x)$: in our previous notations $\mathscr{P}$ should be connected and contained in $\cup_{i=1}^{R} D_{\beta_i}$. In the presence of first-order phase transitions this path may not exist, hence the above methods cannot be applied. As an example let us consider the q-state Potts model on a square lattice. The model is defined in terms of spins (sometimes called colors) s_i defined at the sites of the lattice. Each s_i can assume q integer values between 1 and q. The Hamiltonian is given by

$$H_q(\{\sigma\}) = -\sum_{\langle ij \rangle} \delta_{s_i, s_j} \ ,$$

where the sum is over all nearest-neighbor lattice pairs $\langle ij \rangle$, $\delta_{s,s} = 1$ and $\delta_{s,t} = 0$ if $s \neq t$. As probability distribution we consider the usual Boltzmann-Gibbs distribution

$$\pi \propto e^{-\beta H_q} \ .$$

This model shows two different phases depending on β. For $\beta = \beta_c$ a phase transition occurs. For $q > 4$ such a transition is of first order and the energy has a bimodal distribution at $\beta = \beta_c$. A sketch of the energy distributions close to the transition point is reported in Fig. 6.2. Typical high-temperature (HT) distributions are unimodal and overlap with only one of the peaks appearing at the critical point, that with the highest energy. Analogously, low-temperature (LT) distributions are also unimodal; they only overlap with the low-energy peak of the critical-point distribution. This particular behavior of the energy distributions implies that any US or ST (these considerations also apply to the parallel tempering method which will be discussed in the next section) algorithm with local updates of the spins cannot move rapidly between LT and HT typical configurations. For the mean-field case (Potts model on a complete graph) and the Metropolis algorithm, this is indeed a rigorous theorem [22]: the exponential autocorrelation time of Metropolis ST algorithms increases exponentially with the size of the system. The origin of

the phenomenon is easily understood qualitatively. Suppose we use any of the previously mentioned methods and consider a set of temperatures such that β_1 is in the HT phase and β_R is in the LT phase. Start the simulation in the HT phase. Provided that the temperatures are finely spaced, one would eventually reach the critical point. Since the configuration has been obtained by cooling a HT configuration, it has an energy that belongs to the HT peak. Because of the bimodal nature of the energy distribution at β_c, local updates at β_c would only generate new configurations with energy belonging to the HT peak. Hence, any attempt to further reduce the temperature would fail, since the configuration would never be a typical LT configuration. Hence, LT configurations would never be visited. This argument is quite general and shows that US and ST, when used in combination with local algorithms, only work when the configuration path does not go through first-order transitions. A second-order transition should not be a limitation, since at the transition distributions are broader but usually still unimodal.[6]

To solve the problem one might consider an enlarged parameter space that allows one to go from the LT phase to the HT phase without intersecting the first-order transition point. In the Potts model this could be obtained by adding, for instance, a magnetic field, but this should in any case be done carefully, to be sure that all low-temperature degenerate states are equally visited. In practice, these extensions are usually not efficient.

We now discuss a family of methods that generalize the umbrella sampling method and are appropriate for the study of first-order transitions. They also work with a nonphysical distribution function $\pi(x)$ which is constructed in such a way to allow good sampling of both phases. Sometimes that are called *multicanonical* algorithms following Berg and Neuhaus [25, 26] that applied these methods to the study of first-order transitions.

Let us consider again the Potts model and suppose that one is at the transition point β_c, or at least very close to it. For $q > 4$ (the case we are considering now) the distribution of the energy $h(E)$ is bimodal, with two maxima at $E_1 < E_2$. If $h_i = h(E_i)$ is the value of the distribution at the maximum i, one defines the multicanonical distribution $\pi(x)$ as follows

$$\begin{aligned} \pi(x) &= \frac{e^{-\beta H}}{Z h_1} && E(x) \le E_1 \,, \\ &= \frac{e^{-\beta H}}{Z h(E)} && E_1 < E(x) < E_2 \,, \\ &= \frac{e^{-\beta H}}{Z h_2} && E_2 \le E(x) \,, \end{aligned}$$

[6] There are instances of second-order transitions which show bimodal distributions in finite volume [23, 24]: however, in these cases the two peaks get closer and the gap decreases as the volume increases. ST should work efficiently in these instances. Note, however, that the algorithm may not work in some disordered systems, even if the transition is of second order. One example is the random field Ising model.

where Z is the partition function for π. If we now compute the distribution of the energy in the new ensemble, we find

$$\begin{aligned} h_\pi(E) &= \alpha\, h(E)/h_1 && E(x) \le E_1\ , \\ &= \alpha && E_1 < E(x) < E_2\ , \\ &= \alpha\, h(E)/h_2 && E_2 \le E(x)\ , \end{aligned}$$

where α is a normalization constant. The probability is now flat for $E_1 < E(x) < E_2$ and thus local algorithms should have no problem in going from one phase to the other.

The main problem of the method stays in the fact the β_c as well as $h(E)$ are not known beforehand. In practical implementations one may work as follows. First, one roughly determines the position of the transition point. This can be obtained by running a hysteresis cycle. One thermalizes a configuration at a value of β which is deep in the HT phase and measures its energy. Then, one slightly increases β, thermalizes the configuration at this new temperature and recomputes the energy. One keeps repeating these steps until the configuration "jumps" in the LT phase: this is signalled by a big decrease of the energy. Let us call $\beta_{\max}$ this value of β. Then, one begins a series of runs in which β is decreased until the configuration (for $\beta = \beta_{\min}$) jumps back in the HT phase. The cycle allows one to infer that β_c lies in the interval $[\beta_{\min}, \beta_{\max}]$. In the absence of any other information we can just take the midpoint as the value of β at which the multicanonical simulation is performed. Note that it is not needed that such value be an accurate estimate of β_c. It is only crucial that at this value of β the distribution is bimodal, i.e. that there is a significant overlap with both phases.

Once the value of β at which the simulation should be performed has been chosen, one must determine $\pi(x)$. This can be done recursively. We will illustrate the procedure with an example, considering the liquid-gas transition in a fluid. Here the number N of molecules present in the system plays the role of order parameter in the transition (it is the analogue of E in the Potts model), while the grand canonical distribution $\pi_0 = e^{-\beta H + \beta\mu N}/(N!Z)$ plays the role of the Boltzmann-Gibbs distribution. The gas and liquid phases are the analog of the HT and LT Potts phases. The iterative procedure starts by performing two runs: one run starts from a gas configuration, while the other run starts from a liquid (dense) configuration. For each of the two runs (discarding the equilibration transient) we measure the histograms $h_{0G}(N)$ and $h_{0L}(N)$ of N, see Fig. 6.3 (top, left). We observe two clearly separated peaks centered around $N \approx 30$ and $N \approx 200$. Then, we choose an interval $I = [N_{\min}, N_{\max}]$ that contains the two peaks. In the present case, we choose $N_{\min} = 0$ and $N_{\max} = 220$. Then, we modify the updating step so that N always belongs to the interval I. This is a crucial modification to have a stable recursion; of course, this restriction should be eliminated at the end, once $\pi(x)$ has been determined.

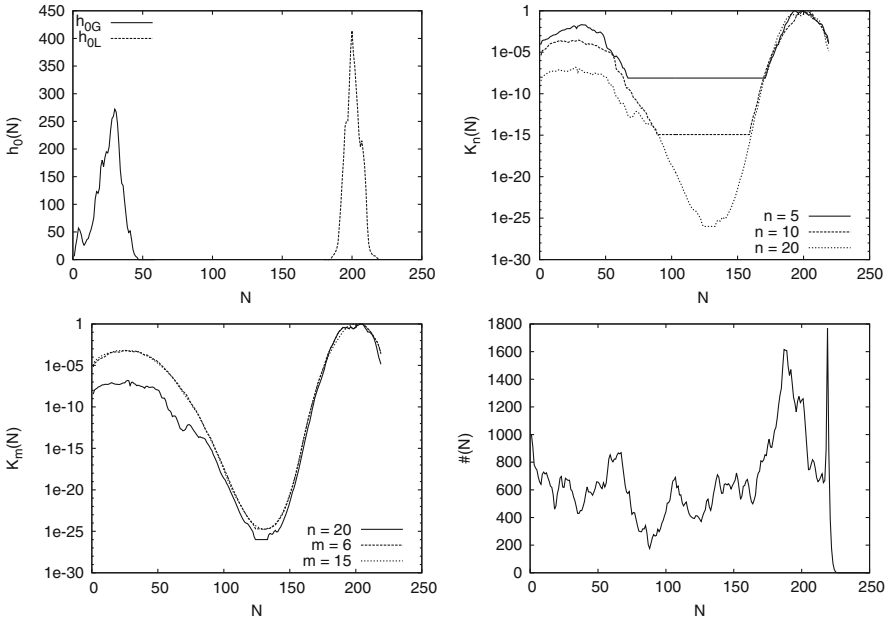

Fig. 6.3 *Top*, *left*: we report the distributions $h_{0G}(N)$ and $h_{0L}(N)$ of N at the beginning of the iterative procedure. *Top*, *right*: function $K_n(N)$ after several iterations ($n = 5, 10, 20$) during the first part of the procedure. *Bottom*, *left*: function $K_n(N)$ at the end of the first part of the procedure ($n = 20$) and after other m iterations following Eq. (6.23). *Bottom*, *right*: histogram of N obtained in a MC simulation using the final umbrella distribution $\pi(x)$

The recursion method determines at each step a function $K_n(N)$ and uses $\pi_{n+1} \propto \pi_0/K_n(N)$ as the distribution function for the next MC simulation. The function $K_n(N)$ should be such that the new distribution π_{n+1} is as flat as possible in the range $[N_{\min}, N_{\max}]$. Let us first determine the zeroth-order approximation $K_0(N)$. If $M_{0G} = \max h_{0G}(N)$ and $M_{0L} = \max h_{0L}(N)$, we define $H_{0G}(N) = h_{0G}(N)/M_{0G}$ and $H_{0L}(N) = h_{0L}(N)/M_{0L}$. Then, we set

$$
\begin{aligned}
K_0(N) &= \varepsilon && \text{if } H_{0G}(N) \le \varepsilon \text{ and } H_{0L}(N) \le \varepsilon\,, \\
K_0(N) &= H_{0G}(N) && \text{if } H_{0G}(N) > \varepsilon \text{ and } H_{0L}(N) \le \varepsilon\,, \\
K_0(N) &= H_{0L}(N) && \text{if } H_{0G}(N) \le \varepsilon \text{ and } H_{0L}(N) > \varepsilon\,.
\end{aligned}
$$

We have introduced a lower cutoff ε on the histograms to discard noisy data (the longer the runs, the smaller ε can be). In the example we use $\varepsilon = 1/200$, hence we use all data except those for which $h_{0G}(N) \le \varepsilon\, M_{OG} \simeq 1$ and $h_{0L}(N) \le \varepsilon\, M_{OL} \simeq 2$. Once $K_0(N)$ is defined, we perform two runs using $\pi_1 \propto \pi_0/K_0(N)$ and again determine the distributions $h_{1G}(N)$ and $h_{1L}(N)$. The successive approximations $K_n(N)$ are obtained as

$$
\begin{aligned}
K_n(N) &= K_{n-1}(N)\,\varepsilon && \text{if } H_{nG}(N) \le \varepsilon \text{ and } H_{nL}(N) \le \varepsilon\,, \\
K_n(N) &= K_{n-1}(N)\,H_{nG}(N) && \text{if } H_{nG}(N) > \varepsilon \text{ and } H_{nL}(N) \le \varepsilon\,, \\
K_n(N) &= K_{n-1}(N)\,H_{nL}(N) && \text{if } H_{nG}(N) \le \varepsilon \text{ and } H_{nL}(N) > \varepsilon\,,
\end{aligned}
$$

where $H_n(N) = h_n(N)/M_n$ and M_n is the maximum of $h_n(N)$. The procedure is repeated several times until the distributions $h_{nG}(N)$ and $h_{nL}(N)$ overlap, i.e., there is an $\bar{N}$ such that $H_{nG}(\bar{N}) > \varepsilon$ and $H_{nL}(\bar{N}) > \varepsilon$. In the example 20 iterations are needed. In Fig. 6.3 (top, right) we show $K_n(N)$ for $n = 5, 10$, and 20. To allow a better comparison, we have multiplied the functions by a constant (irrelevant in the definition of π_n) so that the maximum of $K_n(N)$ is always 1. Note how the double-peak structure emerges as the number of iterations is increased, in spite of the fact that there are 26 orders of magnitude between maximum and minimum. From a practical point of view the procedure can be improved and speeded up in several ways. First, one can smooth the histograms to eliminate noise. Second, after a few iterations one can try to guess $K(N)$: one can fit the peaks with Gaussians and restart the iterations from the fitted function. Third, one can perform a different number of iterations in the two phases if the efficiency of the algorithm is phase dependent. Finally, note that thermalization is needed only in the first run. Then, one can restart the simulation from the last configurations generated in the previous iteration.

Once the gas and liquid distributions overlap, there is no longer need of two different simulations. One performs a single run m times, determines the distribution $h_m(N)$, its maximum M_m, defines $H_m(N) = h_m(N)/M_m$, and updates K_m as follows:

$$
\begin{aligned}
K_m(N) &= K_{m-1}(N)\,\varepsilon && \text{if } H_m(N) \le \varepsilon\,, \\
K_m(N) &= K_{m-1}(N)\,H_m(N) && \text{if } H_m(N) > \varepsilon\,.
\end{aligned}
\tag{6.23}
$$

In this second part of the procedure it is usually a good idea to increase both ε and the number of iterations, to increase the precision on $h_m(N)$. The obtained $K_m(N)$ for the specific example are reported in Fig. 6.3 (bottom, left). After $m = 6$ iterations following Eq. (6.23), the function $K_m(N)$ reaches its asymptotic form. Note that this iterative procedure is quite stable: if we increase the number of iterations, $K_m(N)$ does not change (see the curve for $m = 15$ in the figure). Once $K(N)$ has been determined, we can eliminate the restrictions on N, setting $K(N) = K(N_{\max})$ for $N > N_{\max}$ and $K(N) = K(N_{\min})$ for $N < N_{\min}$. In Fig. 6.3 we report the histogram of N obtained by using the final $\pi \propto \pi_0/K_m(N)$. All values of N are visited and in particular we are sampling in both phases. We can thus use the final $\pi(x)$ to analyze in detail the behavior at coexistence.

It is important to stress that this procedure correctly works for first-order transitions with two single minima and for which the relevant order parameter is known, but cannot be applied to study the LT phase of disordered systems, like spin glasses.

6.6 Parallel Tempering

6.6.1 General Considerations

In the previous section we have discussed multicanonical sampling, which is appropriate for the study of first-order transitions. In that case, sampling correctly all free-energy minima requires the system to visit also the barrier region, where the probability distribution is extremely small, of the order of e^{-aN^p}, where N is the system size. In the presence of second-order phase transitions, the behavior is quite different, since the different free-energy minima characterizing the ordered phase merge at the critical point, giving rise to a single thermodynamic state. Hence, if one wishes to visit all ordered states, there is no need to go over the barriers. For instance, consider a thermal second-order transition, as it occurs in the Ising model. To sample the LT magnetized phases, one can adopt an algorithm in which temperature is varied. Starting from a LT configuration, one can rise the temperature till that of the critical point, where all minima merge, then move into the HT phase, where a single thermodynamic state exists. If the system spends enough time in the HT phase, it loses memory of the thermodynamic LT phase it was coming from. Hence, when temperature is decreased again, it may well fall into a different LT thermodynamic state. This simple argument should convince the reader that algorithms that allow temperature changes are powerful tools for the study of the ordered phases in the presence of second-order phase transitions. ST was indeed devised with this motivation in mind [17]. However, as we discussed in Sect. 6.4.2, ST has a serious shortcoming: a ST simulation requires some free-energy differences to be determined before starting the simulation; moreover, the efficiency of the simulation depends on the accuracy with which these quantities are determined. These problems can be avoided by using a variant of ST, the parallel tempering (PT) method, which is, at present, the most efficient general-purpose algorithm for studying models undergoing second-order phase transitions. The PT method works well even in very complex models, like spin glasses, that have a very large number of LT local minima. It is also very useful in systems which, even in the absence of phase transitions, cannot be simulated efficiently due to the presence of geometric constraints, like complex molecules in dense systems, or in the presence of boundaries, or in porous systems, just to name a few examples. In computer science and statistics, PT is often used in connection with multimodal distributions.

PT has a quite interesting history. It was first introduced in the computer-science/statistics community by Geyer in 1991 [27], as an efficient method to sample multimodal probability distributions and it was named Metropolis-coupled Markov chain Monte Carlo. The work of Geyer stirred a lot of interest in the statistical physics community working on polymer physics and PT was carefully analyzed and compared with US by Tesi et al. [28]. Independently, in 1996 the PT algorithm was introduced by Hukushima and Nemoto [29] with the name of replica-exchange algorithm, and found widespread application in spin-glass simulations. At the same time, thanks to the works of Hansmann [30] the algorithm found its

way in the chemical physics and biophysics community, as a more efficient and simpler alternative to US and multicanonical algorithms (for a list of applications in this field, see the review by Earl and Deem [31]). At present the name "parallel tempering" is apparently the most widely used name in the physics community, while mathematicians prefer to indicate it as "swapping algorithm".

The PT algorithm is a simple generalization of ST. The state space S' is formed by R replicas of the original state space S: $S' = S \times \ldots \times S$. On S' one takes as probability

$$\Pi(x_1, \ldots, x_R) = \pi_1(x_1)\pi_2(x_2) \ldots \pi_R(x_R) \ .$$

In the standard case, $\pi_1(x), \ldots, \pi_R(x_R)$ are the Boltzmann-Gibbs distributions at R different values of the inverse temperatures $\beta_1 < \ldots < \beta_R$. The algorithm usually works as follows:

(a) If $(x_1, \ldots, x_R)$ is the present configuration, one updates each x_i using any MC algorithm that leaves $\pi_i(x)$ invariant.
(b) One proposes a swapping move[7]:

$$(x_1, \ldots, x_i, x_{i+1}, \ldots x_R) \to (x_1, \ldots, x_{i+1}, x_i, \ldots x_R) \ ,$$

which is accepted with probability

$$p_{\text{swap}} = \min\left(1, \frac{\pi_{i+1}(x_i)\pi_i(x_{i+1})}{\pi_{i+1}(x_{i+1})\pi_i(x_i)}\right) = \min\left(1, e^{(\beta_{i+1}-\beta_i)(E_{i+1}-E_i)}\right) \ .$$

It is immediate to verify that the algorithm satisfies the stationarity condition with respect to Π, though it may not necessarily satisfy detailed balance (this depends on how i and $i+1$ are chosen).

As in the US or ST case, in order to perform a PT simulation, one must decide the number R of inverse temperatures and their values. We note that one of the two conditions we discussed in the case of US and ST should hold also here: temperatures should be close enough, so that the typical configuration domains at nearby temperatures overlap. If this does not occur, no swap is accepted. For an efficient simulation it is important to discuss how close temperatures should be. This will be discussed in Sect. 6.6.3.

Whenever a PT run is performed, it is important to make checks to verify that the algorithm is working correctly. The simplest quantity to measure is the swapping rate $a_{i,i+1}$ between adjacent temperatures, that is the fraction of accepted swaps. The algorithm works efficiently only if, for all i, $a_{i,i+1}$ is not too small. As we discuss in Sect. 6.6.3, the optimal value for $a_{i,i+1}$ lies between 0.2 and 0.3, but larger, or

[7] In principle the swapping can be attempted among any pair of replicas, but only for nearby replicas the swap has a reasonable probability of being accepted.

slightly smaller values, although not optimal, are still acceptable. A reasonable swapping rate is, however, not enough to guarantee that the algorithm is working correctly. Indeed, there are situations in which the swapping rates take the desired values, but the PT simulation is inefficient. This typically occurs when there is a "bottleneck" at a certain temperature β_K (usually it is the closest to the critical temperature). In this case $a_{K-1,K}$ and $a_{K,K+1}$ are both reasonable, but the algorithm is unable to move a LT configuration to the other, HT side. In this case, HT replicas mix very slowly with the LT replicas, so that the dynamics, which is based on the idea that LT replicas rapidly move into the HT phase, becomes very slow. To identify bottlenecks, it is not enough to compute the swapping acceptances. One should measure quantities that take into account how temperature changes for each individual replica. Often one considers the average round-trip time, i.e., the time for a replica to start from the lowest temperature, reach the highest one, and finally go back to the lowest one. If the swapping procedure is working efficiently, the round-trip time should be comparable to the return time of a random walker moving among temperatures with the swapping rates actually measured in the simulation. On the contrary, if the swapping procedure has a bottleneck, then the round-trip time becomes large and is essentially controlled by the time it takes for a replica to go through the bottleneck.[8]

As in all MC simulations, also in PT simulations one should thermalize the system before measuring. Two checks should be performed: first, one should check that equilibrium has been attained at all temperatures. Note that it is not enough to check convergence at the lowest temperature. For instance, in PT simulations of non-disordered systems that go through a second-order phase transition, the slowest mode is controlled by the behavior at the critical point, not at the lowest-temperature point (see the discussion in Sect. 6.6.2). Second, the thermalization time should be larger than the time needed to go through any bottleneck present in the model: typically a few round-trip times suffice.

6.6.2 Some General Rigorous Results

The PT algorithm has been studied in detail by mathematicians which have proved theorems [32–34] confirming the general arguments given at the beginning of Sect. 6.6.1. These theorems give bounds on the spectral gap λ of the Markov chain associated with the PT algorithm. In physical terms λ is related to the exponential autocorrelation time $\tau_{\rm exp} = -1/\ln(1-\lambda)$, which gives the number of iterations needed to generate an independent configuration. An efficient algorithm requires λ to be significantly different from zero.

[8] If the PT method is applied to a system undergoing a first-order transition, the swapping procedure would be highly inefficient, because HT replicas would hardly swap with LT replicas. The two sets of replicas would remain practically non-interacting.

To establish the notation, let $P_k(x, y)$ be a Markov chain defined on the state space S which leaves invariant π_k: $\sum_x \pi_k(x) P_k(x, y) = \pi_k(y)$. The basic idea used in the theorems is the state-space decomposition of Madras and Randall [35]. If (a) the state space is decomposable as $S = \cup_l A_l$ such that all π_k are unimodal in each A_l,[9] (b) swaps occur with sufficient frequency along a configuration path that connects all sets A_l, and (c) P_1 is a fast update on S, then the size of the spectral gap is essentially controlled by the spectral gap of the restrictions P_{kl} of P_k on A_l. In other words, PT is, at most, as fast as the slowest of the P_{kl} [34]. To clarify this result, let us consider the Ising model and a PT simulation with β_1 in the HT phase and β_R in the LT phase. Suppose we use the Metropolis algorithm to update the configurations at each temperature. In the LT phase the Metropolis algorithm is of course inefficient (it cannot go through the barriers). However, if we partition $S = M_+ \cup M_-$, where M_+ and M_- are the positive and negative magnetization configurations, respectively, the restrictions P_{k+} and P_{k-} of P_k to M_+ and M_- are efficient algorithms that sample correctly each free-energy minimum. With this decomposition, the slowest dynamics occurs at the critical point, which represents the bottleneck of the simulation. Hence, the theorem essentially states that the autocorrelation time of the PT simulation is of the order of the autocorrelation time of the algorithm at the critical point, which is also the typical time it takes for a HT configurations to become a LT one and viceversa. Note that the improvement is enormous. We are able to sample the LT phase with autocorrelations that increase polynomially as N^z when the system size N goes to infinity ($z \approx 2$ for the Ising model with Metropolis update) and not exponentially in $N^{1-1/d}$, where d is the space dimension (for the two-dimensional Ising model one can prove $\tau \approx e^{aN^{1/2}}$ for a standard MC simulation [36]).

6.6.3 Optimal Choice of Temperatures

Let us now discuss how to choose optimal temperatures in a PT simulation. First of all, the set of temperatures must extend enough in the HT phase in order to allow replicas at the highest temperatures to decorrelate fast. More precisely, we would like the autocorrelation time τ at the highest temperature to be smaller than the typical time a replica spends in the HT regime, so that, when a replica goes back to the LT phase, it has completely forgotten the previous free-energy minimum. This condition fixes the highest temperature, while the lowest temperature is usually determined by the problem we wish to study (e.g., critical properties of the model or the nature of its LT phase).

Once $\beta_{\min}$ and $\beta_{\max}$ have been fixed, what is the best sequence for the remaining temperatures? Under the hypothesis that there are no bottlenecks and thus the

[9] The condition of unimodality is not required in the proofs of the theorems. However, the theorems have physically interesting consequences only if a unimodal decomposition is possible.

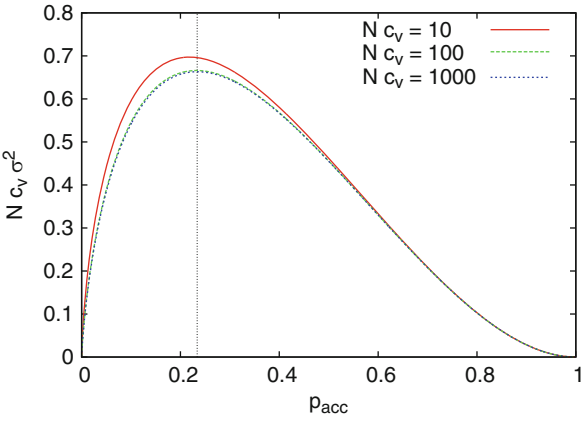

Fig. 6.4 Graph of $Nc_V\sigma^2$ with $\sigma^2 = (\ln r)^2\, p_{\rm acc}$ versus $p_{\rm acc}$ for three different values of Nc_V. The results corresponding to $Nc_V = 100$ and 1,000 cannot be distinguished as they are one on top of the other. The *vertical dotted line* corresponds to $p_{\rm acc} = 0.23$

round-trip time is mainly determined by the swapping rate, the optimal solution is to keep swapping rates constant in the whole temperature range, so that the diffusion of the replicas in temperature space is maximal. The optimal value of the swapping rate depends on the system under study, but in general one has to avoid too small values (replicas almost do not swap) and also too large ones (in this case a smaller number of temperatures would be enough). With the random-walk picture in mind, in order to obtain the largest diffusion rate in temperature space (more precisely in the variable $\ln\beta$), one would like to maximize $\sigma^2 = \ln^2(\beta_i/\beta_{i+1})\, p_{\rm acc}(\beta_i, \beta_{i+1})$, where $p_{\rm acc}(\beta_i, \beta_{i+1})$ is the average acceptance rate for the swap between β_i and β_{i+1}. If the specific heat is constant, the average acceptance rate is well represented for $N \to \infty$ by the formula [37–39]

$$p_{\rm acc}(\beta_i, \beta_{i+1}) = \mathrm{erfc}\left[\frac{1-r}{1+r}(Nc_V)^{1/2}\right],$$

where $r = \beta_i/\beta_{i+1} < 1$ (we assume $\beta_{i+1} > \beta_i$). If we require a constant acceptance rate, r should be constant, hence temperatures should increase geometrically, i.e. $\beta_{i+1} = r\,\beta_i$. The optimal value for r can be found by maximizing σ^2. It turns out, see Fig. 6.4, that the average acceptance rate for the optimal r is very close to 0.23, with essentially no dependence on Nc_V [38–40]. This gives rise to the so-called 0.23 rule, according to which temperatures should be spaced in such a way to guarantee a 0.23 average acceptance rate. Note also that $Nc_V\sigma^2$ is essentially a universal function of $p_{\rm acc}$, see Fig. 6.4, that converges very quickly to its large Nc_V limit

$$Nc_V\sigma^2 = 4\, p_{\rm acc}\left[\mathrm{erfc}^{-1}(p_{\rm acc})\right]^2.$$

This function has a maximum of height 0.6629 at $p_{\rm acc} = 0.2338$. Hence

$$(\ln r_{\text{opt}})^2 = \frac{0.6629}{0.2338}\frac{1}{Nc_V}\,, \qquad r_{\text{opt}} = 1 - \frac{1.684}{\sqrt{Nc_V}}\,.$$

As already found in Sect. 6.2 when discussing data reweighting, also in this case $\Delta\beta \propto (1 - r_{\text{opt}}) \propto (Nc_V)^{-1/2}$. If the specific heat is not constant, $\Delta\beta \propto (Nc_V)^{-1/2}$ should still hold, hence temperatures should be denser where the specific heat is larger.

6.6.4 Improving Parallel Tempering

Sometimes, even with an optimal choice of the temperatures, the PT simulation may show up a bottleneck in temperature, unexpectedly. The problem is that the analytical computation of the swapping rate is made under the hypothesis that each configuration at inverse temperature β is generated according to $\pi_\beta(x)$ with no memory of its past trajectory; this assumption is valid if the time Δt between two consecutive swapping attempts is larger than the autocorrelation time τ_β at β. On the contrary, if $\tau_\beta > \Delta t$, then a replica is likely to swap back to the temperature it came from, since its energy is still correlated with its old temperature. This phenomenon of swapping forward and then immediately backward is exactly what makes diffusion in temperature space much slower.

Recently there have been some proposals to overcome this problem and improve the PT method. In Ref. [41] a method called feedback-optimized PT has been proposed, which iteratively readjusts the temperatures in order to minimize the average round-trip time. The outcome of this procedure is an increase of the density of temperatures (and thus of the swapping rate) where the autocorrelation time τ is larger. In some sense this solution can be viewed as a brute-force one, because forces replicas to spend more time where τ is larger by adding temperatures there. A more elegant solution has been proposed in Ref. [42] and it consists in adapting the time Δt between consecutive swapping attempts to the autocorrelation time τ. Indeed, results for the 2D Ising model show that, by taking $\Delta t \sim \tau$, the resulting time series are nearly uncorrelated and replicas make an unbiased diffusion among temperatures; unfortunately this choice makes the simulation too long, so the final suggestion is to have the ratio $\Delta t/\tau$ more or less fixed to a small number.

Let us finish this overview of the PT method with a comment on its use for disordered systems. Certainly the numerical study of disordered models (e.g., spin glasses) has benefited very much from the PT algorithm in the last decades. Nonetheless, it is important to recall that models with strong quenched disorder show impressive sample-to-sample fluctuations. As a consequence, the optimizations illustrated above should be performed separately on each different sample: indeed, we would expect a very different scheduling of temperatures and swapping times for a strongly frustrated sample with respect to a weakly frustrated one. Since this sample-by-sample optimization is not easy to do, in practice one usually fixes a common scheduling of temperatures and times for all samples, based on average

properties (e.g., on the sample-averaged specific heat). However, thermalization checks and autocorrelation-time analyses should be performed on each sample separately, allowing the simulation to run longer for the slower samples [43].

6.7 Conclusions

In this contribution we present several numerical methods which are used to compute large-deviation observables, that is quantities that require a proper sampling of rare configurations. First, we discuss the problem of data reweighting and the optimal multiple-histogram method [6, 13]. Then, we introduce a family of algorithms that rely on non-Boltzmann-Gibbs distributions and which are able to sample the typical configurations corresponding to a large temperature interval. We present the umbrella sampling [15] and the simulated tempering method [16, 17] and show that these two algorithms are equivalent [18] if configurational updates are performed by using the Metropolis method. The main difficulty in the implementation of the US and ST methods is the determination of the constants α_i that parametrize the probability distribution, see Eqs. (6.12) and (6.15). This problem can be overcome by using the PT algorithm [27–29], which is at present the most efficient algorithm to sample the low-temperature phase of systems undergoing a second-order phase transition, even in the presence of quenched disorder—hence, it can be applied successfully to, e.g., spin glasses. None of these methods can be employed directly in the presence of first-order phase transitions. Multicanonical methods, in which the non-Boltzmann-Gibbs distribution is determined recursively, can be used instead [25, 26].

References

1. N. Metropolis, A.W. Rosenbluth, M.N. Rosenbluth, A.H. Teller, E. Teller, J. Chem. Phys. **21**, 1087 (1953)
2. M.N. Rosenbluth, A.W. Rosenbluth, J. Chem. Phys. **22**, 881 (1954)
3. B.J. Alder, S.P. Frankel, V.A. Lewinson, J. Chem. Phys. **23**, 417 (1955)
4. B.J. Alder, T.E. Wainwright, J. Chem. Phys. **27**, 1208 (1957)
5. S.R.S. Varadhan, Ann. Prob. **36**, 397 (2008)
6. A.M. Ferrenberg, R.H. Swendsen, Phys. Rev. Lett. **61**, 2635 (1988); Erratum ibid. **63**, 1658 (1989)
7. R.H. Swendsen, A.M. Ferrenberg, in *Computer Studies in Condensed Matter Physics II*, ed. by D.P. Landau, K.K. Mon, H.B. Schüttler (Springer, Berlin, 1990), pp. 179–183
8. A.M. Ferrenberg, D.P. Landau, R.H. Swendsen, Phys. Rev. E **51**, 5092 (1995)
9. B. Efron, Ann. Stat. **7**, 1 (1979)
10. B. Efron, Biometrika **68**, 589 (1981)
11. L. Onsager, Phys. Rev. **65**, 117 (1944)
12. B.M. McCoy, T.T. Wu, *The Two-Dimensional Ising Model* (Harvard University Press, Cambridge, 1973)

13. A.M. Ferrenberg, R.H. Swendsen, Phys. Rev. Lett. **63**, 1195 (1989)
14. C.H. Bennett, J. Comp. Phys. **22**, 245 (1976)
15. G.M. Torrie, J.P. Valleau, J. Comp. Phys. **23**, 187 (1977)
16. A.P. Lyubartsev, A.A. Martsinovski, S.V. Shevkunov, P.N. Vorontsov-Velyaminov, J. Chem. Phys. **96**, 1776 (1991)
17. E. Marinari, G. Parisi, Europhys. Lett. **19**, 451 (1992)
18. N. Madras, M. Piccioni, Ann. Appl. Prob. **9**, 1202 (1999)
19. R.H. Swendsen, J.-S. Wang, Phys. Rev. Lett. **58**, 86 (1987)
20. R.G. Edwards, A.D. Sokal, Phys. Rev. D **38**, 2009 (1988)
21. W.K. Hastings, Biometrika **57**, 97 (1970)
22. N. Bhatnagar, D. Randall, in *Proceeding of the Fifteenth Annual ACM-SIAM Symposium on Discrete Algorithms*, New Orleans (ACM, New York, 2004), pp. 478–487
23. M. Fukugita, H. Mino, M. Okawa, A. Ukawa, J. Phys. A **23**, L561 (1990)
24. J.F. McCarthy, Phys. Rev. B **41**, 9530 (1990)
25. B. Berg, T. Neuhaus, Phys. Lett. B **267**, 249 (1991)
26. B. Berg, T. Neuhaus, Phys. Rev. Lett. **68**, 9 (1992)
27. C.J. Geyer, in *Computing Science and Statistics, Proceedings of the 23rd Symposium on the Interface*, ed. by E.M. Keramidas, S.M. Kaufman (American Statistical Association, New York, 1991), pp. 156–163
28. M.C. Tesi, E.J. Janse van Rensburg, E. Orlandini, S.G. Whittington, J. Stat. Phys. **82**, 155 (1996)
29. K. Hukushima, K. Nemoto, J. Phys. Soc. Jpn. **65**, 1604 (1996)
30. U.H.E. Hansmann, Chem. Phys. Lett. **281**, 140 (1997)
31. D.J. Earl, M.W. Deem, Phys. Chem. Chem. Phys. **7**, 3910 (2005)
32. N. Madras, Z. Zheng, Random Struct. Alg. **22**, 66 (2003)
33. Z. Zheng, Stoch. Proc. Appl. **104**, 131 (2003)
34. D.B. Woodard, S.C. Schmidler, M. Huber, Ann. Appl. Prob. **19**, 617 (2009)
35. N. Madras, D. Randall, Ann. Appl. Prob. **12**, 581 (2002)
36. F. Martinelli, E. Olivieri, R. Schonmann, Comm. Math. Phys. **165**, 33 (1994)
37. D.A. Kofke, J. Chem. Phys. **117**, 6911 (2002)
38. A. Kone, D.A. Kofke, J. Chem. Phys. **122**, 206101 (2005)
39. C. Predescu, M. Predescu, C.V. Ciobanu, J. Chem. Phys. **120**, 4119 (2004)
40. D. Sabo, M. Meuwly, D.L. Freeman, J.D. Doll, J. Chem. Phys. **128**, 174109 (2008)
41. H.G. Katzgraber, S. Trebst, D.A. Huse, M. Troyer, J. Stat. Mech. P03018 (2006)
42. E. Bittner, A. Nußbaumer, W. Janke, Phys. Rev. Lett. **101**, 130603 (2008)
43. R. Alvarez Baños et al. (Janus collaboration), J. Stat. Mech. P06026 (2010)

Chapter 7
Large Deviations Techniques for Long-Range Interactions

Aurelio Patelli and Stefano Ruffo

Abstract After a brief introduction to the main equilibrium features of long-range interacting systems (ensemble inequivalence, negative specific heat and susceptibility, broken ergodicity, etc.) and a recall of Cramèr's theorem, we discuss in this chapter a general method which allows us to compute microcanonical entropy for systems of the mean-field type. The method consists in expressing the Hamiltonian in terms of global variables and, then, in computing the phase-space volume by fixing a value for these variables: this is done by using large deviations. The calculation of entropy as a function of energy is, thus, reformulated as the solution of a variational problem. We show the power of the method by explicitly deriving the equilibrium thermodynamic properties of the three-state Potts model, the Blume-Capel model, an XY spin system, the ϕ^4 model and the Colson-Bonifacio model of the free electron laser. When short range interactions coexist with long-range ones, the method cannot be straightforwardly applied. We discuss an alternative variational method which allows us to solve the XY model with both mean-field and nearest neighbor interactions.

7.1 Long-Range Interactions

In this chapter we will present some applications of the large deviations technique to the calculation of entropy and free-energy of systems with long-range interactions [1]. Indeed, most of the examples we will treat are simple mean-field models.

A. Patelli
Dipartimento di Fisica e Astronomia, INFN, Università di Firenze, via G. Sansone 1, Sesto Fiorentino, I-50019, Florence, Italy
e-mail: oreca85@gmail.com

S. Ruffo (✉)
Dipartimento di Fisica e Astronomia, INFN, CNISM, Università di Firenze, via G. Sansone 1, Sesto Fiorentino, I-50019, Florence, Italy
e-mail: stefano.ruffo@unifi.it

A. Vulpiani et al. (eds.), *Large Deviations in Physics*, Lecture Notes in Physics 885,
DOI 10.1007/978-3-642-54251-0_7,

However, it can be shown that some of the methods we discuss here are applicable to all systems for which the interaction decays slowly with the distance.

There is not a unique definition of long-range interactions in the literature [2]. Some authors extend the definition to those interactions that decay with a power of the interparticle distance, therefore including within the definition the van der Waals interaction. We are here interested in the definition which is related to the additive property of the energy. Not all interactions that decay with a power induce non additivity of the energy, which is the important property we want to stress here. Let us therefore adopt the following definition of long-range two-body potential

$$V(r) \sim Jr^{-\alpha} , \qquad (7.1)$$
$$0 \leq \alpha \leq d, \quad r \gg r_s ,$$

with d the dimension of the embedding space and J the coupling strength. The short-distance scale r_s is related to the size of the particle itself. Mean-field systems correspond to $\alpha = 0$.

In nature one finds many examples of this kind of potential: the Newtonian potential between massive bodies, the Coulomb potential between charged particles such as in a plasma, the hydrodynamic interactions between vortices in dimension $d = 2$.

Extensivity, meaning that thermodynamic potentials (energy, entropy, free-energy, etc.) scale with system size, is an essential property in the construction of thermodynamics. Energy per particle $\epsilon = E/N$ should converge to a constant in the thermodynamic limit: $N \to \infty$,$V \to \infty$ with $\rho = N/V \sim const$. The energy per particle can be roughly estimated as

$$\epsilon = \lim_{N\to\infty} \frac{E}{N} = \int_{\delta}^{R} d^d r \rho \frac{J}{r^\alpha} = \frac{\rho J \Omega_d}{d-\alpha} \left[R^{d-\alpha} - \delta^{d-\alpha} \right] , \qquad (7.2)$$

where R is the size of the system, δ is a small distances cut-off and Ω_d the angular volume in dimension d. It is then straightforward to check that

- If $\alpha > d$ then $\epsilon \to const$ when $R \to \infty$.
- If $0 \leq \alpha \leq d$ then $\epsilon \sim V^{1-\alpha/d}$ ($V \sim R^d$).

The first case shows that the limit $R \to \infty$ can be safely performed and defines an intensive energy per particle. In the second case, the energy per particle is not intensive and diverges with the volume, it is super-extensive. Thus, in terms of the energy $E = \epsilon V$, one finds the scaling

$$\alpha \leq d \quad E \sim V^{2-\alpha/d} . \qquad (7.3)$$

Typically, the entropy scales linearly with the volume $S \sim V$, and the free-energy is defined as

$$F = E - TS , \qquad (7.4)$$

with T the intensive temperature. Therefore, the thermodynamic properties of long-range systems are dominated by the energy E, because it scales with volume V faster than linear. A way out from this energy dominance was proposed by Mark Kac. It consists in scaling the coupling constant

$$J \to JV^{\alpha/d-1} \,. \tag{7.5}$$

After this "unphysical" rescaling, the free energy turns out to be extensive in the volume

$$F \sim V \,. \tag{7.6}$$

However, this is a mathematical trick and doesn't correspond to any physical effect. It can be used only for the sake of performing a meaningful large volume limit, in order to get thermodynamic behavior. Once the free energy per particle is obtained, the physical description can be retrieved by scaling back the coupling constant. An alternative would be to rescale temperature with volume

$$T \to TV^{1-\alpha/d} \,. \tag{7.7}$$

With this choice, free energy scales superlinearly with the volume

$$F \sim V^{2-\alpha/d} \,, \tag{7.8}$$

exactly like the energy. The two approaches are both possible, but the first one, rescaling the coupling, is more common in the literature [2].

The need to use Kac's trick teaches that the thermodynamic limit is not trivial for long-range systems. Moreover, although the use of this trick restores extensivity of the energy, this does not mean that the energy is necessarily additive. An observable of a given system is additive if it can be expressed as a sum of the observables of every subsystem. Let us consider a system divided in two subsystem, with given energies E_I and E_{II}. In general, the total energy is

$$E_{tot} = E_I + E_{II} + E_{int} \,, \tag{7.9}$$

where E_{int} is the interaction energy between the two subsystems. For short-range systems the interaction energy scales as the contact area between system I and system II, while the two energies E_I and E_{II} scale with the volume. It is then straightforward that, in the thermodynamic limit, the interaction energy is sub-dominant and can be neglected. On the contrary, for long-range systems, the interaction energy scales with the volume exactly as the energies of the two subsystems and, therefore, cannot be neglected.

The violation of additivity is crucial in determining the thermodynamic properties of systems with long-range interactions [1]. For instance, it determines a violation of convexity of the domain of accessible macrostates. An example is

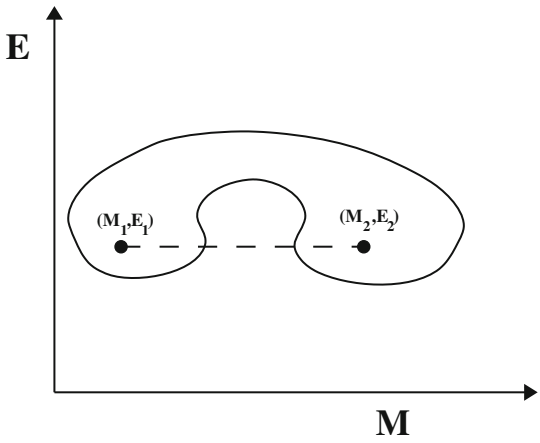

Fig. 7.1 Non convex shape of the region of admissible macrostates in the magnetization/energy plane for long-range systems

shown in Fig. 7.1 where the boundary of admissible macrostates is represented by the thick line with the shape of a bean. In standard thermodynamics, for short range interactions, all states should satisfy the condition

$$E = \lambda E_1 + (1-\lambda)E_2 \quad , \quad M = \lambda M_1 + (1-\lambda)M_2 \quad , \quad 0 \leq \lambda \leq 1 \, , \tag{7.10}$$

at the macroscopic level, because additivity is satisfied. This is in general not true for long-range interactions and can have important consequences, like the violation of ergodicity in the microcanonical ensemble [3,4].

The microcanonical ensembles describe the thermodynamic behaviour of an isolated system. The probability that the system lies in a macrostate at a given energy E depends on the degeneracy of its microstates. The number of microstates with a given energy is the microcanonical partition function

$$\Omega_N(E) = \int \frac{d^{3N}q \, d^{3N}p}{h^{3N}} \delta(E - H(p,q)) \, , \tag{7.11}$$

where (q, p) are canonically conjugate variable, H is the Hamiltonian and h is Planck's constant. Boltzmann's formula gives the microcanonical entropy

$$S(E) = \kappa_B \ln \Omega_N(E) \, . \tag{7.12}$$

where κ_B is the Boltzmann constant. Thanks to additivity of the entropy and of the energy, one can define the probability density that a subsystem of $N_1 \ll N - N_1$ particles has energy E_1, as follows

$$p(E_1) = \frac{\Omega_1(E_1)\Omega_2(E-E_1)}{\int dE_1 \Omega_1(E_1)\Omega_2(E-E_1)} \sim \frac{e^{-\beta E_1}}{Z} \, . \tag{7.13}$$

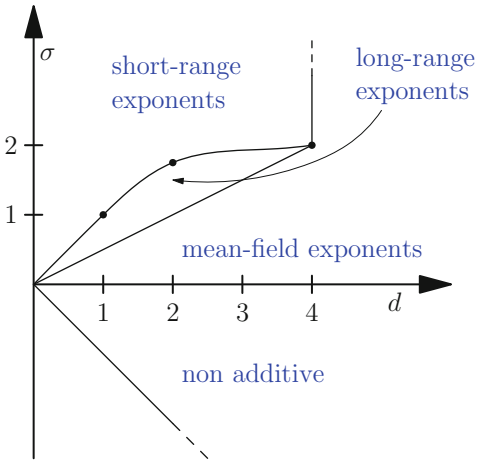

Fig. 7.2 Different behaviors of long-range systems depending on dimension d and the exponent $\sigma = \alpha - d$

The parameter $\beta = \partial S_2/\partial E_2$ is the inverse of the temperature times the Boltzmann constant. This is the canonical ensemble and physically describes a closed system in contact with a thermal bath. Contrary to the microcanonical ensemble, the energy of a canonical system fluctuates around a mean value.

The lack of additivity forbids the classical derivation of the canonical ensemble from the microcanonical one sketched above. However, in the following, we wish to consider the canonical distribution (7.13) also for long-range systems. In order to justify its use for systems with long-range interactions, that are non additive, one must resort to an alternative physical interpretation. For instance, one can consider that the system is in interaction with an external bath of a different nature. One can for instance add damping and noise to the dynamical equations.

The main difference among ensembles arises in the behavior at phase transitions, as we will see in the following sections. Continuous phase transitions can be classified by their behaviors near criticality by a set of critical exponents which govern the divergence of physical quantities. These exponents show universal features depending only on the dimension of the system and on the nature of the interaction potential. Let us briefly show the different behaviors of long-range interacting systems when the exponent $\sigma = \alpha - d$ is varied. One can identify different regions in the d, σ plane (see Fig. 7.2). The non additive long-range region has $-d \leq \sigma \leq 0$, as discussed above. However, the long-range behavior extends to $\sigma > 0$, although the energy is here additive. It can be shown that, if $0 < \sigma \leq d/2$ the critical behavior is characterized by mean-field (classical) exponents, exactly as for the full region $d > 4$ (any value of σ) [5]. Moreover, in a region $\sigma > d/2$ and below a given line which is only partially known, the systems preserves some long-range features, but with non classical σ-dependent critical exponents. Some points along this line are known. At $d = 1$ the line passes through $\sigma = 1$, and in the whole range $0 \leq \sigma \leq 1$ one can find phase transitions in one dimension, which is a strong feature of the long-range nature of the interaction [6, 7]. For $d = 2$, numerical

simulations show that the line passes through $\sigma = 7/4$. Finally, renormalization group techniques suggest that the line reaches $\sigma = 2$ from below at $d = 4$. Above this line and below $d = 4$ the system becomes short-range.

7.2 Some Useful Results of Large Deviations Theory

Let us consider a set of N $d-$dimensional random variables $\mathbf{X}_i$, $i = 1, \ldots, N$, whose probability distribution function (PDF) is $p(\{\mathbf{X}_i\})$. In large deviation theory, one is interested in deriving the PDF of extensive observables

$$\mathbf{M}_N = \frac{1}{N} \sum_{i=1}^{N} f(\mathbf{X}_i) \,, \tag{7.14}$$

in the limit of large N. The function f defines the single variable observable and, for example, when it is the identity, $\mathbf{M}_N$ corresponds to the sample mean.

A *large deviation principle* is formulated, according to which the following limit exists [8]

$$I(x) = \lim_{N \to \infty} -\frac{1}{N} \ln P(\mathbf{M}_N \in [x, x + dx]) \,, \tag{7.15}$$

and defines the rate function $I(x)$. This means that, at leading order, the PDF takes an exponential form $P(\mathbf{M}_N \in [x, x + dx]) \sim \exp(-NI(x))$.

Let us define the scaled cumulant generating function

$$\psi(\boldsymbol{\lambda}) = \lim_{N \to \infty} \frac{1}{N} \ln E \left[\exp(\boldsymbol{\lambda} \sum_{i=1}^{N} f(\mathbf{X}_i)) \right] \,, \tag{7.16}$$

where $\boldsymbol{\lambda} \in R^d$ and the average $E[]$ is performed over the PDF of $\mathbf{X}_i$.

The Gärtner-Ellis' theorem [8] states that, for the sample mean, the rate function is obtained by solving the following variational problem

$$I(\mathbf{x}) = \sup_{\boldsymbol{\lambda} \in R^d} \{\boldsymbol{\lambda}\mathbf{x} - \psi(\boldsymbol{\lambda})\} \,, \tag{7.17}$$

when $\psi(\boldsymbol{\lambda}) < \infty$ and is differentiable everywhere. When the random variables $\mathbf{X}_i$ are independent and identically distributed (i.i.d.) the scaled cumulant generating function is differentiable and assumes the form

$$\psi(\boldsymbol{\lambda}) = \ln\langle \exp(\boldsymbol{\lambda}\mathbf{X}) \rangle \,, \tag{7.18}$$

where $\langle\,\rangle$ is the average with respect to distribution of the single variable. This generating function is differentiable everywhere, because the exponential is an analytic

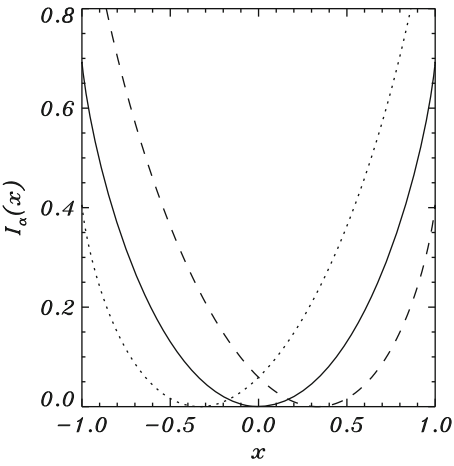

Fig. 7.3 The rate function of coin tossing for $\alpha = 1/3$ (*dashed line*), $1/2$ (*solid line*), $2/3$ (*dotted line*)

function, and the rate function satisfies Gartner-Ellis' theorem. A generalization of this theorem to other observables is given by Varadhan's theorem [8].

Let us consider the example of coin tossing, which physically corresponds to a model of non-interacting spins. The one-dimensional, i.i.d. random variables X_i take the value -1 with probability α and $+1$ with probability $1-\alpha$, with $\alpha \in [0,1]$. The scaled cumulant generating function is

$$\psi_\alpha(\lambda) = \ln\{\exp(\lambda) - 2\alpha \sinh(\lambda)\} . \tag{7.19}$$

When $\alpha = 1/2$ coin tossing is unbiased. In Fig. 7.3 we show the rate function for $\alpha = 1/3, 1/2, 2/3$.

The rate function $I(x)$ determines the number of microstates $\{\mathbf{X}_i\}$ which correspond to a macroscopic configuration characterized by a fraction x of up-spins. In the statistical mechanics vocabulary $I(x)$ is the opposite of Boltzmann entropy.

7.3 Thermodynamic Functions From Large Deviations Theory

In this section we will show how large deviation theory can be used to compute entropy of long-range systems within the microcanonical ensemble and free energy in the canonical ensemble, in particular when the usual microstate counting procedure cannot be used.

Let us illustrate this approach, which we divide in three steps. The first step consists in the definition of the global variables γ. They play the role of the observables for which we compute the PDF. The Hamiltonian, in terms of global variables, is composed by two parts

$$H_N(\omega_N) = \tilde{H}_N(\gamma(\omega_N)) + R_N(\omega_N) \,, \tag{7.20}$$

where $\tilde{H}$ is the extensive part, while R_N is a sub-extensive rest. The variable ω_N represents a phase-space configuration of the N particles, and it can be a vector of all the local variables. Hence, we are naturally led to take the following limit of infinite number of particles

$$h(\gamma) = \lim_{N\to\infty} \frac{H_N}{N} = \lim_{N\to\infty} \frac{\tilde{H}_N}{N} \,. \tag{7.21}$$

The second step relies on the computation of entropy in terms of the global variables

$$s(\gamma) = \lim_{N\to\infty} \frac{1}{N} \log \Omega_N(\gamma) \,, \tag{7.22}$$

where $\Omega_N(\gamma)$ is the number of microscopic configurations ω_N with a fixed value of γ. This entropy is the opposite of the rate function (7.15). If one assumes that the local variables are i.i.d. random variables, then the entropy, can be evaluated using the Gartner-Ellis theorem [8].

The third step amounts to solve either the microcanonical

$$s(\varepsilon) = \sup_{\gamma}\{s(\gamma)|h(\gamma) = \varepsilon\} \,, \tag{7.23}$$

or the canonical

$$\beta f(\beta) = \inf_{\gamma}\{\beta h(\gamma) - s(\gamma)\} \,, \tag{7.24}$$

variational problem. Free energy (7.24) is the Legendre-Fenchel transform of microcanonical entropy (7.23). On the other hand, the Legendre-Fenchel transform of free energy is not the microcanonical entropy, but rather its concave envelope. When the concave envelope coincides with microcanonical entropy (7.23), the two ensembles are equivalent, because there exists a bijective map between microcanonical and canonical macrostates.

Let us discuss these results in the context of phase transitions. Some phase transition are characterized by an order parameter which is zero in a phase and non-zero in the other. For instance, in the case of ferromagnetic phase transition the order parameter is the magnetization of the system along a given direction, denoted by m. In the paramagnetic phase magnetization vanishes ($m = 0$) while in the ferromagnetic phase it assumes values between zero and one ($m \in (0, 1]$).

Second order phase transitions, which imply discontinuities in second order derivatives of thermodynamic functions, have an involutive microcanonical entropy (see Fig. 7.4), i.e. entropy can be obtained either directly or by Legendre-Fenchel transform of the free-energy. This involution property is a simple consequence of

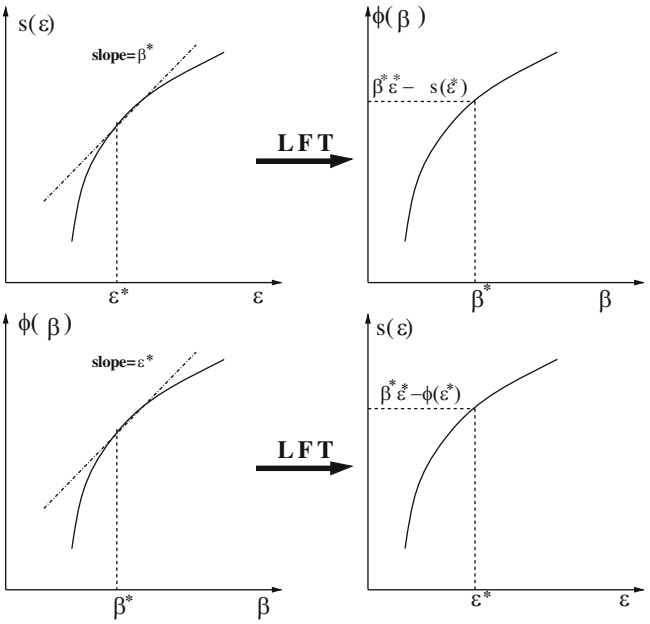

Fig. 7.4 *Upper panel*: Free energy from entropy by a Legendre-Fenchel transform; *Lower panel*: Entropy from free energy

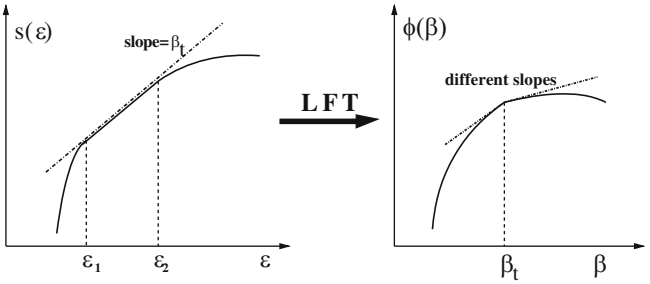

Fig. 7.5 Relation between entropy and free energy at a first order phase transition

the fact that the Legendre-Fenchel transform implies only first order derivatives. Here, the two ensembles are equivalent.

At a first order phase transition, entropy shows a constant slope in the energy range $[\varepsilon_1, \varepsilon_2]$, which is the phase coexistence region. The free energy has a cusp at the transition inverse temperature β_t, see Fig. 7.5, for which there is a continuum of microcanonical states with different energies and the same temperature.

A first order phase transition is thus the extreme case of equivalence between ensembles. Specific heat turns out to be ill defined and one must introduce the concept of latent heat.

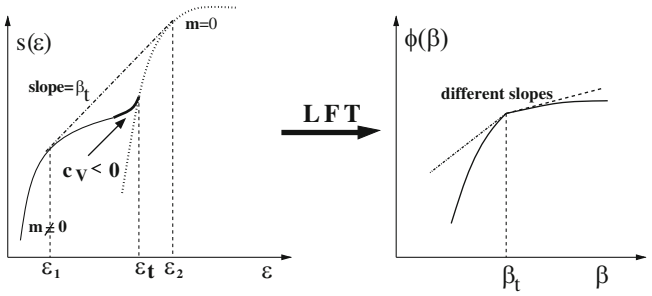

Fig. 7.6 *Left panel*: Microcanonical entropy with negative specific heat and temperature jump in a system with symmetry breaking. *Right panel*: Corresponding free energy in the canonical ensemble

The two ensembles become inequivalent when microcanonical entropy is non concave. The Legendre-Fenchel transform is no more involutive and one can define a canonical entropy which is the concave envelope of microcanonical entropy. This is the basic feature causing ensemble inequivalence. In the microcanonical ensemble the order parameter changes its value with continuity, while it has a discontinuity in the canonical ensemble. Due to the presence of a convex region of the entropy, specific heat can become negative in the microcanonical ensemble.

Phase transition with symmetry breaking, like ferromagnetic phase transitions, show an entropy with two branches at high and low energies, characterized by a different value of the order parameter. The two branches of the entropy generically cross at the transition with different slopes. At the transition energy ε_t two different microcanonical temperatures coexist and one find a *temperature jump*. Conceptually this behavior is similar to the energy jump, due to latent heat, found in the canonical ensemble. Convexity is the main feature which allows for this behavior, because a temperature jump appears only when entropy is convex in a given energy range. In Fig. 7.6 we show a situation where also a region of negative specific heat is present, but this is not necessary for the existence of a temperature jump.

The Legendre-Fenchel transform washes out these behaviour in the canonical ensemble, as shown in Fig. 7.6, and one recovers free energies similar to those at first order phase transitions. It has indeed been conjectured that a necessary condition in order to have negative specific heat and temperature jumps in the microcanonical ensemble is the presence of a first-order transition in the canonical ensemble [9].

7.4 Applications

In this section we show how to apply large deviations methods to find the thermodynamic functions of some model of physical interests. This will illustrate on simple examples the counter intuitive thermodynamic behaviors that appear due to long-range interactions.

7.4.1 Three-States Potts Model

In order to show the application of the method of solution discussed in the previous section to a concrete example, we consider the mean-field three-states Potts model. This is a lattice model where at every site i we associate a spin variable $S_i = a, b, c$. The Hamiltonian is

$$H_N^{Potts} = -\frac{J}{2N} \sum_{i,j=1}^{N} \delta_{S_i,S_j} \ , \tag{7.25}$$

where δ is the Kronecker's δ-symbol, it returns one only when $S_i = S_j$. We identify the spins as the local random variables. The first step of the procedure consists in the identification of the global variables. The form and the symmetries of the Hamiltonian suggest to define the following vector

$$\boldsymbol{\gamma} = (n_a, n_b, n_c) \ , \tag{7.26}$$

where

$$n_\alpha = \frac{1}{N} \sum_i \delta_{S_i,\alpha}, \quad \alpha = a, b, c \ , \tag{7.27}$$

represents the fraction of local random variables populating a given state α. Using these global variables, the extensive part of the Hamiltonian reads

$$\tilde{H}_N^{Potts} = -\frac{JN}{2}(n_a^2 + n_b^2 + n_c^2) = Nh(\gamma) \ , \tag{7.28}$$

and the sub-extensive part vanishes in this case because the Hamiltonian is pure mean-field. The second step deals with the calculation of the entropy in terms of the global variables. Assuming that the three values of the local random variable are equally probable (this corresponds to the principle of "maximal ignorance" often used in statistical mechanics [10]), the scaled cumulant generating function is

$$\psi(\lambda) = \ln\left(\frac{1}{3}\left(e^{\lambda_a} + e^{\lambda_b} + e^{\lambda_c}\right)\right) \ , \tag{7.29}$$

where $\lambda = (\lambda_a, \lambda_b, \lambda_c)$ are Lagrange multipliers. The corresponding rate function is then given by formula (7.17)

$$I(\gamma) = \sup_{\lambda}\{\lambda_a n_a + \lambda_b n_b + \lambda_c n_c - \psi(\lambda)\} \ . \tag{7.30}$$

The extrema of the bracketed expression are obtained when $\lambda_\alpha = \ln n_\alpha, \alpha = a, b, c$. Entropy, as a function of the global variables, is then

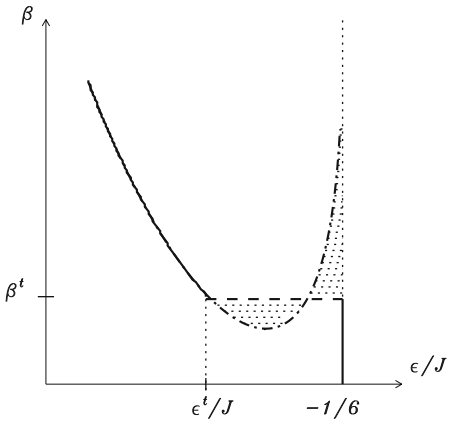

Fig. 7.7 Inverse temperature vs. energy for the mean-field three-state Potts model in both the microcanonical and the canonical ensemble. The microcanonical solution coincides with the canonical one for $\varepsilon \leq \varepsilon^t$ and is otherwise shown by the *dash-dotted line* for $\varepsilon^t \leq \varepsilon < -J/6$. The increasing part of the microcanonical *dash-dotted line* corresponds to a negative specific heat region. In the canonical ensemble, the model displays a first order phase transition at β^t

$$s(\boldsymbol{\gamma}) = -I(\boldsymbol{\gamma}) + \ln \mathscr{N} \,, \tag{7.31}$$

where $\ln \mathscr{N}$ derives from the normalization of the probability, and in this case is $\ln \mathscr{N} = \ln 3$.

In the third step one evaluates the microcanonical entropy from the variational formula

$$s(\varepsilon) = \sup_{n_a, n_b} \Big\{ -n_a \ln n_a - n_b \ln n_b - (1 - n_a - n_b) \ln(1 - n_a - n_b) \\ |h(n_a, n_b) = \varepsilon \Big\} \,. \tag{7.32}$$

The solution of this variational problem is necessarily numerical, because it requires the solution of an implicit equation. However, both the derivation of the entropy and of the microcanonical temperature are straightforward. The dependence of microcanonical temperature on energy is shown in Fig. 7.7: it has a parabolic shape and in the energy range where β grows with energy $\varepsilon \in [-0.215J, -J/6]$, one finds a negative specific heat. By solving the canonical variational problem

$$\beta f(\beta) = \inf_{n_a, n_b, n_c} \Big\{ \sum_{\alpha} n_\alpha \ln n_\alpha - \frac{\beta J}{2} (n_a^2 + n_b^2 + n_c^2) \Big\} \tag{7.33}$$

one can get the average energy ε as a function of β from $\varepsilon = \partial(\beta f)/\partial\beta$. This curve is also plotted in Fig. 7.7. It coincides with the microcanonical curve for energies below $\varepsilon^t = -0.255J$. At the inverse temperature value $\beta^t = 2.75$ the

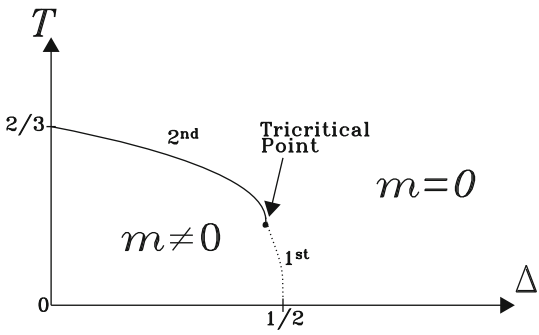

Fig. 7.8 Phase diagram of the Blume-Capel model

model undergoes a first order phase transition, with an associated latent heat in the canonical ensemble. Hence, the results are quite different in the two ensembles: a first order phase transition in the canonical ensemble and no phase transition in the microcanonical one with an associated negative specific heat region in energy.

7.4.2 The Blume-Capel Model

A paradigmatic system showing ensemble inequivalence is the Blume-Capel model. It is a lattice system with both a mean-field coupling and an on-site potential. The model has been used to reproduce the relevant features of superfluidity in He^3–He^4 mixtures and was also proposed as a realistic model of ferromagnetism [11]. Its Hamiltonian reads

$$H_N^{BC} = \Delta \sum_{i=1}^{N} S_i^2 - \frac{J}{2N} \sum_{i=1}^{N} \sum_{j \neq i}^{N} S_i S_j \qquad S_i = 0, \pm 1 \,. \tag{7.34}$$

The canonical ensemble shows first and second order phase transitions. The crossover, which separate the two phases, occurs at the tricritical point. In the phase diagram, this point is located at $\Delta/J = \ln 4/3, T/J = 1/3$, see Fig. 7.8. The coupling constant can be set to $J = 1$ without loss of generality. The first order phase transition point at zero temperature can be computed by equating the paramagnetic and ferromagnetic energies, then $E_{ferro} = \Delta - 1/2$, $E_{para} = 0$. On the other hand, the second order phase transition at $\Delta = 0$ is the usual Curie-Weiss transition for a spin one system, typical of mean-field models. It is obtained by solving the consistency equation

$$m = \frac{\exp(\beta m) - \exp(-\beta m)}{\exp(\beta m) + \exp(-\beta m) + 1} \,, \tag{7.35}$$

where m is the modulus of magnetization.

The entropy of the model can be obtained either by a direct counting of the number of microstates, or by using the large deviation method. We show both these methods, starting from the most common one based on counting of microstates. An example of a typical configuration of the model is pictorially shown below for $N = 30, N_+ = 11, N_- = 9, N_0 = 10$.

$$++++++----00000-------++0000++ \tag{7.36}$$

Fixing the number of up-spins, down-spins and zeros, one can exchange any pair in the group without changing the energy, because the range of interaction covers the whole lattice. Therefore, the number of configurations with given energy is the usual Boltzmann weight

$$\Omega_\varepsilon = \frac{N!}{N_+!N_-!N_0!} . \tag{7.37}$$

Using Stirling approximation, $\ln n! = n \ln n - n$ for large n, one obtains the entropy

$$\begin{aligned} S(q, m, N) = -\kappa_B N[(1-q)\ln(1-q) + \frac{1}{2}(q+m)\ln(\frac{q+m}{2}) \\ +\frac{1}{2}(q-m)\ln(\frac{q-m}{2})] , \end{aligned} \tag{7.38}$$

where $m = (N_+ - N_-)/N$ is magnetization and $q = (N_+ + N_-)/N$ the so-called quadrupolar moment. This latter can be expressed in terms of the energy per spin using the relation

$$\varepsilon = \frac{E}{N} = \Delta(q - Km^2) , \tag{7.39}$$

where $K = J/2\Delta$. This entropy (7.38) is the same as the entropy of the second step of the large deviation procedure. Maximizing it with respects to magnetization m at fixed ε one obtains the microcanonical entropy, which is the third step in large deviations.

We want to show here how to obtain the same entropy using the large deviations procedure that we have introduced previously. The local random variables are $\mathbf{X}_i = (S_i^2, S_i)$, where $S_i = 0, \pm 1$. The identification of the global variables is straightforward, they are magnetization m and quadrupolar moment q. The extensive Hamiltonian, in terms of the global variables, is

$$h(\gamma) = \Delta(q - Km^2) . \tag{7.40}$$

With the assumption that the local variables are i.i.d, the scaled cumulant generating function is also easily computed using the formula (7.16)

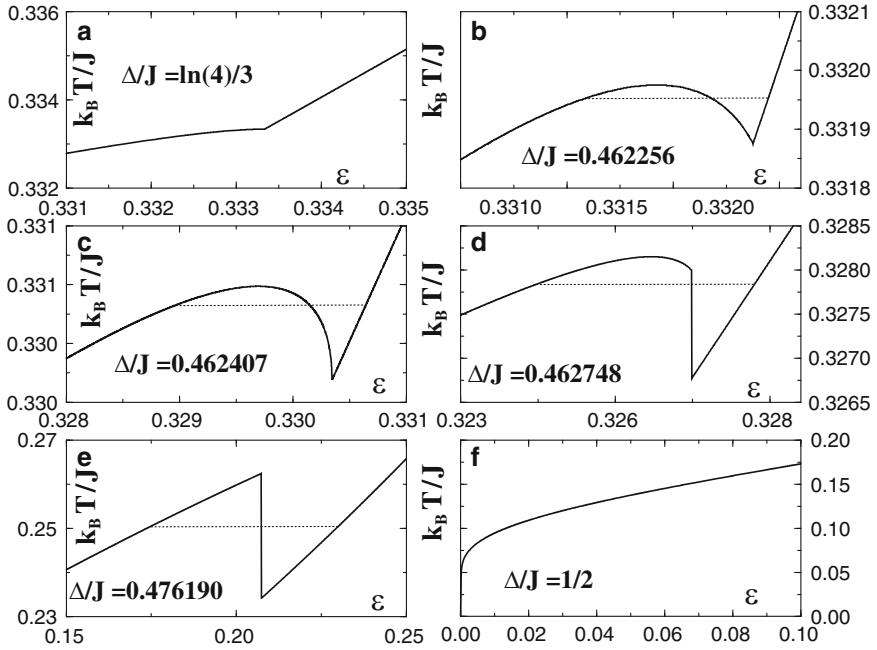

Fig. 7.9 Temperature versus energy for the Blume-Capel model for different values of Δ/J, showing how negative specific heat and temperature jumps develop when entering the region where the phase transition is first order in the canonical ensemble

$$\psi(\lambda, \rho) = \ln\langle \exp\{\lambda S^2 + \rho S\}\rangle = \ln\left(1 + 2e^{\lambda}\cosh(\rho)\right) - \ln 3\,, \tag{7.41}$$

where λ and ρ are Lagrange multipliers. The rate function then reads

$$I(\gamma) = \sup_{\lambda,\rho}\{\rho m + \lambda q - \psi(\lambda, \rho)\}\,. \tag{7.42}$$

The solution of this variational problem gives $\rho = \tanh^{-1}(q/m)$ and $\lambda = -\ln(2\cosh(\rho(q, m))) + \ln(m/(1-m))$. Finally, the substitution of these values into (7.42) returns the rate function in terms of the global variables, and gives the formula (7.38). Hence, the use of large deviations method is a powerful alternative to the direct counting method, whenever the global variables can be identified.

Let us summarize the main features of ensemble inequivalence in this model and give some details about the difference in the thermodynamic states. The inverse temperature is the derivative of entropy with respect to the energy in the microcanonical ensemble. Microcanonical temperature vs. energy is plotted in Fig. 7.9 for decreasing values of the coupling constant Δ/J. It shows how the first order transition appears and induces negative specific heat and temperature jumps. Panel (a) shows a kink in the slope of the temperature at the critical energy. Negative specific heat shows up in panel (b), while the transition is still second order in

the microcanonical ensemble. The transition becomes first order in panel (c) at the microcanonical tricritical point. Panel (d) shows the emergence of the temperature jump and in panel (e) the specific heat region disappears in favor of the temperature jump itself.

The microcanonical tricritical point can be found by expanding the entropy in series of m

$$s = \kappa_B(s_0 + Am^2 + Bm^4 + \ldots) \,. \tag{7.43}$$

The coefficients of the expansion are

$$s_0 = -(1-\epsilon)\ln(1-\epsilon) - \epsilon \ln \epsilon + \epsilon \ln 2 \,, \tag{7.44}$$

$$A = -K \ln(\frac{\epsilon}{2(1-\epsilon)}) - \frac{1}{2\epsilon} \,, \tag{7.45}$$

$$B = -\frac{K^2}{2\epsilon(1-\epsilon)} + \frac{K}{2\epsilon^2} - \frac{1}{12\epsilon^3} \,, \tag{7.46}$$

where $\epsilon = \varepsilon/\Delta$. In order to obtain the second order transition line one has to impose that $A = 0$ with $B < 0$. This line coincides with the canonical second order line in Fig. 7.8 and ends at the microcanonical tricritical point, which is determined by the condition $A = B = 0$. We can now compare the two tricritical points

- Canonical $K_{tr} \approx 1.0820$, $\beta_{tr}\Delta = 1.3995$,
- Microcanonical $K_{tr} \approx 1.0813$, $\beta_{tr}\Delta = 1.3998$.

Although these two points are quite close for this model, they do not coincide. For other models the distance between these two points is larger as for the XY model described below. The region of the phase diagram near the canonical (CTP) and microcanonical (MTP) tricritical points is pictorially represented in Fig. 7.10. This pattern of transitions is found in many different models [2].

7.4.3 A System with Continuous Variables: The XY Model

We will now deal with a model whose Hamiltonian depends on continuous variable, to show the efficiency of the large deviation method also in a case in which one cannot use direct counting of microstates. Let us consider the following Hamiltonian, which describes N XY-spins on a fully connected lattice

$$H_N^{XY} = \sum_{i=1}^{N} \frac{p_i^2}{2} - \frac{J}{2N}\left(\sum_i \mathbf{s}_i\right)^2 - \frac{K}{4N^3}\left[\left(\sum_i \mathbf{s}_i\right)^2\right]^2 \,, \tag{7.47}$$

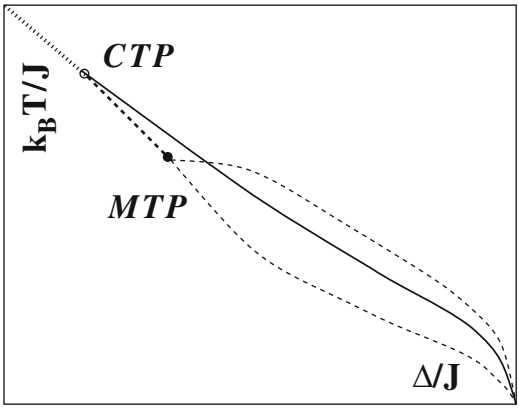

Fig. 7.10 Zoom of the phase diagram of the Blume-Capel model in the tricritical region. CTP and MTP are the canonical and microcanonical tricritical points, respectively. The *dotted line* above CTP is the canonical/microcanonical second-order line. The full line is the canonical first-order line. In the microcanonical ensemble, the second-order line continues below CTP (*dashed line*) and reaches MTP, from there it splits in two lines, a signature of temperature jumps. The two lines join together, and the canonical first-order line, at $T = 0$. In the region between the two microcanonical lines one finds only metastable and unstable states of the microcanonical ensemble (coexistence region)

where $\mathbf{s}_i = (\cos\theta_i, \sin\theta_i)$ is a spin vector with constant modulus and direction $\theta_i \in [-\pi, \pi]$. The local variable p_i is the conjugated momentum of the angle θ_i. The two coupling constants J and K are scaled differently: the first one by $1/N$ following Kac's prescription and the second one by $1/N^3$, in order to make the contribution of the last term of the same size as the others in the $N \to \infty$ limit. We will here sketch how to get microcanonical entropy using the large deviation approach. The three-step procedure begins with the identification of the local random variable: it is here natural to choose $\mathbf{X} = (\cos\theta, \sin\theta, p^2)$. We then define the X and Y directions of the magnetization

$$m_x = \frac{1}{N}\sum_i \cos\theta_i, \quad m_y = \frac{1}{N}\sum_i \sin\theta_i \ . \tag{7.48}$$

The modulus of the corresponding magnetization vector $\mathbf{m} = (m_x, m_y)$ is the order parameter of the paramagnetic-ferromagnetic phase transition taking place in this model. As global variables we identify the three-vector composed by the two magnetizations and by the averaged kinetic energy $E_K = \sum_i p_i^2/N$

$$\boldsymbol{\gamma} = (m_x, m_y, E_K) \ . \tag{7.49}$$

In terms of the global variables, energy density can be written as

$$h(\boldsymbol{\gamma}) = \frac{1}{2}(E_K - Jm^2 - \frac{K}{2}m^4) \ . \tag{7.50}$$

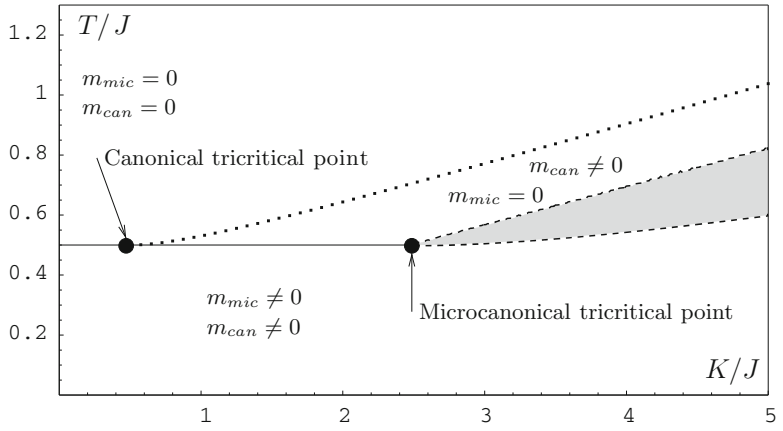

Fig. 7.11 Phase diagram of the XY model (7.47) for both the canonical and microcanonical ensemble. The canonical second order transition line (*solid line* at $T/J = 1/2$) becomes first order (*dotted line*, determined numerically) at the canonical tricritical point. The microcanonical second order transition line coincides with the canonical one below $K/J = 1/2$ but extends further to the right up to the microcanonical tricritical point at $K/J = 5/2$. At this latter point, the transition line bifurcates in two first order microcanonical lines, corresponding to a temperature jump. The region within these lines is forbidden in the microcanonical ensemble. In the figure we also report the magnetization in the different parts of the diagram

The second step of the procedure consists in the evaluation of the scaled cumulant generating function. Its approximate expression, neglecting subleading terms, is the following

$$\psi(\lambda) \simeq \ln \left[\frac{I_0(\sqrt{\lambda_x^2 + \lambda_y^2})}{\sqrt{-\lambda_K}} \right] , \tag{7.51}$$

where I_0 is the modified Bessel function of order zero and $\lambda_x, \lambda_y, \lambda_K$ are Lagrange multipliers. The corresponding rate function, which depends on the global variables, is evaluated by using formula (7.17). From the rate function, which is nothing but the opposite of entropy, one can again obtain microcanonical entropy by solving the corresponding variational problem. Similarly for canonical free energy.

Let us summarize the main features of this model. By varying the value of the ratio between the coupling constants $K \geq 0$ and $J > 0$ the system shows different behaviours. For $K = 0$ the model has a second order phase transition at $T/J = 1/2$, and the ensembles are equivalent in this limit. The second order transition line extends to $K > 0$ for both the canonical and the microcanonical ensemble, see Fig. 7.11. Above that line both the ensembles show the paramagnetic phase ($m = 0$), while below the line the system is ferromagnetic ($m \neq 0$). The canonical second order line remains at the temperature $T/J = 0.5$ along the segment with $K/J \in [0, 0.5)$, until it reaches the canonical tricritical point at $K/J = 0.5$, $T/J = 0.5$.

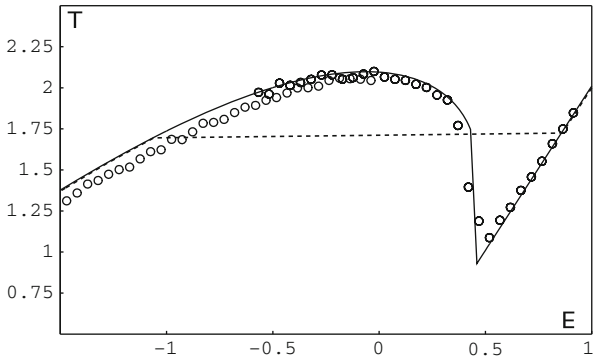

Fig. 7.12 Caloric curve for the XY model (7.47) with $K/J = 10$. The *solid line* is the theoretical prediction in the microcanonical ensemble. It shows a phase transition where temperature has a jump. A negative specific heat region is present, where temperature has a negative slope. The points correspond to the results of microcanonical simulations of a system composed by $N = 100$ spins. The transition is smoothed by finite size effects. The *dashed line* represents the first order phase transition in the canonical ensemble

For larger values of K/J the predictions of the two ensembles differ: in the canonical ensemble the transition becomes first order (see the upper dotted line in Fig. 7.11), while in the microcanonical ensemble the line remains of second order up to the microcanonical tricritical point, located at $K/J = 5/2, T/J = 0.5$. Between the canonical first order line and the microcanonical second order line the ensembles give different predictions for the order parameter. This is zero (paramagnetic phase) in the microcanonical ensemble and non zero (ferromagnetic phase) in the canonical one. Increasing the coupling, $K/J > 5/2$, the difference between the predictions of the two ensembles becomes even more peculiar. While in the canonical ensemble the transition remains first order, in the microcanonical ensemble temperature jumps appear. The coexistence of two temperatures at the transition energy is shown by the two dotted lines in Fig. 7.11. No stable microcanonical states exist between these two lines.

Figure 7.12 shows the caloric curve for $K/J = 10$: both a region of negative specific heat and a temperature jump are presents in the microcanonical ensemble.

Another important feature of this model appears in presence of a competition between ferromagnetic and anti-ferromagnetic terms. This competition can induce a violation of ergodicity. We set $J = -1$ and $K > 0$. Intuitively, we expect that for large values of $|K/J|$ the system is ferromagnetic, while for small values of this ratio the antiferromagnetic term dominates and the system becomes paramagnetic for all energies. For some intermediate values of the ratio, the system shows a phase transition between a paramagnetic and a ferromagnetic phase. In both these phases, due to the competition, there are gaps in the accessible value of magnetization at a fixed energy, and this breaks ergodicity. A convenient parameter plane where to discuss ergodicity breaking for this model is (ε, K). For some values of these parameters, as those in panel (a) of Fig. 7.13, entropy is well defined for all values

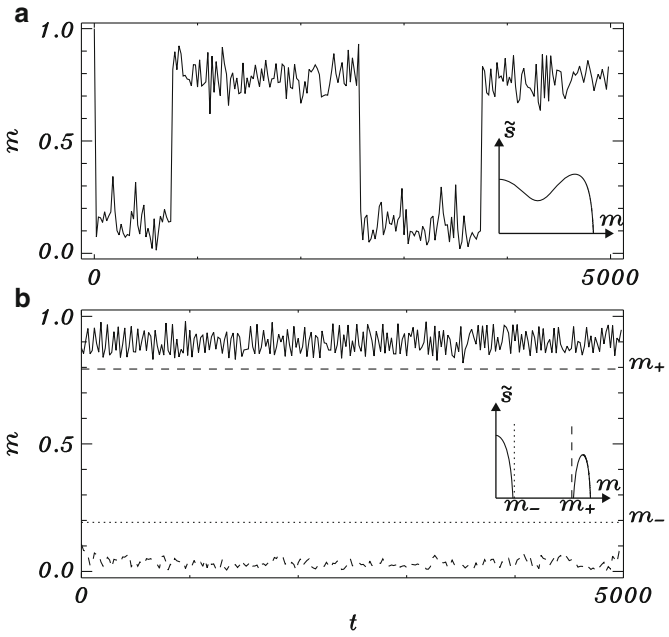

Fig. 7.13 Time evolution of the magnetization for the XY model (7.47) with $J = -1$. Panel (**a**) corresponds to the case $\varepsilon = 0.1$, $K = 8$, panel (**b**) to $\varepsilon = 0.0177$, $K = 3$. In panel (**a**) magnetization flips from a value close to zero to a non zero value, showing that the phase space is connected. The corresponding entropy vs. magnetization curve is shown in the *inset*: it has, as expected, a double hump. In panel (**b**) two different trajectories, started at initially different values of the magnetization, are shown. No flip is observed over a very long time stretch, proving that phase space is indeed disconnected. This is confirmed by the shape of the entropy in the *inset*, which shows that no accessible macrostate is present in the interval $[m_-, m_+]$

of magnetization in a given range. A microcanonical dynamics shows flips among the most probable values, corresponding to entropy maxima. For other values of (ε, K) entropy is not a surjective function of magnetization and it is well defined only for disconnected values of m, as shown in the inset of panel (b) in Fig. 7.13. Equilibrium states, which are maxima of the entropy, can exist in each range of accessible values of magnetization, but the system cannot visit both these ranges with a continuous dynamics because there are no intermediate states. This effect, shown in the main plot of panel (b) of Fig. 7.13, is a direct consequence of the violation of the additivity.

7.4.4 Negative Susceptibility: ϕ^4 Model

Ensemble inequivalence can also determine a negative magnetic susceptibility. As for specific heat, this quantity is positively defined in the canonical ensemble, while it can be negative in the microcanonical ensemble.

Let us recall the first law of thermodynamics for magnetic systems, $TdS = dE - hdM$. This expression can be a guide for the interpretation of the following formula

$$h(\varepsilon, m) = -\frac{\partial s}{\partial m} \Big/ \frac{\partial s}{\partial \varepsilon} = -\frac{1}{\beta(\varepsilon, m)} \frac{\partial s}{\partial m} , \tag{7.52}$$

which defines the external field h in terms of magnetization m and energy ε. The function $s(\varepsilon, m)$ is the entropy as a function of the global variables (7.22). Microcanonical entropy is given by the formula (7.23) and the stability of the resulting equilibrium states is a consequence of the requirement that the entropy is maximal. Then,

$$s_{mm} = \frac{\partial^2 s(\varepsilon, m)}{\partial m^2} < 0 . \tag{7.53}$$

We use here the convention that subscripts correspond to derivatives with respect to the corresponding variable. On the contrary the canonical ensemble has a different stability criterion

$$s_{mm} < 0, \quad s_{\varepsilon\varepsilon} < 0, \quad s_{\varepsilon}^2 - s_{mm} s_{\varepsilon\varepsilon} > 0, \tag{7.54}$$

because the variational problem is here defined as a function of two variables. These difference in stability determines different thermodynamic states in the two ensembles.

Susceptibility χ measures the variation of magnetization induced by an external field of size h. Its expression is the same in the two ensembles,

$$\chi = \frac{\partial m}{\partial h} = \beta \frac{s_{\varepsilon\varepsilon}}{s_{\varepsilon m}^2 - s_{\varepsilon\varepsilon} s_{mm}} . \tag{7.55}$$

It is clear from this formula that in the canonical ensemble susceptibility can be only positive, due to the stability conditions discussed above. On the other hand, in the microcanonical ensemble stability requires only that $s_{mm} < 0$. As a result, microcanonical susceptibility is negative whenever the entropy is non concave in m.

To illustrate the concept of negative susceptibility on a concrete example, let us introduce the ϕ^4 mean-field model, which is in the same universality class of the Curie-Weiss model of magnetism [12]

$$H_N^{\phi^4} = \sum_{i=1}^{N} \left(\frac{p_i^2}{2} - \frac{1}{4} q_i^2 + \frac{1}{4} q_i^4 \right) - \frac{1}{4N} \sum_{i=1}^{N} \sum_{j \neq i}^{N} q_i q_j , \tag{7.56}$$

where (q_i, p_i) are conjugate variables. The global variables are

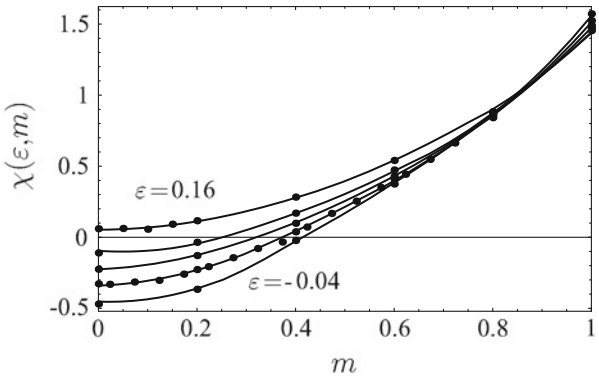

Fig. 7.14 Susceptibility vs. magnetization for different energies for the mean-field ϕ^4 model (7.56). The *full lines* are theoretical results, while the *points* are the results of numerical simulations

$$m = \frac{1}{N}\sum_i q_i\,, \quad z = \frac{1}{4N}\sum_i q_i^4 - q_i^2\,, \quad u = \sum_i p_i^2\,. \tag{7.57}$$

The quantity m corresponds to the magnetization of the system while z is related to the nature of on-site potential, here a double well. The variable u is nothing but twice the average kinetic energy. The scaled cumulant generating function reads

$$\psi(\lambda) = -\frac{\ln \lambda_u}{2} + \ln \int dq\, e^{-\lambda_m q - \lambda_z (q^4 - q^2)} + \texttt{const}\,. \tag{7.58}$$

Microcanonical entropy in terms of the global variables is given by

$$s(u, z, m) = \inf_{\lambda_u, \lambda_z, \lambda_m} \{\lambda_u u + \lambda_z z + \lambda_m m - \psi(\lambda)\}\,, \tag{7.59}$$

and in terms of energy and magnetization

$$s(\varepsilon, m) = \sup_{u,z} \left\{ s(u, z, m) | \varepsilon = \frac{u}{2} + z - \frac{m^2}{4} \right\}. \tag{7.60}$$

Although this function cannot be obtained in explicit form, because the full analytical treatment implies the solution of an implicit equation, it can be obtained numerically with any precision. Using then formula (7.55), one can derive an explicit expression of the susceptibility for the mean-field ϕ^4 model. Figure 7.14 shows a comparison of this formula with the numerical results obtained directly from Hamiltonian (7.56). Below a given energy value, corresponding to the ferromagnetic transition, a range of m appears where susceptibility becomes negative.

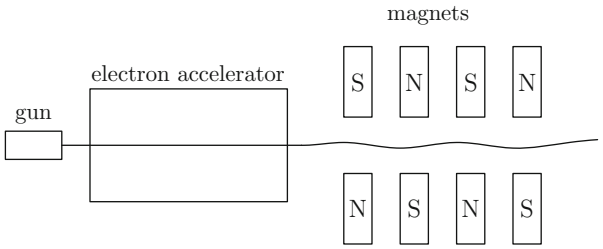

Fig. 7.15 Pictorial representation of a linear free electron laser

7.4.5 The Free Electron Laser

An experimental apparatus where long-range forces are at play is the free electron laser [13]. In the linear free electron laser, a relativistic electron beam propagates through a spatially periodic magnetic field, interacting with the co-propagating electromagnetic wave, see Fig. 7.15. Lasing occurs when the electrons bunch in a subluminar beat wave [14].

After scaling away the time dependence of the system and introducing appropriate variables, it is possible to catch the essence of the asymptotic state by studying the following equations of motion

$$\frac{d\theta_j}{dz} = p_j \ , \tag{7.61}$$

$$\frac{dp_j}{dz} = -\mathbf{A}e^{i\theta_j} - \mathbf{A}^* e^{-i\theta_j} \ , \tag{7.62}$$

$$\frac{d\mathbf{A}}{dz} = i\delta\mathbf{A} + \frac{1}{N}\sum_j e^{-i\theta_j} \ , \tag{7.63}$$

which derive from the Hamiltonian

$$H_N = \sum_{j=1}^{N} \frac{p_j^2}{2} - N\delta A^2 + 2A\sum_{j=1}^{N} \sin(\theta_j - \varphi). \tag{7.64}$$

The p_i's are related to the energies relative to the center of mass of the N electrons and the conjugated variables θ_i characterize their positions with respect to the co-propagating wave. The complex electromagnetic field variable, $\mathbf{A} = A\, e^{i\varphi}$, defines the amplitude and the phase of the dominating mode ($\mathbf{A}$ and $\mathbf{A}^\star$ are canonically conjugate variables). The parameter δ measures the average deviation from the resonance condition.

This model can be solved using the large deviations method. The global variables are $\gamma = (m, A, \sigma, u)$, where m is the magnetization as defined in (7.48), A is the modulus of the field, u twice the average kinetic energy and

$$\sigma = \frac{1}{N}\sum_i p_i + A^2 \,, \tag{7.65}$$

is the total momentum. This last quantity is conserved by the dynamics, as the energy of the system. In the others examples we have derived microcanonical entropy only as a function of energy, because we have supposed that energy is the only non zero conserved quantity of the dynamics. Here, we deal with a microcanonical entropy which depends on both energy and momentum, the two conserved quantities of the dynamics. The extensive part of the Hamiltonian reads

$$h(\gamma) = \frac{u}{2} - \delta A^2 + 2A\Big(m_y \cos(\varphi) - m_x \sin(\varphi)\Big) \,. \tag{7.66}$$

The second and third steps of the procedure lead us to solve the variational problem which defines microcanonical entropy as

$$s(\varepsilon,\sigma,\delta) = \sup_{A,m}\Big\{ \frac{1}{2}\ln\left[\left(\varepsilon - \frac{\sigma^2}{2}\right) + 4Am + 2(\delta-\sigma)A^2 - A^4\right] + s_{conf}(m)\Big\} \,, \tag{7.67}$$

where the configurational entropy $s_{con}(m)$ is given by

$$s_{conf}(m) = -\sup_{\lambda}\{\lambda m - \ln I_0(\lambda)\} \,, \tag{7.68}$$

and I_0 is the modified Bessel function of order zero. Numerical solutions of this variational problem show that the model displays a second order phase transition at the critical energy $\varepsilon_c = -1/(2\delta)$ for $\delta < 0$. Microcanonical and canonical ensemble are equivalent for this model.

7.5 The Min-Max Procedure and a Model with Short and Long-Range Interactions

There are cases in which it is not straightforward to identify the global variables and, therefore, the large deviations method cannot be applied. One can alternatively rely on a procedure that has been called *Min-Max* [15]. This method allows us to obtain microcanonical entropy from canonical free energy, providing a better understanding of how ensemble inequivalence occurs.

The starting point is to assume that there exist a function $G(\beta, x)$ such that the canonical partition function can be written as follows

$$Z(\beta, N) = \int_R dx \exp\{-NG(\beta, x)\} \,, \tag{7.69}$$

where x is a dummy variable. This is for instance the form that the partition function Z takes as a result of the Hubbard-Stratonovich transformation in a mean-field system. The free energy is then defined as $\phi(\beta) = \beta f(\beta) = \inf_x G(\beta, x)$. Let us introduce the Legendre-Fenchel transform of G by the relation

$$s(\varepsilon, x) = \inf_{\beta}\{\beta\varepsilon - G(\beta, x)\} . \tag{7.70}$$

We cannot identify this function as the large deviation function because it is always concave in x. Instead, $s(\varepsilon, m)$ can be non concave in m, as shown by the presence of negative susceptibility. The dummy variable x cannot be interpreted as a magnetization m. On the other hand, one can define a microcanonical entropy from the following variational problem

$$s(\varepsilon) = \sup_{x}\{s(\varepsilon, x)\} = \sup_{x}\inf_{\beta}\{\beta\varepsilon - G(\beta, x)\} . \tag{7.71}$$

Inverting *inf* with *sup* one gets the concave envelope of $s(\varepsilon)$

$$s^*(\varepsilon) = \inf_{\beta}\sup_{x}\{\beta\varepsilon - G(\beta, x)\} , \tag{7.72}$$

which defines a canonical entropy. The Legendre-Fenchel transform of both $s(\varepsilon)$ and $s^*(\varepsilon)$ returns the free energy $\phi(\beta)$. Indeed $\sup\inf \leq \inf\sup$ and the equality holds when the function G is differentiable everywhere.

The XY-model with both long and short-range interactions is an example where the identification of the global variable is not straightforward [4]. Its Hamiltonian is

$$H_N^{XYs} = \sum_i \frac{p_i^2}{2} + \frac{J}{2N}\sum_{i,j}[1 - \cos(\theta_i - \theta_j)] - K\sum_i \cos(\theta_{i+1} - \theta_i) . \tag{7.73}$$

In the long-range term of the Hamiltonian the sum is extended over all pairs of spins, while in the short-range term it is restricted to nearest-neighbour spins on a one-dimensional lattice. The microcanonical thermodynamics of this model can be obtained using the *Min-Max* procedure.

The first step of this method consists in writing the canonical partition function in the form of (7.69). Performing a Hubbard-Stratonovich transformation, the function Z become

$$Z \sim \int z dz \prod_i d\theta_i \exp\Big(-\frac{N\beta}{2}z^2 + \beta z\sum_i \cos\theta_i + \beta K\sum_i \cos(\theta_{i+1} - \theta_i)\Big) . \tag{7.74}$$

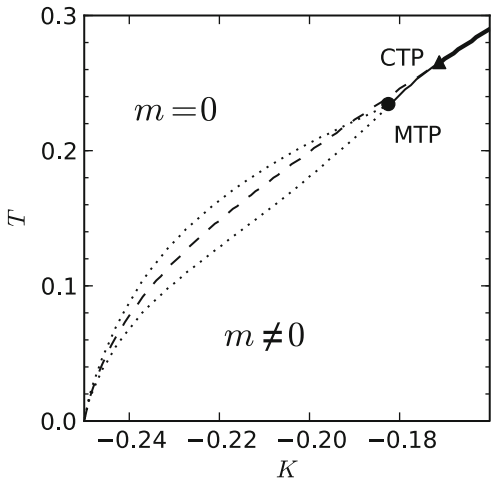

Fig. 7.16 Phase diagram of the XY model with long and short-range interactions. The *full line* is the second order line in both the canonical and microcanonical ensemble. The *triangular point* corresponds to the canonical tricritical point. Below it, the *dashed line* is the first order transition line in the canonical ensemble. The *circular point* is the microcanonical tricritical point and the two *dotted lines* correspond to temperature jumps

The integral over the θ_i can be performed using the transfer operator method. This operator is defined by the following integral eigenvalue equation

$$\mathscr{T}\psi(\theta) = \int d\alpha \exp\left(\beta\frac{z}{2}(\cos\theta + \cos\alpha) + \beta K\cos(\theta-\alpha)\right)\psi(\alpha)\,. \tag{7.75}$$

In the following we suppose that the transfer operator is diagonalizable. We denote by $\lambda(\beta z, \beta K)$ its largest eigenvalue and we suppose that its logarithm is well defined. The partition function is the N-times iterate of the transfer operator and is given by

$$Z = \int z dz \exp\left(-\frac{N\beta}{2}z^2 + N\ln\lambda(\beta z, \beta K)\right)\,. \tag{7.76}$$

Here, the partition function shows the required form in order to apply the *Min-Max* procedure. The function G does not depend explicitly on the number of particles, hence its $N \to \infty$ limit is straightforward. Finally, microcanonical entropy reads

$$s(\varepsilon) = \sup_z \inf_\beta \left[\beta u - \beta\frac{1+z^2}{2} + \ln\lambda(\beta z, \beta K) + \frac{1}{2}\ln\frac{2\pi}{\beta}\right]\,, \tag{7.77}$$

which can be obtained, as usual, by solving numerically the variational problem.

Figure 7.16 shows the phase diagram of this model. Both the canonical and microcanonical ensemble predict a second order transition line for large T and K, till the canonical tricritical point is reached. Below it, the two ensembles become inequivalent. The canonical ensemble shows a first order transition line, while the microcanonical one predicts a second order line until the microcanonical tricritical point is reached. As discussed for the previous XY model, in the microcanonical ensemble the model shows temperature jumps.

7.6 Conclusions and Perspectives

In this chapter we have introduced and illustrated for simple mean-field systems a method, based on large deviations techniques, which allows us to compute entropy in the microcanonical ensemble. This direct computation is necessary because for such systems, and in general for systems with long-range interactions, entropy cannot be obtained as a Legendre-Fenchel transform of free-energy. This feature is in turn determined by the fact that entropy can be non concave as a function of energy. This latter property is at the origin of ensemble inequivalence, whose physical consequence is the presence of negative specific heat and negative susceptibility in the microcanonical ensemble.

The tools discussed in this chapter could be extended to systems with interactions that decay with the distance, as defined in formula (7.2), although not much progress has been made along this direction. However, it has been recently claimed that equilibrium mean-field states are not always entropy maximizers for weakly decaying interactions [16], a remark that points out the difficulty of treating such systems.

Large deviations techniques have been also used to study systems driven out of equilibrium. In some cases, long-range correlations can be described by Hamiltonians with mean-field interactions, as shown in Ref. [17]. For such models, all the features of ensemble inequivalence discussed here show up in the context of non equilibrium.

References

1. T. Dauxois, S. Ruffo, L. Cugliandolo, *Long-Range Interacting Systems* (Oxford University Press, Oxford, 2010)
2. A. Campa, T. Dauxois, S. Ruffo, Statistical mechanics and dynamics of solvable models with long-range interactions. Phys. Rep. **480**, 57 (2009)
3. F. Borgonovi, G.L. Celardo, M. Maianti, E. Pedersoli, Broken ergodicity in classically chaotic spin systems. J. Stat. Phys. **116**, 1435 (2004)
4. D. Mukamel, S. Ruffo, N. Schreiber, Breaking of ergodicity and long relaxation times in systems with long-range interactions. Phys. Rev. Lett. **95**, 240604 (2005)
5. J. Sak, Recursion relations and fixed points for ferromagnets with long-range interactions. Phys. Rev. B **8**, 281 (1973)
6. F.J. Dyson, Existence of a phase-transition in a one-dimensional Ising ferromagnet. Commun. Math. Phys. **12**, 91 (1969)
7. D. Ruelle, Statistical mechanics of a one-dimensional lattice gas. Commun. Math. Phys. **9**, 267 (1968)
8. H. Touchette, The large deviation approach to statistical mechanics. Phys. Rep. **478**, 1 (2009)
9. J. Barré, D. Mukamel, S. Ruffo, Inequivalence of ensembles in a system with long-range interactions. Phys. Rev. Lett. **87**, 030601 (2001)
10. R.S. Ellis, The theory of large deviations: from Boltzmann's 1877 calculation to equilibrium macrostates in 2D turbulence. Physica D **133**, 106 (1999)

11. M. Blume, Theory of the first-order magnetic phase change in UO_2. Phys. Rev. **141**, 517 (1966); H.W. Capel, On the possibility of first-order phase transitions in Ising systems of triplet ions with zero-field splitting. Physica **32**, 966 (1966)
12. R. Desai, R. Zwanzig, Statistical mechanics of a nonlinear stochastic model. J. Stat. Phys. **19**, 1 (1978)
13. R. Bonifacio, F. Casagrande, G. Cerchioni, L. De Salvo Souza, P. Pierini, N. Piovella, Physics of the high-gain FEL and superradiance. Riv. Nuovo Cimento **13**, 1 (1990)
14. G. Robb, Collective instabilities in light-matter interactions, in *Long-Range Interacting Systems*, ed. by T. Dauxois, S. Ruffo, L. Cugliandolo (Oxford University Press, Oxford, 2010), p. 527
15. F. Leyvraz, S. Ruffo, Ensemble inequivalence in systems with long-range interactions. J. Phys. A: Math. Gen. **35**, 285 (2002)
16. T. Mori, Microcanonical analysis of exactness of the mean-field theory in long-range interacting systems. J. Stat. Phys. **147**, 1020 (2012)
17. O. Cohen, D. Mukamel, Ensemble inequivalence: Landau theory and the ABC model. J. Stat. Mech.: Theory Exp. P12017 (2012)

Chapter 8
Large Deviations of Brownian Motors

Alessandro Sarracino and Dario Villamaina

Abstract We review some recent results on the behavior of fluctuations in the framework of molecular motors. We present both theoretical and experimental studies, pointing out some interesting analogies shown by the large deviations of quantities such as work and entropy production in different systems. These common features reveal some underlying symmetry properties governing the nonequilibrium behavior of Brownian motors.

8.1 Introduction

One of the most amazing phenomenona peculiar to nonequilibrium dynamics is the possibility of rectifying unbiased fluctuations. First pointed out by Smoluchoswki in 1912 [1] as "molecular phenomenon opposing the conventional thermodynamics", this observation was later discussed and explained by Feynman in one of his Lectures on Physics [2]. According to the Curie principle, rectification of unbiased noise, also called "ratchet effect", requires to break the spatial symmetry and the time reversal symmetry associated with equilibrium (detailed balance) [3].

As a matter of fact, from microscopic transport in cells to muscle fibers, from micro-organisms to every human activity, the conversion of different forms of energy to mechanical work plays a central role for living beings. Thermodynamics provides precise and well established rules for energy conversion in macroscopic

A. Sarracino (✉)
Istituto dei Sistemi Complessi, Consiglio Nazionale delle Ricerche, and Dipartimento di Fisica, Università "Sapienza", Piazzale Aldo Moro 5, Rome, I-00185, Italy
e-mail: alessandro.sarracino@roma1.infn.it

D. Villamaina
Laboratoire de Physique Théorique et Modèles Statistiques, UMR 8626, Université Paris Sud 11 and CNRS, Bât. 100, Orsay F-91405, France
e-mail: villamaina@gmail.com

A. Vulpiani et al. (eds.), *Large Deviations in Physics*, Lecture Notes in Physics 885,
DOI 10.1007/978-3-642-54251-0_8,

systems but these rules become blurred at small scales when thermal fluctuations play a decisive role [4]. Extracting work under such conditions requires subtle strategies radically different from those effective in the macroscopic world. Within this framework, the theory of Brownian motors (or ratchet systems) deals with the rectification of thermal fluctuations [5–7], a goal which can only be achieved in the presence of dissipation.

Nature possesses an excellent command of these subtle processes, as shown in the cellular world: sophisticated mechanisms can realize the required conversion of chemical energy into mechanical one, allowing unidirectional motion, for instance of proteins and other macro-molecules [8]. In recent years, the study of nonequilibrium fluctuations in small systems has become directly accessible and has raised a great interest due to new experimental techniques, based on micromanipulation technology, allowing one to perform experiments on micro- and nanosystems [9]. In small systems, thermodynamic quantities such as internal energy, work and heat exchanged with the environment, are fluctuating variables, due to the presence of thermal noise, and therefore the study of the probability distributions of such quantities is central to characterize and understand the properties of these systems. For instance, the symmetry properties of these distributions can provide important information about the system response to external perturbations or under specific experimental protocols. In particular, work and heat exchanged with the environment in a given time interval are extensive quantities in time and it is important to characterize their large fluctuations, often playing a central role in the behavior of the system.

From a general theoretical point of view, the study of nonequilibrium fluctuations in the systems mentioned above can be carried on exploiting the mathematical formalism of the large deviations theory (LDT). In the field of nonequilibrium statistical mechanics, for instance, this theory underlies nonequilibrium fluctuating hydrodynamics discussed in [10] which also describes transformations in nonequilibrium stationary states (see contribution by Jona-Lasinio in the present volume). The LDT is also useful to characterize the symmetry relations for the probability density functions of entropy production, work and heat, observed in several nonequilibrium processes and generally referred to as Fluctuation Relations (FR) [11–16] (see contribution by Adamo et al. in the present volume). See also the review by Touchette [17], and reference therein, for the connection between nonequilibrium and LDT. Due to the mathematical difficulty, exact results for large deviations functions (LDF) in nonequilibrium systems are very few (see for instance [14, 18–22]), while general studies on the work and current fluctuations in nonequilibrium models can be found in [23–27].

In this chapter we review and discuss some recent analytical and experimental results concerning the study of large deviations of the nonequilibrium dynamics of Brownian motors, tracing some analogies which have not been noticed before.

According to the second principle of thermodynamics, a basic ingredient for the construction of a ratchet device is the presence of nonequilibrium conditions. These induce a continuous energy flux in the system, breaking the time-reversal symmetry of the dynamics. Nonequilibrium conditions can be realized in different ways,

and they are characterized by many interesting phenomena, such as violations of the equilibrium fluctuation-dissipation theorem [28–32], positive entropy production [14, 33, 34], velocity cross-correlations [35–37], and so on.

Since the presence of dissipation is a fundamental ingredient to induce nonequilibrium conditions, a natural framework where ratchet systems have been studied is the realm of granular media [38], where interactions do not conserve energy due to inelastic collisions. Moreover, fluctuations are always relevant in the framework of granular systems, because of the relatively small number of particles involved. Indeed, several experimental [39–42] and theoretical results [43–46] have been obtained for granular ratchets directly inspired by the Smoluchowski-Feynman model.

More in general, instances of nonequilibrium conditions, relevant to the following discussion, can be induced by the presence of

- Time-dependent temperature: noise amplitude is periodically varied in time, so that the system is prevented from reaching any equilibrium state;
- Temperature gradients: if the system is in contact with two (or more) *reservoirs* at different temperatures a stationary heat flux is present in the systems, flowing from the hot source to the cold one;
- Chemical reactions: conversion of chemical energy (derived for instance from the hydrolysis of ATP) into mechanical work;
- Dissipative (granular) interactions: a gas of macroscopic granular particles, which is characterized by dissipative interactions where a certain amount of energy is lost in each collision, can be kept in a nonequilibrium stationary state by the coupling with an energy source (e.g. a vibrating wall);
- Active particles: self-propelling agents (e.g. bacteria) are out of equilibrium due to the internal conversion of energy into motion;
- Aging: a ferromagnet or a glass-forming liquid quenched to below the critical temperature shows a nonequilibrium non-stationary dynamics;
- Dry friction: solid-on-solid friction (also known as Coulomb friction) is a source of dissipation which induces nonequilibrium behaviors.

In all the situations mentioned above a ratchet device can be realized if a spatial asymmetry is introduced in the system, as illustrated below for some specific examples. A spatial anisotropy can be introduced by the presence of asymmetric potentials, asymmetric shape of the probe, or some asymmetric interactions. In these systems, work against external loads can be extracted by unbiased fluctuations. The study of work fluctuations is therefore a central issue in order to assess some recent results in the context of general nonequilibrium processes and the LDT provides a useful tool to this aim.

In Sect. 8.2 we review, with some explicative examples, two main classes of Brownian motors: kinetic ratchets, which are macroscopic devices where the fluctuations are induced by collisions with gas particles, and molecular motors, which play a fundamental role in transport phenomena in biological systems. In particular, we report analytical results for the LDF of some solvable models within these classes. In Sect. 8.3 we review two experiments where work fluctuations and

large deviations are measured, in the framework of granular media. Finally, in Sect. 8.4 some conclusions are drawn.

8.2 Nonequilibrium Fluctuations and Brownian Motors

Before describing in detail several examples of Brownian motors, we present some general considerations on nonequilibrium stochastic models, relevant in this context. In particular, let us notice that exact results on large deviations in nonequilibrium dynamics are very scarce. In this direction, it is crucial to make some approximations to obtain the LDF and its dependence on the effective parameters of the models considered. In the present literature this kind of approximations can be divided in two different classes:

(a) In the first class, a time scale separation between an asymmetric intruder and the component of the rest of the system can be exploited. Then, the whole system can be reduced to a single particle problem: an intruder (slow degree of freedom) interacting with an external nonequilibrium environment (fast degrees of freedom) and with the additional presence of some effective asymmetric potential. From a mathematical point of view, this approximation corresponds to pass from a many variables master equation to some effective stochastic Langevin equation, where it is possible to calculate explicitly the entropy production and its associated LDF and fluctuation relation.
(b) In the second case, the key point is given by passing from a continuous to a discrete space. This approximation is frequently used to treat the so called flashing ratchet, often an effective model for molecular motors. This kind of models are characterized by a stochastic (equilibrium) dynamics on some proper potential, for instance $V_A(\mathbf{r})$, that can change to $V_B(\mathbf{r})$ according to some transition rates and viceversa. In this class of processes all the irreversibility is contained in the transition rates of the switching potential and the details of the dynamics are not relevant for the nonequilibrium properties of the whole system. It is natural, then to pass from a continuous description to a discrete one where the position of the particle is on a lattice, together with another discrete variable identifying the state of the external potential (A or B in our example). Within this approximation the dynamics is described by some master equation and it is often possible to explicitly calculate the LDF and evaluate the corresponding FR.

The case (a) is typical of the kinetic motors and it is illustrated in Sect. 8.2.1. On the contrary, the discrete approximation (b) is often used in the context of biological applications in order to obtain minimal models for molecular motors, as shown in Sect. 8.2.2. The purpose of this sections is not to review neither the FR nor the molecular motors (the interested reader can refer to the recent review [47]), but rather to mention the main theoretical issues of this research. As examples, two specific models in which it is possible to calculate the LDF will be considered.

8.2.1 Kinetic Ratchets

This class of ratchet models includes systems where the fluctuations of an asymmetric probe are induced by collisions with gas particles, as originally proposed by Smoluchowski and Feynman.

Many examples of kinetic ratchets have been studied in the literature, where nonequilibrium conditions are realized in one of the forms enumerated in the Introduction. For instance, a ratchet working in contact with two thermostats at different temperature has been studied in [48, 49]. A different realization has been introduced by Costantini et al. [44] and by Cleuren et al. [43], where a driven granular gas is the source of fluctuations. Moreover, other ratchets exploiting granular interactions have been studied in [45, 50, 51]. Recently, the dry (or Coulomb) friction has also been considered as unique source of dissipation which is able to drive a ratchet effect in models where the asymmetric probe is in contact with a thermal bath at equilibrium [52]. Kinetic ratchets have been also realized in numerical simulations exploiting aging properties of glasses [53] and in experiments with active matter (bacteria) [54]. In the large part of the cases cited above, the asymmetric intruder is largely bigger than the surrounding particles. This induces a time scale separation and it is possible to consider the gas particles weakly perturbed by the presence of the intruder. Within this strong assumption, the gas distribution is fixed and independent of the motion of the probe, and the dynamics can be described by a master equation for the probability density function $P(V,t)$ of the velocity V of the probe at time t

$$\frac{\partial P(V,t)}{\partial t} = \int dV' [W(V|V')P(V',t) - W(V'|V)P(V,t)] + \frac{\partial}{\partial V} F(V)P(V,t), \tag{8.1}$$

where $W(V'|V)$ are the transition rates for the jump from V to V' due to the collisions, which depend on the mass M of the probe and on the gas parameters (such as density, temperature T, mass of particles and coefficient of restitution for inelastic collisions), and $F(V)$ is an external force (generally dependent on the velocity, for instance due to the presence of friction affecting the motion of the probe). In order to calculate the large deviation function, it is necessary to specify the transition rates W, that depend on the geometry of the problem. Let us now focus on the specific case of the asymmetric piston in the presence of a constant force field ($F(V) \equiv F$). For this example we mainly refer to [51, 55].

We consider a piston of mass M undergoing collisions with bath particles of mass m and the velocity of the particles is distributed according to some distribution $\phi(v)$. The peculiarity of the piston is given by the fact that it has two different inelasticity coefficients (α_- and α_+) on its two different faces (see Fig. 8.1). Then the collision rules can be written in the following way:

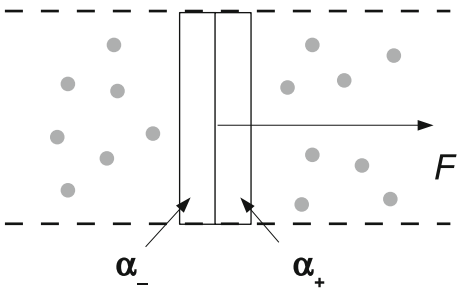

Fig. 8.1 Scheme of the asymmetric inelastic piston, where the two faces have different restitution coefficients and an external force is applied

$$V'_{\pm} = V + (1+\alpha_{\pm})\frac{\epsilon^2}{1+\epsilon^2}(v-V) \qquad v' = v - \frac{1+\alpha_{\pm}}{1+\epsilon^2}(v-V), \tag{8.2}$$

where the parameter $\epsilon = \frac{m}{M}$ has been introduced. The transition rates reflect this asymmetry and are given by

$$W(V|V') = \rho L \int dv (V'-v)\phi(v)\left[\Theta(V'-v)\delta(C_+) - \Theta(v-V')\delta(C_-)\right] \tag{8.3}$$

where

$$C_{\pm} = V - V' + \frac{(1+\alpha_{\pm})\epsilon^2}{1+\epsilon^2}(V'-v). \tag{8.4}$$

The large deviations properties, for instance of the work done by the force F, cannot be deduced in this general case and some approximation is necessary. Then, by assuming a large difference of masses (i.e. $\epsilon \ll 1$) the master equation (8.1) can be simplified with the standard Fokker-Planck expansion [56], yielding the statistical properties of the process described by the stochastic equation:

$$M\frac{dV}{dt} = -a(V) + F + \sqrt{b(V)}\xi(t), \tag{8.5}$$

where $\xi(t)$ is an uncorrelated white noise with unitary variance and

$$a(V) = \rho \int_0^{\infty} dv v^2 \left[(1+\alpha_-)\phi(V-v) - (1+\alpha_+)\phi(V+v)\right] \tag{8.6}$$

$$b(V) = \rho \int_0^{\infty} dv v^3 \left[(1+\alpha_-)^2\phi(V-v) + (1+\alpha_+)^2\phi(V+v)\right]. \tag{8.7}$$

Considering the case $F = 0$, the steady state velocity V_l is given by the solution of $a(V) = 0$. In the symmetric case, when $\alpha_+ = \alpha_-$, it is evident from Eq. (8.6) that $V_l = 0$, but in general $V_l \neq 0$. Consistently with the time scale separation, an expansion for small fluctuations around the average velocity can be considered, yielding

$$M\frac{dV}{dt} = -\Gamma(V - V_l) + F + \sqrt{2\Gamma T_g}\xi(t). \tag{8.8}$$

In this limit it is evident that the position $\Delta X_\tau = X(t+\tau) - X(t)$ is a Gaussian variable. If we consider the work done in the time interval $[t, t+\tau]$ than it is given by

$$W = F\Delta_\tau X, \tag{8.9}$$

the work W is a Gaussian variable

$$P(W = w) \propto \exp\left(-\frac{(w - \langle w\rangle)^2}{2\sigma_w^2}\right), \tag{8.10}$$

where, for large times (i.e. for $t \gg \frac{M}{\Gamma}$)

$$\langle w\rangle = F\left(V_l + \frac{F}{\Gamma}\right)t \qquad \sigma_w^2 \simeq \frac{2F^2T_g}{\Gamma}t. \tag{8.11}$$

Thanks to the Gaussianity of the process, from Eq. (8.11) it is easy to prove the following FR

$$\ln\left(\frac{P(W_\tau = w)}{P(W_\tau = -w)}\right) = \frac{2\langle w\rangle w}{\sigma_w^2} \simeq \left(\frac{\Gamma V_l + F}{F}\right)\frac{w}{T_g}. \tag{8.12}$$

In conclusion, Eq. (8.12) quantifies the probability of exploiting nonequilibrium fluctuations in order to perform work on the system. Let us note that, in the symmetric limit, when $V_l \to 0$, and the slope of the FR approaches the inverse granular temperature of the surrounding gas, but this is true only in this specific case. Some experimental works defined a sort of "effective temperature" from the measure of the entropy production [57] on a vibrating granular gas. Actually it has been shown that this interpretation is not convincing for several reasons [58]. Indeed, a generalization of Eq. (8.12) to more realistic cases meets different problems. Apart from the limit case (8.12), the Gaussian approximation fails and non-symmetric fluctuations are present as soon as the mass of the piston is comparable with that one of the gas particles [51]. Moreover, at higher densities, velocity correlations and memory effects play a crucial role [34] and a generalization of Eq. (8.12) for molecular motors in these cases has not yet been investigated.

8.2.2 Molecular Motors

Molecular motors are small biological devices (size from few to some hundreds nanometers) that can convert chemical energy into mechanical work. Using sophisticated intramolecular amplification mechanisms [8], these motors transport a wide

variety of cargo, power cell locomotion, drive cell division and, when combined in large ensembles, allow organisms to move. An example is kinesin, which is a molecule that uses the energy of bond hydrolysis (ATP) to perform replication, transcription and repair of DNA and the translation of RNA. Other examples are myosins, which move on actin filaments, and dyneins [59].

An important issue to address is to understand the nonequilibrium thermodynamics of these systems. Because of their nanometric size and their incessant exchanges with the surrounding environment, large fluctuations are present and their behavior is thus stochastic as observed experimentally. Accordingly, their motion is unidirectional only on average and random steps in the direction opposite to their mean motion can occur. The study of the deviations from the average motion can be important to characterize the behavior of these systems.

Avoiding biological complexity and focusing on the physical mechanisms, these systems can be modeled as simple stochastic processes [60]. In particular, the underlying chemical processes can be described by Langevin equations in the presence of fluctuating forces with non-Gaussian correlation functions and time-dependent potentials or introducing other degrees of freedom, such as transitions between different states. Being more specific, one can start from the motion of a Brownian particle in an effective potential

$$\gamma \dot{x} = F - \frac{\partial U^{eff}(x,t)}{\partial x} + \eta(t), \tag{8.13}$$

where

$$U^{eff}(x,t) = \begin{cases} U_1(x) & r(t) = 0 \\ U_2(x) & r(t) = 1 \end{cases}, \tag{8.14}$$

where $r(t)$ is a stochastic process defined below.

Usually, in this kind of ratchet (called flashing ratchet in literature) the potentials $U_i(x)$ have some asymmetric shape (a typical case is depicted in Fig. 8.2). All the time dependence of the process is ruled by $r(t)$, a stochastic process that can take only the values between 0 and 1 and its transition rates can be written as:

$$\frac{\omega_2(x)}{\omega_1(x)} = e^{\beta(U_2(x)-U_1(x))+\Delta\mu(x)}. \tag{8.15}$$

By summing up, there are two different sources of nonequilibrium conditions in this model. First, there is the external force F and, secondly, there is the factor $\Delta\mu(x)$ that violates detailed balance for the hopping process $r(t)$. Both of these elements can produce a net drift of the particle, since the detailed balance is violated (time symmetry breaking) and the potentials $U_i(x)$ are asymmetric (space symmetry breaking). These kinds of models have been studied for a long time (see [7] for a review) and have been proposed as candidates for modeling molecular motors. In particular, $\Delta\mu$ mimics the chemical activity of the motor, for instance the ATP consumption.

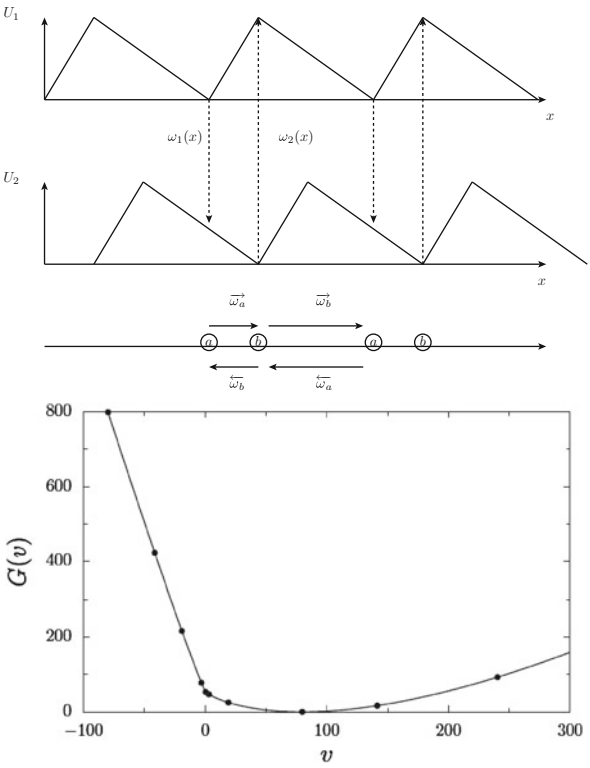

Fig. 8.2 *Top*: Scheme of the flashing ratchet and reduction to the discrete variables (The picture is taken from [61]). *Bottom*: Large deviations function $G(v)$ for some specific values of the parameters (From [62])

A possible way to tackle the problem from an analytical point of view is to construct a proper discrete version of the model, as recently proposed by Lacoste et al. [62]. Their main approximation consists in considering only transitions occurring in the minima of the potentials and essentially a vanishing occupation time for all the other possible positions. In this way, the continuous process can be recast in a discrete random walk, the relevant parameters being n (the distance of the walker) and y (the number of changes of the potential, that is supposed to be related to the ATP consumption). The effective evolution equation for the probability $P_n(y,t)$ that the motor, at time t, has consumed y units of ATP and is at position n is given by:

$$\partial_t P_n(y,t) = -\left(\overleftarrow{\omega}_n + \overrightarrow{\omega}_n\right) P_n(y,t) + \sum_{l=-1,0,1} \left[\overleftarrow{\omega}^l_{n+1} P_{n+1}(y-l,t) + \overrightarrow{\omega}^l_{n-1} P_{n-1}(y-l,t)\right], \tag{8.16}$$

where $\overleftarrow{\omega}_n = \sum_l \overleftarrow{\omega}^l_n$ and $\overrightarrow{\omega}_n = \sum_l \overrightarrow{\omega}^l_n$, and $\overleftarrow{\omega}^l_n$ and $\overrightarrow{\omega}^l_n$ are the transition rates for the motor to jump from site n to $n-1$ or to $n+1$, respectively, with $l(=-1,0,1)$ ATP molecules consumed. These transition rates are properly related

to their continuous version described in Eq. (8.15), see Fig. 8.2 (top) for a visual explanation. We omit here their complete expression, and refer the interested reader to [63] for details. Within this model it is possible to easily calculate the average velocity:

$$\bar{v} = \lim_{t\to\infty} \frac{\langle n(t)\rangle}{t} = 2\frac{\overrightarrow{\omega}_a \overrightarrow{\omega}_b - \overleftarrow{\omega}_a \overleftarrow{\omega}_b}{\overrightarrow{\omega}_a + \overrightarrow{\omega}_b + \overleftarrow{\omega}_a + \overleftarrow{\omega}_b}. \tag{8.17}$$

As evident from Eq. (8.17), $\bar{v}$ is zero if detailed balance is satisfied, namely when one has $\overrightarrow{\omega}_a \overrightarrow{\omega}_b = \overleftarrow{\omega}_a \overleftarrow{\omega}_b$. By using Eq. (8.17) and the corresponding average consumption rate $\bar{r}$, the authors has been able to connect this model to some experiments on kinesin [63].

Going beyond the average velocity, it is possible to study large fluctuations. Then, it is possible to show that [62] the probability for a particle to have a velocity v, after it has gone a distance n from the origin in a time t, is given by

$$P\left(\frac{n}{t} = v\right) \sim e^{-G(v)t}. \tag{8.18}$$

This large deviations property follows directly from the property of the master equation (8.16). In order to see that, one has to consider the probability $P_i(n,t)$ that the motor is on the site $i = a$ or b and at a distance n, which is obtained by integrating over y in the quantity $P_n(y,t)$. The LDF $G(v)$ is the Legendre transform of the largest eigenvalue of the evolution matrix for the process $F_i(\lambda,t) = \sum_n e^{-\lambda n} P_i(n,t)$.

Note that the function $G(v)$ has a strong asymmetric shape as shown in Fig. 8.2 (for its analytical expression, see [62]). This is a quite common feature in ratchet models, and, noticeably, it has been also recovered in experiments on other kinds of motors, as described in Sect. 8.3.1. Associated with this large deviations principle it is possible to derive the corresponding FR:

$$\lim_{t\to\infty} \frac{1}{t} \ln\left(\frac{P(\frac{n}{t} = v)}{P(\frac{n}{t} = -v)}\right) = G(-v) - G(v) = -\Psi v, \tag{8.19}$$

where

$$\Psi \equiv \frac{1}{2} \ln\left(\frac{\overrightarrow{\omega}_a \overrightarrow{\omega}_b}{\overleftarrow{\omega}_a \overleftarrow{\omega}_b}\right). \tag{8.20}$$

As already shown for the kinetic ratchets, Eq. (8.19) puts a strong constraint on the positive or negative fluctuations of velocity. Remarkably, the coefficient ψ is a measure of the irreversibility of the cycle $a \rightleftarrows b$ and it is a particular example of a more general related quantity called affinity [64]. Such a relation has been pointed out also in other models of molecular motors [65]. An experimental test of this single motor theory is still undone, and the FR could help to have access to the

microscopic parameters (ψ) by means of a measure of the asymmetry in the velocity. Moreover, in terms of perspectives, both from a theoretical and experimental point of view, the study of many interacting molecular motors is still a challenging and open issue [66, 67].

8.3 Experiments in Granular Systems

An ideal framework where the role of nonequilibrium fluctuations can be studied is the realm of vibrated granular systems [38]: the dissipation due to inelastic collisions is balanced by some energy injection mechanism, so that a nonequilibrium stationary state with energy fluxes is attained. For a general review about the experimental study of nonequilibrium fluctuations in this context we refer the reader to [68].

The context of granular systems paves the way to the realization of experiments aimed at validating some important general relations derived for nonequilibrium systems, mentioned in Sect. 8.1. In particular, in granular systems, where noise and time-scale separation are often not fully under control and where usually the accessible quantities are somehow coarse-grained, the experimental study of FR is very useful to assess such results in a more general framework [69–71].

Here we focus on the study of systems where the presence of dissipation coupled with some spatial anisotropy induces a macroscopic ratchet effect, namely a finite average drift of a probe which is subjected to collisions with granular particles. In these cases, the more natural, and directly accessible, fluctuating quantity to study is the displacement of the probe over a given time interval. This quantity can be related to the work performed by the ratchet and, therefore, the study of its large deviations is important to characterize general nonequilibrium behaviors in these systems.

The first experimental realization of a ratchet device in the context of granular media was obtained by Eshuis et al. [40]. In this experiment a rotor consisting of four vanes was put in contact with a vibrofluidized granular gas. The spatial symmetry breaking was obtained by applying a soft coating to one side of each vane. Above a certain threshold of the shaking amplitude of the granular medium, a net unidirectional rotation of the probe was observed.

Next, Joubaud et al. [69] studied a similar experiment, measuring the injected work and the entropy production in the system. Generally, the identification of the observable quantities directly related to the entropy production is not easy, due to the difficulty of assessing and measuring the relevant degrees of freedom in the system. However, as discussed more in detail in the following examples, in some limits such an identification is possible. In particular, this is the case when an underlying Langevin description is shown to be valid for the system: then, the amount of injected work is proportional to the displacement of the probe in a time interval. Exploiting this observation, the authors of [69] verified the FR for this granular ratchet.

Another source of dissipation has been shown to play an important role in the dynamics of kinetic ratchets: the Coulomb (or dry) friction [50, 52, 72, 73]. Its main effect is the introduction of two dynamical regimes: one is dominated by the effect of collisions, while the other by the dissipation due to friction. More surprisingly, it has also been shown that the Coulomb friction itself can be sufficient to drive a motor effect, even if the probe is in contact with a molecular fluid at equilibrium [52, 73].

In the following we report two experimental results concerning the study of the fluctuations and large deviations of nonequilibrium currents in the framework of granular systems. The first experiment studies the motion of a self-propelled polar particle in contact with a dense granular medium, while the second analyzes the dynamics of an asymmetric rotor interacting with a dilute granular gas.

8.3.1 Velocity Fluctuations of a Self-Propelled Polar Particle

In the experiment reported in [74], Kumar et al. studied the symmetry properties of the LDF of the velocity of a self-propelled polar particle. The authors considered the motion of a geometrically polar tracer in a dense (packing fraction $\phi \approx 0.8$) monolayer of granular particles on a vertically agitated horizontal surface, see Fig. 8.3. Due to its geometrical asymmetry, the behavior of the polar particle shows a noisy self-propelled motion, with a finite average drift.

The quantity of interest in this system is the fluctuating velocity defined as

$$W_\tau(t) = (1/\tau) \int_t^{t+\tau} \left[V(t') / \langle V \rangle \right] dt' \tag{8.21}$$

where $V(t) \equiv \mathbf{v}(t) \cdot \hat{\mathbf{n}}(t)$, with $\mathbf{v}(t)$ and $\hat{\mathbf{n}}(t)$ the particle velocity and orientation vector in the plane, respectively, and $\langle \ldots \rangle$ denotes an average over the time t. Introducing the probability density function $P(W_\tau)$ the LDF is defined as $F(W_\tau) \equiv \lim_{\tau \to \infty} (-1/\tau) \ln P(W_\tau)$. As shown in Fig. 8.4, the LDF measured in the experiment presents a peculiar shape, far from a Gaussian, and, interestingly, satisfies a symmetry relation similar to the FR, $F(W_\tau) - F(-W_\tau) \propto W_\tau$. Data collapse of the empirical LDF is found for $\tau > 0.12$ s. Figure 8.4 (top panel) shows $F(W_\tau)$ for $\tau = 0.20$, 0.30 and 0.40 s, covering almost the entire range of W_τ. Notice that $F(W_\tau)$ shows a sharp kink at zero, remaining almost flat between 0 and 1. Figure 8.4 (bottom panel) also shows the LDF obtained for lower shaking amplitude: the distribution is again non-Gaussian and a kink at zero is observed. The asymmetric shape of the LDF reflects the unidirectional self-propelled motion of the polar particle.

In order to understand the shape observed, in [74] it is also discussed a comparison to the LDF of the entropy production rate for a colloidal particle driven by a constant force through a periodic potential obtained theoretically in [22], where the same qualitative behavior, namely the presence of a kink in the LDF, is found. A similar behavior of the entropy production has been also observed numerically

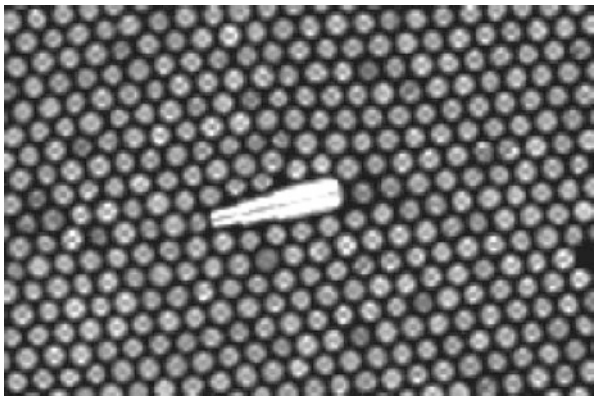

Fig. 8.3 Polar tracer in a dense monolayer of granular particles (From Kumar et al. [74])

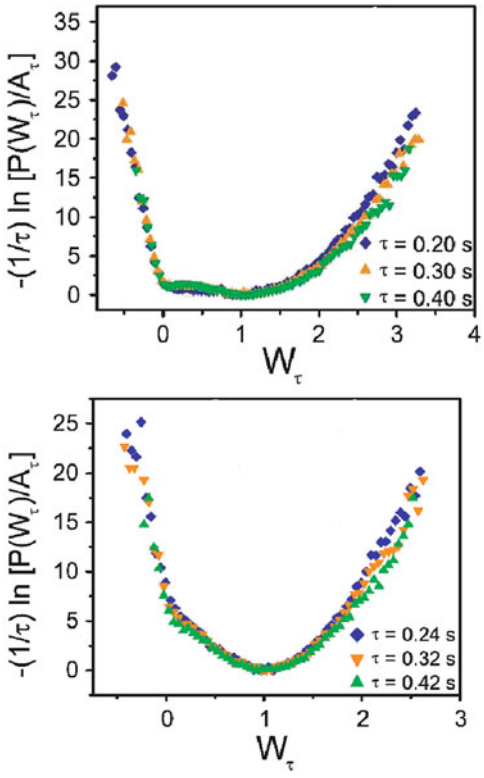

Fig. 8.4 Large deviations functions of the velocity fluctuations, $(-1/\tau)\ln P(W_\tau)/A_\tau$ where A_τ is the maximum value of $P(W_\tau)$, measured in the experiments [74], for high (*top*) and low (*bottom*) shaking accelerations (From Kumar et al. [74])

in the stationary state of a one-dimensional kinetic model where a probe particle is driven by an external field and collides with a bath of particles at a certain temperature [75]. However, as noticed in [74], it has to be pointed out that the LDF measured in the experiment is the LDF for the velocity, not for the entropy production. The results of the experiment can be compared to the predictions of [22] only if the motion of the polar particle can be approximated as propelled by a

constant force. This is not clear in the experiment, where the propulsive force could have significant time dependence. Furthermore, we would also stress the close similarity with the shape of the LDF for the model of molecular motor described in Sect. 8.2.2, see Fig. 8.2 (bottom). In that case, the similarity is more clear because the LDF for the same quantity, namely the velocity, is computed.

This experiment shows that the LDF of the velocity fluctuations, in some cases, share the same symmetry relations as the entropy production. This could indicate that the validity of the FR, proven under well defined hypotheses, may also hold in more general situations. Therefore, the study of the extension of such relations to wider context is very important in order to assess their real meaning. Such a point is also illustrated in the experiment described in the following section.

8.3.2 Asymmetric Rotor in a Granular Gas

In the experiment reported in [76] a new setup for a frictional granular kinetic ratchet is considered in order to get closer to conditions where kinetic theory can be applied. In particular, the study focuses on the nonequilibrium fluctuations of the angle spanned in a time interval by an asymmetric rotator in contact with a granular gas. This quantity is related to the work done by the ratchet against frictional forces present in the system.

The two main components of the setup are the granular gas and the rotator, as sketched in Fig. 8.5. The granular gas is made of small spheres contained in a cylinder which is vertically shaken at fixed frequency with maximum rescaled acceleration Γ. Suspended into the gas, a rotator of mass M turns around a vertical axis, see Fig. 8.5 (right). The spatial asymmetry is introduced by applying insulating tape to the rotator, partially covering its two largest surfaces.

The central quantity to study is the angular velocity ω of the rotator which can be described by the following equation of motion:

$$\dot{\omega}(t) = -\Delta\sigma[\omega(t)] - \gamma_a\omega(t) + \eta_{coll}(t) \tag{8.22}$$

where $\Delta = F_{frict}/I$ is the frictional force rescaled by inertia, γ_a is some viscous damping rate related to air, and $\eta_{coll}(t)$ is the random force due to collisions with the granular gas particles. It is useful to introduce the "equipartition" angular velocity $\omega_0 = v_0\epsilon/R_I$ where $\epsilon = \sqrt{\frac{m}{M}}$ and $R_I = \sqrt{I/M}$. The single particle probability density function (PDF) $p(\omega, t)$ for the angular velocity of the rotator is fully described, under the assumption of diluteness which guarantees Molecular Chaos, by a Boltzmann equation [45, 50, 52].

As mentioned above, the presence of Coulomb friction in the support bearing the rotator introduces two time scales in the system. An estimate of the ratio between the stopping time due to dissipation (dominated by dry friction) $\tau_\Delta \sim \frac{\omega_0}{\Delta}$ and the collisional time $\tau_c \sim \frac{1}{n\Sigma v_0}$, where Σ is the surface of the sides and n is the gas

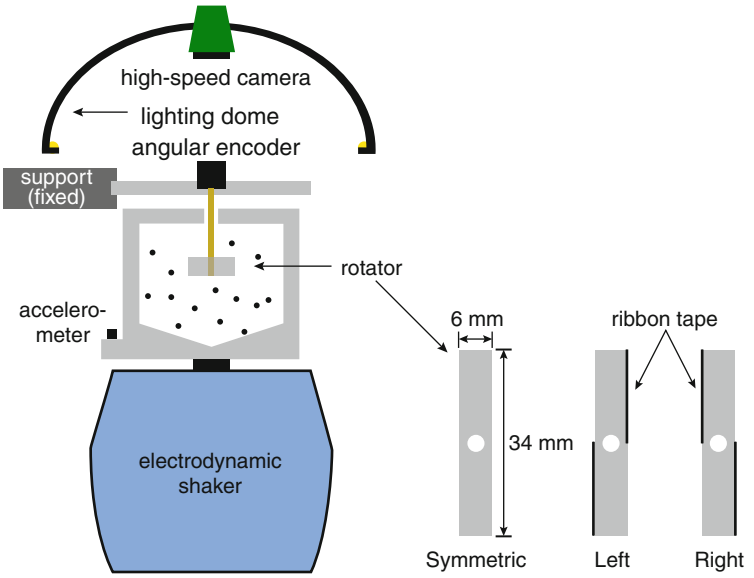

Fig. 8.5 The experimental setup of the experiment of Gnoli et al. [76]

density, is given by the parameter $\beta^{-1} = \frac{\epsilon n \Sigma v_0^2}{\sqrt{2}\pi R_I \Delta} \approx \frac{\tau_\Delta}{\tau_c}$. This parameter controls the transition from a regime (at $\beta^{-1} \ll 1$) with fast stopping due to dissipation, called RC (rare collisions), and a regime (at $\beta^{-1} \gg 1$) with the rotator always in motion, continuously perturbed by collisions, called FC (frequent collisions). A steady drift, signaling the presence of a Brownian motor effect, is observed both in the friction dominated regime ($\beta^{-1} < 1$) and in the collisions dominated regime ($\beta^{-1} > 1$).

A further simplification of the model can be obtained when the mass of the rotator is large with respect to the mass of the granular gas particles, so that the collisional noise in Eq. (8.22) can be cast into the sum of a white noise $\eta(t)$ plus a viscous drag and a systematic force inducing the motor effect:

$$\eta_{coll}(t) \to \eta(t) - \gamma_g \omega(t) + \tau_{motor}, \tag{8.23}$$

with $\langle \eta \rangle = 0$ and $\langle \eta(t)\eta(t') \rangle = \Gamma_g \delta(t - t')$. The expression for γ_g, τ_{motor} and Γ_g are reported in [50]. Notice that the collisional noise η_{coll} is in general not white, and, even more importantly, *it is not independent* of the instantaneous velocity ω. In the FC limit, $\beta^{-1} \gg 1$, the Coulomb friction term and the external viscosity may be neglected, i.e. $\gamma_a \omega + \Delta\sigma(\omega) \ll \gamma_g \omega$, so that Eq. (8.22) is cast into the much simpler form

$$\dot{\omega}(t) = -\gamma_g \omega(t) + \eta(t) + \tau_{motor}. \tag{8.24}$$

From the above equation one may estimate the average velocity of the Brownian motor to be $\langle\omega\rangle = \tau_{motor}/\gamma_g$ [50,72]. Equation (8.24) also allows one to characterize the fluctuations $P(\Delta\theta)$ of the spanned angle in a time interval of length Δt, $\Delta\theta = \theta(t + \Delta t) - \theta(t)$ for any t in the steady state. For the particularly simple linear Langevin case it can be shown, see Sect. 8.2.1, that such fluctuations obey, for large Δt, the following FR:

$$\phi(\Delta\theta) = \log\left[\frac{P(\Delta\theta)}{P(-\Delta\theta)}\right] \approx s\Delta\theta, \tag{8.25}$$

with

$$s = \frac{\gamma_g \tau_{motor}}{\Gamma_g} \approx \frac{\tau_{motor}}{\langle\omega^2\rangle}. \tag{8.26}$$

We mention that such an FR is closely related to the FR for the entropy produced in the time Δt, which in this system is approximated by the work done by the "Brownian motor force" $W \approx \tau_{motor}\Delta\theta$ divided by the "temperature" $\langle\omega^2\rangle$ [33].

In the RC regime, on the other hand, one may assume that the dynamics of the probe is a sequence of independent kicks received at zero velocity, resulting in an explicit formula for the adimensional average angular velocity [50]. In this regime the behavior of $\phi(\Delta\theta)$ is unknown in principle. A FR for the entropy production certainly exists, but there is not a simple relation between $\Delta\theta$ and the entropy produced in a given time interval.

Once stated the possibility of extracting useful work from nonequilibrium fluctuations, it is important to characterize the statistical behavior of the system, by studying the large deviations for the spanned angle in a time interval. Indeed, the PDF of such a quantity contains important information on the underlying symmetry relations for the ratchet currents. The empirical LDF $F(\Delta\theta) = -\log[P(\Delta\theta)]/\Delta t$ of the PDF $P(\Delta\theta)$ for different choices of the time window Δt, are reported in Fig. 8.6 for two experiments with a small and a large value of β^{-1}. In both experiments deviations from the parabolic fit, i.e. slightly non-Gaussian tails, can be appreciated, signaling the large deviations of the PDF of $\Delta\theta$. In particular, the asymmetric shape of the LDF reflects the unidirectional motion of the ratchet effect. In order to point out the symmetry properties of the PDF of $\Delta\theta$, in Fig. 8.7 the asymmetry function $\phi(\Delta\theta) = \log\left[\frac{P(\Delta\theta)}{P(-\Delta\theta)}\right]$ is shown for the same two experiments. At values of Δt large enough, but smaller than those necessary to achieve a stable large deviation rate, the asymmetry functions already display a linear behavior $\sim s\Delta\theta$ with an almost constant slope s.

This study unveils some important information: (1) for large values of β^{-1} the system is described by Eq. (8.24), which is confirmed by the good agreement of the slope with Eq. (8.26); (2) at moderate and small values of β^{-1} the "simplified" Langevin description of Eq. (8.24) is not expected to hold, and indeed discrepancy is found between experimental slopes of $\phi(\Delta\theta)$ and those predicted by Eq. (8.26); nevertheless (3) such experimental values of the slope appear to depend only *weakly*

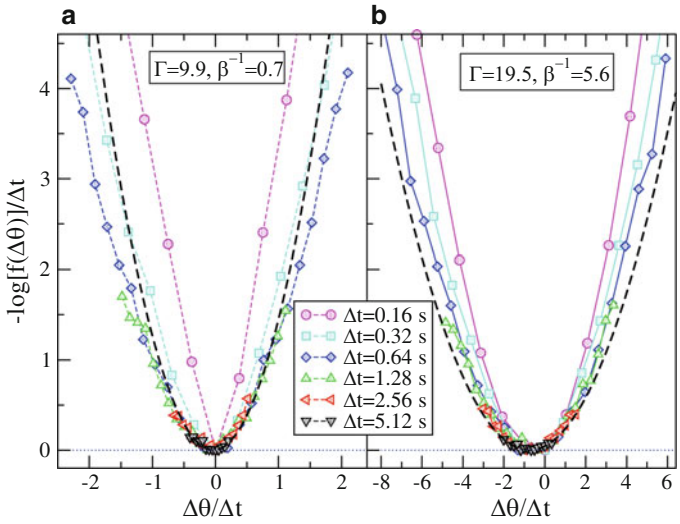

Fig. 8.6 Empirical LDF for the fluctuations of $\Delta\theta$ for two experiments in the RC regime (*left*) and in the FC regime (*right*), at several values of Δt (From Gnoli et al. [76])

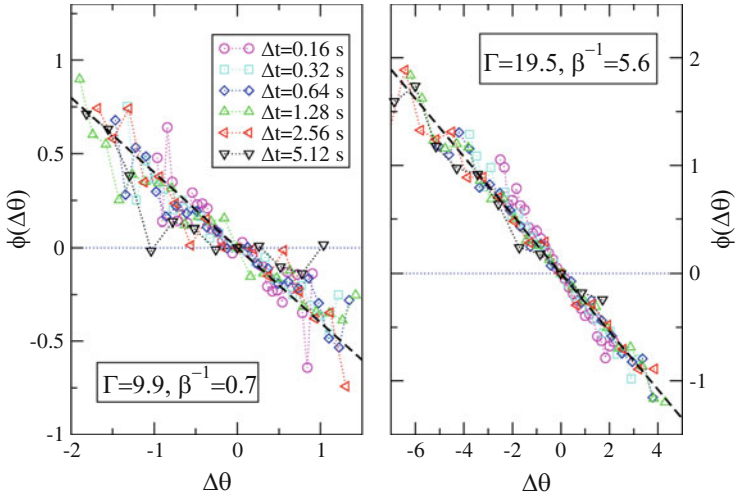

Fig. 8.7 Asymmetry function $\phi(\Delta\theta)$ for the PDFs of $\Delta\theta$ for two experiments in the RC regime (*left*) and in the FC regime (*right*), at several values of Δt (From Gnoli et al. [76])

upon β^{-1} [76], so that they do not differ too much from the values at large β^{-1}. This empirical observation cannot be easily explained: indeed, at small values of β^{-1}, the discontinuous nature of noise due to collisions prevents one from describing the average drift as the effect of a continuous torque (as it is τ_{motor} in the FC limit). Therefore it is not clear at all how to define a work or an injected power and,

consequently, a candidate for the entropy production. A theory for the fluctuations of $\Delta\theta$ in such a situation has to be developed and the discovery of the validity of the FR with a slope similar to a very different regime is largely unanticipated. We mention that in the Gaussian approximation, i.e. assuming a parabolic form for the LDF of $\Delta\theta$ or equivalently

$$P(\Delta\theta) \sim \exp\left[-\frac{(\Delta\theta - \langle\omega\rangle\Delta t)^2}{2D\Delta t}\right], \tag{8.27}$$

leads to the identification $s = 2\langle\omega\rangle/D$, see Sect. 8.2.1. Again, no general theoretical expectations exist for the ratio between the average drift and the angular "diffusion" coefficient D. The empirical observation that such a ratio is somehow independent of the relative importance between collisions and dry friction (controlled by β^{-1}) is quite surprisingly. This suggests that some properties of the LDF for driven systems share general symmetry relations, which are valid in wider contexts.

8.4 Conclusions

Ratchet systems, in their several different realizations, provide an interesting context where nonequilibrium fluctuations play a central role. Since such systems are characterized by the continuous conversions of "thermal" energy into work, they provide us a suitable framework where transformations between nonequilibrium steady states can be studied, with the final aim to extend and assess the validity of general thermodynamic relations in nonequilibrium systems.

As the last decades have shown, a powerful tool to characterize nonequilibrium fluctuations is the theory of large deviations, which describe the behavior of the system beyond the Gaussian approximation, pointing out the role of large fluctuations and rare events in the dynamics. As shown in this chapter, analytical results on the large deviations function for the displacement in ratchet models are very few, due to the mathematical difficulty of the problem. Still, such results shed some light on the underlying mechanisms which produce the general symmetry relations in the fluctuations distributions.

The experimental study of large deviations of velocity currents in ratchet systems is also very intriguing. Results in this framework show that some nonequilibrium relations, which are mathematically proven under strict hypotheses, can be verified also in more general regimes. We have discussed two examples where the velocity statistics of a probe has been observed to verify a symmetry relation like the FR, which is expected to hold for the entropy production in the system. The experimental observations call for a deeper analysis of these relations in a wider and more general framework.

Acknowledgements The authors thank G. Gradenigo, D. Lacoste and J. Talbot for useful discussions and A. Puglisi, D. Vergni and A. Vulpiani for a careful reading of the manuscript.

References

1. M.V. Smoluchowski, Experimentell Nachweisbare, der Üblichen Thermodynamik Widersprechende Molekularphänomene. Phys. Z. **13**, 1069 (1912)
2. R.P. Feynman, R.B. Leighton, M. Sands, *The Feynman Lectures on Physics* (Addison-Wesley, Reading, 1963)
3. M.O. Magnasco, Forced thermal ratchets. Phys. Rev. Lett. **71**, 1477 (1993)
4. C. Bustamante, J. Liphardt, F. Ritort, The nonequilibrium thermodynamics of small systems. Phys. Today **58**, 43 (2005)
5. R.D. Astumian, Thermodynamics and kinetics of a brownian motor. Science **276**, 917 (1997)
6. P. Reimann, Brownian motors: noisy transport far from equilibrium. Phys. Rep. **361**, 57 (2002)
7. P. Hanggi, F. Marchesoni, Artificial Brownian motors: controlling transport on the nanoscale. Rev. Mod. Phys. **81**, 387 (2003)
8. M. Schliwa, G. Woehlke, Molecular motors. Nature **422**, 759 (2003)
9. F. Ritort, Nonequilibrium fluctuations in small systems: from physics to biology. Adv. Chem. Phys. **137**, 31 (2007)
10. L. Bertini, A. De Sole, D. Gabrielli, G. Jona-Lasinio, C. Landim, Macroscopic fluctuation theory for stationary non-equilibrium states. J. Stat. Phys. **107**, 635 (2002)
11. G. Gallavotti, E.G.D. Cohen, Dynamical ensembles in nonequilibrium statistical mechanics. Phys. Rev. Lett. **74**, 2694 (1995)
12. D.J. Evans, D.J. Searles, The fluctuation theorem. Adv. Phys. **52**, 1529 (2002)
13. C. Jarzynski, Nonequilibrium equality for free energy differences. Phys. Rev. Lett. **78**, 2690 (1997)
14. J.L. Lebowitz, H. Spohn, A Gallavotti-Cohen-type symmetry in the large deviation functional for stochastic dynamics. J. Stat. Phys. **95**, 333 (1999)
15. C. Maes, The fluctuation theorem as a Gibbs property. J. Stat. Phys. **95**, 367 (1999)
16. T. Hatano, S. Sasa, Steady-state thermodynamics of Langevin systems. Phys. Rev. Lett. **86**, 3463 (2001)
17. H. Touchette, The large deviation approach to statistical mechanics. Phys. Rep. **478**, 1 (2009)
18. B. Derrida, Non-equilibrium steady states: fluctuations and large deviations of the density and of the current. J. Stat. Mech. P07023 (2007)
19. J. Farago, Injected power fluctuations in Langevin equation. J. Stat. Phys. **107**, 781 (2002)
20. R. van Zon, E.G.D. Cohen, Extension of the fluctuation theorem. Phys. Rev. Lett. **91**, 110601 (2003)
21. P. Visco, Work fluctations for a Brownian particle between two thermostats. J. Stat. Mech. P06006 (2006)
22. J. Mehl, T. Speck, U. Seifert, Large deviation function for entropy production in driven one-dimensional systems. Phys. Rev. E **78**, 011123 (2008)
23. F. Ritort, Work and heat fluctuations in two-state systems: a trajectory thermodynamics formalism. J. Stat. Mech. P10016 (2004)
24. W. De Roeck, C. Maes, Symmetries of the ratchet current. Phys. Rev. E **76**, 051117 (2007)
25. A. Kundu, S. Sabhapandit, A. Dhar, Large deviations of heat flow in harmonic chains. J. Stat. Mech. P03007 (2011)
26. A. Baule, H. Touchette, E.G.D. Cohen, Stick-slip motion of solids with dry friction subject to random vibrations and an external field. Nonlinearity **24**, 351 (2011)
27. S. Sabhapandit, Work fluctuations for a harmonic oscillator driven by an external random force. EPL **96**, 20005 (2011)
28. A. Crisanti, F. Ritort, Violation of the fluctuation-dissipation theorem in glassy systems: basic notions and the numerical evidence. J. Phys. A **36**, R181 (2003)
29. U.M.B. Marconi, A. Puglisi, L. Rondoni, A. Vulpiani, Fluctuation-dissipation: response theory in statistical physics. Phys. Rep. **461**, 111 (2008)
30. E. Lippiello, F. Corberi, M. Zannetti, Off-equilibrium generalization of the fluctuation dissipation theorem for ising spins and measurement of the linear response function. Phys. Rev. E **71**, 036104 (2005)

31. M. Baiesi, C. Maes, B. Wynants, Fluctuations and response of nonequilibrium states. Phys. Rev. Lett. **103**, 010602 (2009)
32. U. Seifert, T. Speck, Fluctuation-dissipation theorem in nonequilibrium steady states. Europhys. Lett. **89**, 10007 (2010)
33. U. Seifert, Entropy production along a stochastic trajectory and an integral fluctuation theorem. Phys. Rev. Lett. **95**, 040602 (2005)
34. A. Sarracino, D. Villamaina, G. Gradenigo, A. Puglisi, Irreversible dynamics of a massive intruder in dense granular fluids. Europhys. Lett. **92**, 34001 (2010)
35. A. Puglisi, A. Baldassarri, A. Vulpiani, Violations of the Einstein relation in granular fluids: the role of correlations. J. Stat. Mech. P08016 (2007)
36. A. Ziehl, J. Bammert, L. Holzer, C. Wagner, W. Zimmermann, Direct measurement of shear-induced cross-correlations of brownian motion. Phys. Rev. Lett. **103**, 230602 (2009)
37. A. Crisanti, A. Puglisi, D. Villamaina, Nonequilibrium and information: the role of cross correlations. Phys. Rev. E **85**, 061127 (2012)
38. H.M. Jaeger, S.R. Nagel, R.P. Behringer, Granular solids, liquids and gases. Rev. Mod. Phys. **68**, 1259 (1996)
39. Z. Farkas, P. Tegzes, A. Vukics, T. Vicsek, Transitions in the horizontal transport of vertically vibrated granular layers. Phys. Rev. E **60**, 7022 (1999)
40. P. Eshuis, K. van der Weele, D. Lohse, D. van der Meer, Experimental realization of a rotational ratchet in a granular gas. Phys. Rev. Lett. **104**, 248001 (2010)
41. R. Balzan, F. Dalton, V. Loreto, A. Petri, G. Pontuale, Brownian motor in a granular medium. Phys. Rev. E **83**, 031310 (2011)
42. M. Heckel, P. Müller, T. Pöschel, J.A.C. Gallas, Circular ratchets as transducers of vertical vibrations into rotations. Phys. Rev. E **86**, 061310 (2012)
43. B. Cleuren, C. Van den Broeck, Granular Brownian motor. Europhys. Lett. **77**, 50003 (2007)
44. G. Costantini, A. Puglisi, U.M.B. Marconi, A granular Brownian ratchet model. Phys. Rev. E **75**, 061124 (2007)
45. B. Cleuren, R. Eichhorn, Dynamical properties of granular rotors. J. Stat. Mech. P10011 (2008)
46. G. Costantini, A. Puglisi, U.M.B. Marconi, Models of granular ratchets. J. Stat. Mech. P07004 (2009)
47. U. Seifert, Stochastic thermodynamics, fluctuation theorems and molecular machines. Rep. Prog. Phys. **75**, 126001 (2012)
48. C. Van den Broeck, M. Kawai, P. Meurs, Microscopic analysis of a thermal Brownian motor. Phys. Rev. Lett. **93**, 090601 (2004)
49. C. Van den Broeck, P. Meurs, R. Kawai, From Maxwell demon to Brownian motor. New J. Phys. **7**, 10 (2005)
50. J. Talbot, R.D. Wildman, P. Viot, Kinetics of a frictional granular motor. Phys. Rev. Lett. **107**, 138001 (2011)
51. G. Costantini, U.M.B. Marconi, A. Puglisi, Noise rectification and fluctuations of an asymmetric inelastic piston. Europhys. Lett. **82**, 50008 (2008)
52. A. Gnoli, A. Petri, F. Dalton, G. Gradenigo, G. Pontuale, A. Sarracino, A. Puglisi, Brownian ratchet in a thermal bath driven by coulomb friction. Phys. Rev. Lett. **110**, 120601 (2013)
53. G. Gradenigo, A. Sarracino, D. Villamaina, T.S. Grigera, A. Puglisi, The ratchet effect in an ageing glass. J. Stat. Mech. L12002 (2010)
54. R. Di Leonardo, L. Angelani, D. Dell'Arciprete, G. Ruocco, V. Iebba, S. Schippa, M.P. Conte, F. Mecarini, F. De Angelis, E. Di Fabrizio, Bacterial ratchet motors. Proc. Natl. Acad. Sci. U.S.A. **107**, 9541 (2010)
55. J. Talbot, P. Viot, Effect of dynamic and static friction on an asymmetric granular piston. Phys. Rev. E **85**, 021310 (2012)
56. H. Risken, *The Fokker-Planck Equation: Methods of Solution and Applications* (Springer, Berlin, 1989)
57. K. Feitosa, N. Menon, Breakdown of energy equipartition in a 2d binary vibrated granular gas. Phys. Rev. Lett. **88**, 198301 (2002)

58. A. Puglisi, P. Visco, A. Barrat, E. Trizac, F. van Wijland, Fluctuations of internal energy flow in a vibrated granular gas. Phys. Rev. Lett. **95**, 110202 (2005)
59. T. Elston, H. Wang, G. Oster, Energy transduction in atp synthase. Nature **391**, 510 (1998)
60. F. Jülicher, A. Ajdari, J. Prost, Modeling molecular motors. Rev. Mod. Phys. **69**, 1269 (1997)
61. D. Lacoste, K. Mallick, Fluctuation relations for molecular motors, in *Biological Physics: Poincarâe Seminar 2009*, ed. by B. Duplantier, V. Rivasseau (Springer, Basel AG, 2010)
62. D. Lacoste, A.W.C Lau, K. Mallick, Fluctuation theorem and large deviation function for a solvable model of a molecular motor. Phys. Rev. E **78**, 011915 (2008)
63. A.W.C. Lau, D. Lacoste, K. Mallick, Nonequilibrium fluctuations and mechanochemical couplings of a molecular motor. Phys. Rev. Lett. **99**, 158102 (2007)
64. P. Gaspard, Time-reversed dynamical entropy and irreversibility in markovian random processes. J. Stat. Phys. **117**, 599 (2004)
65. D. Andrieux, P. Gaspard, Fluctuation theorems and the nonequilibrium thermodynamics of molecular motors. Phys. Rev. E **74**, 011906 (2006)
66. F. Slanina, Interacting molecular motors: efficiency and work fluctuations. Phys. Rev. E **80**, 061135 (2009)
67. P. Malgaretti, I. Pagonabarraga, D. Frenkel, Running faster together: huge speed up of thermal ratchets due to hydrodynamic coupling. Phys. Rev. Lett. **109**, 168101 (2012)
68. S. Ciliberto, S. Joubaud, A. Petrosyan, Fluctuations in out-of-equilibrium systems: from theory to experiment. J. Stat. Mech. P12003 (2010)
69. S. Joubaud, D. Lohse, D. van der Meer, Fluctuation theorems for an asymmetric rotor in a granular gas. Phys. Rev. Lett. **108**, 210604 (2012)
70. A. Naert, Experimental study of work exchange with a granular gas: the viewpoint of the fluctuation theorem. EPL **97**, 20010 (2012)
71. A. Mounier, A. Naert, The Hatano-Sasa equality: transitions between steady states in a granular gas. EPL **100**, 30002 (2012)
72. J. Talbot, A. Burdeau, P. Viot, Kinetic analysis of a chiral granular motor. J. Stat. Mech. P03009 (2011)
73. A. Sarracino, A. Gnoli, A. Puglisi, Ratchet effect driven by coulomb friction: the asymmetric Rayleigh piston. Phys. Rev. E **87**, 040101(R) (2013)
74. N. Kumar, S. Ramaswamy, A.K. Sood, Symmetry properties of the large-deviation function of the velocity of a self-propelled polar particle. Phys. Rev. Lett. **106**, 118001 (2011)
75. G. Gradenigo, A. Puglisi, A. Sarracino, U.M.B. Marconi, Nonequilibrium fluctuations in a driven stochastic lorentz gas. Phys. Rev. E **85**, 031112 (2012)
76. A. Gnoli, A. Sarracino, A. Puglisi, A. Petri, Nonequilibrium fluctuations in a frictional granular motor: experiments and kinetic theory. Phys. Rev. E **87**, 052209 (2013)

Chapter 9
Stochastic Fluctuations in Deterministic Systems

Antonio Politi

Abstract The unavoidable presence of inhomogeneities in the phase space of a chaotic system induces fluctuations in the degree of stability, even when long trajectories are considered. The characterization of such fluctuations requires to go beyond average indicators: this is achieved with the help of the multifractal formalism which contributes to: (i) establishing a general connection between the positive Lyapunov exponents and the Kolmogorov-Sinai entropy; (ii) identifying and quantifying deviations from a purely hyperbolic dynamics; (iii) characterizing anomalous bifurcations, where the attractor looses progressively its stability. In the context of spatially extended dynamical systems, the study of Lyapunov exponent fluctuations leads to a non conventional assessment of the extensivity of the resulting dynamics. Finally, a careful study of the fluctuations allows clarifying the odd phenomenon of "stable chaos", where an irregular dynamics is accompanied by a negative (average) Lyapunov exponent.

9.1 Introduction

A dynamical system is said to be deterministic if the perfect knowledge of its current state allows, in principle, to determine any future state. The (possibly finite) number N of variables that is necessary to know to specify the current configuration is the dimension of the corresponding phase-space. The *deterministic* evolution rule is typically given as a relationship linking the configurations in two consecutive instants. If the time variable is assumed to be discrete, we are before a so-called recursive map [1, 2]

$$\mathbf{x}_{n+1} = \mathbf{F}(\mathbf{x}_n)\,, \tag{9.1}$$

A. Politi (✉)
Institute for Complex Systems and Mathematical Biology, Kings College, University of Aberdeen, Aberdeen AB24 3UE, UK
e-mail: a.politi@abdn.ac.uk

A. Vulpiani et al. (eds.), *Large Deviations in Physics*, Lecture Notes in Physics 885,
DOI 10.1007/978-3-642-54251-0_9,

where $\mathbf{x}_n$ is an N-dimensional vector that identifies the configuration at time n. In the case of a continuous-time variable (and a finite-dimensional phase space), the evolution is typically determined by a set of ordinary differential equations (ODEs). After introducing a suitable surface of section $\mathscr{S}$, a set of ODEs can, in principle, be reduced to a recursive map linking two consecutive crossings with the section $\mathscr{S}$. Accordingly, from now on, I assume that the time is discrete and refer to an evolution rule of the type (9.1). Although the knowledge of the initial condition $\mathbf{x}_0$ suffices to determine the future (and the past, if the system is invertible), the requested configuration can be obtained only by composing a chain of operators. Since in practical applications, the current state is never known with a perfect accuracy, it is convenient to introduce the uncertainty $\delta\mathbf{x}_n$. As long as $\delta\mathbf{x}_n$ is small enough, it can be treated as an infinitesimal quantity and thereby linearize the evolution equation, obtaining [1,2]

$$\delta\mathbf{x}_{n+1} = \mathbf{F}_{\mathbf{x}}\delta\mathbf{x}_n \,, \tag{9.2}$$

where the subscript $\mathbf{x}$ denotes the derivative with respect to the set of variables. By looking at the evolution of $\delta\mathbf{x}_n$, it is possible to infer some general properties of the deterministic evolution rule. In particular, as long as $\delta\mathbf{x}_n$ does not grow (too rapidly) with time, one can claim that future states are predictable. However, if $\delta\mathbf{x}_n$ grows, e.g., exponentially in time, it is obvious that there exists a time scale beyond which the *knowledge of principle* of the future is practically useless. This is indeed the case of deterministic chaos, a rather general phenomenon in nonlinear systems. Deterministic chaos is basically characterized by the stretching of one or more directions, accompanied by the squeezing along other directions (the confinement in phase space is ensured by suitable folding processes). The reader interested in the mechanisms that lead to the onset of a chaotic dynamics may read Refs. [1,2]. In this chapter, I am mainly interested in the fluctuations that unavoidably accompany chaotic motion. With the help of a series of dynamical systems of increasing complexity, I illustrate in Sect. 9.2 a distinctive property of deterministic chaos: the existence of a multitude of different orbits and its quantification with the Kolmogorov-Sinai entropy [3]. A close look at the problem reveals that different definitions may give different results. This circumstance, which seems to reveal the presence of an ill-defined quantity, is instead the consequence of fluctuations, whose treatment requires the combination of a large-deviation formalism, with a suitable encoding of the trajectories. Given the practical difficulty to fully carry out this strategy in generic models, it is, however, more convenient to make use of (finite-time) Lyapunov exponents which are indeed introduced in Sect. 9.3, where their relationship with the Kolmogorov-Sinai entropy is also briefly illustrated.

An important property of a chaotic dynamics is hyperbolicity, i.e. the transversality between stable and unstable manifold (see Ref. [3] for a precise definition), as it allows for rigorous proofs of many properties, starting from the structural stability of a chaotic dynamics [3]. The fluctuations of the Lyapunov exponents help to reveal deviations from a perfectly hyperbolic dynamics. In Sect. 9.4, I present several

examples, starting from the very existence of a negative tail in the distribution of the maximal Lyapunov exponent. Other examples are: (i) the bubbling transition which accompanies the synchronization of chaotic systems; (ii) a fluctuating number of unstable directions. The same formalism can be extended to spatio-temporal systems (although within a Gaussian approximation), where it allows recognizing a strong form of extensivity (see Sect. 9.5). Finally, in Sect. 9.6, I show that the study of large-deviations allows reconciling an atypical form of irregular dynamics, "stable chaos" (characterized by a negative maximum Lyapunov exponent), with standard chaos: the existence of a positive tail in the distribution of the maximum Lyapunov exponent signals the presence of a lower-dimensional strange repeller, a condition that is believed to be a necessary prerequisite for the occurrence of stable chaos.

9.2 Kolmogorov-Sinai Entropy

The simplest setup where one can speak of deterministic chaos is that of 1D maps; the prototypical model is the piece-wise linear Bernoulli map $x_{n+1} = 2x_n \mathrm{mod}\ 1$. It is linear, as it involves only a multiplication by a constant and the possible subtraction of yet another constant; it is "piecewise", since the constant that is being subtracted is either 0 (if $x < 1/2$) or 1 (if $x > 1/2$). The evolution is rather trivial, especially if referred to the binary expansion of x_n: $b_n b_{n+1} b_{n+2} \ldots$, where $b_n \in \{0, 1\}$. In fact, the mth iterate of x_n, is nothing but $b_{n+m} b_{n+m+1} b_{n+m+2} \ldots$. For this reason, it is called a shift dynamical system: the complexity of the time evolution is entirely contained in the complexity of the sequence of bits in the initial condition. Although rather simple, this model allows illustrating some basic concepts and properties that can be encountered in general dynamical system. In particular: (i) one can recognize the existence of infinitely many periodic orbits that are attained when starting from eventually periodic binary sequences (i.e. any rational number); (ii) initial conditions with a larger fraction of 0s in their expansion produce trajectories that stay closer to $x = 0$ than to $x = 1$. In other words, the model is compatible with many different orbits.

The most convenient way to quantify the abundance of different orbits is by counting the number of distinct trajectories of a given length. This is the approach that eventually leads to the introduction of the so-called Kolmogorov-Sinai or metric entropy: here I proceed by first illustrating the problem in a simple setup and thereby progressively refining the definition. As a first step, it is necessary to introduce a partition $\mathbb{P}_\varepsilon$ of the phase space, i.e. a collection of cells (atoms) $\mathscr{C}_m$ of size ε such that $\bigcup_m \mathscr{C}_m$ covers all the accessible phase space. As a result, the state x_n can be turned into the symbol $\mathscr{C}_m$, depending whether $x_n \in \mathscr{C}_m$. Here, it is clear that ε plays the role of the observational resolution: giving the sequence of cells $\mathscr{C}_m$ is equivalent to locating the phase point with an approximation that corresponds to the cell size. Now, one can introduce the number $N(\varepsilon, n)$ of distinct orbits (i.e. different symbol sequences) of length n that can be generated by our dynamical system. In the

specific case of the Bernoulli map, if $\mathscr{C}_0 \equiv [0, 1/2]$, and $\mathscr{C}_1 \equiv [1/2, 1]$, assigning the sequence of $\mathscr{C}_0/\mathscr{C}_1$ is equivalent to assigning the 0 and 1 bits. We are now in the position to define a dynamical entropy as

$$K_0 = \lim_{n\to 0} \frac{\log N(\varepsilon, n)}{n} \tag{9.3}$$

A value of $K_0 > 0$ means that the number of distinct trajectories of length n grows exponentially with the time span n. This property is the landmark of chaos, as it implies an extraordinary richness in the type of trajectories that may be actually generated by the (deterministic) system. Again with reference to the Bernoulli map, since there is no restriction in assigning 0s and 1s in the initial condition, it is easy to verify that the $K_0 = \log 2$.

In order to make the above definition more appealing, one should ascertain whether the exponent K_0 is independent of the partition adopted. This is indeed the case, provided that, either the limit of infinitesimal boxes ($\varepsilon \to 0$) is taken, or the definition is restricted to the so-called generating partitions [4]. A partition is said to be *generating* if, given the infinitely long sequence of cells visited by any trajectory, it is possible to identify the trajectory itself with infinite accuracy. The Bernoulli map can help to clarify how this is possible: in fact, if one knows the (approximate) future positions, it is possible to refine the knowledge of the current state. This is a consequence of the fact that the x axis is stretched (by a factor 2) at every iterate, so that an uncertainty δ_{n+1} implies an uncertainty $\delta_{n+1}/2$ at the previous time. The main obstacle to the refinement is the folding process, which, in the case of the Bernoulli map, is provided by the modulus operation. It implies that two distinct points with the same binary expansion (but the first symbol) are mapped onto the same point. As a result, there must be some care in selecting the borders of the atoms of the partition, as they must coincide with the points where the folding occurs. For instance, had one decided to split the unit interval into two uneven cells (e.g. [0, 0.6] and [0.6, 1]), it would be easily seen that the (periodic) trajectory stemming from 0.6 (0.2,0.4,0.8,0.6 ...) and from 1/15 (2/15,4/15,8/15,1/15,...) would be encoded in the same way. If the atoms of the partition are not properly selected, the number of different trajectories and K_0 are underestimated. Although very difficult to achieve in practice, symbolic encoding is conceptually very appealing, since it allows to map the evolution of a generic dynamical system onto a shift of a sequence of symbols. What could not emerge from the trivial example of the Bernoulli map is that, in general, once a meaningful encoding has been introduced, it is not generally true that all sequences of symbols are allowed, or that the various symbols have equal probabilities. One dimensional maps can again help to clarify the general expectations. I start with the simple asymmetric tent map that is depicted in Fig. 9.1a. Given the partition made of the two atoms $\mathscr{C}_0$ and $\mathscr{C}_1$, that can, for simplicity, be identified with 0 and 1, it is clear that since the image of $\mathscr{C}_0$ coincides with $\mathscr{C}_1$, any symbol 0 is followed by the symbol 1 and no two consecutive 0s can be generated. This is a minimal example of the complexity that is to be expected in more generic dynamical systems. In full generality, there may be very complicate

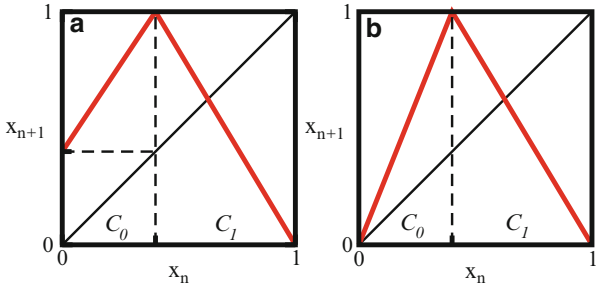

Fig. 9.1 Two examples of tent maps: (**a**) no two consecutive 0s can be generated; (**b**) 0s and 1s have a different probability

constraints which forbid the appearance of symbols of various lengths. This implies that the legal trajectories of an encoded dynamical system represent a nontrivial subset of all possible sequences. The problem of characterizing a dynamical system could be formulated as that of identifying the proper language that is generated by the given dynamical system [5]. Less striking, but nevertheless enlightening is the map illustrated in Fig. 9.1b. In this case there are no forbidden sequences, but the two symbols 0 and 1 have a different probability. In fact, one can see that a flat distribution $P(x) = 1$ is left invariant by the map transformation; accordingly the probability of each symbol is equal to the length of the corresponding interval.

Therefore, one learns that the problem of characterizing the dynamics of a given chaotic system is equivalent to that of studying ensembles of (infinitely) long symbolic sequences. Before proceeding along this direction, it is useful to remind that almost rigorous methods to build generating partitions have been developed also for two dimensional maps. In this case, the key ingredients that allow identifying the borders of the atoms are the primary homoclinic tangencies, which correspond to the folding points [6], and various kinds of symmetry lines, which allow incorporating the islands of order in Hamiltonian systems [7].

Altogether, symbolic encoding allows reducing the study of a dynamical system to that of symbol sequences. The first problem that is encountered is that different averaging strategies may lead to different results. Going back to the counting of distinct trajectories invoked in Eq. (9.3), one can appreciate this ambiguity by invoking the so-called Renyi entropies [8],

$$H_q = -\frac{\log \sum_i p_i^q}{q-1} \,. \tag{9.4}$$

For $q = 0$, H_0 coincides with $\log N$, while for $q = 1$, H_1 reduces to the standard Shannon entropy. In practice, Eq. (9.4) allows extending Eq. (9.3) to a generic q value,

$$K_q = \lim_{n \to 0} \frac{H_q}{n} \,. \tag{9.5}$$

For $q = 1$, one obtains the celebrated Kolmogorov-Sinai or metric entropy. In the Bernoulli map, since all p_i's are equal to one another, the K_q entropies are also equal to one another and it is a matter of taste the selection of the q value one wishes to consider. However, in the slightly more realistic tent map plotted in Fig. 9.1b, the various definitions yield different results, simply because the two symbols have different probabilities. One can turn the q-dependence into a tool to extract more detailed information on the underlying dynamical system.

This is quite evident by following an equivalent but more enlightning approach. Let us rewrite Eqs. (9.4) and (9.5), as

$$\mathrm{e}^{-(q-1)K_q n} = \sum_i p_i^q \,, \tag{9.6}$$

where n is assumed to be large enough. The r.h.s. can be conveniently rewritten as an integral over all possible values taken by the probability p. Moreover, it is convenient to replace the integration variable p with the so-called pointwise entropy,

$$\alpha = -\frac{\log p}{n} \tag{9.7}$$

which tells us how should the probability of a box scale with n in order to take the current value, $p = \exp(-\alpha n)$. Next, let us introduce the number $N(\alpha, n)d\alpha$ of sequences of length n that are characterized by the same pointwise entropy α, and introduce a suitable scaling Ansatz,

$$N(\alpha, n) = \mathrm{e}^{f(\alpha)n} \tag{9.8}$$

where the "multifractal" distribution $f(\alpha)$ identifies the range of possible α values. The name multifractal comes from the theory of fractals, where this approach was first developed [9]: it understands the fact that a simple fractal is characterized by a single scaling exponent α. By assembling all of the above ingredients, one eventually obtains

$$\mathrm{e}^{-(q-1)K_q n} = \int d\alpha \; \mathrm{e}^{(f(\alpha)-q\alpha)n}. \tag{9.9}$$

In the Bernoulli map, all sequences of length n are characterized by the same exponent $\alpha = \log 2$ that is also the value of the Kolmogorov-Sinai entropy. In this case, the domain of $f(\alpha)$ is restricted to a single value and, for this reason, it is called a uniform attractor. In general, the integral can be solved by invoking the saddle point technique, i.e. by looking for the maximum value of the exponent. This leads to a standard Legendre transform structure,

$$(q-1)K_q = q\alpha - f(\alpha) \quad ; \quad f'(\alpha) = q \tag{9.10}$$

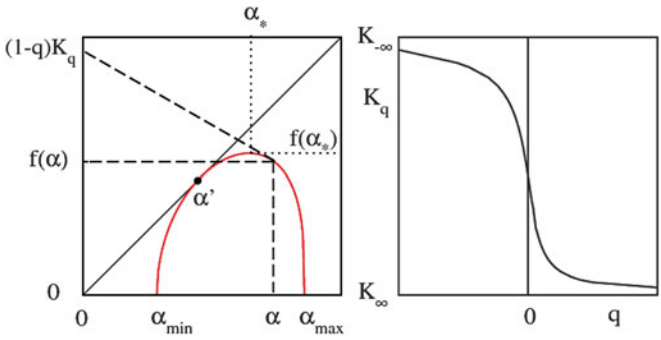

Fig. 9.2 Schematic illustration of the Legendre transform linking $f(\alpha)$ with $(q-1)K_q$

which allows determining $(q-1)K(q)$, once the multifractal distribution $f(\alpha)$ is given. The corresponding geometrical construction is illustrated in Fig. 9.2, where a generic distribution $f(\alpha)$ is plotted together with the corresponding spectrum $K(q)$. In practice, once $f(\alpha)$ is known, it is sufficient to draw the tangent to the curve in α and thereby identify the intersection with the vertical axis as $(q-1)K_q$, while the slope of the curve corresponds to q. One expects $f(\alpha)$ to vanish in correspondence of the minimum α_{min} and maximum α_{max}, since the multiplicity of the extremal values does not typically increase with n. Moreover, it is easy to verify that K_∞, and $K_{-\infty}$ coincide with the minimal and maximal pointwise entropies, respectively. Another special value is the abscissa α_* of the maximum: $f(\alpha_*)$ corresponds to the topological entropy K_0. Finally, the point $q = 1$ is the most important one, as it identifies the metric entropy: it coincides with the tangency of the multifractal distribution with the bisectrix. The reason why it is so can be understood by introducing the probability $P(\alpha, n)$ to observe a sequence with pointwise entropy α while generating a natural trajectory. It is given by $pN(\alpha, n)$ and invoking the same scaling arguments as before, one expects that

$$P(\alpha, n) \approx \mathrm{e}^{-s(\alpha)n} \tag{9.11}$$

where $s(\alpha) = \alpha - f(\alpha)$ is nothing but a large-deviation function. Obvious properties of probability distributions imply that $s(\alpha) \geq 0$ and the minimum value $s(\alpha')$ is equal to zero. From the very definition of $s(\alpha)$, we then conclude that $f(\alpha)$ touches the bisectrix at $\alpha = \alpha'$. Moreover, the central limit theorem implies that the minimum is generally a quadratic function. In fact, by expanding s up to second order, one can write $P(\alpha, n) = \exp[-(\alpha - \alpha')^2/(\sigma^2/n)]$, where σ^2, related to the second derivative of $f(\alpha)$, measures the multifractality of the underlying attractor. As a result, we see that the distribution is Gaussian and the standard deviation decreases as $1\sqrt{n}$. This is consistent with the expectation that a chaotic dynamics is characterized by a short-term memory. One should be anyway warned that there are regimes such as intermittency, where anomalous distributions are expected as

the consequence of long-range correlations [2]. In any case, the minimum of $s(\alpha)$ must be always equal to zero. Finally, Eqs. (9.10) can be inverted. Given K_q, one can determine the multifractal distribution by invoking the relationship $[(q-1)K_q]' = \alpha$. This means that $f(\alpha)$ and $K(q)$ provide equivalent descriptions of the chaotic dynamics.

9.3 Lyapunov Exponents

So far we have considered probabilities of symbolic sequences, but it is not generally easy to determine them, since they require constructing a generating partition. Fortunately, there exists a tight relationship between dynamical entropies and another class of indicators that are more easily accessible to numerical studies: the Lyapunov exponents. Analogosly to fixed points, whose linear stability is quantified by the N eigenvalues of a suitable Jacobian matrix, chaotic attractors can be characterized by N expansion factors $\Lambda_i(n)$ $(i = 1, \ldots, N)$ over a time n. The rates $\lambda_i = \Lambda_i(n)/n$ are the so-called finite-time Lyapunov exponent (FTLE)[10]. For finite n, the FTLEs exhibit fluctuations that become smaller and smaller upon increasing the time span n. In the infinite-time limit, λ_i converges to the standard Lyapunov exponent $\overline{\lambda}_i$ (whenever, it is necessary to distinguish between the FTLE and the asymptotic value, the latter is identified by an overline). Altogether, a complete characterization of the fluctuations can be obtained by invoking the theory of large deviations, which suggests that, in the long-time limit, the probability distribution $P(\boldsymbol{\lambda}, n)$ (where $\boldsymbol{\lambda} = \{\lambda_1, \lambda_2, \ldots, \lambda_N\}$) scales as

$$P(\boldsymbol{\lambda}, n) \underset{n\to\infty}{\propto} \mathrm{e}^{-S(\boldsymbol{\lambda})n} \tag{9.12}$$

where $S(\boldsymbol{\lambda})$ is a positive-defined large deviation function.

In practice, there are at least two different methods to define FTLEs: (i) by repeatedly applying the QR decomposition (by either implementing the Gram-Schmidt orthogonalization procedure or the Householder transformation) to a set of linearly independent perturbations [11]; (ii) by determining the expansion rates of the so-called covariant Lyapunov vectors [12]. The former (standard) approach is essentially based on the computation of the expansion of volumes; the latter one is based on the idea of determining the expansion rate along suitably selected directions, the covariant vectors $\mathbf{v}_c(n)$, that are the natural extension of the eigenvectors. I start by considering the maximum Lyapunov exponent, in which case, the two methods are equivalent over all times. I consider one of the most popular dynamical systems, the 2d Hénon map, $x_{n+1} = a - x_n^2 + bx_{n-1}$, which has the advantage over the above mentioned 1d maps of being invertible. Besides, the Hénon map is a typical example of low-dimensional systems, so that it can be used as testbed for general ideas. It is easy to check that volumes are contracted by a factor b at each time step. This implies that the sum of the two FTLEs is constant

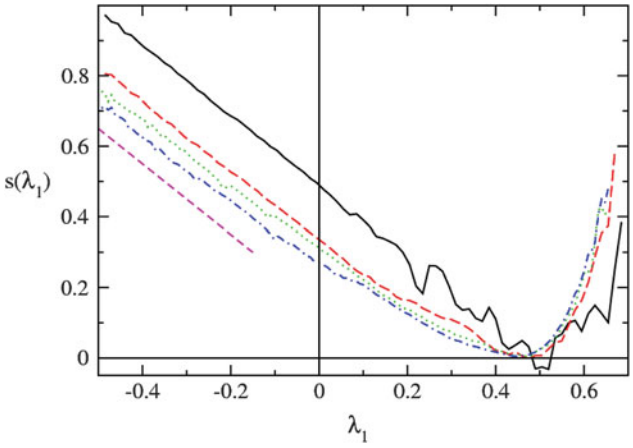

Fig. 9.3 The large deviation function $s(\lambda_1)$ fore the Hénon map with the standard parameter values ($a = 1.4$, $b = 0.3$). The *solid*, *dashed*, *dotted*, and *dotted-dashed curves* correspond to $n = 10$, 15, 20, and 25, respectively. The *dashed purple straight line* has slope 1

($\lambda_1 + \lambda_2 = \log b$), so that the fluctuations in phase space can be captured by studying only the first exponent. By inverting Eq. (9.12), one obtains

$$S(\boldsymbol{\lambda}) = -\lim_{n\to\infty} \frac{\log P(\boldsymbol{\lambda}, n)}{n}. \tag{9.13}$$

Accordingly, one can infer the very existence of an n-independent $S(\boldsymbol{\lambda})$ from the overlap of the functions obtained by implementing Eq. (9.13) for different values of n. In Fig. 9.3, I have plotted $s(\lambda_1)$ for the usual parameter values ($a = 1.4$, $b = 0.3$) as estimated from finite trajectories (the various curves correspond to $n = 10$, 15, 20 and 25, respectively). There is a clear tendency to converge towards a given shape (that is approximately asymptotic already for $n = 15$). The most striking feature is that although the distribution refers to the maximum (positive) Lyapunov exponent, it extends to negative as well as to positive values. This is a consequence of occasional tangencies between the unstable and the stable manifold, where, as a matter of fact, nearby points along the unstable manifold are not expanded but rather contracted. Such points are a manifestation of a non-hyperbolicity, which in general, represents a major obstacle towards the characterization of chaotic systems and the proof of rigorous theorems. In fact, it is typically assumed that the stable and unstable directions are everywhere transversal (hyperbolic systems) and even the factorization (transversality) of the various directions may be required. Accordingly, numerical analysis is very welcome as it can help to identify any signature of a non-hyperbolic behaviour, such as the extension of the maximum FTLE domain to negative values. In particular, it is interesting to notice that the negative tail of $s(\lambda_1)$ exhibits a slope that saturates to a value $q_c \approx 1$ [13]. By adopting the language of thermodynamic formalism [14] this is the signature of a so-called

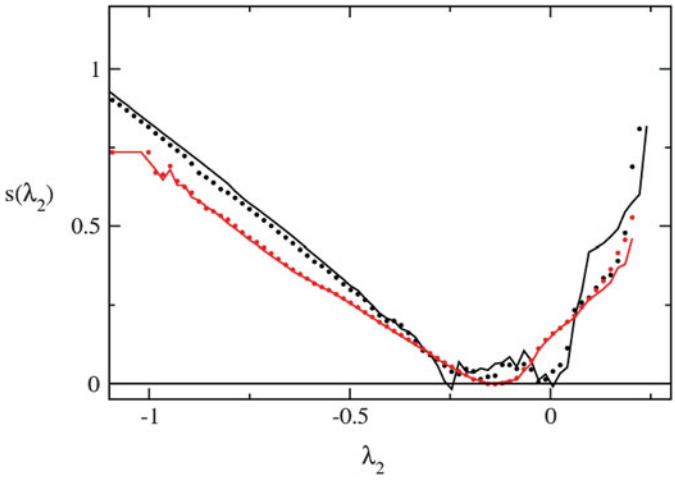

Fig. 9.4 The large deviation function $s(\lambda_2)$ for the generalized Hénon map ($a = 1.4$ and $b = 0.1$). *Solid* and *dotted lines* refer to the FTLEs as computed with the Gram-Schmidt procedure and covariant vectors, respectively. *Black* and *red lines* correspond to $n = 10$, and $n = 20$, respectively

phase transition. In fact, it implies that the Legendre transform is not a smooth function of q: it exhibits a cusp in correspondence of $q = q_c$[13]. This means that the attractor is characterized by two phases, the "hyperbolic" and "non-hyperbolic" one. As the non-hyperbolic phase emerges for $s(\lambda_1)$ larger than some finite value, one can (at least numerically) conclude that it is restricted to a subset of negligible (vanishing) measure. This result authorizes to conjecture that the general theorems proved for hyperbolic systems should apply to generic physical systems, in spite of the fact they are not uniformly hyperbolic. One important example is the fluctuation theorem in Ref. [15].

For all, but the maximal Lyapunov exponent, the above definitions of FTLE are not a priori formally equivalent. A minimal setup where it makes sense to explore the relationship between the two methods is that of 3d maps. I have selected the generalized Hénon map $x_{n+1} = a - x_{n-1}^2 - bx_{n-2}$, as a possible testbed. The model has been studied in Ref. [16], where the authors have found that the model may exhibit hyperchaos (more than one positive Lyapunov exponent) as well as "normal" chaos. In this case too, volumes are contracted by a factor b at each time step. However, since there exist three Lyapunov exponents, the second exponent is allowed to fluctuate, when the first one is known. The large deviation function $s(\lambda_2)$ as computed with the two approaches is plotted in Fig. 9.4. For $n = 10$ there are clear differences (notice that the fluctuations are real and not due to a lack of statistics), but upon increasing n, the differences tend to disappear, not only in the vicinity of the minimum, but also away from it. This suggests that, over long times, the two methods are equivalent. A possible explanation comes from the periodic orbit theory [17]. In fact, the very reason for observing fluctuations of the FTLE

even over long times is the existence of periodic orbits (embedded in the chaotic attractor) that are characterized by a different stability. For instance, referring to the asymmetric tent map in Fig. 9.1b, it is clear that there are two fixed points (identified by the crossing with the diagonal), whose stability is determined by the local slope of the map: the two corresponding Lyapunov exponents coincide with the minimum and maximum value of λ_1. Once the stability of the periodic orbits is known, there are powerful methods (typically based on the so-called dynamical zeta-function formalism [17]) that allow reconstructing the entire large-deviation function, although this is more the case when all sequences are allowed. Accordingly, since the fluctuations can be attributed to the presence of periodic orbits with a different degree of stability, it is implicitely reasonable to expect that any method to compute FTLEs yields the same result. What this argument leaves out is the fluctuations of the non-hyperbolic phase which, nevertheless, seem to be captured in the same way by both approaches. Finally, let us notice that the relationship with periodic orbits, that are, by definition, dynamical invariants, implies that the function $s(\boldsymbol{\lambda})$ is a dynamical invariant too.

9.3.1 Pesin Relation

The metric entropy and the positive Lyapunov exponents are related to one another. This is expressed by the Pesin relation [18],

$$H_{KS} \leq \sum_{i=1}^{D_u} \overline{\lambda}_i \tag{9.14}$$

where D_u is the number of unstable directions. In the following, I describe an insightful, though not mathematically rigorous, approach to derive the above formula. The first step consists in estimating the probability $P(\varepsilon, n)$ to select a bunch of trajectories that stay closer than ε over a time n. In order to ensure that the distance is smaller than ε along an expanding direction, it is sufficient that the inequality is satisfied at the final time n. This means that the probability for this to happen is on the order of $\varepsilon \mathrm{e}^{-\lambda_i n}$ at the initial time, where we have used that the invariant measure is smooth along the unstable directions. On the contrary, along a stable direction, it is sufficient to impose that the trajectories are closer than ε in the very beginning. Altogether, one can then write

$$P(\varepsilon, n) = \exp\left[-\sum_{i}^{D_u} \lambda_i n\right] \varepsilon^{D_u} G(\varepsilon)\,, \tag{9.15}$$

where the function $G(\varepsilon)$ accounts for the (unknown) scaling along the stable directions. A comparison with Eq. (9.11) shows that $\sum \lambda_i$ is equivalent to α and

this in turn implies not only the Pesin formula, but suggests also that the formula can be extended to the entire spectrum of pointwise entropies, by defining

$$s(\alpha) = \min \left\{ S(\boldsymbol{\lambda}) | \sum_{i}^{D_u} \lambda_i = \alpha \right\} \tag{9.16}$$

A more rigorous proof of the Pesin formula leads to the inequality (9.14), since the factorization hypothesis among the unstable directions need not be satisfied.

Finally, I recall another famous formula which links Lyapunov exponents with the information dimension D_1 of a chaotic attractor. This is the Kaplan-Yorke formula, which states that [19]

$$D_1 = n_+ + \frac{\sum_i^{n+} \lambda_i}{|\lambda_{n_+ +1}|} \tag{9.17}$$

where n_+ is the maximal number such that $\sum_i^{n+} \lambda_i > 0$. Analogously to the Pesin relationship, such a formula can be extended to link the spectrum of generalized fractal dimension with that of the Lyapunov exponents, although the resulting formula is less straightforward [20].

9.4 Non Hyperbolicity

The lack of a clear separation between stable and unstable directions is a source of non-hyperbolicity as well as of a more complex dynamics. A relatively simple example that can be accurately analysed is the *bubbling transition* [21], a phenomenon that emerges in systems where an invariant manifold progressively looses transversal stability. The typical context where this can happen is that of *synchronization transitions*. Let us consider two identical coupled maps,

$$\begin{aligned} x_{n+1} &= f(x_n) + \varepsilon(f(y_n) - f(x_n)) \\ y_{n+1} &= f(y_n) + \varepsilon(f(x_n) - f(y_n)) \end{aligned} \tag{9.18}$$

where $f(x)$ is a 1d map and ε measures the coupling strength. Upon introducing $u_n = (x_n + y_n)/2$ and $v_n = (x_n - y_n)/2$, the evolution equations can be written as

$$\begin{aligned} u_{n+1} &= \frac{1}{2}[f(u_n + v_n) + f(u_n - v_n)] \\ v_{n+1} &= \left(\frac{1}{2} - \varepsilon\right)[f(u_n + v_n) - f(u_n - v_n)]\,. \end{aligned} \tag{9.19}$$

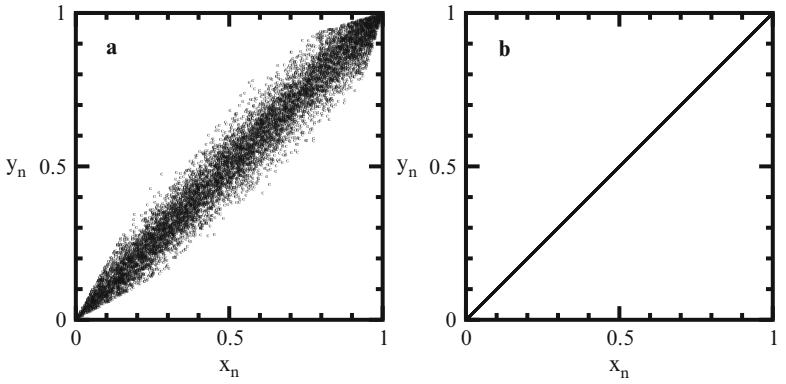

Fig. 9.5 Phase portrait for two tent maps coupled as in Eq. (9.18) for two coupling strengths: panel **a** and **b** refer to $\varepsilon = 0.23$ and $\varepsilon = 0.27$, respectively

It is easy to see that the synchronized regime $v_n = 0$ ($x_n = y_n$) is an invariant state for any ε value. It is characterized by two Lyapunov exponents: the maximal $\overline{\lambda}_1$ (along u), which coincides with that of the uncoupled map, and the transversal one $\overline{\lambda}_2$ (along v), that is determined by the linearized equation

$$\delta v_{n+1} = (1 - 2\varepsilon) f'(u_n) \delta v_n \,. \tag{9.20}$$

As a result,

$$\overline{\lambda}_2 = \log|1 - 2\varepsilon| + \overline{\lambda}_1 \,. \tag{9.21}$$

The critical coupling, where $\overline{\lambda}_2$ changes sign is $\varepsilon_c = [1 - \exp(-\overline{\lambda}_1)]/2$. For the tent map depicted in Fig. 9.1b with an atom $\mathscr{C}_0$ of length $\ell = 0.4$, the critical value is $\varepsilon_c = 0.2499\ldots$. In Fig. 9.5, the attractor is plotted below (panel a) and above (panel b) the transition, showing that in the latter case, the measure is indeed confined along the diagonal. However, the overall scenario is more complicated than it looks [22]. In fact, the relation (9.21) extends to FTLE. Therefore, the fluctuations of the two FTLEs are strictly correlated and the domain of $S(\lambda_1, \lambda_2)$ is restricted to a segment in the (λ_1, λ_2) plane, as shown in Fig. 9.6 for different coupling strengths. There we see that in a finite ε-interval, the transversal FTLEs range from positive to negative values, meaning that some (periodic) orbits are transversally stable, while other are unstable. This is quite a general scenario that is likely to arise whenever the synchronous regime is characterized by a distribution of exponents with $\lambda_{max} > \lambda_{min}$. In such cases, if a second attractor exists, outside the diagonal (this does not happen in model (9.18)) this mixed transversal stability implies that trajectories originating nearby an unstable periodic orbit escape, while those starting near a stable orbit are attracted back to the attractor. Altogether, since the two kinds of orbits are intimately interlaced, so are the basins of attractions of the synchronous and asynchronous attractors. The specific term of *riddled basin*

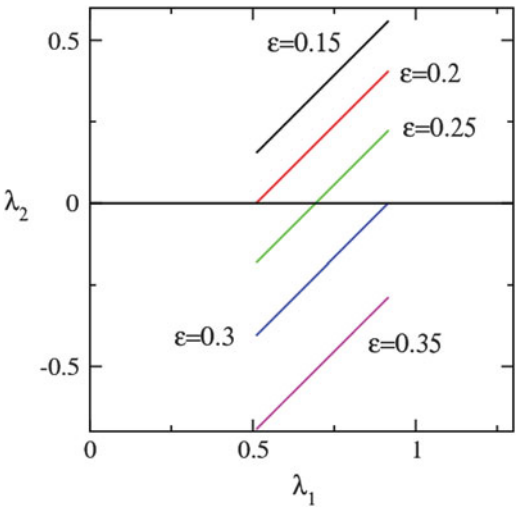

Fig. 9.6 Range of possible (λ_1, λ_2) values for different coupling strengths. Upon increasing ε, λ_2 progressively assumes negative values

has been coined [23], to mean that the points of the two basins are arbitrarily and systematically close to each other. Furthermore, the standard notion of attractor becomes questionable, since arbitrarily close to it, there are points that may escape: the weaker form of Milnor attractor [24] has to be adopted in such cases.

9.4.1 A 3d Map

3d maps offer another source of complex deterministic behaviour, with two directions that may be simultaneously unstable in an invertible dynamics. Here, I illustrate the scenario that emerges in the generalized Hénon map $x_{n+1} = a - x_{n-1}^2 - bx_{n-2}$ (again for $a = 1.4$ and $b = 0.1$). At variance, with the two coupled 1d maps, here, the first two FTLEs may be independent of each other. The domain of values taken by λ_1 and λ_2 is plotted in Fig. 9.7. The picture has been built by partitioning the (λ_1, λ_2) plane into boxes of size $10^{-3} \times 10^{-3}$ and plotting only those boxes which contain at least one point. The white circle identifies the (average) Lyapunov exponents, revealing that only the first one is positive in this case. Nevertheless, both FTLEs can be simultaneously positive, indicating that the unstable manifold is two-dimensional, but also simultaneously negative, indicating the presence of several homoclinic tangencies with the stable manifold, a property that makes the model strongly nonhyperbolic. Finally it is interesting to notice that in many places the second exponent is larger than the first one, indicating that another property of hyperbolic dynamics is violated: i.e. the ordering of the finite-time Lyapunov exponents. In fact, in uniformly hyperbolic systems, the transversality between stable and unstable manifolds implies that the positive FTLEs are strictly separated from the negative ones. This is the concept of dominated Oseledec splitting [25].

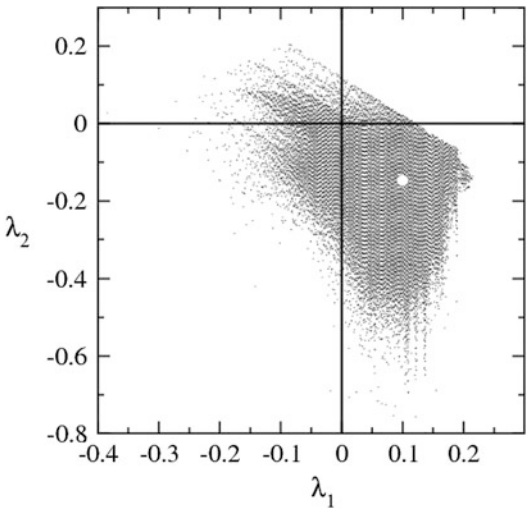

Fig. 9.7 Lyapunov exponent domain for the generalized Henon map ($a = 1.4$ and $b = 0.1$). The numerical values are obtained by computing the FTLE over 25 iterates

9.5 Space-Time Chaos

In spatially extended systems it is known that, in the thermodynamic limit, i.e. for the size $L \to \infty$, the Lyapunov exponents $\overline{\lambda}_i$ depend on the scaled variable $\rho = i/L$. This means that the chaotic dynamics is extensive, i.e., for instance, the Kolmogorov-Sinai entropy is proportional to the system size [14,26]. From the point of view of the fluctuations, the scenario is less clear. If a dynamical system were the Cartesian product of uncoupled ones (perfect extensivity with the typical meaning of the word), $S(\boldsymbol{\lambda})$ would be the sum of various contributions, each dependent on a few variables (those which characterize the single systems). To what extent, does this naive idea apply to a generic space-time system? A direct and reliable numerical analysis is out of question, as it would require a prohibitive statistics. A possible way out consists in focusing on not-too-large deviations, in practice, on Gaussian fluctuations. In practice, this amounts to consider a parabolic approximation of S around the minimum [27],

$$S(\boldsymbol{\lambda}) \approx \frac{1}{2}(\boldsymbol{\lambda} - \overline{\boldsymbol{\lambda}})\mathbf{Q}(\boldsymbol{\lambda} - \overline{\boldsymbol{\lambda}})^{\dagger} \tag{9.22}$$

where † denotes the transpose. This approximation is equivalent to assuming a multivariate Gaussian distribution. In practice, instead of referring to $\mathbf{Q}$, it is preferable to consider the equivalent, symmetric, matrix, $\mathbf{D} = \mathbf{Q}^{-1}$. In fact, the elements D_{ij} can be estimated from the (linear) growth rate of the (co)variances of $(\Lambda_i(\tau) - \overline{\lambda}_i \tau)$,

$$D_{ij} = \lim_{\tau \to \infty} \left(\overline{\Lambda_i(\tau)\Lambda_j(\tau)} - \overline{\lambda}_i \overline{\lambda}_j \tau^2 \right) / \tau. \tag{9.23}$$

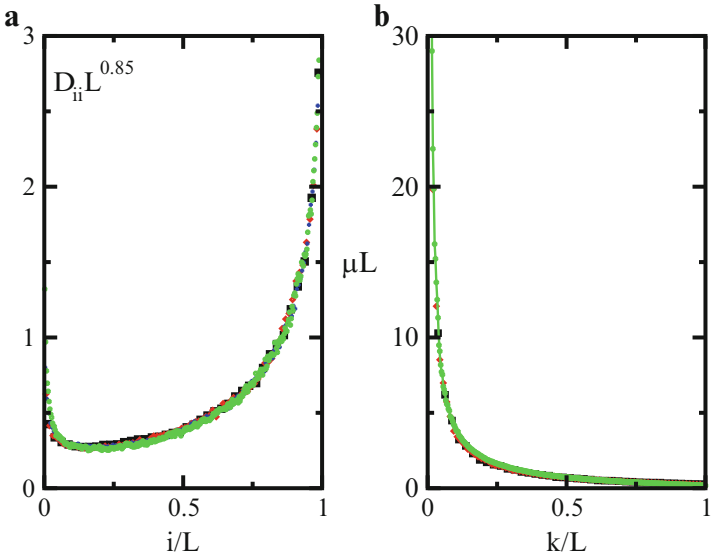

Fig. 9.8 (Panel **a**): diffusion coefficients along the diagonal for a chain of Hénon maps (lengths 80, 160 and 320); (panel **b**) principal components of the covariance matrix for the same system

In the following, I briefly illustrate the general scenario by referring to a specific model, a chain of Hénon maps,

$$x_{n+1}(i) = a - \left[x_n(i) + \varepsilon\big(x_n(i-1) - 2x_n(i) + x_n(i+1)\big)\right]^2 + b\,x_{n-1}(i)\,, \quad (9.24)$$

where ε represents the diffusive coupling strength. The scaling behaviour of the diagonal elements D_{ii} is reported in Fig. 9.8a for $a = 1.4$, $b = 0.3$, $\varepsilon = 0.025$ and periodic boundary conditions. The nice overlap of the rescaled elements reveals a rather anomalous behaviour, $D_{ii} \approx L^{-0.85}$, whose degree of universality is still to be settled. Much clearer is the scaling behaviour of the eigenvalues μ_k of the covariance matrix $\mathbf{D}$. Such eigenvalues allow characterizing in a compact way the fluctuations in spatio-temporal systems, as they represent the amplitudes along the most prominent directions. First of all the μ spectrum captures the presence of more or less hidden constraints. For instance, in the case of a symplectic dynamics, the FTLEs come in pairs whose sum is zero ($\lambda_i + \lambda_{N-i+1} = 0$). As a result, the fluctuations of the negative FTLEs are anticorrelated with those of the positive ones, so that $D_{N+1-i,j} = D_{i,N+1-j} = -D_{ij}$. This implies that half of the μ_k eigenvalues are equal to zero. It turns out that this property holds also in the case of the above Hénon maps [27]. As for the L eigenvalues that are different from zero, it can be seen in Fig. 9.8b that they scale as $1/L$. Since the matrices $\mathbf{Q}$ and $\mathbf{D}$ are diagonal in the same basis, the eigvenvalues of $\mathbf{Q}$ are the inverse of those of $\mathbf{D}$. This implies that the eigenvalues of $\mathbf{Q}$ scale also as $1/L$ and this eventually implies that the large deviation function S (in the vicinity of the minimum) is proportional

to the number L of degrees of freedom. This is a different way of assessing the extensivity of space-time chaos from the standard way mentioned in the beginning of this section. In fact, in the trivially extensive case of uncoupled maps, there would be a perfectly degenerate μ_k spectrum with exponents that do not scale at all with L. The only reminiscence of this behaviour can be observed in the beginning of the spectrum, where one can notice a divergence which is due to the existence of one and only one direction along which the fluctuations remain finite in the thermodynamic limit. Altogether, the implications of this form of extensivity are still to be fully appreciated.

9.6 Stable Chaos

Another example, where large deviations are responsible for an intriguing dynamical behaviour is that of the so-called *stable chaos*, i.e. a dynamics that is characterized by a negative Lyapunov exponent and yet is irregular [28]. This phenomenon has been recently observed in models of neural networks [29], but for the sake of coherence with the other models discussed in this chapter, I consider a 1d coupled map lattice,

$$x_i(t+1) = (1-\varepsilon) f(x_i(t)) + \frac{\varepsilon}{2}[f(x_{i-1}(t)) + f(x_{i+1}(t))] \tag{9.25}$$

where $\varepsilon \in [0,1]$ is the coupling constant and the map of the interval f is piecewise linear,

$$f(x) = \begin{cases} x/\alpha_1 & 0 \le x \le \alpha_1 \\ 1-(1-\beta)(x-\alpha_1)/\eta & \alpha_1 < x < \alpha_1 + \eta \\ \beta + (x - x_c - \eta)/\alpha_2 & \alpha_1 + \eta < x \le 1, \end{cases} \tag{9.26}$$

This continuous map is composed of three branches, one of which (the middle one) is highly expanding, but rarely visited if $\eta \ll 1$. For $\alpha_1 = 1/2.7$, $\beta = 0.07$, $\alpha_2 = 10$, and $\eta \ll 1$, the single map evolves towards a stable period-3 solution, while large lattices of such maps typically (for a broad range of coupling values) exhibit an irregular dynamics in spite of a negative maximal Lyapunov exponent. The paradox can be resolved by noticing that the chaotic behaviour exhibited by this model is akin to that of (chaotic) cellular automata [30]. In fact, in both cases, in finite systems, generic initial conditions, sooner or later, collapse onto periodic orbits: in a cellular automaton, this is because there exists a finite number of different configurations; in the coupled-map model, this is because of the contraction in phase-space. On the other hand, the average time needed to approach the final attractor grows exponentially with the system size. Therefore, in infinitely extended systems it is legitimate to claim that the genuine invariant measure is that one generated by the chaotic dynamics, although it is characterized by a negative Lyapunov exponent.

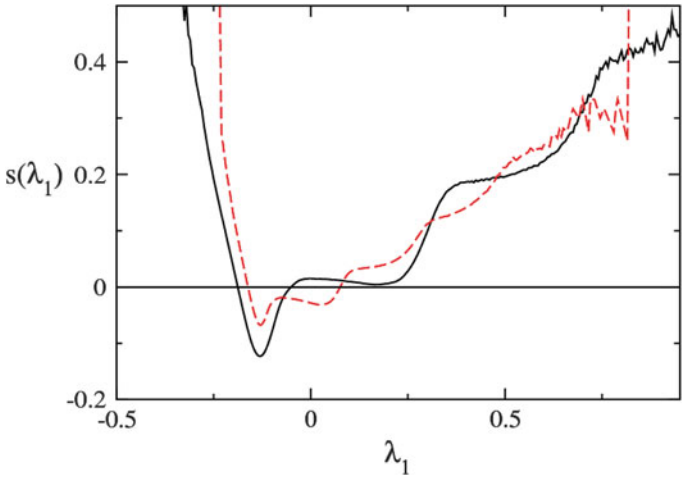

Fig. 9.9 Distribution of FTLEs for the map (9.25) and (9.26) for $\varepsilon = 2/3$ and $\eta = 10^{-4}$, where the average Lyapunov exponent is negative (the chain length is $L = 200$). *Solid* and *dashed curves* refer to $n = 20$ and 40, respectively

Roughly speaking the reason why this awkward phenomenon is able to self-sustain is that small but finite perturbations can be suddenly amplified and become of order 1. The reader interested in a more detailed description of the phenomenon can look at Ref. [28]. Here, I limit myself to comment on the role of large deviations. In fact, the reference to finite perturbations seems to indicate that one cannot extract relevant information from the evolution of infinitesimal perturbations (i.e. from Lyapunov exponents). This is indeed true for the strictly discontinuous case ($\eta = 0$). Nevertheless, in the more realistic case of a continuous rule, interesting discoveries can be made by looking at $s(\lambda_1)$. The results obtained for $n = 20$ and 40 iterates are plotted in Fig. 9.9.

There one can notice a reasonable overlap, although finite-size corrections are still large. The smoothed step are indeed a manifestation of the still relatively small number of visits of the sample trajectory to the expanding branch of the map. It is nevertheless clear that the most probable (negative) Lyapunov exponent is accompanied by a positive tail of the large deviation function which thus reveals a signature of standard deterministic chaos. The origin of such a signature resides in the existence of a chaotic repeller and to the fact that the trajectory occasionally comes arbitrarily close to it. The very existence of a chaotic repeller can be traced back to the presence of the highly expanding branch of the single map. How the expansion, sporadically experienced in the vicinity of the repeller, can sustain an overall chaotic dynamics still needs to be clarified, but it is encouraging to notice that a large deviation approach may help to bridge seemingly contradictory observations.

References

1. E. Ott, *Chaos in Dynamical Systems* (Cambridge University Press, Cambridge, 2002)
2. H.G. Schuster, W. Just, *Deterministic Chaos: An Introduction* (Wiley-VCH, Weinheim, 2005)
3. J-P. Eckmann, D. Ruelle, Rev. Mod. Phys. **57**, 617 (1985)
4. Y. Sinai, Scholarpedia **4**, 2034 (2009)
5. R. Badii, A. Politi, *Complexity: Hierarchical Structures and Scaling in Physics* (Cambridge University Press, Cambridge, 1998)
6. P. Grassberger, H. Kantz, Phys. Lett. A **113**, 235 (1995)
7. F. Christiansen, A. Politi, Nonlinearity **9**, 1623 (1996)
8. A. Renyi, *Probability Theory* (North-Holland, Amsterdam, 1970)
9. R. Benzi, G. Paladin, G. Parisi, A. Vulpiani, J. Phys. A **17**, 3521 (1984)
10. H. Fujisaka, Prog. Theor. Phys. **70**, 1264 (1983)
11. I. Shimada, T. Nagashima, Prog. Theor. Phys. **61**, 1605 (1979); G. Benettin, L. Galgani, A. Giorgilli, J.M. Strelcyn, Meccanica **15**, 9 (1980)
12. F. Ginelli, P. Poggi, A. Turchi, H. Chaté, R. Livi, A. Politi, Phys. Rev. Lett. **99**, 130601 (2007)
13. P. Grassberger, R. Badii, A. Politi, J. Stat. Phys. **51**, 135 (1988)
14. D. Ruelle, *Thermodynamic Formalism* (Cambridge University Press, Cambridge, 2004)
15. G. Gallavotti, E.G.D. Cohen, Phys. Rev. Lett. **74**, 2694 (1995)
16. G. Baier, M. Klein, Phys. Lett. A **151**, 2811 (1990)
17. W. Parry, M. Pollicott, *Zeta Functions and the Periodic Orbit Structure of Hyperbolic Dynamics*. Astérisque, vol. 187–188 (Société mathématique de France, Montrouge, 1990); P. Cvitanovic, Chaos **2**, 1 (1992)
18. Y. Pesin, Russ. Math. Surv. **32**, 55 (1977)
19. J.L. Kaplan, J.A. Yorke, in *Functional Dierential Equations and Approximations of Fixed Points*, vol. 2049, ed. by H-O. Peitgen, H-O. Walther (Springer, Berlin, 1979)
20. R. Badii, A. Politi, Phys. Rev. A **35**, 1288 (1987)
21. P. Ashwin, J. Buescu, I. Stewart, Phys. Lett. A **193**, 126 (1994)
22. A. Pikovsky, P. Grassberger, J. Phys. A **24**, 4587 (1991)
23. J. Alexander, J.A. Yorke, Z. You, I. Kan, Int. J. Bifurc. Chaos **2**, 795 (1992)
24. J.W. Milnor, Scholarpedia **1**, 1815 (2006)
25. C. Pugh, M. Shub, A. Starkov, Bull. Am. Math. Soc. **41**, 1 (2004); J. Bochi, M. Viana, Ann. Math. **161**, 1423 (2005)
26. P. Grassberger, Phys. Scr. **40**, 346 (1989)
27. P. Kuptsov, A. Politi, Phys. Rev. Lett. **107**, 114101 (2011)
28. A. Politi, A. Torcini, Stable chaos, in *Nonlinear Dynamics and Chaos* (Springer, Heidelberg, 2010)
29. R. Zillmer, R. Livi, A. Politi, A. Torcini, Phys. Rev. E **74**, 036203 (2006)
30. S. Wolfram, Rev. Mod. Phys. **55**, 601 (1983)

Chapter 10
Anomalous Diffusion: Deterministic and Stochastic Perspectives

Roberto Artuso and Raffaella Burioni

Abstract Normal diffusion arises in a natural way from random walks with uncorrelated steps of bounded variance, or, in the deterministic setting, from wandering trajectories of a chaotic map. There are many ways in which such a picture fails, and, for instance, the variance of the traveller's position does not grow linearly with time. We review the basic mechanisms that induce deviations from normal transport (long waiting times, broad step length distributions, intermittency, topological issues), and we describe how their origin can be traced back in stochastic and deterministic settings, illustrating a few techniques that allow for a quantitative analysis of such anomalies.

10.1 Introduction

In this contribution we illustrate how to deal with systems where a transport process sets in with profound differences with respect to the paradigmatic – normally diffusing – case, where the variance of the position grows linearly with time, and a description in terms of a diffusion equation becomes asymptotically correct. In the last few decades it has been realized that systems which behave anomalously are not to be considered as cumbersome examples, but rather are both representative of important physical issues, and, on a more conceptual perspective, they witness the physical import of generalized central limit theorem, where the "attracting"

R. Artuso
Dipartimento di Scienza e Alta Tecnologia, Università degli Studi dell'Insubria, Via Valleggio 11, Como, I-22100, Italy
e-mail: roberto.artuso@uninsubria.it

R. Burioni (✉)
Dipartimento di Fisica and INFN, Gruppo collegato di Parma, Viale G.P. Usberti 7/A, 43124 Parma, Italy
e-mail: raffaella.burioni@unipr.it

A. Vulpiani et al. (eds.), *Large Deviations in Physics*, Lecture Notes in Physics 885,
DOI 10.1007/978-3-642-54251-0_10,

distribution is not Gaussian. The settings where such anomalies have been invoked are simply too many to mention, ranging from 2-d fluid flows [1], to the description of human travels [2]: we here concentrate on a very small set of examples, with a twofold purpose: first we want to stress the basic mechanisms that give rise to anomalies (long waiting times, broad step length distributions, ballistic flights, topological issues), secondly we want to emphasize how stochastic methods can play an important role in deterministic examples, where, however, they have to be supplemented by more appropriate techniques.

10.2 Stochastic Anomalous Transport

We start by introducing the relevant quantities we will use in the rest of the chapter, then we provide the simplest examples of anomalous transport, pointing out the relationships with a generalized form of the central limit theorem.

10.2.1 Moments and Scaling

For simplicity, we consider transport in one dimension, and let X represent the diffusing variable, while t denotes the (either continuous or discrete) time. We will denote by $\mathscr{P}(X,t)$ the probability distribution function (PDF), of being at position X at time t. The moments of the distribution are thus defined by

$$M_n(t) = \langle X^n \rangle(t) = \int_{-\infty}^{\infty} dX\, X^n \mathscr{P}(X,t). \tag{10.1}$$

More generally we can define moments for any real order q, as

$$\sigma_q(t) = \langle |X|^q \rangle = \int_{-\infty}^{\infty} dX\, |X|^q \mathscr{P}(X,t); \tag{10.2}$$

we will be interested in the large t asymptotics of such moments, so we define the corresponding spectrum $\beta(q)$ as

$$\sigma_q(t) \sim t^{\beta(q)}, \tag{10.3}$$

or, equivalently,

$$\beta(q) = \lim_{t\to\infty} \frac{\ln \sigma_q(t)}{\ln t}; \tag{10.4}$$

(actually there are more sophisticated ways of defining the algebraic growth of moments, that eliminate problems which may arise in (10.4) due to subleading contributions, see for instance [3]). The "normal" case, random walk being the paradigmatic example, leads to the spectrum $\beta(q) = q/2$ (and in particular a linearly growing variance), characterized by a Gaussian PDF

$$\mathscr{P}_G(X,t) = \frac{1}{\sqrt{4\pi Dt}} e^{-\frac{X^2}{4tD}}, \tag{10.5}$$

where the diffusion constant D is defined as

$$D = \lim_{t\to\infty} \frac{M_2(t)}{2t}. \tag{10.6}$$

Notice that (10.5) may be rewritten in the scaling form:

$$\mathscr{P}_G(X,t) = \frac{1}{t^{1/2}} \mathscr{H}_G(|X|/t^{1/2}), \tag{10.7}$$

where

$$\mathscr{H}_G(z) = \frac{1}{\sqrt{4\pi D}} e^{-\frac{z^2}{4D}}. \tag{10.8}$$

Since $|z|^q \mathscr{H}_G(z)$ is integrable for any non negative q, the scaling form (10.7) automatically yields the normal spectrum $\beta(q) = q/2$.

The usual way in which the diffusing variable arises is via a partial sum (our notation refers to discrete t case, but it is easily generalizable):

$$X_t = \sum_{\tau=0}^{t-1} x_\tau, \tag{10.9}$$

i.e. a sum of i.i.d. random variables in the simplest probabilistic setting (like a random walk), or a Birkhoff sum for instantaneous displacements, in the deterministic case. The form of the PDF (10.5), is then dictated by the Central Limit Theorem. Some care has to be taken in using the asymptotic PDF when evaluating moments asymptotics, since no uniform convergence is guaranteed in the CLT: more precisely let X be the sum of t i.i.d. variables, σ being the (finite) width of the distribution: once the scaled variable

$$Y = \frac{X - t < x >}{\sigma\sqrt{t}} \tag{10.10}$$

is introduced we have that, as regards fluctuations,

$$\lim_{t\to\infty} P(Y > H) = \int_H^\infty \frac{dw}{\sqrt{2\pi}} e^{-w^2/2} \tag{10.11}$$

but, for finite t indeed deviations occur [4–6]. In the case where the original PDF of the x variable has sufficiently fast tails decay, this is immaterial, since deviations are expressed as a perturbative series in $1/\sqrt{t}$, which provide subleading corrections to the asymptotic behavior.

Anomalous diffusion is generally associated to a second moment which does not grow linearly (i.e. $\beta(2) \neq 1$),

$$\langle X^2 \rangle(t) \sim t^\gamma \qquad \gamma \neq 1; \tag{10.12}$$

subdiffusion concerns the case $\gamma < 1$, while the opposite case ($\gamma > 1$) is referred to as superdiffusion: more generally anomalies may also arise in the form of logarithmic corrections.

Anomalous diffusion represents a much studied issue in the last decades, and several reviews have been devoted to the subject (see for example [7–10]): here our focus is on a slightly different perspective: through the analysis of model systems we will try to show how features of anomalous transport are closely linked to other dynamical and topological issues both in the deterministic and in the stochastic approach. One of the features we will consider in some detail is connected to the notion of *strong* anomalous diffusion, which arises when the whole moments spectrum is considered: according to [11] a remarkably interesting case is the one in which a single scaling fails to account for the whole behavior so that

$$\beta(q) \neq \alpha \cdot q \qquad \forall q; \tag{10.13}$$

differently from the standard situation for "normal", Gaussian transport.

Notice that a "weak" anomalous transport is quite easily obtained from a scaling form of the PDF: if

$$\mathscr{P}(X,t) = \frac{1}{t^{\alpha/2}} \mathscr{H}(|X|/t^{\alpha/2}), \tag{10.14}$$

and the condition

$$|z|^q \mathscr{H}(z) \in \mathrm{L}(\mathrm{R}_+) \qquad \forall q \geq 0 \tag{10.15}$$

is satisfied (i.e. the functions in (10.15) are integrable on the positive half line), we get

$$\beta(q) = \alpha/2 \cdot q, \tag{10.16}$$

that, whenever $\alpha \neq 1$, leads to (weak, single-scale) anomalous behavior. This observation is however rather formal, if we think about it in terms of the central

limit theorem: as a matter of fact if the starting probability is in the basin of attraction of the Gaussian distribution then property (10.15) is satisfied, but this is not the case for other stable distributions that are relevant to the present context: namely Lévy stable laws.

10.2.2 A Few Observations About Lévy Stable Laws

Lévy distributions appear in the problem of finding *stable* laws, namely PDF which do not change shape (apart from a dilation and, eventually, a translation) when passing from a single random variable y, to the sum $Y_t = \sum_{i=0}^{t-1} y_i$ of i.i.d. random variables: this means that for some constants Γ_t and Δ_t one has

$$\mathscr{P}(Y', t)dY' = P_1(y)dy, \tag{10.17}$$

where $Y' = \Gamma_t y + \Delta_t$ and $P_1(y)$ is the common PDF of the random variables y_i. A physically interesting interpretation of (10.17) is as a fixed point of a renormalization group transformation [6], which originates the following picture: if we start from a single variable distribution P_1 and consider higher and higher sums of independent random variables all distributed according to P_1, the process leads asymptotically to a stable law: the attracting fixed points have different basins of attraction, that are essentially determined by the tails of P_1. The Gaussian fixed point has a large basin of attraction, consisting of all P_1 decaying at least as $|y|^{-3}$ as $y \to \pm\infty$. Broad distributions (with weaker asymptotic decay) fall into the basin of attraction of Lévy stable laws [4]: a complete account of this class is outside the scope of the present contribution, we will just say a few words about the symmetric (zero average) case, where the distribution depend just on a single exponent μ (once we fix an overall scale). The exponent μ is obviously related to the decay law: both Lévy laws and the set of P_1 in their basin of attraction fall as $|y|^{-(1+\mu)}$ as $y \to \pm\infty$: $\mu > 0$ has to be imposed in order to get a bona fide (normalizable) probability distribution, while if $\mu \geq 2$ we enter the basin of attraction of the Gaussian distribution, since the variance of the distribution function is finite. In general we have no explicit analytic form for the Lévy stable laws $L_\mu(z)$, except when $\mu = 1$:

$$L_1(z) = \frac{1}{z^2 + \pi^2} \tag{10.18}$$

(Cauchy distribution), and $\mu = 1/2$:

$$L_{1/2}(z) = \frac{2}{\sqrt{\pi}} \frac{e^{-1/(2z)}}{(2z)^{3/2}} \tag{10.19}$$

(Smirnov distribution) (see [4]). From an analytic point of view a key result is that an explicit expression is available for the Fourier transform:

$$\hat{L}_\mu(k) = \int_{-\infty}^{+\infty} dz\, e^{ikz} L_\mu(z) = e^{-\gamma_\mu |k|^\mu} \tag{10.20}$$

(see [4] for full details, and explicit expressions of pre factors γ_μ). The generalized CLT in this case take the following form:

$$\mathscr{P}_\mu(X,t) \asymp \frac{1}{t^{1/\mu}} L_\mu(X/t^{1/\mu}), \tag{10.21}$$

where again we are considering symmetric distributions (otherwise we should have treated on different footing the case where $\mu > 1$, where $zL_\mu(z)$ is integrable, and $\mu \in (0,1]$, where the average diverges). Though the scaling form in (10.21) is as (10.14), condition (10.15) holds just when $q < \mu$, so we have a very peculiar (anomalous) moments spectrum

$$\sigma_q(t) \sim \begin{cases} t^{q/\mu} & q < \mu \\ \infty & q \geq \mu \end{cases} \tag{10.22}$$

This is indeed related to the fact that Lévy laws exhibit themselves divergence of moments: this motivated the introduction of different truncation of L_μ (see for instance [7, 12, 13]): notice that as soon as we correct for fat tails in the original P_1, we shift to the basin of attraction of Gaussian distribution in the CLT. In order to give an example of a non trivial spectrum of moments we introduce the following heuristic model: we use Lévy asymptotic for moments, but introduce a cutoff corresponding to a maximal speed of transport, so that at finite time t, the corresponding sum of increments $X_t \leq v \cdot t$: the corresponding moments are then expressed as

$$\sigma_q(t) = \frac{2}{t^{1/\mu}} \int_0^{v \cdot t} dX\, L_\mu(X/t^{1/\mu}) X^q. \tag{10.23}$$

While for all $q < \mu$ the spectrum (10.22) is reproduced, the cutoff avoid divergences for $q > \mu$, and we may estimate

$$\sigma_q(t) \sim t^{q/\mu} \int_0^{t^{1-1/\mu}} dz\, L_\mu(z) z^q \sim t^{q/\mu} \cdot t^{(1-1/\mu)\cdot(q-\mu)}, \tag{10.24}$$

with corresponding scaling function:

$$\beta(q) = \begin{cases} q/\mu & q < \mu \\ q - (\mu - 1) & q > \mu \end{cases} \tag{10.25}$$

which is typical for "strong" anomalous diffusion [11].

10.2.3 An Extension: Continuous Time Random Walks

Up to now we have considered processes in which the events' clock is regular, and anomalies arise only from a fat distribution of step lengths. Continuous time random walks (CTRW) [14, 15] are stochastic processes in which jumps occur at times t_i, chosen according to some waiting time distribution. In their more general attire (again for simplicity we consider a 1-d setting) they are described by a probability density function $\wp(l, t)$ that a step of length l takes place at a time t. In their simplest version, space and time distributions are decoupled

$$\wp(l, t) = \omega(l)\psi(t). \tag{10.26}$$

Given such a probability density, once again we want to construct $\mathscr{P}(X, T)$, the PDF that a walker is at the position X at time T.

We assume that the process starts at $x = 0$ at time $t = 0$, and use the decomposition

$$\mathscr{P}(X, T) = \sum_{n=0}^{\infty} \Omega_n(X)\Xi_n(T), \tag{10.27}$$

where $\Omega_n(X)$ is the probability density that the walker reaches the position X exactly in n steps, while $\Xi_n(t)$ is the probability density that the physical time to perform exactly n steps equals T. We will instead denote by $\Psi_n(T)$ the probability that the same number of jumps occurs ending the sequence just before a jump. Now:

$$\Omega_n(X) = \int_{-\infty}^{+\infty} dx_1 \ldots \int_{-\infty}^{+\infty} dx_n\, \omega(x_1)\cdots\omega(x_n)\delta(X - x_1 - \cdots - x_n) \tag{10.28}$$

and a particularly simple expression is obtained in the Fourier representation:

$$\hat{\omega}(k) = \int_{-\infty}^{+\infty} dx\, e^{ikx}\, \omega(x), \tag{10.29}$$

that is

$$\hat{\Omega}_n(k) = \hat{\omega}(k)^n; \tag{10.30}$$

as regards the time distribution, we have to modify the argument a little bit, by taking into account the possibility that once the walker jumped the n-th time, it waits there up to the observation time t. The probability that a jump does not take place up to time t is

$$\varphi(t) = 1 - \int_0^t d\tau\, \psi(\tau); \tag{10.31}$$

and so

$$\Xi_n(T) = \int_0^T d\,\tau\, \Psi_n(\tau)\varphi(T-\tau). \tag{10.32}$$

As time distributions are supported on the positive real axes, the proper representation is in terms of Laplace transform:

$$\tilde{\psi}(s) = \int_0^\infty dt\, e^{-st}\, \psi(t)\, : \tag{10.33}$$

so

$$\Psi_n(t) = \int_0^\infty dt_1 \ldots \int_0^\infty dt_n\, \psi(t_1)\cdots\psi(t_n)\delta(t - t_1 - \cdots - t_n), \tag{10.34}$$

and, in terms of the Laplace transform,

$$\tilde{\Psi}_n(s) = \tilde{\psi}(s)^n. \tag{10.35}$$

Now, from Eq. (10.31)

$$\tilde{\varphi}(s) = \frac{1-\tilde{\psi}(s)}{s}, \tag{10.36}$$

and we finally get

$$\tilde{\Xi}_n(s) = \frac{(1-\tilde{\psi}(s))}{s}\tilde{\psi}(s)^n, \tag{10.37}$$

so, once we sum the geometric series in (10.27), we get, for the Fourier-Laplace transform of $\mathscr{P}(X,t)$, the following representation

$$\breve{\mathscr{P}}(k,s) = \frac{(1-\tilde{\psi}(s))}{s}\frac{1}{(1-\hat{\omega}(k)\tilde{\psi}(s))} \tag{10.38}$$

which is the key expression to deal with in applications of (factorized) CTRW. In particular moments of integer order may be straightforwardly derived from the (space) Fourier transform of $\mathscr{P}$, the so called generating function:

$$\mathscr{G}_t(k) = \hat{\mathscr{P}}(k,t) = \frac{1}{2\pi i}\int_{a-i\infty}^{a+i\infty} ds\, e^{st}\breve{\mathscr{P}}(k,s), \tag{10.39}$$

since

$$M_n(t) =< X^n > (t) = (-i)^n \left.\frac{d^n}{dk^n}\hat{\mathscr{P}}(k,t)\right|_{k=0} = \frac{1}{2\pi i}\int_{a-i\infty}^{a+i\infty} ds\, e^{st}\tilde{M}_n(s); \tag{10.40}$$

a, as usual, has to be chosen larger than the real part of all the singularities of the transform. The last identity plays an important technical role, since we are interested in the large time behavior of $M_n(t)$, which is connected to small s behavior of $\tilde{M}_n(s)$ by means of Tauberian theorems [5]:

$$\tilde{\eta}(u) \sim \frac{1}{u^\rho} L\left(\frac{1}{u}\right) \quad u \to 0 \iff \eta(t) \sim \frac{1}{\Gamma(\rho)} t^{\rho-1} L(t) \quad t \to \infty \tag{10.41}$$

for $\rho > 0$, and L slowly varying (i.e. $L(ty)/L(t) \to 1$ when $t \to \infty$).

Let us discuss a specific example (somehow complementary to the one we discussed in the former section): we consider a Gaussian distribution in the jump lengths

$$\omega(x) = \frac{1}{\sqrt{2\pi}} e^{-x^2/2} \qquad \hat{\omega}(k) = e^{-k^2/2}, \tag{10.42}$$

and waiting times with fat tails:

$$\psi(t) \sim \frac{\alpha}{\Gamma(1-\alpha)} \frac{\tau^\alpha}{t^{1+\alpha}} \qquad 0 < \alpha < 1; \tag{10.43}$$

in order to evaluate the small s behavior of the transform $\tilde{\psi}(s)$ we cannot use directly a Tauberian argument (10.41), since $\psi(t)$ vanishes too fast as $t \to \infty$. We may however use the following argument: we introduce

$$G(t) = \int_t^\infty d\tau\, \psi(\tau) \qquad \psi(t) = -\frac{dG}{dt}, \tag{10.44}$$

and use integration by parts:

$$\tilde{\psi}(s) = -\int_0^\infty dt\, e^{-st} \frac{dG}{dt} = G(0) + s\int_0^\infty dt\, e^{-st} G(t), \tag{10.45}$$

and use the Tauberian theorem to estimate the last integral in (10.45); so we obtain

$$\tilde{\psi}(s) \sim 1 - \tau^\alpha s^\alpha, \tag{10.46}$$

and the small s expression for $\breve{\mathscr{P}}(k,s)$ is

$$\breve{\mathscr{P}}(k,s) \sim \frac{\tau^\alpha s^{\alpha-1}}{(1 - e^{-k^2/2}(1 - \tau^\alpha s^\alpha))}. \tag{10.47}$$

If we consider the variance, we are led to evaluate (10.40)

$$\tilde{M}_2(s) = -\frac{d^2}{dk^2}\breve{\mathscr{P}}(k,s)\Big|_{k=0} \sim \frac{1}{\tau^\alpha s^{1+\alpha}}, \tag{10.48}$$

so that, for large t we get by (10.41)

$$M_2(t) \sim t^\alpha, \tag{10.49}$$

which provides an example of subdiffusion.

10.2.4 Topological Effects in Subdiffusion: Weak Anomalous Diffusion and Random Walks on Graphs

In the previous section, we have seen an example of subdiffusion generated by a CTRW with Gaussian distributed step lengths and heavy tailed traps, leading to a non trivial scaling form of the probability distribution and of the moments.

A key point in the previous analysis is the scaling form of the PDF (10.14), that, together with the condition (10.15), leads to anomalous diffusion with a single scaling length, that rules all the moments of the distribution.

To get a further insight on the scaling properties of the probability distribution functions involved in anomalous diffusion, we will now consider a typical case of subdiffusion generated by topological effects, that is random walks on graphs [16]. This is still a very general approach, as it is well known that large scale behavior of random walks exhibits the same phenomena as that of diffusions on manifolds or fractals. Now the diffusing variable X can take discrete values, defined to be the vertices of the graph, and jumps can occur between vertices which are connected by a link, through a simple random walk [17]. There is therefore a topological effect induced by the underlying structure.

We will always be interested in the long time behavior of the PDF and we will consider its scaling form in this limit. Interestingly, rigorous results can be obtained for the scaling form of the $\mathscr{P}(X,t)$ in particular cases, through the so called sub-Gaussian estimates [18]. These bounds allow to give, under precise topological conditions for the diffusion process on the graph, a general scaling form for $\mathscr{P}(X,t)$, in terms of relevant exponents. Moreover, this approach provides a direct link, through the Einstein relation, with the resistance of the equivalent electric problem on the graph [19]. In these cases, which can be rigorously controlled, a weak anomalous diffusion is always observed, and a scaling dominated by a single scale is detected in the moments. Analogous estimate can be obtained by Flory arguments [7].

In the simple random walk, the walker can occupy positions on the sites of the graph $\mathscr{G}$, which is a countable set $V_{\mathscr{G}}$ of vertices (or sites) X connected pairwise by a set $L_{\mathscr{G}}$ of unoriented edges (or links) $(X, Y) = (X, Y)$. The connectivity of the site X, i.e. the number of its nearest neighbors, is denoted with z_X, and the graph is assumed to be locally finite. A path in $\mathscr{G}$ is a sequence of consecutive edges $\{(X, Y)(Y, K) \dots (K, M)\}$ and its length is the number of edges in the sequence. In connected graphs, for any two vertices $X, Y \in V_{\mathscr{G}}$, there is always a path joining them. This allows to define an intrinsic distance $r_{X,Y}$, as the length of the shortest path connecting the vertices X and Y. The intrinsic distance in turn defines on the graph the balls of radius $r \in N$ and center $o \in V_{\mathscr{G}}$, as the subgraph of $\mathscr{G}$, given by the set of vertices $V(o, r) = \{X \in V | r_{X,o} \leq r\}$ and by the set of edges $L(o, r) = \{(X, Y) \in L | X \in V(o, r), Y \in V(o, r)\}$. An important requirement for the graph is that the volume growth is polynomial. If we denote by $|S|$ the number of elements of a set, then $|V(o, r)|$, as a function of the distance r, describes the growth rate of the graph at the large scales. In particular, a graph is said to have polynomial growth if $\forall o \in V_{\mathscr{G}}$, at large r:

$$|V(o, r)| \sim r^d. \tag{10.50}$$

This is a global relation on the volume growth of the graph. Interestingly, in recent works this can sometimes be replaced by a weaker local condition of *volume doubling* that is:

$$|V(o, 2r)| \leq C |V(o, r)| \tag{10.51}$$

where C is a suitable constant, and this condition is used linked to the Harnack inequalities [20]. The parameter d is the connectivity dimension of the graph, and it coincides with the Euclidean dimension in regular lattices and in Euclidean spaces. It also coincides with the fractal dimension when the graph is embedded by preserving its topological structure.

The adjacency matrix $A_{X,Y}$, that fully describes the topology of the graph is:

$$A_{XY} = \begin{cases} 1 \text{ if } (X, Y) \in E_{\mathscr{G}} \\ 0 \text{ if } (X, Y) \notin E_{\mathscr{G}} \end{cases} \tag{10.52}$$

The (simple) random walk on the graph $\mathscr{G}$ is then defined by the jumping probabilities p_{XY} between nearest neighbors sites X and Y:

$$p_{XY} = \frac{A_{XY}}{z_X} = (Z^{-1} A)_{XY} \tag{10.53}$$

where $Z_{XY} = z_X \delta_{XY}$ and z_X is the number of nearest neighbors of site X. We assume the graph to be locally finite. Then the probability distribution of reaching in t steps site Y starting from X is:

$$\mathscr{P}(XY, t) = (p^t)_{XY} \ . \tag{10.54}$$

As the graph can in general be highly inhomogeneous, we will include in the notation also the dependence on the starting point, which will be useful in the following discussion. An interesting quantity for the random walks is the exit time from a set A:

$$T_A = min\{t : X_t \in \mathscr{G}\backslash A\} \tag{10.55}$$

and let us denote its average value from the starting point X_0, the mean exit time from set A, as $E_{X_0}(A)$. Then, once defined the ball of radius r and centre $oV(o,r)$, let us denote as $E(o,r)$ the average exit time from $A = V(o,r)$ starting in $X_0 = o$ at $t = 0$. The discrete Laplace transform of $\mathscr{P}(XY,t)$, which maps the time function into its generating function, is then:

$$\tilde{\mathscr{P}}(XY)(\lambda) = \sum_{t=0}^{\infty} \lambda^t \mathscr{P}(XY,t) \tag{10.56}$$

where λ is a complex number. The function $G(X,Y) = \lim_{\lambda\to 1} \tilde{\mathscr{P}}(XY)(\lambda)$ is called the Green kernel of the problem, which can also be infinite in low dimensional graphs.

Given the random walk process on the graph, which is now entirely encoded in the topology by mean of the adjacency matrix, an interesting question is then to prove and to characterize the scaling form of the PDF, as a function of some parameters related to the topological structure of the graph. Interestingly, this can be done by sub-Gaussian estimates [18]. In these cases, the probability distribution satisfies the following relation, providing a specific scaling form:

$$\mathscr{P}(XY,t) \sim \frac{1}{|V(X,t^{1/\beta})|} \exp\left[-\left(\frac{r_{X,Y}^{\beta}}{ct}\right)^{1/(\beta-1)}\right] \tag{10.57}$$

Notice that the previous relation introduces a scaling length in the process, growing as $t^{1/\beta}$. An important result [18] is then that the scaling form is satisfied if the graph has polynomial growth with connectivity dimension d and the average exit time has a power law behavior:

$$E(o,r) \sim r^{\beta} \qquad \forall o \in V_{\mathscr{G}}. \tag{10.58}$$

The exponents in the scaling form (10.57) can be related to usual random walks quantities. We expect to recover from the scaling form the general definition of the spectral dimension of a graph, which describes the asymptotic behavior of the return probability to the starting site on graphs [21]. We have then $\mathscr{P}(X,X,t) \sim t^{-d_s/2}$. Therefore $d/\beta = d_s/2$, or $\beta = 2d/d_s$.

There are many ways of stating the sub-Gaussian results. An interesting one, holding in the case $d > \beta \geq 2$, i.e. on transient graphs, is in term of the Green kernel,

and it states that the sub-Gaussian estimate is satisfied if and only if the Green kernel has a polynomial decays:

$$G(X;Y) \sim r_{X,Y}^{-(d-\beta)}. \tag{10.59}$$

The powerful sub-Gaussian estimate is in general not easy to derive, and it has been rigorously proven for a class of deterministic fractal graphs [20]. There are many ways of stating it, beside relating it to the average exit time of to the Green kernel [18]. Let us give here a simple and not rigorous derivation, based on scaling, implying the so called Einstein relation, which correspond to the results (10.57) and (10.58) in terms of scaling exponents. Interestingly, the Einstein relation links the spectral dimension, the exponents for the resistance $R(N) \sim N^{\alpha}$ between sites at large distance N in the equivalent electric network problem, and the connectivity dimension [22] for recurrent graphs, with $d_s < 2$. This is obtained by the well known analogy between the master equation of the random walk and the Kirchhoff equations [19], that maps the graph in a networks of resistors. Let us briefly recall this mapping [23].

The PDF can be written as a function of the dynamical scaling length of the process in the following form:

$$\mathscr{P}(XY,t) = t^{-d_s/2} f\left(r_{X,Y}/\ell(t)\right) \tag{10.60}$$

where $\ell(t)$ is the scaling length on the process.

The equation for the electric potential V_X on a network of unitary resistors with a unitary current flowing from site 0 to site N reads:

$$-\sum_Y L_{Y,X} V_Y = \delta_{X0} - \delta_{XN} \tag{10.61}$$

where $L_{X,Y} = z_X \delta_{XY} - A_{XY}$ is the Laplacian matrix of the graph. This equation simply corresponds to the fact that the sum of all the currents entering a node with their sign must be zero, apart the two nodes where the current is injected and extracted. Now, the master equation of the random walk process on the graph can be written as:

$$\mathscr{P}(0X,t+1) - \mathscr{P}(0X)(t) = -\sum_Y L_{Y,X}\mathscr{P}(0Y,t)/z_Y + \delta_{X0}\delta_{t0}. \tag{10.62}$$

Denoting with $\tilde{\mathscr{P}}(0X,\omega)$ the Fourier transform of $\mathscr{P}(0X,t)$ we get

$$\tilde{\mathscr{P}}(0X,\omega)(e^{i\omega}-1) = -\sum_Y L_{Y,X}\tilde{\mathscr{P}}(0Y,\omega)/z_Y + \delta_{X0} \tag{10.63}$$

and, comparing Eqs. (10.61) and (10.63)

$$V_X = \frac{1}{z_X} \lim_{\omega \to 0} (\tilde{\mathscr{P}}(0X, \omega) - \tilde{\mathscr{P}}(NX, \omega)). \tag{10.64}$$

The potential difference between sites 0 and N as a function of their distance N, can be, hence, obtained introducing in $\lim_{\omega \to 0} \tilde{\mathscr{P}}(0N, \omega)$ the scaling form of the PDF:

$$V(N) \sim \lim_{\omega \to 0} \int dt e^{i\omega t} t^{-d_s/2} f\left(\frac{r}{\ell(t)}\right) \tag{10.65}$$

Changing the variable of integration into $t' = \omega t$ we obtain

$$V(N) \sim N^{2d/d_s - d} \lim_{\omega \to 0} g\left(\frac{r}{\tilde{\ell}(\omega)}\right) \tag{10.66}$$

where g is a suitable function and $\tilde{\ell}(\omega) = \omega^{-d_s/(2d)}$ is the correlation length in terms of the frequency ω. Therefore, one has:

$$\alpha = \frac{2d}{d_s} - d \tag{10.67}$$

holding for $d_s < 2$. For transient graphs, with $d_s > 2$, the sub-Gaussian estimate based on Green kernels can be used [24, 25]. If α is known, the scaling exponents follow. Notice that the scaling of the resistance is a static problem on the graph, and it is in general much easier to solve.

There are many open problem in proving sub-Gaussian estimate on highly inhomogeneous graphs. An interesting example is provided by combs, where it can be shown that it is impossible to rigorously derive an uniform sub-Gaussian estimates for the PDF [26].

Another very interesting case of an inhomogeneous graph where it is difficult to obtain a sub-Gaussian estimate is the so called NT_d graph, introduced in [19] and studied in terms of random walks in [27]. This is a tree graph, built recursively by starting from an origin point, and connecting it to another site a by a link, then splitting the tree from a in k branches of length 2^1, then splitting every end point of the branches into other k branches of length 2^2 and so on. On this graph, the spectral dimension can be exactly determined, and the mean square displacement grows diffusively. Due to the long 1 dimensional branches, the NT_d graph features a strong inhomogeneity, and the scaling form of the PDF is difficult to determine, even if the scaling of the moments appears to be weak and determined by a single length.

10.2.5 Topological Effects in Superdiffusion: Strong Anomalous Diffusion and Quenched Lévy Walks

In the framework of CTRW, we have considered the case of simple Lévy walks with decoupled space and time distributions. We will now consider a process where topology effects comes into play to modify this decoupling, once again crucial for the general scaling picture of the PDF. In this case the transport process can still be described by a Lévy walk, but with correlations induced by the mutual position of the steps. The general scaling form of the probability distribution can still be determined through estimates that closely follows the sub-Gaussian estimates of the previous section. However in this case the scaling of the moments is strongly modified.

In this Lévy process, scatterers are placed and spaced according to a Lévy-type distribution, so that the probability density for two consecutive scatterer to be at distance l is

$$\omega(l) \equiv \mu l_0^{\mu} \frac{1}{l^{\mu+1}}, \quad l \in [l_0, \infty), \tag{10.68}$$

where l_0 is a cutoff fixing the scale-length of the system. Then, the continuous time random walk CTRW naturally defined on this structure is a walker that moves ballistically (at constant velocity v) until it reaches one of the scatterers, and then it is transmitted or reflected with probability $1/2$. The underling structure is therefore quenched, the steps are correlated and the choice of the starting point of the walker can influence the long time behavior of the PDF.

Interestingly, this model features strong anomalous diffusion with a non trivial form of the $\beta(q)$, as the (single) scaling violation introduced by the physical cut off at finite velocity is modified due to a long tail developed in the PDF. To determine the scaling form of the PDF, one can use the same approach considered in the subdiffusive case, in the previous section, mapping the problem into the equivalent electric problem [28]. Once again, the problem is translated into the exact calculation of the scaling exponent for the resistance [29].

Then, in order to obtain the correct form of the function $\beta(q)$ it is necessary to estimate the effect of the physical cut off by a "single long jump" hypothesis, an approximation that allows to extract the most important contribution of the long tail [28]. The general picture obtained within this method applies also to higher dimension but in that case an exact calculation leading to the explicit value of the scaling exponent for the resistance is lacking. However, if this is measured from experiments or from numerical data [30], this provides the scaling form of the PDF.

For the calculation of the PDF, several initial conditions can be considered. If one averages over all the starting point of the structure at $t = 0$, and then one averages over all stochastic processes and realizations of the disorder, this is general called an *equilibrium average*, and it has been analyzed in details in [31]. Let us briefly recall the main steps of the results. For $\mu < 1$ the motion is always ballistic, while

for $\mu > 1$ a crucial point is the calculation of the probability of reaching a site at distance l at the first step. This decays as $1/l^{\mu}$ (i.e. much more slowly than $\omega(l)$) and therefore the motion is dominated by the first jump (called ballistic peak). In particular, for $1 \leq \mu \leq 2$ the first step provides the major contribution to the mean square displacement, which can be estimated to be $\langle X^2(t) \rangle \sim t^{3-\mu}$. As a matter of fact, what it happens is that the single length scaling is violated precisely by the ballistic peak and the estimate closely follows that performed in Sects. 10.2.2 and 10.2.3.

If the processes start with a scattering event, and then one averages over scattering points, a so called *non equilibrium average*, the probability of reaching a distance l at the first step is the same as that of any other scattering event. Therefore, the first-jump does not determine the behavior of the mean square displacement [31]. We will consider this case in detail, discussing the scaling form of the distribution and the strong anomalous picture arising for the moments of the PDF.

A particular care must be taken in identifying the scaling properties of the PDF, including the subleading terms that can violate the single length scaling. To be precise, the most general scaling hypothesis for $\mathscr{P}(X,t)$ is given by:

$$\mathscr{P}(X,t) = \ell^{-1}(t) f(X/\ell(t)) + g(X,t) \tag{10.69}$$

defined by a convergence in probability

$$\lim_{t\to\infty} \int_0^{vt} |\mathscr{P}(X,t) - \ell^{-1}(t) f(X/\ell(t))| dX = 0 \tag{10.70}$$

where the physical cut off $X \leq vt$ has been introduced in the upper limit of the integral. The two parts in Eq. (10.69) give their contribution in different regions: the leading contribution to $\mathscr{P}(X,t)$ is $\ell^{-1}(t) f(X/\ell(t))$, which is significantly different from zero only if X is of the order or less than $\ell(t)$. The subleading term $g(X,t)$, with $\lim_{t\to\infty} \int |g(X,t)| dX = 0$, describes the behavior at larger distances, i.e. $\ell(t) \ll X < vt$. The function $g(X,t)$ does not contribute to the PDF in the infinite time limit; however, if it does not vanish rapidly enough, it can nevertheless provide important contributions to $\langle X^2(t) \rangle$ and to the other moments.

Let us now consider the Einstein relation derived in the previous section. If we now use this new scaling form for the probability distribution, since $g(X,t)$ is relevant only in the regime $X \gg \ell(t)$ and the resistance is evaluated at a finite distance N and for a diverging characteristic length $\ell(t)$ (i.e. $\omega \to 0$), $g(X,t)$ does not provide significant contributions to the resistance $R(N)$. Therefore, recalling that the system is in 1 dimension, the scaling of the resistance is given by

$$R(N) \sim N^{2/d_s - 1}. \tag{10.71}$$

The stationary problem and the calculus of the resistance are a much more simple task than the direct solution of random walks and its spectral dimension, so that the asymptotic behavior of R at large distances can be calculated analytically [29]

obtaining $R(N) \sim N^{\mu}$ for $\mu < 1$ and $R(N) \sim N$ for $\mu > 1$. Putting this result into Eq. (10.71) we obtain the value of d_s as a function of μ. Then, the asymptotic behavior of $\ell(t)$ is obtained from the following general consideration. From the normalization of the PDF, and from its scaling form we have:

$$t^{-d_s/2} \int f\left(\frac{X}{\ell(t)}\right) K X^{d-1} dX \; = \; 1. \tag{10.72}$$

and changing the integration variable to $r/\ell(t)$ we finally obtain, in 1 dimension:

$$\ell^d(t) \sim t^{d_s/2}. \tag{10.73}$$

By using this relation, together with the result on the scaling of the resistance [29] and the Einstein relation (10.71), we finally obtain the scaling length of the process:

$$\ell(t) \sim t^{\frac{1}{1+\mu}} \quad \text{if } 0 < \mu < 1 \tag{10.74}$$

and

$$\ell(t) \sim t^{\frac{1}{2}} \quad \text{if } 1 \leq \mu. \tag{10.75}$$

Let us now consider the mean square displacement, and the other moments of the PDF. The mean square displacement reads, introducing also the physical cut off as in Sect. 10.2.2

$$\langle X^2(t) \rangle = \int_0^{vt} \ell^{-1}(t) f(X/\ell(t)) X^2 dX + \int_0^{vt} g(X,t) X^2 dX. \tag{10.76}$$

We have to take into account two anomalies with respect to the usual behavior $\langle X^2(t) \rangle \sim \ell^2(t)$. The second term $g(X,t)$ in the probability distribution can be dominant with respect the first one, as it happens precisely when averaging over any starting site [31] due to the contribution of the ballistic peak. A different anomaly can be present if the scaling function $f(x)$ decays too slowly for $x \to \infty$, as it happens in the case of the standard Lévy walk [32, 33]. Here, depending on the value of μ, both contribution can arise [28].

As we expect that the scaling violations arise from the regime where $X \gg \ell(t)$, the estimate is based on a *single long jump* hypothesis, providing the most important contribution to the moments in this region. In averages over all starting sites the probability of long jumps is much higher at the first step, hence the single long range event occurs at $t = 0$, through the contribution of the ballistic peak. Here on the other hand, it can happen, with equal probability, at any scattering site. In particular, neglecting the possibility of multiple "long jumps" we obtain, for $X \gg \ell(t)$, $P(X,t) \sim N(t)/X^{1+\mu} \ll 1$, where $N(t)$ is the number of scattering sites visited by the walker in a time t and $1/X^{1+\mu}$ is the probability for a scatterer to be followed by a jump of length X, as described by the $\omega(l)$. If one does not take into

account the single long jump, the distance crossed by the walker in time t is always of order $\ell(t)$. According to the results in [29], the number of scattering sites visited in this time is the resistance of a segment of length $\ell(t)$, i.e. $\ell(t)^\mu$ for $\mu < 1$ and $\ell(t)$ for $\mu \geq 1$. This implies that $N(t) \sim t^{\mu/(1+\mu)}$ for $\mu < 1$ and $N(t) \sim t^{1/2}$ for $\mu \geq 1$.

For $\mu < 1$ and $r \gg \ell(t)$, the $\mathscr{P}(X,t)$ reads:

$$\mathscr{P}(X,t) \sim t^{\frac{\mu}{1+\mu}} \frac{1}{X^{1+\mu}} \sim \frac{1}{\ell(t)} \left(\frac{X}{\ell(t)} \right)^{-(1+\mu)} \tag{10.77}$$

Hence the scaling function $f(x)$ features a long tail for large x decaying as $x^{-1-\mu}$. On the other hand for $\mu \geq 1$ and $X \gg \ell(t)$:

$$\mathscr{P}(X,t) \sim t^{\frac{1}{2}} \frac{1}{X^{1+\mu}} \sim \frac{1}{t^{(\mu-1)/2}\ell(t)} \left(\frac{X}{\ell(t)} \right)^{-(1+\mu)} \sim g(X,t) \tag{10.78}$$

Now $g(X,t)$ provides a subleading contribution to $\mathscr{P}(X,t)$. Indeed it is easy to see that $\lim_{t\to\infty} \int_{\ell(t)}^{vt} g(X,t) = 0$ ($\mu > 1$). This clearly indicates that the scaling is violated both from the subleading term in the scaling form of the PDF, and by the long tail developed in the PDF directly.

The contribution to $\langle X^2(t) \rangle$ of lengths X of the order or less than $\ell(t)$ is always of order $\ell(t)^2$, while, at larger distances, the dominant contribution is provided by probabilities (10.77) and (10.78). The contributions coming from these tails are, for $\mu < 1$

$$\int_{\ell(t)}^{vt} t^{\frac{\mu}{1+\mu}} \frac{X^2}{r^{1+\mu}} dX \sim t^{\frac{2+2\mu-\mu^2}{1+\mu}} \tag{10.79}$$

and for $\mu > 1$

$$\int_{\ell(t)}^{vt} t^{\frac{1}{2}} \frac{X^2}{X^{1+\mu}} dX \sim t^{\frac{5}{2}-\mu}. \tag{10.80}$$

The first part (10.79), at large times is always greater than $\ell^2(t)$, while (10.80) is dominant with respect $\ell^2(t)$ only for $\mu < 3/2$. The overall behavior of the mean square displacement is therefore given by:

$$\langle X^2(t) \rangle \sim \begin{cases} t^{\frac{2+2\mu-\mu^2}{1+\mu}} & 0 < \mu < 1 \\ t^{\frac{5}{2}-\mu} & 1 \leq \mu \leq 3/2 \\ t & 3/2 < \mu \end{cases} \tag{10.81}$$

Notice that for $0 < \mu < 3/2$ the scaling is strongly anomalous and the standard single length scaling behavior $\langle r^2(t) \rangle \sim \ell(t)^2$ is violated.

Analogously we can estimate the moments of the PDF:

$$\langle X^q(t)\rangle \sim \begin{cases} t^{\frac{q}{1+\mu}} \sim \ell(t)^q & \mu < 1,\ q < \mu \\ t^{\frac{q(1+\mu)-\mu^2}{1+\mu}} & \mu < 1,\ q > \mu \\ t^{\frac{q}{2}} \sim \ell(t)^q & \mu > 1,\ q < 2\mu - 1 \\ t^{\frac{1}{2}+q-\mu} & \mu > 1,\ q > 2\mu - 1 \end{cases} \tag{10.82}$$

The strong anomalous picture arising from the correlated Lévy walk process described in this section is expected to play a role also in higher dimensions. Interestingly, the correlation induced by the mutual position of the steps should influence experimental settings where superdiffusion appears to take place [34].

10.3 Deterministic Anomalous Transport

While the former section was based on a underlying stochastic process, it is well known that interesting transport features may be observed also in deterministic systems. For the sake of simplicity we will consider only *discrete* deterministic evolution, labelled by an integer time t, induced by a mapping T from the phase space to itself. Namely a trajectory of the system, corresponding to the initial condition x_0, will be

$$x_0,\ x_1 = T(x_0),\ x_2 = T^2(x_0),\ \ldots,\ x_n = T^n(x_0), \tag{10.83}$$

where powers indicate functional composition $T^2(y) = T(T(y))$, and so forth.

This also provides the opportunity to mention how concepts like the central limit theory or large deviations appear in a deterministic setting.

10.3.1 A Brief Tour of Intermittency

From a dynamical point of view, intermittency is characterized by long laminar, regular sequences punctuated by chaotic bursts. A paradigmatic example of such a behavior is provided by a family of one-dimensional maps on the unit interval (the phase space) [35], which we write in the following form [36] (see Fig. 10.1).

$$x_{t+1} = T_\gamma(x_t) = \begin{cases} x_t(1 + 2^\gamma x_t^\gamma) & x_t \in [0, 1/2) \\ 2x_t - 1 & x_t \in [1/2, 1] \end{cases} \tag{10.84}$$

When $\gamma = 0$ the Bernoulli map is recovered, which provides the simplest example of complete (and uniform) chaos: as soon as $\gamma > 0$ global hyperbolicity is lost, as $x = 0$ is an indifferent fixed point of (10.84): though elsewhere instability is

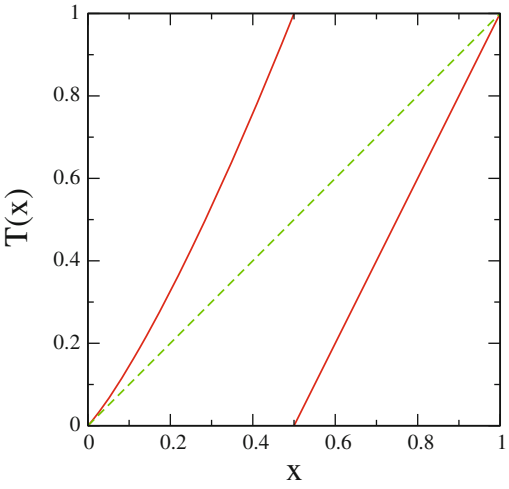

Fig. 10.1 The map (10.84), for $\gamma = 0.5$

maintained ($T'_\gamma(x) > 1 \; \forall x > 0$), the influence of the indifferent fixed point is very deep. This can be seen in a number of ways: we will just emphasize those related to the subject of the present volume. For small enough γ the map is still ergodic, though the invariant measure $d\mu_\gamma$ is quite different from the Lebesgue (flat-density) invariant measure in the Bernoulli limit. More precisely for $\gamma \in (0, 1)$ an absolutely continuous invariant probability measure exists, but its density diverges as $\rho_\gamma(x) = d\mu_\gamma/dx \sim x^{-\gamma}$ as $x \to 0$ [35, 37]; when $\gamma > 1$ no normalizable absolutely continuous invariant measure exists, and we enter the realm of *infinite ergodic theory* [38], which lies outside the scope of the present contribution. The way in which the nature of the indifferent fixed point modifies dynamical properties can be appreciated if we consider correlation decay: for generic observables A, correlations decay polynomially where the power law depends on the intermittency exponent γ:

$$\mathscr{C}_A(t) = \int_0^1 d\mu_\gamma(x) A(x)(A \circ T_\gamma^t)(x) - \left(\int_0^1 d\mu_\gamma(x)\, A(x) \right)^2 \sim t^{-\Theta_\gamma}, \quad (10.85)$$

where [36, 37, 39]:

$$\Theta_\gamma = \frac{1}{\gamma} - 1. \quad (10.86)$$

In the range $\gamma \in (0, 1/2)$, thus correlations are integrable, and the CLT is expected to hold (for a rigorous approach see [40]; we notice that the CLT holds for mixing systems once observables decorrelate with sufficient speed): when $\gamma \in [1/2, 1)$ (thus still in the ergodic – and mixing – regime), for zero average (smooth) observables G, with $G(0) \neq 0$, (10.86) shows that correlations are no more

integrable, and a CLT holds only in a generalized sense [41], where both the scaling of Birkhoff sums and the limit law are different from the usual form of the law of large numbers. Indeed the rigorous results states that

$$\frac{1}{t^\gamma}\sum_{k=0}^{t-1} G \circ T_\gamma^k \longrightarrow L_{1/\gamma,c,\beta} \tag{10.87}$$

where the convergence is in distribution according to the invariant measure $d\mu_\gamma$, and $L_{1/\gamma,c,\beta}$ is a (non-symmetric) Lévy distribution of order $1/\gamma$. The slow decay of correlations influences all statistical properties: in particular as regards large deviations. Exponential large deviations are indeed known to hold for systems with strong chaotic properties [42], but intermittent maps enjoy weaker statistical properties, and generally exhibit *polynomial* large deviations, where the exponent is exactly Θ_γ [43,44]. More precisely the result in [43,44] states that for an observable G, whose correlations decay according to a power law with exponent Θ_γ, (and with $\int G\, d\mu_\gamma = 0$) we get

$$\mu_\gamma\left\{x \in [0,1] : \left|\frac{1}{t}\sum_{i=0}^{t-1} G(T_\gamma^i x)\right| \geq \epsilon\right\} = O(t^{-\Theta_\gamma}). \tag{10.88}$$

Incidentally, we notice that such a result holds for a large class of dynamical systems exhibiting power law correlations, and it has been implemented as a numerical tool to get precise estimates of the polynomial rate of mixing [45]. From a qualitative point of view, the most striking way in which the marginal fixed point influences the dynamics is a sort of *stickiness*, namely generic trajectories, once they pass in the vicinity of the fixed point typically spend a long time there: this is quantified by long time tails in the waiting time distribution, like in the CTRW we examined in the previous section. The asymptotic form of the distribution can be obtained explicitly [46]: the idea is of partitioning the "laminar" branch ($\mathscr{I}_0 = [0, 1/2)$), by inverse images of the "chaotic" branch $\mathscr{I}_1 = [1/2, 1]$. Let's call $\xi_0 = 1/2$, and denote by $\Upsilon_\epsilon \quad \epsilon = 0, 1$ the inverse mappings of T ($\Upsilon_{0,(1)}$ map the unit interval onto $\mathscr{I}_{0,(1)}$, respectively). We now define $\xi_n = \Upsilon_0^n(\xi_0)$: then the interval (ξ_n, ξ_{n-1}) is mapped onto $\mathscr{I}_1$ exactly in n iterations. The asymptotic location of the sequence of points $\{\xi_n\}$ is obtained by a continuous time approximation [46], as follows: since

$$\xi_{k-1} = \xi_k + 2^\gamma \xi_k^{1+\gamma} \tag{10.89}$$

in a continuous time approximation we may write

$$d\left(\frac{1}{\xi^\gamma}\right) = \gamma 2^\gamma dk \qquad \xi(0) = \frac{1}{2}, \tag{10.90}$$

from which we get

$$\xi_k = \frac{1}{(2^\gamma(1+\gamma\cdot k))^{1/\gamma}} \qquad \xi_k \sim \frac{1}{k^{1/\gamma}} \quad k \gg 1. \tag{10.91}$$

This allows us to estimate the size Δ_k of intervals where exactly k iterations are needed to be mapped to the chaotic branch:

$$\Delta_k = \xi_{k-1} - \xi_k \sim \frac{1}{k^{1+1/\gamma}} : \tag{10.92}$$

this is the crucial estimate, since linearity of the chaotic branch implies a uniform reinjection from $\mathscr{I}_1$ to the laminar branch $\mathscr{I}_0$ and thus the waiting time distribution in the laminar region behaves like

$$\psi(t) \sim \frac{1}{t^{1+1/\gamma}} \quad t \gg 1. \tag{10.93}$$

Such a distribution has to satisfy the normalization condition

$$\int_0^\infty dt\, \psi(t) = 1, \tag{10.94}$$

and we also notice that, in the ergodic regime $\gamma \in (0,1)$, the average waiting time is finite

$$\langle \tau \rangle = \int_0^\infty dt\, t\, \psi(t) < \infty; \tag{10.95}$$

in the infinite ergodic case $\gamma > 1$ this is no longer true, and this leads to peculiar dynamical features (see for instance [47]). Notice that when $\gamma \in [0, 1/2)$ also the variance is finite, while we have that

$$\int_0^\infty dt\, t^2 \psi(t) = +\infty \qquad \gamma \in [1/2, 1). \tag{10.96}$$

10.4 Chain of Intermittent Maps

The first example of deterministic dynamics yielding anomalous transport (both subdiffusive [48] and superdiffusive [46]) was obtained by lifting intermittent maps over the whole real line. Such a procedure, which we will shortly describe, follows closely the way early models of deterministic transport were indeed designed [49]. Again we consider a discrete time dynamics induced by a mapping F, defined on the whole real line, and satisfying the translation property $F(x+m) = m + F(x)$ (see Fig. 10.2), we will also consider the associated torus (interval) map $\hat{F}$, as discussed

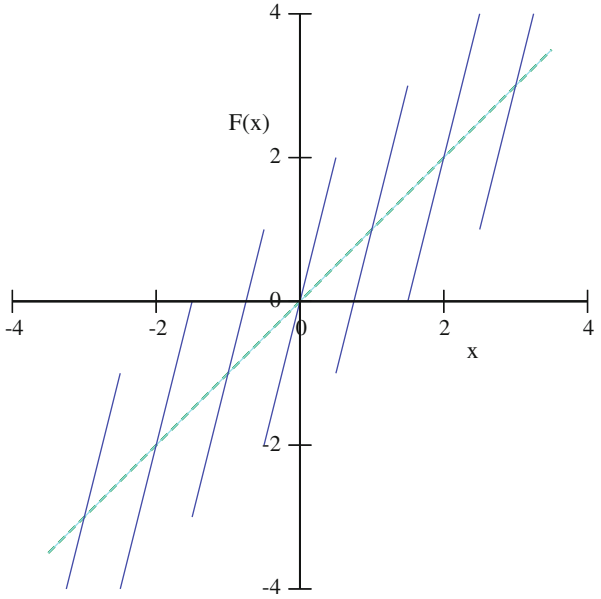

Fig. 10.2 A chaotic map leading to normal diffusion

in a few lines. To get a map of this form we may start by defining the lift F on a finite interval, as $I_0 = [0, 1]$: a particularly simple example is [50]

$$F(x) = \frac{1}{2} + \Lambda \left(x - \frac{1}{2} \right), \tag{10.97}$$

with $\Lambda > 2$. We then extend the map on the whole real line by defining it on each $I_k = [k, k + 1]$ as $F(y) = k + F(y - k)$ (see Fig. 10.2); finally, the torus map on $\mathcal{T}_1$ is $\hat{F}(\theta) = F(\theta)|_{mod\ 1}$. Lifting hyperbolic maps on the real line usually leads to normal diffusion, even though the relationship between dynamical properties and the diffusion coefficient may be rather complex [50, 51]. To provide models for anomalous diffusion we consider intermittent rather than hyperbolic maps: the lift can be devised in such a way to lead to long waiting times (as in Fig. 10.3), or the marginal fixed points can be associated to "running" modes (as in Fig. 10.4, in such a way that motion is characterized by long sequences of ballistic transport). In this section we discuss how CTRW models may describe such anomalous deterministic transport: we will discuss in the next section how well such a stochastic technique is able to cope with the present truly deterministic setting, where the only statistical average is over a set of initial conditions.

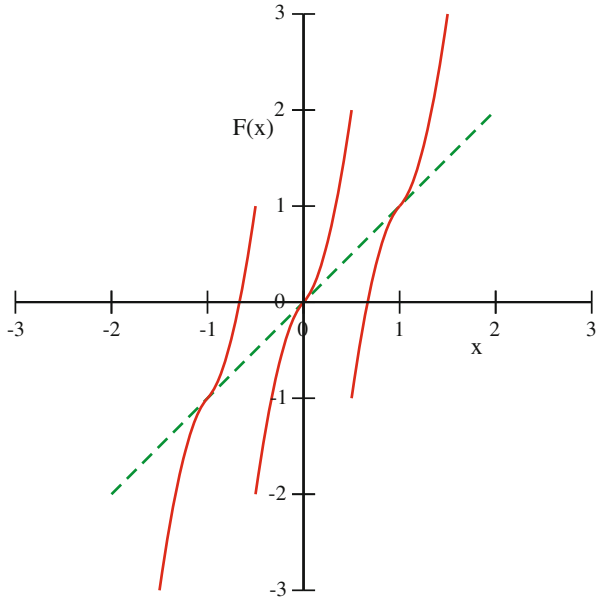

Fig. 10.3 An intermittent map leading to slowed diffusion

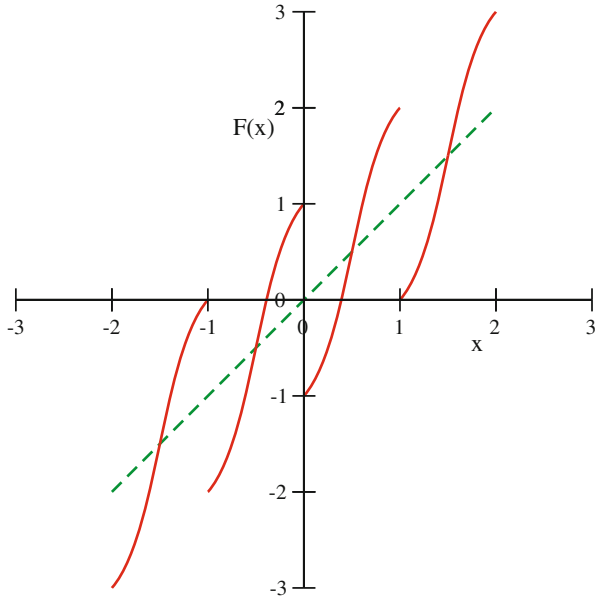

Fig. 10.4 An intermittent map leading to superdiffusion

10.4.1 Subdiffusion

Let's consider the case of Fig. 10.3: dynamically it consists in finite size jumps occurring after a long time tailed distribution of waiting times: the analysis in terms of CTRW is quite similar to the discussion after Eqs. (10.42) and (10.43), but, if we consider the ergodic case, we are not getting any anomaly: they come only in the infinite ergodic case, where, as in (10.43) the distribution yields an infinite waiting time [48, 52].

10.4.2 Superdiffusion

We now consider the case in which laminar sequences correspond to ballistic segments. The simple CTRW expression (10.26) in this case is not appropriate, and we must take into account a more sophisticated picture, given by the *velocity* model [33, 53] (Lévy walks). Again we start from the probability density function that a step of length l takes place at time t: but we suppose that t is chosen from a broad distribution, and that during that period the walker travels with a unit velocity:

$$\wp(l,t) = \psi(t)Q(l|t), \tag{10.98}$$

where

$$Q(l|t) = \frac{1}{2}\left(\delta(l-y) + \delta(l+t)\right); \tag{10.99}$$

and we choose the "ballistic" time distribution according to the intermittent dynamics:

$$\psi(t) \sim \frac{1}{t^{1+\frac{1}{\gamma}}}. \tag{10.100}$$

We assume that the processes starts at the position $x = 0$ at time $t = 0$, and we decompose the probability density $\mathscr{P}(X,T)$ in a sum over the "number of events". First of all consider the probability of being at position X at time T in a single motion event:

$$\mathscr{P}_1(X,T) = \frac{1}{2}(\delta(X-T) + \delta(X+T)) \int_T^\infty d\tau \psi(\tau), \tag{10.101}$$

where we have taken into account also cases in which the ballistic segment does not end at X: notice that this has a form similar to (10.98) where instead of ψ we have the function

$$\Psi(t) = \int_t^\infty d\tau\, \psi(\tau) \qquad \Psi(0) = 1 \qquad \Psi(t) \sim \frac{1}{t^{\frac{1}{\gamma}}} \quad t \gg 1. \tag{10.102}$$

Higher order contributions are easily evaluated: for instance

$$\mathscr{P}_2(X,T) = \int d\xi \int d\tau\, \wp(\xi,\tau)\mathscr{P}_1(X-\xi, T-\tau), \tag{10.103}$$

and

$$\mathscr{P}_3(X,T) = \int d\xi_1\, d\xi_2 \int d\tau_1\, d\tau_2\, \wp(\xi_1,\tau_1)\wp(\xi_2,\tau_2)\mathscr{P}_1(X-\xi_1-\xi_2, T-\tau_1-\tau_2). \tag{10.104}$$

When we take the Fourier-Laplace transform we get the following structure:

$$\check{\mathscr{P}}_1(k,s) = \frac{1}{2}\int_0^\infty dt\, \left(e^{-(s+ik)t} + e^{-(s-ik)t}\right)\Psi(t) = \frac{1}{2}(\tilde{\Psi}(s+ik) + \tilde{\Psi}(s-ik)). \tag{10.105}$$

By summing over all terms we finally get:

$$\check{\mathscr{P}}(k,s) = \frac{\check{\mathscr{P}}_1(k,s)}{1-\check{\wp}(k,s)} = \frac{\frac{1}{2}(\tilde{\Psi}(s+ik) + \tilde{\Psi}(s-ik))}{1-\frac{1}{2}(\tilde{\psi}(s+ik) + \tilde{\psi}(s-ik))}. \tag{10.106}$$

In order to get the moments' spectrum we need to estimate the leading behavior of (10.106) for small arguments, and this depends crucially on the range of intermittency exponent γ we are taking into account. Let us briefly consider the case $\gamma \in (1/2, 1)$, which corresponds to a genuine ergodic case, where, however, ballistic duration times have an infinite variance. Usual tauberian theorems cannot once again be directly applied to get the small argument behavior of either $\tilde{\psi}$ or $\tilde{\Psi}$, but asymptotic expressions easily come out by using integration by parts. Take for instance $\tilde{\psi}$, where the large t behavior of $\psi(t)$ is with a power law exponent in the range $1 + \frac{1}{\gamma} \in (2,3)$: if we consider the following function

$$\mathscr{W}(t) = \int_t^\infty dt_1 \int_{t_1}^\infty dt_2 \psi(t_2) \qquad \frac{d^2\mathscr{W}}{dt^2} = \psi(t) \qquad \frac{d\mathscr{W}}{dt} = -\Psi(t), \tag{10.107}$$

we get, for small arguments,

$$\tilde{\psi}(u) \sim 1 - <\tau> u + \tilde{c}u^{\frac{1}{\gamma}} \tag{10.108}$$

and

$$\tilde{\Psi}(u) \sim <\tau> - \tilde{c}u^{\frac{1}{\gamma}-1}, \tag{10.109}$$

so, if we put

$$q = s + ik \qquad \Lambda = \tilde{c}/ < \tau >, \tag{10.110}$$

we have, for small q,

$$\check{\mathscr{P}}(k,s) = \frac{2 - \Lambda\left(q^{\frac{1}{\gamma}-1} + q^{*\frac{1}{\gamma}-1}\right)}{q + q^* - \Lambda\left(q^{\frac{1}{\gamma}} + q^{*\frac{1}{\gamma}}\right)}. \tag{10.111}$$

Moments can be then evaluated according to (10.40), and, for instance, we have that

$$\langle X^2 \rangle(t) \sim t^{3-\frac{1}{\gamma}}, \tag{10.112}$$

namely an accelerated diffusion. When considering the whole spectrum we have to take care that velocity is finite, and this leads to a nontrivial behavior of the whole spectrum, like the one described in Sect. 10.2.2. As a matter of fact we have from the very beginning that $\mathscr{P}(X,T) = 0$ for $|X| > T$, while the tight relationship with Lévy distributions may be appreciated by the fact that for very small arguments (10.111) may be approximated by

$$\check{\mathscr{P}}(k,s) = \frac{A}{s + B|k|^{\frac{1}{\gamma}}}, \tag{10.113}$$

whose Laplace transform gives the conventional Fourier transformed form of a Lévy distribution.

10.5 Deterministic vs Stochastic Approximation

The natural questions to ask, since we considered a crude stochastic modeling of a deterministic dynamics, is whether hypotheses like independence of successive steps are reasonably satisfied for deterministic systems, and whether crisply deterministic techniques, not relying on probabilistic hypotheses can be introduced to evaluate in a quantitative way the asymptotic growth of moments', the average over which they are computed being over a suitable set of initial conditions. In the case of intermittent systems, the approximation in which successive laminar sequences are supposed to be uncorrelated has been widely investigated [54,55]: in particular [55] contains an analysis of correlation functions for the infinite horizon Lorentz gas: here a trajectory is partitioned into independent events defined by collisions with the array of disks: the approximation is shown to be quite accurate for long times, while short time correlations are obviously missed.

The most satisfying theoretical framework in which anomalous transport is quantitatively analyzed for intermittent systems is periodic orbit theory [56–58] (see [59] for an exhaustive presentation of periodic orbit theory). We will only sketch very briefly the idea: for a full account see [60, 61].

The theory applies to systems enjoying periodicity properties like the maps in Figs. 10.3 and 10.4 (or like a periodic Lorenz gas): the strategy is to introduce a generalized transfer operator whose spectral properties determine the asymptotics for large times, in analogy with statistical mechanics evaluation of leading behavior in the thermodynamic limit through eigenvalues of transfer matrices. We will again denote by T the map on the real line and by $\hat{T}$ the corresponding torus map (in the Lorenz gas case the corresponding reduced system would be a Sinai-like billiard). The generating function of the diffusing variable is

$$\mathscr{G}_n(\beta) \;=\; \langle e^{\beta(T^n(x_0)-x_0)}\rangle_0, \tag{10.114}$$

where angular brackets denote an average over a suitable set of initial conditions: moments can be computed through derivatives of (10.114) with respect to β. As we mentioned before, the generating function may be expressed at the trace of a generalized transfer operator $\mathscr{L}_\beta$ in the following way:

$$\begin{aligned}\mathscr{G}_n(\beta) &= \int_0^1 dx \int_0^1 dy\, \mathscr{L}_\beta^n(x,y) \\ &= \int_0^1 dx \int_0^1 dz_{n-1} \cdots \int_0^1 dz_1 \int_0^1 dx\, \mathscr{L}_\beta(x,z_1)\cdots\mathscr{L}_\beta(z_{n-1},y),\end{aligned} \tag{10.115}$$

where the transfer operator is defined as:

$$\left(\mathscr{L}_\beta h\right)(x) \;=\; \int_0^1 dz\, h(z)\, e^{\beta(\hat{T}(z)+n_z-z)}\delta(x-\hat{T}(z)), \tag{10.116}$$

where h is chosen in an appropriate space of smooth functions, and n_z denotes the jump once the orbit is unfolded on the real line: namely $T(z) = \hat{T}(z) + n_z$.

Periodic orbits come into play when we evaluate the leading eigenvalue of the transfer operator (which, in view of (10.115) will dominate the large t behavior of the generating function). In particular the leading eigenvalue $\lambda_0(\beta)$ is the inverse of the smallest $z(\beta)$ solving the secular equation

$$\det\left(1 - z(\beta)\mathscr{L}_\beta\right) \;=\; 0. \tag{10.117}$$

Manipulations on (10.117) (details are provided in [60, 61]) show that $z(\beta)$ is a zero of the dynamical zeta function:

$$\zeta_\beta^{-1}(z) \;=\; \prod_{\{p\}}\left(1 - z^{n_p}\frac{e^{\beta\cdot\sigma_p}}{|\Lambda_p|}\right), \tag{10.118}$$

where $\{p\}$ denotes the set of periodic orbits of the map $\hat{T}$, and for any of such orbits p, n_p is the prime period, Λ_p the instability and the integer σ_p is the unfolded jump: for any orbit point x_i we have that $\hat{T}^{n_p}(x_i) = x_i$, while $T^{n_p}(x_i) = x_i + \sigma_p$. Calculations of moments are then carried out through

$$M_k(n) = \langle (x_n - x_0)^k \rangle_0 = \left. \frac{\partial^k}{\partial \beta^k} \mathcal{G}_n(\beta) \right|_{\beta=0}$$
$$\sim \left. \frac{\partial^k}{\partial \beta^k} \frac{1}{2\pi \mathrm{i}} \int_{a-\mathrm{i}\infty}^{a+\mathrm{i}\infty} ds\, \mathrm{e}^{sn} \frac{d}{ds} \ln \left[\zeta_\beta^{-1}(\mathrm{e}^{-s}) \right] \right|_{\beta=0} \tag{10.119}$$

What makes such calculations delicate in the intermittent case (and originates anomalies) is that the transfer operator does not have a spectral gap [62], and this is reflected in the analytic behavior of ζ_β^{-1} near the first zero. Once again, the dynamical origin is the behavior around the marginal fixed point. Like in our former analysis it led to polynomial tails in the waiting time distribution, here it leads to polynomial growth of instability Λ_p of orbits that approach more and more closely the marginal fixed point.

From the point of view of the present review, the most significant point is that periodic orbit theory reproduces exactly the results we derived in the former section by using a stochastic approximation.

10.6 A Final Warning

As we mentioned in the introduction, the present contribution does not want to be exhaustive, and many important issues have been left out. We hope to have conveyed the idea on the basic mechanisms leading to anomalous transport, and how models can be devised to a quantitative study of their effects both in the stochastic and in the deterministic framework.

References

1. T.H. Solomon, E.R. Weeks, H.L. Swinney, Phys. Rev. Lett. **71**, 3975 (1993)
2. D. Brockmann, L. Hufnagel, T. Geisel, Nature **439**, 462 (2006)
3. D. Bessis, J.S. Geronimo, P. Moussa, J. Stat. Phys. **34**, 75 (1984); G. Mantica, S. Vaienti, Ann. Inst. Poinc. **8**, 265 (2007)
4. B.V. Gnedenko, A.N. Kolmogorov, *Limit Distributions for Sum of Independent Random Variables* (Addison-Wesley, Reading, 1954)
5. W. Feller, *An Introduction to Probability Theory and Its Applications*, vol. II (Wiley, New York, 1970)
6. D. Sornette, *Critical Phenomena in Natural Sciences* (Springer, Berlin, 2000)
7. J-P. Bouchaud, A. Georges, Phys. Rep. **195**, 127 (1990)

8. R. Metzler, J. Klafter, Phys. Rep. **339**, 1 (2000)
9. R. Metzler, J. Klafter, J. Phys. A **37**, R161 (2004)
10. R. Klages, G. Radons, I.M. Sokolov (eds.), *Anomalous Transport* (Wiley-VCH, Berlin, 2008)
11. P. Castiglione, A. Mazzino, P. Muratore-Ginanneschi, A. Vulpiani, Physica D **134**, 75 (1999)
12. R.N. Mantegna, H.E. Stanley, Phys. Rev. Lett. **73**, 2946 (1994)
13. B. Podobnik, P.Ch. Ivanov, Y. Lee, H.E. Stanley, Europhys. Lett. **52**, 491 (2000)
14. E.W. Montroll, G.H. Weiss, J. Math. Phys. **6**, 167 (1965)
15. J. Klafter, I.M. Sokolov, *First Steps in Random Walks* (Oxford University Press, Oxford, 2011)
16. R. Burioni, D. Cassi, J. Phys. A **38**, R45 (2005)
17. G.H. Weiss, *Aspects and Applications of the Random Walk* (North-Holland, Amsterdam, 1994)
18. A. Grigor'yan, A. Telcs, Math. Ann. **324**, 521 (2002)
19. P.G. Doyle, J.L. Snell, *Random Walks and Electric Networks* (The Mathematical Association of America, Washington, 1999)
20. A. Telcs, *The Art of Random Walks*. Lecture Notes in Mathematics (Springer, Berlin/New York, 2006)
21. S. Alexander, R. Orbach, J. Phys. Lett. **43**, L62 (1982)
22. M.E. Cates, J. Phys. **46**, 1059 (1985)
23. R. Burioni, L. Caniparoli, S. Lepri, A. Vezzani, Phys. Rev. E **81**, 011127 (2010)
24. A. Grigor'yan, A. Telcs, Duke Math. J. **109**, 451 (2001)
25. A. Telcs, Ann. Inst. Poinc. **44**, 169 (2008)
26. D. Bertacchi, F. Zucca, J. Aust. Math. Soc. **75**, 325 (2003)
27. R. Burioni, D. Cassi, Phys. Rev. E **49**, 1785 (1994); R. Burioni, D. Cassi, Phys. Rev. E **51**, 2865 (1995)
28. R. Burioni, L. Caniparoli, A. Vezzani, Phys. Rev. E **81**, 060101 (2010)
29. C.W.J. Beenakker, C.W. Groth, A.R. Akhmerov, Phys. Rev. B **79**, 024204 (2009)
30. P. Buonsante, R. Burioni, A. Vezzani, Phys. Rev. E **84**, 021105 (2011)
31. E. Barkai, V. Fleurov, J. Klafter, Phys. Rev. E **61**, 1164 (2000)
32. M.F. Shlesinger, G.M. Zaslavski, J. Klafter, Nature **363**, 31 (1993)
33. G. Zumofen, J. Klafter, Phys. Rev. E **47**, 851 (1993)
34. P. Barthelemy, J. Bertolotti, D.S. Wiersma, Nature **453**, 495 (2008)
35. P. Gaspard, X-J. Wang, PNAS **85**, 4591 (1988); X-J. Wang, Phys. Rev. A **40**, 6647 (1989)
36. C. Liverani, B. Saussol, S. Vaienti, Ergod. Theory Dyn. Syst. **19**, 671 (1999)
37. H. Hu, Ergod. Theory Dyn. Syst. **24**, 495 (2004)
38. J. Aaronson, *An Introduction to Infinite Ergodic Theory* (AMS, Providence, 1997); R. Zweimüller, *Surrey Notes on Infinite Ergodic Theory* (2009). Available at (http://homepage.univie.ac.at/roland.zweimueller); S. Isola, Chaos Solitons Fractals **44**, 467 (2011)
39. L-S. Young, Isr. J. Math. **110**, 153 (1999); O. Sarig, Invent. Math. **150**, 629 (2002); S. Gouëzel, Isr. J. Math. **139**, 29 (2004)
40. C. Liverani, in *Pitman Reseach Notes in Mathematics*, vol. 362, ed. by F. Ledrappier, J. Levovicz, S. Newhouse (Addison-Wesley, Reading, 1996)
41. S. Gouëzel, Probab. Theory Relat. Fields **128**, 82 (2004)
42. L-S. Young, Trans. Am. Math. Soc. **318**, 525 (1990)
43. M. Pollicott, R. Sharp, Nonlinearity **22**, 2079 (2009)
44. I. Melbourne, Proc. Am. Math. Soc. **137**, 1735 (2009)
45. R. Artuso, C. Manchein, Phys. Rev. E **80**, 036210 (2009)
46. T. Geisel, J. Nierwetberg, A. Zachary, Phys. Rev. Lett. **54**, 616 (1985)
47. M. Thaler, R. Zweimüller, Probab. Theory Relat. Fields **135**, 15 (2006); G. Bel, E. Barkai, Europhys. Lett. **74**, 15 (2006); N. Korabel, E. Barkai, Phys. Rev. Lett. **102**, 050601 (2009)
48. T. Geisel, S. Thomae, Phys. Rev. Lett. **52**, 1936 (1984)
49. T. Geisel, J. Nierwetberg, Phys. Rev. Lett. **48**, 7 (1982); M. Schell, S. Fraser, R. Kapral, Phys. Rev. A **26**, 504 (1982); H. Fujisaka, S. Grossmann, Z. Phys. B **48**, 261 (1982)
50. R. Klages, J.R. Dorfman, Phys. Rev. Lett. **74**, 387 (1995)
51. G. Cristadoro, J. Phys. A **39**, 1285 (2006)
52. T. Akimoto, T. Miyaguchi, Phys. Rev. E **82**, 030102 (2010)

53. M.F. Schlesinger, B. West, J. Klafter, Phys. Rev. Lett. **58**, 1100 (1987)
54. V. Baladi, J-P. Eckmann, D. Ruelle, Nonlinearity **2**, 119 (1989); P. Dahlqvist, J. Phys. A **27**, 763 (1994); P. Dahlqvist, Nonlinearity **8**, 11 (1995); P. Dahlqvist, Physica D **83**, 124 (1995); P. Dahlqvist, J. Stat. Phys. **84**, 773 (1996)
55. P. Dahlqvist, R. Artuso, Phys. Lett. A **219**, 212 (1996)
56. R. Artuso, G. Casati, R. Lombardi, Phys. Rev. Lett. **71**, 63 (1993)
57. R. Artuso, G. Cristadoro, Phys. Rev. Lett. **90**, 244101 (2003)
58. R. Artuso, G. Cristadoro, J. Phys. A **37**, 85 (2004)
59. P. Cvitanović, R. Artuso, R. Mainieri, G. Tanner, G. Vattay, *Chaos, Classical and Quantum* (Niels Bohr Institute, Copenhagen, 2009). ChaosBook.org
60. R. Artuso, in *The Mathematical Aspects of Quantum Chaos*. Springer Lecture Notes in Physics, vol. 618, ed. by M.D. Esposti, S. Graffi (Springer, Berlin, 2003)
61. R. Artuso, G. Cristadoro, in *Anomalous Transport*, ed. by R. Klages, G. Radons, I.M. Sokolov (Wiley-VCH, Berlin, 2008)
62. V. Baladi, *Positive Transfer Operators and Decay of Correlations* (World Scientific, Singapore, 2000); T. Prellberg, J. Phys. A **36**, 2455 (2003); S. Isola, Nonlinearity **15**, 1521 (2002)

Chapter 11
Large Deviations in Turbulence

Guido Boffetta and Andrea Mazzino

Abstract We give a survey of the use of the multifractal method, as a manifestation of the large deviation theory, to study the scaling behavior in fully developed turbulence. Particular emphasis is reserved to the phenomenon of intermittency, i.e., the most relevant manifestation of the break-down of mean field arguments in turbulence. To explain intermittency, the statistical role of fluctuations are explicitly accounted for by means of the multifractal formalism. Its application to the statistics of velocity gradients and acceleration will be discussed. A remark related to the use of large deviation theory in multifractal formalism will be emphasized. Also, the presentation of the famous Refined Similarity Hypothesis due to Kolmogorov and Obukhov in 1962 to account for the statistical role of fluctuations will be reviewed.

11.1 Introduction

The multifractal approach to fully developed turbulence stands, technically speaking, on the shoulders of the large deviation theory and is one of the most fruitful idea which allowed to physically understand the phenomenology of intermittency and anomalous scaling in turbulence [1–3].

From a technical point of view, one can say that multifractal analysis is a large deviation theory of self-similar measure [4]. The so-called multifractal spectrum and structure function, which are related by Legendre transforms, are the analogs of an entropy and a free energy function, respectively.

G. Boffetta (✉)
Dipartimento di Fisica and INFN, University of Torino, via P. Giuria 1, Torino, I-10125, Italy
e-mail: boffetta@to.infn.it

A. Mazzino
INFN and CINFAI Consortium, DICCA – University of Genova, Via Montallegro 1, Genova, I-16146, Italy
e-mail: andrea.mazzino@unige.it

A. Vulpiani et al. (eds.), *Large Deviations in Physics*, Lecture Notes in Physics 885,
DOI 10.1007/978-3-642-54251-0_11,

These important relationships permitted to gain a rigorous formulation of multifractals, as well as to provide a guide for deriving new results. As pioneering works which anticipated some aspects of the the multifractal approach to turbulence we can cite the lognormal theory of Kolmogorov [5], the contributions of Novikov and Stewart [6] and Mandelbrot [7]. In the lognormal model of Kolmogorov, the anomalous scaling of structure functions was attributed to large fluctuations of the velocities which, in turn, were supposed to be triggered by "intermittent" nature of the coarse grained energy dissipation rate. Since then, a number of models have been proposed to understand the essential features of these fluctuations. Among these models, the multifractal model represents the most general approach to intermittency and anomalous scaling in turbulence.

Our main aim here is to give a survey of the use of the multifractal method, as a manifestation of the large deviation theory, to study the scaling behavior of fully developed turbulence.

The material of the chapter is organized as follows. In Sect. 11.2 we introduce the concept of scale invariance in turbulence and how it is related to the famous $4/5$-th law for fully developed turbulence. In Sect. 11.3 the statistical role of fluctuations are explicitly accounted for by means of the multifractal formalism. A remark related to the use of large deviation theory in multifractal formalism will be also discussed. Sect. 11.4 is devoted to the presentation of the Refined Similarity Hypothesis due to Kolmogorov and Obukhov in 1962. Conclusions are reserved to Sect. 11.5.

11.2 Global Scale Invariance and Kolmogorov Theory

Turbulence in fluids is described by the Navier-Stokes equations for an incompressible ($\boldsymbol{\nabla} \cdot \boldsymbol{v} = 0$) velocity field $\boldsymbol{v}(\boldsymbol{x}, t)$

$$\partial_t \boldsymbol{v} + \boldsymbol{v} \cdot \boldsymbol{\nabla} \boldsymbol{v} = -\boldsymbol{\nabla} p + \nu \nabla^2 \boldsymbol{v} + \boldsymbol{f} \tag{11.1}$$

where p represents the pressure, ν is the kinematic viscosity of the fluid and $\boldsymbol{f}$ is a forcing terms necessary to have a statistically stationary state. Turbulence appears spontaneously as the dimensionless Reynolds number $Re = UL/\nu \to \infty$ (U is a typical velocity in the flow and L a typical scale, e.g. the scale at which the forcing is acting). The nonlinearity of the equation, together with the non-locality (due to the pressure term), implies that in general an analytical treatment of (11.1) is a formidable task, while some special, time-independent solutions, for small Re are known [8]. A confirmation of this difficulty comes from the fact that for the three-dimensional case, and given some initial conditions, mathematicians have not yet proved that smooth solutions always exist, or that if they do exist they have bounded kinetic energy. This is called the Navier-Stokes existence and smoothness problem. The Clay Mathematics Institute in May 2000 made this problem one of its seven Millennium Prize problems in mathematics. It offered a US 1,000,000 prize to the first person providing a solution for a specific statement of the problem.

In two dimensions it is possible to prove that in the deterministic case the solution of the Cauchy problem exists and is unique [9] and, very recently, that in the stochastic case (see, e.g., [10]) the solution is a Markov process exponentially mixing in time and ergodic with a unique invariant (steady state) measure even when the forcing acts only on two Fourier modes [11].

For an inviscid fluid ($\nu = 0$) and in the absence of external forces (i.e. $\boldsymbol{f} = 0$), the evolution of the velocity field (11.1) becomes the Euler equation, which conserves kinetic energy. In such a case, introducing an ultraviolet cutoff K_{max} on the wave numbers, it is possible to build up an equilibrium statistical mechanics simply following the standard approach used in Hamiltonian statistical mechanics. However, because of the so-called dissipative anomaly [3, 12], in $3D$ the limit of zero viscosity is singular and cannot be interchanged with $K_{max} \to \infty$. In other words, given any viscosity as small as possible, there exist a wavenumber $k < K_{max}$ at which the dissipative term in (11.1) is not negligible and the energy dissipation rate reaches a value which is independent on ν. This basic empirical property of turbulent flows implies that the statistical mechanics of an inviscid fluids has a rather limited relevance for the Navier-Stokes equations at very high Reynolds numbers Re (which is equivalent to very small ν).

In addition, mainly as a consequence of the non-Gaussian statistics, even a systematic statistical approach, e.g. in term of closure approximations, is very difficult [3, 12]. In the fully developed turbulence (FDT) limit, i.e. $Re \to \infty$, and in the presence of forcing at large scale, one has a non equilibrium statistical steady state, with an inertial range of scales, where neither energy pumping nor dissipation acts, which shows strong departures from the equipartition [3, 12].

The main features of FDT are described by the statistical theory of Kolmogorov developed in three papers published in 1941 (now called K41 theory) [13, 14]. At the basis of the K41 theory [3, 13] there is the idea of turbulent *cascade* (introduced by Richardson in [15]): energy fluctuations, introduced at large scale by a mechanical forcing, reach the smallest scale (where they are converted into heat) via a scale-by-scale cascade process. As a conseguence, one may expect that small scale turbulence, at sufficiently high Reynolds numbers, is statistically independent on the large scales and can thus locally recover homogeneity and isotropy. This implies that small scale features of turbulence are universal, i.e. independent on the particular flow and forcing mechanism. The concept of homogeneous and isotropic turbulence was already introduced by Taylor [16] for describing grid generated turbulence. The important step made by Kolmogorov in 1941 was to postulate that small scales are statistically isotropic, no matter how turbulence is generated.

This hypothesis is based on intrinsic properties of the dynamics, i.e. the invariance of Navier-Stokes equations (11.1) under space translations, rotations and scaling transformation:

$$\boldsymbol{x} \to \lambda\, \boldsymbol{x} \quad , \boldsymbol{v} \to \lambda^h \boldsymbol{v} \quad , t \to \lambda^{1-h}\, t \quad , \quad \nu \to \lambda^{h+1} \nu \ , \tag{11.2}$$

for any $\lambda > 0$ and h (and we have neglected the contribution of forcing). A classical example of scaling symmetry is the so-called similarity principle of fluid mechanics

which states that two flows with the same geometry and the same Reynolds number are similar. The similarity principle is at the basis of laboratory modeling of engineering and geophysical flows where, because usually the fluid is water, its application requires $h = -1$ in (11.2) in order to keep the value of ν.

Kolmogorov's treatment of small scale turbulence is based on the hypothesis that, in the limit of high Reynolds numbers and far from boundaries, the symmetries of Navier-Stokes equation are restored for statistical quantities. To be more precise, let us consider the velocity increment $\delta \boldsymbol{v}(\boldsymbol{x}, \boldsymbol{\ell}) \equiv \boldsymbol{v}(\boldsymbol{x} + \boldsymbol{\ell}) - \boldsymbol{v}(\boldsymbol{x})$ over the scales $\ell \ll L$. Restoring of homogeneity in statistical sense requires that $\delta \boldsymbol{v}(\boldsymbol{x} + \boldsymbol{r}, \boldsymbol{\ell}) \stackrel{law}{=} \delta \boldsymbol{v}(\boldsymbol{x}, \boldsymbol{\ell})$, where equality in law means that the PDF of $\delta \boldsymbol{v}(\boldsymbol{x} + \boldsymbol{r}, \boldsymbol{\ell})$ and $\delta \boldsymbol{v}(\boldsymbol{x}, \boldsymbol{\ell})$ are identical. Similarly, statistical isotropy, also used by Kolmogorov in his 1941 papers, requires $\delta \boldsymbol{v}(A\boldsymbol{x}, A\boldsymbol{\ell}) \stackrel{law}{=} \delta A \boldsymbol{v}(\boldsymbol{x}, \boldsymbol{\ell})$ where A is a rotation matrix. Because we will consider homogeneous, isotropic turbulence, in the following for simplicity we will use the notation $\delta \boldsymbol{v}(\boldsymbol{\ell})$ for the velocity increment.

In the limit of large Reynolds number, Kolmogorov made the hypothesis that for separation in the inertial range of scales $\ell_D \ll \ell \ll L$ (where the dissipative scale is $\ell_D \simeq LRe^{-3/4}$) the PDF of $\delta \boldsymbol{v}(\boldsymbol{\ell})$ becomes independent on viscosity ν. As a consequence, in this limit and in this range of scales, scaling invariance (11.2) is statistically recovered without fixing the value of the scaling exponent h:

$$\delta \boldsymbol{v}(\lambda \boldsymbol{\ell}) \stackrel{law}{=} \lambda^h \delta \boldsymbol{v}(\boldsymbol{\ell}). \tag{11.3}$$

The values of the scaling exponent, h are now limited only by the requiring that the velocity fluctuations do not break incompressibility, which is equivalent to $h \geq 0$ [3].

Starting from (11.1) Kolmogorov was able to derive an exact relation, known as the "4/5-th law" [3, 13], which, under the assumption of stationarity, homogeneity and isotropy, and in the inertial range of scales $\ell_D \ll \ell \ll L$ states

$$\langle \delta v_{||}^3(\ell) \rangle = -\frac{4}{5} \bar{\varepsilon} \ell \,, \tag{11.4}$$

where $\delta v_{||}(\ell)$ is the longitudinal velocity difference, i.e. $\delta v_{||}(\ell) = \delta \boldsymbol{v}(\ell) \cdot \boldsymbol{\ell} / \ell$ (which, under homogeneity and isotropy, depends on ℓ only). Assuming global scaling invariance, i.e. a unique exponent h in (11.3), the 4/5-law (11.4) fixes its value to $h = 1/3$. As a consequence, one expects a power-law behavior in the inertial range for any structure function of velocity difference

$$S^{(p)}(\ell) \equiv \langle \delta v_{||}^p(\ell) \rangle = C_p \bar{\varepsilon}^{p/3} \ell^{p/3} \tag{11.5}$$

where the C_p are dimensionless, universal constant, not determined by the theory except for $C_3 = -4/5$.

We remark that the fact that the third moment of velocity differences does not vanish is a consequence of the directional transfer (from large to small scales) of energy on average. An important consequence, which will be discussed in details, is that the PDF of velocity differences in turbulence cannot be Gaussian.

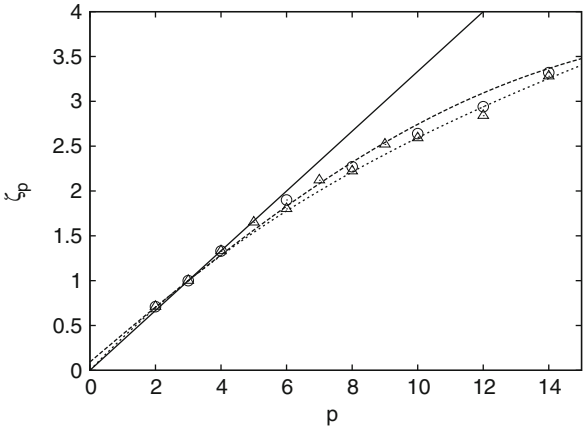

Fig. 11.1 Structure function scaling exponents ζ_p plotted vs. p. *Circles* and *triangles* correspond to the data of different experiments (Anselmet et al. [17]). The *solid line* corresponds to Kolmogorov scaling $p/3$; the *dashed line* is the random beta model prediction (11.25) with $B = 1/2$ and $x = 7/8$; the *dotted line* is the She-Leveque prediction (11.29) with $\beta = 2/3$

11.3 Accounting for the Fluctuations: The Multifractal Model

Kolmogorov 41 theory is not exact because both experiments and numerical simulations show that higher order structure functions display unambiguous departure from the scaling exponents (11.5). Indeed one has

$$S^{(p)}(\ell) \sim \left(\frac{\ell}{L}\right)^{\zeta(p)} \tag{11.6}$$

with $\zeta(p) \neq p/3$. We remark that in (11.6) and in the following we do not include, for notation simplicity, the terms built on ε and needed in order to make these expressions dimensionally correct. In Fig. 11.1 we report a collection of scaling exponents $\zeta(p)$ extracted from different experimental data [17]. Let us recall that the scaling exponents are not completely free as (11.4) requires $\zeta(3) = 1$. Under very general hypothesis, one can also demonstrate that ζ_p has to be a concave and nondecreasing function of p [3]. From Fig. 11.1 it is evident that the $\zeta(p)$ exponents are firstly *universal* and secondarily *anomalous*, i.e. they are expressed by a non-linear function of p. This also means that the PDF's of velocity differences $\delta \boldsymbol{v}(\ell)$ not only deviate from the Gaussian (as required by (11.4)), but also that at different scales the PDF's are differents and that the skewness of velocity differences increases going to small scales.

The deviation of scaling exponents ζ_p from $p/3$ goes under the name of intermittency [3], and is physically due to the fact that the turbulent intensity and local energy dissipation ε are strongly fluctuating in physical space. One consequence is that, for example, $\overline{\varepsilon^{p/3}} \neq \bar{\varepsilon}^{p/3}$ and therefore (11.5) is not justified (apart from $p = 3$, of course).

A simple way to modify the K41 consists in assuming that the energy dissipation ε is distributed uniformly on a subset $S \subset \mathscr{R}^3$ of fractal dimension $D_F < 3$. This is equivalent to assume that $\delta \boldsymbol{v}(\boldsymbol{x}, \boldsymbol{\ell}) \sim (\ell/L)^h$ with $h = (D_F - 2)/3$ for $\boldsymbol{x}$ on the fractal set S and $\delta \boldsymbol{v}(\boldsymbol{x}, \boldsymbol{\ell})$ non singular otherwise. The relation between h and D_F is obtained by the request that $\zeta_3 = 1$. This assumption leads to the so-called absolute curdling or β-model for which

$$\zeta_p = \frac{D_F - 2}{3} p + (3 - D_F) \,. \tag{11.7}$$

Such a prediction, with $D_F \simeq 2.83$, is in fair agreement with the experimental data for small values of p, but higher order scaling exponents give a clear indication of a non linear behavior in p (see Fig. 11.1).

One generalization of the (fractal) β-model is the multifractal model of turbulence [1, 3, 18]. The multifractal model relaxes the assumption of global scale invariance for a more general local invariance, i.e. the existence of a continuous set of exponents h such that $\delta v(\ell) \sim (\ell/L)^h$ where, as in the β-model, each exponent is realized on a different fractal set of dimension $D(h)$. More precisely one assumes that in the inertial range of scales ℓ one has

$$\delta \boldsymbol{v}(\boldsymbol{x}, \boldsymbol{\ell}) \sim \left(\frac{\ell}{L} \right)^h \,, \tag{11.8}$$

if $\boldsymbol{x} \in S_h$, where S_h is a fractal set with dimension $D(h)$ and $h \in (h_{min}, h_{max})$. The probability to observe a given scaling exponent h at the scale ℓ is determined by the codimension $3 - D(h)$ of the fractal set as $P_\ell(h) \sim \ell^{3-D(h)}$ and therefore

$$S_p(\ell) \sim \int_{h_{min}}^{h_{max}} \ell^{hp} \ell^{3-D(h)} \mathrm{d}h \sim \ell^{\zeta_p} \,. \tag{11.9}$$

For $\ell \ll 1$, a steepest descent estimation gives the scaling exponent

$$\zeta_p = \min_h \{hp + 3 - D(h)\} = h^* p + 3 - D(h^*) \tag{11.10}$$

where $h^* = h^*(p)$ is the solution of the equation $D'(h^*(p)) = p$. The Kolmogorov 4/5-th law (11.4) imposes $\zeta_3 = 1$ which implies that

$$D(h) \le 3h + 2 \,, \tag{11.11}$$

with the equality realized by $h^*(3)$. We remark that the Kolmogorov similarity theory $\zeta_p = p/3$ corresponds to the case of only one singularity exponent $h = 1/3$ with $D(h = 1/3) = 3$.

It is important to remark that the multifractal model is not predictive in a strict sense as it depends on an infinite set of parameters (the function $D(h)$) which are

not derived from the Navier-Stokes equations. Nonetheless, it is able to reproduce the set of scaling exponents ζ_p on the basis of simple phenomenological arguments, as it will be discussed in the next section. Moreover, once $D(h)$ has been obtained from a model or from experimental data, the multifractal model can be used to make predictions on other statistical quantities in turbulence [19].

Let us now discuss an important issue related to the use of large deviation theory in the multifractal formalism. To obtain the scaling behavior of $S_p(\ell) \sim (\ell/L)^{\zeta_p}$ given by (11.9) with ζ_p obtained from (11.10), one has to assume that the exponent $ph + 3 - D(h)$ has a minimum, ζ_p, which is a function of h, and that such an exponent behaves quadratically with h in the vicinity of the minimum. This is the basic assumption to apply the Laplace's method of steepest descent. The point we would like to discuss here is that, for small separations ℓ, indeed $S_p(\ell) \sim (\ell/L)^{\zeta_p}$ but with a logarithmic prefactor:

$$S_p(\ell) \sim \left[-\ln\left(\frac{\ell}{L}\right)\right]^{-1/2} \left(\frac{\ell}{L}\right)^{\zeta_p} . \tag{11.12}$$

Such a prefactor is usually not considered in the naive application of Laplace method leading to (11.10). Moreover, the presence of logarithmic correction would clearly invalidate the $4/5$-th law (11.4), which is an exact results obtained from the Navier-Stokes equations.

The problem to reconcile logarithmic corrections in the multifractal model with the $4/5$-th law has been quantitatively addressed by Frisch et al. [20]. There, exploiting the refined large-deviations theory, the Authors were able to show in which way logarithmic contributions cancel out thus giving a prediction compatible with the naive (and a priory not justified) procedure to extract the scaling behavior (11.9). The key point is that the leading order large deviation result for the probability $P_\ell(h)$ to be within a distance ℓ of the set S_h carrying singularities of scaling exponent h must be extended to take into account next subleading order. As a result one obtains [20]

$$P_\ell(h) \sim \left(\frac{\ell}{L}\right)^{3-D(h)} \left[-\ln\left(\frac{\ell}{L}\right)\right]^{1/2} , \tag{11.13}$$

which contains subleading logarithmic correction. It is worth observing that despite the multiplicative character of the logarithmic correction one speaks of "subleading correction". This is justified by the fact that the correct statement of the large-deviations leading-order result involves the logarithm of the probability divided by the logarithm of the scale. The correction is then a subleading additive term.

Once the expression (11.13) is plugged in the integral

$$S_p(\ell) \sim \int dh P_\ell(h) \left(\frac{\ell}{L}\right)^{ph} \tag{11.14}$$

and the saddle point estimation is carried out according to [21], logarithms disappear and the 4/5-th law is correctly recovered.

It is worth mentioning that the presence of a square root of a logarithm correction in the multifractal probability density had already been discussed in [22] on the basis of a normalization requirement. In that paper, the Authors also pointed out that a similar correction has been proposed by [23] in connection with the measurement of generalized Renyi dimensions.

We conclude this section by observing that anomalous scaling for the velocity differences implies that the local dissipative scale, ℓ_D, does not take a unique value. The latter scale is indeed determined by imposing the effective Reynolds number to be of order unity:

$$Re(\ell_D) = \frac{\delta v_D \ell_D}{\nu} \sim 1\,, \tag{11.15}$$

therefore the dependence of ℓ_D on h is thus

$$\ell_D(h) \sim L Re^{-\frac{1}{1+h}} \tag{11.16}$$

where $Re = Re(L)$ is the large scale Reynolds number [18]. The fluctuation of the dissipative scale has important consequences on the statistics of small scale quantities, such as velocity gradients and acceleration, which will be discussed in the next sections. Another consequence is that it predicts the existence of an *intermediate dissipation range* at the lower bound of the inertial range, where the inertial range contributions of the various scaling exponents h are successively turned off [24].

11.3.1 The Statistics of Velocity Gradient

Let us denote by s the longitudinal velocity gradient, e.g. $s = \partial u_x/\partial x$. On the basis of the above considerations, this quantity can be expressed in terms of the singularity exponents h as

$$s \sim \frac{\delta v_D}{\ell_D} = v_0 \ell_D^{h-1} = v_0^{\frac{2}{1+h}} \nu^{\frac{h-1}{h+1}} \tag{11.17}$$

where we used the fact that $\delta v_D \simeq v_0 (\ell_D/L)^h$ and we have exploited (11.16). From (11.17) we realize that we can easily express the probability density function (PDF) of s (for a fixed h), $P_h(s)$, in terms of the PDF, $\Pi(V_0)$, of the large-scale velocity differences V_0, with $v_0 \equiv |V_0|$. The latter PDF is indeed known to be in general well described by a Gaussian distribution [25]. The link between the two PDFs is given by the standard relation:

$$P_h(s) = \Pi(V_0) \left| \frac{dV_0}{ds} \right| \tag{11.18}$$

from which one immediately gets:

$$P_h(s) \sim \frac{\nu}{|s|}^{\frac{1-h}{2}} e^{-\frac{\nu^{1-h}|s|^{1+h}}{2\langle V_0^2 \rangle}}. \tag{11.19}$$

The K41 theory corresponds to $h = 1/3$, therefore (11.19) predicts a stretched exponential form for the PDF with an exponent, $1+h$, larger than one. Experimental data (see e.g. [26,27]) are not consistent with this prediction and indicate for the tail of the PDF a stretched exponential with exponent smaller than one. In this respect, the multifractal description has been used to describe correctly these experimental evidences (see, e.g., [19] for a derivation).

11.3.2 The Statistics of Acceleration

Acceleration in fully developed turbulence is an extremely intermittent quantity which displays fluctuations up to 80 times its root mean square [28]. These extreme events generate very large tails in the PDF of acceleration which is therefore expected to be very far from Gaussian.

We remark that even within non-intermittent, Kolmogorov scaling turbulence, acceleration PDF is expected to be non-Gaussian. Indeed acceleration can be estimated from velocity fluctuations at the Kolmogorov scale as

$$a = \frac{\delta v(\tau_D)}{\tau_D} \tag{11.20}$$

where $\tau_D = \ell_D/\delta v_D$ and the Kolmogorov scale ℓ_D is given by the condition $\ell_D \delta v_D/\nu = 1$. Using the relation $\delta v(\ell) \simeq v_0(\ell/L)^h$ (with $h = 1/3$ for Kolmogorov scaling) one obtains

$$\frac{\ell_D}{L} \sim \left(\frac{v_0 L}{\nu} \right)^{-\frac{1}{1+h}} \tag{11.21}$$

and finally

$$a = \frac{v_0^2}{L} \left(\frac{v_0 L}{\nu} \right)^{\frac{1-2h}{1+h}} \tag{11.22}$$

Similarly to the derivation of the velocity gradient, assuming a Gaussian distribution for large scale velocity fluctuations v_0, and taking $h = 1/3$, one obtains for the PDF of a a stretched exponential tail $p(a) \sim \exp(-Ca^{8/9})$.

In the presence of intermittency the above argument has to be modified by taking into account the fluctuations of the scaling exponent and of the dissipative scale. In the recent years, several models have been proposed for describing turbulent acceleration statistics, on the basis of different physical ingredients. In the following we show that the multifractal model of turbulence, when extended to describe fluctuation at the dissipative scale, is able to predict the PDF of acceleration observed in simulations and experiments with high accuracy [29]. Moreover the model does not require the introduction of new parameters, besides the set of Eulerian scaling exponents. In this sense, multifractal model become a *predictive* model for the statistics of the acceleration.

Accounting for intermittency in the above argument is simply obtained by weighting (11.22) with both the distribution of v_0 (still assumed Gaussian, as intermittency is not expected to affect large scale statistics) and the distribution of scaling exponent h which can be rewritten, using (11.21), as

$$p(h) \sim \left(\frac{\ell_D}{L}\right)^{3-D(h)} \sim \left(\frac{v_0 L}{\nu}\right)^{\frac{D(h)-3}{1+h}} \tag{11.23}$$

The final prediction, when written for the dimensionless acceleration $\tilde{a} = a/\langle a^2\rangle^{1/2}$, becomes [29]

$$p(\tilde{a}) \sim \int_h \tilde{a}^{[h-5+D(h)]/3} R_\lambda^{y(h)} \exp\left(-\frac{1}{2}\tilde{a}^{2(1+h)/3} R_\lambda^{z(h)}\right) dh \tag{11.24}$$

where $y(h) = \chi(h-5+D(h))/6 + 2(2D(h)+2h-7)/3$ and $z(h) = \chi(1+h)/3+4(2h-1)/3$. $R_\lambda = v_{rms}\lambda/\nu$ is the Reynolds number based on the Taylor scale $\lambda = v_{rms}/\langle(\partial_x v_x)^2\rangle^{1/2}$. The coefficient χ is the scaling exponent for the Reynolds dependence of the acceleration variance, $\langle a^2\rangle \sim R_\lambda^\chi$. Its expression is given by $\chi = \sup_h (2(D(h)-4h-1)/(1+h))$. For the non-intermittent Kolmogorov scaling ($h = 1/3$ and $D(1/3) = 3$) one obtains $\chi = 1$ and (11.24) recovers the stretched exponential prediction discussed above.

We note that (11.24) may show an unphysical divergence for $a \to 0$ for many multifractal models of $D(h)$ at small h. This is not a real problem for two reasons. First, the multifractal formalism cannot be extended to very small velocity and acceleration increments because it is based on arguments valid only to within a constant of order one. Thus, it is not suited for predicting precise functional forms for the core of the PDF. Second, small values of h correspond to very intense velocity fluctuations which have never been accurately tested in experiments or DNS. The precise functional form of $D(h)$ for those values of h is therefore unknown.

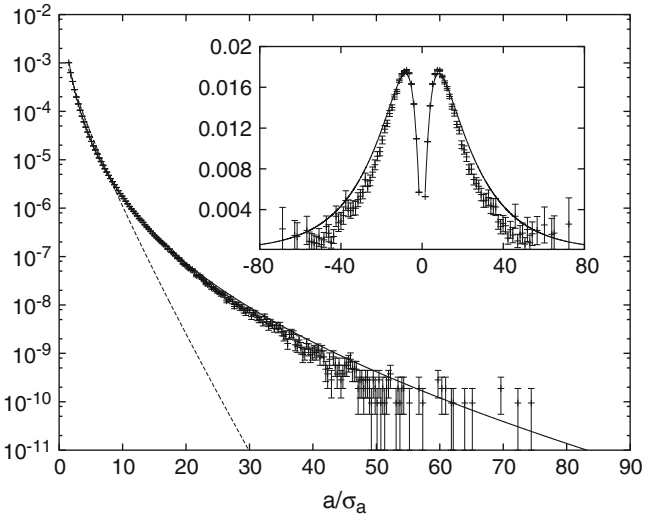

Fig. 11.2 Log-linear plot the PDF of the acceleration. Points are obtained from Direct Numerical Simulations of homogeneous-isotropic turbulence at $R_\lambda \simeq 280$ [29] with the statistics of 10^{10} events. The *dashed line* represents the K41 prediction $p(a) \sim exp(-Ca^{8/9})$. The *continuous line* is the multifractal prediction. *Inset*: $\tilde{a}^4\, p(\tilde{a})$ for the DNS data (*crosses*) and the multifractal prediction

Figure 11.2 shows the comparison between the PDF of the acceleration obtained from high-resolution Direct Numerical Simulations [29] together with the theoretical prediction obtained from K41 and the multifractal models. The figure clearly shows that the multifractal model is able to capture accurately the shape of the PDF. It is remarkable is that (11.24) agrees with the DNS data over a wide range of fluctuations – from the order of one standard deviation σ_a up to order $70\sigma_a$. We emphasize that the only free parameter in the multifractal formulation of $p(\tilde{a})$ is the minimum value of the acceleration, $\tilde{a}_{\min}$.

11.3.3 Multiplicative Processes for the Multifractal Model

We have seen in the previous section that the knowledge of the function $D(h)$ allows to predicts several features of a turbulent flow. An analytic computation of $D(h)$, or equivalently ζ_p, from the Navier-Stokes equations is a prohibitive task. In the past years a different approach has been developed, based on a phenomenological approach which gives closed expression for $D(h)$ on the basis of multiplicative processes. The use of multiplicative processes is inspired again from the Richardson cascade picture and the log-normal theory of Kolmogorov.

Let us briefly remind the so-called random β-model [2], generalization of the β-model discussed at the beginning of Sect. 11.3. This model describes the energy

cascade in real space looking at eddies of size $\ell_n = 2^{-n}L$, with L the length at which the energy is injected. At the n-th step of the cascade a mother eddy of size ℓ_n splits into daughter eddies of size ℓ_{n+1}, and the daughter eddies cover a fraction β_j ($0 < \beta_j < 1$) of the mother volume. The β_j's are independent, identically distributed random variables (the probabilistic nature of β_j reflects the complex dynamics generated by the Navier-Stokes equations). Therefore the velocity fluctuations $v_n = \delta v_{\ell_n}$ at the scale ℓ_n receive contributions only on a fraction of volume $\prod_j \beta_j$. Taking into account the fact that the energy flux must be constant throughout the cascade (i.e. the $4/5$-th law), one has

$$v_n = v_0 \ell_n^{1/3} \prod_{j=1}^{n} \beta_j^{-1/3} . \tag{11.25}$$

As stated above, all the physics is contained in the distribution of the coefficients β_j. A simple, and somehow phenomenologically motivated choice is to take $\beta_j = 1$ with probability x and $\beta_j = B = 2^{-(1-3h_{min})}$ with probability $1-x$ (we remark that the distribution is independent on the scale). This multiplicative process generates a two-scale Cantor set, which is a common structure in chaotic systems. The resulting scaling exponents are given by

$$\zeta_p = \frac{p}{3} - \ln_2[x + (1-x)B^{1-p/3}] \tag{11.26}$$

corresponding to

$$D(h) = 3 + (3h-1)\Big[1 + \ln_2\Big(\frac{1-3h}{1-x}\Big)\Big] + 3h \ln_2\Big(\frac{x}{3h}\Big) . \tag{11.27}$$

The two limit cases of interest are $x = 1$, i.e. K41 theory with $\zeta_p = p/3$, and $x = 0$ which gives the β-model with $D_F = 2 + 3h_{min}$. Using $x = 7/8$, $h_{min} = 0$ (i.e. $B = 1/2$) one has a good fit for the ζ_p of the experimental data (see Fig. 11.1).

There are many others different models which fit well the experimental scaling exponents, all based on some physical arguments. A popular model is the so-called She-Leveque model [30] where vortex filaments are a fundamental ingredient for intermittency. In terms of the multifractal model, the She-Leveque model is obtained by taking

$$D(h) = 1 + \frac{2\beta - 3h - 1}{\ln \beta}\left[1 - \ln\left(\frac{2\beta - 1 - 3h}{2\ln\beta}\right)\right] \tag{11.28}$$

and gives for the scaling exponents

$$\zeta_p = \frac{2\beta - 1}{3} p + 2(1 - \beta^{p/3}) . \tag{11.29}$$

The set of exponents given by (11.29) are close to the experimental data for $\beta = 2/3$ (see Fig. 11.1). Another important model, which was introduced by Kolmogorov himself without reference to the multifractal model, is the recalled log-normal model which will be discussed in the next section.

11.4 Fluctuations of the Energy Dissipation Rate

On September 1961, Kolmogorov gave a famous talk at a turbulence colloquium organized in Marseille. In this talk he presented new hypotheses, due to himself and to Obukhov which constitute the basis of what is known as the Kolmogorov-Obukhov 62 (KO62) theory [5].

At that time, there were not strong experimental motivations to call for an improvement of the K41 theory. The main criticisms were based on a theoretical ground and were due to a remark by Landau. The Landau's remark, as reported for instance by Frisch [3], states that the constants in (11.5), for example the constant C_2 for the second order longitudinal structure function, cannot be universal. As $\overline{\varepsilon^{2/3}}$ differs from $\overline{\varepsilon}^{2/3}$, the former depends from the distribution of ε at large scales, close to the integral one, which cannot be universal, as it depends on the forcing mechanism. This remark applies to all the structure functions and implies that C_p (a part C_3 which depends only on the average $\overline{\varepsilon}$) cannot be universal. The point that Kolmogorov emphasized, starting from this remark, is that dissipation is concentrated on very tiny regions of the flow. This may lead to anomalous values for the scaling exponents of velocity structure functions.

To take into account this point, Kolmogorov introduced the coarse grained energy dissipation on a ball of radius ℓ centered on $\mathbf{x}$

$$\varepsilon_\ell(\boldsymbol{x}, t) = \frac{1}{4/3\pi\ell^3} \int_{|y|<\ell} d\,\boldsymbol{y}\, \varepsilon(\boldsymbol{x} + \boldsymbol{y}, t) \tag{11.30}$$

and postulated that the dimensionless quantity

$$\frac{\delta v(\ell)}{\varepsilon_\ell^{1/3} \ell^{1/3}} \tag{11.31}$$

has a probability distribution independent of the local Reynolds number $Re_\ell = \delta v(\ell)\ell/\nu$ in the limit $Re_\ell \to \infty$. This is what is called the Refined Similarity Hypothesis (RSH). This hypothesis links the scaling laws of velocity structure functions with the scaling properties of the energy dissipation:

$$S_p(\ell) \sim \langle \delta v^p(\ell) \rangle \sim C_p \overline{\varepsilon_\ell^{p/3}} \ell^{p/3} \tag{11.32}$$

Kolmogorov then introduces a simple multiplicative model for the statistics of ε_ℓ. This leads to a Gaussian distribution for the logarithm of ε_ℓ with variance (for $\ln \varepsilon_\ell$)

$$\sigma_\ell^2 = A + 9\mu \ln(L/\ell) \tag{11.33}$$

The lognormal model leads to a parabolic prediction for scaling exponents

$$\zeta_p = \frac{p}{3} + \frac{\mu}{18} p(3-p) \tag{11.34}$$

in which the value of the free parameter can be fixed by experimental data as $\mu \simeq 0.025$.

The lognormal model KO62 can be described within the general framework of multifractal model by taking a quadratic $D(h)$

$$D(h) = -\frac{9}{2\mu} h^2 + 3\frac{2+\mu}{2} h - \frac{4 - 20\mu + \mu^2}{8\mu} \tag{11.35}$$

which, inserted in (11.10), leads to (11.34).

It can be useful to highlight the relationship between the multifractal model for fully developed turbulence and the description of singular measures (e.g. in chaotic attractors) based on the so-called $f(\alpha)$ spectrum [12]. For this purpose, let us introduce the measure $\mu(\mathbf{x}) = \varepsilon(\mathbf{x})/\bar{\varepsilon}$, based on the local energy dissipation rate, a partition of non overlapping cells Λ_ℓ of size ℓ and the coarse graining probability

$$P_i(\ell) = \int_{\Lambda_\ell(\mathbf{x}_i)} d\mu(\mathbf{x}) \tag{11.36}$$

where $\Lambda_\ell(\mathbf{x}_i)$ is a cube of edge ℓ centered in $\mathbf{x}_i$.

The coarse grained energy dissipation averaged over Λ_ℓ is given by $\varepsilon_\ell \sim \bar{\varepsilon}\ell^{-3} P(\ell)$. Denoting by α the scaling exponent of P_ℓ and with $f(\alpha)$ the fractal dimension of the subfractal with scaling exponent α, we can introduce the Renyi dimensions [18] d_p:

$$\sum_i P_i(\ell)^p \sim \ell^{(p-1)d_p} \tag{11.37}$$

where the sum is over the non empty boxes. A simple computation gives

$$(p-1)d_p = \min_\alpha [p\alpha - f(\alpha)] \ . \tag{11.38}$$

Noting that from the definition

$$\langle \varepsilon_\ell^p \rangle = \ell^3 \sum \varepsilon_\ell^p \tag{11.39}$$

we finally have

$$\langle \varepsilon_\ell^p \rangle \sim \ell^{(p-1)(d_p-3)} \tag{11.40}$$

In conclusion, we have the following correspondence between the multifractal model and the $f(\alpha)$ spectrum

$$h \leftrightarrow \frac{\alpha - 2}{3} \ , \ D(h) \leftrightarrow f(\alpha) \ , \ \zeta_p = \frac{p}{3} + \left(\frac{p}{3} - 1\right)\left(d_{\frac{p}{3}} - 3\right) . \tag{11.41}$$

which, as it should, gives $\zeta_3 = 1$ independently on the form of $f(\alpha)$.

11.5 Conclusions

The experimental study of fully developed turbulence led to the introduction of large deviation theory, in the form of the multifractal model, in order to describe the intermittent nature of the turbulent flow. The multifractal model has been successfully used to describe many features of turbulent flows: from scaling exponents of the structure functions to the statistics of the velocity gradients and acceleration, to the scaling of Lagrangian quantities. Despite the fact that the model is not predictive, once the function $D(h)$ is given, or measured from experimental data, all the other quantities are given without free parameters. In this sense we can see at the multifractal model as a tool which provides, within the general framework of large deviations, a general and consistent comprehension of different aspects of turbulence.

References

1. G. Parisi, U. Frisch, in *Turbulence and Predictability of Geophysical Fluid Dynamics*, ed. by M. Ghil, R. Benzi, G. Parisi (Amsterdam, North-Holland, 1985), p. 84
2. R. Benzi, G. Paladin, G. Parisi, A. Vulpiani, J. Phys. A Math. Gen. **17**, 3521 (1984)
3. U. Frisch, *Turbulence: The Legacy of A.N. Kolmogorov* (Cambridge University Press, Cambridge, 1995)
4. D. Harte, *Multifractals: Theory and Applications* (CRC, New York, 2001)
5. A.N. Kolmogorov, J. Fluid Mech. **13**, 82 (1962)
6. E.A. Novikov, R.W. Stewart, Izv. Akad. Nauk SSSR Geofiz. **3**, 408 (1964)
7. B.B. Mandelbrot, J. Fluid Mech. **62**, 331 (1974)
8. P.K. Kundu, I.M. Cohen, D.R. Dowling, *Fluid Mechanics* (Academic, Waltham, 2012)
9. O.A. Ladyzhenskaya, *The Mathematical Theory of Viscous Incompressible Flow* (Gordon and Breach, New York, 1969)
10. J. Bricmont, A. Kupiainen, R. Lefevere, Commun. Math. Phys. **230**, 87 (2002)
11. M. Hairer, J.C. Mattingly, Ann. Math. **164**, 993 (2006)
12. T. Bohr, M.H. Jensen, G. Paladin, A. Vulpiani, *Dynamical Systems Approach to Turbulence* (Cambridge University Press, Cambridge, 1998)

13. A.N. Kolmogorov, Dokl. Akad. Nauk. SSSR, **30**, 299 (1941); reprinted in A.N. Kolmogorov, Proc. R. Soc. Lond. A **434** 9 (1991)
14. A. Monin, A. Yaglom, *Statistical Fluid Dynamics* (MIT, Cambridge, 1975)
15. L.F. Richardson, *Weather Prediction by Numerical Processes* (Cambridge University Press, Cambridge, 1922)
16. G.I. Taylor, Proc. R. Soc. Lond. A **151**, 421 (1935)
17. F. Anselmet, Y. Gagne, E.J. Hopfinger, R.A. Antonia, J. Fluid Mech. **140**, 63 (1984)
18. G. Paladin, A. Vulpiani, Phys. Rep. **156**, 147 (1987)
19. G. Boffetta, A. Mazzino, A. Vulpiani, J. Phys. A Math. Theor. **41**, 363001 (2008)
20. U. Frisch, M.M. Afonso, A. Mazzino, V. Yakhot, J. Fluid Mech. **542**, 97 (2005)
21. C.M. Bender, S.A. Orszag, *Advanced Mathematical Methods for Scientists and Engineers* (Springer, New York, 1999)
22. C. Meneveau, K.R. Sreenivasan, Phys. Lett. A **137**, 103 (1989)
23. W. van de Water, P. Schram, Phys. Rev. A **37**, 3118 (1988)
24. U. Frisch, M. Vergassola, Europhys. Lett. **14**, 439 (1991)
25. U. Frisch, Z.S. She, Fluid Dyn. Res. **8**, 139 (1991)
26. B. Castaing, Y. Gagne, E.J. Hopfinger, Physica D **46**, 177 (1990)
27. A. Vincent, M. Meneguzzi, J. Fluid Mech. **225**, 1 (1991)
28. A. La Porta, G.A. Voth, A.M. Crawford, J. Alexander, E. Bodenschatz, Nature **409**, 1017 (2001)
29. L. Biferale, G. Boffetta, A. Celani, B.J. Devenish, A. Lanotte, F. Toschi, Phys. Rev. Lett. **93**, 064502 (2004)
30. Z.S. She, E. Lévêque, Phys. Rev. Lett. **72**, 336 (1994)

Index

Additivity principle, 82
Anomalous fluctuations, 149
Anomalous scaling, 296, 299, 300, 302, 306, 307
Anomalous transport, 264
Atomic theory, 2
Avogadro number, 2

Bernoulli map, 246, 281
β-model, 18, 300, 305, 306
Birkhoff-Khinchin theorem, 34
Blume-Capel model, 205
Boltzmann equation, 93
Boltzmann-Gibbs distribution, 162
Boundary condition, 73–75, 82–84, 86
Breathers, 50
Brownian motion, 2, 95
Brownian motors, 222, 224, 225

Canonical ensemble, 17
Cellular automata, 259
Central limit theorem, 3, 4, 9–11, 264, 267
Chaotic hypothesis, 119
Chaotic systems, 9, 19
Chemical potential, 73–75, 83, 86–88
Clustering, 56
Complex viscosity, 102
Concave envelope of microcanonical entropy, 200
Connected configuration path, 178
Connectivity dimension, 273
Conservation law, 73
Continuous time random walk, 269, 277, 283
Coulomb friction, 225, 232, 234, 235
Covariance matrix, 258
Cramér function, 4, 11–13, 15–17, 20, 21, 25, 26, 136, 167, 230, 232, 236
Critical exponents, 197
Cumulant generating function, 12
Current, 71–75, 77–84, 87–89

Data reweighting, 163, 164, 166
Detailed balance, 24, 25, 230
Detailed balance violation, 228
Deterministic anomalous transport, 281
Discrete nonlinear Schrödinger Equation, 47
Disordered systems, 9, 136, 142
Dissipation function, 121
Dobrushin-Lanford-Ruelle condition, 60
Dynamical system, 21, 33, 103, 243
Dynamical zeta function, 290

Einstein formula, 94
Einstein relation, 73, 86
Energy dissipation rate, 18, 299, 300, 307, 308
Energy histogram, 164, 169
Ensemble theory, 32
Entropy production, 26, 223, 231, 232, 236
Ergodicity. *See* ergodic problem
Ergodicity (violation of), 36, 40, 52, 56, 196, 211
Ergodic hypothesis, 5–7, 30, 34
Ergodic problem, 4, 5, 7, 8, 30, 107
Extensivity, 194
External field, 71, 73–77, 83, 84, 86–88

Fermi-Pasta-Ulam model, 37
Finite-time Lyapunov exponent, 20, 250, 252, 253, 255

A. Vulpiani et al. (eds.), *Large Deviations in Physics*, Lecture Notes in Physics 885,
DOI 10.1007/978-3-642-54251-0, © Springer-Verlag Berlin Heidelberg 2014

First-order phase transitions, 201
Fluctuation(s), 1, 2, 304
Fluctuation-dissipation relation, 78, 93, 98, 99
  of first kind, 102
  of second kind, 102
Fluctuation-Dissipation Theorem, 2
Fluctuation relations, 25, 26, 118
Fourier-Laplace transform, 288
Fractal dimension, 300, 308
Free-electron laser, 215
Free energy, 17, 22, 23

Gallavotti-Cohen theory, 119, 120
Gärtner-Ellis theorem, 157, 198, 200
Gaussian random matrices, 154
Generalized admittance, 102
Generalized impedance, 102
Generalized Lyapunov exponents, 23
Generating function, 290
Granular systems, 223, 231
Green-Kubo relations, 95, 101, 118, 125, 126

Hamilton-Jacobi equation, 72, 78, 80, 89
Helmhotz free energy, 164, 165
Hénon map, 250
High-temperature distributions, 179–181, 184
Hyperbolic, 252

Importance sampling, 162, 163
Inelastic collisions, 223, 231
Inequivalence of ensembles, 201, 207
Inertial range, 297, 298, 300
Infinite ergodic theory, 282
Intermediate dissipative range, 302
Intermittency, 18, 19, 281, 296, 299, 304
Intermittent maps, 283, 284
Ising model, 167

Jackknife method, 168
Jarzynski equality, 95, 126, 127
Johnson-Nyquist noise, 99

Kac's scaling of couplings, 195
KAM theory, 42
Kaplan-Yorke formula, 254
Kinetic ratchet, 225, 232, 234
Kolmogorov refined similarity hypotheis, 307
Kolmogorov-Sinai entropy, 244, 248, 257
Komogorov theory, 296–298, 300
Kullback-Leibler divergence, 14

Langevin equation, 96, 228
Laplacian matrix, 275
Large deviation(s), 78, 118, 301
  formalism, 244
  functional, 75, 77, 78, 85
  theory, 3, 4, 11–13
Large deviation function. *See* Cramér function
4/5-th law, 296, 298, 300–302
Law of large numbers, 3, 4, 7, 136
Legendre transform, 12, 138, 200
Lévy stable laws, 267
Lévy walks, 277, 287
Linear response, 108
Liouville equation, 105, 109
Liquid-gas transition, 181
Local equilibrium, 71, 72
Local invariance, 300
Lognormal approximation, 16
Lognormal model, 308
Long-range interactions, 194
Long range correlations, 80, 81
Lorentz gas, 289
Low-temperature distributions, 179–181
Lyapunov exponents, 19–22, 144, 244, 257
Lyapunov vectors, 250

Macroscopic correlation, 80
Macroscopic Fluctuation Theory, 72, 74, 84, 89
Macroscopic state, 31
Markov chain, 6, 7
Markovian microscopic dynamics, 80
Markov processes, 24
Maximal ignorance principle, 203
Mean field Ising model, 139
Mean field spin glass, 151
Mean-field systems, 194
Metastable states, 137
Metrically indecomposable, 7
Metrically transitive, 7
Metropolis algorithm, 162, 176
Min-Max procedure, 216
Mixing, 35, 107, 129
Mobility, 97, 101
  complex mobility, 102

Molecular motors, 224, 227
Moments, 268
Monte Carlo method, 162
Multicanonical sampling, 178
Multifractal, 18, 19, 248, 250
Multifractal model, 295, 299–301, 304–306, 308, 309
Multiple histogram method, 168
Multiplicative process, 9, 18, 305

Navier-Stokes equations, 296–298, 301
Negative magnetic susceptibility, 212
Negative specific heat, 202, 205
Negative temperature, 47, 49
Nonequilibrium dynamics, 221, 224
Nonequilibrium fluctuations, 224, 231
Nonequilibrium states, 71, 72, 74, 84, 90, 222, 231
Nonequilibrium thermodinamics, 71
Non-extensivity, 194, 197
Non-hyperbolic, 252

One-dimensional maps, 281
Onsager-Machlup theory, 72, 112
Onsager relations, 95, 118
Oseledec splitting, 256
Oseledec theorem, 9, 21–23, 144, 156
Overlap parameter, 155

Parallel tempering, 184, 185
Partition, 245
Partition function, 17, 22, 163
Periodic orbit theory, 290
Pesin relation, 253
Phase transition, 17, 81, 82, 84, 89
ϕ^4 model, 212
Pointwise entropy, 248, 249
Potts model, 179, 203
Power spectrum, 100, 101
Product of random matrices, 21, 144
Product of random variables, 15, 18
Pure state, 59

Quasi potential, 75, 78, 80, 85–89

Random β-model, 305, 306
Random directed polymer, 151
Random field Ising model, 158
Random Ising chain, 143, 147, 156
Random walks on graphs, 272, 277
Ratchet effect, 221, 231
Rate function. *See* Cramér function
Reaction-diffusion systems, 85
Regression hyptothesis, 113
Relative entropy. *See* Kullback-Leibler divergence
Renyi dimensions, 308
Renyi entropies, 247
Repeller, 260
Replica method, 143, 145
Replica Symmetry Breaking, 153
Response function, 3
Reynolds number, 296–298, 302, 304, 307

Scale invariance, 296
Scaling, 268, 272
Scaling exponent, 300–302, 304
Second-order phase transitions, 200
Self-averaging property, 22, 23, 143, 155, 157
Sensitive dependence on initial conditions, 19, 20
Shannon entropy, 247
Shear fluid model isoenergetic, 118
Sherrington-Kirkpatrick model, 146, 151
Simulated tempering, 173
Space-time chaos, 257
Spatial asymmetry, 221, 228, 230–232, 234
Specific heat, 165, 166
Spectral dimension, 274, 276
Spherical spin-glass model, 154
Spin glass transition, 152
Stable chaos, 259
Statistical error, 164, 165
Steady state fluctuation relation, 26
Stochastic stability, 62, 65
Strong anomalous diffusion, 277
Structure functions, 298, 299, 307
Subdiffusion, 266, 272, 287
Sum functions, 8
Superdiffusion, 266, 277, 287
Synchronization transitions, 254

Tauberian theorems, 271
Thermodynamic limit, 257
Thermostat, 118
Time reversal, 72, 78–80, 89, 221
Time-reversal dynamics, 24, 103
t-mixing, 127
Toda model, 43, 45
Transfer matrix formalism, 22, 23

Transfer operator, 290
Transport coefficient, 71–73, 82
Turbulence, 18, 295–305, 307, 309
Turbulent acceleration, 303–305

Ultrametricity, 67
Umbrella sampling, 172
Universality, 83

Varadhan's theorem, 199
Velocity gradients, 302

Weak anomalous diffusion, 272
Wiener-Khinchin theorem, 100

XY-model, 208